

ST&B

U 393

.S7

CP

v. 1

Copy 1







Return To  
**SCIENCE AND TECHNOLOGY DIVISION**  
Library of Congress







SUMMARY TECHNICAL REPORT  
OF THE  
NATIONAL DEFENSE RESEARCH COMMITTEE



Manuscript and illustrations for this volume were prepared for publication by the Summary Reports Group of the Columbia University Division of War Research under contract OEMsr-1131 with the Office of Scientific Research and Development. This volume was printed and bound by the Columbia University Press.

Distribution of the Summary Technical Report of NDRC has been made by the War and Navy Departments. Inquiries concerning the availability and distribution of the Summary Technical Report volumes and microfilmed and other reference material should be addressed to the War Department Library, Room 1A-522, The Pentagon, Washington 25, D. C., or to the Office of Naval Research, Navy Department, Attention: Reports and Documents Section, Washington 25, D. C.

Copy No.

3

This volume, like the seventy others of the Summary Technical Report of NDRC, has been written, edited, and printed under great pressure. Inevitably there are errors which have slipped past Division readers and proofreaders. There may be errors of fact not known at time of printing. The author has not been able to follow through his writing to the final page proof.

Please report errors to:

JOINT RESEARCH AND DEVELOPMENT BOARD  
PROGRAMS DIVISION (STR ERRATA)  
WASHINGTON 25, D. C.

A master errata sheet will be compiled from these reports and sent to recipients of the volume. Your help will make this book more useful to other readers and will be of great value in preparing any revisions.



SUMMARY TECHNICAL REPORT OF THE  
COMMITTEE ON PROPAGATION, NDRC  
VOLUME 1

# HISTORICAL AND TECHNICAL SURVEY

OFFICE OF SCIENTIFIC RESEARCH AND DEVELOPMENT  
VANNEVAR BUSH, DIRECTOR

NATIONAL DEFENSE RESEARCH COMMITTEE  
JAMES B. CONANT, CHAIRMAN

COMMITTEE ON PROPAGATION  
CHAS. R. BURROWS, CHAIRMAN

---

WASHINGTON, D. C., 1946

WAR DEPARTMENT  
LIBRARY  
WASHINGTON, D. C.



# NATIONAL DEFENSE RESEARCH COMMITTEE

James B. Conant, *Chairman*

Richard C. Tolman, *Vice Chairman*

Roger Adams

Army Representative<sup>1</sup>

Frank B. Jewett

Navy Representative<sup>2</sup>

Karl T. Compton

Commissioner of Patents<sup>3</sup>

Irvin Stewart, *Executive Secretary*

<sup>1</sup>*Army Representatives in order of service:*

Maj. Gen. G. V. Strong

Col. L. A. Denson

Maj. Gen. R. C. Moore

Col. P. R. Faymonville

Maj. Gen. C. C. Williams

Brig. Gen. E. A. Regnier

Brig. Gen. W. A. Wood, Jr.

Col. M. M. Irvine

Col. E. A. Routheau

<sup>2</sup>*Navy Representatives in order of service:*

Rear Adm. H. G. Bowen

Rear Adm. J. A. Furer

Capt. Lybrand P. Smith

Rear Adm. A. H. Van Keuren

Commodore H. A. Schade

<sup>3</sup>*Commissioners of Patents in order of service:*

Conway P. Coe

Casper W. Ooms

## NOTES ON THE ORGANIZATION OF NDRC

The duties of the National Defense Research Committee were (1) to recommend to the Director of OSRD suitable projects and research programs on the instrumentalities of warfare, together with contract facilities for carrying out these projects and programs, and (2) to administer the technical and scientific work of the contracts. More specifically, NDRC functioned by initiating research projects on requests from the Army or the Navy, or on requests from an allied government transmitted through the Liaison Office of OSRD, or on its own considered initiative as a result of the experience of its members. Proposals prepared by the Division, Panel, or Committee for research contracts for performance of the work involved in such projects were first reviewed by NDRC, and if approved, recommended to the Director of OSRD. Upon approval of a proposal by the Director, a contract permitting maximum flexibility of scientific effort was arranged. The business aspects of the contract, including such matters as materials, clearances, vouchers, patents, priorities, legal matters, and administration of patent matters were handled by the Executive Secretary of OSRD.

Originally NDRC administered its work through five divisions, each headed by one of the NDRC members. These were:

Division A—Armor and Ordnance

Division B—Bombs, Fuels, Gases, & Chemical Problems

Division C—Communication and Transportation

Division D—Detection, Controls, and Instruments

Division E—Patents and Inventions

In a reorganization in the fall of 1942, twenty-three administrative divisions, panels, or committees were created, each with a chief selected on the basis of his outstanding work in the particular field. The NDRC members then became a reviewing and advisory group to the Director of OSRD. The final organization was as follows:

Division 1—Ballistic Research

Division 2—Effects of Impact and Explosion

Division 3—Rocket Ordnance

Division 4—Ordnance Accessories

Division 5—New Missiles

Division 6—Sub-Surface Warfare

Division 7—Fire Control

Division 8—Explosives

Division 9—Chemistry

Division 10—Absorbents and Aerosols

Division 11—Chemical Engineering

Division 12—Transportation

Division 13—Electrical Communication

Division 14—Radar

Division 15—Radio Coordination

Division 16—Optics and Camouflage

Division 17—Physics

Division 18—War Metallurgy

Division 19—Miscellaneous

Applied Mathematics Panel

Applied Psychology Panel

Committee on Propagation

Tropical Deterioration Administrative Committee



## NDRC FOREWORD

AS EVENTS of the years preceding 1940 revealed more and more clearly the seriousness of the world situation, many scientists in this country came to realize the need of organizing scientific research for service in a national emergency. Recommendations which they made to the White House were given careful and sympathetic attention, and as a result the National Defense Research Committee (NDRC) was formed by Executive Order of the President in the summer of 1940. The members of NDRC, appointed by the President, were instructed to supplement the work of the Army and the Navy in the development of the instrumentalities of war. A year later, upon the establishment of the Office of Scientific Research and Development [OSRD], NDRC became one of its units.

The Summary Technical Report of NDRC is a conscientious effort on the part of NDRC to summarize and evaluate its work and to present it in a useful and permanent form. It comprises some seventy volumes broken into groups corresponding to the NDRC Divisions, Panels, and Committees.

The Summary Technical Report of each Division, Panel, or Committee is an integral survey of the work of that group. The first volume of each group's report contains a summary of the report, stating the problems presented and the philosophy of attacking them, and summarizing the results of the research, development, and training activities undertaken. Some volumes may be "state of the art" treatises covering subjects to which various research groups have contributed information. Others may contain descriptions of devices developed in the laboratories. A master index of all these divisional, panel, and committee reports which together constitute the Summary Technical Report of NDRC is contained in a separate volume, which also includes the index of a microfilm record of pertinent technical laboratory reports and reference material.

Some of the NDRC-sponsored researches which had been declassified by the end of 1945 were of sufficient popular interest that it was found desirable to report them in the form of monographs, such as the series on radar by Division 14 and the monograph on sampling inspection by the Applied Mathematics Panel. Since the material treated in them is not

duplicated in the Summary Technical Report of NDRC, the monographs are an important part of the story of these aspects of NDRC research.

In contrast to the information on radar, which is of widespread interest and much of which is released to the public, the research on subsurface warfare is largely classified and is of general interest to a more restricted group. As a consequence, the report of Division 6 is found almost entirely in its Summary Technical Report, which runs to over twenty volumes. The extent of the work of a division cannot therefore be judged solely by the number of volumes devoted to it in the Summary Technical Report of NDRC; account must be taken of the monographs and available reports published elsewhere.

Though the Committee on Propagation had a comparatively short existence, being organized rather late in the war program, its accomplishments were definitely effective. That so many individuals and organizations worked together so harmoniously and contributed so willingly to the Committee's efforts is a tribute to the leadership of the Chairman, Chas. R. Burrows. The latest information in this field was gathered from the four corners of the earth, organized, and dispatched to the points where it would aid most in the prosecution of the war.

Much credit must be given, not only to the members of the Committee and its contractors, but also to the many other individuals who gave so generously of their time and effort. This group included a number of our Canadian and British allies. In addition to the assistance given the war effort, a considerable contribution has been made to the knowledge of short-wave transmission and especially to the interrelation of this phenomenon with meteorological conditions. Such information will be most valuable in weather forecasting and in furthering the usefulness of the whole radio field.

VANNEVAR BUSH, Director

*Office of Scientific Research and Development*

J. B. CONANT, Chairman

*National Defense Research Committee*







## FOREWORD

THE SUCCESS of the propagation program was the result of the wholehearted cooperation of many individuals in the various organizations concerned, not only in this country but in England, Canada, New Zealand, and Australia. The magnitude of the research work accomplished was possible only because of the willingness of the workers in many organizations to undertake their parts of the overall program. In fact, the entire program of the Committee on Propagation was carried out without the necessity of the Committee exercising directive authority over any project.

Dr. Hubert Hopkins of the National Physical Laboratory in England and Mr. Donald E. Kerr of the Radiation Laboratory at the Massachusetts Institute of Technology, who were working on this phase of the war effort when the Propagation Committee was formed, were instrumental in giving a good start to its activities. The largest single group working for the Committee was under Mr. Kerr.

The existence of a common program for the united nations in radio wave propagation resulted from the splendid cooperation given the Propagation Mission to England by Sir Edward Appleton and his Ultra Short Wave Panel. Later, through the cooperation of Canadian engineers and scientists, Dr. W. R. McKinley of the National Research Council of Canada and Dr. Andrew Thomson of the Air Services Meteorological Division, Department of Transport, Toronto, Canada, undertook to carry on a part of the program originally assigned to the United States. The program was further rounded out by the willingness of the New Zealand government to undertake an experiment for which their situation was particularly favorable. Dr. F. E. S. Alexander of New Zealand and Dr. Paul A. Anderson of the State College of Washington initiated this work. Needless to say, the labor of the Committee on Propagation could hardly have been effective without the cooperation of the Army and Navy. Maj. Gen. H. M. McClelland personally established Army coopera-

tion, and Lt. Comdr. Ralph A. Krause and Capt. Lloyd Berkner were similarly helpful in organizing Navy liaison and help.

Officers and scientific workers of the U. S. Navy Radio and Sound Laboratory at San Diego, California, altered their program on propagation to fit in with the overall program of the Committee. Capt. David R. Hull, Bureau of Ships, understanding the importance of the technical problems, paved the way for effective cooperation by this laboratory.

Dr. Ralph Bown, Radio and Television Research Director, Bell Telephone Laboratories, integrated the research program undertaken by Bell Telephone Laboratories for the Committee on Propagation. This joint research program included meteorological measurements on Bell Telephone Laboratories property by meteorologists of the Army Air Forces working with Col. D. N. Yates, Director, and Lt. Col. Harry Wexler of the Weather Wing, Army Air Forces. The accomplishments of the Committee on Propagation are a good example of the effectiveness of cooperation—all parts were essential and none more than the rest.

I want to thank Dr. Karl T. Compton, President of the Massachusetts Institute of Technology, who was always willing to discuss problems of the Committee and who helped me to solve many of the more difficult ones, and also, Prof. S. S. Attwood, University of Michigan, whose continual counsel throughout my term of office was in no small way responsible for the success of our activity.

Credit is also due Bell Telephone Laboratories, which made my services available to the government and paid my salary from August 1943 to September 1945, and to Cornell University, which has allowed me time off with pay to complete the work of the Committee on Propagation since September 1945.

CHAS. R. BURROWS

Chairman, Committee on Propagation







## PREFACE

IN THIS SERIES of three volumes, which is part of the Summary Technical Report of NDRC, the Committee on Propagation is presenting a record of its activities and technical developments. The material presented, concerning as it does the propagation of radio waves through the troposphere, is of permanent value both in war and in peace.

The present volume is divided into four parts. Part I outlines the organization and activities of the NDRC Committee on Propagation, gives the mechanism used for coordinating the various Service and civilian organizations interested in propagation, and makes recommendations for continued activity in studying propagation phenomena.

Part II gives a critical overall view of the technical developments in the study of tropospheric propagation. Outlined is the general theory of both standard and nonstandard propagation together with descriptions and results of transmission experiments carried out in widely separated parts of the earth and designed to test the theory. Included also is a résumé of the meteorological factors affecting propagation of waves and their attenuation in the atmosphere.

The second, third, and fourth Conferences on Propagation, under the auspices of the NDRC Committee on Propagation, were held in February 1944,

November 1944, and May 1945, respectively. The bulk of the technical material presented at the conferences is published in Volume 2 of this series and in Part III and Part IV of the present volume. These comprise the material dealing with the theory of both standard and nonstandard propagation. Certain reports have been omitted, primarily because the material was superseded by later studies or is covered adequately elsewhere.

The General Bibliography lists reports on tropospheric propagation issued by numerous Service and civilian organizations of both the United States and the British Empire. With a few exceptions, original reports listed in the Bibliography for this volume have been microfilmed. A few, such as summary reports issued by the Columbia University Wave Propagation Group and the compiled Propagation Conference Reports, are included in the present series.

Acknowledgment is due to the many authors who have contributed to this series, not only for the material and its oral presentation at the conferences, but also for their willingness to prepare the material in form for permanent record.

STEPHEN S. ATTWOOD  
Editor







# CONTENTS

CHAPTER

PAGE

Summary . . . . .	1
-------------------	---

## *PART I*

### *HISTORY*

1	Origin and Organization . . . . .	5
2	Objectives and Research Agencies . . . . .	9
3	Chronological Record . . . . .	13
4	Results and Recommendations . . . . .	25

## *PART II*

### *SUMMARY*

5	Standard Propagation . . . . .	31
6	Elementary Theory of Nonstandard Propagation . . . . .	42
7	Meteorological Measurements . . . . .	50
8	Transmission Experiments . . . . .	58
9	General Meteorology and Forecasting . . . . .	75
10	Scattering and Absorption of Microwaves . . . . .	82

## *PART III*

### *CONFERENCE REPORTS ON STANDARD PROPAGATION*

11	A Graphical Method for the Determination of Standard Coverage Charts . . . . .	93
12	Nomographic Solutions for the Standard Case . . . . .	95
13	Theoretical Analysis of Errors in Radar Due to Atmospheric Refraction . . . . .	106
14	Diffraction of Radio Waves over Hills . . . . .	110
15	Siting and Coverage of Ground Radars . . . . .	113
16	Variations in Radio Coverage . . . . .	178



*PART IV**CONFERENCE REPORTS ON NONSTANDARD  
PROPAGATION*

17	Tropospheric Propagation and Radio Meteorology . . . . .	189
18	Theoretical Treatment of Nonstandard Propagation in the Diffraction Zone . . . . .	226
19	Characteristic Values for the First Mode for the Bilinear <i>M</i> Curve . . . . .	228
20	Incipient Leakage in a Surface Duct . . . . .	233
21	The Solution of the Propagation Equation in Terms of Hankel Functions . . . . .	237
22	Attenuation Diagrams for Surface Ducts . . . . .	240
23	Approximate Analysis of Guided Propagation in a Nonhomogeneous Atmosphere . . . . .	244
24	Some Theoretical Results on Nonstandard Propagation . . .	247
25	Perturbation Theory for an Exponential <i>M</i> Curve in Nonstandard Propagation . . . . .	249
26	First Order Estimation of Radar Ranges over the Open Ocean . . . . .	256
27	Convergence Effects in Reflections from Tropospheric Layers . . . . .	258
	Bibliography—Volume 1 . . . . .	261
	General Bibliography . . . . .	277
	OSRD Appointees . . . . .	310
	Contracts . . . . .	311
	Service Projects . . . . .	312
	Index . . . . .	313

# INTRODUCTION

THIS REPORT IS a summary of the activities of the Committee on Propagation, NDRC. It is divided into three parts, each of which deals with a particular type of activity or record.

Part I is an account of the administrative activities of the Committee, its origin, organization, and work, with a description of the needs of the armed forces which called it into being. It is divided into four chapters for convenient reference. In general, the technical aspects of the problems set before the Committee, and of the work undertaken to solve those problems, are touched on in Part I only sufficiently to make clear the needs of the Services and the steps taken to satisfy those needs. Actual chronology is adhered to as far as possible with any departures indicated where they occur. This part of the report is designed to serve not only as a record of the Committee's work but to assist any future group in the organization of a similar program, should the occasion arise. Chapters 1 and 2 describe the organizational setup, liaison channels, objectives, the changes which occurred, and the reasons for making them. Chapter 3 relates the chronological activities of the organization. Chapter 4 summarizes the results accomplished and also contains a critique of the organization and its work, as evaluated by the chairman, with recommendations for future investigation in this field.

Part II is a technical description of the development of propagation work during World War II and the results obtained by the various organizations engaged in this work. Chapter 5 begins with a definition of certain basic concepts and proceeds with a review of so-called standard propagation as known at the beginning of the war. For a rapid survey of the vast body of information that has since been acquired, Chapter 6 reviews nonstandard propagation from an elementary theoretical viewpoint. The principal discovery made during the war is that the effective range of radar and short-wave radio equipment depends essentially and critically on the distribution of the refractive index in the lower strata of the atmosphere. In Chapter 7 the newly developed methods for the measurement of the refractive index variation are described, and a collection of typical refractive index curves resulting from actual measurements in various parts of the world is presented.

Chapter 8, the central chapter of Part II, gives a brief chronological record and the principal results of

the major propagation experiments performed in Great Britain, Canada, and the United States. Because short and microwave propagation characteristics are determined by the physical condition of the lower atmosphere, they are intimately connected with the evolution of the weather on a large scale as studied by the forecasting meteorologist. The relationships between the dynamics of the air and the distribution of refractive index are presented in Chapter 9. A review of the climatic and seasonal conditions involved in various parts of the world and of the bearing of all these factors upon the forecasting of radio propagation conditions is included. Finally, in Chapter 10, the results of investigations on the atmospheric absorption of microwaves and of the scattering of short and microwaves by radar targets and by raindrops are summarized.

The data given in this report refer only to the transmission of the higher frequency bands, above about 30 mc.

Parts III and IV are devoted to the presentation of 18 reports, out of 61 published in the Summary Technical Report, which were presented before the second, third and fourth conferences on propagation held in February, 1944, November 1944, and May 1945, or were published by the Columbia University Wave Propagation Group. Those appearing in Chapters 11 through 15 are concerned with standard propagation; Chapters 16 through 27 with nonstandard propagation. The remaining 43 reports are published in Volume 2.

One of the main functions of the Committee was to bring about a rapid exchange of information between the laboratories and Service units working on the subject, thus making the results available to all workers technically concerned with the military application of radar and other short wave radio equipment. To fulfill this function the Columbia University Wave Propagation Group operating under contract with the Committee periodically published a comprehensive bibliography on propagation, beginning in the spring of 1944. Its fifth and last edition, issued in August 1945, is included in this volume. This bibliography is a rather exhaustive documentation of the efforts made during the war in this field by Great Britain, Canada, New Zealand, Australia, and the United States. Reference to papers and reports is made in the main body of this summary by superior numbers.





*PART I*  
*HISTORY*





## Chapter 1

### ORIGIN AND ORGANIZATION

#### 1.1

#### ORIGIN

IN AUGUST 1943, Dr. K. T. Compton, a member of the National Defense Research Committee [NDRC], in the course of discharging his duties resulting from his "radar mission" to England, asked Dr. Chas. R. Burrows of the Bell Telephone Laboratories if he would undertake the coordination of research work on radio wave propagation in the United States under the auspices of NDRC. This was the initial step in the formation of the Committee on Propagation. During the Compton radar mission the urgent need for radar information in the armed forces was discussed by Dr. Compton and Sir Edward Appleton.

The Committee on Propagation of the National Defense Research Committee was organized in August 1943, under the chairmanship of Dr. Burrows. This body was created for the purpose of coordinating American scientific investigation of the propagation of electromagnetic waves through the lower atmosphere (troposphere), correlating the United States research with that being carried out in Great Britain and other countries of the United Nations and transmitting the information obtained to the Armed Forces in usable form, as speedily as possible.

It was decided that the propagation phenomena referred to could be divided into two classes: one, the effects of the troposphere itself on electromagnetic radiation of the wavelengths under discussion and, two, the effects of the earth's land and water surfaces in reflecting radiation incident at various angles. A British memorandum dated April 28, 1943 was drawn up, inviting specific United States cooperation in investigation of the following problems:

1. The entire question of effects of tropospheric conditions near and over a continental land mass similar in size, climate, and topography to Europe, on radiation of radar frequencies, in meteorological environments ranging from polar to tropical, with particular emphasis on obtaining quantitative data. British facilities and environments for this investigation were limited.

2. An exhaustive study of propagation under desert and moist tropical conditions, particularly with transmitter and receiver at heights of less than 100 ft.

3. Propagation under temperate climatic conditions with either the receiver or transmitter at heights from 5,000 to 10,000 ft.

4. Experiments to determine the dependence of the reflection coefficient on the angle of incidence with the surface of a rough sea.

5. Experiments along nearly optical paths over various kinds of topography likely to be encountered in field operations. Exhaustive knowledge of this aspect of the general propagation problem appeared to be an urgent necessity, and comparison of United States and United Kingdom experience was considered highly desirable.

It was felt that such investigations, correlated with parallel work on those aspects of the research which could be carried out in Great Britain, would produce early results of great importance to the successful prosecution of the war.

It was extremely important for the armed forces to know with reasonable accuracy the coverage to be expected with given radar or radio communication equipment under various conditions of terrain and meteorology. In order that this coverage could be determined it was necessary to know the laws governing electromagnetic wave propagation, and these laws could be derived only by an extensive theoretical and experimental research program. The urgency and importance of the entire matter of coverage become obvious when the following pertinent aspects of modern warfare are considered:

1. The development of highly mobile and powerful instruments (such as the improved tank and other surface combat vehicles, and of long range, high speed bombardment aircraft employed for strategic attacks on the means of production and civilian morale, as well as for tactical purposes) which permitted the principal belligerents to readopt a war of movement, instead of one of static fortification and attrition, and made the development of devices for detecting the presence and movements of enemy mobile units vitally necessary.

2. The necessity of protecting extremely extended sea and land supply lines from successful attack by enemies who early realized that their major hope of ultimate victory lay in cutting those lines.

3. The enormous extent and diversity of the various theaters of operations, necessitating inte-



grated global communications over vast areas of unfavorable terrain and with thousands of mobile units.

Very early in the conflict it was realized that only the British development and organized employment of radar had permitted that country, with a numerically inferior air force, to defeat the Luftwaffe decisively in the Battle of Britain, in which the German High Command had hoped to destroy the Royal Air Force and open the way for a successful invasion of Great Britain. Early warning radar permitted the British commanders to conserve their small resources of men and matériel by sharply reducing air patrolling, and by conducting interceptions with an exactitude which conserved men and aircraft flying hours to the utmost.

With the importance of radar thus established, its use was rapidly expanded and extended into new applications. To protect the extremely long sea supply lines from crippling submarine attacks, radar detection devices were developed expressly to detect surfaced submarines as the only practicable means of searching wide areas of ocean under varying conditions.

With the entry of the Japanese into the struggle, the field of operations became truly global, and the demands made on detection and communication equipment became more severe in all respects. Rapid improvement was made in the performance and reliability of radio and radar equipment to meet these increased demands.

With these advances in design and manufacture and the speedy accumulation of a large amount of factual data on equipment performance in the field, it soon became apparent that meteorological conditions in the troposphere had very serious influence on the operational efficiency of such apparatus. In particular, it was noted that the reliable coverage area of a given installation varied considerably with weather conditions, with the result that confidence in early warning radar and very high-frequency communication links was reduced, and this loss of confidence affected field operations seriously. It thus became vitally necessary to investigate as rapidly and completely as practicable the causes of such variations, with a view to discovering ways of minimizing reductions of coverage and reliability and to improving the general overall performance.

The need for this investigation was communicated from units in the field through regular liaison channels to the National Defense Research Committee

[NDRC] in the United States, and to the Department of Scientific and Industrial Research in Great Britain. Certain researches into the problem were begun independently in the two countries. During the course of the discussion previously referred to between Dr. Compton and Sir Edward Appleton, the need for a body to coordinate these researches was revealed. The magnitude and complexity of the problem, occasioned by the extreme variations in equipment, siting, terrain, and meteorology in the various theaters of operations, made it essential to divide the investigation so as to avoid gaps or duplication of effort. This could be achieved only by integrating research programs through a coordinating body.

Accordingly the radar mission under the chairmanship of Dr. Compton, upon its return to the United States strongly recommended the formation of such a body.

1.2

## ORGANIZATION

A preliminary conference on propagation was held July 1 and 2, 1943 at the Massachusetts Institute of Technology, at which most of the interested United States agencies were represented. This conference was held under the chairmanship of Donald E. Kerr, leader of the propagation group of the Radiation Laboratory and was called specifically for the following purposes:

1. To make those attending acquainted with each other and with the work then in progress.
2. To review and summarize the general status of microwave propagation knowledge in the United States.
3. To compare general measurement techniques.
4. To standardize terminology and methods of presenting data.
5. To formulate a program for future research and recommend any necessary redistribution of emphasis.

The general conclusion reached by this conference was that the following subjects were of greatest importance:

1. Perfection of the technique of radar range forecasting to a degree which would make it immediately useful to the services, even if this had to be done in a preliminary form.
2. Continuation of both theoretical and experimental investigation of the mechanism by which the properties of the atmosphere and earth affect micro-



wave propagation, under widely varying conditions of climate and terrain.

3. Measurement of the reflection coefficients of land and sea surfaces over a wide range of angles of incidence, for the entire radar frequency spectrum, with a view to immediate application to radar coverage problems in the services.

4. Establishment in the immediate future of an agency which could perform the following functions:

- a. Serve as a clearing house for all microwave propagation information in the United States and organize future conferences of representatives of agencies working in the propagation field.
- b. Review the available knowledge from time to time and recommend any necessary redistributions of effort by investigating bodies.
- c. Act as responsible agency for the entire United States propagation investigation in dealing with groups working in similar fields in the United Kingdom and other Allied countries.

Following this conference, Dr. I. I. Rabi, Head of the Research Division of the Massachusetts Institute of Technology Radiation Laboratory, suggested that Division 14 of NDRC take the initiative in setting up a microwave propagation committee to organize the more adequate program outlined in paragraph 4 of the preliminary conference's conclusions. During a subsequent consultation between Dr. Compton and Dr. Ralph Bown, Radio Research Director of the Bell Telephone Laboratories, Dr. Burrows was suggested as chairman of the proposed NDRC Committee on Propagation. Dr. Burrows was chairman of the Radio Wave Propagation Committee of the Institute of Radio Engineers and had made numerous contributions to the knowledge of propagation.

Under the NDRC Committee on Propagation a nation-wide program was proposed, to coordinate the work of such investigative bodies as the Radiation Laboratory, Bureau of Standards, Weather Bureau, various Army and Navy agencies, certain institutions cooperating with Division 13 of NDRC on direction finder problems, the Wave Propagation Committee of the Joint Communications Board [JCB], and such other bodies as the Committee on Propagation, after its official organization, might find helpful in furthering its program.

On August 24, 1943, Dr. Burrows agreed to accept the chairmanship of the proposed Committee and at once began the work of organization and of surveying

the activities of groups in the United States already engaged in propagation studies.

The initial membership of the Committee as proposed by Dr. Burrows, after consultation with the men concerned and heads of the NDRC Divisions directly interested, was as follows:

Dr. J. A. Stratton, Office of the Secretary of War.

Dr. J. H. Dellinger, National Bureau of Standards. (Chief of Section 13.2 and representing Division 13, NDRC.)

Dr. H. H. Beverage, Radio Corporation of America (representing Division 15, NDRC).

D. E. Kerr, Radiation Laboratory, MIT (representing Division 14, NDRC).

A recommendation for these appointments was submitted to Dr. James B. Conant on October 5, 1943. The Committee on Propagation was originally planned to be a part of Division 14, but shortly after its formation it was raised to the level of an NDRC committee, because the broadened scope of its directive, as issued in November, clearly took in aspects of the propagation problem outside the field of Division 14 alone. Prior to this crystallization of the Committee personnel and while the group was in the formative stage and still under the jurisdiction of Division 14, Professor S. S. Attwood of the University of Michigan also served as a member. Later Prof. Attwood was detached from the Committee to direct the Columbia University Division of War Research Wave Propagation Group [CUDWR-WPG], which was responsible under a contract to the Committee for the preparation of reports. This and other contracts are discussed in Chapter 2.

During the closing months of 1944, Dr. Stratton resigned from membership. Shortly thereafter the membership was enlarged to include Dr. T. J. Carroll of the War Department and (somewhat later) M. Katzin of the Naval Research Laboratory.

During the first year the Committee operated without the services of a technical aide. Late in the summer of 1944, Dr. A. F. Murray and S. W. Thomas served temporarily in this capacity until a full-time aide could be obtained. This post was filled by R. J. Hearon from December 1944 until January 1946.

The Committee retained the services of Dr. C. E. Buell, Chief Meteorologist of American Air Lines, who served as a consultant from March 15, 1944. Following completion of his work as director of the CUDWR-WPG, in October 1945, Prof. Attwood was made a consultant to the Committee.



## LIAISON CHANNELS

In general, liaison between the Committee and those organizations directly represented on it was through the individual concerned. Thus Dr. Dellinger provided liaison with Division 13, Mr. Kerr performed the same service for Division 14, and Dr. Beverage acted in this capacity for Division 15. Dr. Stratton served as liaison with the Office of the Secretary of War.

In order to provide a similar close link with the Wave Propagation Committee of the Combined Communications Board [CCB], Dr. Burrows was appointed to membership on this Committee.

In addition to these direct channels, a number of specialists from various Service organizations were appointed as liaison officers, in order to keep the work of the Committee closely coordinated with Service requirements and to speed the dissemination of information.

Captain D. R. Hull acted in this capacity for the Navy, with R. S. Baldwin as alternate. Later Lt. Comdr. W. B. Chadwick was appointed as an addi-

tional liaison officer for the Navy Department.

Lieutenant Colonel J. J. Slattery served in this capacity for the Army, to supplement the liaison already provided through Dr. Stratton.

Also, at the request of the chairman of the Committee on Propagation, Comdr. F. W. Reichelderfer, Chief of the Weather Bureau and Chairman of the Combined Meteorological Committee, assigned Lt. Col. H. Wexler to the Committee in the dual capacity of technical advisor on meteorology and as liaison officer for the CCB.

Somewhat later Dr. Carroll and Comdr. D. H. Menzel were appointed to transmit propagation problems of the Army and Navy, respectively, to the Committee on Propagation under a directive of the JCB.

In addition, use was made of established channels for contact with many agencies, including those in Allied countries. These channels included the Office of Scientific Research and Development Liaison Office, the Naval Coordinator of Research and Development, the War Department Liaison Officer, and the Office of Field Service.



## Chapter 2

# OBJECTIVES AND RESEARCH AGENCIES

### 2.1 DIRECTIVE AND OBJECTIVES

THE ORIGINAL DIRECTIVE for the Committee on Propagation was issued by Dr. James B. Conant, NDRC Chairman, in November 1943 and read as follows:

It shall be the duty of the Propagation Committee of the NDRC to organize and coordinate a program designed to secure the answers to problems on propagation of importance to the war effort. Its recommendations of contracts should be transmitted to the NDRC through Divisions 13, 14, and 15, and the supervision of the contracts remains with the Divisions which transmit the recommendations to the NDRC. It shall give consideration to the needs of Divisions 13, 14, and 15 within the field in which it is limited. Information secured by this Committee and by corresponding sections of Divisions 13, 14, and 15 shall be made mutually available as desired by the groups and may be used by the groups for the purpose of carrying out their missions. It is further understood that one of the duties of the Committee on Propagation is to assemble and analyze, and make available to appropriate agencies, all information in regard to propagation of importance to the war effort.

The directive was purposely made broad enough to permit investigation in any direction promising useful results. In view of this breadth, it was necessary to establish a priority list of specific problems for immediate attack. Proper choice of the problems on this list was of great importance to the successful accomplishment of the Committee's objectives and accordingly was taken up at the first regular meeting, held on October 13, 1943. During the course of this meeting the specific functions of the Committee were also defined, as follows:

1. To coordinate the research then going forward in the United States and to initiate any new work necessary to round out the program.

2. To review completely the existing data on propagation, correlate it, put it into a form usable in the Services, and disseminate it through authorized liaison channels being set up for the purpose.

3. To cooperate with similar agencies in the United Kingdom and other Allied nations for exchange of information and coordination of research, with a view to avoiding duplication of effort or of gaps in the investigation.

With the establishment of these specific functions, two operational problems were selected as being of the highest priority. These were the tracking of

storms and estimation of their properties with radar equipment and the prediction of range for all types of radio equipment employing that part of the electromagnetic spectrum above 30 mc.

The additional problems of determining necessary radar facilities, radar navigation along a shore line, and siting of direction finder equipment, were discussed, but it was decided that these subjects were either outside the province of the Committee or were being adequately considered by other agencies.

The following research problems were also agreed upon:

#### 1. Propagation in nonhomogeneous media.

a. Meteorology. (1) A thorough review of available instruments and methods for making atmospheric soundings and initiation of a program of manufacture of suitable types. (2) Development of techniques for employing these instruments by means of sounding balloons, aircraft, etc. (3) Determination of the dielectric constant of the troposphere as a function of height, at locations within the United States or possessions where conditions in strategically important war theaters are reasonably well simulated. (4) Repetition of operations of (3) in selected strategically important regions or their meteorological equivalent, to obtain sample refractive index distributions. (5) Conduction of meteorological weather analysis concurrently with functions under (3) and (4). (6) Sponsorship of further research into world-wide meteorological conditions, their diurnal and seasonal variations, and their effect on propagation.

b. Theoretical analysis of propagation. (1) Extension of analytical methods to permit better physical understanding of the effects of varying refractive index distribution. (2) Preparation of working formulas for determining field strength and fading characteristics.

c. Establishment of experimental propagation measuring circuits in locations where results of (4) above make such experiments advisable, these experiments to be correlated with simultaneous meteorological observation and



weather analysis. Three frequencies were considered the minimum number capable of yielding a useful result. Those selected were 24,000, 3,000, and 200 mc, with 10,000 mc considered as an alternate for 24,000, if equipment for the higher frequency was unavailable. The characteristics of both one-way and two-way continuous wave and pulse transmissions were to be considered.

- d. Development of a technique for forecasting propagation conditions in the field, suitable for tactical and strategic use.
  - e. Application of points mentioned above to specific operational problems in selected regions.
2. Measurements of absorption of K-band radiation by atmospheric moisture in various forms and by dust or other scatterers.
  3. Study of the effects of the earth's land and water surface on propagation.
    - a. Determination of reflection coefficients of various surfaces for specular reflection and its effect on coverage of various radar and radio equipments.
    - b. Study of back-scattering echoes from land and sea surfaces (ground clutter and sea return), with particular emphasis on effects at the highest frequencies to be employed.
  4. Investigation of storm echoes.
  5. Study of the shielding, diffraction, absorption, and depolarization effects of trees, hills, man-made structures, and other topographical features.
  6. Compilation, analysis, integration, and publication of propagation information obtained, in forms suitable for use by the armed forces.

This extensive program of investigation necessarily required agreement on an appropriate division of effort among United States, British, and other agencies available for the work. This division is discussed in the chronological record of the Committee's activities in Chapter 3.

## INVESTIGATING BODIES

Very early in its existence the Committee considered at length how best to implement the required research program. The conclusion was reached that making use of existing research agencies qualified to work in the propagation field, rather than setting up an independent research agency, would be most

productive. This decision was influenced considerably by the serious shortages of personnel and equipment, and it was estimated that setting up a separate agency would have retarded progress of the investigation six months to one year.

During the course of its investigations the Committee maintained connections with a total of about 66 separate agencies in the United States, Britain, Canada, New Zealand, and Australia, including the principal organizations within the armed forces of the Allied countries interested in propagation phenomena.

Reports, recommendations, and requests from all these various agencies were received, analyzed, acted upon, and filed. This accumulated body of information on propagational phenomena is listed in the Bibliography. These papers are referred to again in Chapter 4 under a summarization of the results of the Committee's work.

Of the agencies conducting actual theoretical or experimental research on radiowave propagation, the principal ones in the United States were as follows:

1. Bell Telephone Laboratories [BTL].
2. Camp Evans Signal Laboratory.
3. Columbia University Division of War Research [CUDWR].
  - a. Radiation Laboratory.
  - b. Wave Propagation Group.
4. National Bureau of Standards, Interservice Radio Propagation Laboratory, [IRPL].
5. Radiation Laboratory, Massachusetts Institute of Technology [MIT-RL].
6. U. S. Naval Research Laboratory.
7. U. S. Navy Radio and Sound Laboratory.
8. U. S. Army Signal Corps Operational Research Branch.
9. Radio Corporation of America.
10. Radio Research Laboratory, Harvard University.
11. U. S. Army Air Forces, Weather Division.

There were also 2 agencies in Australia, about 21 in Britain, 2 in Canada, and 2 in New Zealand. The number of agencies investigating propagation phenomena in the Allied countries totaled about 39. This relatively large number was necessitated by the importance, urgency, diversity, and complexity of the problem, and the physical difficulties of conducting direct experimental investigation with usable accuracy under war, and at times under combat conditions.

During the course of the Committee's work,



members visited the various investigating agencies to correlate the work when necessary, obtain first-hand information of the special aspects under investigation, or suggest a line of attack. Such visits are described in Chapter 3.

## 2.3 CONTRACTS AND PROJECTS

The entire organization and work of the Committee was carried on under the auspices of Army and Navy Project AN-16, pursuant to a recommendation of the Combined Meteorological Committee [CMC] of the Combined Chiefs of Staff, dated December 7, 1943. This recommendation was made to the National Defense Research Committee in response to a request by the Combined Chiefs of Staff dated December 4, 1943 and channeled jointly through the War Department Liaison Officer and the Coordinator of Research and Development. The Combined Chiefs of Staff asked specifically that:

1. The Committee on Propagation of NDRC be requested to act as a coordinating agency for all meteorological information associated with short wave propagation.

2. The Committee on Propagation be requested to forward periodically to the CMC a list of all reports and papers dealing with the meteorological aspects of short wave propagation which have been received or transmitted by that Committee.

Originally contracts arranged with various agencies for research into propagation phenomena were handled through the contract machinery of the appropriate division of NDRC, specific recommendations for the terms of the contract being drawn up by the Committee.

The NDRC later changed the manner of arranging contracts of the Committee on Propagation so that the Committee would recommend, and assume direct responsibility for, the contracts. At the same time the contracts that had already been let by Divisions 13, 14, and 15 involving radio wave propagation were transferred to the Committee on Propagation. Such further extensions to these contracts as were required were arranged and recommended by the Committee on Propagation.

Contract OEMsr-1207, let for the Committee, with Columbia University through the contract machinery of Division 14, was active from November 1, 1943 to October 31, 1945. This contract was for collecting, analyzing, and integrating data on

radio and radar wave propagation. Under its terms the CUDWR set up a Wave Propagation Group, directed by Professor S. S. Attwood, who had served on the Committee while that body was a part of Division 14. This group consisted of a scientific staff and stenographic and clerical personnel, and it handled the work described above, as well as periodic publication of reports for distribution according to a list approved by the NDRC chairman's office.

Contract OEMsr-728, with the State College of Washington, which was originally let through Division 14 and taken over by the Committee on Propagation after its formation, terminated on October 31, 1945. Work under this contract was under the direction of Dr. Paul A. Anderson of this college. The contract was a general one for the purpose of "carrying on experimental and analytical investigations in connection with the study of microwave propagation." The first research conducted under its terms was a study of propagation along an overland path in the Pacific Northwest, where climatic and topographical conditions differed from those at San Diego and on the East Coast.

Another project under this contract was the development of a portable low-level sounding instrument for measuring temperature and humidity gradients in the lower atmosphere. Subsequently this apparatus was adopted by the U. S. Navy and several other United Nations military and scientific agencies.

Production of an improved model of this equipment was also carried out, with subsequent deliveries to the Army Air Forces [AAF], the Naval Research Laboratory [NRL], the Department of Scientific and Industrial Research in New Zealand, and to Dr. Paul C. T. Kwei and Dr. Eugene T. Hsu for use in China.

Performance of the sounding apparatus under tropical conditions and tests to determine the feasibility of predicting nonstandard radar coverage by means of atmospheric soundings were the objects of another project, which was carried out in Panama in collaboration with the NRL.

Another very important project under this contract was Office of Field Service Project SWP-3 which was for the purpose of exploring meteorological conditions in the Southwest Pacific theater to determine their effects on radar coverage, and to assist the AAF in establishing a forecasting service for the tactical exploitation of nonstandard propagation in that region.

A member of the State College of Washington group working under this contract was loaned to



the NRL staff to assist in an experiment at Antigua early in 1945. This experiment investigated and established the existence of surface air layers having significant effects on radar coverage over large areas of the ocean.

Contract OEMsr-1502 between the Committee and the Jam Handy Organization of Detroit was in force from May 7, 1945 to December 31, 1945. The contractor undertook the production of a motion picture and various other training aids, designed primarily for use by the armed forces in educating personnel concerned with propagation phenomena, and secondarily to acquaint all agencies concerned with progress made.

Contract OEMsr-1496 between the Committee and the University of Texas was in force from June 1, 1945 to October 31, 1945. This contract required the contractor to develop equipment for, and make measurements of, deviations in angle-of-arrival of microwaves propagated through the lower atmosphere. It was designed also to supplement and expand knowledge of the deviations in angle-of-arrival already obtained through experiments conducted by the BTL. These deviations were considered large enough to affect the accuracy of gunlaying radars and similar equipments.

Contract OEMsr-1497 with the Humble Oil Company of Texas was in force from June 2, 1945 to October 31, 1945. Under its terms the contractor undertook construction of certain field strength measuring equipments for use in experiments being carried on as part of Project AN-16 in the Naval

Research Laboratory, Navy Radio and Sound Laboratory, and the Army's Camp Coles, Camp Evans, and Watson Laboratories, and by the New Zealand Joint Communications Board.

These five contracts make up the total of direct contractual relationships entered into by or on behalf of the Committee on Propagation but represent only a small portion of the work on propagation problems carried on in the United States. The bulk of actual research was conducted under contracts let by Divisions 13, 14, and 15 and by the Service in conjunction with laboratories and industrial companies. The Committee served as the integrating, analyzing, and disseminating body for the results of all such work bearing on the propagation problem.

In addition to carrying on the general integration of reports and papers from all sources (see list of sources in the Bibliography), the Committee sponsored three conferences which were attended by representatives of most of the agencies investigating propagation phenomena. A similar conference was held before the Committee was in being, and a report of the proceedings was published by the Wave Propagation Group of the MIT Radiation Laboratory. The fourth and last conference on propagation, the third held under sponsorship of the Committee, was attended by 236 persons, representing approximately 59 separate agencies in and out of the armed forces of the Allied nations. This meeting took place May 7, 8, and 9, 1945 in Washington, D. C. Full reports of this and previous conferences are listed in the Bibliography.



## Chapter 3

# CHRONOLOGICAL RECORD

3.1

### COMMITTEE ACTIVITIES

THE COMMITTEE ON PROPAGATION was organized in Division 14 of the National Defense Research Committee, in response to an urgent request by Sir Edward Appleton, Director of the Department of Scientific and Industrial Research of Great Britain. This request was specifically for United States cooperation in a more adequate investigation of radio wave propagation. Observed variations of radar coverage and performance over a considerable range of climatic and meteorological conditions had already revealed the need for a thorough understanding of the influences of such conditions on radio wave propagation, particularly at frequencies above 30 mc. Also, the effects of back scattering of radiation from the sea surface (sea return) under various wind and wave conditions and of land surface topographies of various types on radio wave propagation, particularly at angles approaching the horizontal, were already known to be serious. These and similar factors had been established by reports from operational installations as having profound significance in the operational employment of radio devices, and the fundamental mechanisms producing these effects were not well understood.

A preliminary conference on propagation was held at the Massachusetts Institute of Technology [MIT] Radiation Laboratory [RL], July 1 and 2, 1943. A report of this conference was published by the Laboratory. It contained a statement of the general program of investigation held desirable and recommendations for setting up a body to coordinate the activities of research agencies with needs of the armed forces and with work on the problem already in progress in Allied countries. This body, which became known as the Committee on Propagation, was organized as explained in Chapter 2, with Dr. Chas. R. Burrows as chairman.

Dr. Burrows accepted the chairmanship on August 24, 1943, proceeded immediately with organization of the full Committee, and began the task of establishing and correlating a program of research.

Dr. Burrows and Donald E. Kerr, head of the Wave Propagation Group at the Radiation Laboratory and a member of the Committee on Propaga-

tion, conferred in Washington on September 2 with Dr. A. F. Murray of NDRC and with Doctors H. Hopkins and W. Ross of the British Central Scientific Office. A complete set of reports of British work on propagation was available in this office, and this was placed at the disposal of Dr. Burrows and the Committee. The desirability of extending the investigation down to 27 mc was discussed in connection with improving the efficiency of certain equipments using those frequencies.

On September 3, Dr. Burrows and D. E. Kerr conferred with Dr. J. A. Stratton in the Office of the Secretary of War regarding Dr. Stratton's serving on the Committee and the possibility of minimizing or eliminating ground return in radar operation at low angles. Comdr. F. W. Reichelderfer, head of the Weather Bureau, was also contacted, and the use of radar in locating storm areas was taken up.

During the remainder of September the organization of the Committee was pushed forward, with the result that the names of Stratton, Dellinger, Beverage, and Kerr were formally proposed for membership to the Office of the Chairman, NDRC.

The first official meeting of the Committee on Propagation was held on October 13, 1943, with the following members and representatives of interested agencies: Dr. Chas. R. Burrows, Chairman; Dr. J. H. Dellinger, Division 13, NDRC; D. E. Kerr, Division 14, NDRC; Dr. H. H. Beverage, Division 15, NDRC; Dr. J. A. Stratton, War Department; J. H. Teeter, representing the Chairman, NDRC; Dr. H. G. Hopkins, representing the British Central Scientific Office; and Lt. (jg) J. M. Bridger, representing Captain D. R. Hull of the Navy Department.

The field of propagation was reviewed, the specific functions of the Committee were defined, and a list of definite problems for both immediate and longer term consideration was drawn up. It was agreed that the Committee would confine itself to the study of tropospheric propagation, at least at first, with special emphasis on problems of nonstandard propagation.

On October 15 Professor S. S. Attwood of the University of Michigan agreed to assist Dr. Burrows in directing the activities of the Committee. Later



Prof. Attwood was appointed Director of the Columbia University Wave Propagation Group [CUDWR WPG] which operated under contract OEMsr-1207, to integrate, analyze, and disseminate reports of research. This contract went into force on November 1, 1943.

Dr. Burrows, Prof. Attwood, and D. E. Kerr flew to England November 22, 1943, to confer with British investigators and secure integration of the United States and British programs. As a result of this visit, a unified program of research was agreed upon, with certain divisions of effort to prevent duplication of particular phases of the work, and to insure covering all practical aspects of the problem. The British agreed to continue experiments on wavelengths of 9, 6, and 3 cm, with parallel measurements of meteorological factors, and also to undertake measurements at 1.25 cm when equipment became available. The effects of hills and trees on the shorter wavelengths was also to be studied. They were also to continue theoretical investigations already under way with special emphasis on use of the Manchester University differential analyzer.

It was agreed that American agencies would make detailed measurements to determine the characteristics of water vapor diffusion in a warm air mass blowing over cold water, with accompanying radio transmission tests at wavelengths of roughly 10 and 50 cm. A team of research workers was to be organized and equipped to make simultaneous propagation and meteorological measurements at locations providing conditions similar to those encountered by radar-using personnel of the armed forces. Tests on 1.25-cm waves were to be made along the eastern coast of the United States as apparatus permitted, to provide data on propagation conditions typical of the eastern coast of a large continent.

It was agreed also that Dr. John E. Freehafer of MIT-RL would be sent to Britain in order to obtain closer cooperation in theoretical attacks being made on these problems.

It was further agreed to make a study of atmospheric absorption, particularly at 3-cm and shorter wavelengths, and of absorption by rain, fog, dust, and other such phenomena. The reflection coefficient of the sea for radiation of 10-cm and possibly 3-cm and shorter wavelengths was to be studied for grazing angles less than 5 degrees, and the back-scattering effect was also to be investigated. Storm echoes and their possible tactical uses were also to be treated. In addition, the United States was to set up

and maintain a group to compile, analyze, integrate, and disseminate propagation information.

It was jointly agreed to interchange samples of meteorological instruments most useful for measurements in connection with propagation studies.

Upon return to the United States of this mission, in January 1944, offices were occupied in the Empire State Building, New York City, jointly with the Wave Propagation Group of Columbia University Division of War Research.

On February 12, 1944, a meeting was held at which liaison representatives from the armed forces presented certain urgent Service requirements and outlined experimental programs that the respective branches were prepared to undertake in cooperation with the Committee.

One of the most urgent needs in the Services was for a handbook and other instructional aids, prepared in the simplest practicable form for the use of operational personnel with limited technical background. It was proposed that the Columbia University Wave Propagation Group, which had been set up in accord with the program agreed on with the British, should undertake the preparation of such aids to instruction.

At a meeting held February 15, 1944, a statement outlining the propagation problem was drawn up, with proposals for Service cooperation in experiments devised to provide solutions to the most urgent aspects of the question. This statement set forth the NDRC Committee's view that the problem of "non-ionospheric propagation in a nonstandard atmosphere" should be given highest priority, and it gave details of experiments proposed or already under way. Five specific experiments were outlined, in each of which the assistance of the Services was required. These were as follows:

1. Organization and equipment of a complete transportable field unit for conducting propagation experiments, which could be sent to any region considered likely to yield results useful in the operational theaters. This experiment would require considerable apparatus and a team of trained research, operational, and maintenance personnel. Dr. Paul Anderson of the State College of Washington provided a considerable amount of material on this project.

2. An over-water experiment along a path between Cape Ann and Cape Cod was to be carried out by MIT-RL, to obtain information on propagation characteristics along the eastern coast of a continent. These data would be applicable to similar regions in



war theaters, particularly near the Chinese north-east coast.

3. A detailed experiment was considered desirable in a region where stable temperature inversions were produced in the atmosphere by subsidence of upper layers of air. Such experiments were already being conducted by the U. S. Navy Radio and Sound Laboratory [NRSL] along several over-water paths near San Diego, California.

4. An experiment near the Panama Canal Zone was planned by the Navy in cooperation with the State College of Washington group under Anderson, to establish a correlation between meteorological conditions of that region and radar performance. It was expected that this would provide a good test of equipment and methods under tropical conditions and that the information obtained would apply in other similar regions.

5. An experiment was proposed to be conducted in Florida, with the aid of Signal Corps and Air Force personnel utilizing equipment already in the area. It was expected that this project would yield considerable information on means of predicting propagation characteristics for localities climatically similar.

Meantime the Columbia University Division of War Research Wave Propagation Group [CUDWR WPG], directed by Prof. Attwood and operating under contract OEMsr-1207, was preparing a report on tropospheric propagation for radar operators, officers, and other operating personnel, at the request of the Combined Communications Board [CCB] and Combined Meteorological Committee [CMC]. This report, compiled from all established data on variations in radar coverage available, was prepared in as non-technical and popular a style as possible. It received the approval of the Wave Propagation Committee of the CCB, and about 30,000 copies were distributed to the armed forces of the United Nations during June 1944 under the title *Variations in Radar Coverage* (JANP-101). This report helped to clarify the problem of nonstandard propagation for Service personnel and to throw light on certain peculiarities in radar performance and coverage variations caused by newly discovered meteorological conditions (see Chapter 16). During early 1944, a bibliography of publications on propagation was prepared and published by the CUDWR WPG.

At a meeting on February 28, 1944, a direct request from General MacArthur to NDRC was laid before the Committee, which asked that a group of scien-

tists be sent to Australia to study radar and communication problems in that area of the Pacific theater. It was finally arranged that the communication part of this request would be handled by the Signal Corps and that the radar portion would be fitted into the general research program already in process of organization.

Out of the series of meetings and conferences held during February, a program of four principal points was developed which was presented on March 4, 1944, to the Wave Propagation Committee of the Joint Communications Board. This program was accepted and put into effect soon afterward, as follows.

1. A working group under the direction of Dr. Anderson proceeded to the Canal Zone to conduct meteorological measurements in cooperation with the Navy. Following completion of this work, the group proceeded to Australia and performed similar investigations as requested by General MacArthur. This work was carried on under contract OEMsr-728, with the State College of Washington. Arrangements were also made for training a group of about 20 Army and Navy officers in use of the meteorological measurement technique and apparatus developed by Dr. Anderson. These officers were later to be sent into the field to organize teams for making meteorological soundings.

2. The Wave Propagation Group of the MIT-RL under D. E. Kerr conducted a study along an over-water path on the east coast of the United States, as outlined previously.

3. The NRSL investigation of propagation under subsidence conditions was continued.

4. Propagation conditions over land were planned for study by Canadian Army research groups. Preliminary discussions were held with these groups early in 1944.

On March 13, Dr. Burrows and Prof. Attwood conferred with the staff of the NRSL in San Diego in connection with the investigation of propagation under subsidence conditions. The research was integrated into the general program and reported to the Joint Communications Board [JCB] on March 29.

As a result of this visit the NRSL agreed to modify and expand its propagation research extensively to include tests over a number of different paths, using both one-way and radar transmissions, with simultaneous meteorological measurements. These experiments were to be measurements of propagation on three representative frequencies along a 108-mile



over-water path between Los Angeles and San Diego, and comparable frequencies between San Diego and San Pedro, a distance of 80 miles over water, using suitable antenna heights. Atmospheric soundings were to be taken from a ship at a point midway along such paths and also on shore as near the midpoint as possible. Measurements with a blimp to determine the extent of uniformity of the inversion layer were also projected.

Measurements were to continue on fixed radar targets located at various altitudes and along various azimuthal bearings. Field strength measurements were also to be made from an aircraft flown at significant altitudes over the transmission paths, the results to be correlated with meteorological data. The chairman assisted inauguration of this expanded program by using the Committee's powers and influence in obtaining additional apparatus required. In addition, information was exchanged with members of a British scientific delegation who were present, and considerable effort was directed to obtaining a meteorologist for full-time work with the NRSL group conducting the experiment.

On April 3, Dr. Burrows, Comdr. J. L. Reinartz, and Lt. Comdr. D. H. Menzel visited Panama to observe the experiments being conducted jointly by Dr. Anderson's group and the Navy.

As a result of this visit, substantially better and more extensive cooperation between the scientific group and Service forces in the area was obtained, and an analysis of the data obtained to date was secured, which revealed occurrence of a predictable surface duct condition.

A conference was held in Washington on May 2, 1944, at which representatives of the various research agencies of the United States interested in propagation were present. A large amount of propagation information was exchanged by presentation of many papers describing various experimental and theoretical researches going on in various countries. The complete record of papers and proceedings was published by the CUDWR WPG and is contained in the Bibliography at the end of this volume.

Special consideration was given to the question of symbols and nomenclature by a committee headed by Prof. Attwood. A list of such symbols was prepared by this committee and was accepted without dissent by the Wave Propagation Committee of the CCB on May 17, 1944.

On May 23 the chairman of the Committee on Propagation presented to the NDRC a report on

what had been accomplished up to that time by the Committee and its plans for the ensuing year, together with budget requirements. The budget was approved with minor deletions in the items covering contingencies.

On June 29, 1944, a meeting was held at which the progress of the various experimental projects was reviewed in some detail. Two Armed Service requests were also taken up. The first, submitted by Comdr. Menzel and Dr. T. J. Carroll, dated June 12, 1944, outlined the general needs of the Services. Copies of this letter were forwarded to the Committee members for their consideration before the meeting convened. The second was received from General Colton, in the Office of the Chief Signal Officer, and specifically requested a theoretical investigation of the effects of low-level tropospheric layers on propagation at wavelengths near 10 and 3 cm.

After discussing specific requirements of the services as laid down in the Menzel-Carroll letter, certain of the questions were referred to appropriate agencies for solution. In particular, MIT-RL undertook to study the effects of refraction on gunfire control radars operating in the 10- and 3-cm bands. Most of the other questions raised were already under investigation but were not yet sufficiently advanced to permit of conclusive answers. General Colton's request was considered to be covered by the action taken in connection with the Menzel-Carroll letter.

In addition to progress reports from United States research agencies, a report on British work was submitted, particularly on the status of 9-6-3-cm experiments over the Irish Sea. Little useful correlation between propagation and meteorological factors had yet been obtained in this experiment. Projected British experiments included investigation of absorption and attenuation of 10- and 3-cm band radiation in oxygen, in water in all forms occurring in the atmosphere, and in salt spray.

Late in June 1944, the need for closer liaison between the Committee and CMC was met by the appointment of Major H. Wexler of the Army Air Forces, Weather Division, as a technical advisor. This also strengthened the meteorological representation associated with the Committee, which had not formerly been completely adequate.

The Committee met at the Radiation Laboratory on August 4, 1944. During this meeting plans were laid for an extensive conference on propagation to be held in Washington, D. C., on November 16 and 17, at which representatives of research agencies in



all the countries engaging in propagation research could present findings to date.

Plans were laid for Dr. Anderson's trip to the Southwest Pacific theater in response to General MacArthur's request for investigation of propagation phenomena. This project was of considerable importance and is more fully described elsewhere in this report.

A report by Dr. Svein Rosseland, assistant to Prof. Attwood in the CUDWR WPG, was heard, on work going on in England and on data brought back to that country by Dr. Booker. These data described radar echoes from points more than 1,500 miles from the 200-mc Bombay, India, station, which had been observed during the season following the northeast monsoon.

Other reports were heard on Bell Telephone Laboratories [BTL] experiments on K band along a path to Atlantic Highlands and similar experiments by MIT-RL near Boston. No nonstandard propagation had been observed at Atlantic Highlands, but some had occurred in the Boston area.

Experiments of MIT-RL along a ten mile path had indicated the impossibility of measuring the effect of oxygen and water vapor outside the laboratory itself.

Dr. W. H. Furry described the work of preparing coverage diagrams for radar and VHF (very high frequency) communication equipment under ground-based duct conditions. Owing to the volume of calculations required in this work it was decided to obtain use of the Harvard University automatic sequence-controlled calculating machine, which would effect a probable reduction in the time required from an estimated nine or ten months to about three weeks. This proposal was subsequently carried out.

Dr. Beverage presented certain problems of Division 13, particularly the need for supplying the best information on probable coverage to signal officers in the field at the earliest possible date. Estimates based on the  $\frac{4}{3}$  earth radius formula tended to be pessimistic.

Dr. H. Goldstein presented information on the problem of fluctuating signals. Instability in the equipment was a source of great difficulty, but, when this had been overcome, such results as were obtained indicated that most fluctuation was due to interference.

Plans were made for a field trip to observe the extensive MIT-RL experiments proceeding on four different wave bands along a path between Race

Point and Gloucester. On this trip the entire apparatus and organization of the experiment were inspected and discussed.

A detailed memorandum of the Committee's current work was submitted on August 10 to the Chiefs of NDRC Divisions 13, 14, and 15, in order to keep these groups informed of developments. The breakdown of activities described five well-controlled experiments which were under way in different meteorological environments and the theoretical attack proceeding in Britain and the United States. These experimental attacks on the problem have been described earlier in outlining the Committee's program for the year. The memorandum referred to here specifically invited Division comment on the program in progress and requests for other investigations if additional ones seemed desirable.

A Committee meeting on September 21, 1944 considered new humidity measuring instruments and reviewed progress of the work under way at RL. This was reported by D. E. Kerr as nearing the conclusion of the experimental work. The matter of educational films to disseminate propagation information to the Services was brought up, and the need for a technical aide to the Committee who should be familiar with NDRC procedure was discussed. Dr. Burrows stated that efforts were being made to obtain a contractor who would make meteorological measurements along the BTL to Mt. Neshanic propagation path, for correlation with the transmission data available at BTL. These measurements were later undertaken by the Airborne Instruments Laboratory [AIL] of Mineola, Long Island. The matter of eventual demobilization of OSRD was discussed, particularly as to effects of such demobilization on investigations of propagation then in progress.

The Committee met again on November 15, 1944 to consider replies received from Divisions 13, 14, and 15 to the memorandum outlining its program in progress submitted on August 10 and to transact other business. The matters of calculation of radar coverage diagrams for nonstandard conditions, of the range and reliability of very high frequency [VHF] and ultra high frequency [UHF] communications links, and the choice of frequencies for such links were taken up in detail. After thorough consideration, a reply was drafted for the Divisions concerned, particularly Division 13, stating that available information on propagation did not permit preparation of accurate coverage diagrams for such communications circuits on any other basis than



that of  $\frac{4}{3}$  earth radius, as was already being done. It was expected that work then in progress would modify the limitation as it progressed. In the matter of choice of VHF, UHF, and super high frequencies [SHF], information was not yet available, but surveys under way were expected to provide some background, although the intricacy of the problem did not encourage hope of an early complete solution.

The difficulties involved in the preparation of field strength contours appeared so formidable that requests from the Services for preparation of such contours was withdrawn, and a new request was substituted. This asked that workers on theoretical or observational and experimental programs forward as informal memoranda such examples of correlations between meteorological conditions and propagation characteristics as could be applied directly in the field, with suggestions for possible tactical applications. This substitute request was received by the Committee in November.

In addition, an important report by Dr. Anderson from the Southwest Pacific theater was considered which described the progress of project PDRC-647 which members of the State College of Washington staff had undertaken under Contract OEMsr-728. Its objectives were to explore meteorological conditions in the Southwest Pacific theater to determine their effects on propagation, and to assist the Army in establishing a forecasting service for the tactical exploitation of nonstandard propagation in that region.

After several conferences between Dr. Anderson's group, various Australian agencies, and representatives of the Air Signal Office, Far East Air Force [FEAF], headquarters for the mission was established at the Radio Physics Laboratory at Sydney. Meetings were held here with Professor F. W. G. White and representatives of the Royal Australian Air Force and Royal Australian Navy. The following facts were brought out. The Australian and NDRC programs supplemented each other without duplication of effort, making revision of plans unnecessary. An acute need existed for definite information concerning low-level meteorological conditions in the oceanic areas of the Southwest and Central Pacific. This information could best be obtained by NDRC and United States Army groups.

Rough forecasting of nonstandard propagation along the southeast, south and southwest coasts of Australia was possible, correlating superrefraction

data collected from radar stations with synoptic meteorological data.

Observations from North Australia showed no similar clearcut correlations. Reports from New Guinea and the Solomon Islands were too meager to be useful.

A Radio Physics Laboratory [RPL] experimental program was projected at a location near Darwin, Australia, which would be correlated with land, ship-based, and aircraft soundings and synoptic weather. A low-level sounding equipment was delivered to RPL for use in these experiments.

A conference was held at the Radio Development Laboratory in New Zealand at which a low-level sounding equipment was delivered and trial soundings taken by Dr. Anderson. As a result of this meeting, a long-range program was agreed on in addition to the work already being conducted by New Zealand agencies. This program would take advantage of the unusual conditions offered by the persistent Föhn winds which override the cold water at the eastern coast.

Dr. Stephenson of Dr. Anderson's group began the collection of meteorological and oceanographic data available in Australia preliminary to the selection of optimum sites for radar-weather observations. New information was available on continental and general equatorial meteorology but very little for the ocean area to the west and north of New Guinea.

Recommendations for establishment of a limited number of radar-weather stations in the Biak-Owi-Noemfoor region were submitted to the FEAF late in August. These recommendations were approved after some discussion, but the plans were changed when FEAF headquarters suggested the usefulness of an Army radar-weather team with sounding equipment in the projected operations at Leyte. Preparations were made to take advantage of this suggestion.

Consideration was given to determination of the low-level conditions characteristic of the Southwest and Central Pacific oceanic areas, with tentative conclusions from data secured during the summer of 1944 that strong ducts to 40 or 50 ft and weaker stratifications to 800 or 1,000 ft were common in the region, especially in late afternoon. In the doldrum region standard conditions were the rule. The need for more complete measurements was pointed out, and the use of PT boats and seaplanes to obtain them was secured.

Approval for measurements in the region near



Saipan was also obtained, and arrangements were begun for the transfer of personnel to that theater.

Further informal conferences were held with Australian and British groups, from which these conclusions were drawn. General meteorological data did not provide sufficient information quickly to be of practical use in forecasting propagation in a given area. Instead, intensive ground-based and aircraft soundings offer the most practical means for setting up a short-range forecasting service for radar and radio communication coverage.

At a formal conference with the same groups a policy to be adopted by the Australian Services was decided upon. An operational program similar to the NDRC Office of Field Service program was outlined by the members and approved for immediate inauguration. A radar-weather school was to be set up in the Meteorological Section of the RAAF for training radar-weather officers. Arrangements for manufacturing sounding equipment were also made, with almost all components planned for production in Australia.

Plans for expanding the operational program at Leyte were laid, and arrangements for observations at Saipan were also concluded. Measurements at Woendi Island were planned to continue until definite results were obtained, and arrangements were also made for transferring direction of the project to an officer of the Fifteenth Weather Region Headquarters, after which all civilian personnel with the exception of Mr. Grover would return to the United States. Mr. Grover would remain for the purpose of maintaining contact between the U. S. Army, Australian, and NDRC programs.

Finally, recommendations for future procedure in this theater were made, which included maintaining at least one civilian research meteorologist in the area, and perhaps a group with the Army in China.

Another conference on propagation was held during November 1944, attended by representatives of the investigating laboratories and armed forces of the Allied Nations. A large number of papers were delivered on propagation and related subjects. A full report of this conference was prepared by the CUDWR WPG and distributed to approved agencies.

At the next meeting of the Committee, held on December 9, 1944, a number of new matters were taken up, as well as the status of work already in progress. A group of British research workers, who had been conferring with United States propagation workers during a tour of laboratories in this country, reported

on their findings. Dr. Booker also gave a detailed account of the work going on in Australia, as seen by him during a visit to that country which he had just concluded. The joint United States-British program was discussed, as well as methods of interpreting results of propagation experiments, calculations of coverage diagrams, and the proper dissemination of a report, *Tropospheric Propagation and Radio Meteorology*, which had been prepared by CUDWR WPG. This report, distributed in December, was a compact but thorough summary of the established information on propagation obtained to the date of its preparation. It was on a practical but much more quantitative level than *Variations in Radar Coverage* issued earlier under auspices of JCB. It proved to be of considerable value to radar officers, particularly in improving the confidence and efficiency of radar operating and siting personnel, who had previously had at best only qualitative conceptions of such effects as superrefraction and trapping of radiation in ducts.

A subcommittee of the Committee on Propagation met on December 30, 1944, and heard a personal report by Dr. Anderson on his mission to the Southwest Pacific during the middle of the year just ending. From the results of this mission it was apparent that low-level ducts existed over substantial areas of the ocean in the trade wind regions which had profound effects on propagation characteristics of radar and VHF radio frequencies. These propagation characteristics were also found to vary markedly with heights of transmitting and receiving antennas. After consideration of these findings, the subcommittee decided that a carefully controlled experiment under similar conditions was an urgent necessity, in order to reduce these qualitative indications to reasonably accurate quantitative data, which could be applied by operational personnel in theaters where similar conditions existed. It was decided that an experiment conducted directly by the Navy at a suitable location in the Caribbean area would be most practicable, and plans were drawn up for a detailed investigation by one-way and radar transmission on several frequencies.

In response to a request from Brigadier General Borden the Committee arranged on December 14 for establishment of a meteorological sounding station in the Southwest Pacific [SWP] area. On December 19 a letter was drafted and despatched to Dr. E. M. Marsden, Director of Scientific Developments in the Department of Scientific and Industrial Research in



New Zealand. This letter commented on the work already accomplished, as reported to the Committee by Dr. Anderson and Dr. Booker, and invited expansion of the investigation, particularly to determine the effects on propagation of a hot, dry, air mass moving from the land out over the sea. This condition existed in many other operationally important regions of the Western Pacific and was known to affect seriously the performance of coastal radar installations.

On January 1, 1945, Dr. Stratton asked to be relieved of his responsibilities as a Committee member and accepted in lieu thereof an appointment as a consultant, which capacity permitted him more time for discharging his duties in the Office of the Secretary of War.

At a meeting held on January 5 many questions were taken up, and progress made in the preceding year was reviewed.

The following projects were reported as proceeding concurrently.

1. The Navy experiment along an over-water path in the Caribbean area, where thin surface ducts were prevalent.

2. Experiments where relatively dry air moved from the land over a water surface. These included the MIT-RL experiment near Cape Cod and analysis of the data obtained, and experiments going on in New Zealand.

3. Propagation over a land surface where radiation cooling produced temperature inversions in the lower air layers. An experiment was being conducted in Arizona by NRSL, and another was being prepared in Canada by the Army Operational Research Group.

4. Experiments along an over-water path where subsidence of an upper air mass produces duct conditions. The NRSL was conducting such experiments near San Diego, which offered conditions typical of certain other areas in the Pacific.

5. Developments of meteorological theory for low-level ducts in purely oceanic air. This work was going on at MIT-RL.

6. Development of atmospheric sounding equipment for the armed forces. This work was going on at the State College of Washington.

7. An educational program designed to provide the Services with up-to-date information on the propagation question. This was being carried out by Columbia University.

8. Mathematical calculations of wave propagation

characteristics. These calculations were being conducted by CUDWR WPG and by MIT-RL.

In addition, certain new questions were taken up with a view to arranging experiments to provide the answers. These were the matters of accuracy of gun-laying radars as affected by variations of the refractive index, the reflection coefficient of open sea surfaces, and radar cross sections of ship and airplane targets. The latter two questions were being undertaken by NRL, and the former was believed possible of solution by BTL.

The business matters of improved liaison with Pacific theaters and of the budget for the ensuing period were also taken up.

At other meetings held during January 1945, organizational, personnel, and equipment matters were taken up and settled as facilities permitted. Dr. Carroll, of the War Department Radio Propagation Section, was appointed a Committee member on January 12. Possible cooperation with China was discussed, following a discussion by Dr. P. C. T. Kwei of Wuhan University, of research carried on in China before and during the retreat from the Japanese invasion.

During the month of February the Committee on Propagation established liaison with the Watson Laboratories of the Army Air Force which had recently begun operations.

In February also the Committee heard an address by Dr. S. K. Mitra of the Council of Scientific and Industrial Research in India and established liaison with that body.

The question of utilizing the services of Dr. Kwei and his assistant, Dr. Eugene Hsu, in obtaining ionospheric information after their return to China was also discussed.

On March 6, 1945, a detailed report by Dr. Carroll on uses of tropospheric propagation in the Army was submitted to the Committee. This report had been prepared during January and provided a great deal of information needed by the Committee in continuing the propagation investigation. At later meetings in March, the matter of utilizing the services of Dr. Kwei and Dr. Hsu was settled affirmatively, and a meeting was held with representatives of the Coast Guard to establish a better liaison link with that service.

Martin Katzin of NRL was appointed a Committee member early in April. Later that month the Chairman prepared a report for Col. D. N. Yates, Chief of the Weather Division, AAF, on the problems



involved in correcting existing errors in fire control radars, due to refractive effects.

The fourth conference on propagation was held in Washington in May 1945. This conference was the largest and most comprehensive yet held and was attended by 236 representatives of about 59 separate agencies of the Allied Nations. A report of this conference was published as usual by the CUDWR WPG and distributed through authorized channels. A great deal of important data was presented at this conference, including showing of a motion picture produced in Britain which presented in effective form much information on nonstandard propagation, particularly propagation in ducts of stratified air layers. Another short motion picture prepared in Canada was presented in which radar echoes from snowstorms were shown on an accelerated time scale. Progress of such storms was readily followed by radar observation, and the importance of microwave propagation for this and similar applications was made apparent.

At the close of the conference the chairman announced that a contract had been negotiated with the Jam Handy Organization for production of a motion picture to present pictorially the uses of propagation data by the armed forces.

With the collapse of the enemy in Europe, little shifting of the Committee's program was required. The Committee was formed too late in the war to be of major help in the European theater so from the start the efforts were aimed at the solution of propagation problems of the war in the Pacific theater.

A meeting late in June 1945 considered advances in theoretical methods of attacking the propagation problem and agreed on certain standard symbols for representing the quantities involved, to avoid confusion between investigating agencies.

Two additional contracts were arranged during June, the first with the University of Texas for the measurement of variations in angle of arrival of microwave radiation under varying meteorological conditions. This question has a very direct bearing on the troublesome question of improving accuracy of radar controlled gunfire, which played such an important part in defense against Japanese suicide plane attacks.

The second contract was negotiated with the Humble Oil Company on July 2, 1945, for the manufacture of a number of field strength measuring equipments which were required by various

Service agencies of the United States and Allied nations.

A particularly important meeting of the Committee took place on July 13 in Washington. This meeting was attended by several representatives of the Allied Nations, including Professor D. R. Hartree, J. M. C. Scott, and Lt. Comdr. F. L. Westwater from England, and Drs. Kwei and Hsu from China. The progress of the theoretical attack on wave propagation through a nonhomogeneous atmosphere was thoroughly discussed by Prof. Hartree and Dr. C. L. Pekeris of the Analysis Section of CUDWR WPG.

Dr. A. T. Waterman of the Office of Field Service reported on work being done in the Southwest Pacific by D. E. Kerr. In the investigation of the difficulties of operation of the MEW radar on Saipan he confirmed the existence of a low-level evaporation duct discovered by Dr. Anderson and Dr. Stephenson in that area. Elevated ducts, the presence of which had been suspected by Dr. Anderson from analyses of radiosonde data, were definitely determined to exist at heights ranging from 1,000 to 2,700 ft, as a result of Kerr's investigations.

Dr. Waterman also described a survey of Service interest in scientific developments conducted in the entire area commanded by General MacArthur, in which a number of ways were found for OSRD to assist the Army Air and Ground Forces. The Pacific Branch of OSRD was organized so as to furnish a consulting staff under a director, a pool of scientists available for emergency field work, and a laboratory for solution of emergency field problems. This work was to be under directorship of Dr. K. T. Compton, and it seemed very desirable to have a representative in close touch with this OSRD unit in the field.

Dr. Anderson stressed the importance of conducting additional research in the Southwest Pacific area, and the need for informing the Services in that theater more fully of the operational advantages to be gained directly from such research. He went on to report progress in development and production of the equipment developed under the State College of Washington contract for making atmospheric soundings.

Lt. Comdr. Westwater reported on the overland propagation experiment going on at Suffield, Alberta, which was not yet completed, and described the meteorological conditions obtaining along the transmission path. These were of the type producing variations in the vertical angle of arrival of microwave radiation transmitted at angles near the hori-



zontal, and Dr. Burrows suggested that this experiment might be integrated with the Committee's angle-of-arrival project for determining refractive errors in gun-laying radar systems.

Methods for taking atmospheric soundings were reviewed, and a new combination kite and balloon was described in a report by M. Katzin of NRL.

Dr. Carroll reported on extensive tests on practically all types of VHF military voice communication sets, which were being planned in California. He reported that radio propagation tests were going to be correlated with meteorological measurements made with wired sondes.

The appointment of Dr. Kwei as the Committee's representative in China was discussed, and Dr. Kwei described the communication facilities to be made available for handling ionospheric propagation data obtained in China for transmission to the Committee. He urged that more scientifically trained personnel be transported to China when possible, to offset the very great lack of such persons to assist in the work.

Dr. Carroll described experiments going on in Florida supplementary to those being conducted in California, designed to answer questions about the maximum reliable range for VHF communications sets under varying conditions.

Meteorological measurements made offshore in the Boston area by the Radiation Laboratory Wave Propagation Group were described by Dr. R. B. Montgomery. These established the existence of ducts and at times substandard layers varying in height from 100 to as much as 700 ft, with complex distributions of refractive index. These measurements were especially important as they were known to parallel conditions to be expected in similar regions off the North China and Japanese coasts.

Work in progress on all other projects was also discussed, including angle-of-arrival experiments and the overland tests going on in New Zealand, Canada, and Arizona. Mr. R. J. Hearon reported on the new contracts, with particular reference to the direct Service interest in each. The whole future of propagation investigation was then considered, particularly with reference to the future employment of the propagation group at MIT-RL. It was the opinion of some Service representatives that the operation of this research establishment should be conducted under joint Army-Navy control. It was found impossible to reach definite conclusions as to a program to continue after eventual demobilization of OSRD, but general opinion was that a contract under the

Chiefs of Staff or other coordinating group might be made with MIT or a similar organization. It was decided to continue discussion at the next meeting.

On July 2, 1945, a summary of projects for consideration by the proposed Research Board for National Security [RBNS] was prepared for presentation when that body should become active. This included a considerable list of propagation, meteorology, and equipment problems requiring further research. At the date of writing, the exact status of this proposal with the RBNS is not known.

With the decisive change in the course of the war which took place during July and August 1945, emphasis was shifted from operational propagation problems to organizational and administrative matters, particularly reports, demobilization, and recommendations for a continuing program.

On July 30, a letter was circulated among the members and representatives of the Services requesting consideration of certain definite questions relating to future propagation research and reviewing such opinion as had already been expressed on the matter. Service interest in a continuing program had already been manifested, and it was felt particularly important that action be taken before the teams of ideally suited research workers at MIT and other laboratories were demobilized.

Upon the Japanese surrender in August 1945, the principal efforts of the Committee were directed to accomplishing contract terminations, preparation and submission of a final report, and demobilization of the organization. At a meeting on August 28, the matter of contract terminations was settled, and additional discussion of future propagation research was held.

A meeting of the Committee on Propagation was held in Washington on October 30, 1945, to discuss termination of the various projects and related matters, including preparation of a Summary Technical Report and a history, and the probable future of propagation research. This was expected to be the last full meeting of the Committee, and a large amount of business was transacted which can be mentioned only briefly here. The entire membership was present, with liaison officers of various Services concerned and several representatives of contractors and of British and Australian research agencies.

Dr. Saxton reported that future work in the United Kingdom was under discussion but that a decision had not yet been reached. He described certain experiments proposed for trial in New Zealand, for



which meteorological equipment was needed, and another which might be handled in South Africa. He also explained that the Canadian experiments along a land path near Suffield, Alberta, were continuing and that Sir Edward Appleton was of the opinion that the Ultra Shortwave Panel in Great Britain would continue to function into the peace.

Dr. Anderson reported that meteorological apparatus consisting of six sets of the lower atmosphere sounding apparatus developed at the State College of Washington was ready for transfer to New Zealand and that about forty sets of castings for the equipment were also available for distribution.

Mr. Munro announced that propagation research was to continue in Australia at the Radio Physics Laboratory and that the Radio Propagation Committee, a subcommittee of the Radio Research Board, would continue to function. He described the postwar policy for this investigation as favoring an expansion of the investigation with transfer of workers from projects. Fields of investigation in which work was proceeding or planned included tropospheric and ionospheric propagation, scattering from clouds and layers in the middle atmosphere, and a study of radio noise levels. Analysis of Service data was being conducted, a report on extra-long range echoes observed near Darwin had been issued, and a statistical survey of superrefraction along the Australian coast was under preparation.

Lieutenant W. E. Gordon, AAF, described angle-of-arrival measurements being conducted in New Jersey by BTL, simultaneously with meteorological measurements by the Weather Division of the AAF. Angles varying from 0.7 degree above to 0.1 degree below the line of sight were observed over the 12½-mile path, the nonstandard angles always coinciding with measured nonstandard atmospheric refractive conditions. On two occasions multiple paths had been observed.

Dr. E. W. Hamlin reported progress of the University of Texas group which was to study angle of arrival by measuring phase difference. He announced that the Office of Research and Inventions of the Navy had agreed to take over the project on an interservice plan of participation, with cooperation of Army and Navy laboratories, and active exchange of information with BTL and other interested agencies. It was also expected that AAF and other field stations would collaborate.

Dr. W. M. Rush described progress in construction of the receivers for field strength measurement under

the Humble Oil Company contract. Of the 24 units scheduled, 18 were to be completed by October 31, 1945. In addition, he announced that the company was interested in geophysical surveys over the Gulf to distances of 30 miles offshore by means of radar measurements and would be glad to cooperate with the University of Texas and Service groups.

The chairman announced that steps were under way to declassify all propagation information and to make it feasible for all organizations interested to obtain copies of pertinent material published by NDRC.

Captain D. R. Hull announced that the name of the NRSL was shortly to be changed to Navy Electronics Laboratory [NEL] and that facilities in Arizona were soon to be available for cooperation with the University of Texas.

D. E. Kerr announced the transfer of signal strength measuring receivers from RL to NRSL [NEL] and went on to describe a field expedition conducted by himself for the Operational Research Section of the Office of Field Service. He stated that the cause of the poor operation of the MEW was poor adjustment of the equipment. He confirmed the existence of strong superrefraction. He also mentioned contacting a part of Dr. Anderson's group in Manila and described the necessity for disseminating knowledge of propagation effects among operating personnel in the field, particularly in the Army. He also described use being made of radar for storm detection by the Southwest Pacific Weather Force and a series of educational talks being conducted with radar officers in the Philippines when the war ended.

Dr. Carroll briefly described results of propagation tests made by the Signal Corps along several over-water and over-land optical paths in California, on 100, 250, 1,450, and 4,500 mc. Elevated ducts had been observed, but surface reflection was found to be of greater importance. General conclusions from these tests indicated the importance of reflection from sea and land surfaces and the desirability of employing diversity reception with antennas spaced vertically.

Dr. Dellinger described his trip to a conference on radio held in Brazil, at which two government departments of that country had expressed willingness to undertake ionospheric observations in cooperation with a world-wide network. These departments had requested equipment and instructions for this work, which were to be supplied.

M. Katzin of NRL referred to the Antigua experiment completed early in the year and described a



similar experiment planned for the Pacific, employing a mobile laboratory and aircraft, with combination one-way and radar transmission. He also mentioned that NRL and NRSL (NEL) were planning a rather extensive propagation investigation which, however, would not interfere with the work planned for the Navy at the University of Texas.

Dr. Beverage announced that the activities of Division 15 of NDRC were to end almost completely on October 31, 1945, and added that some projects were being transferred to the Services but that no propagation studies were active.

Prof. Attwood announced termination of the Columbia contract (OEMsr-1207) as of October 31 and stated that 34 reports had been written under its terms, with some still awaiting distribution. He also mentioned that the Navy was taking over the Analysis Section of the Wave Propagation Group under a new contract with Columbia University.

John Campbell of the Jam Handy Organization described progress in the production of a film covering many aspects of propagation phenomena, which was due for completion about December 10, 1945.

Lt. Comdr. W. B. Chadwick described a Navy plan for predicting radar propagation conditions up to 24 hours in advance and transmitting such information with measured *M* curves to a central station for correlation and dissemination. He was of the opinion that the end of the war would probably halt this project, making it necessary to return the matter to research groups.

Lt. Col. J. J. Slattery and K. A. Norton announced that the Signal Corps planned to extend and continue propagation experimentation in general, in cooperation with other Services and industrial and scientific establishments.

The chairman requested comment on projected future propagation studies.

Dr. Dellinger stated that many questions yet to be answered seemed appropriate for investigation by a national research organization and by the new electronics department of MIT. He added that there

was an organization, the Union Radio Scientifique Internationale, with Sir Edward Appleton as international chairman and himself as chairman of the American section, which would exercise a definite interest in the propagation field.

D. E. Kerr expressed the opinion that MIT would not be in a position to undertake as large a program as had been suggested and added that after current projects were closed there would still be on hand a large amount of unanalyzed data, which could not be used unless an agency were found to make the analysis.

Major Wexler announced that the Army Weather Service would continue to cooperate with groups making propagation measurements and added that the Air Force was negotiating through the Signal Corps for basic research in storm detection by radar to be done at MIT.

The chairman announced that in view of the end of hostilities, no new conference on propagation would be called by the Committee. Following a vote of thanks to the Chairman proposed by Dr. Dellinger the meeting was adjourned. This was the last full meeting held by the Committee, but members remained active for a considerable time longer, carrying on the necessary work of demobilizing the organization.

With general demobilization of the Committee imminent and terminations of contracts already taking effect, the principal work of the Committee was concluded. After termination of the Columbia contract, it was felt advisable to appoint Prof. Attwood a consultant to the Committee to assist with final solution of administrative questions, and this was made effective November 1, 1945. An office for conducting correspondence and preparing this report was maintained in the Empire State Building in New York City, under the auspices of the NDRC Summary Reports Group. With submission of this report for publication, the work of the Committee may be considered closed.



## Chapter 4

# RESULTS AND RECOMMENDATIONS

4.1

### RESULTS

ANY TABULATION of the results of the Committee's work must be based to a degree on certain intangibles difficult to evaluate. This is because a substantial proportion of the overall result was a change in the attitude of agencies and personnel concerned with the performance of radar and radio equipment using the frequencies above about 30 mc. The complete analysis and understanding of propagation of these frequencies through the troposphere still lies in the future and will undoubtedly require much additional experimental and theoretical work, conducted without the restrictions of wartime secrecy and urgency. However, a considerable overall tangible result was also achieved, both in establishing the basic theory of tropospheric propagation and in development of methods and instruments for measuring meteorological factors influencing such propagation.

In the earlier stages of the war, nonstandard (at first called "anomalous") propagation caused several confusing and disconcerting incidents, due to misunderstanding of the phenomena. The instance later called "The Battle of the Pips," which took place near the Aleutians, was paralleled in other theaters many times. In this case echoes returned from islands ordinarily beyond radar range caused such confusion that fire was opened and an attempt made to engage nonexistent enemy units. Such puzzling and exasperating variations in radar and radio performance caused serious loss of confidence in equipment and was of considerable operational significance. This has been considered more fully in Chapter 1, as it was directly related to the origin of the Committee.

The general effect of such publications as *Variations in Radar Coverage*, of which upwards of 30,000 copies were distributed, *Tropospheric Propagation and Radio Meteorology*, and numerous other reports prepared and distributed for the Committee by the Columbia University Division of War Research [CUDWR] Wave Propagation Group [WPG] under contract OEMsr-1207, was to restore confidence in the equipment and its use and to focus attention on other causes of unreliability, which previously were

often masked by or confused with the effects of propagation variations. These other sources of variable performance, principally misadjustment of or defects in equipment caused by the rigors of field service, became easier to track down and eliminate, because they could be distinguished from propagation effects with reasonable success when the latter were understood.

Another general result of the Committee's work was a considerable modification of siting principles for radar and radio equipment. The results of the Caribbean over-water experiment, and of similar tests conducted at San Diego, Cape Cod, and across the Irish Sea, conclusively demonstrated the frequent existence of relatively stable horizontal layers of the lower atmosphere, in which the vertical distribution of refractive index was such as to cause substantial departures of actual radar coverage and radio communication range from the values obtained in a standard atmosphere. In particular, it was determined that, over much of the tropical and semi-tropical areas of the oceans, such layers were prevalent during many months, varying in thickness and intensity with wind speed and other measurable meteorological variables. These surface layers often produced large increases in radar ranges on surface craft and low-flying aircraft for radars of appropriate frequency sited in or close above the duct.

These investigations also revealed that under certain conditions a reverse effect could occur, in which the radiation was refracted downward much less than in a standard well-mixed atmosphere, with the result that coverage was less than normal. In extreme cases the radiation might even be bent upward away from the surface, resulting in ranges less than optical. In the course of arriving at these general results, methods and instruments for measuring the meteorological factors producing these effects were developed, particularly the Massachusetts Institute of Technology [MIT] psychrograph and the State College of Washington [WSC] wired sonde, with techniques for interpreting the data in approximate terms of radar performance. These instruments and techniques were made available to the armed forces of the Allied Nations.

A total of about 550 reports on various aspects of



the propagation problem were received from the numerous investigating laboratories. These reports were analyzed and the essential information contained was put into forms suitable for the use of operational personnel and distributed to the Services of the United States and the other Allied Nations. Such dissemination usually was in the form of publications by the CUDWR WPG, which issued a total of 34 such reports to a large distribution list. These reports and the very much larger number of scientific papers from which they were prepared are listed in the Bibliography.

## 4.2

## CRITIQUE

The greatest handicap to the work of the Committee on Propagation was the delay in recognizing the need for such an organization. In the rush to get electronic equipment that would allow the realization of the many new war inventions, the fact that the tactical use of these equipments depends upon their quantitative performance, which in turn depends upon the transmission medium, was neglected. As a result when this need was finally recognized the few experts in this field were deep in important war work and the committee decided to work with existing laboratories, letting new contracts for specific projects rather than setting up a central laboratory late in the war. The work of the committee should have begun with the conception of the ideas of the new radio systems, radar, loran, VHF (very high frequency) communication systems, guided missiles, etc. Then there would have been time to have established a central laboratory for carrying out propagation research and evaluating the performance characteristics of equipment.

## 4.3 FUTURE PROPAGATION RESEARCH

During the latter part of 1943, Committee members and liaison officers gave considerable attention to the matter of propagation research which would be desirable to have continued into the postwar period. Studies were made of the knowledge already obtained with a view to outlining the principal gaps in that knowledge and developing a general program for filling them, which could be carried on by such organizations as the Service laboratories or the Research Board for National Security. The results

of these studies are given here, divided roughly into suitable categories.

## PROPAGATION PROBLEMS

1. Subnormal propagation through fog and suspended water and ice particles.
2. Modifications of the coverage diagram when the radiation source is located in or below the horizontal layer exhibiting nonstandard variations of refractive index with height.
3. Errors produced in operation of direction finders, navigational equipment, and gunlaying radar by varying factors of tropospheric propagation.
4. Effects on atmospheric reflection of variations of frequency, pulse rate, pulse length, radiated power, and other variable parameters.
5. Correlation of variations of horizontal and vertical angle of arrival of radio waves with simultaneous meteorological measurements and evaluation of resulting variations in propagation characteristics.
6. Determination of frequencies permitting greatest security under various meteorological conditions.
7. Measurements of absolute signal strength and characteristics of the transmitted signal.
8. Determination of atmospheric noise levels in all important regions and the variation with season, frequency, and meteorology.
9. Phenomena responsible for long distance propagation in the 100- to 200-mc region.
10. Characteristics of propagation in the region between 50 and 500 kc.
11. Tropospheric propagation measurements over various types of terrain and water surfaces to determine, more accurately, coverage, angle of arrival, reflection, scattering, and absorption over the range in which the refractive index of the troposphere shows significant change.
12. Further theoretical analysis of propagation phenomena and comparison with observed experimental results.

## METEOROLOGICAL PROBLEMS

1. Particle sizes and distribution for all forms of atmospheric water.
2. Survey of the Pacific area similar to the German *Meteor* study of the Atlantic.

## EQUIPMENT PROBLEMS

1. Development of improved equipment for measuring variations of atmospheric refractive index.
2. Development of improved equipment for gener-



ating, detecting, and measuring radiation in the part of the frequency spectrum under consideration.

3. Required field strengths necessary for satisfactory operation of systems employing this range of frequencies.

4. Types of equipment suitable for determining location, intensity, and movement of storms, and distinguishing them from permanent echoes.

5. Handbooks of standard and nonstandard propagation and of standard performance of radar equipment.

Some of the points listed are not strictly propagation questions, but their investigation will require

the active assistance of propagation experts for solution. It is expected that systematic investigation will do much to eliminate the factors of uncertainty in siting and operation as well as in design of radio equipment operating in the frequency bands considered, particularly when better methods and apparatus have been developed for determining the performance of the equipment itself. Such methods and apparatus were by no means satisfactory during the war, with the result that uncertainty as to the actual condition and performance of equipment in the field further complicated the already formidable problem of determining propagation characteristics.







*PART II*  
*SUMMARY*







## Chapter 5

# STANDARD PROPAGATION

5.1

### INTRODUCTION

BY STANDARD PROPAGATION is meant radio wave propagation through an atmosphere free from irregular stratifications, particularly of vertical distributions of water vapor and temperature. With irregular stratification the propagation is said to be nonstandard and will be treated extensively in the later chapters.

In this chapter the fundamental general relations between transmitted and received power is first reviewed; then the main factors influencing the transmission of electromagnetic waves such as refraction, diffraction, and dielectric properties of the ground are surveyed; and finally the computation of the field at the receiver for various heights of transmitter and receiver above a homogeneous smooth earth of given electromagnetic properties is very briefly discussed. The last subject divides naturally into the determination of the field above the line of sight and the determination of the field below the line of sight in the earth's shadow.

The text of the present chapter largely follows the book, issued by the Columbia University Wave Propagation Group [CUDWR WPG] under the title *Propagation of Radio Waves through the Standard Atmosphere* which is Volume 3 of the Summary Technical Report of the Committee on Propagation.

5.2

### POWER TRANSMISSION

Certain relations occur so frequently in wave propagation problems that it is convenient to summarize them here before entering into a description of the characteristic features of short wave propagation. Some of these are mere definitions; some are consequences of electromagnetic theory.

It is convenient to use, as a standard antenna, one which has a length which is small compared to the wavelength, designated as "doublet." Such doublets may be used for both the transmitting and receiving antennas. In the latter case it is assumed that the load resistance is matched to the output resistance of the antenna. In free space, optimum transmission is achieved when the two doublets are parallel to

each other and perpendicular to the line connecting their centers. If their distance apart,  $d$ , is large compared to the wavelength, the ratio of power transmitted to maximum useful power received is found from electromagnetic theory to be

$$\frac{P_2}{P_1} = \left( \frac{3\lambda}{8\pi d} \right)^2, \quad (1)$$

where  $\lambda$  and  $d$  are measured in the same units. Here  $P_2$  is the power delivered to a matched load at the output terminal of the receiver and  $P_1$  the power fed to the transmitting antenna.

The gain  $G$  of any directive antenna is the ratio of the power transmitted by a doublet to the power transmitted by the antenna in question, to produce the same response in a distant receiver, when both transmitting antennas are adjusted for maximum transfer of power. The gain of a receiving antenna is similarly the ratio of the power delivered to the transmitting antenna when a doublet receiving antenna is used to the power delivered to the transmitting antenna to produce the same response when the antenna in question is used at the receiver.

Two methods of expressing antenna gain are in common use: the one just indicated where the gain is measured as the ratio of the power in the optimum direction relative to that of a doublet, and the other where the gain is that relative to a hypothetical isotropic radiator which is one assumed to radiate the same power density in all directions. Simple geometrical considerations show that the gain of a doublet over that of an isotropic radiator is  $3/2$  so that the gains expressed in the former system are converted into the latter system by multiplying them by  $3/2$ . In the equations below, the gain is expressed relative to the doublet.

If transmission takes place, not in free space, but over a conducting ground, in a refracting atmosphere, etc., the power ratio will be expressed as

$$\frac{P_2}{P_1} = G_1 G_2 \left( \frac{3\lambda}{8\pi d} \right)^2 A_p^2, \quad (2)$$

where  $G_1 G_2$  are the antenna gains of the transmitting and receiving systems, respectively, and  $A_p$  is the



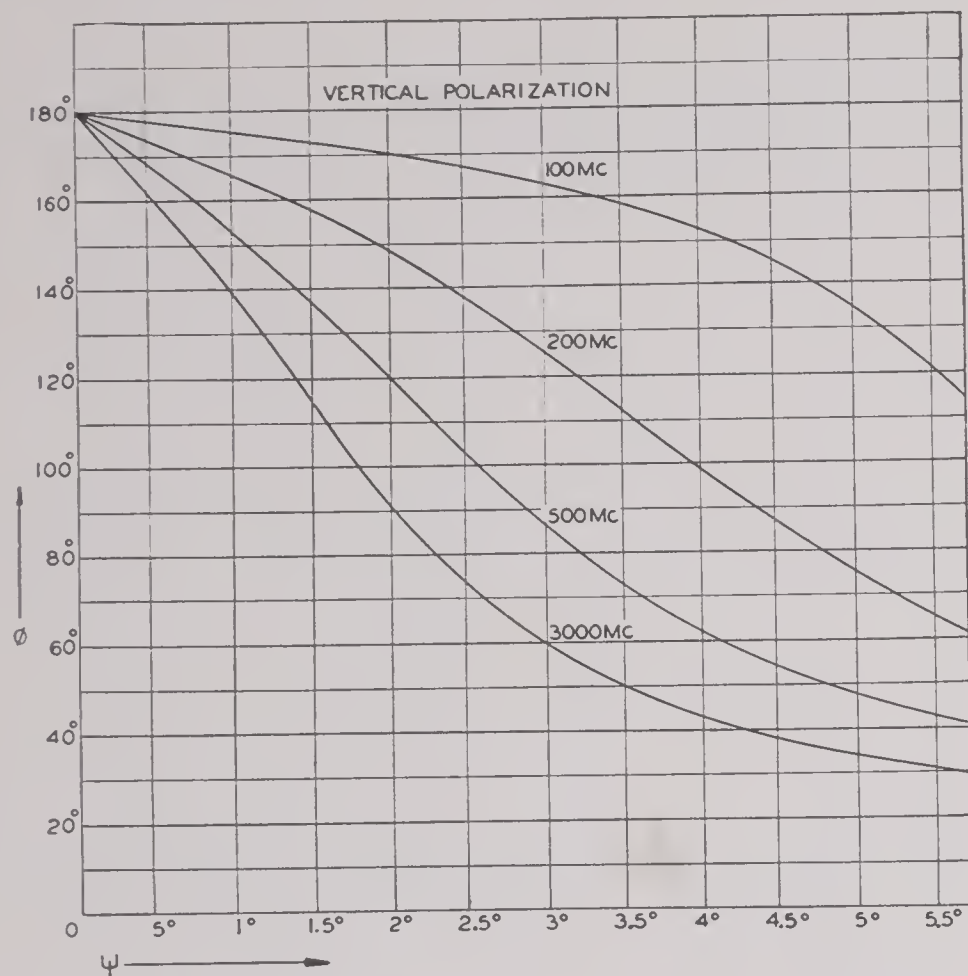


FIGURE 4. Phase lag,  $\phi$ , of the reflection coefficient versus reflection angle,  $\psi$ , from  $\psi = 0$  to  $\psi = 5.5^\circ$  for sea water.

From the practical viewpoint the following summary may give an overall picture of the more outstanding features of ground and sea reflection.

For *horizontal* polarization over the sea the reflection coefficient may be taken as unity and the phase shift as 180 degrees for frequencies up to and including the centimeter range, for practically all angles of reflection. Over land there is a slight decrease of the amplitude of the reflection coefficient with increasing angle; for instance, for a frequency of 200 mc, at an angle of 15 degrees the reflection coefficient has decreased to 0.9 or slightly more for moist soil and to 0.8 or slightly more for dry soil. These statements apply when the ground or sea surface is reasonably smooth. In order to decide whether a surface is smooth or rough, Rayleigh's criterion, explained below, is usually applied. When the surface is rough or wavy, irregular scattering predominates and reduces the intensity to a small part of the value attained with a smooth surface.

For *vertical* polarization the curve of the magnitude of the reflection coefficient versus the angle goes through a minimum (see Figure 2). When the imaginary term of the complex dielectric constant is negligible so that the ground behaves like a pure dielectric material, the reflection coefficient goes to zero at a certain angle (Brewster angle). Ordinary soil nearly fulfills this condition. For instance, at a frequency of 200 mc the Brewster angle occurs at

about 12 degrees with moist soil and at about 21 degrees with dry soil.

For the ocean surface, and vertical polarization, the imaginary part of the dielectric constant cannot be neglected, and the reflection coefficient as a function of the angle does not vanish at any angle but goes through a minimum, the pseudo-Brewster angle. The actual variation of amplitude and phase lag is represented in Figures 2 and 3 for the small angles of reflection which are most important in practice.

When the ground is rough the reflection coefficient for both types of polarization is reduced to a very small value. For 10-cm waves and still more for shorter ones, most types of land are rough. A reflection coefficient of 0.2 may be taken as representative for an average ground covered with vegetation. A slightly ruffled sea is a fairly good reflector for 10-cm waves but appears somewhat rough at shorter wavelengths.

#### STANDARD REFRACTION

Numerous experiments have resulted in the following formula for the refractive index of moist air:

$$(n - 1) \cdot 10^6 = \frac{79}{T} \left( p - e + \frac{4,800e}{T} \right) \quad (9)$$

where  $n$  = the index of refraction,

$p$  = the barometric pressure in millibars

(1 mm mercury = 1.3332 mb),

$e$  = partial pressure of water vapor in millibars,

$T$  = absolute temperature.

The mixing ratio,  $s$ , which is practically equal to specific humidity, is connected with  $e$  by the relation

$$e = 0.00161ps. \quad (10)$$

A recent analysis<sup>278</sup> has shown, moreover, that this expression for refractive index must, on theoretical grounds, be substantially independent of frequency down to the shortest waves employed in microwave engineering.

In an average atmosphere temperature, pressure, and water vapor density decrease with height, and, in the lowest few kilometers where most of the short and microwave propagation takes place, it may be assumed to a good approximation that the decrease of refractive index with height is linear though the rate of decrease is somewhat dependent on the climate. In middle latitudes it is given by



$$\frac{dn}{dh} = -0.039 \cdot 10^{-6} \text{ per meter.} \quad (11)$$

Refraction at the boundary of two media is familiar from optics and is expressed by Snell's law:

$$n_1 \cos \alpha_1 = n_2 \cos \alpha_2, \quad (12)$$

where  $n_1$  and  $n_2$  are the refractive indices of the two media and  $\alpha_1$  and  $\alpha_2$  the angle between the boundary and the direction of the ray in the first and second media respectively. In the atmosphere the refractive index is a continuous function of height, and the sudden change of direction at a boundary is then replaced by a *curvature* of the rays. Equation (12) can be written

$$n \cos \alpha = n_0 \cos \alpha_0, \quad (13)$$

where  $n$  and  $\alpha$  are now continuous functions of the height and the subscript 0 designates a reference level.

The above formulas refer to a plane earth. If the earth's curvature is taken into account so that the planes relative to which the angle  $\alpha$  is measured are replaced by spheres about the earth's center, formula (13) must be modified; and the mathematical analysis shows<sup>442</sup> that it is replaced by

$$nr \cos \alpha = n_0 r_0 \cos \alpha_0 \quad (14)$$

where  $r$  is the distance from the center of the earth to the level considered.

If now we set  $r = r_0 (1 + h/r_0)$  where  $h = r - r_0$  and  $h/r_0$  is a small quantity and, furthermore, if we note that with a linear gradient of  $n$

$$n = n_0 + \frac{dn}{dh} h \quad (15)$$

we obtain on substituting into (14) and neglecting small quantities of the second order

$$\left[ 1 + \left( \frac{1}{r_0} + \frac{dn}{dh} \right) h \right] \cos \alpha = \cos \alpha_0. \quad (16)$$

It results from this equation that a linear gradient of refractive index has the same effect on refraction as the curvature of the earth,  $1/r_0$ . By introducing an effective earth's radius it is possible to eliminate the refraction term entirely and to treat the atmosphere as if it were homogeneous. This device was first introduced by Schelleng, Burrows, and Ferrell,<sup>24</sup> and has since been generally accepted. Some German writers have introduced a quadratic function to represent the variation of refractive index with height in the atmosphere,<sup>443</sup> the coefficients of the quadratic terms being characteristic of the air mass or type of

atmosphere involved. This has the advantage of permitting a close fit with observed refractive index curves up to heights of 6 to 8 km. It seems, however, that the advantage of the greater analytical simplicity of the linear refractive index curves far outweighs the increased accuracy of the quadratic form, and the latter has therefore not found acceptance in this country and Great Britain.

It is customary to designate the effective, or modified earth radius by  $ka$  where  $k$  is a numerical constant and  $a$  replaces  $r_0$  used above and represents the mean radius of the earth. Hence

$$\frac{1}{a} + \frac{dn}{dh} = \frac{1}{ka}, \quad (17)$$

and by comparison with equation (11) it follows that

$$k = \frac{4}{3} \quad (18)$$

since  $dn/dh = -0.039 \cdot 10^{-6} = -1/4a$ . The earth's radius  $a = 6.37 \cdot 10^6$  meters.

In view of this result coverage diagrams of radar and radio communication sets are commonly drawn with a  $\frac{4}{3}$  earth's radius. In such a diagram the rays, which are curved in a "true" geometric representation, appear as straight lines.

The value  $k = \frac{4}{3}$  does not, of course, represent a universal law. It is merely an expression of the fact that the rate of decrease of the refractive index with height has, in the middle geographical latitudes, a certain average value. In arctic climates  $k$  as a rule is somewhat smaller, lying between  $\frac{4}{3}$  and  $\frac{5}{5}$ , while in tropical climates  $k$  is somewhat larger, between  $\frac{4}{3}$  and  $\frac{3}{2}$ . In temperate and tropical climates, the main factor determining the magnitude of  $k$  is the humidity gradient in the lower atmosphere. In Figure 5 is shown a nomogram from which the appropriate value of  $1/k$  can be read directly as function of the gradient of *relative* humidity and air temperature. The table has been computed under the assumption that the temperature gradient has the "standard" value of  $-0.65$  C per 100 m, but the value of  $k$  is relatively insensitive to variations in the temperature gradient.

Usually the value of  $k = \frac{4}{3}$  is referred to as the standard case, but this term is also used to designate more generally an atmosphere with a linear refractive index distribution where  $k$  might differ somewhat from  $\frac{4}{3}$ . Experience shows that the atmospheric conditions under which the refractive index is a linear function of height are quite common, but this



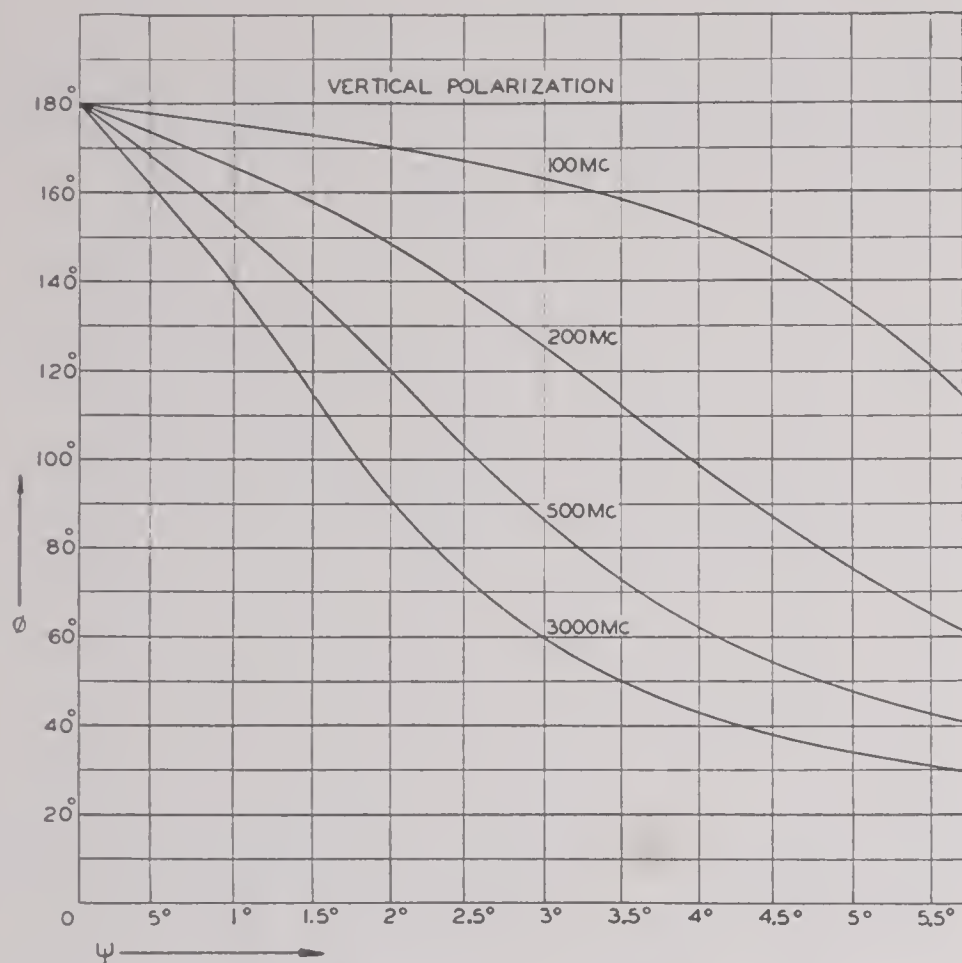


FIGURE 4. Phase lag,  $\phi$ , of the reflection coefficient versus reflection angle,  $\psi$ , from  $\psi = 0$  to  $\psi = 5.5^\circ$  for sea water.

From the practical viewpoint the following summary may give an overall picture of the more outstanding features of ground and sea reflection.

For *horizontal* polarization over the sea the reflection coefficient may be taken as unity and the phase shift as 180 degrees for frequencies up to and including the centimeter range, for practically all angles of reflection. Over land there is a slight decrease of the amplitude of the reflection coefficient with increasing angle; for instance, for a frequency of 200 mc, at an angle of 15 degrees the reflection coefficient has decreased to 0.9 or slightly more for moist soil and to 0.8 or slightly more for dry soil. These statements apply when the ground or sea surface is reasonably smooth. In order to decide whether a surface is smooth or rough, Rayleigh's criterion, explained below, is usually applied. When the surface is rough or wavy, irregular scattering predominates and reduces the intensity to a small part of the value attained with a smooth surface.

For *vertical* polarization the curve of the magnitude of the reflection coefficient versus the angle goes through a minimum (see Figure 2). When the imaginary term of the complex dielectric constant is negligible so that the ground behaves like a pure dielectric material, the reflection coefficient goes to zero at a certain angle (Brewster angle). Ordinary soil nearly fulfills this condition. For instance, at a frequency of 200 mc the Brewster angle occurs at

about 12 degrees with moist soil and at about 21 degrees with dry soil.

For the ocean surface, and vertical polarization, the imaginary part of the dielectric constant cannot be neglected, and the reflection coefficient as a function of the angle does not vanish at any angle but goes through a minimum, the pseudo-Brewster angle. The actual variation of amplitude and phase lag is represented in Figures 2 and 3 for the small angles of reflection which are most important in practice.

When the ground is rough the reflection coefficient for both types of polarization is reduced to a very small value. For 10-cm waves and still more for shorter ones, most types of land are rough. A reflection coefficient of 0.2 may be taken as representative for an average ground covered with vegetation. A slightly ruffled sea is a fairly good reflector for 10-cm waves but appears somewhat rough at shorter wavelengths.

#### STANDARD REFRACTION

Numerous experiments have resulted in the following formula for the refractive index of moist air:

$$(n - 1) \cdot 10^6 = \frac{79}{T} \left( p - e + \frac{4,800e}{T} \right) \quad (9)$$

where  $n$  = the index of refraction,

$p$  = the barometric pressure in millibars

(1 mm mercury = 1.3332 mb),

$e$  = partial pressure of water vapor in millibars,

$T$  = absolute temperature.

The mixing ratio,  $s$ , which is practically equal to specific humidity, is connected with  $e$  by the relation

$$e = 0.00161ps. \quad (10)$$

A recent analysis<sup>278</sup> has shown, moreover, that this expression for refractive index must, on theoretical grounds, be substantially independent of frequency down to the shortest waves employed in microwave engineering.

In an average atmosphere temperature, pressure, and water vapor density decrease with height, and, in the lowest few kilometers where most of the short and microwave propagation takes place, it may be assumed to a good approximation that the decrease of refractive index with height is linear though the rate of decrease is somewhat dependent on the climate. In middle latitudes it is given by



$$\frac{dn}{dh} = -0.039 \cdot 10^{-6} \text{ per meter} . \quad (11)$$

Refraction at the boundary of two media is familiar from optics and is expressed by Snell's law:

$$n_1 \cos \alpha_1 = n_2 \cos \alpha_2 , \quad (12)$$

where  $n_1$  and  $n_2$  are the refractive indices of the two media and  $\alpha_1$  and  $\alpha_2$  the angle between the boundary and the direction of the ray in the first and second media respectively. In the atmosphere the refractive index is a continuous function of height, and the sudden change of direction at a boundary is then replaced by a *curvature* of the rays. Equation (12) can be written

$$n \cos \alpha = n_0 \cos \alpha_0 , \quad (13)$$

where  $n$  and  $\alpha$  are now continuous functions of the height and the subscript 0 designates a reference level.

The above formulas refer to a plane earth. If the earth's curvature is taken into account so that the planes relative to which the angle  $\alpha$  is measured are replaced by spheres about the earth's center, formula (13) must be modified; and the mathematical analysis shows<sup>442</sup> that it is replaced by

$$nr \cos \alpha = n_0 r_0 \cos \alpha_0 \quad (14)$$

where  $r$  is the distance from the center of the earth to the level considered.

If now we set  $r = r_0 (1 + h/r_0)$  where  $h = r - r_0$  and  $h/r_0$  is a small quantity and, furthermore, if we note that with a linear gradient of  $n$

$$n = n_0 + \frac{dn}{dh} h \quad (15)$$

we obtain on substituting into (14) and neglecting small quantities of the second order

$$\left[ 1 + \left( \frac{1}{r_0} + \frac{dn}{dh} \right) h \right] \cos \alpha = \cos \alpha_0 . \quad (16)$$

It results from this equation that a linear gradient of refractive index has the same effect on refraction as the curvature of the earth,  $1/r_0$ . By introducing an effective earth's radius it is possible to eliminate the refraction term entirely and to treat the atmosphere as if it were homogeneous. This device was first introduced by Schelleng, Burrows, and Ferrell,<sup>24</sup> and has since been generally accepted. Some German writers have introduced a quadratic function to represent the variation of refractive index with height in the atmosphere,<sup>443</sup> the coefficients of the quadratic terms being characteristic of the air mass or type of

atmosphere involved. This has the advantage of permitting a close fit with observed refractive index curves up to heights of 6 to 8 km. It seems, however, that the advantage of the greater analytical simplicity of the linear refractive index curves far outweighs the increased accuracy of the quadratic form, and the latter has therefore not found acceptance in this country and Great Britain.

It is customary to designate the effective, or modified earth radius by  $ka$  where  $k$  is a numerical constant and  $a$  replaces  $r_0$  used above and represents the mean radius of the earth. Hence

$$\frac{1}{a} + \frac{dn}{dh} = \frac{1}{ka} , \quad (17)$$

and by comparison with equation (11) it follows that

$$k = \frac{4}{3} \quad (18)$$

since  $dn/dh = -0.039 \cdot 10^{-6} = -1/4a$ . The earth's radius  $a = 6.37 \cdot 10^6$  meters.

In view of this result coverage diagrams of radar and radio communication sets are commonly drawn with a  $\frac{4}{3}$  earth's radius. In such a diagram the rays, which are curved in a "true" geometric representation, appear as straight lines.

The value  $k = \frac{4}{3}$  does not, of course, represent a universal law. It is merely an expression of the fact that the rate of decrease of the refractive index with height has, in the middle geographical latitudes, a certain average value. In arctic climates  $k$  as a rule is somewhat smaller, lying between  $\frac{4}{3}$  and  $\frac{6}{5}$ , while in tropical climates  $k$  is somewhat larger, between  $\frac{4}{3}$  and  $\frac{3}{2}$ . In temperate and tropical climates, the main factor determining the magnitude of  $k$  is the humidity gradient in the lower atmosphere. In Figure 5 is shown a nomogram from which the appropriate value of  $1/k$  can be read directly as function of the gradient of *relative* humidity and air temperature. The table has been computed under the assumption that the temperature gradient has the "standard" value of  $-0.65$  C per 100 m, but the value of  $k$  is relatively insensitive to variations in the temperature gradient.

Usually the value of  $k = \frac{4}{3}$  is referred to as the standard case, but this term is also used to designate more generally an atmosphere with a linear refractive index distribution where  $k$  might differ somewhat from  $\frac{4}{3}$ . Experience shows that the atmospheric conditions under which the refractive index is a linear function of height are quite common, but this



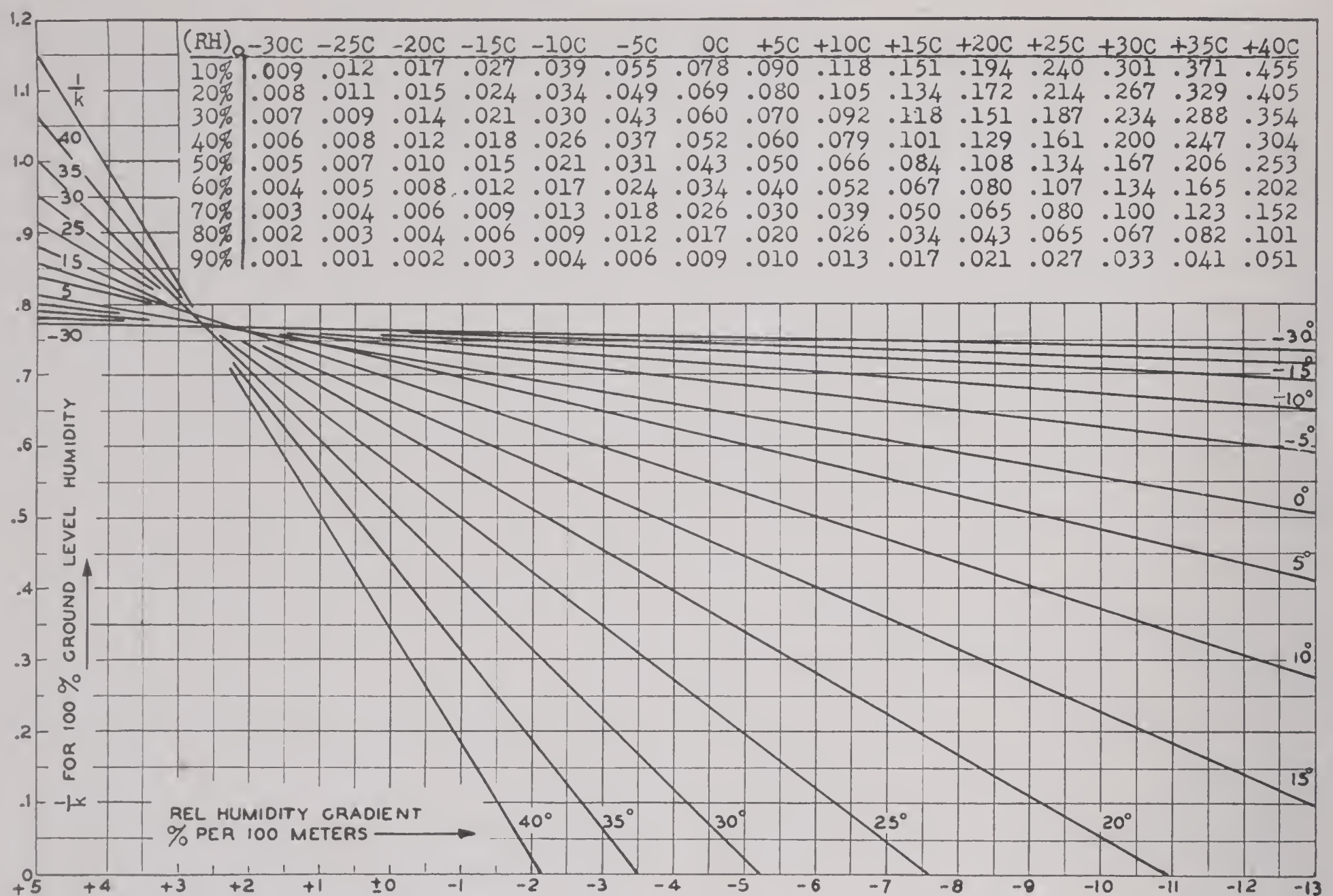


FIGURE 5. Graph:  $1/k$  versus RH gradient and temperature for 100 per cent RH at ground. Add correction tabulated to obtain  $1/k$  for RH at ground  $\neq 100\%$ .

is only one case out of several that may, and do, arise in the atmosphere. A full appreciation of the limitations of the concept of standard refraction requires some knowledge of the phenomena of non-standard propagation which will be dealt with extensively in later chapters.

#### ROUGHNESS OF THE GROUND

In order to estimate how closely the ground approximates the condition of an ideal reflecting surface, a rule is required that gives results sufficiently accurate to be used in radio and radar practice. The subject has not been very thoroughly explored, but Rayleigh's criterion for roughness, originally developed for optical purposes, has been applied with good success. Since it seems to be the only criterion of its kind and since it is often necessary to decide whether the terrain in front of a given radio or radar site is reflecting, it deserves some detailed consideration.

The principle of Rayleigh's criterion is illustrated in Figure 6. The roughness is assumed to be produced by a large number of elevations in the reflecting plane of average height  $H$ . One such "hump"

is shown in the figure together with two rays one of which is assumed to be reflected from the ground surface and one from the top of the "hump." The difference in phase between the two rays is  $2H\psi(2\pi/\lambda)$ .

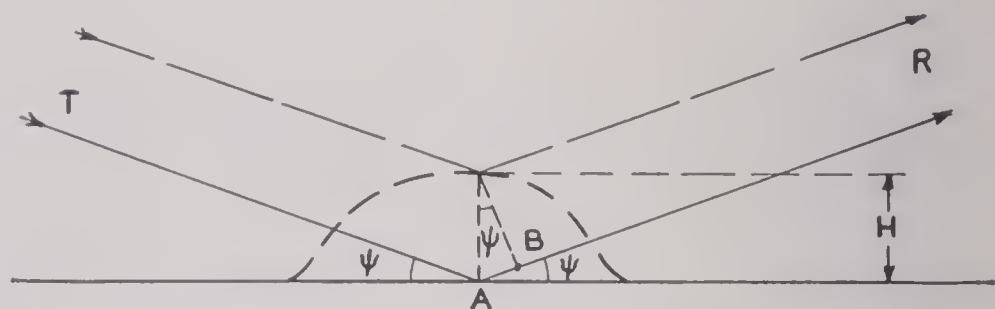


FIGURE 6. Geometry for Rayleigh's criterion for rough ground.

The criterion now requires that the surface be considered as rough when this phase difference exceeds  $\pi/4$  radians. This gives for the critical value of  $H$ , when  $\psi$  is in degrees,  $\lambda$  in meters,

$$H = \frac{\lambda}{16\psi} \quad (19)$$

If  $n$  is the "lobe variable," that is, a quantity equal to 1, 3,  $\dots$   $(2n - 1)$ ,  $\dots$  at the first, second,



$n$ th interference maximum of the direct and ground-reflected rays, namely,

$$n = \frac{4h_1\psi}{\lambda}, \quad (20)$$

where  $h_1$  is the height of the transmitter above the ground, the criterion can be written in the form

$$H = \frac{h_1}{4n}. \quad (21)$$

Although admittedly rough, the criterion indicates the order of magnitude of the angle above which specular reflection will be greatly reduced in favor of diffuse scattering of the type which, in ordinary optics, is produced by a dull, white surface. It is reasonably safe to assume that for angles exceeding the critical angle the amount of specular reflection will be reduced to a small fraction, perhaps to the order of one-fifth, of the value of the reflection under ideal conditions.

#### DIFFRACTION BY TERRAIN

A number of the influences of the earth's surface upon wave propagation have the common characteristic that they represent deviations of the actual earth from the idealized model of a smooth sphere endowed with homogeneous electrical constants. Diffraction by the earth's average curvature is not included among the effects considered here since it is dealt with extensively in Volume 3.

There are two main classes of phenomena that fall under the general heading of diffraction. One is the diffraction by obstacles, such as hills, trees or houses, and the other is the diffraction by the structure of an otherwise fairly level ground, in particular, roughness and horizontal variations of dielectric constant.

The diffraction by hills and similar obstacles of the terrain is commonly treated theoretically by means of the Fresnel-Kirchhoff diffraction theory as found in textbooks on optics. The only problem which is sufficiently simple to admit of a direct application to short wave transmission is that of diffraction by a straight edge. It is not necessary that the edge be perpendicular to the line connecting the transmitter and receiver but for the validity of the theory it is necessary to suppose that the distances from the diffracting obstacle to the transmitter and receiver are large compared to the height of the obstacle, which means that the angles of diffraction are small.

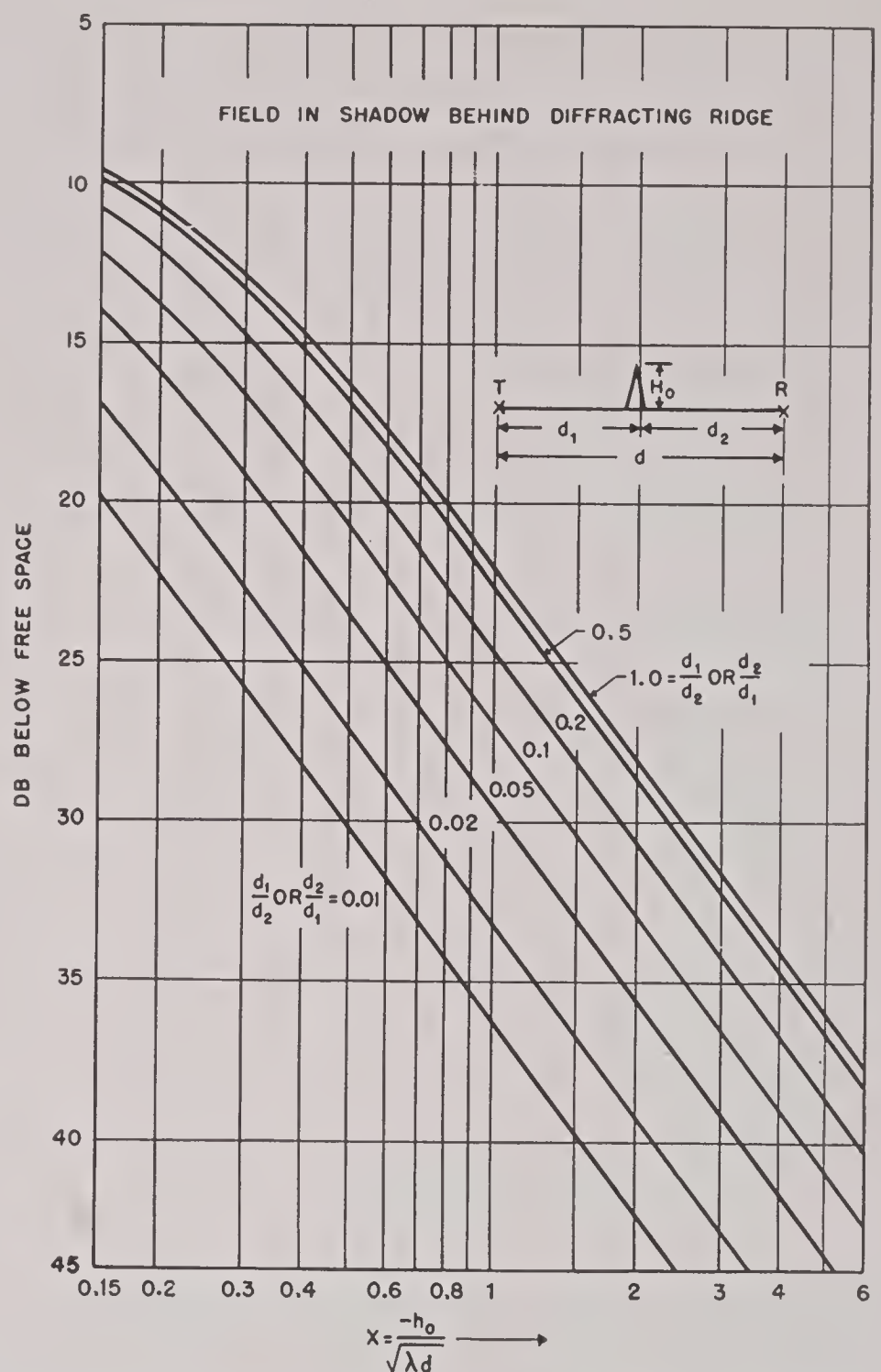


FIGURE 7. Field in shadow behind a diffracting ridge.

Figure 7 shows a nomogram from which the field strength in the shadow of a diffracting edge can be read in decibels below that of free space. The geometrical significance of the quantities used is illustrated on the figure.

Such experiments as have been made show a general agreement with theory, but it is difficult in practice to realize conditions of transmission that approach ideal ones, to which the Fresnel-Kirchhoff theory refers. When appropriate values are taken for the reflection coefficient of the ground and the four components of the resulting field are added vectorially, good agreement has been found between experiment and theory for selected terrain. (See Chapter 15 of this volume.) Sometimes the terrain conditions are often so complicated that they do not readily lend themselves to idealization by simple geometrical models. For these reasons the Fresnel-Kirchhoff diffraction theory has been of only limited value in short wave radio propagation.

A case which quite often can be described ade-



quately by an idealized model is that of a sudden change of the dielectric properties of the ground, as at a coast line.<sup>340-346</sup> If the land is rough while the sea surface produces full specular reflection, the coast line can be considered as a diffracting straight edge with respect to the image antenna, rays of which represent the field reflected by the sea surface. The straight edge serves to cut off that part of the radiation from the image that would represent reflection from the land area. The geometrical conditions are shown schematically in Figure 8. For the details of

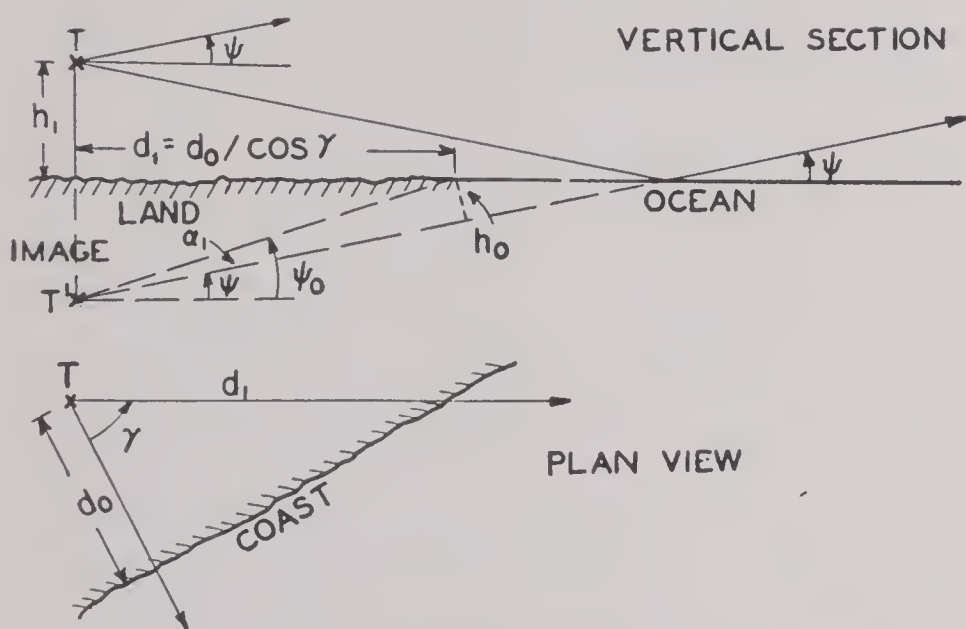


FIGURE 8. Diffraction by a coast line.

the analytical treatment the reader is referred to the comprehensive report on standard propagation contained in Volume 3 of the Summary Technical Report of the Committee on Propagation. The distortion of the coverage diagram of a radar set caused by this type of diffraction is often quite large and becomes important operationally at frequencies of 100 to 200 mc. This is illustrated here by a computed coverage diagram shown in Figure 9. If diffraction is

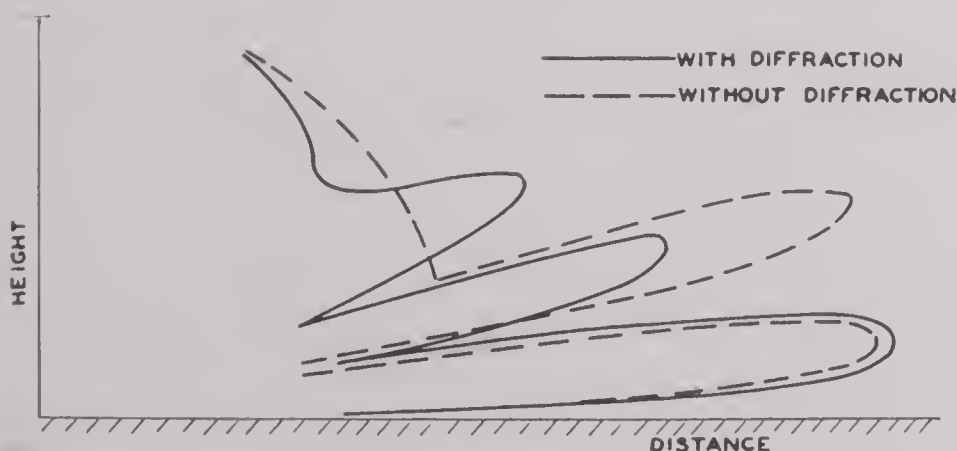


FIGURE 9. Coverage diagram for coast line diffraction (relative field strength). (Heights exaggerated 3.5 to 1.)

not taken into account the coverage pattern shows a constant amplitude through higher angular elevations reached only by the direct rays since the ground reflection is negligible. At lower angular elevations

rays reflected from the sea add to the direct rays, and the "lobe" type of pattern appears. It is clear that if the diffraction effect were neglected very serious errors of the estimated coverage would result.

Similar methods can be used to treat diffraction caused by cliffs, edges of wooded areas, lakes, etc., but these cases are not so often of importance in radar practice.

#### 5.4 THE ELECTROMAGNETIC FIELD

##### FIELD STRENGTH DISTRIBUTION

If a transmitter is erected over a plane, ideally reflecting earth, the well-known lobe pattern results

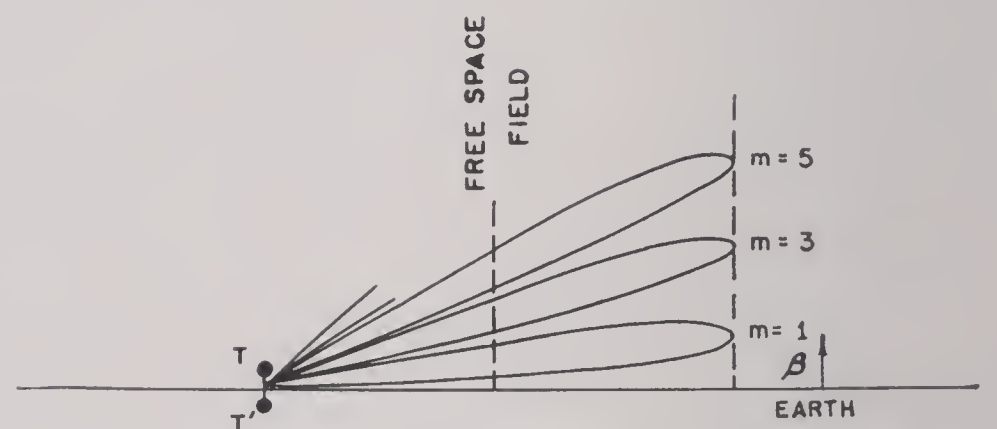


FIGURE 10. Typical coverage diagram (lobes) over plane earth.

(Figure 10), the curves being ones of constant field strength. The field is given by

$$E = E_0 \cdot 2 \sin \left( \frac{2\pi h_1 h_2}{\lambda d} \right) \quad (22)$$

where  $h_1$  and  $h_2$  are the transmitter and receiver heights, and  $d$  the distance from transmitter to receiver. The maxima and minima occur at the positions in space where

$$h_1 h_2 = \frac{n}{4} \lambda d, \quad (23)$$

with  $n=1, 3, 5 \dots$  for the maxima,  
 $n=0, 2, 4 \dots$  for the minima.

If  $h_2 \gg h_1$ , the angle of elevation is  $\psi = h_2/d$  and the formula for the maxima and minima can be written

$$\psi = \frac{n\lambda}{4h_1}. \quad (24)$$

If the earth curvature is taken into account the pattern remains essentially the same above the line of sight, but a number of corrections enter which change somewhat the position and strength of the



lobes. The problem is primarily one of geometry, taking into account the modification of the direction, phase, and intensity of the reflected ray caused by the earth's curvature. It can be solved by suitable numerical and graphical methods such as are given in Volume 3 where the details are extensively treated. It may suffice here to enumerate the main modifying factors.

If a tangent to the earth is drawn at the point of reflection (Figure 11), the distances  $h'_1$  and  $h'_2$  of transmitter and receiver from this line are the equiv-

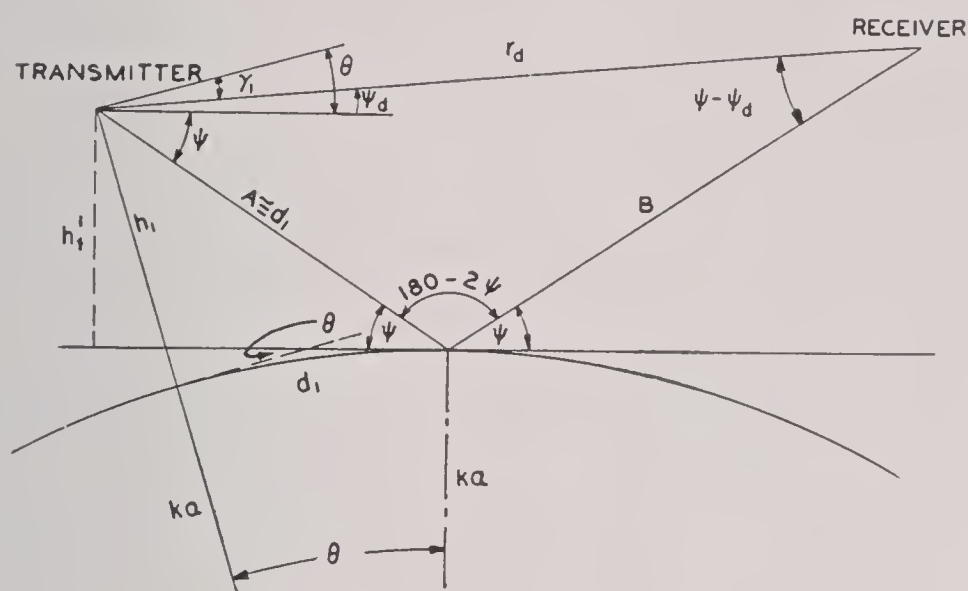


FIGURE 11. Geometry over spherical earth.

alent heights in terms of which the problem is a plane-earth problem for that particular ray. They are smaller than the heights above the ground  $h_1$  and  $h_2$ , but clearly they are functions of the angle of elevation. Thus a set of implicit equations has to be solved for each angle of elevation giving  $h'_1$  and  $h'_2$  as functions of  $h_1$ ,  $h_2$ , and  $d$ , whereupon the interference between the direct and reflected rays is computed as in the case of a plane earth.

In addition to the modification of direction and phase at reflection, there is also a change in intensity of the reflected ray caused by the fact that the reflecting surface is curved. This modification is taken into account by the *divergence factor*, a purely geometrical quantity which is part of the reflection coefficient, reducing the intensity of the reflected ray.

The behavior of the field below the line of sight requires a more powerful line of attack. The line of sight itself is given by a tangent to the earth's surface passing through the transmitter. The distance from the transmitter to the horizon, when a modified earth's radius  $ka$  is used is

$$d_T = \sqrt{2kah_1}. \quad (25)$$

When  $k = \frac{4}{3}$ ,  $h_1$  is in meters and  $d_T$  in kilometers, this becomes

$$d_T = 4.12 \sqrt{h_1}. \quad (26)$$

The diffraction region actually extends at least from the lower surface of the first lobe downward to the earth's surface. In the diffraction region well below the line of sight, the field strength decreases very rapidly and very nearly exponentially with the distance.

Figure 12 shows a typical example for the ground

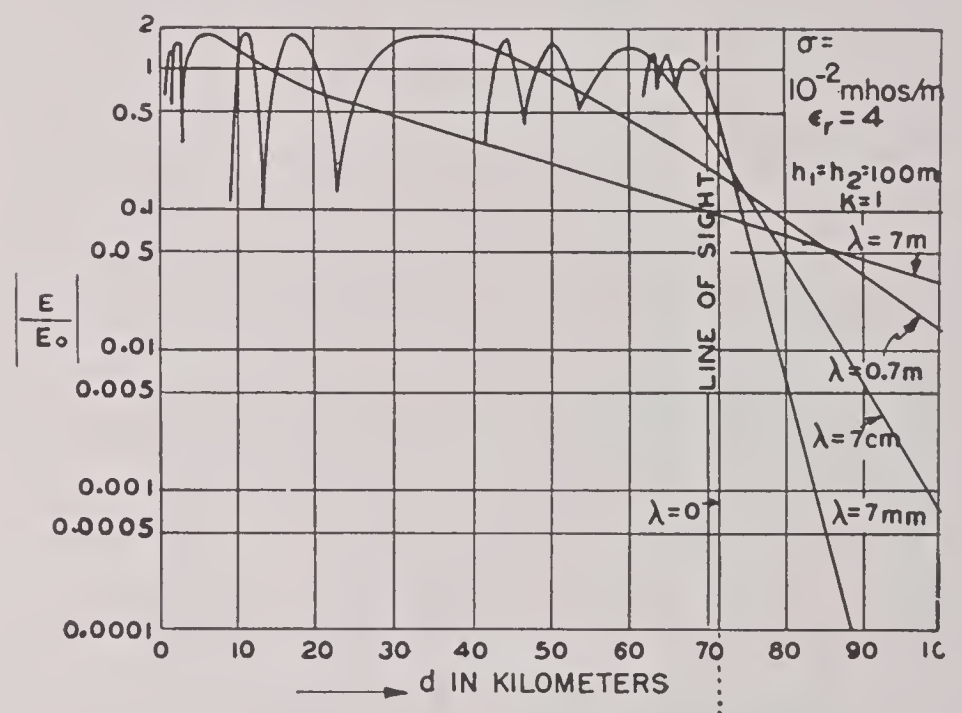


FIGURE 12. Field strength versus distance for fixed height, vertical polarization.

constants indicated. The ordinate is the ratio of field strength to the free space field; the transmitter and receiver heights are fixed and  $d$  is plotted as abscissa. Above the line of sight the typical lobe pattern is exhibited. The decrease of the field in the diffraction region is the more rapid the shorter the wavelength. In the centimeter band this decrease is so rapid that for most practical purposes the field is nonexistent near the ground at distances exceeding the horizon distance by more than a few kilometers. Figure 13 shows a similar diagram for fixed distance and variable receiver height.

## MODES

The description of the electromagnetic field above the line of sight is adequately given by means of rays and their phases as used in optics. This method obviously breaks down in the diffraction region into which the rays do not penetrate. For this region a solution of the wave equation is required. Many distinguished mathematicians have contributed varying techniques for solving the wave equation. The



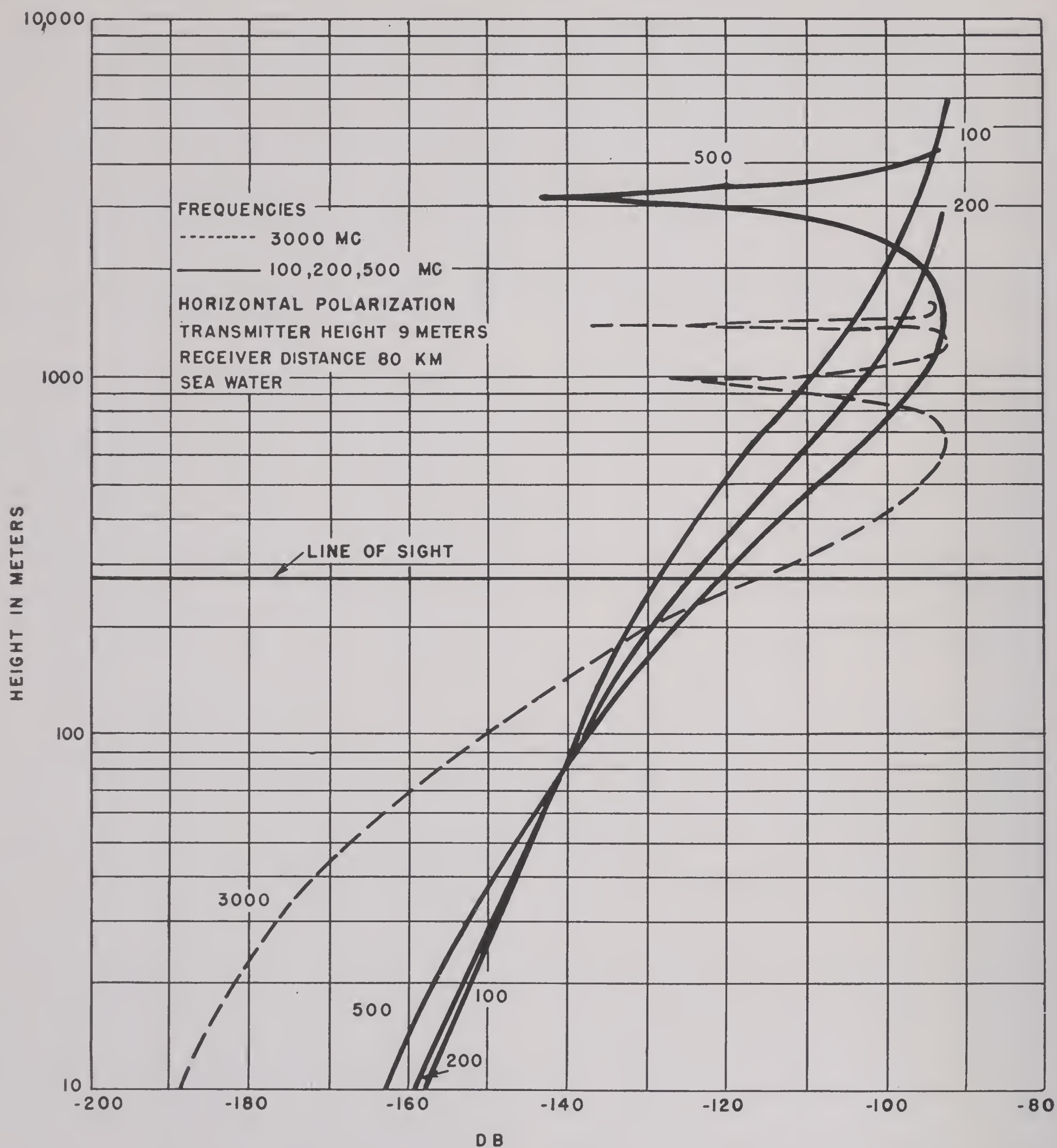


FIGURE 13. Field strength versus height of receiver for fixed distance relative to radiation field at one meter from transmitter.

theory in its present form as applied to short and microwave propagation has been worked out by van der Pol and Bremmer<sup>20</sup> for vertical polarization and Marian C. Gray for horizontal polarization.

The results of the theory may be summarized as follows. The electromagnetic field can be represented as an infinite series of the form

$$E = E_0 \sqrt{d} \sum_m c_m e^{-\zeta_m d} U_m(h_1) U_m(h_2) \quad (27)$$

where  $E_0$  is the free space field and  $c_m$  and  $\zeta_m$  are complex constants depending upon the wavelength and the electromagnetic ground constants.  $h_1$  and  $h_2$  are again the heights of the transmitter and receiver above the ground,  $d$  is the distance between the two;  $U_m$  are the height-gain functions, and  $e$  is the base of natural logarithms. The formula is symmetrical with respect to the interchange of transmitter and receiver, in agreement with the principle of reciprocity.



Each of the terms which compose the sum (27) is called a *mode*. The coefficients  $\zeta_m$  are complex constants with their real parts positive. They represent therefore an exponential decrease of the field strength with distance. The real part of  $\zeta_m$  is the *attenuation factor* of the  $m$ th mode expressed in nepers per unit distance. The height-gain functions  $U_m$  are found to increase with height above the ground. The increase is first slow but eventually becomes exponential and remains that way for large heights.

The real part of  $\zeta_m$ , the attenuation factor, increases with increasing mode number; hence, if the receiver is far enough from the transmitter, all modes except the first one become very small and the sum in equation (27) reduces to its first term which can be computed without much difficulty. This applies when the heights  $h_1$  and  $h_2$  are fairly small. The height-gain functions increase with height the more rapidly the higher their order, and as one approaches the line of sight the number of modes that contribute to the field strength becomes large. It is true that the series (27) converges everywhere,

but above the line of sight the number of terms required for a good approximation is so large that the expression is useless for numerical work. Here the methods of ray optics become applicable. It is usually found that, at a given distance  $d$ , the field in the lower part of the diffraction zone can be computed by using one or a few terms of the series (27). At large heights above the line of sight the field is determined by the methods of ray optics, and the two curves can be joined with a good degree of accuracy by graphical means on a decibel diagram. This has been done in Figures 12 and 13.

The series (27), though simple in external appearance, still proves extremely difficult to evaluate. Burrows and Gray,<sup>23</sup> however, have simplified the mechanics of evaluation to such a degree that numerical data can be obtained by means of a small number of graphs. The detailed procedures employed in computing field strength and contour diagrams by the method of modes are summarized and collected in Volume 3.



## ELEMENTARY THEORY OF NONSTANDARD PROPAGATION

6.1

## HISTORICAL

DURING 1941 AND 1942, short and microwave radar sets became available in England and were installed along the Channel and North Sea coast. Very soon it was found that at certain times these sets were able to pick up targets such as ships and fixed echoes from the French coast which were well below the line of sight and which under the conditions of standard propagation would have given entirely negligible responses. A relationship with the weather soon became apparent. In 1942, enough had become known to establish most of the correlations between excessive ranges and meteorological conditions which have remained fundamental and which are based on the picture of refraction in the lower atmosphere that is now generally accepted.

Later on similar effects with radar sets were discovered all over the world. An example in point is in the Mediterranean where nonstandard propagation, during certain seasons, is the rule rather than the exception. These conditions will be discussed in more detail in the chapter on radiometeorology. The most extraordinary ranges, perhaps, were found in the Indian Ocean where radar sets operating at frequencies of 200 mc were found on occasion to record fixed echoes from as far away as 1,500 miles. The mechanism of this phenomenon is not yet fully understood.

In the Pacific theater extended ranges have also been observed; but, on account of the vast territory covered, the technical difficulty of all operations, and the inadequacy of meteorological coverage, it is difficult to evaluate the results systematically. Up to the present, reports on the conditions responsible for nonstandard propagation have been received from many parts of the world which vary widely in their characteristic features and dependence upon season, weather, time of day, properties of the ground, etc. It is possible to lay down certain general rules, but on the whole the phenomena are exceedingly complex.

During 1943 and 1944, a number of systematic experiments on nonstandard propagation were carried out by the British and American Services and affiliated organizations. Most of these were one-way

transmission experiments that have a number of advantages over radar experiments, but some of the latter also were undertaken. Extensive transmission experiments were conducted by the British in the Irish Sea and the Americans in Massachusetts Bay, the state of Washington, southern California, and Arizona, and in the West Indian Ocean.

These experiments will be described in the next chapter. Because of the nature of the subject, it will be profitable to discuss the theory before the experiments and to give, in this chapter, an outline of our present conceptions of the theory of nonstandard propagation.

6.2

## REFRACTIVE INDEX

Nonstandard propagation takes place whenever the rate of variation of the refractive index in the lower atmosphere deviates considerably from the "standard" linear slope defined by equation (11), Chapter 5. The variation might consist either in a deviation from linearity, which is the most common case, or in a linear slope in the lowest layers that is widely different from the value assumed for the standard. The refractive index is a function of temperature, pressure, and the partial pressure of water vapor, given by equation (9), Chapter 5. The dependence of the refractive index on pressure leads to a regular decrease with height, but the change of barometric pressure with the weather produces only an insignificant effect on the gradient. The variations of refractive index in the lower atmosphere owe their existence to stratifications in which the temperature and moisture changes rapidly with height.

In order to express refraction in quantitative terms Snell's law for a curved earth is used as given by equation (14), Chapter 5:

$$nr \cos \alpha = n_0 r_0 \cos \alpha_0. \quad (1)$$

Now let

$$\begin{aligned} n &= 1 + (n - 1) \text{ with } n - 1 \ll 1 \\ r &= a \left( 1 + \frac{h}{a} \right) \text{ with } \frac{h}{a} \ll 1 \end{aligned} \quad (2)$$

$$\cos \alpha = \left( 1 - \frac{1}{2} \alpha^2 \right) \text{ with } \alpha \ll 1$$



where  $a$  is the earth's radius. Similar expressions are valid for the quantities having the subscript 0. Multiplying out and neglecting quantities that are small of the second order, one obtains

$$n - n_0 + \frac{1}{a} (h - h_0) = \frac{1}{2} (\alpha^2 - \alpha_0^2). \quad (3)$$

It has become customary to introduce the modified refractive index  $M$  by

$$n + \frac{h}{a} = 1 + M \cdot 10^{-6}, \quad (4)$$

whereupon Snell's law assumes the form

$$(M - M_0) \cdot 10^{-6} = \frac{1}{2} (\alpha^2 - \alpha_0^2). \quad (5)$$

This equation indicates how the angle  $\alpha$  between a ray and the horizontal changes as a function of  $M$  which, in turn, is a function of the height, both explicitly by equation (4) and implicitly because  $n$  is a function of the height in a stratified atmosphere.

6.3

### TYPES OF $M$ CURVES

An  $M$  curve is a diagram in which  $M$  as abscissa is plotted against the height  $h$  as ordinate. Extensive experience has led to a classification of  $M$  curves which is shown in Figure 1. The six types exhibited

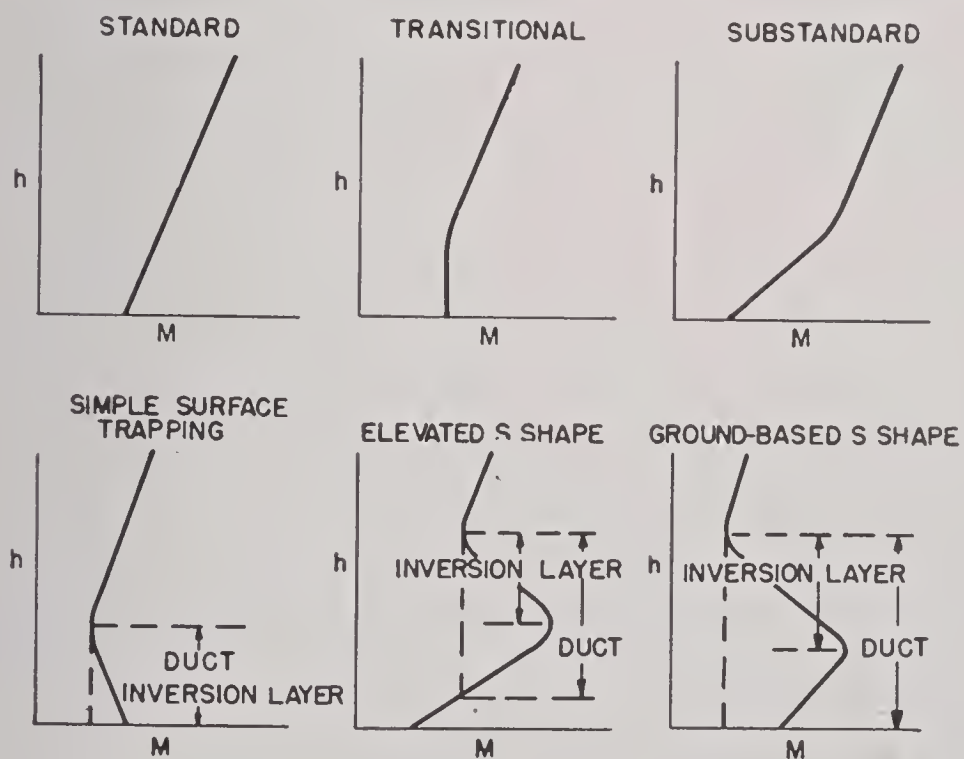


FIGURE 1. Types of  $M$  curves.

comprise all cases that are of practical interest.  $M$  curves of a more involved structure are rare. In all cases it is assumed in accord with experience that at sufficiently high elevations the  $M$  curves become linear and have, or nearly have, the standard slope.

The height at which these variations in refractive index occur may vary from a few feet to several hundred or even a few thousand feet though they are likely to be found at very low elevations in cold climates and at higher elevations in warm climates. The meteorological conditions which yield these curves will be dealt with extensively in Chapter 9, and few indications may suffice here. Ordinarily, on going aloft the temperature decreases at a slow and fairly steady rate. When, instead, the temperature *increases* with increasing height, a phenomenon known to meteorologists as a temperature inversion, equation (9), Chapter 5, shows that  $n$  decreases with increasing height. This does not necessarily imply that  $M$  decreases with height since, by equation (4),  $M$  contains the term  $h/a$ , which increases with height. If, however, the variation of temperature is sufficiently great, a decrease or inversion of  $M$  results. Such an inversion produces a *duct*, a term which refers essentially to certain meteorological phenomena and whose exact significance is explained below. A variation of humidity over the layer has an effect essentially analogous to, but distinctly more pronounced than, the effect of temperature. In this case  $M$  increases with height with a decreasing moisture content and vice versa. Variations of humidity are common in the lower atmosphere, and they constitute the main cause of refractive index variations, with temperature variations frequently a contributing factor.

The six cases shown in Figure 1 are as follows: the standard case which needs no further comment; the transitional case where the moisture or temperature variation is not great enough to produce a true inversion of the  $M$  curve but merely results in a nearly constant value of  $M$  in the lowest strata; the substandard case in which  $M$  increases more rapidly with height than in the standard case; and three cases of ducts. The simple ground-based duct or surface trapping, consists in an  $M$  inversion immediately adjacent to the ground or sea. There are two types of elevated  $M$  inversions distinguished by the position of the *minimum* value of  $M$  aloft. If this minimum is larger than the value of  $M$  at the ground so that the vertical projection from the minimum intersects the  $M$  curve, it is considered a true elevated, S-shaped duct. If this minimum is less than the value of  $M$  at the ground it is an elevated  $M$  inversion but a ground-based duct.

In dealing with these  $M$  curves it is universally assumed that the stratification is the same over the







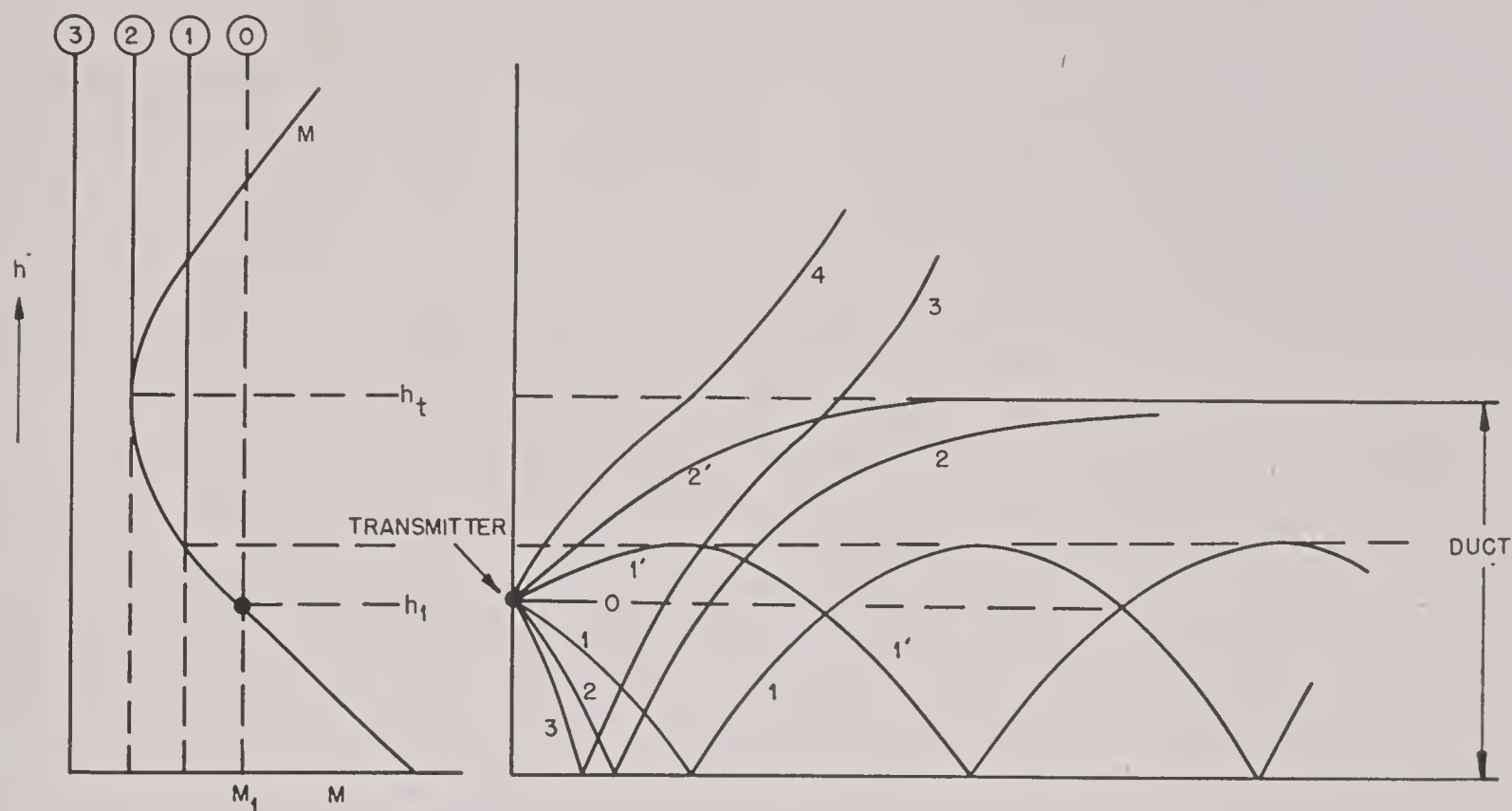


FIGURE 3. Rays with a ground-based duct.

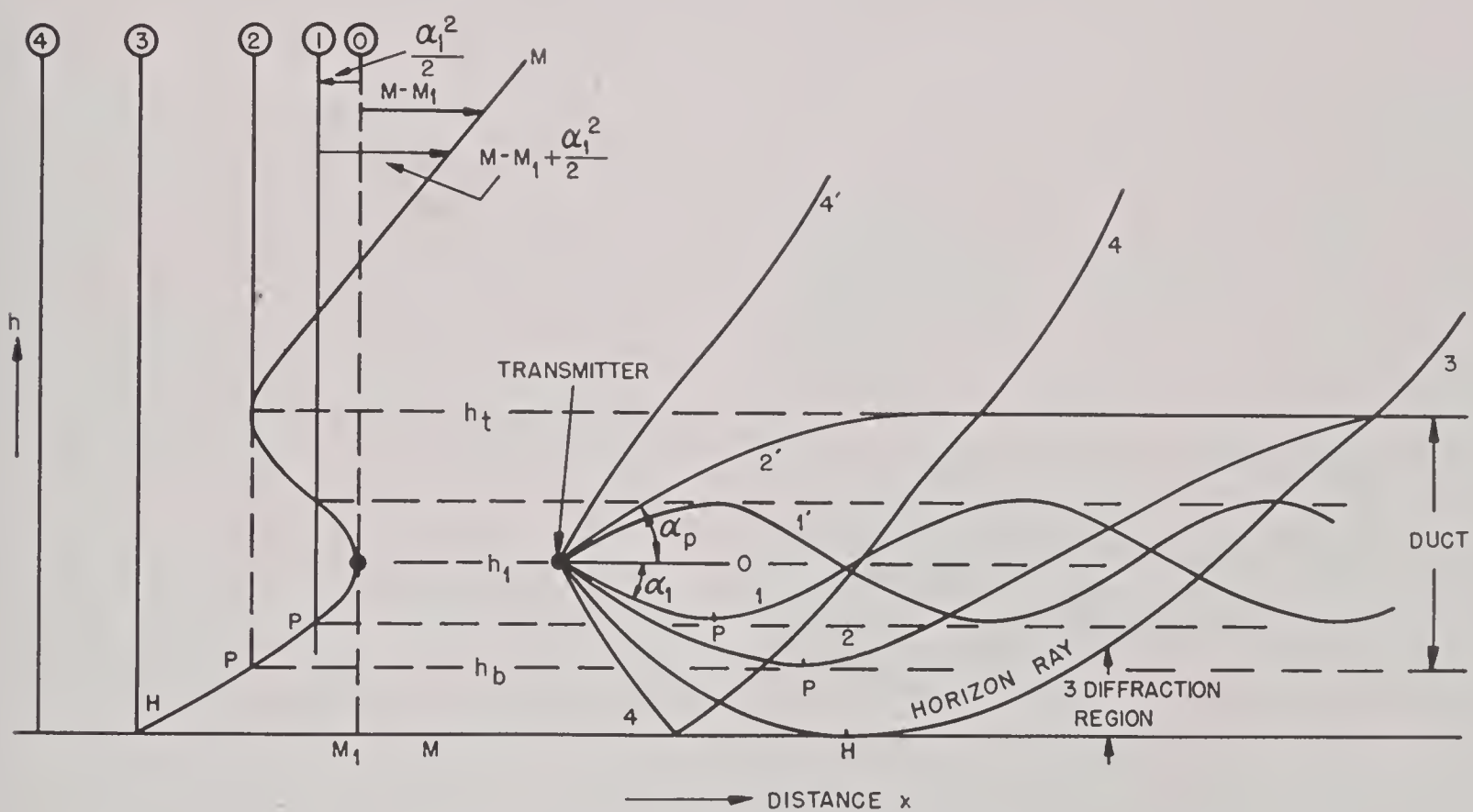


FIGURE 4. Rays with an elevated duct.

basis it is necessary to know the phases associated with the rays so as to determine their mutual interference. If this is done by an appropriate graphical or numerical method, contours of *constant field strength* can be drawn. Figure 5 shows, typical coverage diagrams computed in this way,<sup>146</sup> corresponding to a value of  $h_1/\lambda = 20$ . The lines separating the "detection zones" from the "blind zones" indicate ranges at which a medium bomber would just become visible to the particular radar to which these diagrams apply. Diagram 1 shows the undistorted lobe diagram for standard refraction while diagrams 2, 3, 4, 5 show the coverage diagram for

various types of ground-based and elevated ducts.

In Figure 6 is shown the variation of field strength with height for various distances for the *M* curve shown on the left-hand side of the figure.<sup>73</sup> The transmitter is at a height of 60 m.

In all diagrams shown in this section the vertical scale is vastly exaggerated as compared to the horizontal scale. It may readily be shown that when the representation is such that the earth is curved, the contours of constant height can be represented by parabolas in the approximation where the true vertical elevations are small compared to the horizontal distances involved.



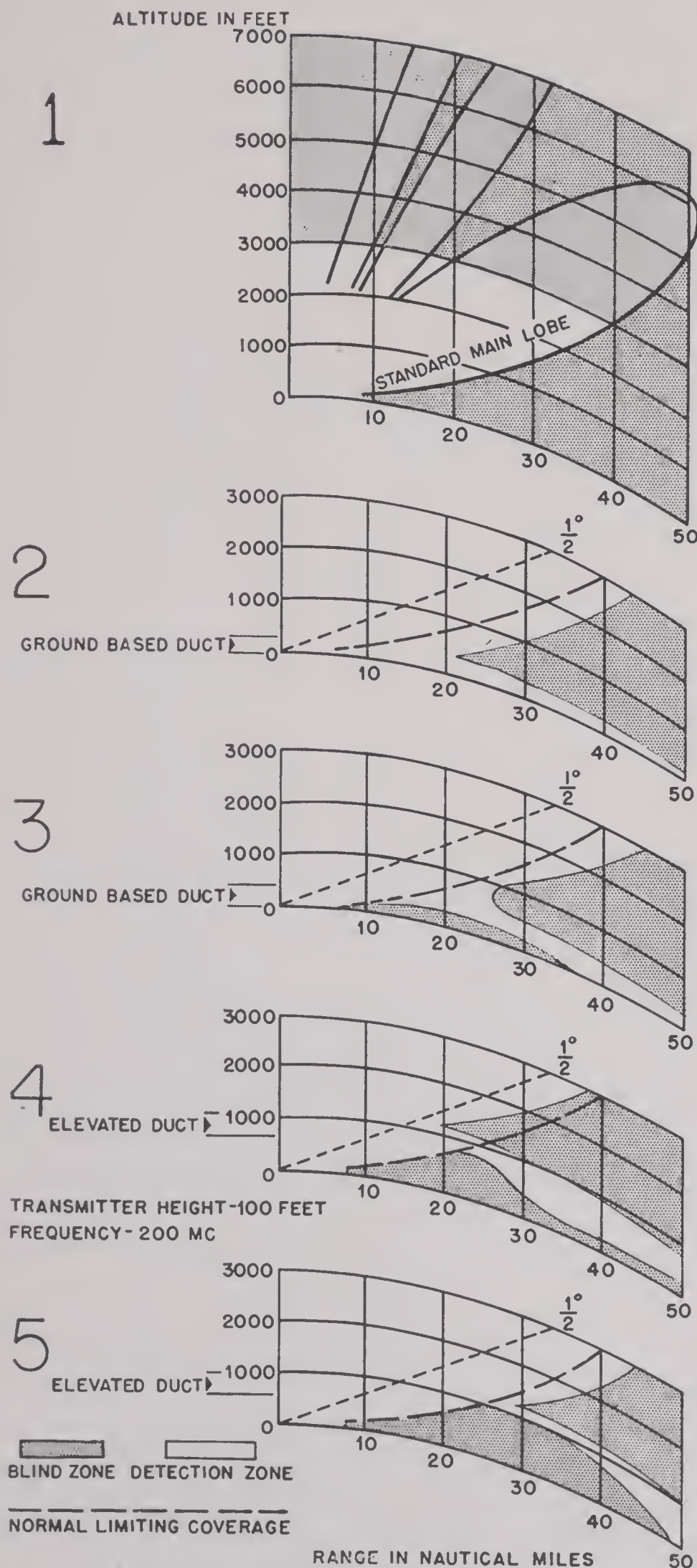


FIGURE 5. Calculated coverage diagram.

6.5

### GENERAL CHARACTERISTICS OF DUCTS

It is evident that the number of types of  $M$  curves that one can construct a priori is almost unlimited. In practice both the types actually occurring and their variability within each type of classification

are severely limited by meteorological conditions.

$M$ , as defined by equation (4), is the sum of two parts, the true refractive part ( $n - 1$ ) and the earth curvature part  $h/a$ . At higher elevations the absolute moisture in the atmosphere decreases, and irregular variations of temperature become more and more exceptional so that eventually, at a relatively great height, any  $M$  curve approaches the standard curve. An additional limitation comes from the fact that both the temperature and moisture variations in any one climate are subject to definite limitations. An extreme moisture change occurs when there is a boundary separating a nearly or fully saturated warm air mass from a very dry cool air mass. Temperature inversions involving differences of more than 10 to 15° C are quite exceptional. As a consequence of this both the actual height of the  $M$  inversion as well as the difference  $\Delta M$  between the maximum of  $M$  at the bottom and the minimum at the top of the  $M$  inversion are limited. The height of the  $M$  inversion layer may be only a few feet if it is close to the ground or sea surface. It frequently is of the order of 50 to 100 ft or even larger. Under particularly favorable conditions in warm climates, elevated  $M$  inversions may have heights of several thousand feet. The duct itself can be appreciably thicker than the  $M$  inversion layer, as may be seen from the structure of the last two  $M$  curves in Figure 1.

Again, the decrease  $\Delta M$  over the height of the inversion is limited for the same reasons. For low ducts values of the order of  $\Delta M = 5$  to 10 are common. Somewhat larger values will sometimes occur. The maximum value observed is about  $\Delta M = 40$  in high-level inversions at San Diego which originate in the singular climatic conditions found there.

An important consideration for the detailed mathematical treatment of duct propagation is the shape of the knees of the  $M$  curve. This, again, depends on the physical nature of the atmospheric stratification. Very often the inflections are so sharp that a succession of two or three straight lines furnishes an excellent approximation. These are known as bilinear and trilinear ducts and are of very common occurrence, especially with elevated ducts and a large class of ground-based ducts. On the other hand, there are also ground-based ducts in which the corners are extremely well rounded.

It follows from the restrictions on the numerical values of  $M$  that there are severe limitations on the angle  $\alpha$  for which duct effects can occur. Thus  $\Delta M =$



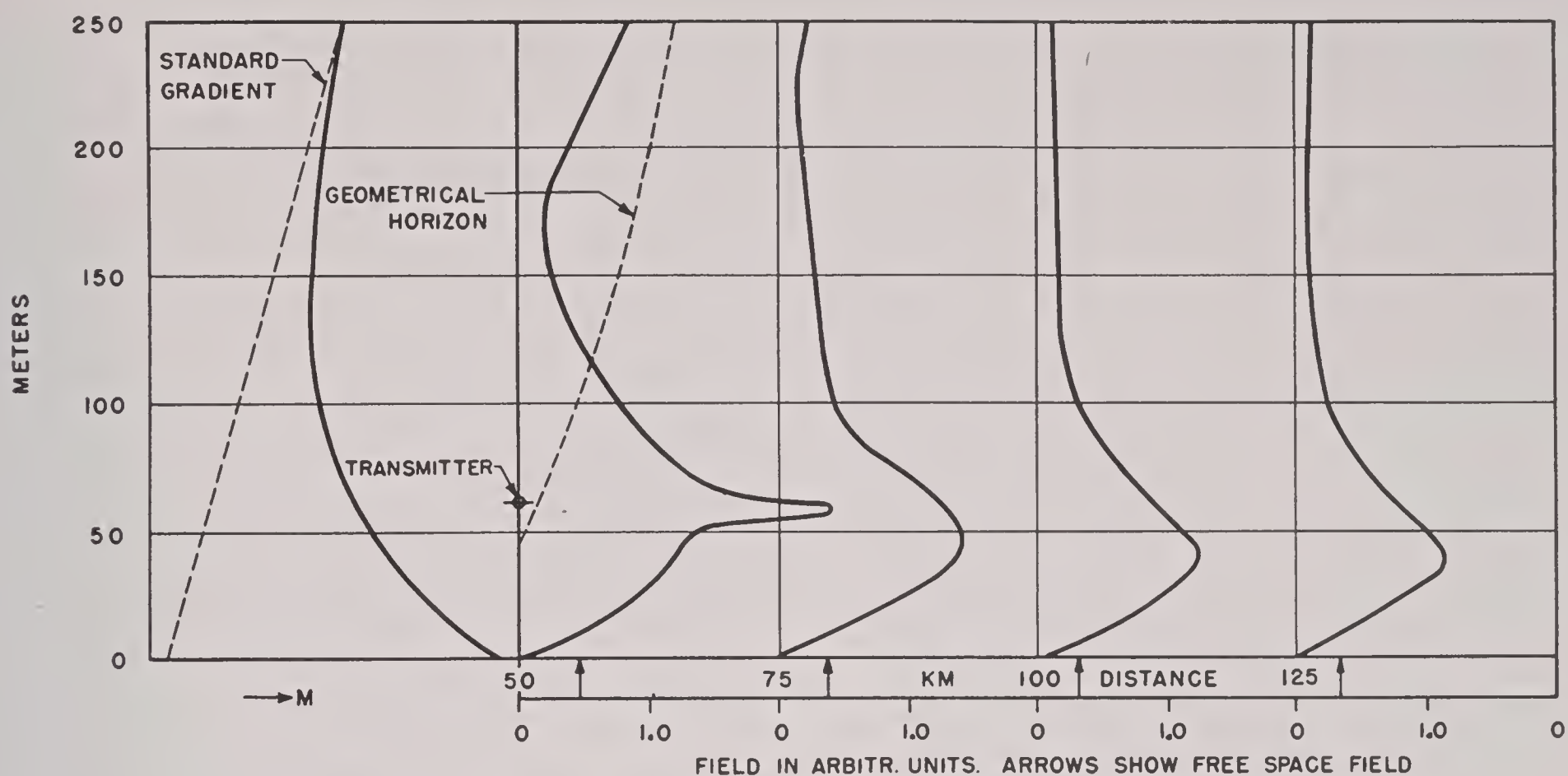


FIGURE 6. Variation of field strength with height for various distances.

10 represents a change of one part in  $10^5$  in the refractive index. Now from equation (5), we have by differentiation

$$\Delta M \cdot 10^6 = \alpha \Delta \alpha. \quad (9)$$

For a complete reversal of a ray we must have  $\Delta \alpha \sim \alpha$ , and then  $\alpha$  is proportional to the square root of  $\Delta M$ . In the above case, where  $\Delta M = 10$ , we find that  $\alpha$  is of the order of  $3 \cdot 10^{-3}$ , or about 10 minutes of arc.

Carrying considerations of this type into a little more detail it is found that the major effects of nonstandard refraction occur only for rays which emerge from the transmitter at an angle of less than  $\frac{1}{2}$  degree. For angles between  $\frac{1}{2}$  and  $1\frac{1}{2}$  degrees the refractive effects produced by the typical nonstandard  $M$  curves consist merely in minor modifications of the standard coverage pattern, while for angles above  $1\frac{1}{2}$  degrees the refractive effects are negligible.

## 6.6 SURVEY OF WAVEGUIDE THEORY

The ray tracing method presented in Section 6.4 is only a rather rough approximation to the true solution of the wave equation. It neglects diffraction, which on closer investigation is found to be very important. In order to visualize this, the waveguide analogue was introduced at an early stage of the development. Consider a two-dimensional wave-

guide consisting, for instance, of two parallel plane sheets of copper of infinite extent. The propagation of an electromagnetic wave in such a guide is somewhat analogous to that in a duct. The reversal of the vertical component of the rays by refraction in the duct corresponds to the reflection by the walls in the case of a metallic waveguide. It is well known that wave propagation under these conditions can be described by the methods of geometrical optics only to a very rough approximation. Soon after the discovery of ducts the accurate theoretical treatment of duct propagation was initiated in England.<sup>67,70,71,73,88,94</sup> The general result of these investigations may be summarized as follows. For an atmosphere of arbitrary stratification the field can be formally expressed by the series development, equation (27) of Chapter 5. The constants appearing therein and the height-gain functions involved are, however, different from the standard case and depend on the particular  $M$  curve involved. The solution, therefore, consists again of a superposition of "modes" which decay exponentially with distance from the transmitter. The height-gain functions do not, in general, increase with altitude all the way up from the ground. In the case of a duct the height-gain functions of the lowest modes have a pronounced maximum in the duct, similar to the curves for the overall field strength shown in Figure 6. This maximum becomes flatter and eventually disappears entirely for the height-gain functions of the higher modes.

It is useful to supplement the rather complex



mathematical development into modes, represented by equation (27) of Chapter 5, by a simpler type of analysis which connects it with the ray picture. For the sake of simplicity let the phenomena be two-dimensional, confined to the horizontal  $x$  direction and the vertical  $z$  direction. If the wavelength is small enough compared to the dimensions of the duct, the electromagnetic field at some distance from the transmitter may, in any sufficiently small volume element, be represented by a plane wave whose wave front is perpendicular to the direction of the rays. Such a plane wave may be written as

$$E = E_0 e^{j\omega t} e^{-j(kx+lz)}. \quad (10)$$

Confining ourselves for the moment to the case of the plane earth, it is found from electromagnetic theory that

$$k^2 + l^2 = \left(\frac{2\pi n}{\lambda}\right)^2, \quad (11)$$

where  $n$  is the refractive index in the volume element considered, and  $\lambda$  is the free space wavelength. Since  $k$  and  $l$  are proportional to the directional cosines between the direction of the ray and the  $x$  and  $z$  axes, we may put

$$k = \frac{2\pi n}{\lambda} \cos \alpha, \quad l = \frac{2\pi n}{\lambda} \sin \alpha \quad (12)$$

where  $\alpha$  is the angle between the ray, or the normal to the wave, and the horizontal.

The further mathematical analysis shows that, for a horizontally stratified medium where  $n$  is a function of  $z$  only, we have  $k = \text{constant}$ . In view of equation (12) this gives us  $n \cos \alpha = \text{constant}$ , which is just Snell's law for a plane earth, as enunciated before.

The ray picture, being a rough approximation, gives an electromagnetic field in some regions and none in others. In the rigorous solution of the wave equation there is some electromagnetic field strength everywhere. Consider in particular the region just above a duct. There are regions of "shadow" above the duct caused by the fact that some of the rays are bent downward in the duct. Clearly, at the point of reversal of a ray,  $\alpha = 0$  and hence  $l = 0$ . If we proceed farther upward in a duct  $n$  decreases, and it follows from equation (11) that if  $n$  decreases sufficiently  $l$  must eventually become imaginary. Instead of a wave component in the  $z$  direction we then have an electromagnetic field which decreases

exponentially as we go upwards. In the top layer of a duct, the decay takes place very gradually because the change in refractive index is extremely slow. Eventually, however,  $n$  must begin to increase again as we go still farther upwards from the duct and there comes a height where  $l$  is again real and an ordinary wave is again possible. This behavior might be likened to that of a metal foil so thin as to be partly transparent for the waves considered. The duct thus may be likened to a waveguide bounded on one side by a solid reflector, the ground, and on the other by a semi-transparent reflector. The mathematical theory of ducts has therefore often been designated as *leaky waveguide* theory.

A closer study of the height-gain functions which appear in the mode formula, equation (27) of Chapter 5, shows that in the presence of a duct the leakage across the upper boundary of the latter is the more pronounced the higher the order of the mode, and that for sufficiently high modes there is almost no confinement of the electromagnetic field within the region of the duct. In consequence of this fact the exponential damping with *horizontal* distance, which is characteristic of each mode, is more pronounced for the higher modes, because for these modes the electromagnetic energy rapidly "leaks away" from the duct. At large distances from the transmitter the field in and near the duct is therefore described by the lowest mode alone. This depends, of course, partially on the relative strength of excitation as well as on the attenuation of the various modes.

Another aspect of the wave theory of ducts which is of great practical importance is the cutoff effect. It is well known that any ordinary metallic waveguide has a cutoff frequency below which the guide cannot transmit an electromagnetic wave. The mathematical treatment of the duct shows that there is a similar lower limit of frequency for transmission through a duct, but, because of the "leakage" phenomenon, it is found that there is no sharply defined cutoff frequency but a gradual decrease of the duct's ability to confine radiation within itself with decreasing frequency. Figure 7 is a graph giving representative values for what may be taken as the cutoff frequency of a duct as a function of its height in feet and  $\Delta M$ , the decrease of  $M$  in the inversion layer. These values are the result of a somewhat crude approximation and should not be taken to indicate more than the order of magnitude of the frequency at which this effect occurs.



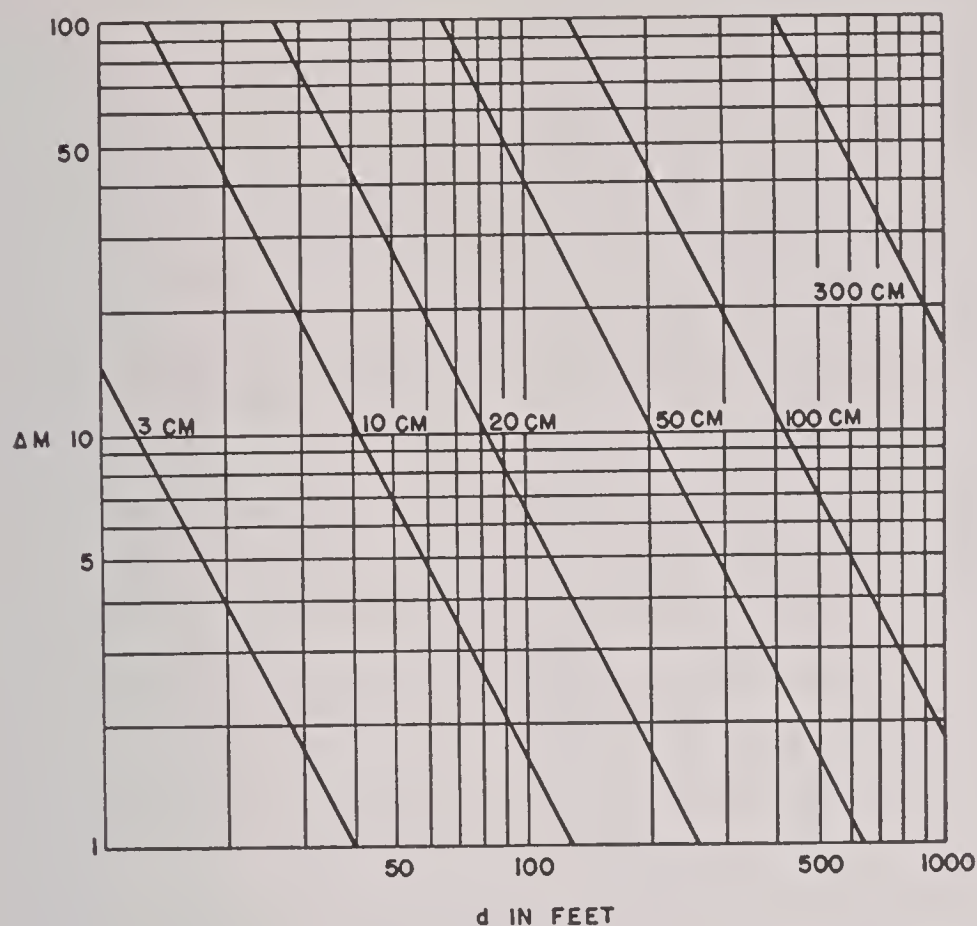


FIGURE 7. Maximum wavelength trapped in a simple surface duct. Duct width  $d$  in feet.  $\Delta M$  is total decrease of  $M$  in duct.  $\lambda_{\max} = 2.5 d \sqrt{\Delta M 10^{-6}}$ .

### 6.7 REFLECTION FROM ELEVATED LAYERS

Reflection from elevated layers has so far been observed systematically only under the rather special meteorological conditions at San Diego, but it probably occurs elsewhere, though with a lesser degree of regularity. It appears when there is a strong elevated  $M$  inversion. Such an  $M$  curve is very nearly equivalent to a true discontinuity of refractive index, and the effect on a wave traversing such a region is similar to that of a boundary between two media, the more nearly so, the larger the  $M$ -inversion gradient. If there is a true discontinuity, an incident wave is split up into a reflected and a transmitted wave. If the discontinuity is replaced by an  $M$  inversion layer, the reflected wave still persists but becomes weaker the less steep the inversion. The distinction between this phenomenon and the apparent reflection in the duct where the

rays become horizontal before turning downward is usually fairly clear-cut. The true reflection described here occurs primarily in waves which are so long as to be below the cutoff.

There exists a case of gradual transition between two media with different refractive indices for which the wave equation can be integrated.<sup>444, 445</sup>

This can be applied qualitatively to the case,<sup>77, 91</sup> in so far as earth's curvature can be neglected. Figure 8 shows the calculated ratio in decibels of

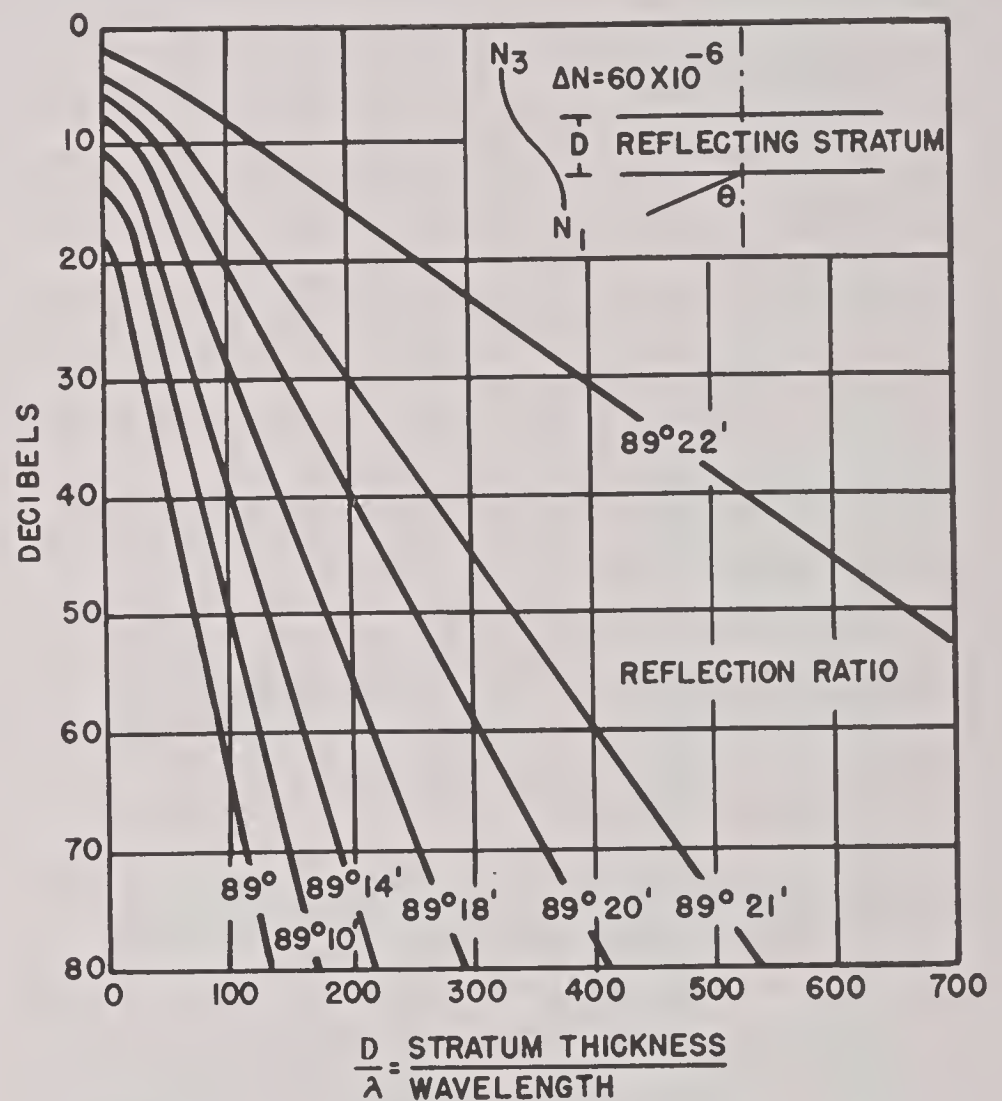


FIGURE 8. Calculated reflection ratio in decibels.

reflected to incident wave for various angles of incidence plotted against the ratio of thickness of the transition layer to wavelength as abscissa.

The verification of this theoretical concept in the San Diego experiments will be discussed in the next chapter.



## Chapter 7

# METEOROLOGICAL MEASUREMENTS

### 7.1 INTRODUCTION

THE DIRECT MEASUREMENT of the refractive index of air is carried out in the laboratory under closely controlled conditions. The variations of the refractive index in the atmosphere which are of paramount importance for propagation problems are determined indirectly by measurements of the temperature and humidity. From the values of these latter the refractive index is computed by equation (9) of Chapter 5. There has been no reason, so far, to doubt the reliability of this procedure, and speculative assumptions of the failure of this relation which have been brought forward at times during the war have not been accepted.

This chapter describes measuring equipment that was especially developed during 1943 to 1945 to study refractive index variations. Following this description is a collection of actual  $M$  curves which have been measured in different parts of the world

### 7.2 TEMPERATURE AND HUMIDITY ELEMENTS

The value of the refractive index  $n$ , or of  $M$  as defined by equation (4), Chapter 6, is sensitive to relatively small changes in temperature and especially in humidity. Both accuracy and speed in determination of  $M$  are required. Speed is especially necessary because a considerable number of points generally are needed to determine the shape of an  $M$  curve. Electrical methods have been used almost exclusively for these measurements, though an ordinary psychrometer will do in the absence of more specialized equipment.

There is no particular difficulty in measuring the temperature with suitable accuracy, such as  $\pm 0.2$  C. The electric resistance element used in the Bureau of Standards radiosonde is well suited to the purpose and is commercially available. More recently thermistors have been used. At stationary installations in England ordinary nickel or platinum resistance thermometers have been installed, primarily for recording purposes.

Humidity may be measured either directly, or indirectly by measuring the wet bulb temperature. Hair hygrometers are unsuitable because of their large time lag. For the direct measurement of humidity electrolytic resistance elements, such as are standard in the U. S. Weather Bureau radiosonde, are used. The active agent in this type of element is an aqueous solution of lithium chloride which is deposited as a film on a small cylinder. The resistance of the solution is highly sensitive to changes in relative humidity of the surrounding air. In England a variant of this principle has been employed where the lithium chloride solution is absorbed in a cotton cloth.

In the indirect method of measuring humidity a thermistor of cylindrical form is surrounded by a moist wick which, with proper aeration, indicates the wet bulb temperature. To insure insulation the element is covered with several coats of insulating lacquer before the wick is attached.

The main problem in all these devices is that of time lag. When mobile carriers such as captive balloons, kites, airplanes, or ships are employed, it is in general necessary to obtain an individual reading within less than a minute, and the response of the measuring elements to the temperature and humidity of the ambient medium must be reasonably close within the time available.

The time lag constant is the time required to attain the fraction  $1 - (1/e) = 0.63$  of the total change, if the temperature (or humidity) is changed suddenly. For the temperature elements the time lag constant is several seconds in an air stream with a velocity of 2 to 5 m per sec. The lag depends somewhat on the position of the element relative to the air stream and is a maximum when the element is perpendicular to the stream. The lag constant of the same element, used as wet bulb indicator with wick applied, is only slightly larger than that of the dry element. The lag constant of the Bureau of Standards humidity element has been measured in several laboratories, and there seems to be some controversy as to its exact value, the results varying from a few seconds to about 45 sec,<sup>228</sup> the latter in an air stream of 2 to 5 m per sec.<sup>238</sup>



## 7.3

In both captive balloon and kite equipment only the measuring elements are carried aloft with fine wires in the cable to connect with the rest of the circuit. The assembly that is carried aloft is therefore quite light, weighing only about a pound in the case of nonaerated instruments and 3 to 4 pounds for aerated ones.

Figure 2 shows a schematic wiring diagram for the dry and wet bulb resistance elements of the Radiation Laboratory instrument. The resistance of the thermal element  $X$  controls the bias of one triode of the double triode 6SN7 which acts as a vacuum tube

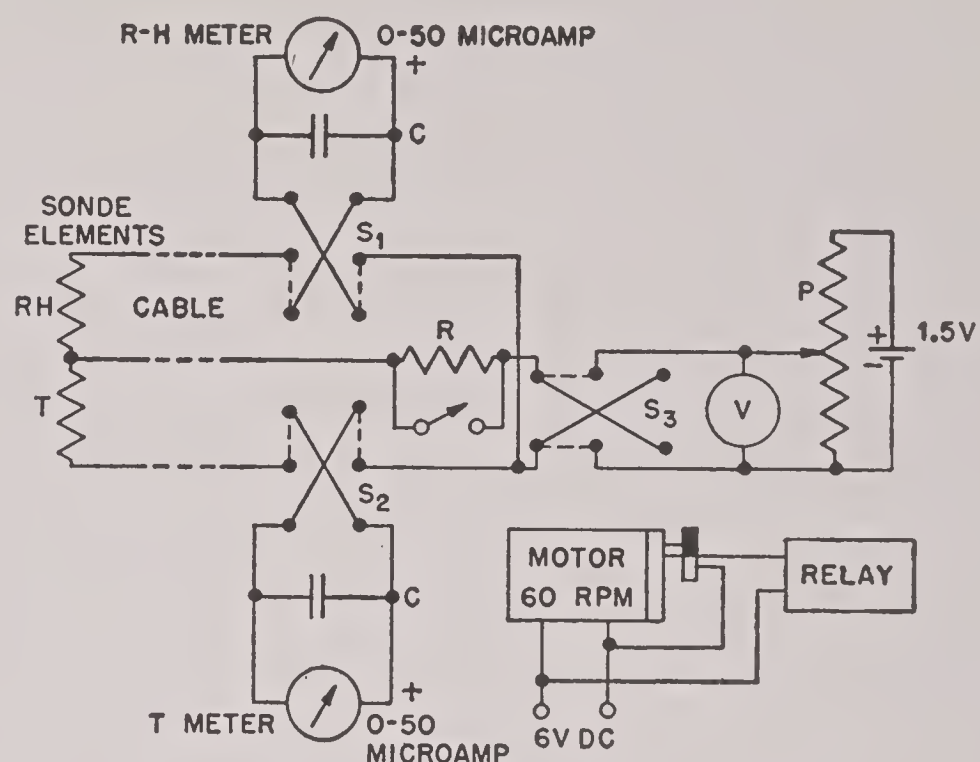


FIGURE 1. Circuit diagram for State College of Washington wired sonde.

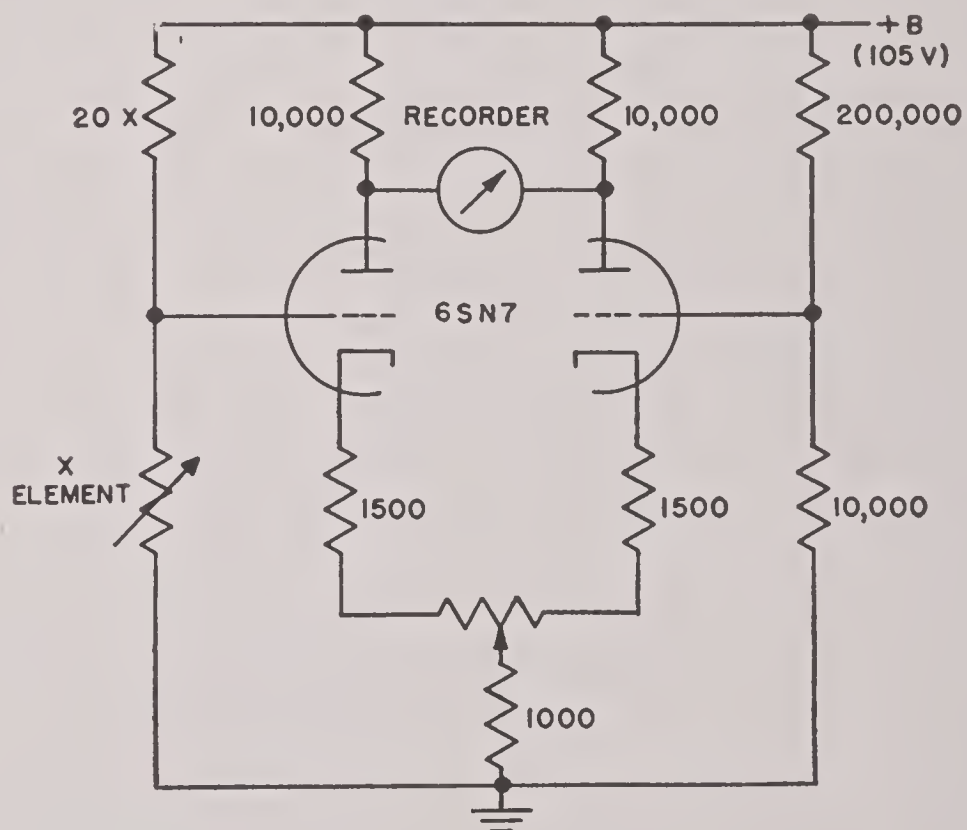


FIGURE 2. Circuit diagram for electronic amplifier for measuring temperature. (Radiation Laboratory, MIT.)

voltmeter to compare the resistance of the thermal element with a standard resistance. A 1-ma recording meter is placed between the two plates. In operation the dry and wet elements are switched into the circuit alternately. Calibration of the amplifier is obtained by switching a series of precision resistors in steps of 1,000 ohms into the circuit in place of the thermal element. The stability of this voltmeter is such that with a change in line voltage between 95 and 120 v there is no observable change of the meter at any given deflection.



#### 7.4 REFRACTIVE INDEX MEASUREMENTS

The methods which have been used to make refractive index measurements in the lower atmosphere are the following:

1. Stationary installations on towers, usually with automatic recording on the ground. Aerated wet and dry bulb instruments are installed at several heights giving a continuous survey of the  $M$  curve between the ground and the top of the tower.

2. Installations similar to (1), on shipboard, with the meters or recording equipment in the ship's cabin. In order to explore the humidity distribution in the lowest layers adjacent to the sea surface, the instruments have been mounted at the end of a beam that pivots about a horizontal axis fastened to the side of the ship. This device has been used extensively in the Irish Sea experiments. Artificial aeration of shipborne installations is not usually necessary because in calm weather the necessary velocity of the air is provided by the motion of the ship.

3. Airborne installations. The unit is mounted at a convenient place on the outside of the plane where it is not affected by motor exhaust or propeller slip stream, with the meters or recorders in the ship's cabin. Comparatively slow-flying planes have been used for such measurements, not only in order to minimize the dynamic temperature correction, but also because in a fast-flying plane too long a column of air will be sampled during the period of relaxation of the instrument. In airplane measurements it is necessary to keep track of the altitude of the plane by means of a carefully calibrated altimeter.

4. Captive balloons and kites. In these devices only the measuring unit is carried aloft, the indicating or recording meters remaining at the ground. Three wires are required when the instrument is nonaerated and two additional ones when an aeration motor is provided. The wires are of thin insulated copper, stranded together into a cable, although more recently aluminum wires have been tried because of their greater mechanical strength.<sup>233</sup> The fine wires of the cable are wound in a high-pitch spiral around a strength member consisting of fishline and then glued to the latter. Considerable effort has been spent on the development of these cables which constitute the most critical part of the balloon sonde equipment. For details the reader is referred to the reports listed under Meteorological Equipment in the Bibliography (Report WPG-14).

Captive balloons are used in calm weather and in

winds not exceeding about 4 m per sec. For higher wind velocities the balloons become difficult to manipulate, and a kite is then used to carry the measuring unit aloft from the ground or even from shipboard. Small barrage balloons have a greater lift than ordinary weather balloons and can be used in the same winds as kites because of their streamline shape. They are, however, less mobile and require more hydrogen than the smaller balloons.

The cable for the balloon or kite is wound on a drum, and connection with the stationary meters is made by means of slip rings. The height of the balloon or kite is determined by the length of cable paid out together with a rough measurement of the angle of the cable.

Captive balloons reach heights of several hundred feet without difficulty and even heights of 1,000 to 2,000 ft are not infrequent.

7.5

#### OTHER METEOROLOGICAL INSTRUMENTS

It is hardly necessary to say that measurements of atmospheric temperature and humidity are possible and have been made, with instruments of a more conventional type. In the early stages of our knowledge of nonstandard propagation, surveys were

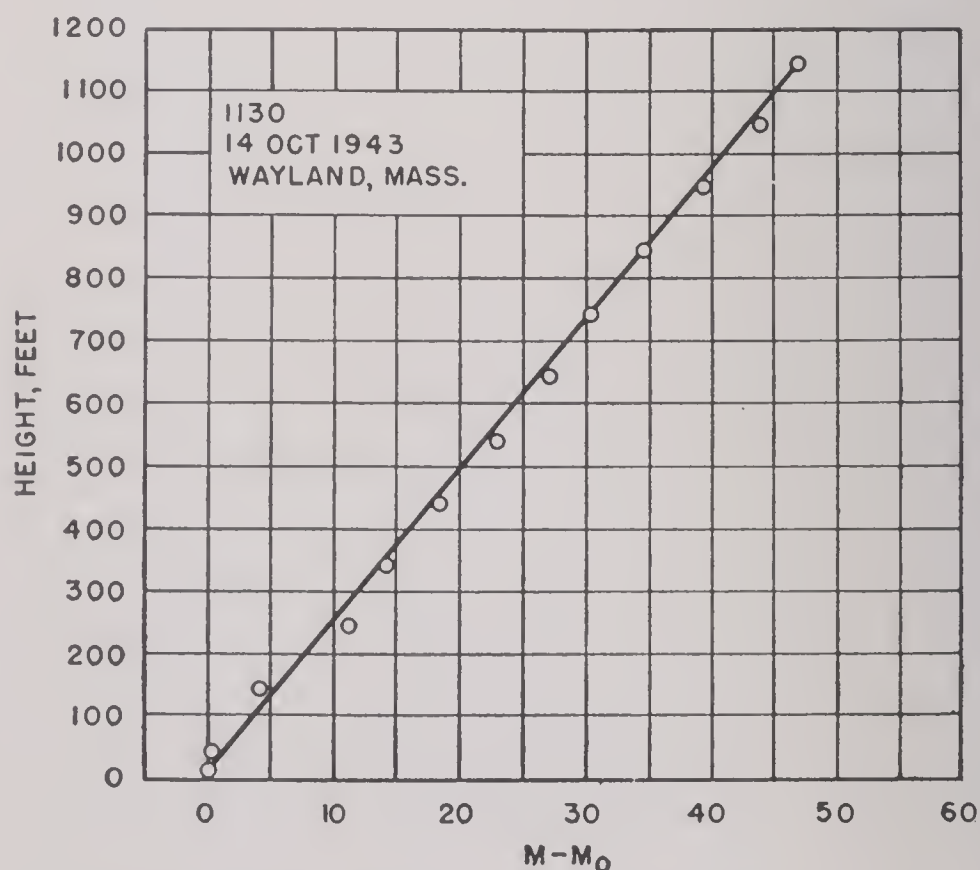
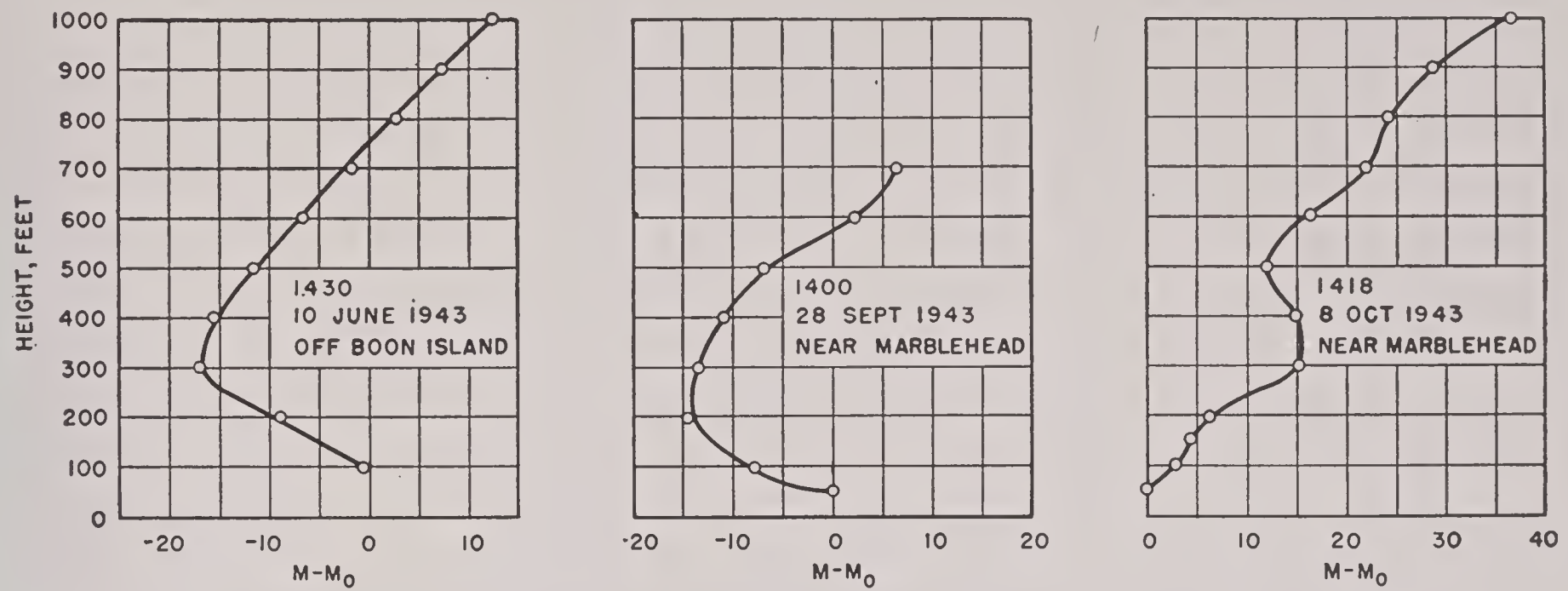
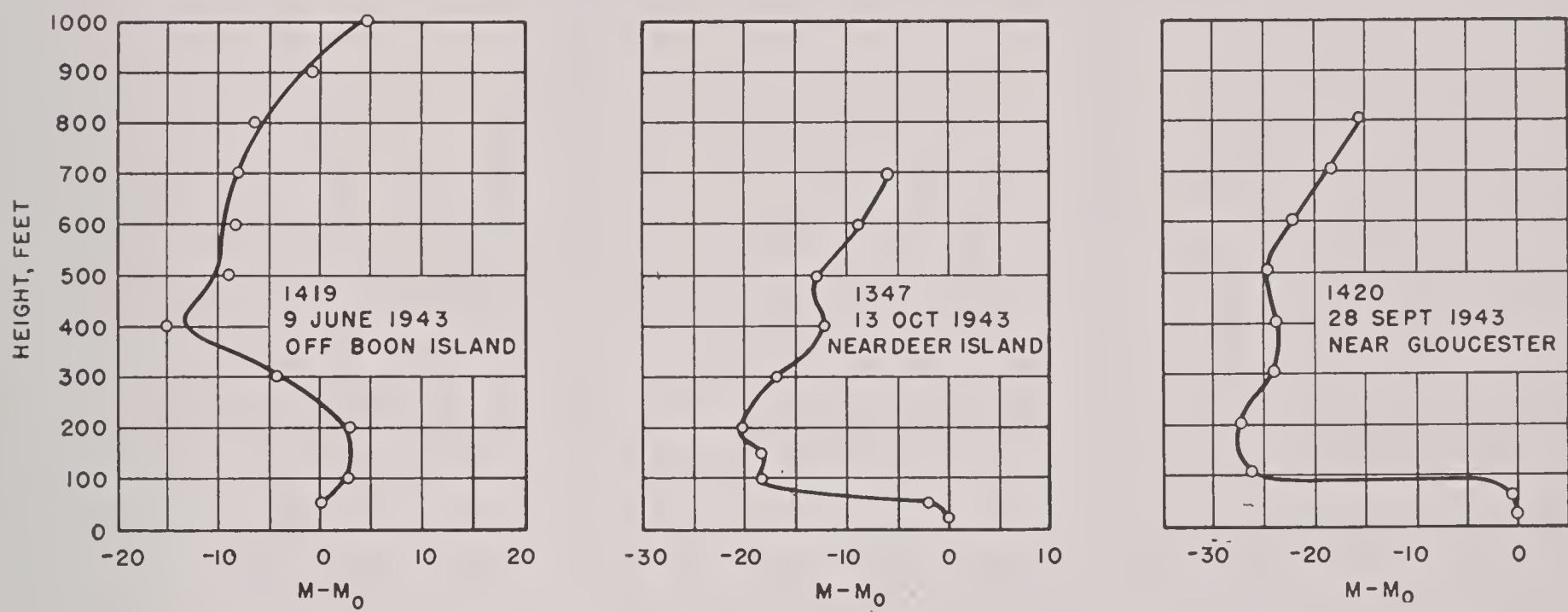
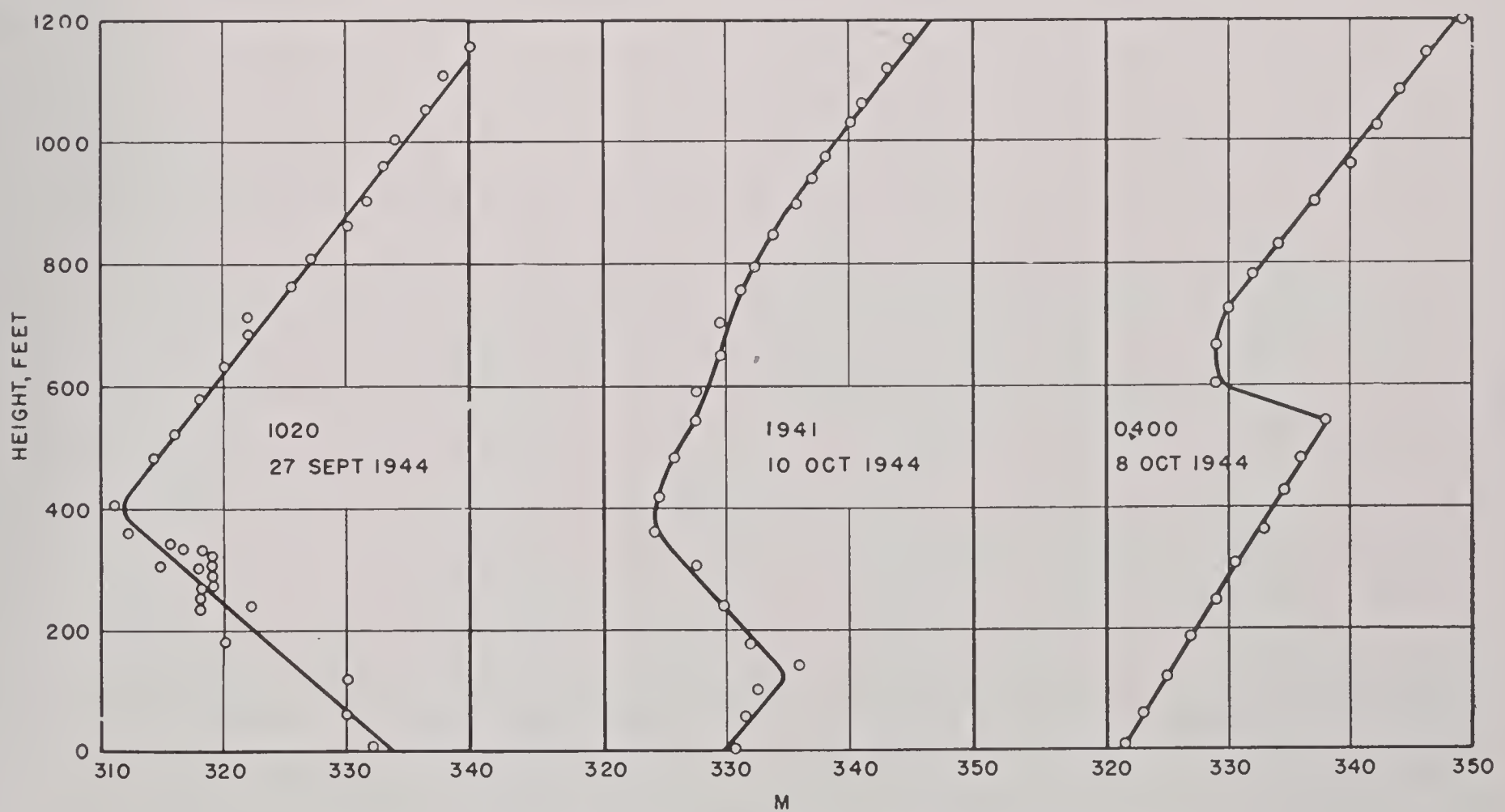


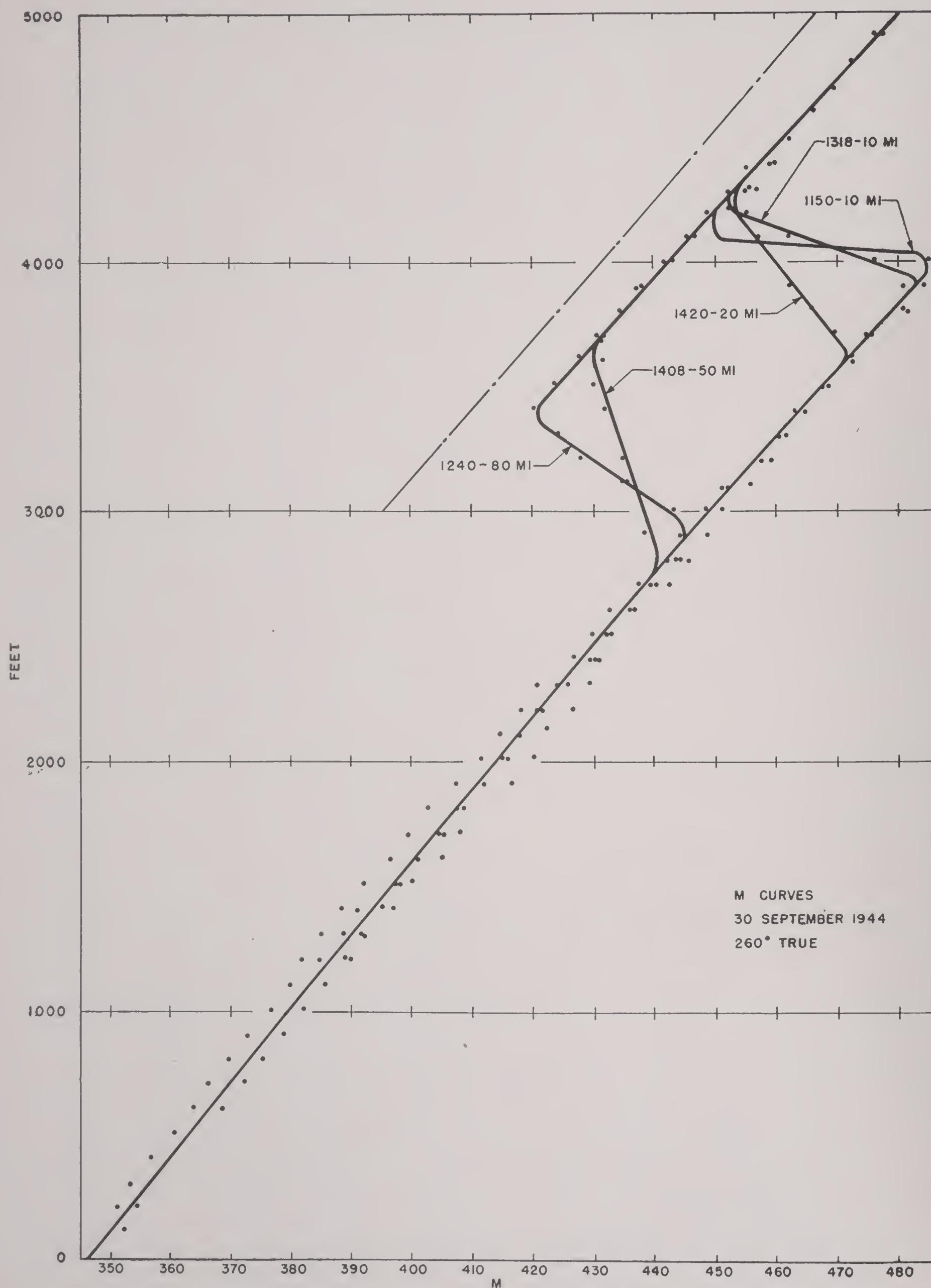
FIGURE 3. Representative standard  $M$  curve. (36  $M$  units per 1,000 ft.)

made by means of an ordinary psychrometer held out of the window of a slowly cruising plane and aerated by the slip stream. The British installations

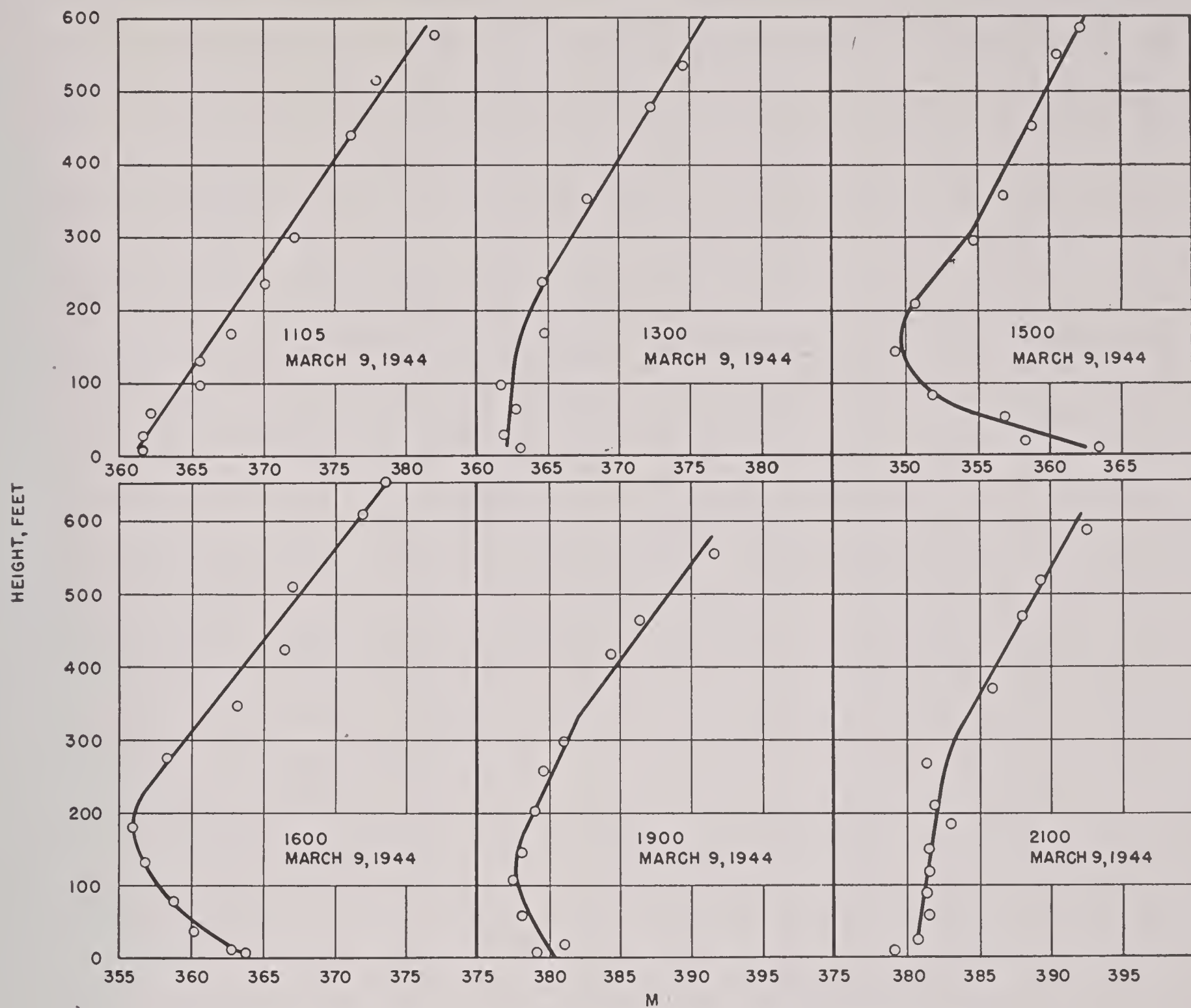


FIGURE 4. Representative nonstandard  $M$  curves from the Massachusetts coast.FIGURE 5.  $M$  curves from the Massachusetts coast showing strong ducts.FIGURE 6.  $M$  curves from New Zealand, east coast near Cook Strait.



FIGURE 7. *M* curves from a flight west of San Diego.




 FIGURE 8.  $M$  curves from Taboga Island near Balboa, Canal Zone.

commonly use multijunction dry and wet thermopiles which have the advantage of not requiring elaborate calibration. In connection with captive balloons this type of equipment is somewhat clumsy in that the cold junctions have to be carried aloft in a Dewar flask.

It should be noted here that the ordinary noncaptive radiosonde as used in the routine meteorological observations of the U. S. Weather Bureau and of the Armed Services is not suitable for radio-meteorological purposes. The reason is that these sondes are designed to give representative data only at definite and fairly large vertical intervals, 100 ft or more. These are too widely spaced to yield a representative  $M$  curve, as the characteristic features of the latter are usually concentrated in the lowest strata of the atmosphere.

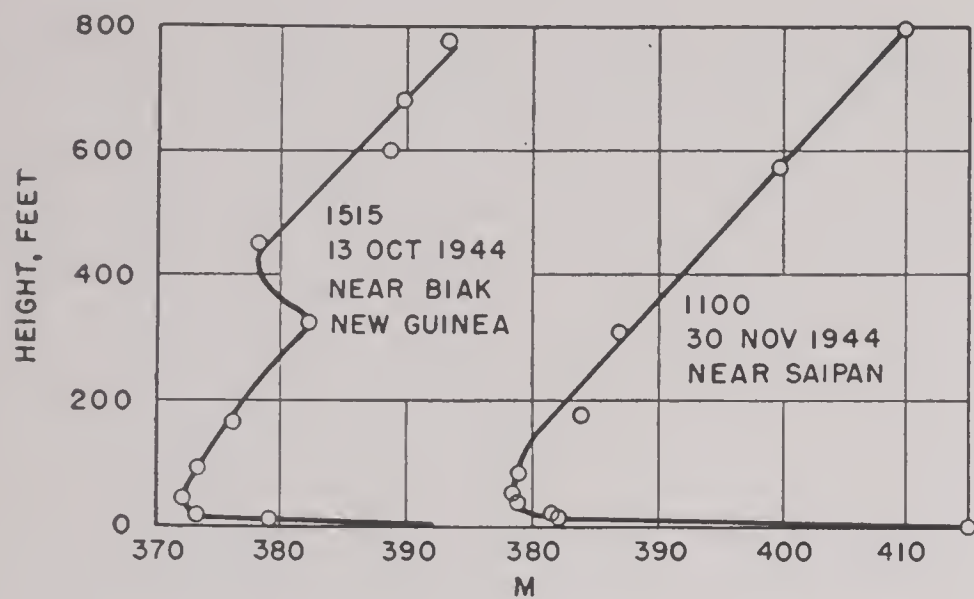
Wind measurements are of importance in connection with propagation problems, for reasons which will be given in detail in the chapter on weather

forecasting. They are particularly significant at coasts when off-shore winds or land and sea breezes are present. Sensitive and carefully calibrated anemometers with ordinary wind vanes prove adequate for measurements of this type. Special equipment such as supersensitive anemometers, developed for particular purposes such as chemical warfare problems, are not usually needed because the large area covered by radio transmission paths or radars renders too detailed measurements useless.

## 7.6 REPRESENTATIVE OBSERVED $M$ CURVES

A small catalogue of  $M$  curves that have been actually measured in various parts of the world by means of the equipment described previously concludes this chapter. Most of the curves presented were taken over the ocean merely because the



FIGURE 9.  $M$  curves from the New Guinea area.

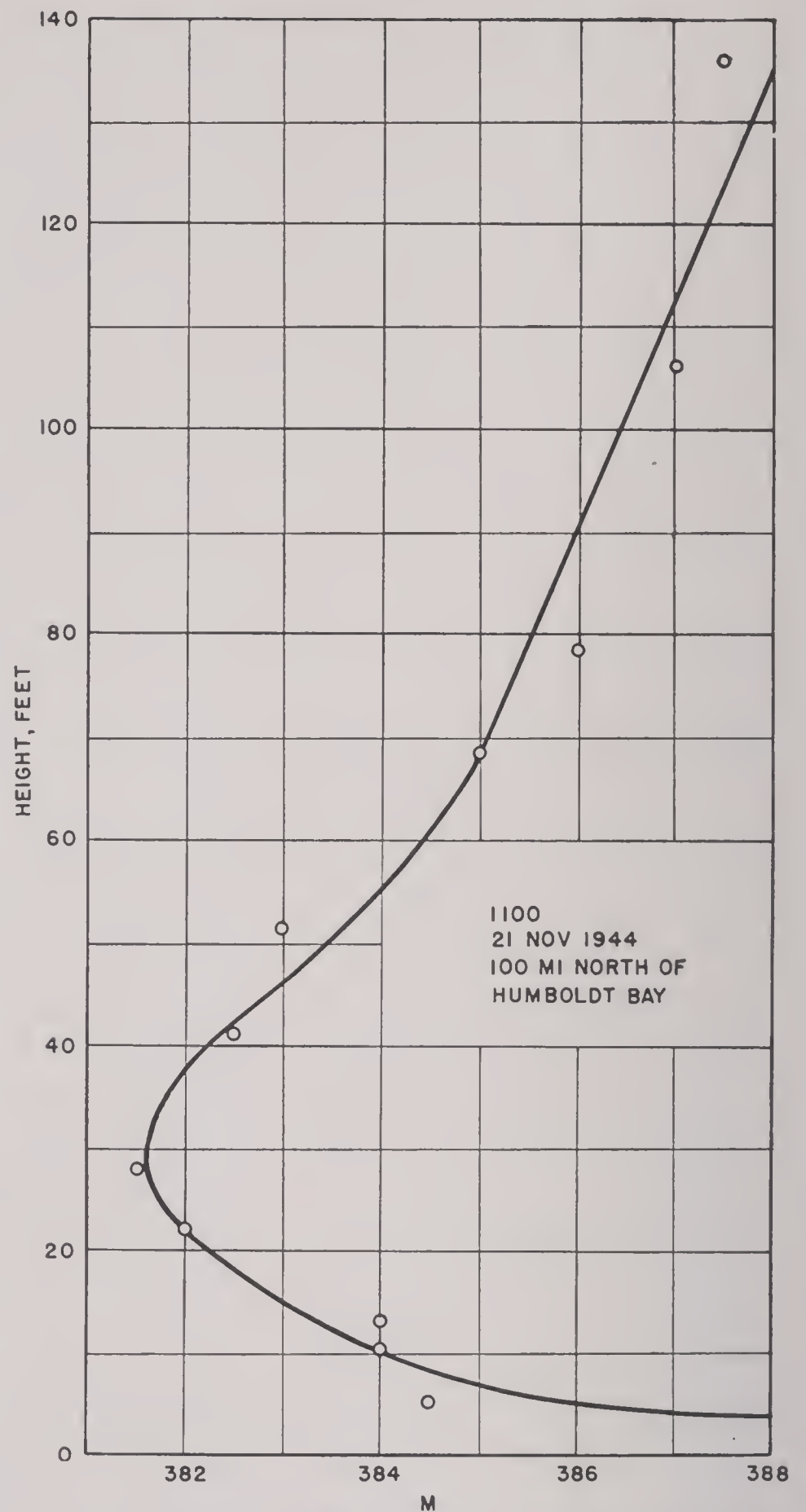
majority of experimental measurements have been made there. Experience indicates that there is not much difference in the types of  $M$  curves over land and over sea except that standard propagation conditions will in general be much more common over land for reasons that will appear in Chapter 9. In all these graphs the actually measured points are entered so that the reader may gain an idea of the degree of accuracy obtained with this equipment.

Figure 3 shows a standard curve as measured at the coast of Massachusetts. The linearity of the refractive index in this case is not an accident but is the result of the definite physical condition of thorough turbulent mixing in the lower atmosphere, as will be explained in more detail in Chapter 9. Since this is a fairly frequent condition, standard curves are actually quite common, and in them the measured points cluster well around a straight line as shown in Figure 3.

Figures 4 and 5 show a set of nonstandard curves selected from a large series of measurements taken on the Massachusetts coast in the summer and fall of 1943.<sup>210</sup> Here the  $M$  curves are quite irregular, perhaps more so than is common at other locations. These curves show various types of ducts, some of them rather weak, others with a decrease of  $M$  as much as 20 units or even more.

Figure 6 is a set of  $M$  curves that were measured on the east coast of New Zealand, at a point some 100 miles south of Cook Strait.<sup>223</sup> These curves provide good examples of the type of  $M$  curves that consist of several very nearly linear sections.

Figure 7 illustrates the typical elevated duct found in the San Diego region. Both below and above the inversion region the  $M$  curve is standard. The various curves shown were measured at several distances on a flight from San Diego outward.

FIGURE 10. Detailed  $M$  curve taken over the ocean near New Guinea.

The curves of Figure 8 were taken at Taboga Island, some 15 miles south of Balboa, at the eastern entrance to the Panama Canal. They show various familiar types of ducts; two of the curves represent transitional cases where the  $M$  curve is steeper than standard but does not bend backward.

Figure 9 shows two soundings from the tropical Western Pacific. The curve at the left was taken at Biak Island, New Guinea, and is remarkable for the presence of two ducts, a ground-based and an elevated one. The curve at the right was taken at Saipan.

Figure 10, taken near New Guinea, shows in more



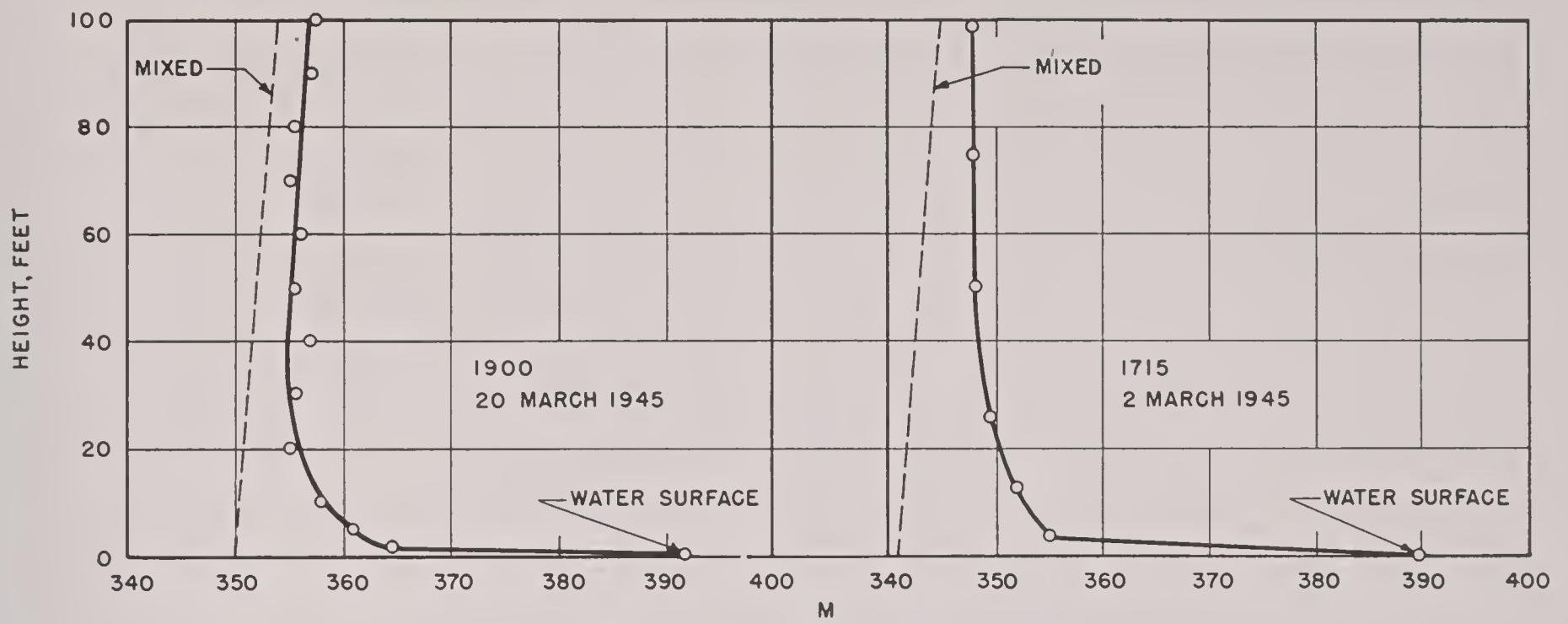


FIGURE 11.  $M$  curves over the ocean at Antigua, British West Indies.

detail the structure of the low maritime duct which in this case is only about 30 ft high.<sup>225</sup> This type of duct has been studied carefully in the transmission

experiments at Antigua in the West Indies which are reported in Chapter 8. Two typical soundings taken near Antigua are reproduced in Figure 11.<sup>194</sup>



## Chapter 8

# TRANSMISSION EXPERIMENTS

8.1

### BRITISH EXPERIMENTS

IN THE DEVELOPMENT of short and microwave communication and radar, the British were first to make systematic transmission experiments on a large scale. A number of such experiments were carried out at wavelengths below 50 cm, beginning about 1936 with some transmission paths over land, some over sea; and experiments in the 10-cm band were undertaken in the early years of the war. These experiments will not be reported individually because the earlier results are reproduced and verified in the later and more elaborate trials. Instead, attention will be confined to two major experiments, one over the sea and one over land.<sup>3,10</sup>

#### THE IRISH SEA EXPERIMENT

This transmission experiment represents a cooperative enterprise undertaken jointly by the Radio Division of the National Physical Laboratory, the Telecommunications Research Establishment, Signal Research and Development Establishment, The Ministry of Supply, The Naval Meteorological Service, The Meteorological Office, and the General Electric Company, Ltd. One-way transmission with stationary apparatus was carried on in the winter of 1943 to 1944 and continued in operation until the end of the war.

Practically all the transmission is over the sea at wavelengths of about 9, 6, and 3 cm. At each frequency the transmitted signal consists of square pulses, with equal on-off periods and a repetition frequency of 1,000. The 1,000 cycle component of the modulation is rectified in the receivers to operate the recording milliammeters, and provision is made for monitoring the transmitter power and the sensitivity of the receivers in terms of a suitable standard. Parabolic mirrors 48 in. in diameter are used for all transmitters and receivers and are permanently mounted inside the station buildings behind large canvas-covered "windows."

There are two transmission paths, 57 and 200 miles in length, which run roughly from south to north, but diverge from each other by about 17 degrees and have the transmitting station in common

at the southern tip in South Wales. There are transmitting stations A and B at 540 and 90 ft above sea level respectively. The receivers, C and D, for the short path are in North Wales at two heights, and E and F, for the long path, in Scotland at two heights. In units of the geometrical horizon distance the lengths of the various transmission paths are as follows.

$\frac{AC}{0.89}$	$\frac{BC}{1.21}$	$\frac{AD}{1.40}$	$\frac{BD}{2.40}$	$\frac{AE}{3.82}$	$\frac{AF}{4.92}$	$\frac{BE}{5.63}$	$\frac{BF}{8.45}$
-------------------	-------------------	-------------------	-------------------	-------------------	-------------------	-------------------	-------------------

It has not been found possible to utilize all these paths at the same time, because the amount of records accumulated proved too great for evaluation, but selected runs at various frequencies and for several paths have been made.

There is an elaborate setup for measuring meteorological conditions simultaneously with the intensity of the transmitted signal. A weather station is located at each of the three terminals, but the main meteorological program is carried out from ships which ply along the transmission paths. The Admiralty has detailed three ships for the sole purpose of making these measurements so that the transmission path is continuously covered by at least one ship on duty. The ships are provided with elaborate meteorological equipment of the type described in Chapter 7.

#### RESULTS

The following is a qualitative summary of some of the results obtained thus far.

1. There is general agreement between signal variations over the two paths, though the short period variations often differ.

2. Signals are obtained over the long path only when the signal strength over the short path *BD* is high. But if the latter condition is fulfilled, the former does not always follow.

3. There is a marked diurnal variation when the general signal level is low or moderate with strong signals in the late afternoon or evening and a minimum between 6 a.m. and 9 a.m.

4. There is evidence of an appreciable seasonal variation with high level for a greater fraction of the time in summer than in winter or spring.



5. Low level occurs commonly, but not always in conditions of fog or low visibility.

6. Low signal level is usually observed at the passage of warm fronts and high level at the passage of cold fronts.

7. Generally speaking, high signal level tends to occur in periods of anticyclonic weather.

A typical record of signal strength for 9-cm waves, representing hourly mean values for a month, is shown in Figure 1. These records are from two

Hatch and the General Electric Laboratories at Wembley. The wavelength is in the 10-cm band, and transmission, monitoring, frequency control, and recording are fully automatic. The path is optical except for some houses and trees near the receiver which introduce a diffraction loss estimated at 30 db. As is generally the case with paths that are optical or nearly so, the fluctuations of received intensity are far less than in the case of long non-optical paths. Figure 2 shows a record for one month

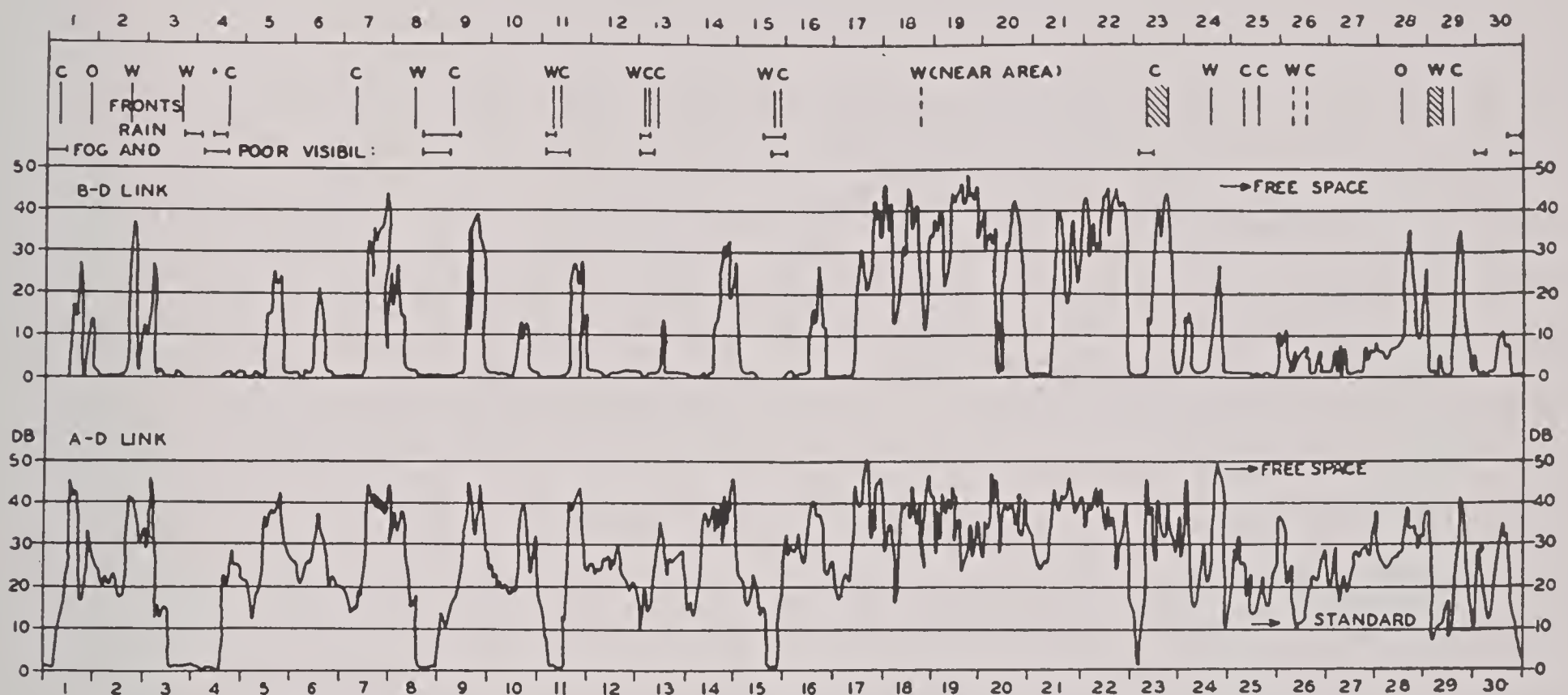


FIGURE 1. Signal strength in decibels above  $1 \mu\text{v}$  receiver input. S band hourly means, June 1944. (Irish Sea experiment.) (C = cold front, W = warm front, O = occluded front.)

links of the short path, both nonoptical. Important meteorological phenomena, especially passage of fronts, are shown at the top of the diagram. W indicates warm, C cold, O occluded. Note in particular the standard and the free space level indicated on the lower record and the free space level on the upper. The standard level for the latter would be about 33 db below the zero line. This record, which is by no means exceptional, gives a fair idea of how vastly the signal exceeds the magnitude calculated for standard conditions. At the same time it shows the highly irregular character of these phenomena and the difficulty of correlating them in a simple way with the weather or other conditions.

#### OVERLAND PATH

An experimental overland path 38 miles has long been operated in the neighborhood of London between the Admiralty Signal Establishment at Whitwell

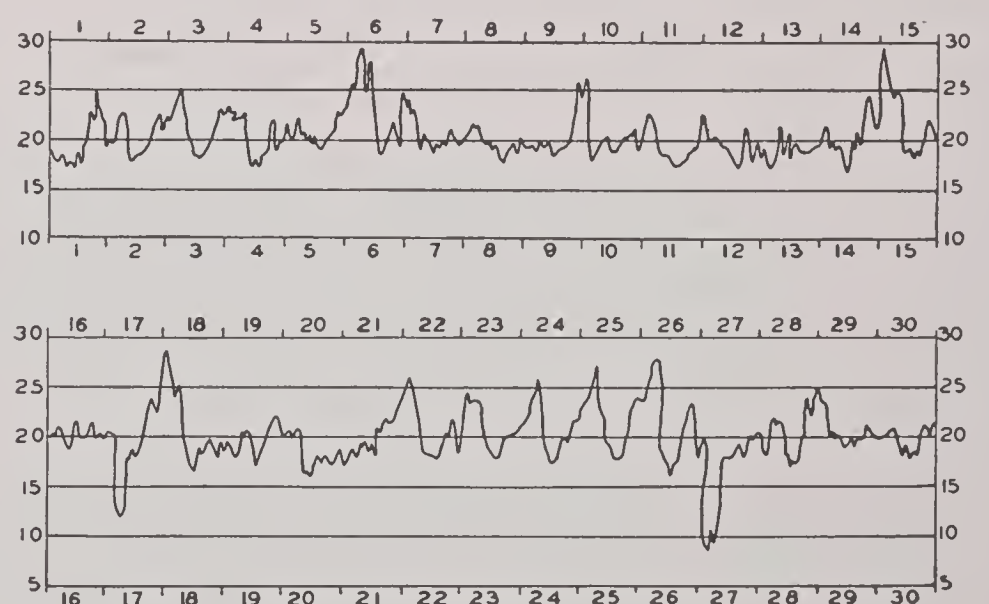


FIGURE 2. Whitwell Hatch-Wembley path, March 1944. S band hourly mean intensities in decibels above  $1 \mu\text{v}$  receiver input.

in 1944. The large diurnal fluctuations in amplitude with maxima above normal in the early morning hours occur in the beginning of the month and at several occasions later, especially from the 21st to the 26th. These are related to weather conditions



with clear skies, as will be explained in Chapter 9.

The work undertaken in England on experimental transmission paths of various types is quite extensive, and the preceding description hardly gives an idea of the variety of experiments made and results obtained. Most of the experiments are of a smaller size than the ones described here.

## 8.2 EXPERIMENTS AT THE EASTERN COAST OF THE U. S.

In the early years of the war a transmission experiment was undertaken by RCA Communications, Inc., between New York and two points on Long Island.<sup>131, 155</sup> The short path of 42 miles was optical, but the long path of 70 miles was nonoptical, the receiver being about 400 ft below the transmitter's line of sight calculated on a  $\frac{2}{3}$  earth's radius basis. Transmission was carried out on 45, 475, and 2,800 mc. The results show what has been confirmed by later experiments, that the amplitude of fluctuations is larger the higher the frequency. On the optical path the range of fluctuations of the 45-mc signal averages only  $\pm 3$  db, whereas over the same path the 475-mc and 2,800-mc signals exhibited fluctuations which were in excess of 40 db, so far as they could be measured. As was to be expected, the 2,800-mc signal fluctuated more than the 475-mc one. Over the nonoptical path all three signals show very wide fluctuations of intensity, the rate and amount again increasing with the frequency.

In the course of these experiments a certain amount of meteorological study was carried out and forecasting of propagation conditions was done on a tentative basis. The general results again fore-shadowed the more complete data obtained by later studies, and a description of the details will be omitted here.

Similar experiments were carried out simultaneously by the Bell Telephone Laboratories [BTL] on optical paths near New York City. The wavelengths employed were 10, 6, and 3 cm.<sup>168, 174</sup> Here we find clearly established the different signal or fading types that are described in detail below.

A very extensive program of transmission measurements was carried out by the Radiation Laboratory of Massachusetts Institute of Technology [MIT]. The meteorological records were made in cooperation with the U. S. Army Air Forces. The first measurements were made in 1942, and experiments on a very large scale were carried out in 1944.<sup>3, 10, 12, 153, 183</sup> Two

optical transmission paths were operated in 1943, a 22-mile path over the sea and a 45-mile path over land. A 10-cm continuous signal was used, and the strength was monitored by means of thermistors. The antennas were dipoles with 30-in. parabolic reflectors. The received signal was automatically recorded on meters having a range of 60 db. The signals received were correlated with meteorological observations, the results of which will be given below.

In the spring of 1944 a new over-water transmission path was installed which was operated simultaneously with the 22-mile one. This path was nonoptical, 41 miles long, and crossed Massachusetts Bay from the southern tip of Cape Ann to the northern tip of Cape Cod near Provincetown. Transmission over this path was carried on with 256-cm waves, 10-cm S band, 3-cm X band, and 1.25-cm K band. The 256-cm equipment used Yagi antennas and operated with continuous waves. The microwave transmitters used pulses with a repetition frequency of 700 c and used parabolic reflectors as antennas.

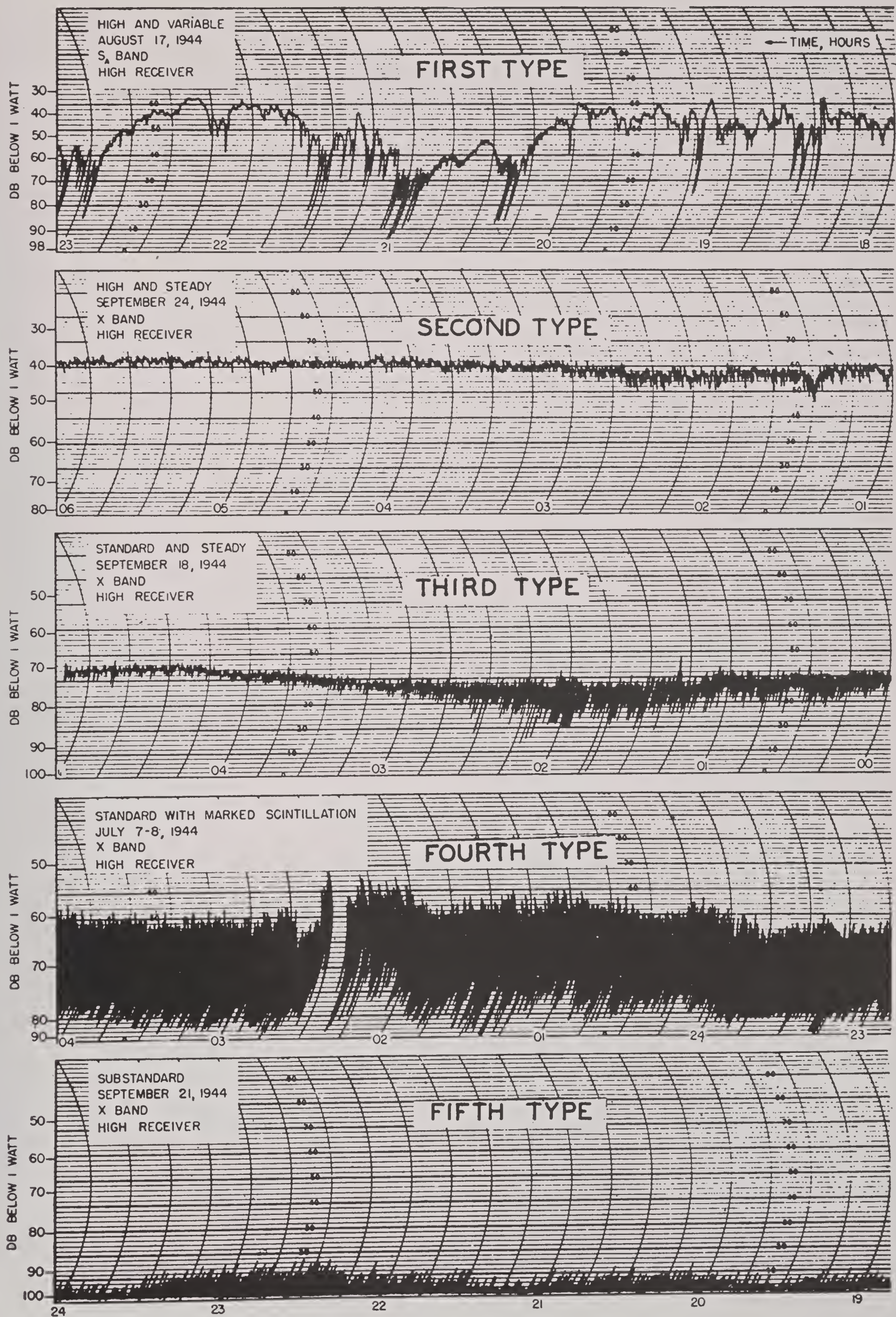
The transmitter for the short path was about 120 ft above mean sea level, and the transmitters for the long path were at a similar height. The two receivers were about 136 and 30 ft above mean sea level. The transmitter power was monitored and continuously recorded during the experiments while the receivers had automatic frequency control with apparatus which searches for the signal if it is lost. The automatic gain control of the receivers was arranged to give a spread of the signal over 70 to 80 db. The receivers were directly calibrated by means of signal generators and a very close check was kept on their performance throughout. The rectified output of all receivers was fed directly into recording milliammeters.

Coincident with the operation of these transmission paths there was a very extensive meteorological program determining sea and air temperatures and atmospheric humidities by means of fixed installations, captive balloons, ships, and airplanes. The distribution of the refractive index along the transmission path was thus known in considerable detail during practically the whole course of the experiments. Concurrently with these measurements, a program of forecasting the transmission conditions was carried out.

## RESULTS

The results obtained on the various transmission paths on the east coast of the United States are



FIGURE 3. Microwave signal types S<sub>A</sub> and X band, Massachusetts Bay.



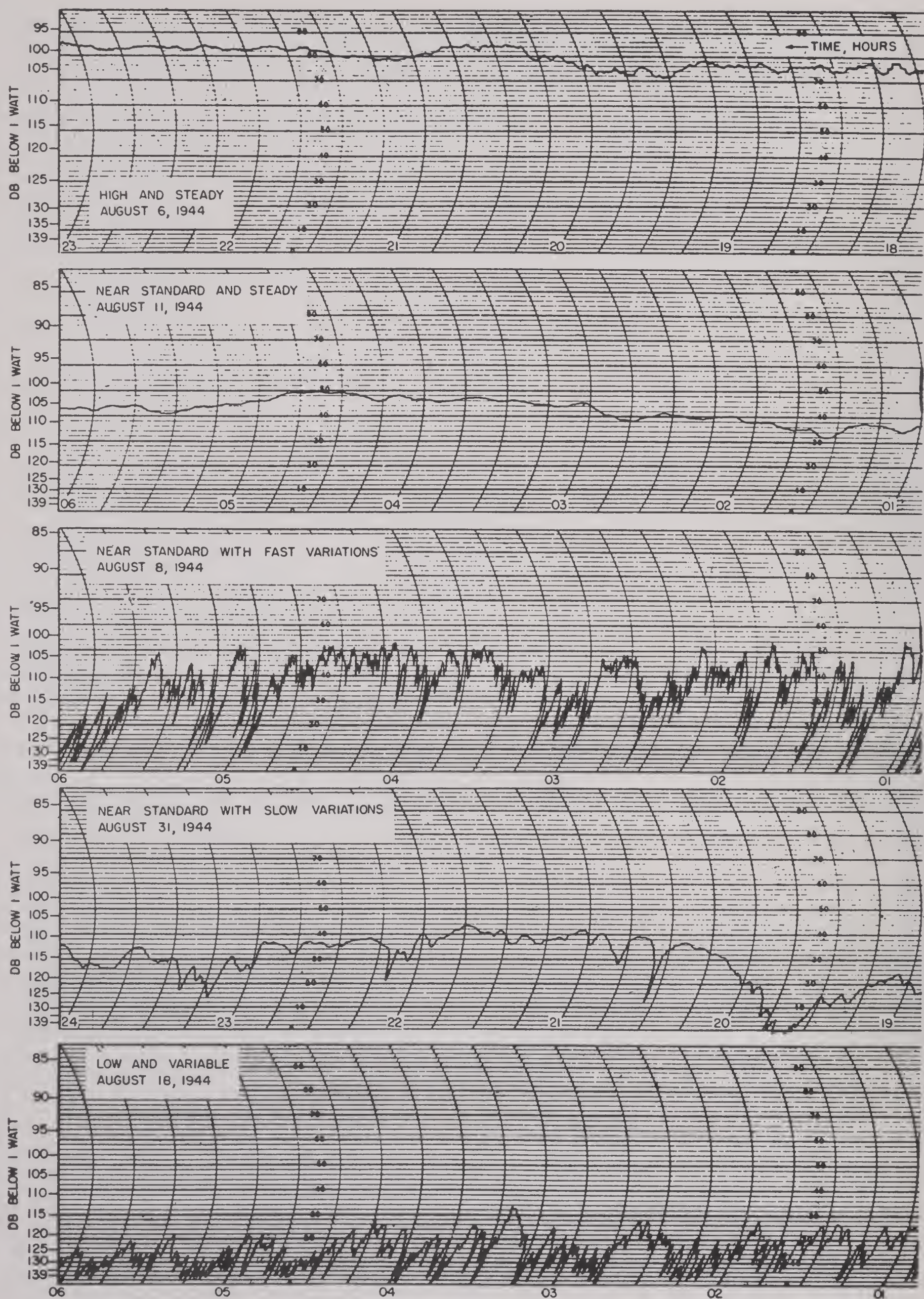


FIGURE 4. Signal types at 256 cm (117 mc per sec), Massachusetts Bay.



rather closely similar to each other, and the graphs presented here may be taken as being characteristic of all of them.

Figure 3 shows the signal types observed at the microwave frequencies, S band and X band. The first type is well above the standard level with high signal on the average. It has roller fades with periods of from 2 min to an hour or so which may go down to the minimum detectable level. These periods are generally shorter at any time on the X than on the S band. When this type of signal was present on the S band, it was almost invariably present on the X band and on both the short and long paths. It always occurred simultaneously on the high and low receivers at any frequency.

The second type is high and steady at anywhere from 5 to 30 db above the standard, generally higher on the X than on the S band. Most of the time this type occurred simultaneously on both bands, but there were some occasions when the S-band signal was of the high and steady type while the X one was of the first type, high with roller fades.

The third type of signal is about standard and fairly steady which may be a limiting case of the high and steady variety. It does not necessarily occur on both frequencies and on both high and low receivers at the same time.

The fourth type is standard on the average, with scintillations of more than 10 db. The reason for the difference between this and the preceding type has not yet been established. The scintillations may occur on either the S or X band while at the same time the other signal is steady.

The fifth type, known as "blackout," is far below standard and shows strong scintillations. In general it occurs simultaneously on both frequencies, both paths, and on both high and low receivers.

Figure 4 shows a similar set of signal types as observed with 256-cm waves. These are distinct from those observed at the microwave frequencies not only in appearance but also in times of occurrence. In general no relation has been found to exist between the signal type at this frequency and that observed simultaneously on S or X band, although on rare occasions such a relation is indicated; the type may remain constant on one frequency and change on the other. Steady signal is most frequent at 256 cm, but the other types shown also occur fairly often. Variations of 30 to 40 db overall take place, and the variations may be fast or slow.

A statistical study of the frequency of occurrence

of various signals reveals some rather interesting features. Table 1 shows the frequency of occurrence of above standard, standard, and below standard types on the S and X bands during three typical weeks in the summer of 1944. In these statistics the range of the standard signal was taken as  $\pm 5$  db for the S band and  $\pm 10$  db for the X band. The behavior of the K-band signal is quite similar to that of the other two.

TABLE 1. S and X bands, July and August.

Date	Per cent of time above standard	Per cent of time below standard	Per cent of time standard
July 10-16	63	36	1
Aug. 21-27	97	3	0
Aug. 28-Sept. 3	80	15	5

As the season progressed into the fall, standard signal became more common and substandard signal less frequent especially in the S band. This is shown in Table 2.

TABLE 2. S and X bands, September and October.

Date		Per cent of time above standard	Per cent of time below standard	Per cent of time standard
Sept. 25-Oct. 1	S	58	15	27
	X	80	10	10
Oct. 16-22	S	76	2	22
	X	92	0	8

These statistical results are characteristic of the over-water path near a coast used in the experiments of the Radiation Laboratory; and, while the signal types shown in Figures 3 and 4 are about the same in overland paths, the relative frequency of incidence for the various types is quite different. This frequency depends not only on the location of the path but, also as shown above, on the season. A more detailed analysis shows that it also depends on the particular weather situation, which may prevail for periods of several days or longer.

It has been mentioned before that the signal patterns on the S and X bands and those on the high and low receivers are closely parallel. Figures 5 and 6 show these correlations graphically; the first is between the S and X bands and the second is between the high and the low S-band receivers. In contradistinction there is practically no correlation between



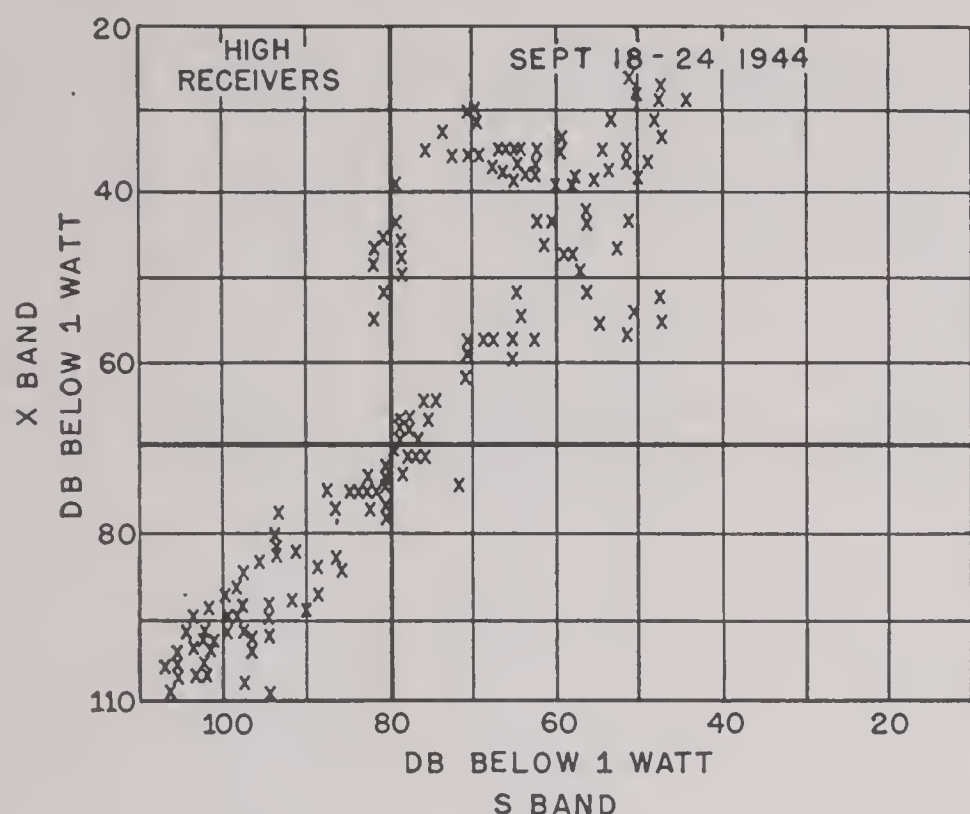


FIGURE 5. Correlation between S- and X-band signal strengths, Massachusetts Bay.

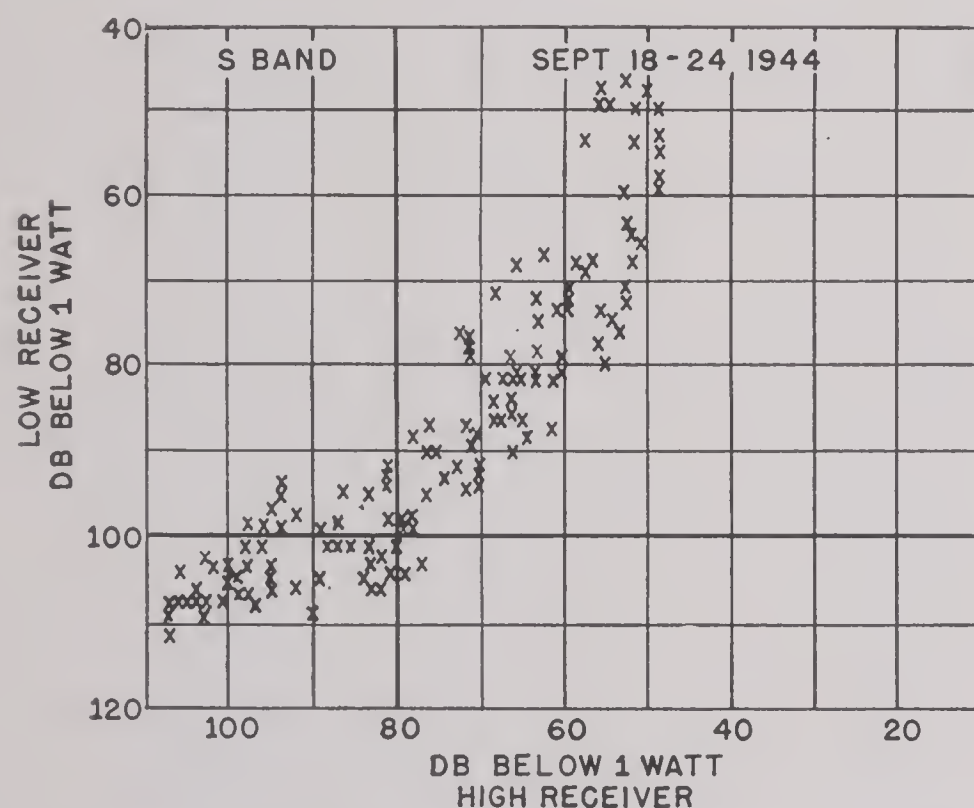


FIGURE 6. Correlation between signal strengths at high and low receivers, Massachusetts Bay.

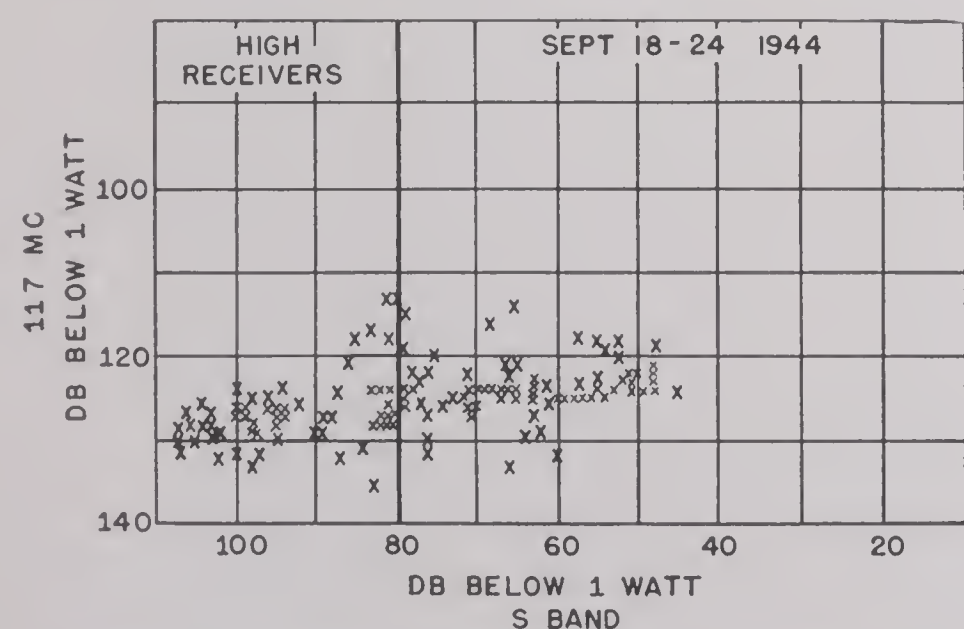


FIGURE 7. Correlation between 117-mc and S-band signal strengths, Massachusetts Bay.

the S-band and 117-mc signal levels, as Figure 7 indicates.

It is hardly necessary to state that the high signal levels occur when the meteorological measurements show the presence of a duct and the substandard signals occur when the  $M$  curve is of the substandard type. It will not be possible, in this summary report, to enter into the detailed relationship between signal strength and  $M$  distribution. In a general way the experimental results confirm the electromagnetic theory in so far as it has been worked out at present.

Another aspect of the short wave transmission that has been studied in these experiments is the relationship between radio and radar transmission. Since radar involves two-way transmission, its path factor, as defined in the beginning of Chapter 5, is the square of the path factor for one-way transmission. Therefore the change with distance in the received-field strength is more rapid with radar than with the one-way radio.

In order to study this relationship, two small mobile radar sets on the S and X bands were set up near the transmitter of the long path, at Provincetown. Echoes from natural targets along the coast of the mainland were studied in connection with the soundings and correlated with the one-way transmission measurements. In Figure 8 is shown a correlation between the signal strength of the X-band radar and the signal strength of the high X-band

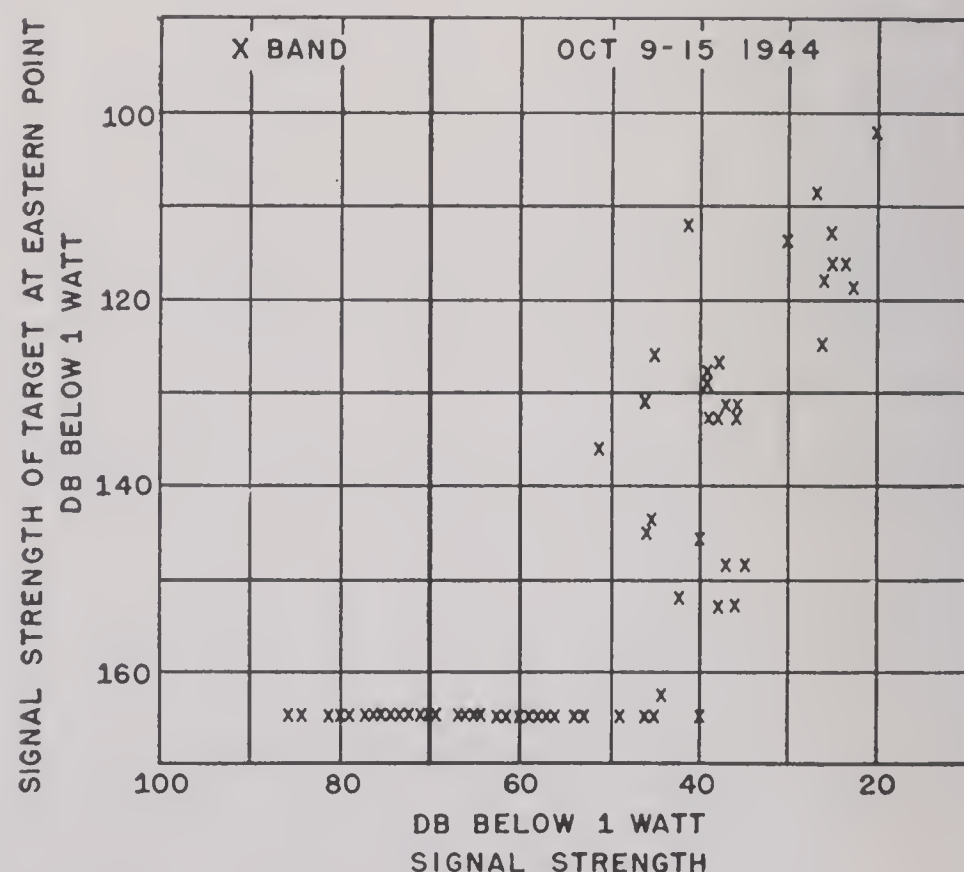


FIGURE 8. Correlation between one-way and radar signal strengths over the same path. X band, Massachusetts Bay.



receiver of the long transmission path. The radar target is near the one-way receiver so that both paths are practically coincident. When the radar signal was below the limit of sensitivity, it is indicated on the graph by this limit so that the lower points of the diagram really have little physical significance. If a straight line is drawn, averaging the variation of the higher points, its slope is roughly 2:1 as should be expected.

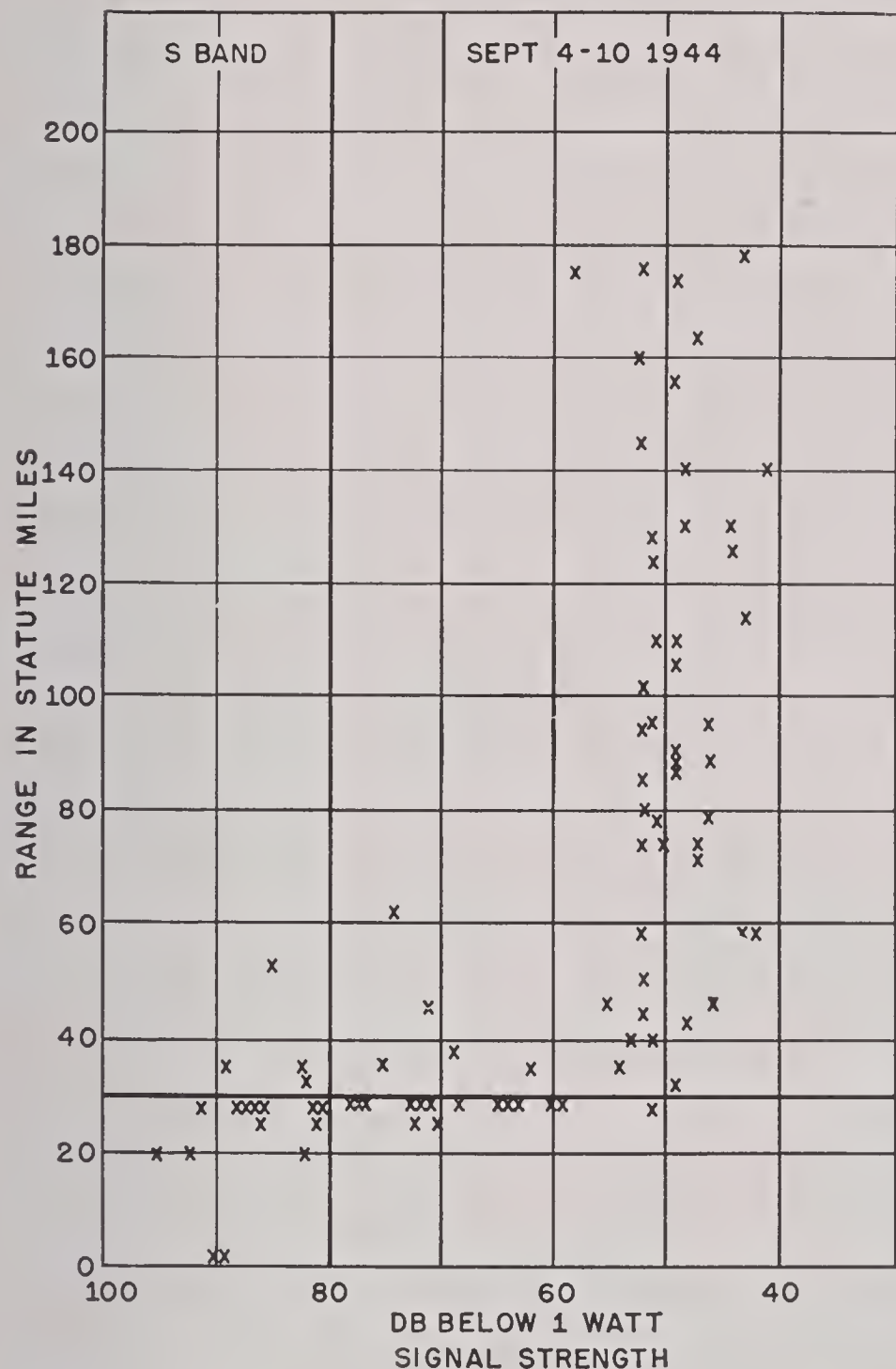


FIGURE 9. Correlation between maximum radar ranges and one-way signal strength. X band, Massachusetts Bay.

Figure 9 shows a correlation between the one-way signal strength on the S band and the maximum range of fixed echoes detected by the S-band radar along the coast. It is interesting to note that super-standard radar ranges do not appear until the one-way signal has reached a certain, rather larger value. The one-way signal does not seem to be able to increase much beyond this value, whereas the range of detectable radar targets rises with extreme rapidity.

### 8.3 EXPERIMENTS IN NORTHWESTERN UNITED STATES AND CANADA

#### STATE COLLEGE OF WASHINGTON PROJECT

During 1943, a series of transmission experiments were carried out by a group of workers from the State College of Washington under the auspices of Division 14, NDRC.<sup>134, 137, 164, 228</sup> The first series of tests were made in the neighborhood of Spokane over 14- and 52-mile optical paths and over a 112-mile nonoptical path. Later in the same year a transmission path 20 miles long with receivers both below and above the optical horizon was installed on the east side of Flathead Lake, Montana.

Among the tests carried out by this group was an experimental telephone communication on 10-cm waves which gave excellent results. The earlier experiments demonstrated the necessity of having detailed data on the refractive index variation in low levels and thus led to the development of the State College of Washington wired balloon sonde, described in the preceding chapter and of basic importance for further propagation work. The first model of the sonde was used systematically in connection with the Flathead Lake transmission path.

The location of these experiments has a climate of a continental type, there being several mountain ranges between these spots and the Pacific coast. The air is comparatively dry, and the structure of the lowest strata is subject to the large variations of temperature and of stability typical of continental conditions.

The general results of these tests are similar in many respects to those found at the east coast of the United States. The signal types are analogous, but the times and frequencies of occurrence are often quite different. In the Flathead Lake experiments, where strong ducts were often present, signal level variations of 50 db were observed for the optical path, 55 db for the nonoptical paths. The correlation between the observed  $M$  curves and the received signal strength was extremely close, high signal levels being observed when the measured  $M$  curves showed the presence of a duct; and standard signal levels, when the  $M$  curve was of the standard type. Similar observations were later made many times over in other experiments such as those at Massachusetts Bay, already described.

Figure 10 shows typical signal records in form of hourly maxima and minima over a three-day period for the 20-mile path on Flathead Lake. Though the



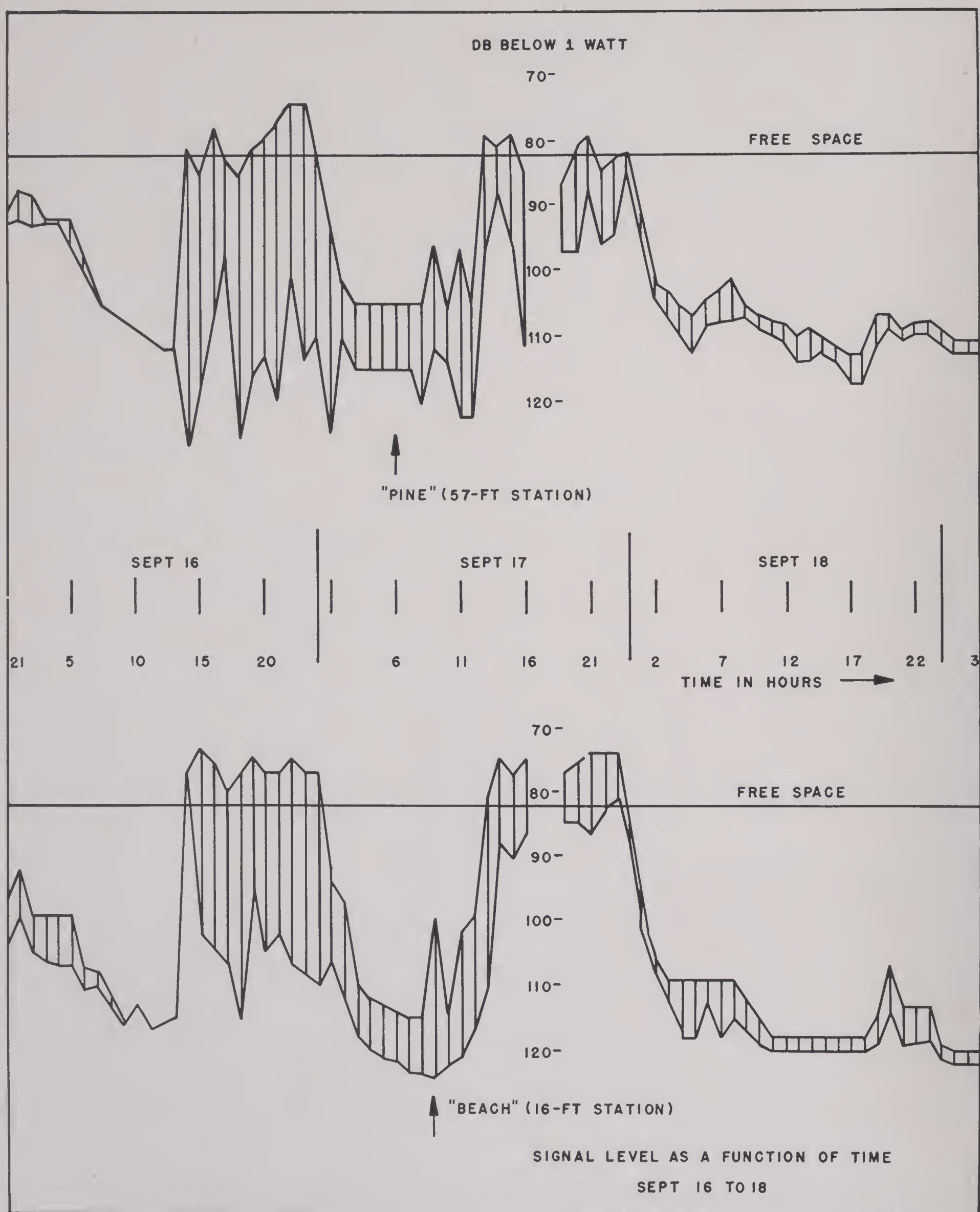


FIGURE 10. Variation of signal strength over 3 days. Two receivers on S band, Flathead Lake, Montana.

path itself is entirely over water, the over-water trajectory of the air is limited by the dimensions of the lake. Both receiving stations are below the line of sight, the upper by 91 ft, the lower by 132 ft.

There is, in this graph, a rather clearcut distinction between periods of standard propagation with a comparatively limited margin of variability of the signal, and periods of superrefraction accompanied



by very deep fades. This behavior is found in most propagation experiments but is perhaps rarely as well marked as in this graph. Another feature of interest is the fact that the maximum signal level is fairly close to the free space level. This has been found to hold approximately in a number of other propagation experiments where, in the presence of a duct, the maximum received level seems to occur not far from the theoretical free space signal level. No explanation for this behavior has been given, and it may be purely accidental.

Figure 11 presents, for part of the same period as

the Canadian Wave Propagation Committee. They were started in the last year of the war and are still under way at the writing of the present report. These tests promise to throw light upon certain aspects of the propagation problem that are difficult to investigate elsewhere. The equipment is located on the prairies of western Canada. The transmission path is over terrain that is as near perfectly level as can be found. The ground is covered with short grass and is without trees or houses. The region forms part of a large flat area in which the atmosphere can be expected to be much more homogeneous than

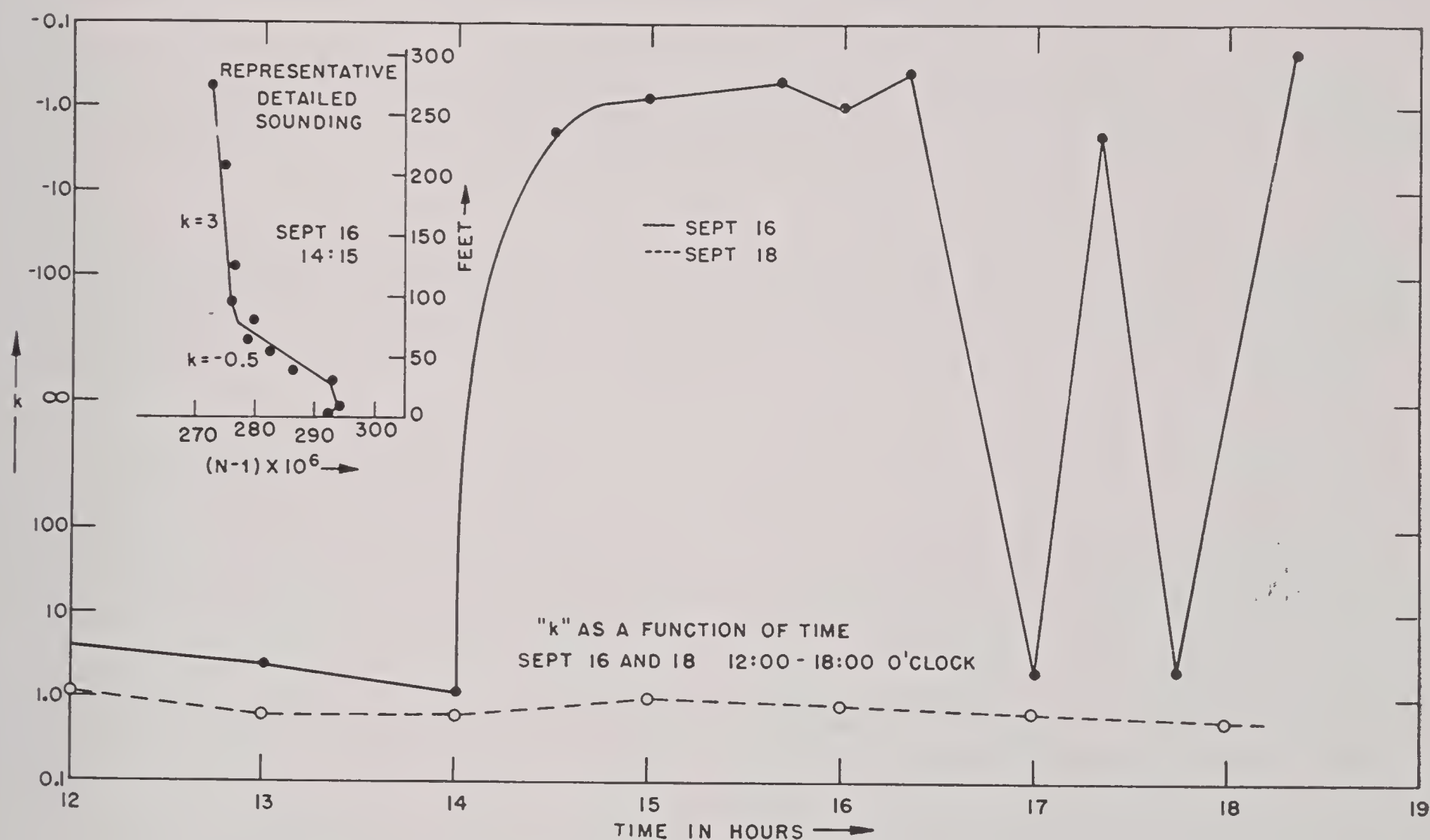


FIGURE 11. Values of  $k$  as a measure of  $M$  or  $N$  gradient for part of period shown in Figure 10.

shown in Figure 10, the value of  $k$  as a function of time at a point on the transmission path. Here  $k$  is a measure of the slope of the  $M$  curve in the lowest strata. Combining equation (17), Chapter 5, and equation (4), Chapter 6, we have  $1/ka = dM/dh \cdot 10^{-6}$ . Thus when  $k$  is negative a duct is present. It will be seen that the incidence of negative values of  $k$  correlates well with high signal strength in Figure 10.

#### CANADIAN EXPERIMENTS

The Canadian transmission experiments are being undertaken by the Tropospheric Subcommittee of

the Canadian Wave Propagation Committee. They were started in the last year of the war and are still under way at the writing of the present report. These tests promise to throw light upon certain aspects of the propagation problem that are difficult to investigate elsewhere. The equipment is located on the prairies of western Canada. The transmission path is over terrain that is as near perfectly level as can be found. The ground is covered with short grass and is without trees or houses. The region forms part of a large flat area in which the atmosphere can be expected to be much more homogeneous than



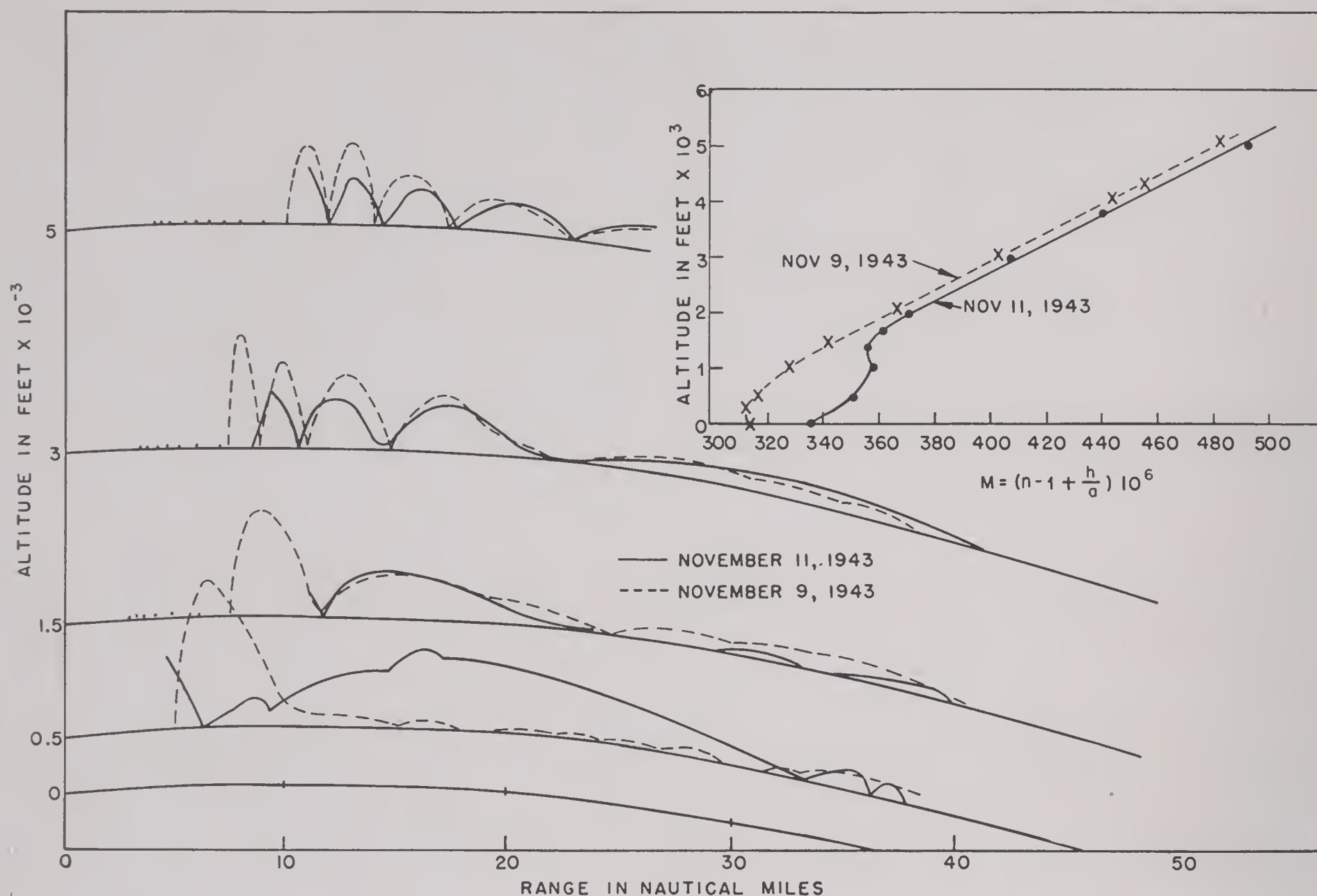


FIGURE 12. Signal strength at several elevations as function of distance. (Near San Diego.)

8.4

#### EXPERIMENTS IN THE SOUTHWESTERN UNITED STATES

The Navy Radio and Sound Laboratory at San Diego has performed a considerable number of propagation experiments which have substantially aided our understanding of the phenomena of guided propagation. Moreover the meteorological conditions found in this part of the United States are rather unique; and, while they are not, perhaps, reproduced at many other places of the earth, they are so clear-cut and regular as to facilitate greatly experimental investigations and their interpretations.

The meteorological conditions at San Diego during most of the year are characterized by the presence of a high-pressure area and high-level subsidence. In more concrete terms, there is a surface stratum of comparatively cool and moist air on top of which there is a layer of very dry, warm air. The transition between the two strata is as sharp as can be found anywhere, and the transitional layer is often no more than a few hundred feet thick. The height of the transition layer above the ground is usually between 1,000 and 3,000 ft and sometimes as much as 4,000 ft.

During the winter of 1942 to 1943, a series of measurements were made on the intensities of artificial fixed echoes of a 700-mc radar located near San Diego,<sup>125,138</sup> and these were compared with measured temperature and humidity gradients in the lower atmosphere. A pronounced correlation between excessive echo ranges and nonstandard  $M$  gradients at once appeared. The quantitative aspects of these correlations will not be discussed here since they are very similar to others of this type already reported.

Another set of observations where the receiver was located in a plane is shown in Figure 12.<sup>3</sup> The receiving antenna was a Yagi, mounted in the nose of the plane, records being made when the plane was flying over the ocean toward the transmitter which was a 500-mc radar. Figure 12 represents the results of flights at various altitudes on two different days, the maxima of the signal strength curves corresponding to the "lobes" of the transmitter pattern. On one of these days a duct was present as shown in the inset where  $M$  is plotted against height. The dot-and-dash straight line in this diagram represents the condition  $dh/dM = \text{constant}$ . The most con-



80 MILE LINK SAN PEDRO TO SAN DIEGO  
TRANSMITTER AND RECEIVER AT 100 FT. ALTITUDE

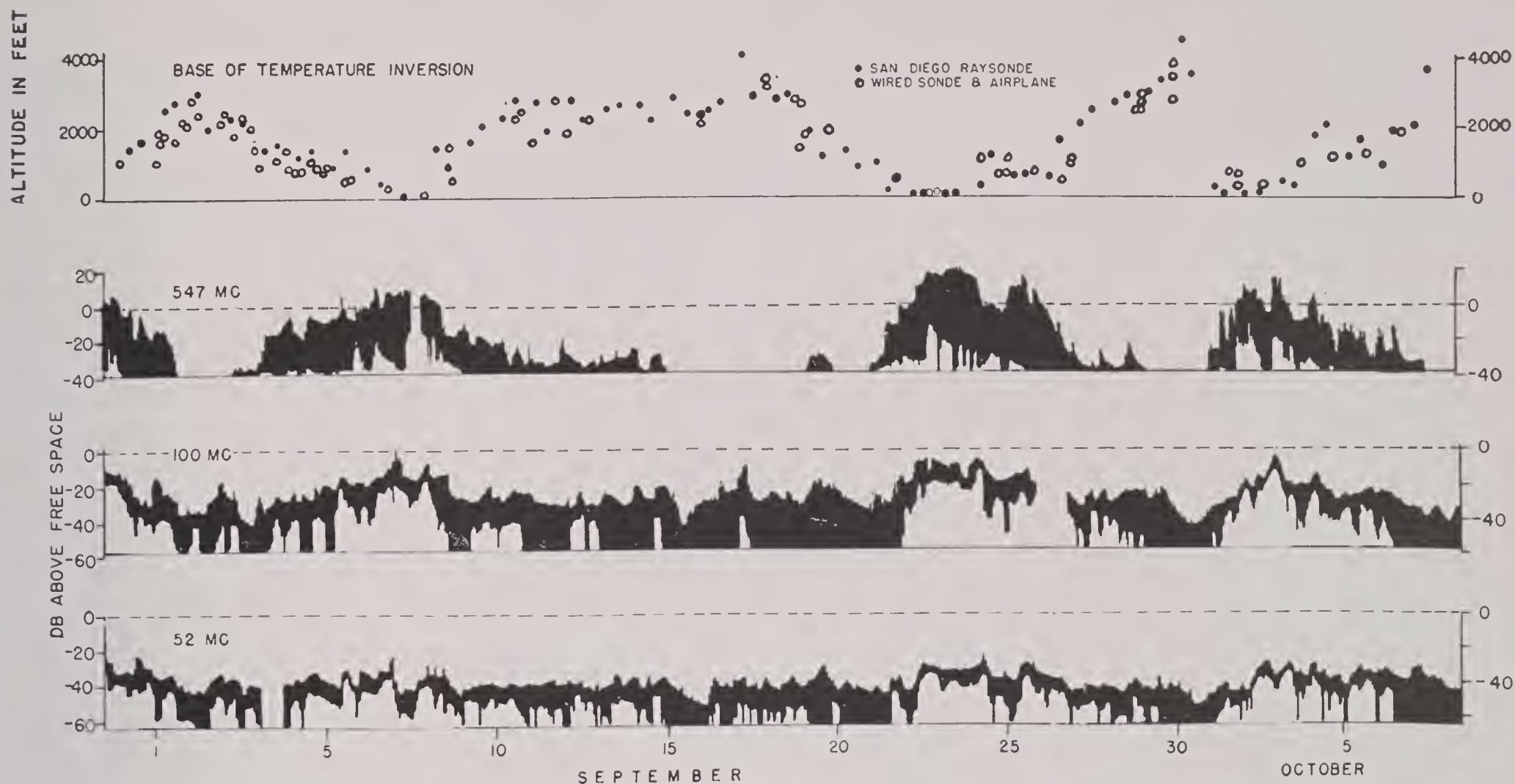


FIGURE 13. Signal strength over 80-mile path, San Diego to San Pedro, correlated with height of temperature inversion.

spicious feature of Figure 12 is the difference between the signal distribution in the absence and presence of a duct at 500 ft, the lowest level measured, whereas the intensities agree fairly well at the higher levels. This behavior is in full agreement with the general predictions of propagation theory. Nevertheless, the detailed interpretation led to a slightly different

result from that expected, as was brought out by subsequent experimental investigations.

In 1944 a one-way transmission path was operated between San Pedro and San Diego, an over-water path<sup>10, 159</sup> 80 miles long with both terminals at an elevation of 100 ft, which were thus well below the optical horizon. Three fairly low frequencies, 52, 100, and 547 mc, were used. Figure 13 shows a field strength diagram of bihourly means for a period of about six weeks in the early fall of 1944. At the top of these diagrams is shown the height of the base of the temperature inversion, which is a quantitative measure of the height of the elevated duct. In order to compare these data with the results of duct theory, Figure 14 shows the number of lowest modes, trapped in the elevated duct, plotted against the signal strength. For each point indicated, the number of trapped modes is calculated by simple waveguide theory from the measured  $M$  curves while the field strength is that simultaneously measured on the transmission path. For the lowest frequency, 52 mc, the duct is always beyond cutoff and no trapping should occur; nevertheless, the field strength record shows considerable fluctuation.

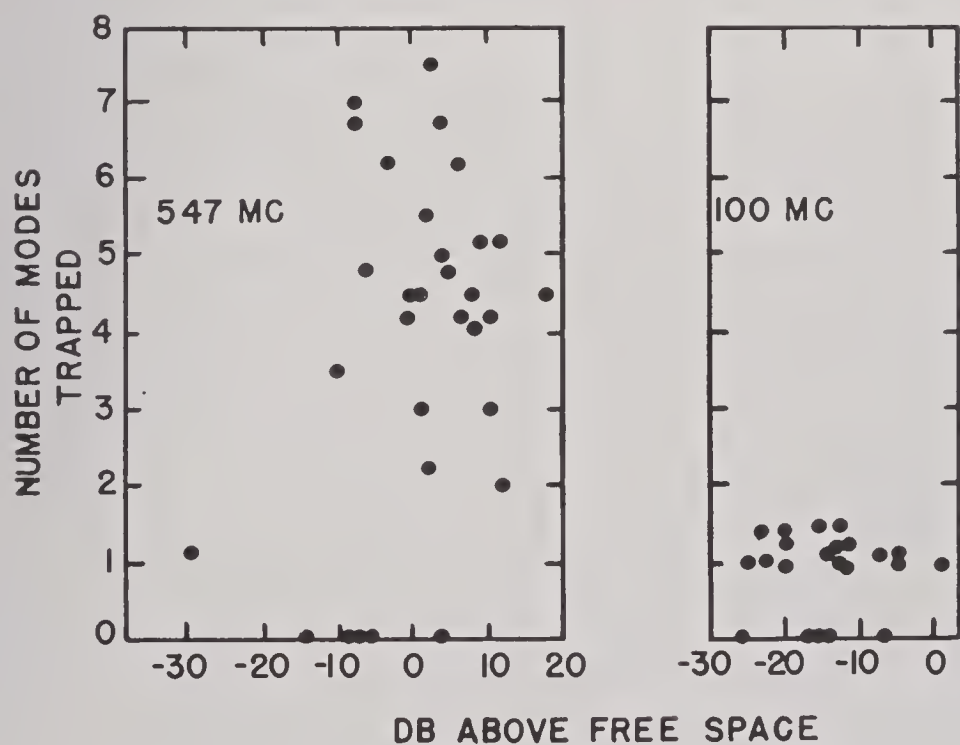


FIGURE 14. Computed number of modes trapped versus observed field strength, San Diego Bay.

As seen from Figure 14 there is no correlation be-



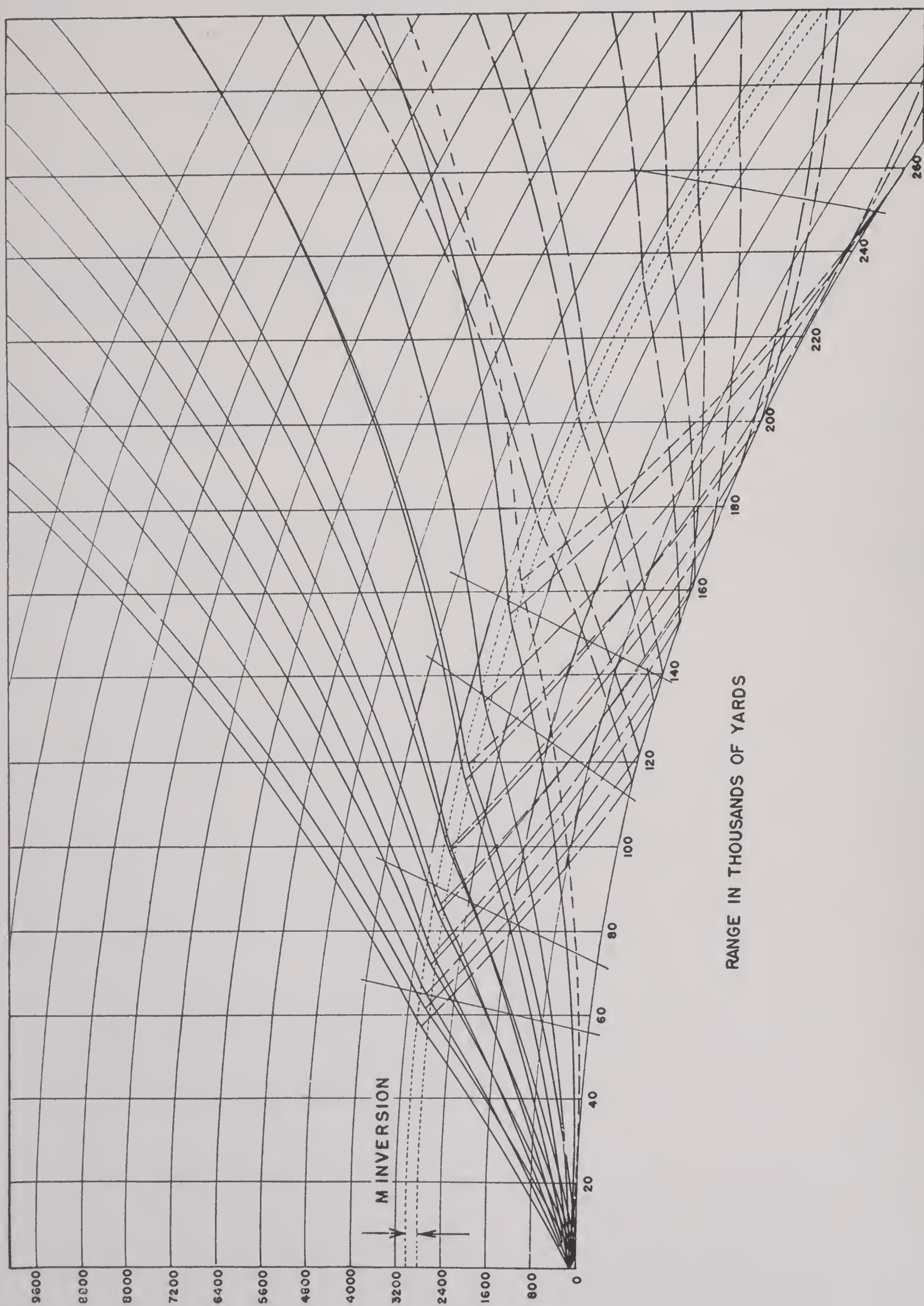


FIGURE 15. Ray tracing diagram including rays reflected from elevated inversion layer, San Diego Bay.  $M$  changes by 50 units through the inversion.



tween the field strength and the number of modes that, theoretically, are transmitted by the duct. On the other hand, there is a very pronounced inverse correlation between the height of the inversion layer and the strength of the received signal. This is just what should be expected on the basis of *reflection*, as distinguished from ray bending, from the elevated layer of  $M$  inversion. The principle of this reflection phenomenon has previously been outlined at the end of Chapter 6, Section 6.7. Further study shows that the rate of change of the field intensity and its variation with frequency are just of the magnitude required by the theory. Figure 15 shows a ray-tracing diagram on which the paths of the reflected rays are indicated. Summarizing the results of this experiment, it may be said that the phenomenon of reflection from an elevated layer has been well established qualitatively and, in some respects, quantitatively. The meteorological conditions at San Diego are rather singular, and so far such reflection occurring in a systematic fashion has not been described elsewhere though indications of similar effects have occasionally been reported.

Another transmission experiment was made by the Navy Radio and Sound Laboratory in the Arizona desert in December 1944.<sup>188</sup> The path was nonoptical, 47 miles long, and the frequency used was 3,200 mc. The desert air is extremely dry so that the contribution of water vapor to the refractive index is small and the change in  $M$  owing to changes in humidity with height is nearly negligible. During the clear nights a pronounced temperature inversion develops from radiative cooling of the ground, a ground-based duct thus being formed. The received field strength varied in close correlation with the formation and disappearance of the duct, with a pronounced diurnal period. The overall results of this experiment are again in excellent qualitative agreement with the predictions of the duct theory. At the same time the experiment also furnished an opportunity for studying the development over land of low temperature inversions which are valuable for radiometeorological forecasting.

dertaken by the Naval Research Laboratory in the spring of 1945.<sup>194</sup> The island of Antigua, one of the Leeward Islands of the Lesser Antilles in the British West Indies, was chosen as the site. The prevailing winds there are northeasterly and the air has an over-water trajectory of several thousand miles before arriving at the island and is therefore considered characteristic of large portions of the central Atlantic and Pacific oceans. There is almost no diurnal and only a limited seasonal variation in the air at the lowest levels.

Equipment for the transmission experiments was comprised of S-band and X-band sets provided by the Radiation Laboratory, MIT. The transmitters with parabolic antennas were mounted on a ship at heights of 16 and 46 ft. There were two parabolas for each height and each frequency, one set pointing to the stern and one to the bow, so that measurements could be made on both the outward and inward runs of the vessel. Receivers were located at heights of 14, 24, 54, and 94 ft on a tower at the edge of the water. Monitoring and automatic recording were similar to those used in the transmission experiments previously described. Records were obtained while the ship was traveling away from the receiving station and again on its return. Signals could usually be detected up to 190 miles for some combination of transmitter and receiver heights. Direction finding equipment was used for keeping the ship on its course, and fading of the signal caused by the ship's being off course could be readily detected and rectified.

An extensive program for measuring low-level  $M$  curves paralleled the transmission measurements. Since the weather conditions at Antigua are quite steady there is little variation in these curves, as shown by two typical ones illustrated in Figure 11 of Chapter 7. The low-level duct indicated by these graphs has been found present at all times in this location.

Typical field strength records for the S band and the X band are shown in Figures 16 and 17, respectively, the most outstanding feature being the variation of field strength with antenna heights. For the S-band transmission, the field strength increases slightly with increasing antenna height but not nearly so fast as it would under standard conditions. For the X band, on the other hand, the field strength, as a rule, is increased by lowering the antennas. This behavior can be explained on the basis of the mode theory of duct propagation as outlined in Chapter 6. For the shorter wavelength X band, we have genuine

Operational experience in the Pacific Ocean led to the conclusion that low ducts are very common over the ocean surface in subtropical and tropical climates. In order to study these ducts, an experiment was un-



trapping, so that the field strength is greatest when the transmitter or receiver or both are in the duct. In terms of the height-gain functions of equation (27), Chapter 5, it appears that these functions of the lowest mode or modes have a pronounced maximum in the duct and decrease rapidly above it. For S-band transmission there is a transition between the complete cutoff, indicated by a highly simplified waveguide theory, and complete trapping. This intermediate effect is caused by some leakage of this wave train from the duct and the retention by the duct of a portion of its wave-guiding properties. The height-gain functions, while still much larger in the duct than in the case of standard propagation, no longer have distinct maxima but show a gradual increase

with height from the ground. This case is particularly interesting because it clearly exemplifies the possible variety of conditions intermediate between trapping, as described by the ray tracing of geometrical optics, and the diffraction around the earth's surface characteristic of standard propagation.

Figure 16 shows two regions with distinctly different slopes in the curves of power versus distance. This probably indicates that two different modes predominate in these two regions. The pattern shown in Figure 16 can occur if for some distance near the ground the height-gain function of the second mode is greater than that of the first mode. The second mode, however, is attenuated more rapidly with distance than the first. At moderate

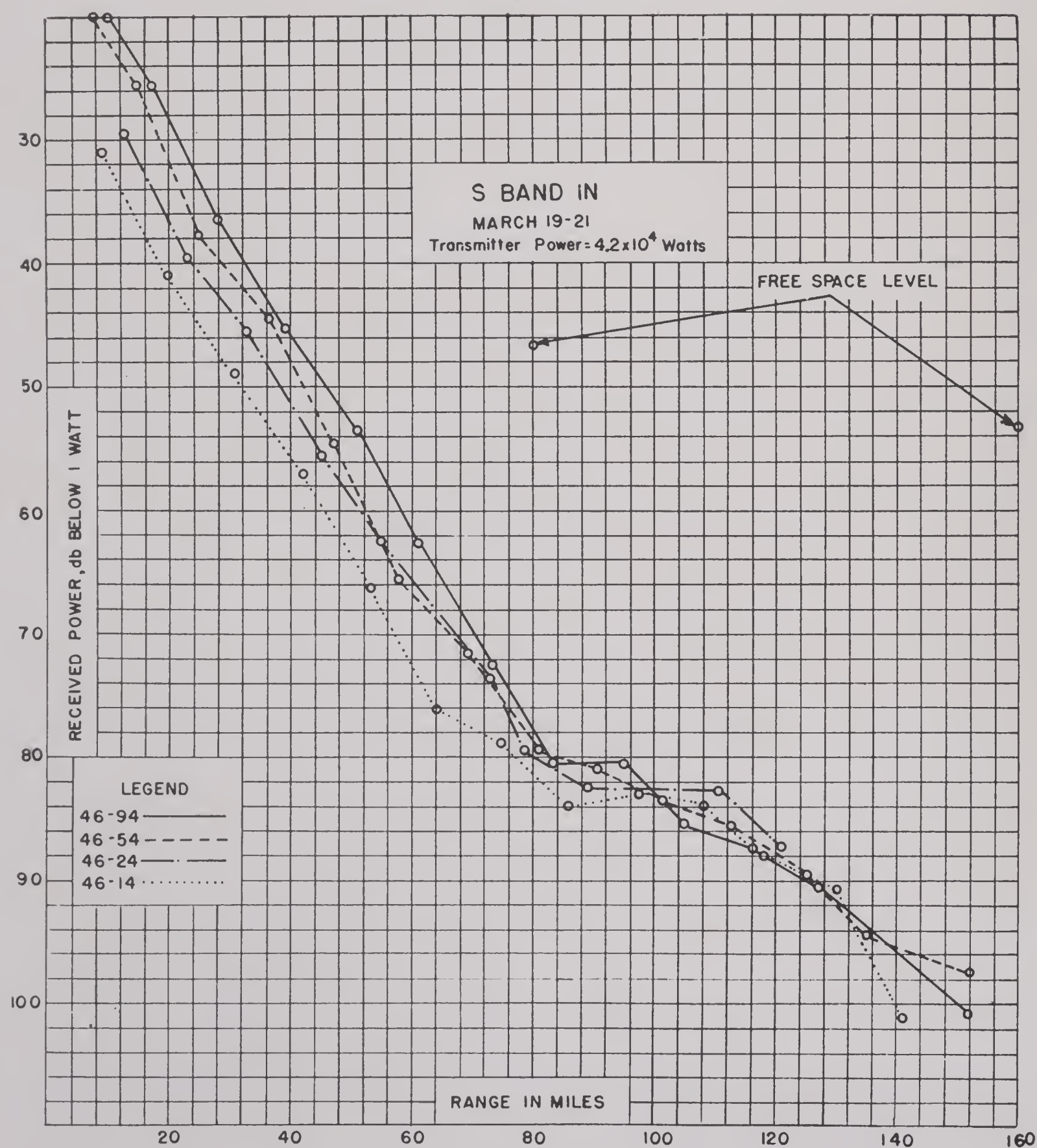


FIGURE 16. Signal strength as function of range. S band, Antigua experiments.



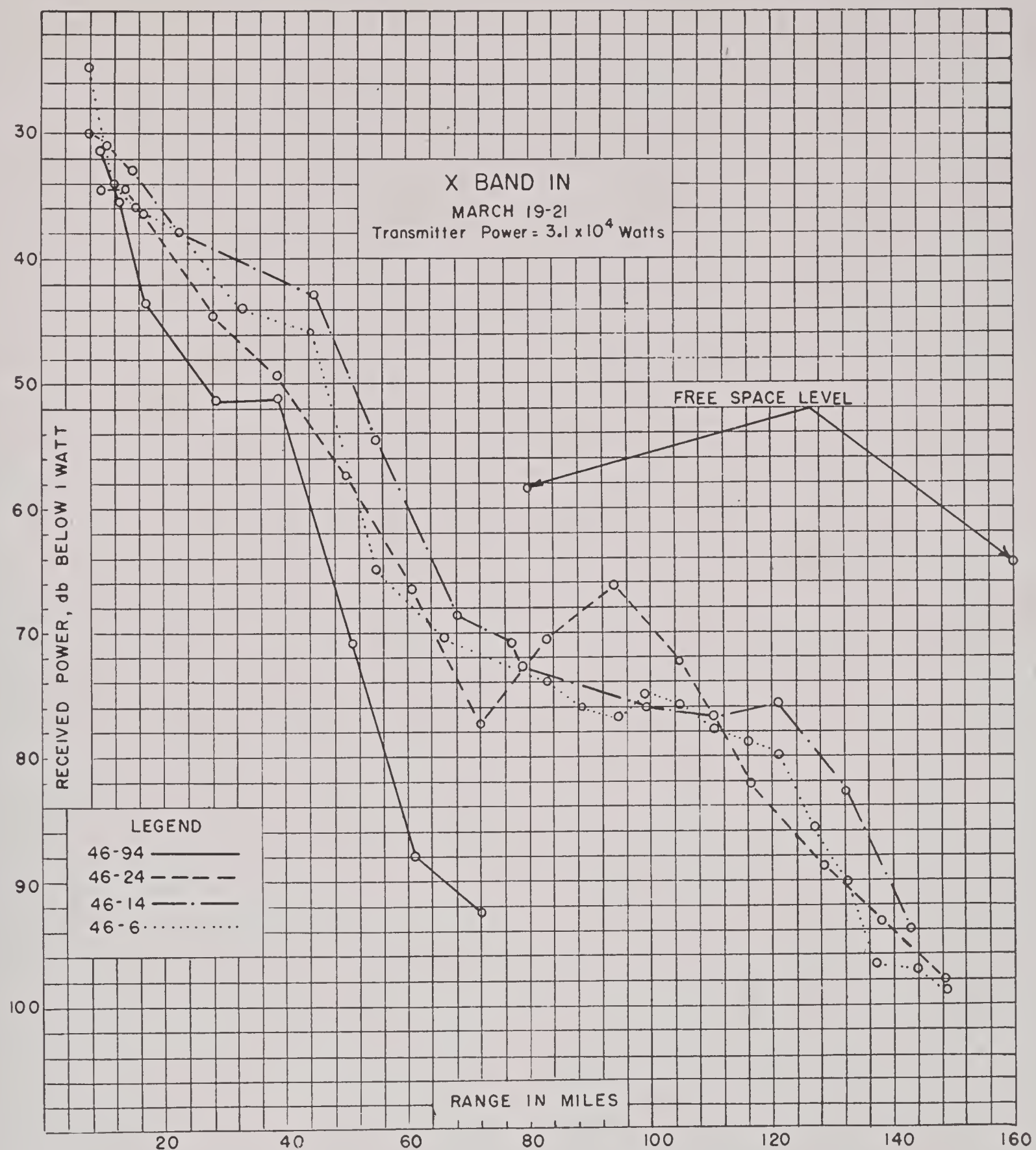


FIGURE 17. Signal strength as function of range. X band, Antigua experiments.

distances from the transmitter the second mode prevails, but at greater distances it will become smaller than that of the first which decreases less rapidly with distance.

Finally Figure 18 shows a set of curves for attenuation versus distance of the target for an X-band radar on Antigua. Again it is evident that, on the whole, the lowest elevation of the radar gives the largest signal strength.

## 8.6 ANGLE-OF-ARRIVAL MEASUREMENTS

Because the effects of nonstandard propagation are most pronounced at great distances from the

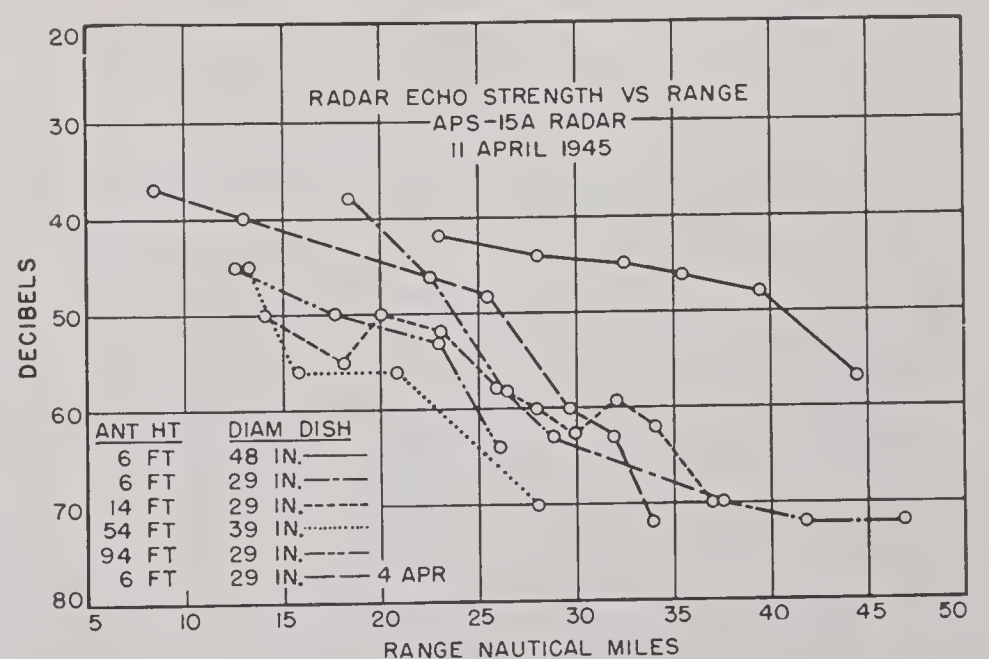


FIGURE 18. Radar echo strength as function of range. X band, Antigua experiments. Target is a PC boat.



transmitter, they are most important for early warning radar and communication work. These effects were investigated earlier than the question of the deviation of the angle of arrival from that prevailing in a standard atmosphere. This deviation, though small, may nonetheless be significant for fire control radars operating in the microwave band. The angle of arrival may vary by several minutes of arc because of ducts, and this effect was first studied systematically by BTL in 1944.<sup>10, 182</sup>

Figure 19 is a schematic view of the receiving

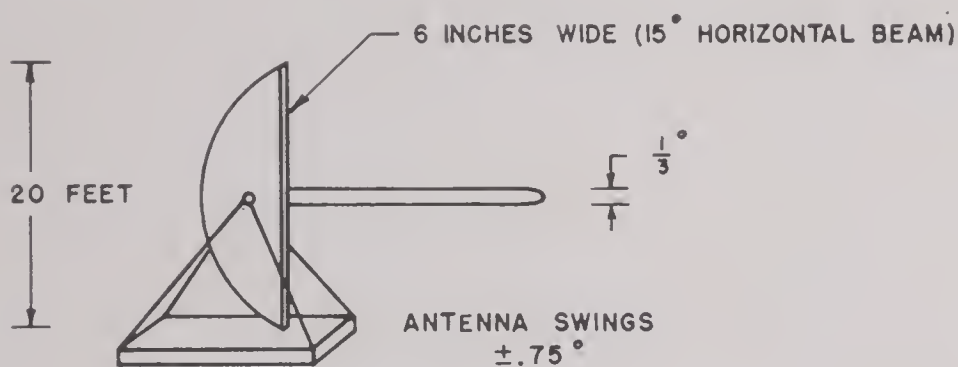


FIGURE 19. Sharp-beamed antenna for angle-of-arrival measurements.

antenna used for such measurements. This antenna is a section of a parabolic cylinder arranged so that its beam, at the center of swing, is directed toward the transmitter, this being the angle at which waves arrive on a day with standard propagation. The antenna measures the vertical angle of arrival, and a duplicate antenna rotates about a vertical axis and measures the horizontal angle. The antennas are periodically swung through an angle which is

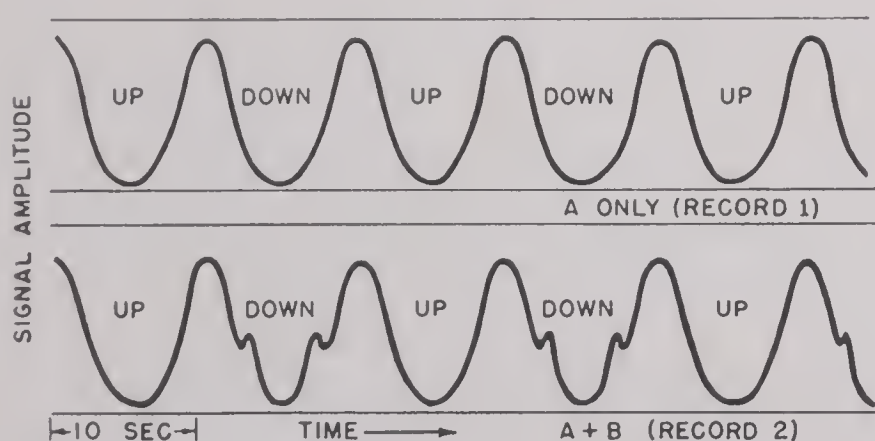


FIGURE 20. Typical record of angle-of-arrival measurements. Top, direct ray only. Bottom, direct and ground-reflected ray.

set to include the largest variations of the angle of arrival. Figure 20 shows a typical record of received field strength versus time for a periodic swing, the upper record representing the presence of a direct

ray only, and the lower indicating both a direct and a ground-reflected ray.

Observations near New York during the summer of 1944 were made on two optical paths 24 and 12.6 miles long with a common receiving antenna. These measurements are estimated to be accurate to 0.04 degree, and they indicate that the greatest variation of the *horizontal* angle of arrival is 0.10 degree. Fluctuations within this magnitude, however, are quite common. The maximum in the *vertical* angle for the long path was 0.46 degree above the standard for the direct ray and 0.17 degree below the standard for the reflected ray. No correlation between departures from the standard of the direct ray and the ground-reflected ray has been observed. When the direct ray was 0.46 degree above the standard, it was apparently being trapped and no reflected ray was observed. The greatest spread observed between the direct and reflected rays was 0.75 degree, as compared to a standard of 0.35 degree. The variation of vertical angle over the short path was less than over the long one, the greatest change in angle being an increase of 0.28 degree over the standard for the direct ray while that of the ground-reflected ray was too small to be observed.

The Evans Signal Laboratory analyzed some low-level meteorological records which were made simultaneously and in the near vicinity of these transmission experiments. The angles of arrival were determined by ray-tracing methods and were in satisfactory agreement with the observations. The difference between angles in standard atmospheres of various climates was also analyzed theoretically, and the results show that the maximum angular deviations are less than the tolerance of present-day fire control equipment.

For early warning radars where the target is perhaps 75 to 100 miles away, the difference in bending of the rays between standard atmospheres of moderate and warm climates becomes appreciable. In this case differences in estimated height vary by as much as 2,000 ft, if the target height is determined by the first signal in the lowest standard lobe.

Measurements of the angle of arrival by BTL were continued in 1945, and the results, though not yet published, give more details and corroborate the previous observations. During the second half of 1945, the Electrical Engineering Department of the University of Texas has embarked on a program to study the angle of arrival.



## Chapter 9

# GENERAL METEOROLOGY AND FORECASTING

9.1

### INTRODUCTION

IN CHAPTER 5, equation (9) was given for the refractive index as

$$(n - 1) \cdot 10^6 = \frac{79}{T} \left( p - e + \frac{4,800e}{T} \right). \quad (1)$$

On adding to this the term  $(h/a)10^6$  the “modified refractive index  $M$ ” of equation (4), Chapter 6 is obtained, namely

$$M = \left( n - 1 + \frac{h}{a} \right) \cdot 10^6. \quad (2)$$

When the temperature increases with height, other things being constant,  $n - 1$  decreases with height and when this decrease is strong enough it will outweigh the increase of  $M$  caused by the term  $h/a$ . Similarly, a decrease of moisture with height will produce a decrease of  $n - 1$  which, if strong enough, will again produce a negative slope of the  $M$  curve. In Chapter 7 we have dealt with these changes purely from the observational viewpoint. Now the origin of these variations owing to the physics and dynamics of the lower atmosphere will be considered. A knowledge of general meteorological conditions may enable a trained weather forecaster to predict, from weather maps and other pertinent data relating to the structure of the lower atmosphere, the presence of ducts and other meteorological factors affecting transmission.

The first attempts at radio forecasting were made as early as 1943 by the British Meteorological Office in conjunction with the services operating the radar sets along the North Sea and Channel Coast. While the correlation between forecasts and observed results was imperfect, results were promising enough to encourage further studies. Since then, the forecasting technique in the British home waters has been developed to a considerable degree of effectiveness. Studies regarding the relationship between the dynamics of the lower atmosphere and radio wave propagation have been initiated by the interested Services in various parts of the British Empire, particularly in Australia where a number of interesting correlations have been discovered. In the United States the problem was first systematically attacked by the propagation group of the Massachusetts

Institute of Technology Radiation Laboratory [MIT-RL], and at about the same time by the Army Air Forces Tactical School in Florida. The latter established a training course for radio meteorological forecasters, a number of whom participated in offensive operations in the Pacific at Leyte and later.

In connection with the transmission experiment across Massachusetts Bay, which was described in Chapter 8, a forecasting unit was established cooperatively by MIT-RL, the AAF, and the U. S. Weather Bureau at Boston. Regular forecasts were made and checked by both meteorological and radio observations. The pertinent information required for radio meteorological forecasting was assembled by a number of agencies in England<sup>244</sup> and in this country. The most extensive American texts on the subject have been issued by Headquarters, Weather Division, AAF,<sup>245</sup> and by the Columbia University Wave Propagation Group.<sup>157</sup> The latter report, *Tropospheric Propagation and Radiometeorology* is published in Volume 2 of the Summary Technical Report of the Committee on Propagation.

9.2

### ATMOSPHERIC STRATIFICATION

From the meteorological viewpoint it is convenient to distinguish three factors which tend to affect the temperature and moisture distribution in the lower part of the atmosphere. These factors are known to meteorologists as (1) advection, (2) nocturnal cooling (over land) and (3) subsidence.

*Advection* is a term that designates the horizontal displacement of an air mass of specific properties over an underlying surface which tends to modify the structure of the mass. Thus one speaks of the advection of dry polar air over a warm water surface. Advection is not the modification of air mass properties but merely a preliminary to such modification.

Advection changes the physical characteristics of the lower strata of the atmosphere through transfer of heat or moisture between the air and the underlying ground or sea surface. The operating factor in this exchange is turbulence, and a brief review of its effects in the atmosphere will be given.

*Nocturnal cooling* over land is caused by a loss of



heat from the ground by infrared radiation. The cooling thus effected is communicated to the lower strata of the atmosphere by means of turbulence. Nocturnal cooling occurs to an appreciable degree only if the sky is clear. Any layer of clouds will exert a "blanketing" effect which reduces the cooling of the ground to a small fraction of that for clear nights.

*Subsidence* is a meteorological term for the slow vertical sinking of air over a very large area. It is usually found in regions where barometric highs are located. By a dynamic process, too complicated to be described here, subsidence often produces a temperature inversion, the air in a subsiding stratum being, as a rule, very dry. Subsidence is usually strongest in a layer somewhat elevated from the ground, and when the dry subsiding mass overlies a moist stratum near the ground, a sharp moisture gradient is created which is favorable for the formation of the duct. The elevated ducts at San Diego are of this type.

*Convection* occurs whenever the vertical temperature gradient exceeds in absolute value the critical gradient of about  $-1$  C per 100 m. It is usually the result of the heating of the ground by the sun's rays, and over land on a hot summer day it may extend to great heights in the atmosphere. Since convection mixes the air thoroughly, it establishes small and constant moisture gradients throughout the lower atmosphere, resulting in a very nearly linear  $M$  curve. Consequently standard conditions of propagation prevail on summer days over land from late morning until late afternoon, this being the time when convection is most likely to be present. Often this applies also to summer days with a light overcast.

*Frictional turbulence* occurs normally in the lowest 1,000 m of the atmosphere even when convection is absent. It is caused by the wind, requires at least light winds, and is fully developed with moderate or strong winds over land. Since turbulence is caused by the roughness of the ground it is less well developed over the sea surface. It can safely be assumed that over land with moderate or strong winds standard propagation conditions prevail because of the regularizing action of turbulence.

*Temperature inversions* occur when the temperature of the sea or land surface is appreciably lower than that of the air. The temperature transition from the ground to the free air takes the form shown in Figure 1. The heat and moisture transfer caused by turbulence in a temperature inversion is less simple than that in a frictional layer. The turbulent processes in inversion regions are highly complex and, as yet, are

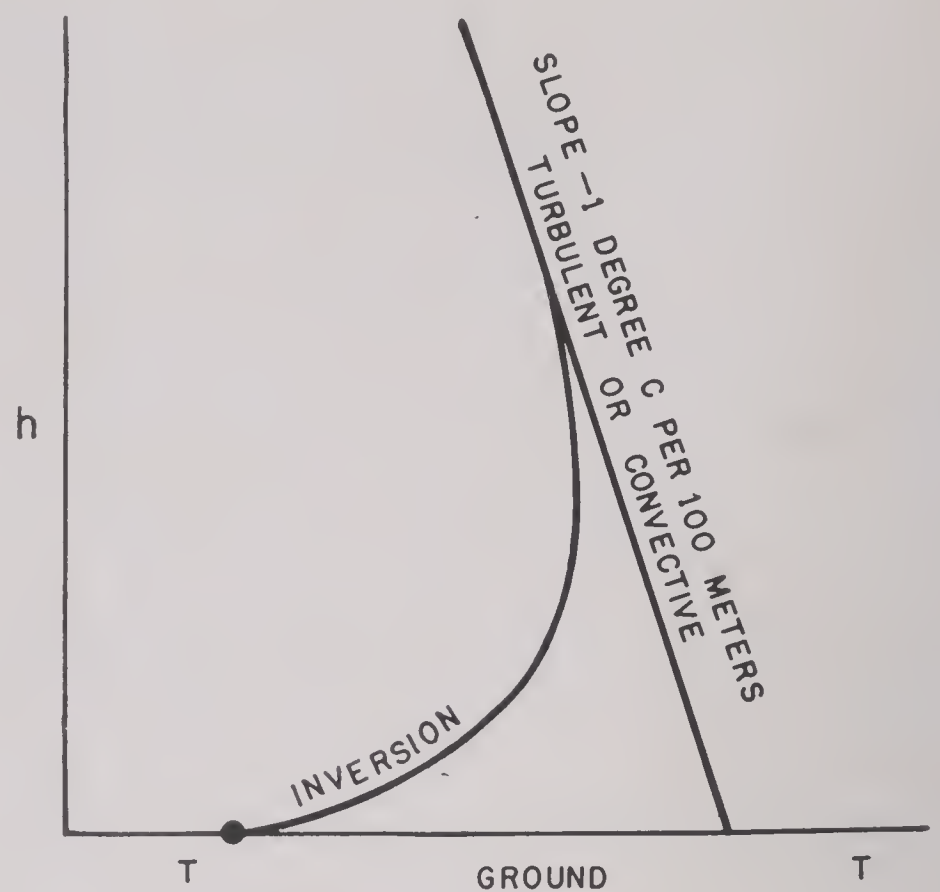


FIGURE 1. Air temperature versus height for a temperature inversion.

not very well explored. It is known, however, that the intensity of the vertical transfer of heat and moisture is much less than the rate of transfer with frictional turbulence and decreases with the vertical increase of temperature. In a steep inversion the rate of transfer may be many times less than in a frictional layer. This tends to produce a vertical stabilization of the air layers in the inversion region. As soon, therefore, as a temperature inversion has begun to form, the rapid mixing in the lowest layers, usually effected by frictional turbulence, stops and is replaced by a much more gradual diffusion.

Assuming that the rate of diffusion has become so slow that the transfer of moisture over a height of a few hundred feet takes many hours or, perhaps, a day or two, when the air in the inversion is dry to begin with and flows over the sea or moist land there will be established, in such an air mass, a steep moisture lapse, since the water vapor that has been taken up by the air near the ground will only gradually diffuse into the dry air aloft. Conditions are then favorable for the formation of an evaporation duct, in addition to whatever tendency toward duct formation may be caused by the temperature inversion itself.

9.3

## CONDITIONS OVER LAND

Because of the considerable variation of the ground temperature by cooling at night and heating during the day, there is to be found over land an alternation



of convection during the day and conditions of a temperature inversion during the night. There is some phase shift in that the atmospheric conditions lag about three to four hours behind the sun. The amount of nocturnal cooling caused by infrared radiation of the ground is very nearly independent of its constitution. It is, however, strongly reduced by the presence of clouds which in turn radiate toward the ground, canceling part of the cooling effect. High moisture content in the lower atmosphere acts partly in the same way and somewhat reduces the heat lost by the ground. With a full overcast, nocturnal cooling is negligible and normally no temperature inversion will be formed.

In temperate climates temperature inversions alone can produce only weak ducts because the effect of temperature upon the refractive index is relatively small. In the fairly common case, however, where the inversion is accompanied by sufficient moisture gradient, a strong duct will result. This occurs when the air is dry enough to allow evaporation into it from the ground. In warmer climates where the transition between night and day is rapid, evaporation may set in early in the morning before the nocturnal inversion has been completely destroyed by the action of the sun. A strong duct will then be formed for a short period.

*Fog.* Contrary to what might perhaps be expected, the formation of fog results generally in a decrease of refractive index. For instance, when fog forms by nocturnal cooling of the ground, the total amount of water in the air remains substantially unchanged, although part of the water changes from the gaseous to the liquid state. It is found that water suspended in the air in the form of drops contributes less to the refractive index than the equivalent amount of vapor. The formation of fog, therefore, reduces the effective contribution of the water vapor to the refractive index. If there is a temperature inversion in the fog layer, the vapor pressure required for saturation increases with height, and a substandard  $M$  curve usually results.

With a substandard  $M$  curve the electromagnetic field near the earth surface is diminished instead of increased, a case opposite to that of superrefraction. In practice this weakening of the field not uncommonly leads to a more or less complete radio blackout.

Fog, however, does not always produce a substandard  $M$  curve although that is usually the case. In certain less frequent types of fog, the temperature and saturation vapor pressure may be constant or

increase with height through the fog layer. In this event propagation will be standard, or ducts may even form occasionally within the fog layer.

#### 9.4 COASTAL AND MARITIME CONDITIONS

Advection is of prime importance near a coast where the wind may blow the air from land to sea or vice versa. The former case, which is the more important in practice, will be considered. A temperature inversion is formed, if the air from above a warmer land surface flows out over a cooler ocean surface. Over the land the air will usually have attained a state of convective equilibrium with correspondingly slow variations of temperature and humidity with height. When this air comes in contact with the cold water surface a temperature inversion is formed which increases gradually as the air proceeds over the water. Thus the inversion is the more pronounced, the greater the distance from the shore. Eventually, however, at very large distances, equilibrium between the air and the water surface will again be reached.

The temperature inversion formed during this process would in itself give rise to only a comparatively weak duct. When, however, the air is dry, evaporation from the sea surface takes place simultaneously with heat transfer, and a fairly strong negative humidity gradient is established in the lowest layers. This combination of temperature inversion and moisture gradient is very favorable for the formation of a pronounced duct off shore.

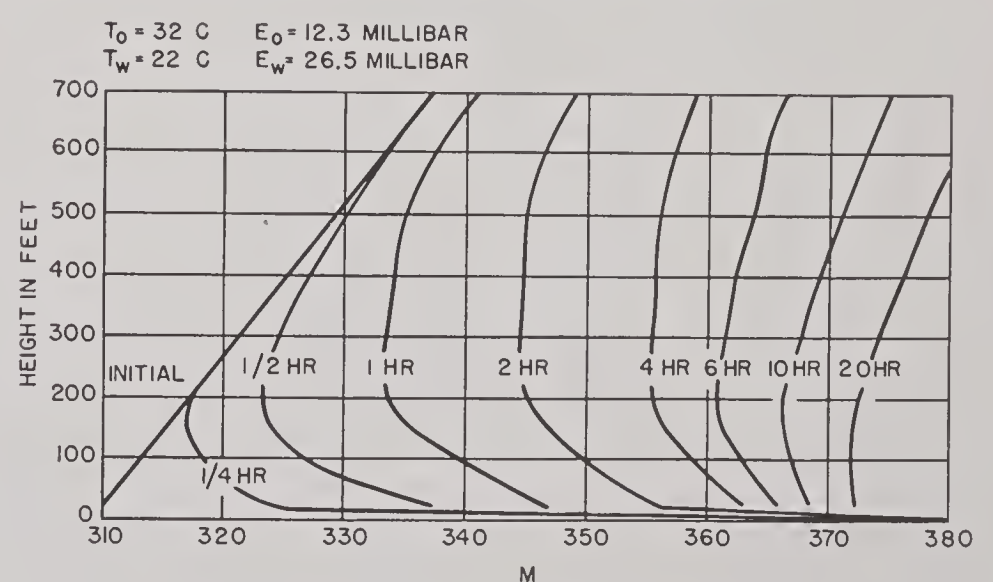


FIGURE 2. Successive  $M$  curves resulting from modification of warm dry air over cool moist surface. Zero time corresponds to the coastline; 1/4 hr, 1/2 hr, etc. refer to the time the air has been over water.

The progressive formation of an advection duct, created by the mechanism just outlined, is shown



schematically in Figure 2. The successive  $M$  curves correspond to a series of time intervals measured from the passage of the air over the shore line. The increase of the duct toward the maximum and the subsequent flattening of the  $M$  curve as the air approaches a new state of equilibrium is clearly seen from the figure.

Duct formation in such a case depends on two quantities: (1) the excess of the unmodified air temperature above the water temperature, and (2) the humidity deficit, that is, the difference between the saturation vapor pressure corresponding to the water temperature and the actual water vapor pressure in the unmodified air. The problem can be treated by means of the mathematical theory of diffusion in a turbulent medium, and a considerable amount of effort has been spent in investigating this type of advective duct. Extensive mathematical work has been carried out in England<sup>200</sup> based primarily on the large body of data on atmospheric diffusion gathered in connection with chemical warfare problems.<sup>197</sup> In the United States such ducts have been studied very extensively in connection with the propagation experiments in Massachusetts Bay where conditions are favorable for their formation.<sup>201, 204</sup>

Another phenomenon often responsible for ducts in coastal regions is the land and sea breeze. This type of wind is of thermal origin and is produced by temperature differences between land and sea. During the day, when the land gets warmer than the sea, the air over the land rises and that over the sea descends, thus causing a circulation in which the air in the lowest layers flows from sea to land. This is the sea breeze. Vice versa, during the night the land becomes colder than the sea, and circulation is in the reverse direction, creating the land breeze. As a rule this type of phenomenon is extremely shallow, and the winds do not extend above a few hundred feet at the most. A sea breeze modifies the advective conditions described above in various ways, and extremely strong ducts have occasionally been observed under sea breeze conditions. The land and sea breezes are of a strictly local nature and in some cases will extend only a few miles to land or sea from the shore. Nevertheless this region may be an important part of the radiation trajectory of coastal radars. These breezes develop only under fairly calm conditions; they are wiped out by a moderate or strong wind.

The advective ducts of the types described here

are by their very nature of only limited horizontal extent. The horizontal variation of refractive index presents a problem that till now has not been systematically studied from either the experimental or the theoretical angle.

A particular type of duct has been discovered in purely maritime air, that is, air which has had an extremely long sea trajectory and thus should have reached an approximately steady state of diffusion relative to the underlying sea surface. The Antigua experiments described in the preceding chapter reveal the existence of a type of low duct which seems to be characteristic of maritime air. It appears probable that similar ducts are permanent in the oceanic regions of many parts of the earth. The relative humidity of the air at Antigua was found to be 60 to 80 per cent, indicating that a continuous upward diffusion of moisture must take place, since the air immediately adjacent to the water surface is always practically saturated. On the other hand, there is little difference between the air and sea temperatures in this case, the ocean being about 25 C while the air temperature varies between 23 and 26 C. The ducts are therefore caused solely by the variation of water vapor in the lowest layers and are much lower than the advective ducts described before, their height rarely exceeding 40 ft. Typical  $M$  curves have been shown in Chapter 7, and, for the particular effects caused by the low height of these ducts, we refer to the discussion of the experimental results.

The diurnal change of ocean temperature is insignificant, except in extremely shallow water, and therefore, at some distance from the coast, propagation conditions do not show any appreciable diurnal variation.

9.5

## DYNAMIC EFFECTS

The physical processes in the lower strata of the atmosphere which determine the formation of ducts are to a considerable extent controlled by the large-scale dynamics of the atmosphere. It is therefore often possible to make at least a qualitative forecast of propagation conditions on the basis of a knowledge of the synoptic weather situation. An example in point is the diurnal variation over land in clear weather from standard conditions during the day to duct conditions in the latter part of the night and the early morning hours.

Conditions in a barometric low pressure area



generally favor standard propagation. Winds are usually strong or at least moderate resulting in a well-mixed layer of frictional turbulence. Local thermal stratifications are destroyed, and abnormal moisture gradients will not develop because of the intense turbulent mixing. The sky is frequently overcast in the low pressure area and nocturnal cooling therefore is often negligible.

On the other hand, meteorological conditions in a high pressure area are frequently favorable for the formation of ducts. The sky is commonly clear, thus giving rise to pronounced nocturnal cooling of the ground and to the attendant formation of a temperature inversion in the lowest layers. This, again, often gives rise, by evaporation, to steep moisture gradients within the inversion layer resulting in the formation of ducts in the manner already described. Winds in high pressure areas are often slight, or a calm prevails, resulting in a formation of local thermal stratifications and of land and sea breezes.

One of the prime phenomena conducive to non-standard propagation conditions in a barometric high is *subsidence*, already described. Subsidence is closely connected to high pressure areas on the weather map and is always found in such areas, but it is not always intense enough to produce an inversion. The typical pattern of air flow in a baro-

If such air is located over a surface capable of evaporation such as the ocean, a steep moisture gradient may be established at some level above the ground. This is the most common mechanism for the formation of elevated ducts. Quite often subsidence combines with some or the other effects mentioned earlier enhancing their tendency toward the formation of the duct. The elevated ducts found in the San Diego region are perhaps the most outstanding example of this type of dynamically induced stratification.

The effect of *fronts* in the atmosphere upon propagation does not seem to be very pronounced. This is probably due to the fact that in a front the transition between warm and cold air is comparatively gradual extending over a height of perhaps 1 km. In the English propagation experiments some effects of fronts have indicated slightly substandard conditions with warm fronts and slightly superstandard conditions with cold fronts. Often, however, the effect of fronts upon radio propagation is negligible. This, of course, refers only to the frontal region itself and not to the change in air mass and attendant propagation conditions connected with the passage of a front.

9.6

## WORLD SURVEY

It clearly appears from the preceding sections that climate has a fundamental influence on the nature of propagation conditions. A systematic attack on the problem of the occurrence of ducts over the ocean has been made in England on a world-wide scale.<sup>250</sup> Monthly maps based on estimates drawn from general low-level weather data, giving regions of the most frequent occurrence of superrefraction and substandard refraction, were issued. However, these need much further checking by actual observations. The propagation features of some important parts of the world where some knowledge has been accumulated is outlined briefly below.

*Atlantic Coast of the United States.* Along the northern part of this coast superrefraction is common in summer, while in the Florida region the seasonal trend is reversed, a maximum occurring in the winter season.

*Western Europe.* On the eastern side of the Atlantic, around the British Isles and in the North Sea, there is a pronounced maximum in the summer months. Conditions in the Irish Sea, the Channel, and East Anglia have been studied by observing the appearance or nonappearance of fixed echoes. Additional

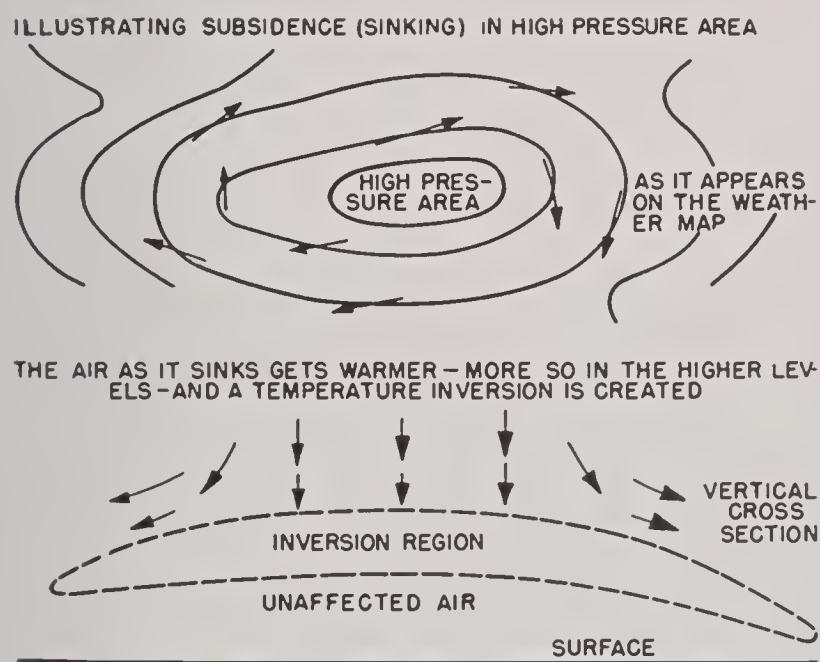


FIGURE 3. Schematic diagram illustrating subsidence in a region of high barometric pressure.

metric high is shown in Figure 3 in both horizontal projection and vertical cross section.

The air in the lower parts of a region of subsidence is very dry because it has descended from a high level in the atmosphere where the temperature is low and hence the saturation vapor pressure is small.



data based on one-way communication confirmed the radar investigations.

*Mediterranean Region.* The campaign in this region provided good opportunities for the study of local propagation conditions. The seasonal variation is very marked, with superrefraction more or less the rule in summer, while conditions are approximately standard in the winter. An illuminating example is provided by observations from Malta, where the island of Pantelleria was visible 90 per cent of the time during the summer months, although it lies beyond the normal radar range.

Superrefraction in the Central Mediterranean area is caused by the flow of warm, dry air from the south (sirocco) which moves across the ocean, thus providing an excellent opportunity for the formation of ducts. In the winter, however, the climate in the Central Mediterranean is more or less a reflection of Atlantic conditions and hence is not favorable for duct formation.

*The Arabian Sea.* Observations covering a considerable period are available from stations in India, the inlet to the Persian Gulf, and the Gulf of Aden. The dominating meteorological factor in this region is the southwest monsoon which blows from early June to mid-September and covers the whole Arabian Sea with moist equatorial air up to considerable heights. Where this meteorological situation is fully developed, no occurrence of superrefraction is to be expected. In accordance with this expectation, all the stations along the west side of the Deccan report normal conditions during the southwest monsoon season. During the dry season, on the other hand, conditions are very different. Superrefraction then is the rule rather than the exception, and on some occasions very long ranges, up to 1,500 miles (Oman, Somaliland), have been observed with fixed echoes on 200-mc radar, based near Bombay.

When the southwest monsoon sets in early in June, superrefraction disappears on the Indian side of the Arabian Sea. However, along the western coasts conditions favoring superrefraction may still linger. This has been reported from the Gulf of Aden and the Strait of Hormuz, both of which lie on the outskirts of the main region dominated by the monsoon. The Strait of Hormuz is particularly interesting as the monsoon there has to contest against the "shamal" from the north. The Strait itself falls at the boundary between the two wind systems, forming a front, with the dry and warm shamal on top, and the colder, humid monsoon

underneath. As a consequence, conditions are favorable for the formation of an extensive radio duct, which is of great importance for radar operation in the Strait.

*The Bay of Bengal.* Such reports as are available from this region indicate that the seasonal trend is the same as in the Arabian Sea, with normal conditions occurring during the season of the southwest monsoon, while superrefraction is found during the dry season. It appears, however, that superrefraction is much less pronounced than on the northwest side of the peninsula.

*The Pacific Ocean.* This region appears to be the one where, up to the present, least precise knowledge is available. There seems, however, to be definite evidence for the frequent occurrence of superrefraction at some locations, e.g., Guadalcanal, the east coast of Australia, around New Guinea, and on Saipan. Along the Pacific coast of the United States, observations indicate frequent occurrence of superrefraction, but no statement as to its seasonal trend seems to be available. The same holds good for the region near Australia.

In the tropics there is a very strong and persistent seasonal temperature inversion, the so-called trade wind inversion. It has no doubt a very profound influence on the operation of radar and short wave communication equipment in the Pacific theater.

## 9.7

## RADAR FORECASTING

The forecasting of propagation conditions for early warning radars is of great operational significance because ranges for airplane as well as ship targets often vary by as much as a factor of 2 or more depending on the weather conditions. Forecasting is based on the general meteorological principles presented above which can be organized into a system of standard procedures for the prediction of propagation in a given area.<sup>244, 253, 255</sup> It is usually quite difficult to make a quantitative forecast of such parameters as duct height, but this has been tried with a fair degree of success.

A radio forecast is made by first taking the general synoptic weather situation as presented on a weather map and including such upper air data as may be available. Usually one forecast cannot be applied to more than a limited area of specific local conditions; fortunately such a forecast is in general adequate for the area covered by one or a few radar sets. The



formation of ducts depends principally on the temperature difference between the air and the ground or sea surface and on the humidity of the air. Data on sea temperature, which is usually fairly constant, are collected while over land it is necessary to obtain data on the diurnal variation of the soil temperature. Wind velocities may be gathered from the weather map, and the trajectory of the air previous to and during the forecast period can then be determined. If the relative humidity of the air is known, it is possible from the theories at hand to draw estimated curves of the temperature and moisture variation in the lowest layers. From these an estimated  $M$  curve is obtained. The success of this method depends to a large degree upon the familiarity of the forecaster with local conditions.

The forecasting of advective ducts over the ocean

is the main problem in which radio forecasting requires other tools than those used for ordinary weather forecasting; but most other problems are closely similar to those presented by conventional practice, among which are the forecasting of subsidence from upper air meteorological data, the forecasting of nocturnal temperature inversions in dry climates, and the forecasting of standard propagation conditions.

In order to facilitate weather forecasting in the Pacific, where data have been very scanty during the war, a system has been worked out whereby localities in the Pacific area are compared to those of closely similar climatic and meteorological character in the Atlantic. A rough estimate of propagation conditions to be expected may be derived therefrom.<sup>25, 215</sup>



## SCATTERING AND ABSORPTION OF MICROWAVES

THE OBJECT of the present chapter is to summarize the status of absorption and scattering of microwaves by different solid obstacles, by liquid water or ice particles floating or falling in the atmosphere like those present in clouds, fog, rain, hail, and snow. The absorption of microwaves by the atmospheric gases as well as the aforementioned meteorological elements will also be summarized here.

The following grouping of the material included suggests itself naturally: absorption and radar cross section; targets (planes, ships); absorption and scattering by rain, hail, snow, clouds, and fog; and absorption by the atmospheric gases, oxygen, and water vapor.

### 10.1 ABSORPTION AND RADAR CROSS SECTION

Any object irradiated by electromagnetic waves will in general remove energy from the incident beam both by absorption and by scattering. The absorbed energy is transformed into heat in the body, while the scattered energy appears in the form of radiation propagated generally in every direction around the scatterer as the source.

Let us call  $P_a$  the power removed from the beam through the internal absorption of the object. Its absorption cross section is defined by

$$A = \frac{P_a}{W_i}, \quad (1)$$

where  $W_i$  is the power density in the incident beam, that is, the power passing a unit cross-sectional area.

Similarly, if  $P_s$  is the total power removed from the beam through scattering in every direction, then the scattering cross section associated with this object is

$$S = \frac{P_s}{W_i}. \quad (2)$$

The value of  $S$  gives information about the total scattered energy, but this is not directly useful in radar work because one is interested only in that fraction of the total scattered power which travels in the direction of the receiver. One wants then a

parameter involving the scattered power per unit area  $W_r$  at the radar receiver instead of the total. If the target is an isotropic scatterer,

$$W_r = \frac{P_s}{4\pi d^2}, \quad (3)$$

$d$  being the distance from the target to the receiver. The scattering cross section can thus be written as

$$S = 4\pi d^2 \frac{W_r}{W_i}. \quad (4)$$

For targets other than isotropic scatterers, however, this procedure fails since one cannot say that the power per unit area at the radar is  $P_s/4\pi d^2$ . Nevertheless, it is useful to define a parameter,

$$\sigma = 4\pi d^2 \frac{W_r}{W_i}, \quad (5)$$

which is called the radar cross section in analogy with the scattering cross section  $S$  of an isotropic scatterer. This cross section  $\sigma$  may be thought of as the scattering cross section which the target in question would have if it scattered as much energy in all directions as it actually does scatter in the direction of the radar receiver. For an isotropic scatterer  $\sigma = S$ , but in general it does not.

It can be shown<sup>a</sup> that the ratio of the received power  $P_2$  to the output power  $P_1$  is given by

$$\frac{P_2}{P_1} = G_1 G_2 \frac{\sigma}{4\pi d^2} \left( \frac{3\lambda}{8\pi d} \right)^2 A_p^4. \quad (6)$$

The gains  $G_1$ ,  $G_2$  and path factor  $A_p$  are defined in Volume 3, Chapter 2, and  $\lambda$  is the wavelength of the radiation used. (See also Volume 3, Chapter 9.) This formula can be used for the determination of  $\sigma$ . Or if  $\sigma$  is known, it may serve to calculate the possible range. (It may be noted here that sometimes  $\sigma A_p^4$  is called radar cross section.) Also, a characteristic length  $L$ , sometimes called the scattering coefficient, is occasionally defined in relation to  $\sigma$  by

$$\sigma = 4\pi L^2. \quad (7)$$

For simple targets  $\sigma$  may be calculated. Table 1 contains a few calculated radar cross sections.

<sup>a</sup>See Volume 3 of the Summary Technical Report of the Committee on Propagation.



TABLE 1. Radar cross sections.

Targets	Condition	Radar cross section
Conducting sphere, radius $a$	$\lambda \ll a$	$\pi a^2$
	$\lambda \gg a$	$\frac{144\pi^5 a^6}{\lambda^4}$
Metallic plate, area $S$	All dimensions $\gg \lambda$	$\frac{4\pi S^2}{\lambda^2}$
Cylinder, diameter = $d$ , length = $l$	Axis of cylinder parallel to electric field, $\lambda \ll d, \lambda \ll l$	$\frac{\pi d l^2}{\lambda}$
Matched load dipole	Oriented parallel to the incident electric field	$\frac{9\lambda^2}{16\pi}$
Shorted dipole	Oriented parallel to the incident electric field	$\frac{9\lambda^2}{4\pi}$
Corner reflector		$\frac{4\pi S^2}{\lambda^2}$
		$S = \text{cross section of triply reflected beam}$
Triangular corner reflector	$L = \text{length of reflector's edge.}$ $\theta = \text{angle between direction of incidence and axis of symmetry of reflector}$	$\frac{4\pi L^4}{3\lambda^2}(1 - 0.0076\theta^2)$
Square corner reflector		$\frac{12\pi L^4}{\lambda^2}(1 - 0.0274\theta)$

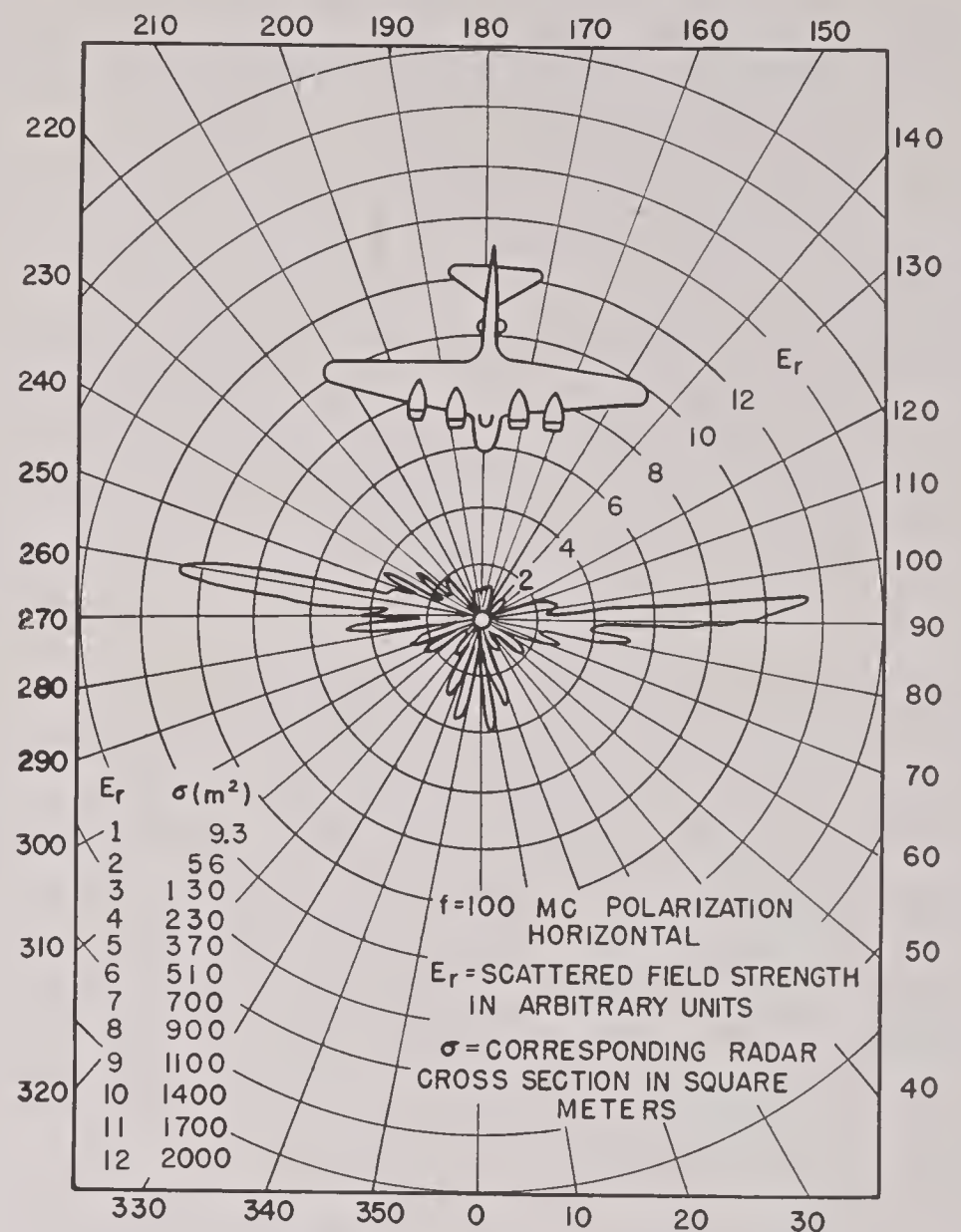


FIGURE 1. Aspect diagram of a B-17E at 5 degrees above horizon.

are independent of wavelength. This result may be interpreted to mean that a plane in motion behaves more or less like a collection of good reflecting surfaces oriented at random. It is worth noting in this connection that the radar cross section of a circular plate of radius  $a$ , whose normal is at an angle  $\theta$  with the direction of incidence, is

$$\sigma = \pi a^2 \left[ \cot \theta \times J_1 \left( \frac{4\pi a}{\lambda} \sin \theta \right) \right]^2, \quad (8)$$

TABLE 2. Airplane radar cross sections.

Airplane	$\sigma$ , sq m	$\sigma$ , sq ft
SNC	3.9	42
SNJ	5.0	54
OS-2U	9.5	100
Taylorcraft	9.5	100
CESSNA	9.5	100
O-47	10	110
AT-11	11	120
SWB	13	140
15-D (Curtiss Wright)	23	250
J2F	25	260
JRF	30	320
PBY	31	340
B-18	36	380
B-17	45	480
B-29	67	710

Diagrams showing the dependence of  $\sigma$  on the orientation of the aircraft indicate very large and irregular fluctuations. The radar cross section can change by 100 to 1 with a change of aspect of only a few degrees. These varying values of the radar cross section are dependent on wavelength, polarization, details of plane design, etc. Reflection patterns such as shown in Figure 1 have been measured in the laboratory for a few simplified models. Actually an observer would see only the time average of the radar cross section of a plane, and it is only this average value which is of operational importance.

Table 2 gives measured values of  $\sigma$  for various aircraft. These are the values to be used in equation (6). As far as is known, these empirical cross sections



where  $J_1$  is the first order Bessel function of the first kind. The maximum of  $\sigma$  occurs for  $\theta = 0$ , when equation (8) reduces to

$$\sigma = \frac{4\pi^3 a^4}{\lambda^2}. \quad (9)$$

This sharp maximum of  $\sigma$  at  $\theta = 0$  is the phenomenon of specular reflection. The average value of  $\sigma$  over all values of  $\theta$  turns out to be

$$\sigma_{\text{avg}} = \frac{1}{2}\pi a^2. \quad (10)$$

This result is independent of wavelength and suggests that a large number of specularly reflecting surfaces oriented at random will have a cross section independent of  $\lambda$ , or that a few surfaces of rapidly changing orientation may have this property. The lack of dependence of wavelength of aircraft radar cross sections might be understood on the basis of these results.

10.3

### SHIP TARGETS

A ship being a collection of both complicated and flat surfaces, a rigorous computation of the radar cross section of any given ship of known design is not feasible. Nevertheless, the Naval Research Laboratory workers have been able to give a good account of these problems.<sup>374,376,388,392,417,421</sup>

The path factor in the formula (6) raised to the fourth power is

$$A_p^4 = 6 \left[ 1 - \frac{\sin \delta_0}{3\delta_0} (4 - \cos \delta_0) \right], \quad (11)$$

where

$$\delta_0 = \frac{4\pi h_1 H}{\lambda d},$$

$h_1$  = antenna height,

$H$  = height of ship above water including superstructure.

The above result follows by integrating the received power over the height  $H$ , assuming perfect reflection from sea.

It is seen in equation (11) that whether  $\delta_0 < \pi$ , the region called the "far zone," or  $\delta_0 > \pi$ , the "near zone" (short ranges), materially affects the qualitative behavior of the factor  $A_p^4$ . In the latter region

$$A_p^4 \cong 6.$$

The radar cross section of a ship which does not exhibit marked specular reflection is given roughly by

$$\sigma = \alpha \frac{B^2 H}{\lambda}, \quad (12)$$

where  $\alpha$  = dimensionless constant dependent on ship design,

$B$  = the breadth of the aspect under observation,

$H$  = height of ship above water including superstructure.

The approximate values of  $\alpha$  to be used are indicated in Table 3.

TABLE 3. Ship targets.

Type of ship	$\alpha$	Remarks
Battleship	0.1	
Cruiser	0.1	
Aircraft carrier	0.05	Except at direct broadside aspect
Submarine	0.01	

In Tables 4 to 7, values of  $\sigma$  computed from equation (12) are called theoretical values. Experimental values are computed from observations made by the Naval Research Laboratory workers with each quantity the mean of several observations. The 200-mc experimental result is unexpectedly low while the values at the higher frequencies are a little higher than would be anticipated. This points to the existence of some specular reflection for this ship, which would not be surprising in view of its great size. Considering the uncertainty in the experimental values, the agreement with the theoretical results is not unsatisfactory and bears out the assumed dependence on wavelength.

The aircraft carrier shows pronounced specular reflection at the direct broadside aspect, particularly at the higher frequencies. These values of  $\sigma$  are

TABLE 4. Radar cross section of a battleship (BB-63), broadside aspect.  $\alpha = 0.1$ ,  $B = 270$  m,  $H = 24$  m.

$f(\text{mc})$	$\sigma$ (exp), sq m	$\sigma$ (theory), sq m
200	$0.12 \times 10^5$	$1.9 \times 10^5$
700	$10.2 \times 10^5$	$6.8 \times 10^5$
970	$15. \times 10^5$	$9.4 \times 10^5$
3,060	$110. \times 10^5$	$30. \times 10^5$

TABLE 5. Radar cross section of a cruiser (CL-87), broadside aspect.  $\alpha = 0.1$ ,  $B = 180$  m,  $H = 24$  m.

$f(\text{mc})$	$\sigma$ (exp), sq m	$\sigma$ (theory), sq m
100	$2.45 \times 10^4$	$2.6 \times 10^4$
200	$5.06 \times 10^4$	$5.2 \times 10^4$
700	$7.79 \times 10^4$	$18.1 \times 10^4$
970	$28.4 \times 10^4$	$25.1 \times 10^4$
3,060	$102.2 \times 10^4$	$79.3 \times 10^4$



TABLE 6. Radar cross section of submarine (SS-171), broadside aspect.  $\alpha = 0.01$ ,  $B = 83$  m,  $H = 7.6$  m.

$f(\text{mc})$	$\sigma(\text{exp})$ , sq m	$\sigma(\text{theory})$ , sq m
200	$3.0 \times 10^2$	$3.5 \times 10^2$
700	$18.7 \times 10^2$	$12.2 \times 10^2$
3,060	$71.4 \times 10^2$	$53.4 \times 10^2$

 TABLE 7. Radar cross section of aircraft carrier (CV-36), near broadside aspect.  $\alpha = 0.05$ ,  $B = 250$  m,  $H = 46$  m.

$f(\text{mc})$	$\sigma(\text{exp})$ , sq m	$\sigma(\text{theory})$ , sq m
200	$0.22 \times 10^5$	$0.96 \times 10^5$
700	$2.6 \times 10^5$	$3.4 \times 10^5$
970	$6.3 \times 10^5$	$4.6 \times 10^5$
3,060	$11.3 \times 10^5$	$14.4 \times 10^5$

typical of the ship for aspects other than direct broadside.

In Table 8, the same ship is analyzed at direct broadside. No theoretical calculation of  $\sigma$  has been attempted because of a lack of sufficient data from other ships of this type. The column  $\lambda^2 \sigma$  is near

TABLE 8. Radar cross section of aircraft carrier (CV-36), direct broadside aspect.

$f(\text{mc})$	$\sigma(\text{exp})$ , sq m	$\lambda^2 \sigma(\text{exp})$
200	$0.055 \times 10^7$	$1.2 \times 10^6$
700	$1.0 \times 10^7$	$1.8 \times 10^6$
970	$5.0 \times 10^7$	$4.8 \times 10^6$
3,060	$7.1 \times 10^7$	$7.1 \times 10^6$

enough to a constant to indicate the existence of specular reflection. Since the hull at broadside can be considered as a flat surface, specular reflection is to be expected under normal incidence with a radar cross section proportional to  $1/\lambda^2$  as indicated by equation (9).

In view of the complicated reflecting properties of targets of operational interest, it may be said that the experimental results can be considered as being in fair agreement with theoretical predictions.

#### 10.4 ABSORPTION AND SCATTERING BY CLOUDS, FOG, RAIN, HAIL, AND SNOW

The theory of the scattering and absorption of microwaves by a collection of spherical particles of known concentration, size, distribution, and given dielectric properties was completely worked out before systematic experimental work was done on these phenomena.<sup>258, 277, 279</sup> The electromagnetic theory predicts that the total scattering cross section of a sphere of given electrical properties is

$$S = \frac{\lambda^2}{2\pi} \sum_{n=1}^{\infty} (2n+1) (|a_n|^2 + |b_n|^2) \text{ cm}^2, \quad (13)$$

where  $\lambda$  is the wavelength in centimeters of the incident radiation in air and  $a_n$  and  $b_n$  are the so-called scattering amplitudes associated with the magnetic and electric  $2n$ -poles induced in the sphere by the incident electromagnetic field. Similarly the absorption cross section of a sphere defined as the ratio of the total power removed from the incident beam both by "internal absorption" (heating) and by scattering is

$$A = \frac{\lambda^2}{2\pi} (-\text{Re}) \sum_{n=1}^{\infty} (2n+1) (a_n + b_n) \text{ cm}^2. \quad (14)$$

Here Re means "Real part of . . . ." The complex scattering amplitudes depend on the dielectric constants of the sphere, its diameter, and the wavelength of the incident radiation. The observations which are available seem to indicate that a collection of spherical particles with random distribution scatter microwaves incoherently, although under certain circumstances, existing for very short time intervals, they may scatter coherently.<sup>419</sup> On the assumption of incoherent scattering, given a collection of spherical particles of diameters  $D_1, D_2, \dots, D_k, \dots, D_n$ , whose number per unit volume or cc is  $n_1, n_2, \dots, n_k, \dots, n_n$ , the scattering cross section of such a collection per unit volume or the absorption coefficient due to scattering is

$$\alpha_s = 4.343 \times 10^5 \sum_{i=1}^n n_i S_i \text{ db/km}, \quad (15)$$

where  $S_i$  is the scattering cross section of one drop of diameter  $D_i$  centimeters, and the summation extends over all possible drops present in the collection. Similarly, the "absorption coefficient" or "attenuation" associated with the absorption cross section  $A_i$  (sphere of diameter  $D_i$ ) defined by equation (14) is

$$\alpha_a = 4.343 \times 10^5 \sum_{i=1}^n n_i A_i \text{ db/km}. \quad (16)$$

#### RAIN AND HAIL ABSORPTION

In order to compute the theoretical absorption coefficient of a rain or thunderhead (heavy storm cloud) one has to know the raindrop size distribution, since the computation of the cross sections for one spherical drop is straightforward provided its dielectric properties are known. The greatest uncertainties



in the theoretical predictions of scattering or absorption by rain are due to the relatively limited knowledge of drop size distributions in rains of different rates of fall. There is no evidence that a rain with a known rate of fall has a unique drop size distribution though the latest studies on this problem seem to indicate that a certain most probable drop size distribution can be attached to a rain of given rate of fall.<sup>446</sup> Results of this study are included in Table 9. On the basis of these results the absorption cross

TABLE 9. Drop size distribution.

$p$ , mm/hr	Percentage of total volume							
	0.25	1.25	2.5	12.5	25	50	100	150
$D$ , cm								
0.05	28.0	10.9	7.3	2.6	1.7	1.2	1.0	1.0
0.10	50.1	37.1	27.8	11.5	7.6	5.4	4.6	4.1
0.15	18.2	31.3	32.8	24.5	18.4	12.5	8.8	7.6
0.20	3.0	13.5	19.0	25.4	23.9	19.9	13.9	11.7
0.25	0.7	4.9	7.9	17.3	19.9	20.9	17.1	13.9
0.30		1.5	3.3	10.1	12.8	15.6	18.4	17.7
0.35		0.6	1.1	4.3	8.2	10.9	15.0	16.1
0.40		0.2	0.6	2.3	3.5	6.7	9.0	11.9
0.45			0.2	1.2	2.1	3.3	5.8	7.7
0.50				0.6	1.1	1.8	3.0	3.6
0.55				0.2	0.5	1.1	1.7	2.2
0.60					0.3	0.5	1.0	1.2
0.65						0.2	0.7	1.0
0.70								0.3

section of raindrops of different size has been computed for use in Table 10. This table gives the decibel attenuation per kilometer in rains of different rates of fall and for radiation of wavelengths between 0.3 and 10 cm. In Table 11, similar to Table 10, another set of results is contained for rains of measured drop size distributions. This table is extended to include radiations of wavelengths up to 100 cm. It seems equally interesting to give a graphical representation of those results. Figure 2 corresponds to Table 10 and Figure 3 to Table 11. All these data refer to raindrops at 18 C.

TABLE 10. Attenuation in decibels per kilometer for different rates of precipitation of rain. Temperature 18 C,  $\lambda$  in cm.<sup>277</sup>

$p$ , mm/hr	Attenuation, db/km.								
	$\lambda = 0.3$	$\lambda = 0.4$	$\lambda = 0.5$	$\lambda = 0.6$	$\lambda = 1.0$	$\lambda = 1.25$	$\lambda = 3.0$	$\lambda = 3.2$	$\lambda = 10$
0.25	0.305	0.230	0.160	0.106	0.037	0.0215	0.00224	0.0019	0.0000997
1.25	1.15	0.929	0.720	0.549	0.228	0.136	0.0161	0.0117	0.000416
2.5	1.98	1.66	1.34	1.08	0.492	0.298	0.0388	0.0317	0.000785
12.5	6.72	6.04	5.36	4.72	2.73	1.77	0.285	0.238	0.00364
25	11.3	10.4	9.49	8.59	5.47	3.72	0.656	0.555	0.00728
50	19.2	17.9	16.6	15.3	10.7	7.67	1.46	1.26	0.0149
100	33.3	31.1	29.0	27.0	20.0	15.3	3.24	2.80	0.0311
150	46.0	43.7	40.5	37.9	28.8	22.8	4.97	4.39	0.0481

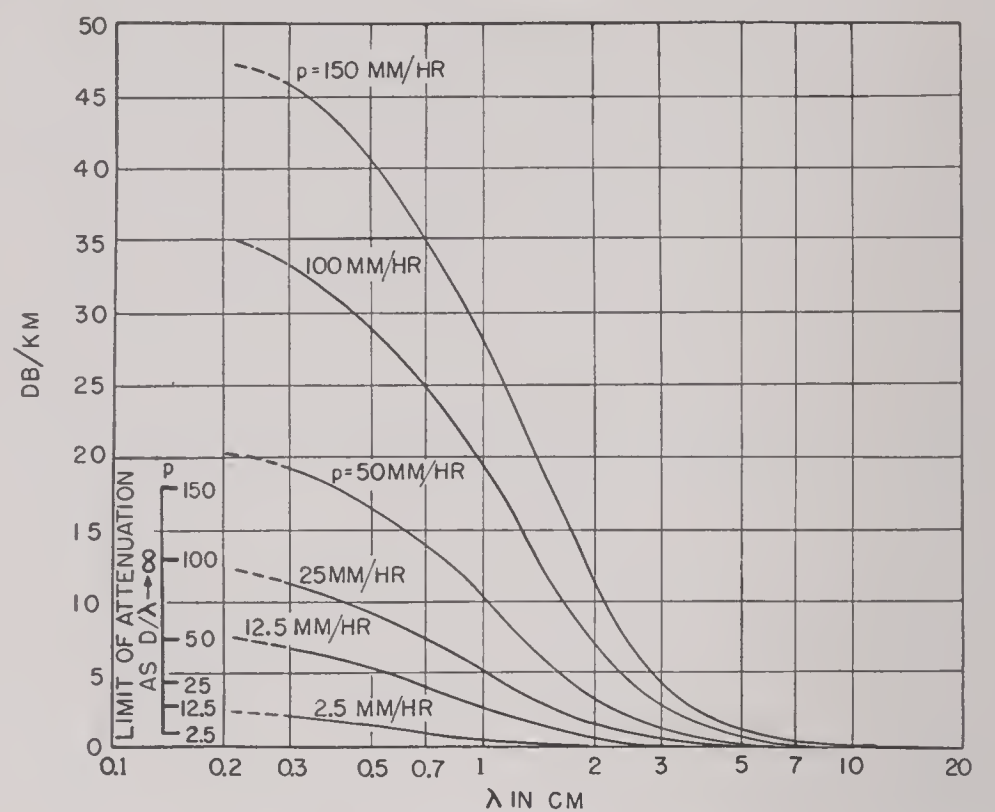


FIGURE 2. Graphical presentation of data given in Table 10.

Since the scattering coefficients  $a_n$  and  $b_n$  depend on the temperature, because of its effect on the dielectric properties of water, it seems important to evaluate the attenuation of rains whose drops are at temperatures different from those included in the preceding tables. Table 12 contains the necessary data relative to the changes of attenuation with temperature and is to be used primarily in connection with Table 10.

It will suffice to mention here that, for waves larger than about 3 cm, the attenuation produced by hail of the same water precipitation rate as a rain will be but a few per cent of the rain attenuation. At shorter waves, in the millimeter region, hail attenuation may become larger than that of rain. Similarly the attenuation of snow should be considerably less than rain; however, Canadian reports indicate approximately the same value for the same water content.

As mentioned above, the whole theory of attenuation is based on equation (14). The formulas giving



TABLE 11. Attenuation in rains of known drop size distribution and rate of fall (decibels per kilometer).

mm/hr	Wavelength $\lambda$ , cm										Distribution		
	1.25		3		5		8		10			15	
2.46	1.93	$10^{-1}$	4.92	$10^{-2}$	4.24	$10^{-3}$	1.23	$10^{-3}$	7.34	$10^{-4}$	2.80	$10^{-4}$	A
4.0	3.18	$10^{-1}$	8.63	$10^{-2}$	7.11	$10^{-3}$	2.04	$10^{-3}$	1.19	$10^{-3}$	4.69	$10^{-4}$	C
6.0	6.15	$10^{-1}$	1.92	$10^{-1}$	1.25	$10^{-2}$	3.02	$10^{-3}$	1.67	$10^{-3}$	5.84	$10^{-4}$	D
15.2	2.12		6.13	$10^{-1}$	5.91	$10^{-2}$	1.17	$10^{-2}$	5.68	$10^{-3}$	1.69	$10^{-3}$	E
18.7	2.37		8.01	$10^{-1}$	5.13	$10^{-2}$	1.10	$10^{-2}$	6.46	$10^{-3}$	1.85	$10^{-3}$	F
22.6	2.40		7.28	$10^{-1}$	5.29	$10^{-2}$	1.21	$10^{-2}$	6.96	$10^{-3}$	2.27	$10^{-3}$	G
34.3	4.51		1.28		1.12	$10^{-1}$	2.32	$10^{-2}$	1.17	$10^{-2}$	3.64	$10^{-3}$	H
43.1	6.17		1.64		1.65	$10^{-1}$	3.33	$10^{-2}$	1.62	$10^{-2}$	4.96	$10^{-3}$	I

mm/hr	Wavelength $\lambda$ , cm										Distribution
	20		30		50		75		100		
2.46	1.52	$10^{-4}$	6.49	$10^{-5}$	2.33	$10^{-5}$	1.03	$10^{-5}$	5.85	$10^{-6}$	A
4.0	2.53	$10^{-4}$	1.08	$10^{-4}$	3.88	$10^{-5}$	1.72	$10^{-5}$	9.75	$10^{-6}$	C
6.0	3.02	$10^{-4}$	1.25	$10^{-4}$	4.34	$10^{-5}$	1.93	$10^{-5}$	1.09	$10^{-5}$	D
15.2	7.85	$10^{-4}$	2.95	$10^{-4}$	9.23	$10^{-5}$	4.15	$10^{-5}$	2.35	$10^{-5}$	E
18.7	9.09	$10^{-4}$	3.60	$10^{-4}$	1.20	$10^{-4}$	5.36	$10^{-5}$	3.03	$10^{-5}$	F
22.6	1.17	$10^{-3}$	4.81	$10^{-4}$	1.66	$10^{-4}$	7.41	$10^{-5}$	4.19	$10^{-5}$	G
34.3	1.75	$10^{-3}$	6.83	$10^{-4}$	2.24	$10^{-4}$	9.95	$10^{-5}$	5.63	$10^{-5}$	H
43.1	2.29	$10^{-3}$	8.71	$10^{-4}$	2.78	$10^{-4}$	1.23	$10^{-4}$	6.98	$10^{-5}$	I

the amplitudes  $a_n$  and  $b_n$  are too complicated to be reproduced here. Their numerical evaluation for spherical drops of given size and temperature is

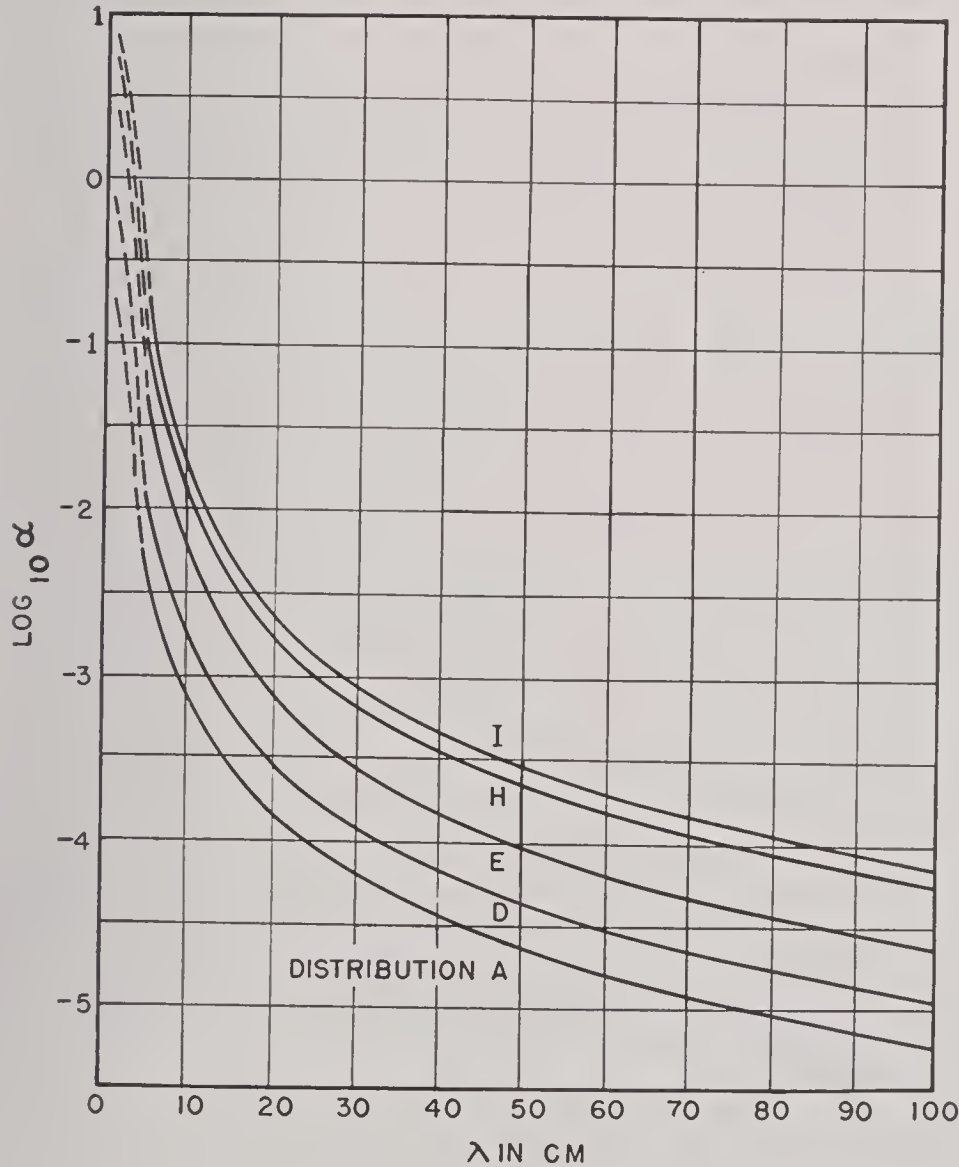


FIGURE 3. Attenuation in rains of known drop-size distribution as a function of the wavelength  $\lambda$  in centimeters. The ordinate scale gives  $\log_{10} \alpha$ , where the attenuation constant  $\alpha$  is expressed in decibels per kilometer. The letters on the curves refer to the drop size distributions given in Table 11.

quite laborious except for small values of the parameter  $\pi D/\lambda$ . They involve Bessel and Hankel functions of half-integer order of the parameter  $\pi D/\lambda$ .

A series of experimental results are given in Table 13. These results are to be regarded as maximum attenuation values.

If these results are compared with those of Table 10 and Figure 2 one sees that, in view of the uncertainty in the temperature of the raindrops and their size distribution, the agreement between theoretical

TABLE 12

Rate of precipitation, mm/hr	$\lambda$ , cm	Correction factor $\theta$ ( $T$ )				
		$T = 0$ C	$T = 10$ C	$T = 18$ C	$T = 30$ C	$T = 40$ C
0.25	0.5	0.85	0.95	1.0	1.02	0.99
	1.25	0.95	1.0	1.0	0.90	0.81
	3.2	1.21	1.10	1.0	0.79	0.55
	10.0	2.01	1.40	1.0	0.70	0.59
2.5	0.5	0.87	0.95	1.0	1.03	1.01
	1.25	0.85	0.99	1.0	0.92	0.80
	3.2	0.82	1.01	1.0	0.82	0.64
	10.0	2.02	1.40	1.0	0.70	0.59
12.5	0.5	0.90	0.96	1.0	1.02	1.00
	1.25	0.83	0.96	1.0	0.93	0.81
	3.2	0.64	0.88	1.0	0.90	0.70
	10.0	2.03	1.40	1.0	0.70	0.59
50	0.5	0.94	0.98	1.0	1.01	1.00
	1.25	0.84	0.95	1.0	0.95	0.83
	3.2	0.62	0.87	1.0	0.99	0.81
	10.0	2.01	1.40	1.0	0.70	0.58
150	0.5	0.96	0.98	1.0	1.01	1.00
	1.25	0.86	0.96	1.0	0.97	0.87
	3.2	0.66	0.88	1.0	1.03	0.89
	10.0	2.00	1.40	1.0	0.70	0.58



TABLE 13. Experimental values of the maximum attenuation per unit precipitation rate.

$\lambda$ , cm	$(\alpha/p)$ db per km/min per hr	References
0.62	0.37	269
0.96	0.15	256
1.089	0.2	262
1.25	0.19	176
	0.09-0.40	276
	0.63	281
3.2	0.032-0.042	261

and observed values is, on the whole, satisfactory. It will be seen that the results reported on K-band rain attenuation in Hawaii by the U. S. Navy Radio and Sound Laboratory workers<sup>281</sup> are higher than those observed by other workers on the same wavelength. The orographic character of these Hawaiian rains which were made up of drops falling about 300 m instead of ordinary rains falling 1,500 to 2,000 m may be one of the reasons for this divergent result.

#### CLOUDS AND FOG

Observations indicate that fair weather clouds and fog are composed of droplets whose diameters do not seem to exceed 0.02 cm. Under these conditions the attenuation formula takes on a remarkably simple form since it becomes independent of the drop size distribution. The attenuation formula in this limit of very small values of the parameter  $\pi D/\lambda$  is

$$\alpha_{ab} = \frac{4.092 m c_1}{\lambda} \text{ db/km}, \quad (17)$$

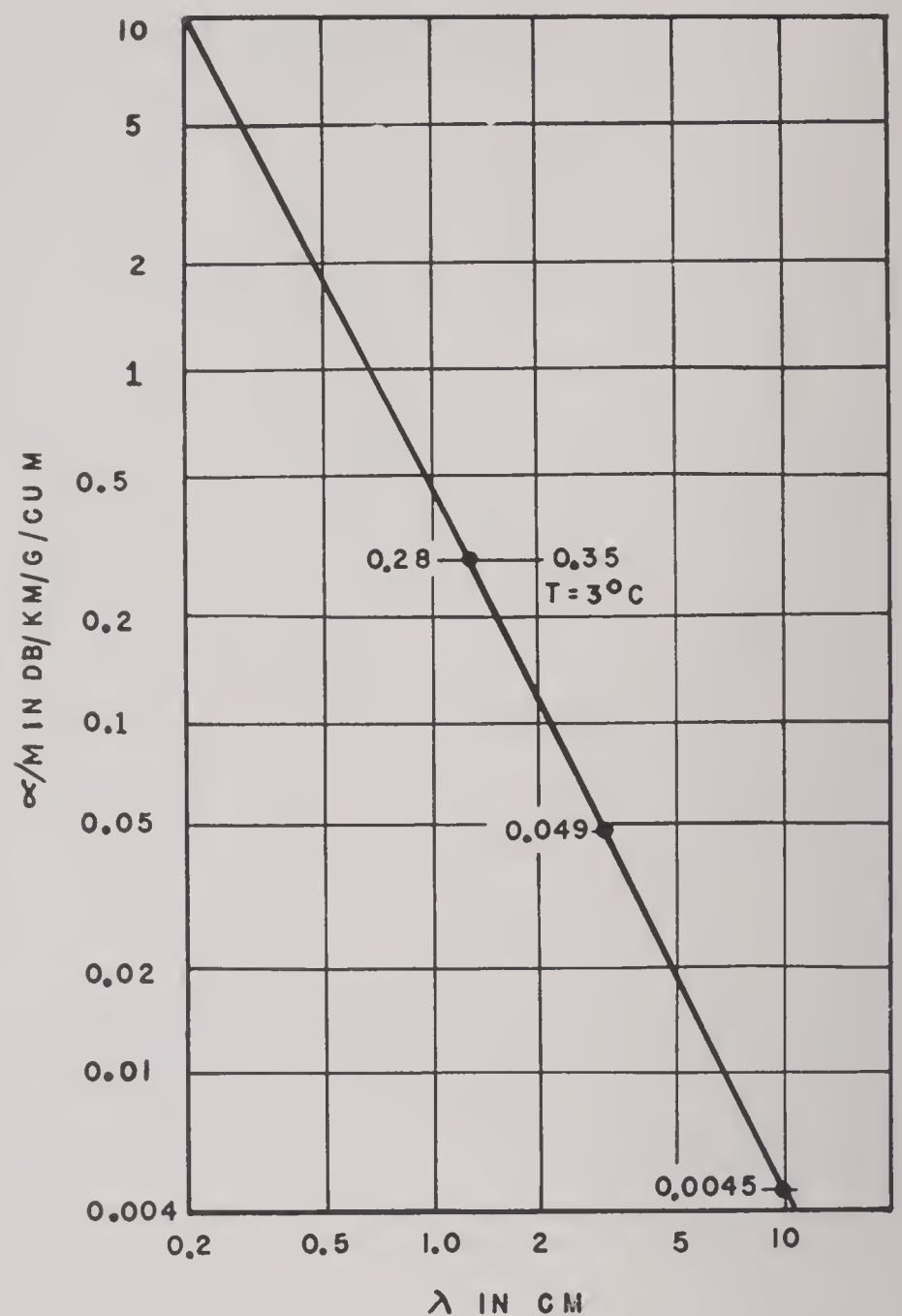
where  $m$  is the mass of liquid water per cubic meter,  $\lambda$  is the wavelength of the radiation in centimeters, and

$$c_1 = \frac{6\epsilon_1}{(\epsilon_r + 2)^2 + \epsilon_i^2}, \quad (18)$$

where  $\epsilon_r$  and  $\epsilon_i$  are the real and imaginary parts of the dielectric constant of water at the temperature in question and for radiation of wavelength  $\lambda$ . Figure 4 represents the attenuation in clouds and fog in the range 0.2 to 10 cm. This graph corresponds to a

TABLE 14. Attenuation in decibels per kilometer for ice crystal clouds.

Shape of crystals	$T = -40^\circ \text{C}$	$T = 0^\circ \text{C}$
Spherules	0.00044 $m/\lambda$	0.0035 $m/\lambda$
Needles	0.00062 $m/\lambda$	0.0050 $m/\lambda$
Disks	0.00087 $m/\lambda$	0.0070 $m/\lambda$

FIGURE 4. Attenuation factor in liquid clouds and fogs.  $T = 18^\circ \text{C}$ .

liquid water concentration of 1 g per cu m, which is undoubtedly rather high. Actually, the observations indicate that the liquid water concentrations in clouds and fog rarely exceed 0.6 g per cu m.

To this may be added the Table 14 for attenuation by ice clouds. In ice clouds  $m$  will rarely exceed 0.5 and will often be less than 0.1 g per cu m.

#### SCATTERING (ECHO)

If we denote by  $\sigma(\pi)$  the back-scattering cross section per unit solid angle of a spherical water drop and if there is a distribution  $n_1, n_2, \dots, n_k, \dots, n_n$  drops per cubic meter, the cloud or rain cross section for scattering is

$$S(\pi) = \sum n_i \sigma_i(\pi) \Delta V \quad (19)$$

where  $\Delta V$  is the scattering volume of the cloud, on the assumption of incoherent scattering on account of the random character of the drop distribution. The summation includes all the drop groups. The



rain front is usually wider than the irradiated area so that the radar beam intersects it. Under these conditions, taking  $\Delta V$  approximately as a spherical shell of thickness  $\Delta d$ , at a distance  $d$  from the radar set, and denoting by  $2\theta$  the half-power beam width of the radar beam, one gets

$$\Delta V = 2\pi d^2 (1 - \cos \theta) \Delta d. \quad (20)$$

The rain echo cross section is then

$$S(\pi) = 2\pi d^2 (1 - \cos \theta) \left( \Delta d \sum_i n_i \sigma_i(\pi) \right). \quad (21)$$

Remembering that  $\sigma_i(\pi)$  or  $S(\pi)$  is precisely the cross section per unit solid angle in the direction of the radar set, one gets instead of equation (6) for the ratio of received to transmitted power

$$\frac{P_2}{P_1} = \frac{G_1 G_2}{4} \left( \frac{3\lambda}{8d} \right)^2 \theta^2 \left( \Delta d \sum_i n_i \sigma_i(\pi) \right) \quad (22)$$

for small angles  $\theta$  which must be given in radians.

TABLE 15. Fraction of incident power scattered backward by a layer of 1 km of rain in different types of rain. (Decibels)

Drop size distrib- ution*	$p$ , mm/hr	Wavelength in centimeters							
		3	5	8	10	15	20	30	50
A	2.46	-45	-54	-61	-65	-72	-77	-84	-93
D	6.0	-38	-46	-54	-58	-65	-69	-76	-85
E	15.2	-32	-37	-45	-48	-55	-61	-68	-77
H	34.3	-29	-35	-42	-46	-53	-58	-65	-74
I	43.1	-27	-33	-40	-44	-51	-56	-63	-71

\*See Table 11 for drop size distributions.

The quantity  $[\Delta d \sum_i n_i \sigma_i(\pi)]$  or its value in decibels for known drop size distributions has been tabulated in Table 15. With this table and the known characteristics of a radar set the ratio  $P_1/P_2$  can be computed at once. In the table  $\Delta d$  is taken as 1 km. Since the maximum thickness  $\Delta d$  cannot exceed the pulse length, the values found in the table can be adapted immediately to any pulse length  $l$  by adding to it  $(10 \log_{10} l)$ ,  $l$  being expressed in kilometers. Using equation (22) for particular radar sets it is found that the theoretically computed echo powers from rains agree well with the observed values, if the uncertainties of the meteorological knowledge of the echoing elements, which are mostly rains and storm clouds, is kept in mind. As expected, the echoing power of snow is very much less than that of rain. The systematic observations on S band by the

Canadian group<sup>402, 422</sup> and on X band by Bent<sup>424</sup> clearly indicate that precipitation either in the form of rain or snow is necessary to produce an echo on the scope of the radar set.

#### ABSORPTION BY THE ATMOSPHERIC GASES

It was predicted that oxygen and water vapor will absorb electromagnetic waves in the microwave range.<sup>259, 275</sup> In particular, oxygen was predicted as having a resonance band around 5 mm and one line at 2.5 mm, while the water vapor absorption is caused mainly by a single rotational line of relatively small strength around 1 cm. Experiments have confirmed both these absorption effects.<sup>272, 273</sup> In Figure 5, the

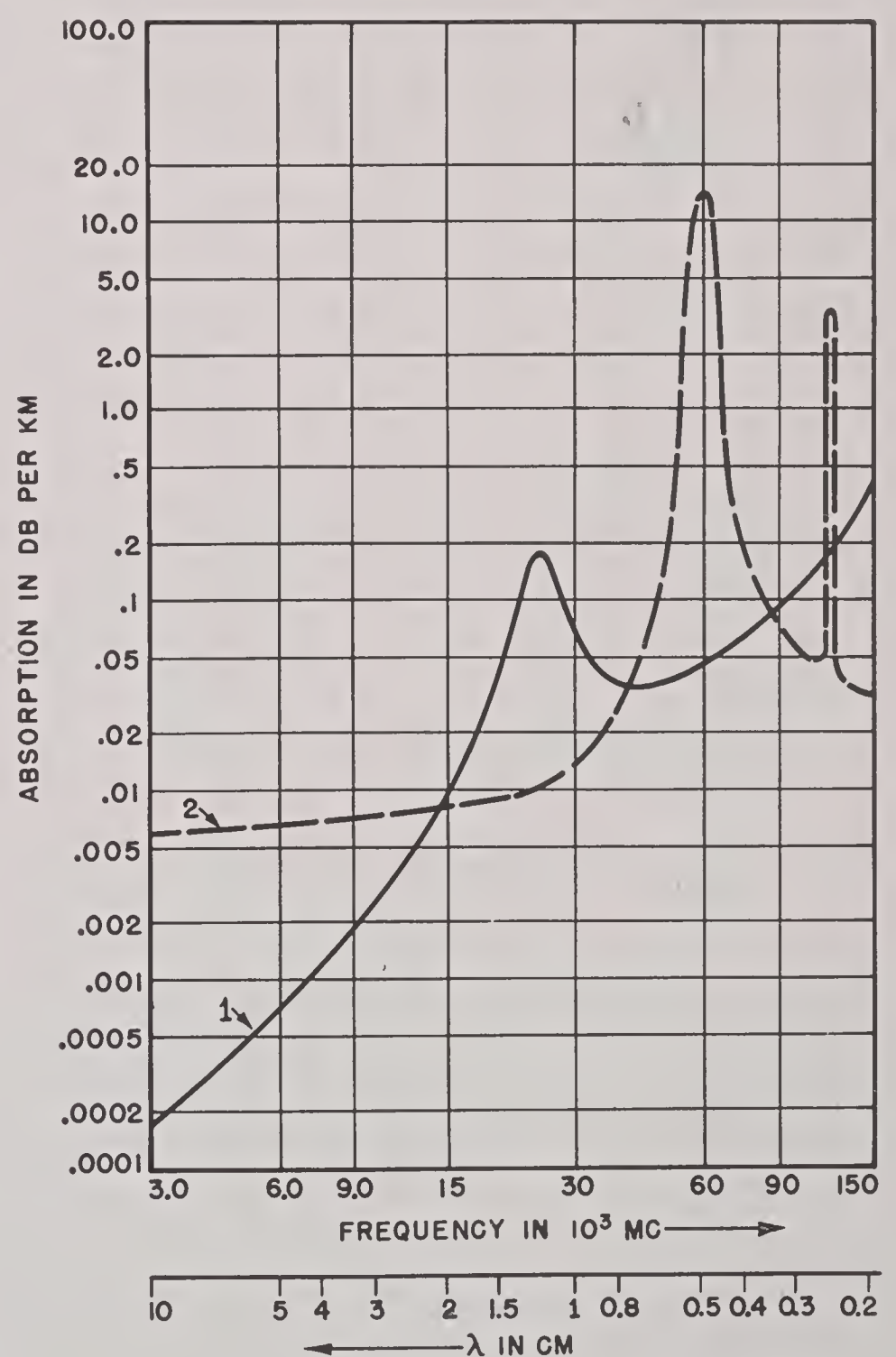


FIGURE 5. (1) Absorption due to water vapor in an atmosphere at 76-cm pressure containing 1 per cent water molecules, or 7.5 g per cu m. The water resonance line is assumed to be at 24,000 mc, and its half width at half maximum (line breadth) is 3,000 mc. (2) Absorption due to oxygen in an atmosphere at 76-cm pressure whose resonance band at 60.10<sup>3</sup> mc is supposed to have a line breadth of 600 mc.



individual oxygen and water vapor attenuation curves have been plotted in the 0.2- to 10-cm wavelength range. Any change in the water vapor content from the one adopted for this graph (7.5 g per cu m or 6.5 g per kg of air) or the total pressure can be taken into account in computing the combined oxygen and water vapor attenuations, since these

at 76-cm pressure, with the same water vapor content as the curve of Figure 5. Curves 2, 3, and 4 are additional rain attenuation curves computed for a moderate rain of rainfall 6 mm per hr, a heavy rain of 22 mm per hr and an excessive rain of 43 mm per hr, which is of cloudburst proportions. In any rain the result of total attenuation is the sum of the oxygen, water vapor, and liquid drop attenuation.

It is thus seen that for waves of 3 cm or shorter the rain attenuation may become prohibitive, whereas the gaseous attenuation loses its practical importance at waves longer than about 2 cm. In this connection it is to be noted that for millimeter waves the rain attenuation begins to level off at waves of a few millimeters, as Table 10 indicates, and would actually decrease at waves shorter than 1 mm. However in this range, the water vapor absorption due to the strong water lines situated at much shorter waves becomes more and more intense, and communication or radar on these bands is almost totally excluded. It is worth noting in this connection that using radiation which is strongly absorbed might, in certain cases, be of great operational interest. In the oxygen band, for example, short-range communication could be achieved without any likely interference by the enemy.

Electromagnetic theory thus gives a satisfactory picture of the absorption and scattering phenomena of microwaves both by floating or falling water drops, or their equivalent in hail and snow, and by the oxygen and water vapor of the atmosphere.

Of the approximately 100 reports which were prepared by the Columbia University Wave Propagation Group or were presented at the second, third, and fourth conferences on propagation held in February 1944, November 1944, and May 1945, 61 have been selected for publication in the Summary Technical Report. Of these, 18 reports, covering standard and nonstandard propagation, are published in this volume; the remainder are published in Volume 2. The reports not included in these two volumes were omitted chiefly because their material was superseded by later documents.

The reports in the remainder of this volume appear in two sections. Chapters 11 through 15 are concerned with standard propagation; Chapters 16 through 27, with nonstandard propagation.

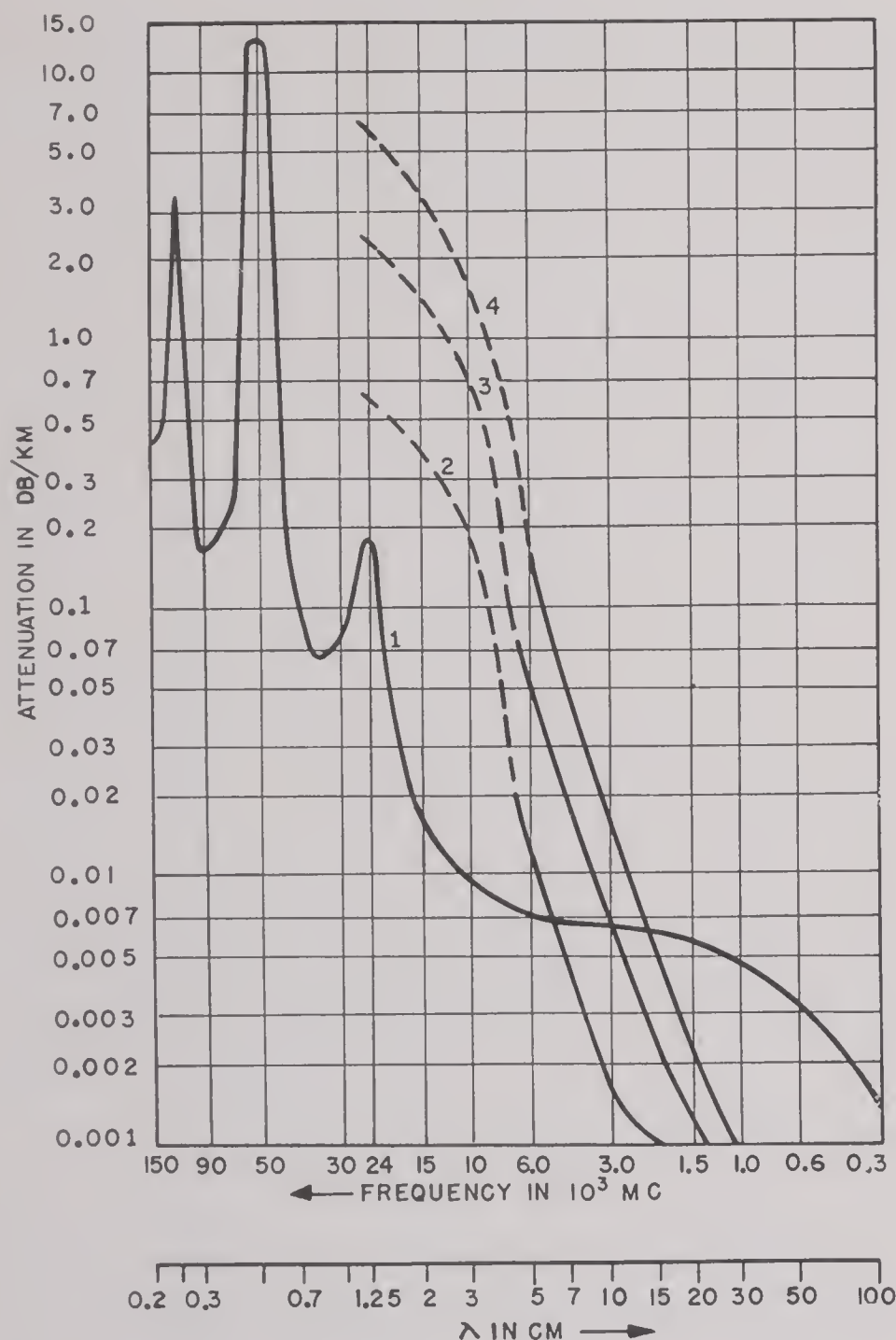


FIGURE 6. Atmospheric one-way attenuation. (1) Oxygen and water vapor (total for  $p = 76$  cm Hg,  $T = 20$  C, water vapor. = 7.5 g per cu m). (Van Vleck.) (2) Moderate rain (6 mm per hr) of known drop size distribution. (3) Heavy rain (22 mm per hr). (4) Rain of cloudburst proportion (43 mm per hr).

are proportional to the partial pressures of oxygen and water vapor. For practical purposes the effect of temperature variations can be neglected.

In Figure 6, curve 1, is plotted the total attenuation of oxygen plus water vapor in an atmosphere



*PART III*  
*CONFERENCE REPORTS ON STANDARD*  
*PROPAGATION*







## Chapter 11

### A GRAPHICAL METHOD FOR THE DETERMINATION OF STANDARD COVERAGE CHARTS<sup>a</sup>

THE POWER DENSITY at distance  $S$  from a transmitter of unit power depends upon  $h_1$  and  $h_2$ , the heights of the transmitting and receiving antennae, and upon  $\lambda$ , the wavelength of the radiation. For the high frequencies under discussion, we assume the earth to be a perfectly conducting sphere, of effective radius  $r$ , equal to  $\frac{2}{3}$  that of the earth. We are to take into account the so-called divergence factor  $D$  resulting from the earth's curvature.

Even with the simplifying assumptions above, one cannot express the power as a simple function of  $S$ ,  $h_1$ ,  $h_2$ , and  $\lambda$  in a single equation. Accordingly, most workers on this problem have introduced various arbitrary parameters, as intermediate steps. Differences in procedure lie primarily in the choice of parameters. Whether a method is simple or difficult depends upon the character of the parameters. Certain procedures suggested are satisfactory for determining the number of decibels by which the signal is below the adopted standard of  $1 \mu\text{w}$  per square meter, designated here by  $A$ ; but if we are given  $A$ ,  $h_1$ , and  $f$  and then are asked to compute  $h_2$  as a function of  $S$ , as for a coverage diagram, some of the methods become very unwieldy. The present method works satisfactorily for either case.

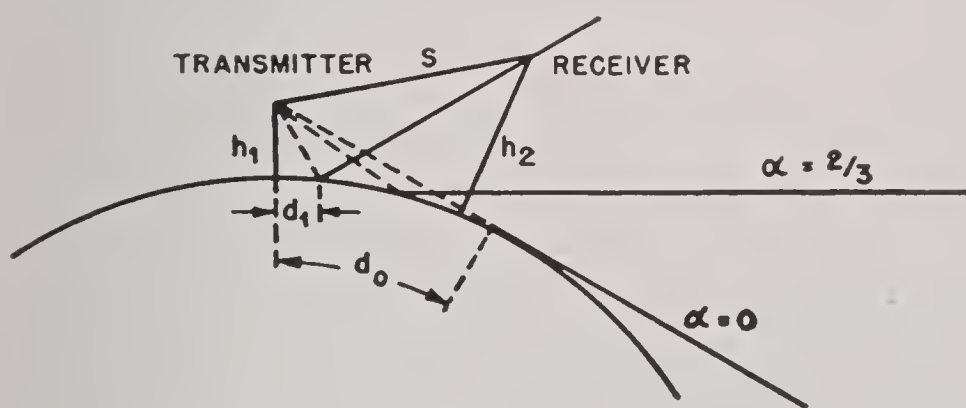


FIGURE 1. Geometry for determination of standard coverage.

In selecting a parameter we have been guided by the following conditions. The number of parameters should be kept to a minimum; the remaining variables  $h_1$ ,  $h_2$ , and  $S$  should appear in the final equations, if possible. Also it should be unnecessary to interchange transmitter and receiver according to

<sup>a</sup>By Lt. Comdr. D. H. Menzel, USNR, Office of the Chief of Naval Operations.

the condition that  $h_2$  is or is not greater than  $h_1$ .

The arbitrary parameter  $\alpha$  is defined as follows. Let  $d_1$  be the distance from the transmitter to the point at which the ray is reflected and  $d_0$  the distance to the point where a ray is tangent. Then

$$d_1^2 = d_0^2(1 - \alpha) = 2h_1r(1 - \alpha). \quad (1)$$

$\alpha$ , therefore, is constant along a reflected ray;  $\alpha = 0$  corresponds to the continuation of the tangent ray;  $\alpha = \frac{2}{3}$  corresponds to a reflected ray perpendicular to the mast of the transmitting antenna;  $\alpha = 1$  is the vertical ray. Thus

$$0 \leq \alpha \leq 1,$$

with  $\alpha > \frac{2}{3}$  over a large portion of the range of interest for the frequencies involved.

Equation (1) leads to the following relationship

$$S^2 + \frac{(-2 + 3\alpha)}{(1 - \alpha)^{\frac{1}{2}}} S \sqrt{2rh_1} + 2rh_1 \cdot (1 - 2\alpha) - 2rh_2 = 0, \quad (2)$$

an irreducible cubic in  $\alpha$ . It is this fact that makes the problem mathematically difficult and makes impossible the explicit elimination of  $\alpha$ .

Additional equations are

$$D^2 = \frac{\alpha}{4 - 3\alpha - 4\sqrt{2rh_1} S^{-1} (1 - \alpha)^{\frac{1}{2}}} \cong \frac{\alpha}{4 - 3\alpha}, \quad (3)$$

an approximation holding well over the region of interest since  $\alpha > \frac{2}{3}$ . The phase difference  $\Phi$ , resulting from the difference in optical path between the reflected and direct rays, is

$$\Phi = \frac{4\pi h_1^2 \alpha^2}{\lambda} \left[ \frac{1}{\sqrt{2rh_1(1 - \alpha)}} - \frac{1}{S} \right], \quad (4)$$

and for the transmitted power

$$10^{-A/10} = \frac{10^6}{\pi} \frac{1}{S^2} \left[ \frac{(1 - D)^2}{4} + D \sin^2 \frac{\Phi}{2} \right]. \quad (5)$$

Here we have four equations. If  $h_1$ ,  $\lambda$ , and  $A$  are specified, there remain five unknowns:  $D$ ,  $\Phi$ ,  $\alpha$ ,  $h_2$ , and  $S$ . Thus we should be able theoretically to elimi-



nate all but  $h_2$  and  $S$ , defining our coverage diagram.

We may substitute the approximate value for  $D$  into equation (5) and also use equation (4) to eliminate  $S$  from the equation

$$10^{-A/20} = \frac{10^3}{\pi} \left[ \frac{1}{\sqrt{2rh_1(1-\alpha)}} - \frac{\lambda\Phi}{4\pi h_1^2 \alpha^2} \right] \times \left\{ \left[ \frac{1 - \left( \frac{\alpha}{4-3\alpha} \right)^{\frac{1}{2}}}{4} \right]^2 \left[ \frac{\alpha}{(4-3\alpha)} \right]^{\frac{1}{2}} \sin^2 \Phi \right\}^{\frac{1}{2}} \quad (6)$$

We may now set

$$\Phi = \left( n - \frac{1}{2} \right) \pi ; \quad n = 1, 2, 3, \dots \quad (7a)$$

which correspond to the maxima of the lobes. We may alternatively take

$$\Phi = n\pi , \quad (7b)$$

corresponding to lobe minima or, more generally

$$\Phi = (n + b) \pi \quad (7c)$$

to represent any specific position on the lobe.

With  $A$ ,  $h_1$ ,  $\lambda\Phi$ , and  $\alpha$  as variables, we may throw equation (6) into the form of a nomogram, from which we determine  $\alpha$ , first for the lobe tips, second for the minima, and third for as many intermediate points as are necessary.

With the  $\alpha$ 's so determined, proceed to equation (4), also in nomographic form, to get  $S$ . Finally, use

equation (2), to determine  $h_2$ . This equation can also be thrown into nomographic form if we set

$$\frac{S^2}{2r} - h_2 = h'_2 \quad (8)$$

where  $h'_2$  is measured vertically from the line tangent to the base of the transmitter.

Another somewhat simpler type of coverage diagram is possible. If we take

$$10^{-A^*/10} = \frac{10^6}{4\pi S^2} \quad (9)$$

as defining the intensity for a transmitter in free space, we get for the ratio of the two

$$10^{-(A-A^*)/10} = 10^{B/10} = \left[ 1 - \left( \frac{\alpha}{4-3\alpha} \right)^{\frac{1}{2}} \right]^2 + 4 \left( \frac{\alpha}{4-3\alpha} \right)^{\frac{1}{2}} \sin^2 \frac{\Phi}{2}, \quad (10)$$

where  $B$  is the number of decibels by which the actual field exceeds the free space value. Coverage diagrams of this type consist of lines radiating from the transmitter, rather than contours. For non-standard propagation the drawings have some complications, but the procedures are clear. This method has the additional advantage of fitting in with the theory used for surface targets, for which it is simpler to use free space intensities and lump the field strength integrated over the target area as an "effective" target area in a uniform field.



## Chapter 12

### NOMOGRAPHIC SOLUTIONS FOR THE STANDARD CASE<sup>a</sup>

THE EQUATIONS GIVEN in the preceding chapter have now been thrown into nomographic form. When these nomograms are employed a rapid method for constructing coverage diagrams results.

Let  $h_1$  denote the height of the transmitter in feet,  $f_{mc}$  be the frequency in megacycles,  $n$  be an integer (1, 2, 3, ...) specifying the number of the lobe,  $b$  ( $0 \leq b < 1$ ) a "phase" factor specifying the position on the lobe, and  $r$  the radius of the earth. Introduce the quantity  $B$  defined as follows.

$$B = \frac{150 (n - b) \sqrt{2N} (3.281)^{\frac{3}{2}}}{h_1^{\frac{3}{2}} f_{mc}}$$

$$= 3.676 \times \frac{10^6 (n - b)}{h_1^{\frac{3}{2}} f_{mc}}, \quad (1)$$

where we have taken  $r = 8.50 \times 10^6$  m, as the approximate  $\frac{4}{3}$  earth value. We have to decide on the interval for  $b$ . By taking  $b = 0, \frac{1}{6}, \frac{2}{6}, \frac{3}{6}, \frac{4}{6}, \frac{5}{6}$ , we actually obtain seven points on each lobe, which should be sufficient for the purpose of drawing a coverage diagram. Hence,  $n - b = 0, \frac{1}{6}, \frac{1}{3}, \frac{1}{2}, \frac{2}{3}, \frac{5}{6}, 1, \frac{7}{6}, \dots$ , etc., spaced at intervals of  $\frac{1}{6}$ .

Equation (1) is represented in the nomogram of Figure 1. We are given  $h_1$  and  $f_{mc}$ , the height and frequency of the transmitter. Connect the appropriate values on the scales by a straight line and mark the point of intersection on the central vertical line.

Define a quantity  $k$  by the equation

$$n - b = \frac{k}{6},$$

so that  $k = 3$  corresponds to the maximum of the first lobe,  $k = 6$  to the minimum,  $k = 9$  to the next maximum,  $k = 12$  to the minimum, etc.  $k = 15, 21$ , and  $27$  correspond to the third, fourth, and fifth maxima, respectively. Other values of  $k$  determine intermediate points on the lobe.

Now draw a straight line from  $k = 1$  through the point previously determined on the central vertical line until it intersects the left-hand axis of  $B$ . Read off  $B$  or  $1/B$ , whichever is given. Repeat the process for  $k = 2, 3, \dots$ , etc., until a value of  $B$  is obtained

that exceeds 10; in other words, continue until the straight line runs off the lower edge of the left-hand scale.

There will be cases, however, usually involving large values of  $h_1$  or  $f_{mc}$ , where  $B$  will still be small ( $1/B$  large) even for  $k = 27$ . When this condition exists, the lobes tend to be so closely spaced that the individual maxima are difficult to define and even more difficult to draw on a coverage chart. For such conditions an alternative procedure is recommended, which will be given later.

If no difficulty is encountered, however, enter the values of  $B$  or  $1/B$  (designate the latter with an asterisk) in a table such as Table 1.

TABLE 1

$f_{mc}$  = Frequency in mc  
 $h_1$  = Height of antenna in ft

$k =$	$B^*$	$n$	$b$
1		1	$\frac{1}{6}$
2		1	$\frac{1}{3}$
3		1	$\frac{1}{2}$ max.
4		1	$\frac{2}{3}$
5		1	$\frac{5}{6}$
6		2	0 min.
7		2	$\frac{1}{6}$
8		2	$\frac{1}{3}$
9		2	$\frac{1}{2}$ max.
10		2	$\frac{2}{3}$
11		2	$\frac{5}{6}$
12		3	0 min.
15		3	$\frac{1}{2}$ max.
21		4	$\frac{1}{2}$ max.
27		5	$\frac{1}{2}$ max.

\*Put an asterisk after an entry if the value read off is equal to  $1/B$ . The corresponding values of  $n$  and  $b$  are entered in columns 3 and 4 of the form sheet.

It should be noted that equation (1) is easy to solve, and the operator familiar with mathematical procedures may prefer to use direct calculation, by slide rule or logarithm tables, as much more accurate. In general, however, the nomogram values are sufficiently accurate for the work.

Next, for the five or six assumed values of decibels for which contours are desired, we solve a subsidiary equation for  $Y$  by means of a nomogram (not reproduced here). We note that

$$Y = db + 60 - 10 \log (2\pi r h_1),$$

<sup>a</sup>By Lt. Comdr. D. H. Menzel and Lt. A. L. Whiteman, Office of the Chief of Naval Operations.





FIGURE 1



and slide-rule calculation is extremely convenient. For each of the selected values of  $b$ , we have prepared a nomogram connecting  $Y$ ,  $B$ , and  $\alpha$ . Although there are six adopted values of  $b$ , the expressions for  $b = \frac{1}{6}, \frac{5}{6}, \frac{1}{3}, \frac{2}{3}$  coincide, so that four charts suffice. A representative sample of these charts, for  $b = 0$ , is given in Figures 2 and 3. Connect each value of  $Y$ , for which a contour is desired, with the value of  $B$  on the appropriate chart, according to the value of  $b$  (or  $k$ ). Read off the corresponding value of  $\alpha$ .

Having determined  $\alpha$  for a given point on the coverage chart, we now calculate  $S$  from the nomogram in Figure 4, with  $\alpha$ ,  $\text{db}$ , and  $S$  as variables. For  $S$  measured in units of 1,000 yd, we have

$$10^{-db/20} = \frac{10^3}{\sqrt{\pi}} \left( \frac{1}{914 S} \right) \left\{ \left[ \frac{1 - \left( \frac{\alpha}{4 - 3\alpha} \right)^{\frac{1}{2}}}{4} \right]^2 + \left( \frac{\alpha}{4 - 3\alpha} \right)^{\frac{1}{2}} \sin^2 \pi b \right\}^{\frac{1}{2}}.$$

A typical example for the selected values of  $b$  is shown, as before.

Finally, we must calculate  $h_2$ . For heights we have

$$H = h_2 + (1 - \alpha)h_1 = \frac{(3.281)(914)^2}{2r} S^2 + \frac{(3.281)^2 (914)(150)(n - b)}{h_1 f_{mc}} \frac{(-2 + 3\alpha)}{\alpha^2} S. \quad (2)$$

This equation, unfortunately, has too many variables for nomographic solution in a single step. We first define a quantity  $C$ , such that

$$C = \frac{(3.281)^2 (914)(150)(n - b)}{h_1 f_{mc}} \frac{(-2 + 3\alpha)}{\alpha^2}.$$

Obtain the simple product  $h_1 f_{mc}$ , which is a characteristic of the set. Then use the nomogram of Figure 5 to obtain the values of  $C$  for the selected ranges of  $k$  and  $\alpha$ . Then we can determine  $H$  from the nomogram of Figure 6, for each value of  $S$  and  $C$ . Finally, from a nomogram (not shown here), representing the equation

$$h_2 = H - (1 - \alpha)h_1$$

we determine  $h_2$ . Actually, for much of the range,  $\alpha \sim 1$  and  $h_2 \sim H$ .

For the upper lobes considerable simplification is possible. We may omit all the steps involving cal-

culatation of  $\alpha$ . We determine the various  $B$ 's as before. Then, as long as  $B \gg 1$  we employ the equation

$$10^{-db/10} = \frac{10^6}{\pi} \left( \frac{1}{914S} \right)^2 \times \left[ \frac{1}{B^4} + \left( 1 - \frac{1}{B^2} \right) \sin^2 \pi b \right].$$

This equation gives  $S$  directly for each decibel value and assumed value of  $b$ . The nomogram for this problem appears in Figure 7. We then obtain  $H$  from equation (2), with  $\alpha$  set equal to unity.

$$H = \frac{(3.281)(914)^2}{2r} S^2 + \frac{(3.281)^2 (914)(150)}{C'} S. \quad (3)$$

In equation (3) we have written  $C'$  instead of  $C$ . For much of the range, wherever  $B$  is very large, we may take  $C' \sim C$ . If greater accuracy is desired, we may compute  $C'$  directly by the equation

$$C' = \frac{(3.281)^2 (914)(150)k}{6 f_{mc} h_1} \left( 1 - \frac{1}{B^2} \right).$$

It is interesting to note that equation (3), apart from the correction factor  $(1 - 1/B^2)$ , which merely serves to improve the accuracy of the result, is familiar to many in the construction of so-called "fade charts." These diagrams depict merely the lobe minima (and sometimes also the maxima). If we set  $b = 0$  we get the former, and if we take  $b = \frac{1}{2}$  we determine the latter.

The total number of lobes  $N$  is approximately

$$N = \frac{2h_1}{\lambda} = \frac{h_1 f_{mc}}{(150)(3.281)} = 2.03 \times 10^{-3} h_1 f_{mc}$$

for  $h_1$  in feet. These will be distributed over an angle of 90 degrees. Hence  $\bar{A}$ , the average angle per lobe, is

$$\bar{A} = \frac{90^\circ}{N} = \frac{4^\circ 43' \times 10^4}{f_{mc} h_1}.$$

Near the horizon, however, the angle per lobe  $A_0$  is somewhat smaller, to wit:

$$A_0 = \frac{360^\circ}{\pi N} = \frac{5^\circ 64' \times 10^4}{f_{mc} h_1}.$$



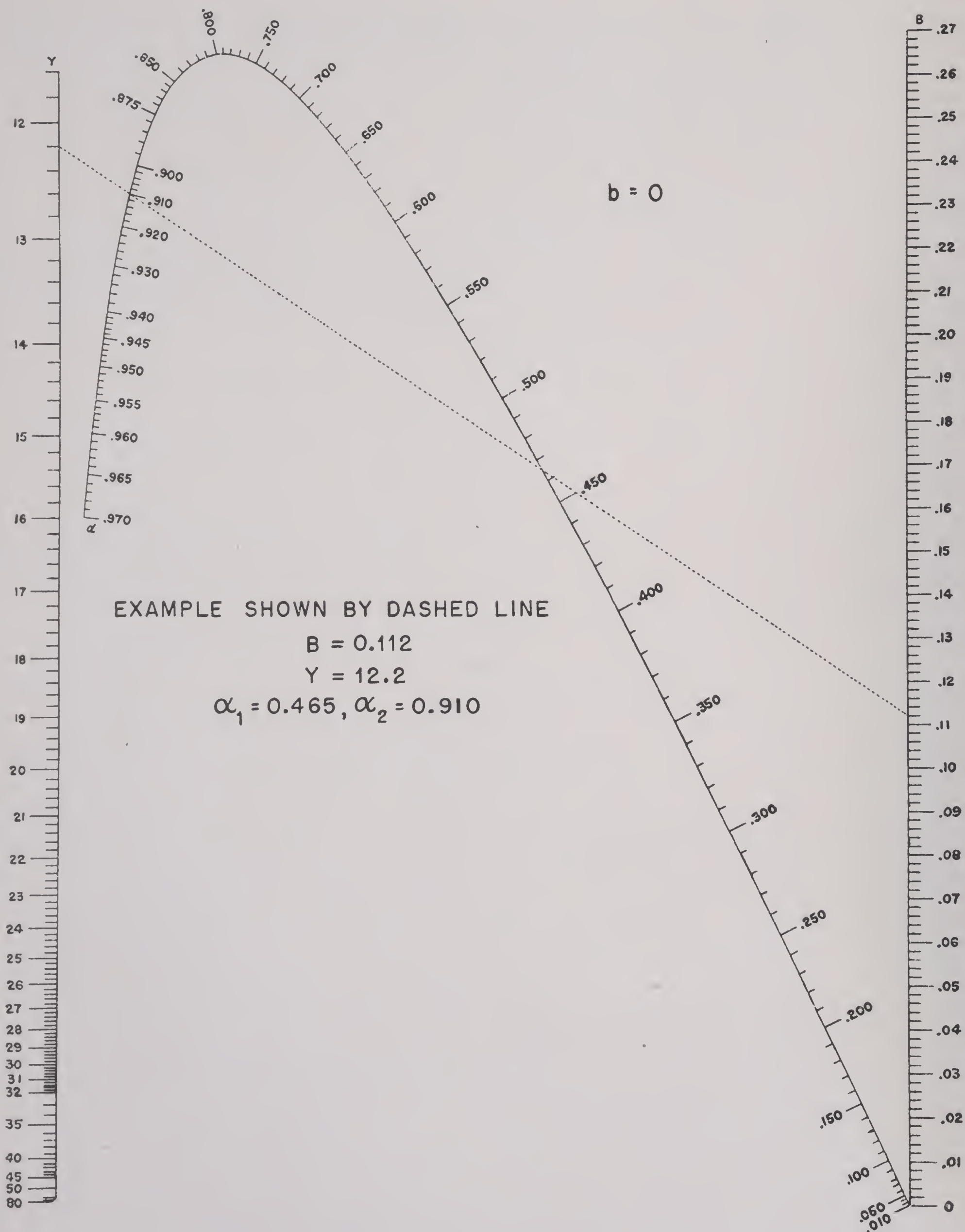


FIGURE 2



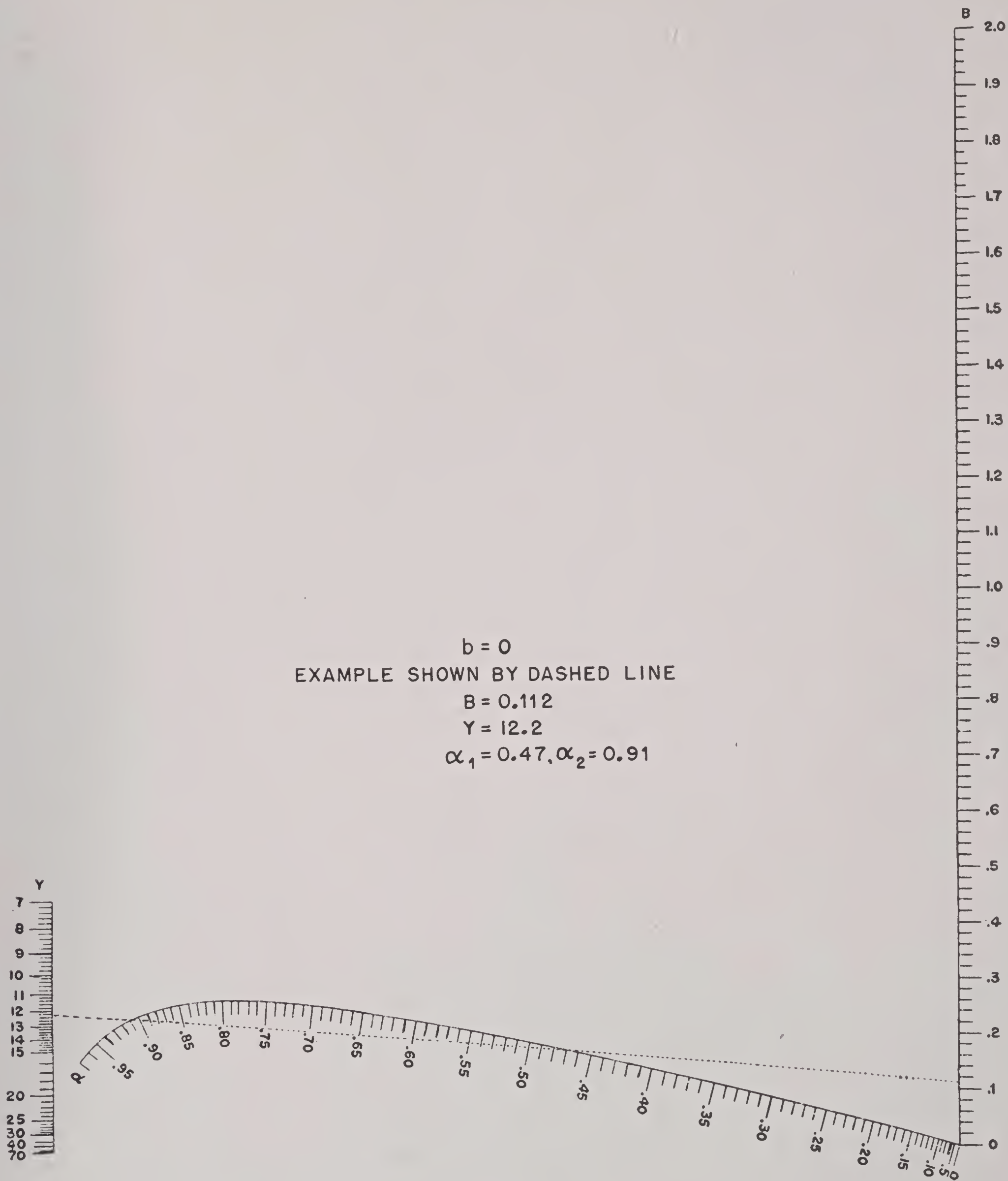


FIGURE 3



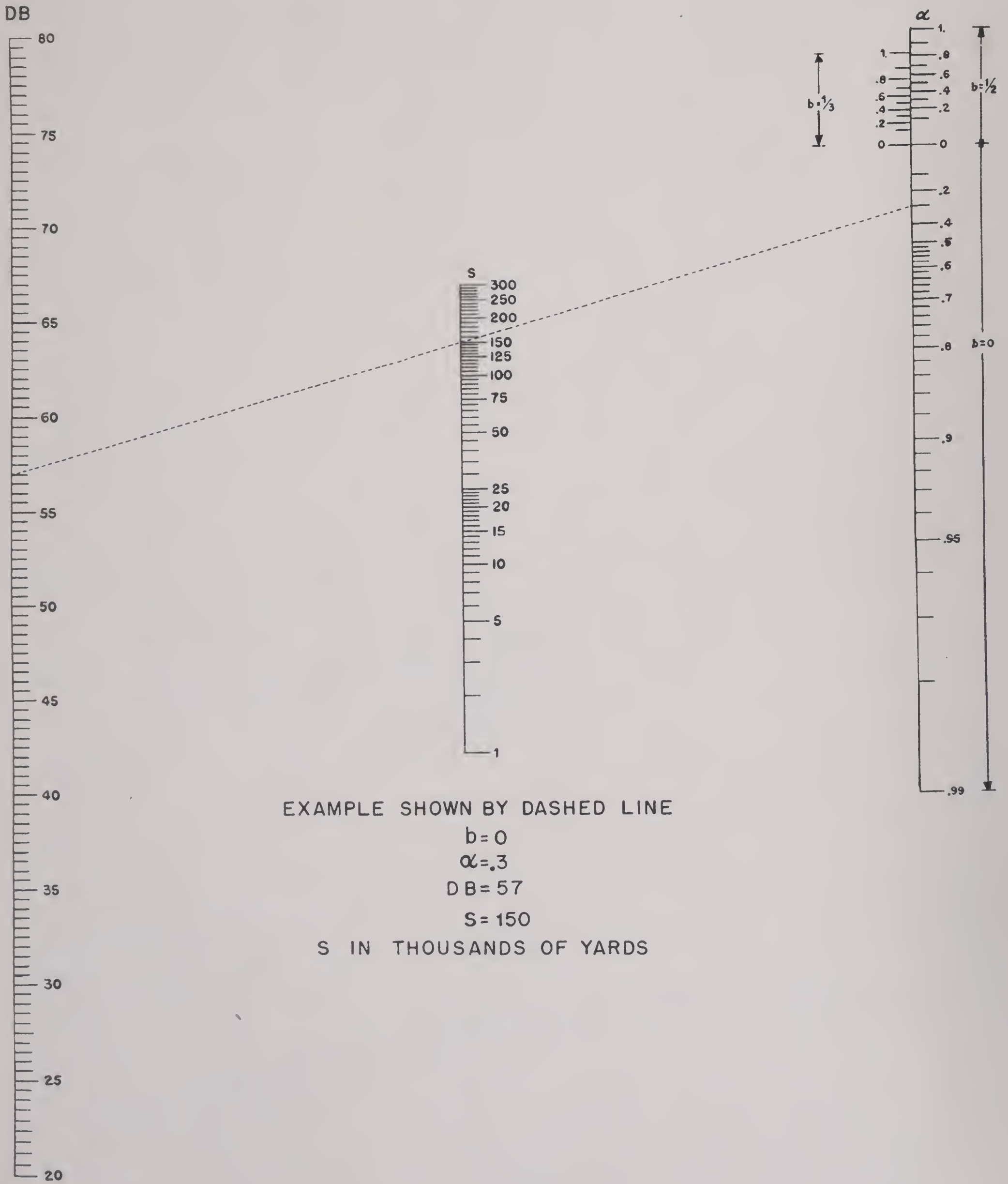


FIGURE 4



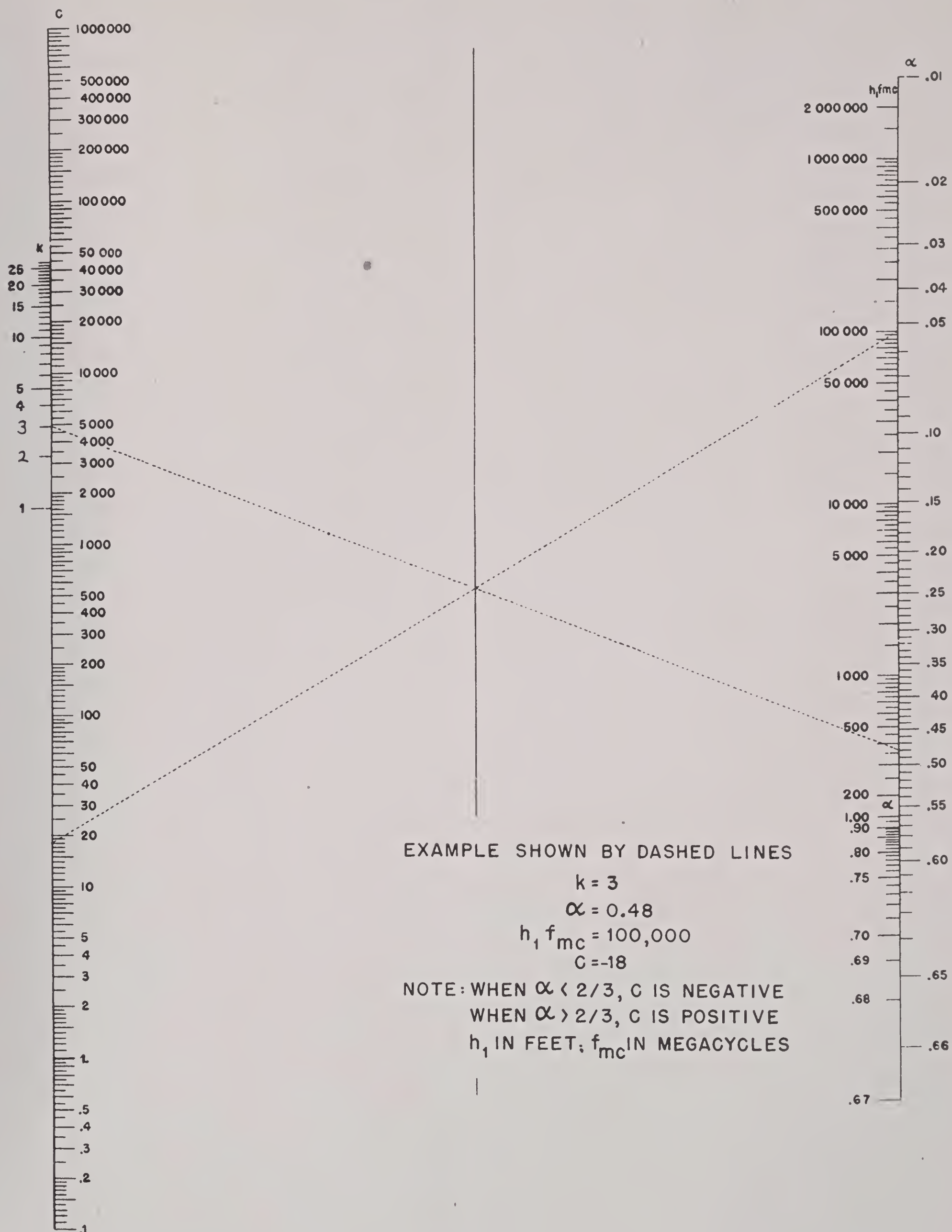


FIGURE 5



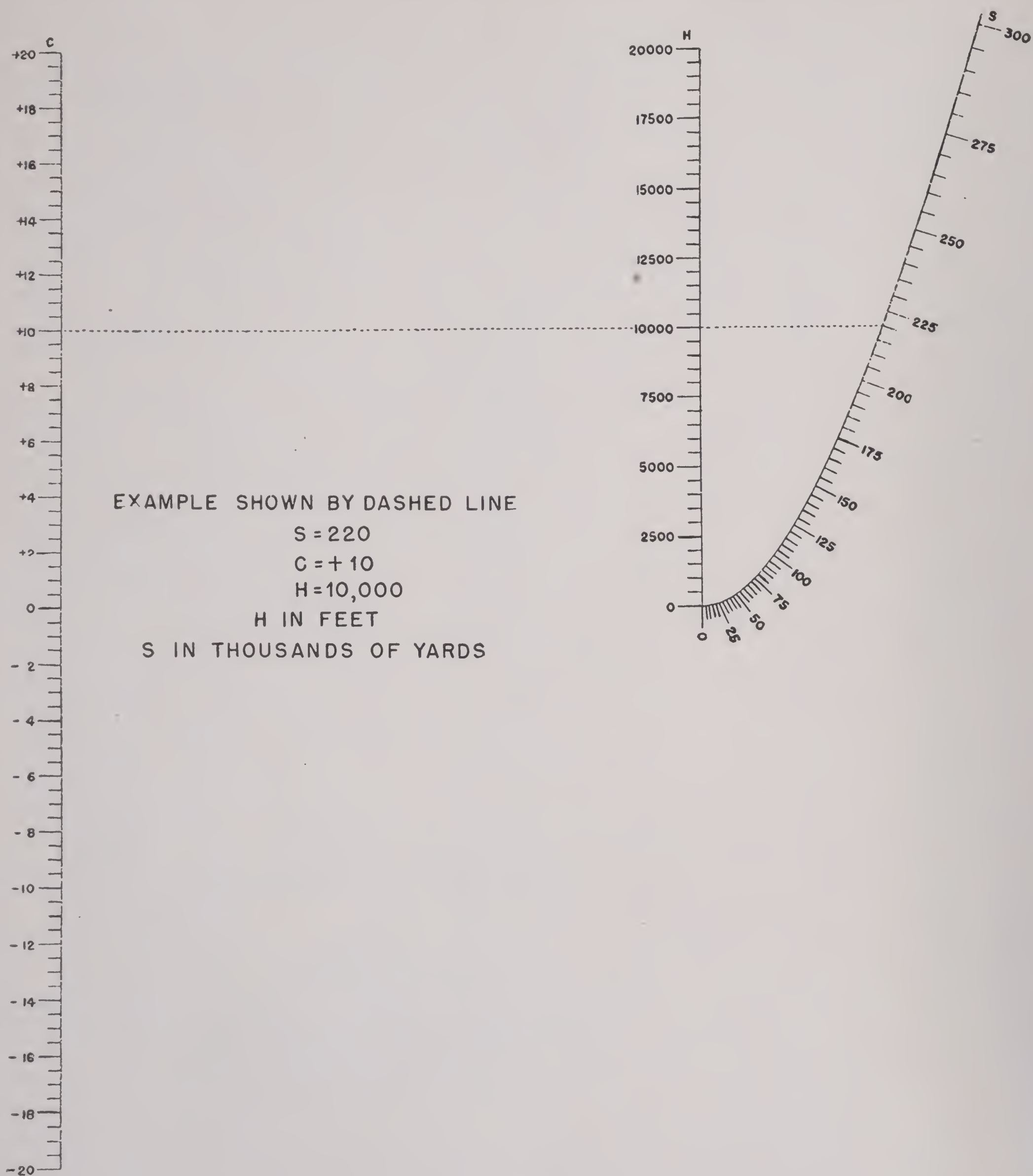


FIGURE 6



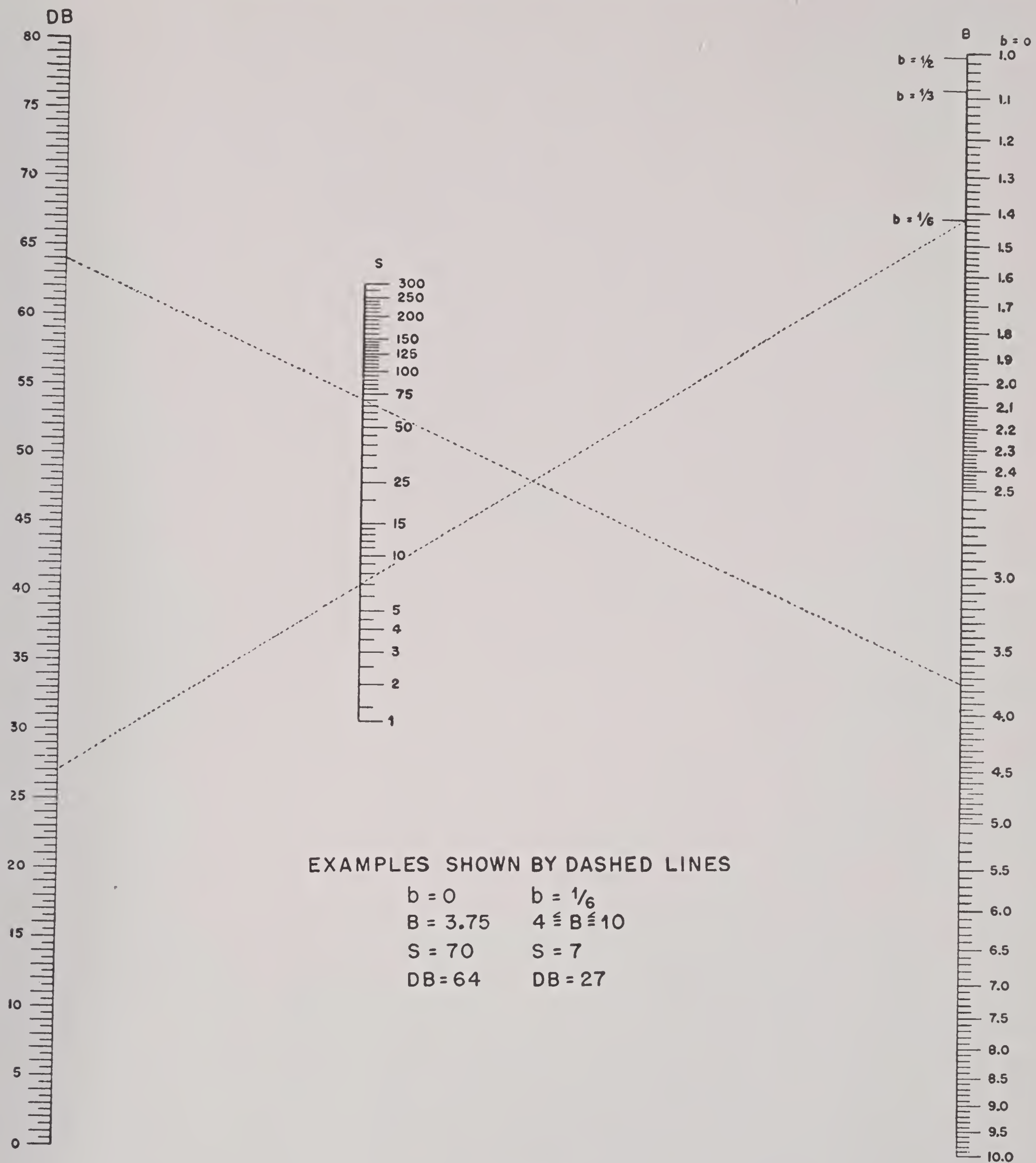


FIGURE 7



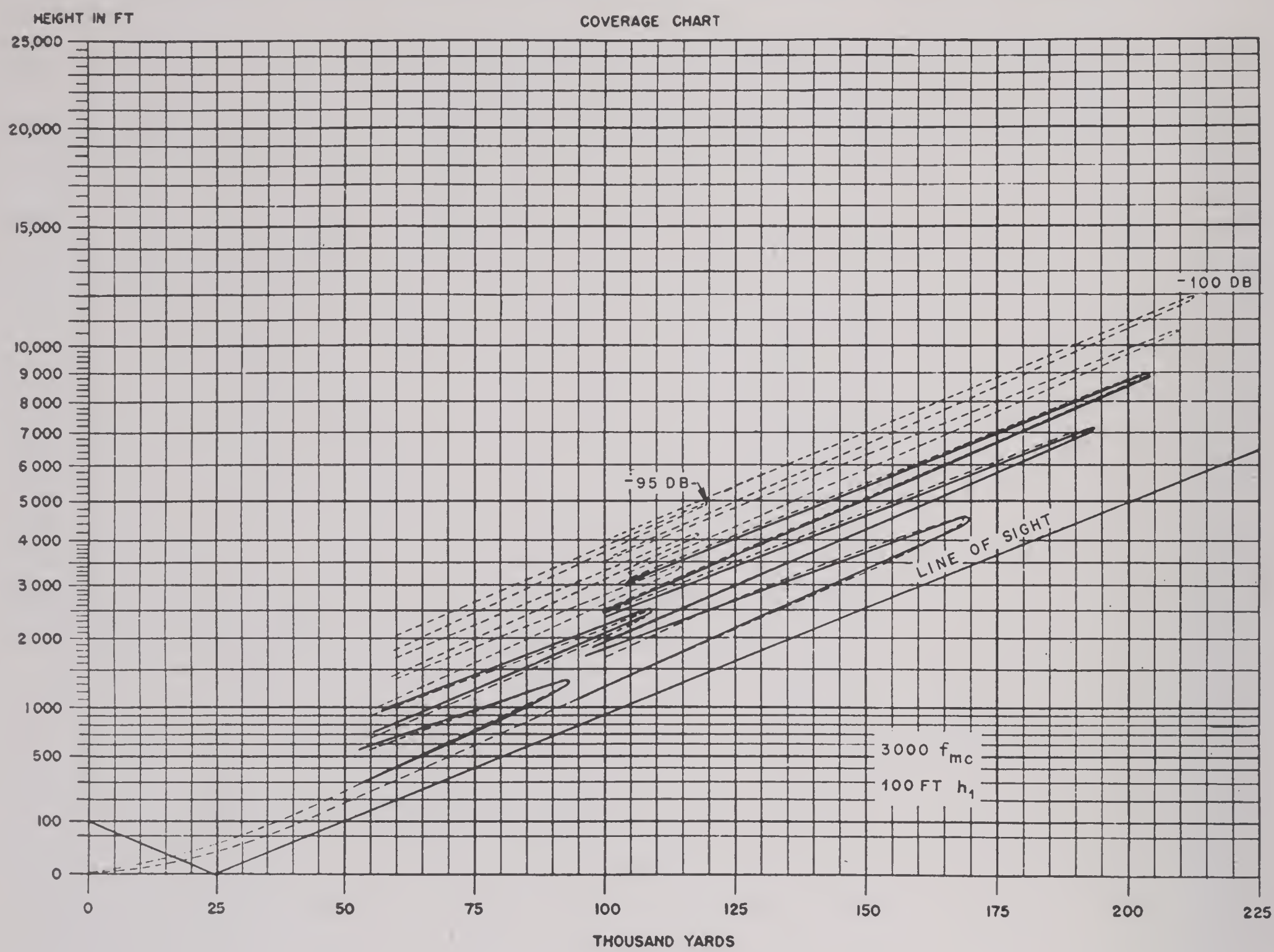


FIGURE 8

TABLE 2. Work sheet for coverage diagram calculations.

db = 46 (MIT - 95 db)  
 $f_{mc} = 3,000$   
 $h_1 = 100 \text{ ft}$   
 $Y = 13.9$   
 $h_1 f_{mc} = 300,000$

<i>k</i>	<i>B</i>	<i>n</i>	<i>b</i>	<i>α</i>	<i>S</i>	<i>C</i>	<i>H</i>	<i>h</i> <sub>2</sub>
1	0.21	1	$\frac{1}{6}$	0.478	53.5	-2.15	350	300
2	0.42	1	$\frac{1}{3}$	0.581	82.5	-1.29	950	908
3	0.63	1	$\frac{1}{2}$	0.655	93.0	- .20	1,350	1,316
4	0.84	1	$\frac{2}{3}$	0.72	85.0	1.07	1,250	1,222
5	1.02	1	$\frac{5}{6}$	0.778	52.5	2.45	600	568
6	1.22	2	0					
7	1.35	2	$\frac{1}{6}$	0.828	56.0	4.10	750	733
8	1.55	2	$\frac{1}{3}$	0.835	94.0	4.70	1,850	1,834
9	1.85	2	$\frac{1}{2}$	0.863	109.0	5.70	2,550	2,536
10	1.95	2	$\frac{2}{3}$	0.873	98.0	6.60	2,200	2,187
11	2.1	2	$\frac{5}{6}$	0.893	57.0	7.80	950	939
12	2.3	3	0					
15	2.9	3	$\frac{1}{2}$	0.923	114.0	10.80	3,300	3,292
21	3.9	4	$\frac{1}{2}$	0.951	118.0	15.40	4,100	4,095
27	5.3	5	$\frac{1}{2}$		119.0	23.5	5,100	5,100



When  $A_0 < 0.1$ , the lower lobes are so closely packed that the drawing of a coverage diagram becomes almost impossible. For such cases one should determine, for a given decibel value, the lower edge of the lowest lobe. Then, with the aid of the nomograms for  $b = 1/2$ , calculate merely the positions of maxima of the other lobes.

A work sheet for coverage diagram calculations is shown in Table 2. As an illustrative example we have selected the case in which

$$h_1 = 100 \text{ ft}, f_{mc} = 3,000 \text{ mc}, db = 46 .$$

Here  $db$  stands for the number of decibels that the power density is *below* standard, where we have assumed a power of 1 w for the transmitter. The symbol  $db$  is defined differently by the MIT group. The correspondence is:

$$db \longleftrightarrow - [db_{MIT} + 49] .$$

The value of  $\lambda$ , which depends only on  $db$  and  $h_1$ , was obtained from the nomogram of Figure 4 and equals 13.9. The product  $h_1 f_{mc}$  is, of course, 300,000. The rest of the table was filled out by the methods just described.

The lobes corresponding to this data were also computed by the MIT method and are shown plotted in dotted lines in Figure 8. In general, these lobes agree completely with our own. In the cases where there is some slight variance, we have also drawn our lobes in heavy lines. Note that the MIT  $db$  of 95 corresponds to our  $db$  of 46. The nomograms presented herein correspond to a reflection coefficient of  $-1$ . For any other value they would have to be redrawn.



## Chapter 13

# THEORETICAL ANALYSIS OF ERRORS IN RADAR DUE TO ATMOSPHERIC REFRACTION<sup>a</sup>

13.1

### PURPOSE

THIS REPORT is a theoretical evaluation of errors in altitude, azimuth, and range caused by atmospheric refraction. These errors are compared with the error tolerance specified in military characteristics for fire control radar equipment. Regional climatological data are utilized to determine probable refractive index gradients used in the determination of the error. Errors in heightfinding resulting from ducts are also treated. An Evans Signal Laboratory [ESL] report now under preparation discusses errors which may occur during specific meteorological situations and which may exceed the errors indicated in this report.

13.2

### PROCEDURE

The variation of the index of refraction perpendicular to the path of a radio wave results in a curvature of the ray toward the higher index. The curvature of the ray is approximately equal to the rate of decrease of the index of refraction with altitude. Errors due to atmospheric refraction will therefore depend on the rate of decrease of the index of refraction perpendicular to the ray path and to the range. A simplified equation for the error in azimuth and altitude is derived below and is utilized in this report. This method has been found to check to within a thousandth of a degree with more accurate methods<sup>b</sup> of ray tracing.<sup>c</sup>

The rate of decrease of the index of refraction in a standard atmosphere is  $12 \times 10^{-6}$  unit per 1,000 ft up to 4,000 ft above mean sea level. This corresponds to a curvature of the path of the ray approximately one fourth the curvature of the earth. The standard atmosphere represents average conditions in temperate zones. In tropical air such as exists in equatorial regions and southeast Asia and southeast

United States in summer, the average rate of decrease of the index of refraction is approximately  $18 \times 10^{-6}$  unit per 1,000 ft up to 6,000 ft corresponding to a curvature of the ray  $\frac{3}{2}$  that of the earth. Over trade wind regions of the ocean (latitude  $10^\circ$  to  $30^\circ$ ) dry subsiding air exists over a moist tropical layer. The rate of decrease of the index of refraction in these regions is approximately  $24 \times 10^{-6}$  unit per 1,000 ft corresponding to a curvature of the ray one-half that of the earth. Within layers of atmosphere designated as "ducts" the curvature of the ray may exceed the earth's curvature and may result in a trapping of the ray within the duct. Errors due to atmospheric conditions in each of the above atmospheres are analyzed. In Table 1 are tabulated values of the index of refraction at selected levels for the standard atmosphere, tropical atmosphere, and tropical dry atmosphere as utilized in this report.

TABLE 1. Values of the index of refraction for selected levels in different air masses.\*

$(n - 1) 10^6$ ;  $n$  = index of refraction.

Elevation above mean sea level (feet)	Standard atmosphere	Tropical atmosphere	Tropical air dry air above
0	324	394	348
2,000	300	358	300
4,000	276	322	260
6,000	255	286	242
8,000	236	255	227
10,000	219	234	216
15,000	191	195	179
20,000	151	159	146
30,000	105	107	105

\*Aerological data for Miami and San Diego for July 1943 were utilized to compute the indices of refraction for the tropical atmosphere and the tropical atmosphere with dry air above, respectively.

13.3

### APPLICATION TO GROUND RADAR EQUIPMENTS

#### GUNLAYING (ANTI-AIRCRAFT) RADAR

Military characteristics for gunlaying radar call for a tolerance of 50-yd error in a range of 29,000 yd and an angle of 1.5 mils in azimuth and elevation. Initial angles of sight are between  $10^\circ$  and  $90^\circ$ .

#### RESULTS

In a standard atmosphere, errors in angle of eleva-

<sup>a</sup>By Raymond Wexler, Signal Corps Ground Signal Agency.

<sup>b</sup>Errors in angle of altitude due to a duct with a standard atmosphere above the duct have been computed by members of Group 42 of the Radiation Laboratory. Values computed by the method outlined below under Derivation of Formulas have been found to agree with their results.

<sup>c</sup>For a more detailed analysis of ray tracing methods, see reference 75.



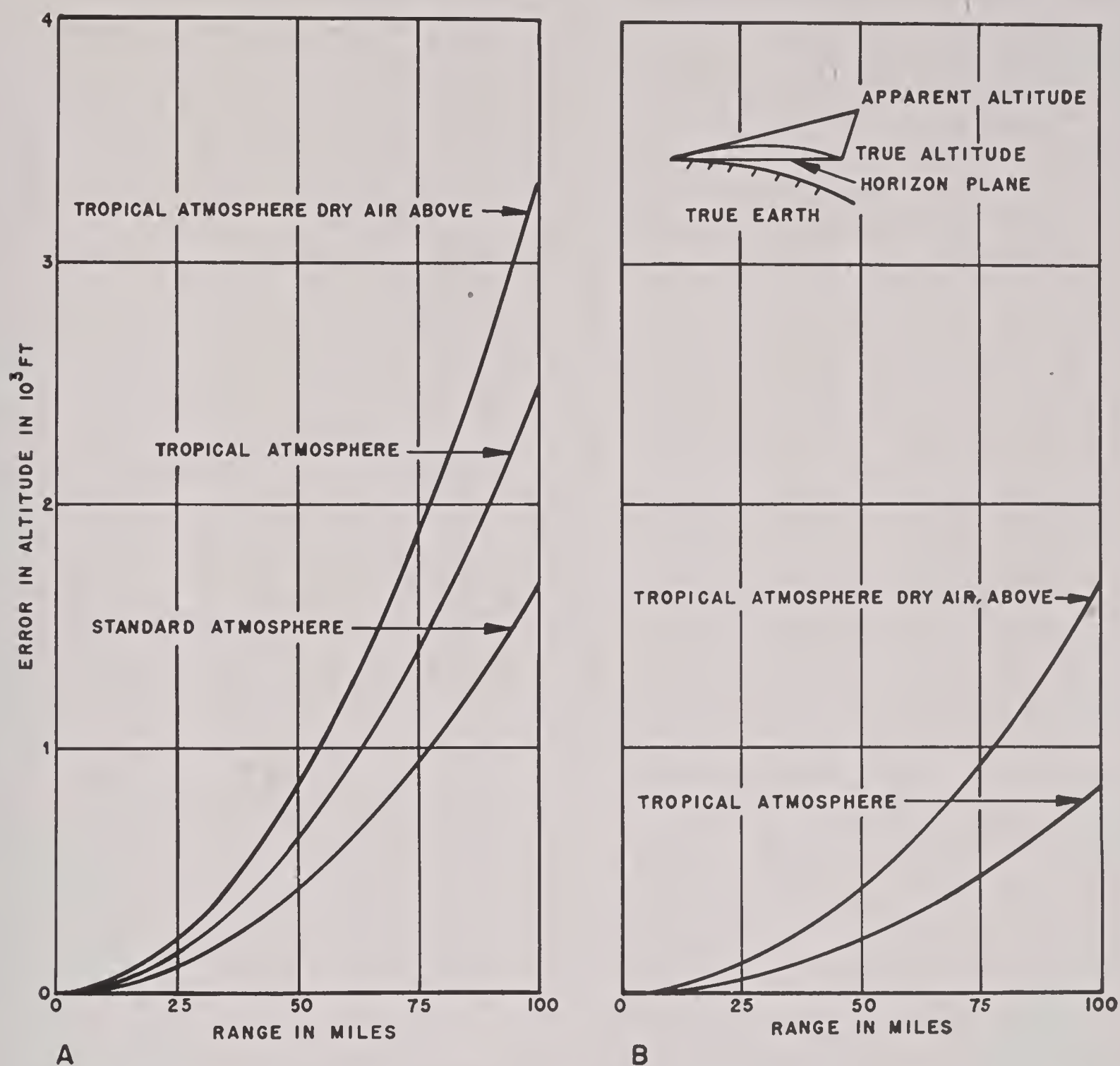


FIGURE 1. Maximum errors in absolute altitude due to atmospheric refraction. A. True earth radius. B.  $\frac{4}{3}$  earth radius. Target assumed to be at true angle of zero degrees.

tion for a range of 29,000 yd and an initial angle of sight  $10^\circ$  are 0.5 mil. A maximum error is obtained at 0.9 mil. For an initial angle of sight of  $20^\circ$  the maximum error is about 0.6 mil as compared to an error in a standard atmosphere of 0.4 mil. Errors in azimuth and range are negligible.

#### EARLY WARNING HEIGHTFINDING RADAR

Military characteristics call for the following tolerances in heightfinding radars.

Set	Freq. Band	Accuracy Required
AN/CPS-4	S	1,000 ft in absolute altitude and 500 ft in relative altitude at 45 miles range, preferably 90 miles.
AN/CPS-6	S	1,000 ft in absolute altitude and 500 ft in relative altitude at 75 miles range, preferably 100 miles.
AN/TPS-10	X	1,500 ft in absolute altitude and 500 ft in relative altitude at 50 miles range.

#### ABSOLUTE ALTITUDE

Figure 1A indicates the errors in absolute altitude for different air masses on the assumption that the target is at a true angle of zero degrees. Thus at a range of 75 miles the error in elevation is 940 ft in a standard atmosphere and 1,880 ft in a tropical atmosphere with dry air above. Figure 1B depicts the errors on the assumption that the standard atmosphere correction ( $\frac{4}{3}$  earth radius) is applied. Thus with the  $\frac{4}{3}$  earth radius correction the error remains under 1,000 ft at 75 miles. However, these atmospheric conditions represent normal conditions so that in specific meteorological situations the error may exceed 1,000 ft in 75 miles especially in the trade wind regions.

Since the maximum error occurs at a true angle of  $0^\circ$ , these errors in absolute altitude for a range of 75 miles are tabulated for true angles of  $0^\circ$  to  $3^\circ$ .



TABLE 2. Errors in absolute altitude for early warning heightfinding. Range 75 miles.

True angle	Angle of sight (degrees)		Errors in altitude (feet)	
	Standard	Tropical	Standard	Tropical
0	0.14	0.20	941	1,412
1	1.12	1.17	823	1,332
2	2.10	2.14	705	970
3	3.09	3.12	626	845

Ducts in the lower layer of the atmosphere will cause errors to exceed those specified by military characteristics. For a duct depth of 25 ft and 1-unit decrease in the modified index of refraction, errors in absolute altitude may exceed 1,000 ft within ranges of 50 miles. A 200-ft duct, in which the modified index of refraction decreases 10 units, may cause an error of more than 2,000 ft in 50 miles range. Figure 2 depicts errors in absolute altitude

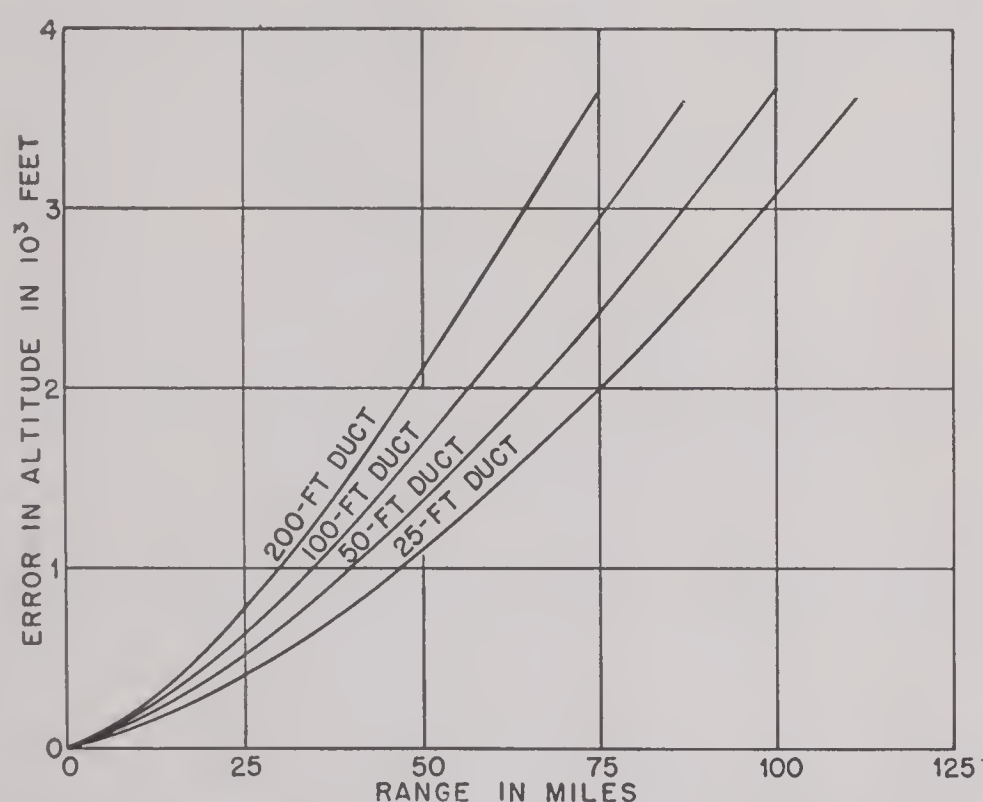


FIGURE 2. Maximum errors in absolute altitude due to surface ducts with standard atmosphere above.

for ducts of various depths on the assumption that the ray just escapes the top of the duct into a standard atmosphere above. The rate of decrease of the modified index of refraction in the duct is 1 unit per 20 ft (corresponding to a curvature of the ray about twice that of the earth).

#### RELATIVE ALTITUDE

As an example, let us assume that five aircraft are located at altitudes of 3,000, 8,000, 13,000, 23,000, and 33,000 ft above mean sea level. Suppose that these planes are detected by radar at ranges of 50, 75, and 100 miles. Errors in relative altitude occur because of differential refraction at high and low

levels. Even in a standard atmosphere errors in relative altitude arise since the rate of decrease of the index of refraction near sea level is  $12 \times 10^{-6}$  unit per 1,000 ft, while at 15,000 ft it is only  $6 \times 10^{-6}$  unit per 1,000 ft. In a tropical atmosphere with dry air aloft the errors are likely to be considerably greater since the rate of decrease of the index of refraction with height is greater.

TABLE 3. Errors in altitude relative to lowest plane located at 3,000 ft above mean sea level.

Separation of planes (feet)	Standard atmosphere (feet)	Tropical atmosphere (feet)	Tropical dry (feet)
<i>Range 50 miles</i>			
5,000	35	24	317
10,000	73	107	380
20,000	131	243	514
30,000	171	306	572
<i>Range 75 miles</i>			
5,000	78	54	713
10,000	164	242	924
20,000	287	539	1,158
30,000	389	693	1,290
<i>Range 100 miles</i>			
5,000	139	97	1,270
10,000	376	431	1,644
20,000	527	960	2,061
30,000	673	1,237	2,296

Thus in a tropical atmosphere with dry air aloft such as exists in the trade wind areas over the ocean errors of some 500 ft relative altitude for planes separated by 20,000 ft would occur in a range of 50 miles. For 100-mile range, errors can be as much as 2,000 ft. Even in a standard atmosphere errors are more than 500 ft for ranges of 100 miles for the higher level planes.

#### AZIMUTH AND RANGE

Errors in azimuth are negligible for all meteorological conditions except possibly for propagation parallel to a sea coast or sharp cold front (see paragraph below). Errors in range are likewise negligible for all possible meteorological conditions.

#### SURFACE SURVEILLANCE RADAR

Military characteristics for sets AN/MPG-1 and AN/FPG-2 specify errors up to  $0.05^\circ$  in azimuth at 28,000 yd and 50,000 yd respectively. Range error toleration is 20 yd in 50,000 yd.



## AZIMUTH

Errors in azimuth arise from horizontal variations in the index of refraction in the atmosphere. Generally these variations are of insufficient magnitude to cause such errors to be appreciable. In order to obtain an error of  $0.05^\circ$  in 50,000 yd it can be shown that a change in the index of refraction of  $1.5 \times 10^{-6}$  unit in 44 yd perpendicular to the path of propagation is required. This corresponds to an increase of 1C temperature and a decrease of 0.1 mb in vapor pressure. Such changes within 44 yd may occur in propagation parallel to a sea coast or to a sharp cold front, or in isolated regions such as between forest and meadow, valley and plain, or land and water surfaces. Except in the vicinity of a cold front or sea coast it is unlikely that such horizontal gradients of the index of refraction exist along the entire path of the ray.

## RANGE

Errors in range due to vertical refraction within a duct are approximately of the order of 1 yd in 50,000 yd. The error in range corresponding to an azimuth error of  $0.05^\circ$  is estimated at less than 0.2 yd in 50,000 yd.

13.4

## CONCLUSIONS

1. For gunlaying (antiaircraft) radar, the maximum error in angle of elevation at 29,000-yd range is 0.9 mil, as compared to a military tolerance of 1.5 mil.

2. In early warning heightfinding radar, errors of 1,000 ft absolute altitude at 75 miles range may be exceeded even with the application of a standard atmosphere ( $\frac{4}{3}$  earth radius) correction. Because of ducts, errors may be as much as 2,000 ft at 50 miles. Errors in relative altitude may likewise exceed 500 ft in 75 miles.

3. Errors in azimuth may exceed  $0.05^\circ$  in 50,000 yd in propagation parallel to a sea coast or a cold front. Errors of this magnitude will, however, be rare.

4. Errors in range are negligible for all possible meteorological situations.

## DERIVATION OF FORMULAS

Let the origin of the coordinate system be the point where a ray is initially tangent to a line of constant index of refraction  $n_0$ , and let the  $Y$  axis

coincide with this line. Since the ray curves toward higher index of refraction  $n$ , according to Snell's law:

$$n \cos \beta = n_0, \quad (1)$$

where  $\beta$  is the angle the ray makes with the line  $n$ . Then from trigonometric relations:

$$\begin{aligned} \tan \beta &= \frac{dX}{dY} \equiv \frac{\sqrt{n^2 - n_0^2}}{n_0} \\ &= \frac{\sqrt{n - n_0} \sqrt{n + n_0}}{n_0}. \end{aligned} \quad (2)$$

Since  $n$  and  $n_0$  are extremely close to unity no appreciable error will result if we assume that  $n + n_0 = 2$ , hence

$$\frac{dX}{dY} = \frac{\sqrt{2}}{n_0} \sqrt{n - n_0}.$$

Assuming a linear variation of the index of refraction in the  $X$  direction,  $n = n_0 + \omega X$ , and

$$\begin{aligned} Y &= \frac{n_0}{\sqrt{2\omega}} \int_0^X \frac{dX}{\sqrt{X}} = n_0 \frac{\sqrt{2X}}{\sqrt{\omega}}, \\ Y^2 &= \frac{2 n_0^2 X}{\omega}. \end{aligned} \quad (3)$$

Equation (3) indicates that the ray follows a parabolic path. Let us convert into polar coordinates by the transformation  $X = r \sin \phi$  and  $Y = r \cos \phi$ , where  $r$  is the actual range. Then the equation of the path becomes

$$r = \frac{2 n_0^2}{\omega} \tan \phi \sec \phi. \quad (4)$$

Since in actual practice,  $\phi$  is extremely small and  $n_0$  is extremely close to unity, equation (4) can be written as

$$\tan \phi = \frac{\omega r}{2}. \quad (5)$$

Here  $\omega$  represents the rate of change of the index of refraction perpendicular to the ray, and  $\phi$  is the error. If the ray were initially at an angle  $\alpha$  to the line of equal index of refraction, then the rate of change of the index of refraction perpendicular to the ray would be  $\omega \cos \alpha$ . Hence, more generally, the equation for the path of a ray at a mean angle  $\alpha$  to the lines of index of refraction can be written as

$$\tan \phi = \frac{\omega r}{2} \cos \alpha. \quad (6)$$

Equation (6) has been utilized to compute errors in azimuth and angle of elevation.



## Chapter 14

### DIFFRACTION OF RADIO WAVES OVER HILLS<sup>a</sup>

EXPERIENCE HAS SHOWN that frequencies in the VHF (very high frequency) range and higher are propagated over hills and behind obstacles more easily than has been commonly expected. Hills or other obstacles in the transmission path cast shadows which may make a radio system unworkable when either antenna is located close to the obstacle, but recent experiments, notably the work of Jansky and Bailey,<sup>334</sup> have shown that hills and mountains can cause constructive interference as well as destructive interference. In other words, *with proper antenna siting, the field intensity beyond the line of sight may be higher than is expected for the same distance over plane earth. This improvement in field intensity may be 5 to 10 db or more.*

One attempt to develop a theory for radio transmission over hills is based on the computed field intensity over the solid triangle shown in Figure 1.

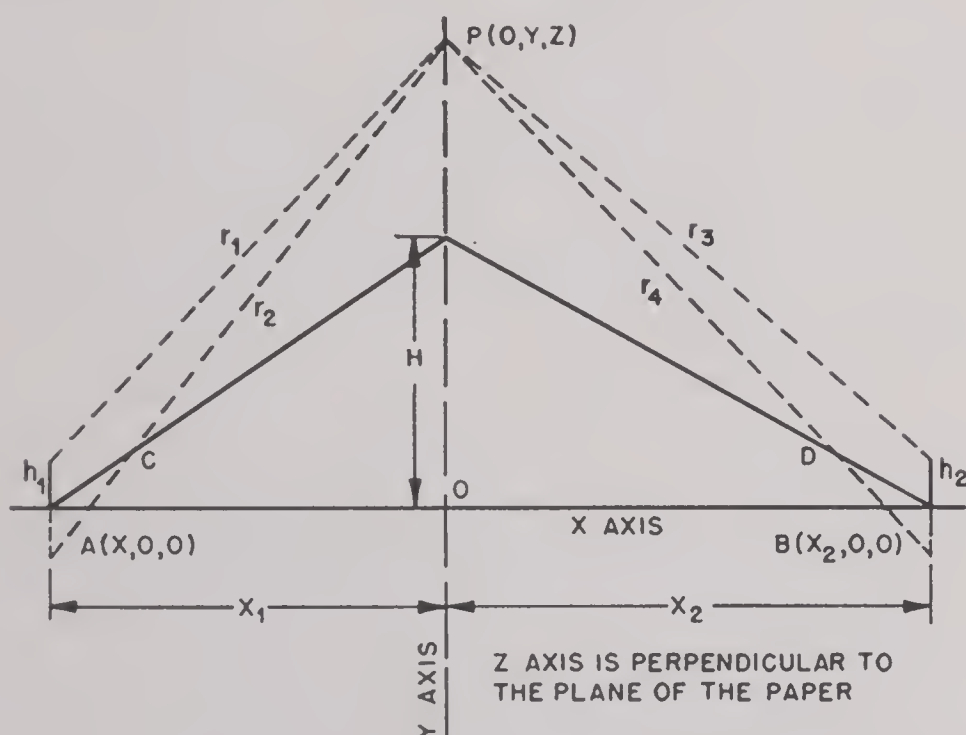


FIGURE 1. Analysis of field intensity over a solid triangle.

It was reasoned that a good approximation to the field over any profile might be obtained from a knowledge of (1) the field over a perfectly smooth earth, (2) the field over the solid triangle that encloses the actual profile, and (3) the field over a knife edge equal in height to the highest point in the profile. The theory of propagation over a perfectly smooth earth is well known; it is the basis of all the published theoretical curves on radio propagation. The corresponding expressions for the field intensity

<sup>a</sup>By K. Bullington, Bell Telephone Laboratories.

over a solid triangle and over a knife edge are indicated in a paper by Schelleng, Burrows, and Ferrell,<sup>447</sup> but some effort is needed to place these expressions in a convenient form for computation.

The method of obtaining an expression for the field over a solid triangle is indicated in Figure 1, and the same analysis applies to each of the ideal profiles shown in Figure 2. The field intensity at any

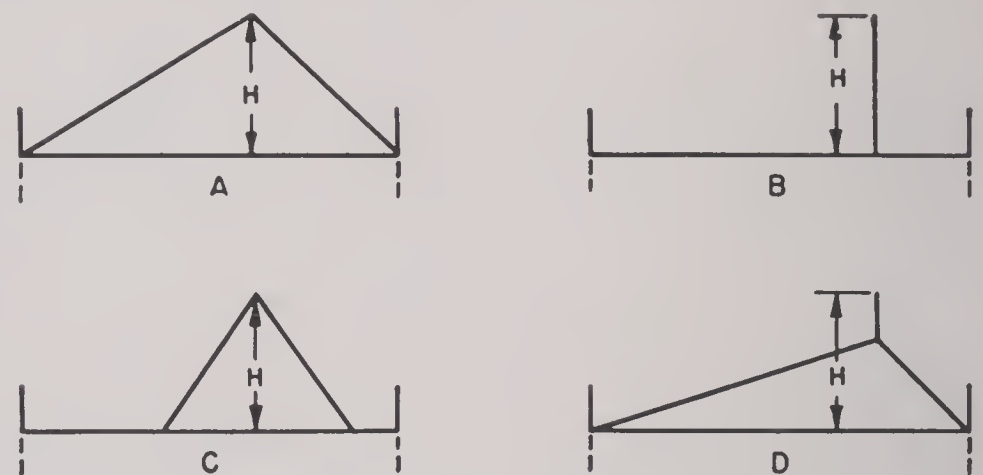


FIGURE 2. Analysis of field intensity over various triangular profiles.

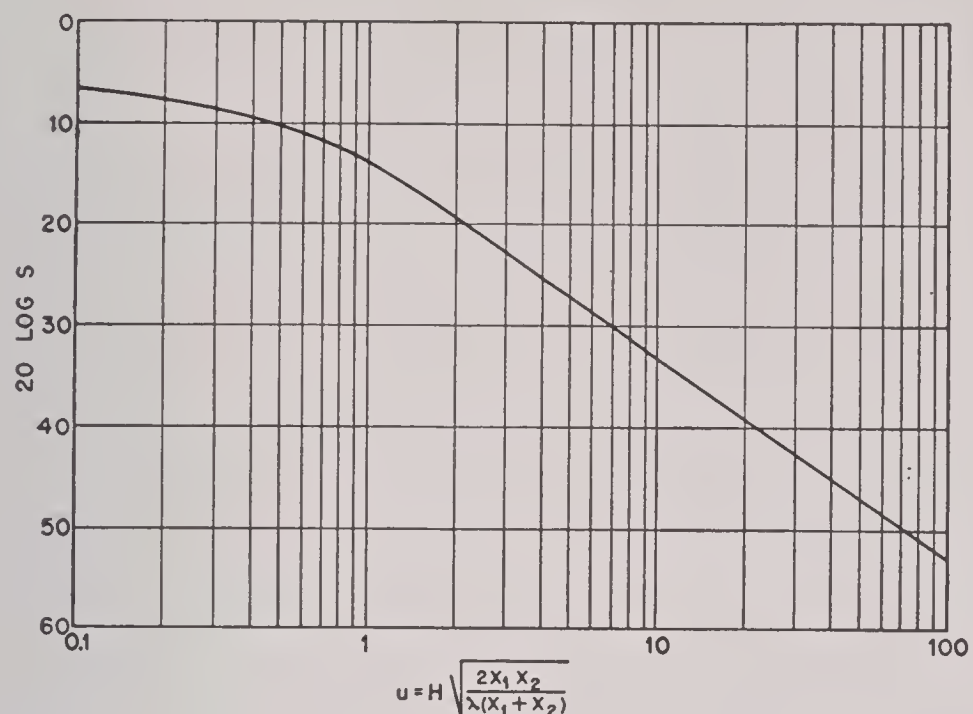
point  $P$  in the vertical plane through the apex of the triangle is assumed to be the sum of a direct ray and a ray reflected from the ground which is equivalent to a ray from an image antenna. In a similar manner the field at point  $P$  is propagated to the receiving antenna by means of a direct ray and a ground reflected ray. By integrating over the plane above the apex of the triangle (that is, from  $y = H$  to  $y = \infty$  and from  $z = -\infty$  to  $z = \infty$ ) an expression for the total received field is obtained. The complete expression is not as complicated as the expression for propagation over a smooth sphere, but two simple approximations will be sufficient for the present discussion. When the height of the hill  $H = 0$  and when the ground reflection coefficient is  $-1$ , the complete expression reduces, as it should, to the well-known formula for VHF propagation over plane earth.

$$E = 2E_0 \sin \frac{2\pi h_1 h_2}{\lambda (x_1 + x_2)}. \quad (1)$$

When the height of the triangle  $H$  is greater than three to five times the average height of the antennas and when the reflection coefficient is  $-1$ , the complete expression reduces to

$$E = 4E_0 S \sin \frac{2\pi H h_1}{\lambda x_1} \sin \frac{2\pi H h_2}{\lambda x_2}. \quad (2)$$




 FIGURE 3. Shadow-loss factor  $S$ .

The factor  $S$  is the shadow loss shown in Figure 3 as a function of

$$u = H \sqrt{\frac{2x_1 x_2}{\lambda(x_1 + x_2)}}$$

The other symbols in the above expressions have the following meanings:

$E$  = field intensity in microvolts per meter,  
 $E_0$  = free space field intensity in microvolts per meter

$$= \frac{3 \sqrt{5P} \times 10^6}{x_1 + x_2},$$

$P$  = radiated power in watts,

$\lambda$  = wavelength in meters,

$H$  = height of the obstruction in meters,

$h_1, h_2$  = antenna heights in meters,

$x_1, x_2$  = distances as shown in Figure 1 in meters.

The approximate expression given in equation (2) indicates that the field intensity for points well beyond the line of sight may be greater than the field over a plane earth which is given in equation (1). The sine terms in equation (2) indicate interference patterns beyond the line of sight which seem to offer an explanation for the experimental fact that behind hills raising the antenna may cause a loss, or lowering the antenna may result in a gain, in signal intensity.

A comparison between theory and experiment is shown in Figure 4. These data, which were taken from the previously mentioned NDRC report prepared by Jansky and Bailey, show measured values at 116 mc for horizontally polarized waves propagated over the profile shown in the bottom of the

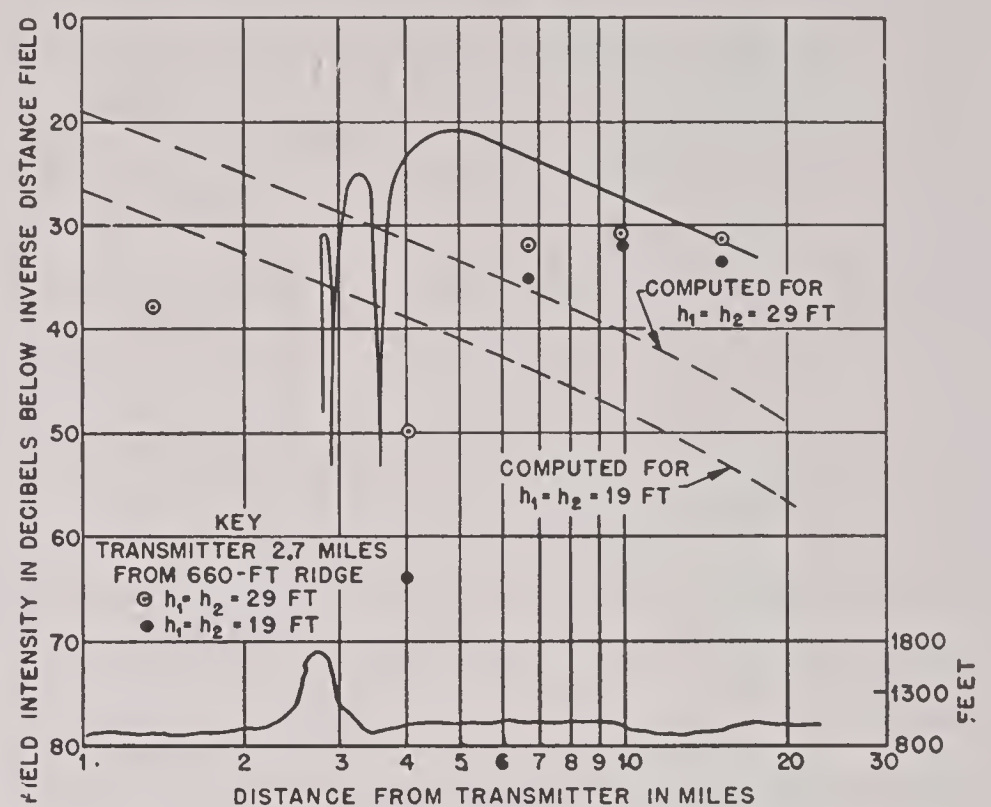


FIGURE 4. Theoretical and experimental results in measuring field intensity of horizontally polarized waves. Frequency 116 mc.

drawing. The open circles show the field intensity in decibels below the free space value when both antennas are 29 ft in height, and the dots give similar data for 19-ft antennas. The two dashed lines running from upper left to lower right are the computed values for smooth earth for 29-ft and 19-ft antennas, respectively. The solid line with the interference fringes is obtained from equation (2) for the case of 29-ft antennas. The correlation between theory and experiment is not complete, but at least the theory may be a step in the right direction. Similar theoretical and experimental results are obtained with vertical polarization.

Thus far the only type of profile considered has been one with a single prominent hill, and it is natural to ask what happens over profiles containing several hills. There are less experimental data available on this point than for propagation over a single hill, and consequently the remainder of this discussion is more speculative than the preceding part.

An ideal profile consisting of two hills of equal height is shown in Figure 5. The complete mathematical solution for this case is difficult, but an approximation can be obtained in the following manner. The field at any point  $P$  midway between the two hills can be obtained by means of the expression for the diffraction over a single hill. The field at this point is then propagated over the second hill to the receiver. The total received field is obtained by mechanical integration, that is, by adding the effect (magnitude and phase) of many evenly spaced points in the vertical plane midway between the two hills.



The net result is that the total received field is represented more closely by the path  $ACB$  than by the path  $ADEB$ . The energy received over any given

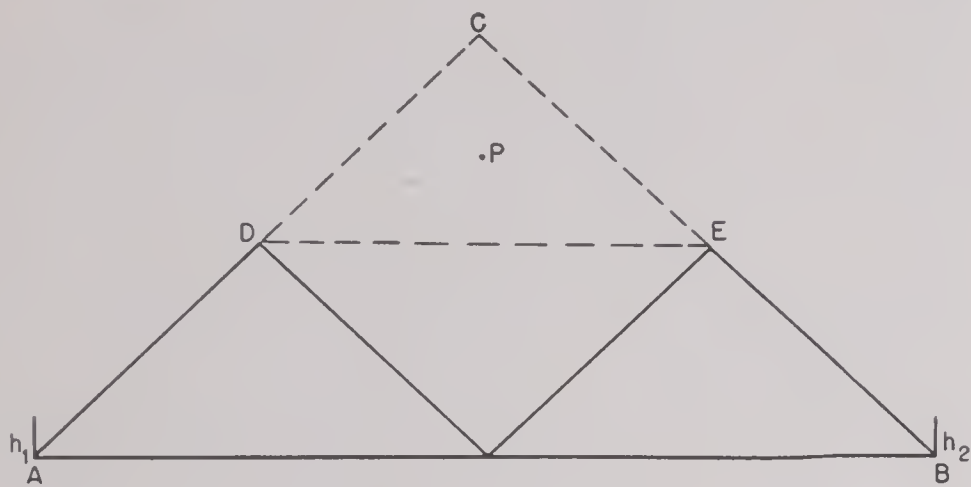


FIGURE 5. Field intensity computation for a profile of two hills by a solid triangle.

path such as path  $ADEB$  decreases rapidly as the number of diffractions in that path increases. However, for any profile there is always at least one path between transmitter and receiver such as path  $ACB$  that requires no more than one diffraction, and the field intensity over this path is usually controlling. In other words, the profile consisting of two hills can be approximated for computation purposes by a solid triangle which is formed by a line from the base of the transmitting antenna to the base of the receiving antenna and lines from the base of each antenna tangent to the hill that blocks the line of sight. By the same reasoning it appears that a profile which includes any number of hills can be represented approximately by the circumscribing triangle.

The principal assumptions that are basic to this method of treating radio propagation over hills and other obstructions are as follows: (1) the height of antennas is greater than about one-half wavelength, (2) the size of obstructions is large compared with the wavelength, and (3) the distance between antennas is large compared with either the antenna height or the size of the obstructions. These assumptions

limit the application of this theory to wavelengths shorter than a few meters.

The principal differences between the diffraction over an irregular earth and the diffraction over a smooth sphere is illustrated in Figure 6 for trans-

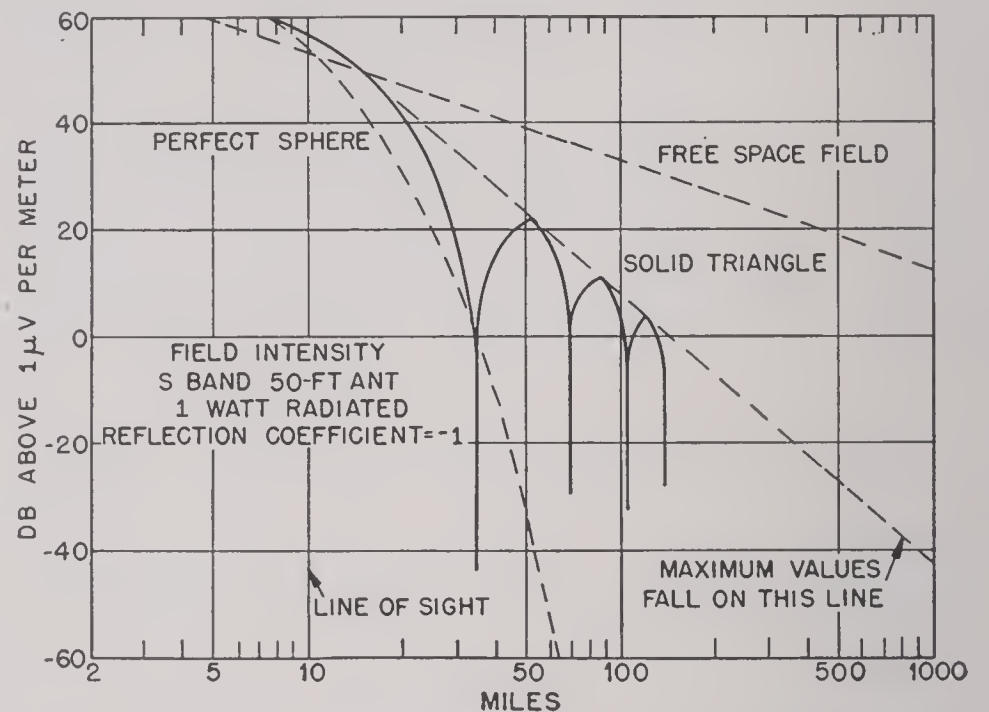


FIGURE 6. Comparison of diffraction over irregular earth and over a smooth sphere for S-band waves over sea water.

mission of S-band waves over sea water. The dashed line shows the field intensity versus distance over a perfectly smooth earth. The solid line shows diffraction over a solid triangle which represents what is expected when the sea is rough, that is, when the height of the water waves is large compared with the S-band radio waves. It will be noted that there is little difference between the two methods for distances less than about twice the optical range, but at greater distances the solid triangle theory indicates that some energy will be received at appropriate distances.

These views on the transmission of meter and centimeter radio waves over multiple obstacles are speculative. There is little experimental evidence to support them, but also there appears to be even less experimental evidence to contradict them.



## Chapter 15

# SITING AND COVERAGE OF GROUND RADARS<sup>a</sup>

15.1

### INTRODUCTION

THIS IS A GENERAL discussion of the effects of terrain on the operation of ground radar systems. Written to supplement a Signal Corps publication *Radar Performance Testing*, it is intended to provide a practical, engineering type of solution of siting problems. The principal emphasis is on early warning and other very high frequency [VHF] systems although application may be made to microwave and other types of radio equipment.

The objective has been to enable field personnel to compute coverage and other characteristics of a given site and radar and reduce the number of test flights required to a minimum. Thus the terrain factors may be evaluated, and a definite, numerical description of the capabilities of a site may be stated.

Since it is not possible to anticipate all problems that may arise in the field, sufficient theory has been included to cover a fairly wide scope. In most cases several types of solutions are provided so that the accuracy and detail required may be related to the labor involved. A number of fully worked examples are included with a discussion of significant features. The drawings are made to scale and to fit practical situations.

15.2

### RADAR SYSTEMS

15.2.1

#### Types of Ground Radar

Tactical requirements and intensive technical development have led to the introduction of numerous types of ground radar equipment. The characteristics and descriptions of these units are given in several Service publications.

Ground radars may be divided into two classes: (1) those which utilize ground reflection; (2) those which use only the direct ray. Sets which are sited so that ground reflection influences their performance usually have stringent siting requirements and the coverage is dependent on the site. This report is concerned chiefly with this type of radar. Equipment that uses only direct rays is relatively free from site

restrictions, and the terrain has little effect on the coverage.

15.2.2

#### Radar Systems—Tactical Aspects

In most cases radar stations are operated in groups for the defense of a region of considerable extent. The several stations are assigned sectors in which searches are conducted for designated targets, and these, when located, are reported to a central agency for tactical disposition. Technical operation of such groups requires close study of the topography of the region so that available equipment and personnel may be used to the best advantage. In this way adjacent stations may support each other in the event of outage due to maintenance or enemy activity, and other factors may be taken into account, such as jamming, atmospheric effects, and permanent echoes.

The nature of the region to be protected and the type of application for which the radar equipment is to be employed are controlling factors determining the number, location, and kind of sets which must be used. Thus, harbors, islands, and inland mountainous regions present problems with widely differing operational characteristics. Early warning [CHL], fighter control [GCI], gunlaying (coast defense), gunlaying (antiaircraft), and searchlight control radars all have different siting requirements. This report deals mainly with the first three types of equipment listed above, but the methods have general application to other problems such as the siting of direction finding sets [DF].

The early warning radar usually has the mission of reporting and identifying enemy aircraft (at say 20,000 ft) 45 minutes before they can reach the vital defense area. This is based on the time required to alert the area and to give the defense aircraft time to take off and make their attack. Other missions may be assigned, such as detection of ships or observation of friendly aircraft for purposes of control and air-sea rescue. Using the moderate plane speed of 240 miles per hour it is apparent that the early warning radar must have a range of 180 miles if located near the defense area. Sometimes suitable outlying sites, such as islands, are available, and the

<sup>a</sup>By Capt. E. J. Emmerling, detailed by Signal Corps to the Columbia University Wave Propagation Group.



coverage may be extended accordingly. The disadvantages of outlying sites presented by communication and supply difficulties, exposure to enemy attack, etc., should be carefully considered. More often, however, the success of the warning system depends on effective long-range operation of radars located relatively close to the defense area. The early warning stations give periodic reports of the grid position of an aircraft and its response to interrogation signals.

The GCI radar is used to direct from the ground the operation of friendly fighters against enemy aircraft. It has a range of about 50 miles and is capable of handling a large volume of traffic. In addition to the grid position and identification of the target it also determines the height. Surrounding the defense area is a region whose width depends on the time required to make an interception on an incoming enemy plane. The siting objective of the GCI stations is the continuous and effective coverage of the interception region. Close coordination is maintained between early warning and fighter stations, and the coverage deficiencies of one station are counteracted by favorable characteristics of the other stations.

The coast defense gunlaying radar is concerned primarily with accurate location of ships. It has a range up to 100,000 yd and must be sited fairly high and within a few miles of the coast defense guns which it directs. This radar supplies accurate data on the azimuth and range of the target.

The antiaircraft gunlaying radar is used primarily for directing the guns. Long-range search features are usually provided so that they may function also as early warning radars, at least to a limited extent. They are sited near the guns which are located to meet artillery requirements. These units provide a continuous flow of data to the gun director giving the azimuth, elevation, and range with great accuracy.

The searchlight control radar is a short-range high angle set which is located near the light it directs. It furnishes the azimuth, angular elevation, and altitude of the target.

### 15.2.3 Radar Siting—Technical Aspects

In the past some elaborate air warning systems have been set up without a competent analysis of terrain effects. This resulted in a waste of time and money and in failure to adequately provide urgently needed radar screens. This failure was caused in

many cases by the use of prepared coverage diagrams, furnished with the equipment, which were computed for idealized sites. In mountainous regions where only limited reflection areas occur and where the sites are very much higher than those used in laboratory tests, such diagrams are likely to be very misleading. A result of this experience is an unfortunate tendency to explain variations from expected coverage by resort to various abstruse speculations, with weather not infrequently bearing the brunt of the odium.

It is the purpose of this report to provide an engineering type of solution for the bulk of the problems that arise in siting and in field computation of coverage. A more accurate analysis, with increased attention to detail, probably is not warranted at this time in view of the relatively rough measurements which now are made in the field of radar.

The common early warning radar uses horizontal polarization and operates in the VHF band. It must be sited from several hundred to several thousand feet high in order to obtain sufficiently low angles for the range and low coverage desired. Suitable sites of the required height may be far inland so that an important part of the reflecting surface may be rough land or sloping flat areas. Such features and also cliff edges, ridges, hills or other obstacles, nearby towers and structures will, in general, produce a marked effect on the coverage pattern.

The GCI radar uses horizontal polarization, operates in the VHF band and should be sited on a large, flat area. The determination of the height of an airplane is accomplished by comparing signals from two antennas of different heights. If reasonable accuracy is to be attained the lobe structure in the vertical plane must be known with considerable precision. Best results are obtained by using a site of the extent and flatness prescribed in the instruction manual. In practice it may be necessary to operate on rough ground or limited areas. The question may then arise concerning the benefit that will be obtained by grading the surrounding areas, or how much forest or vegetation should be removed for acceptable operation.

Similar problems arise in siting DF stations. Large errors may be introduced by reflection from sloping land or other terrain features.

The effects described above, involving reflection from limited areas or rough land or passage of waves past an edge, may all be treated as problems of



diffraction, for which solutions are well known or may be readily computed. This subject is unfamiliar to most Service personnel; but a working knowledge of the methods of computation may be obtained by anyone who has the usual engineering education. Since it is not possible to anticipate all problems which may arise in the field, a fairly comprehensive discussion of diffraction has been included in this report so that even in the absence of other references the majority of problems may be treated.

Other important considerations such as orientation, visibility, permanent echoes, interference, and test methods are discussed. There have been many ingenious developments in these subjects in different theaters, and where available they have been included in this report. Only standard atmosphere propagation has been considered. Those who are interested in nonstandard propagation should refer to the articles on this subject published in this series.

## 15.3 TOPOGRAPHY OF SITING

### 15.3.1 Introduction

The performance of equipment which utilizes radio propagation depends upon the character of the intervening land or sea and in particular upon the local terrain at the terminals of the propagation path. Siting refers to the general problem of selecting and utilizing available locations for the best operation of the equipment involved. With some types of equipment the effects of local conditions are minor, and with other types the requirements are most exacting. In many cases practical and tactical considerations will compel the use of unfavorable locations. Performance may then be considerably below that obtained in the laboratory or under ideal conditions, and familiar characteristics may be drastically modified.

Field personnel are frequently called upon to predict or explain abnormal operation, to devise methods of improving poor performance, and to make modifications to fit local requirements. This discussion will be limited to general principles, and reference is made to the instructions furnished with the individual equipment for specific details.

Elements of a communication or radar network should ordinarily be viewed as parts of a system and not as isolated, self-sufficient units. From this point of view a site that gives outstanding results would not be satisfactory if it did not help achieve the

mission of the *system*. This interrelation between various parts of a system, which may extend over hundreds of miles, raises numerous problems of orientation, visibility, and coverage.

### 15.3.2

## Maps and Surveys

Where available, topographic maps of a scale on 1 or 2 miles to the inch and contour intervals of not more than 100 ft, preferably 20 ft, should be secured. Hydrographic charts are valuable in coastal areas. If there are no reliable maps, aerial photographs may be used to a limited extent.

Due consideration should be given to the suitability of the map projection for the purposes for which it is to be used. The grid system used for reporting should be based on the Lambert polyconic projection, and not on the Mercator projection. Otherwise important errors in azimuth may occur. This is especially true at high latitudes. If in coordinating with other services, such as the Navy, it is required to use the Mercator projection, the transfer from the Lambert projection may be made with a transparent overlay of one grid system on the other.

A transit and a stadia rod are most useful for orientation, surveys, profiles, etc. Compasses, clinometers, and other surveying instruments should be provided. In the absence of some of this equipment much may be done with improvised devices made with plumb bobs and protractors. Rough surveys may be made with only a sketching board and by pacing off distances. Navigation instruments may be used for approximate determination of position. Engineer and artillery publications describe orientation methods in detail. Close attention should be given to the grid system used for reporting nets so that all stations are accurately located. Grid errors may be minimized by making all charts from a master copy.

### 15.3.3

## Profiles

The height of the center of the antenna should be determined to within a few per cent. The reference level is the main reflecting surface, which is normally the sea. Heights given on maps should be checked against available bench marks and the terrain. Barometers or airplane altimeters are useful for height determinations, but their readings should be corrected for temperature.

Where the reflection surface is part or all land, a



profile is usually necessary for estimation of the effective antenna height and the reflection characteristics of the terrain. Profiles should be prepared of several representative azimuths in the operating sector. The accuracy required decreases with the distance from the transmitter. In most cases sufficient detail is not available on maps so that a personal inspection of the terrain should be made to become familiar with the nature of the soil and the degree of roughness. Special attention should be given to ridges, flat areas, bodies of water, distance to the shore, hills to the rear, obstacles in the operating area and at the boundaries. A knowledge of the antenna pattern in both the vertical and horizontal planes is necessary for judging what parts of the terrain should be more closely examined.

## 15.3.4

**Orientation**

Where long distances and directive beams are involved fairly accurate orientation is required. This is especially true of the narrow beam, precision type radars. Of the many ways of determining the direction of north, one of the most convenient is observation of the azimuth of the sun. Care must be taken when using compasses because of local attractions or inadequate information of the declinations. Star observations are capable of good accuracy, but where Polaris is not visible they require the same procedure as solar shots. Caution must be used in aligning on permanent echoes because nonstandard refraction may bring in confusing distant echoes, or side lobes may give false echoes. In general several methods should be used in order to obtain independent checks. When an accurate orientation has been obtained reference marks should be provided so that the azimuth may be readily checked.

Solar azimuths, correct to the nearest quarter of a degree, may be determined from the date, time to the nearest minute, and the latitude and longitude to the nearest degree. Two methods will be given for obtaining the azimuth of the sun: (1) by calculation, (2) from tables. A third method gives true south only.

The azimuth of the sun may be calculated from the formula:

$$\tan \beta = - \frac{\sin HA}{\cos \Phi \tan \delta - \sin \Phi \cos HA} \quad (1)$$

$\beta$  = bearing of the sun.

The bearing is east or west of south when  $\Phi - \delta$  is

positive. The bearing is east or west of north when  $\Phi - \delta$  is negative. The bearing is east in the morning ( $\beta$  will be negative), and west in the afternoon ( $\beta$  will be positive).

$HA$  = hour angle of the sun.

During the morning hours when the hour angle is greater than 12 hours, its value should be subtracted from 24 hours for use in the formula.

$\Phi$  = latitude of the place of observation.

$\delta$  = declination of the sun at the time of observation.

The signs of  $\Phi$  and  $\delta$  are important and each is positive when north of the equator and negative when south.

The hour angle  $HA$  is the local apparent time [LAT] minus 12 hours. To convert the observed time into LAT the civil time at Greenwich [GCT] must be found and combined with the equation of time to correct for the apparent irregular motion of the sun. This gives Greenwich Apparent Time [GAT] which is converted to LAT by allowing for the longitude. The equation of time and the declination of the sun are plotted in Figure 1 for 1945. The annual change is small, and these curves may be used for radar work without regard to the year. Standard time meridians are every  $15^\circ$  east or west of Greenwich, each zone corresponding to 1 hour. Care should be used to take daylight saving, or other changes from standard, into account correctly.

*Example 1.* It is desired to compute the azimuth of the sun.

*Given:*

Date	March 16
Time	1345 hours PWT
Latitude	$40^\circ$ North
Longitude	$118^\circ$ West

*Solution:*

The hour angle will be determined first:

Observed time PWT	13 <sup>h</sup>	45 <sup>m</sup>
Zone difference	+	7 <sup>h</sup>
Greenwich civil time	20 <sup>h</sup>	45 <sup>m</sup>
Equation of time (Figure 1)		− 9 <sup>m</sup>
Greenwich apparent time	20 <sup>h</sup>	36 <sup>m</sup>
Longitude difference for $118^\circ$ W	−	7 <sup>h</sup> 52 <sup>m</sup>
Local apparent time	12 <sup>h</sup>	44 <sup>m</sup>
LAT − 12 = $HA$	−	12 <sup>h</sup>
Hour angle of sun	+	0 <sup>h</sup> 44 <sup>m</sup>
$HA$ in arc ( $4^m = 1^\circ$ )		+ 11 <sup>°</sup>
Latitude $\Phi$		+ 40 <sup>°</sup>
Declination of sun $\delta$ (Figure 1)		− 2 <sup>°</sup>

Substituting in equation (1):

$$\begin{aligned} \tan \beta &= - \frac{\sin 11^\circ}{\cos 40^\circ \tan (-2^\circ) - \sin 40^\circ \cos 11^\circ} \\ &= - \frac{0.19}{0.766 \times (-0.0349) - 0.643 \times 0.982} \end{aligned}$$



$$= 0.29,$$

$$\beta = 16^{\circ}10'.$$

Since  $\Phi - \delta$  is positive,  $\beta$  is the bearing from the south. The bearing is west of south since  $\beta$  is positive (p.m.). The azimuth of the sun is

$$180^{\circ} + 16^{\circ}10' = 196^{\circ}10'.$$

A quicker solution may be obtained from a book *Azimuths of the Sun*, H. O. 71, published by the U. S. Navy, Hydrographic Office. The equation of time may be obtained from a current copy of *The American Nautical Almanac*, United States Naval Observatory, Washington, D. C.

This method will be illustrated by the data from Example 1. The LAT is obtained as before. Between September 23 and March 21 the sun is in south declination and since the latitude in this case is north, the second part of the book labeled "Declination Contrary Name to Latitude" is used. For latitude  $40^{\circ}$  an interpolation is made between 12:40 and 12:50 obtaining  $164^{\circ}$ . The table is marked "the angular departure of the sun west of north" for readings in the afternoon, and the tabular value is therefore subtracted from  $360^{\circ}$ , giving  $196^{\circ}$  as the azimuth of the sun. It is usually more convenient

to plot a curve of azimuth against time for the hours during which it is expected that the observation will be made. Such a curve may be used for several days without much error.

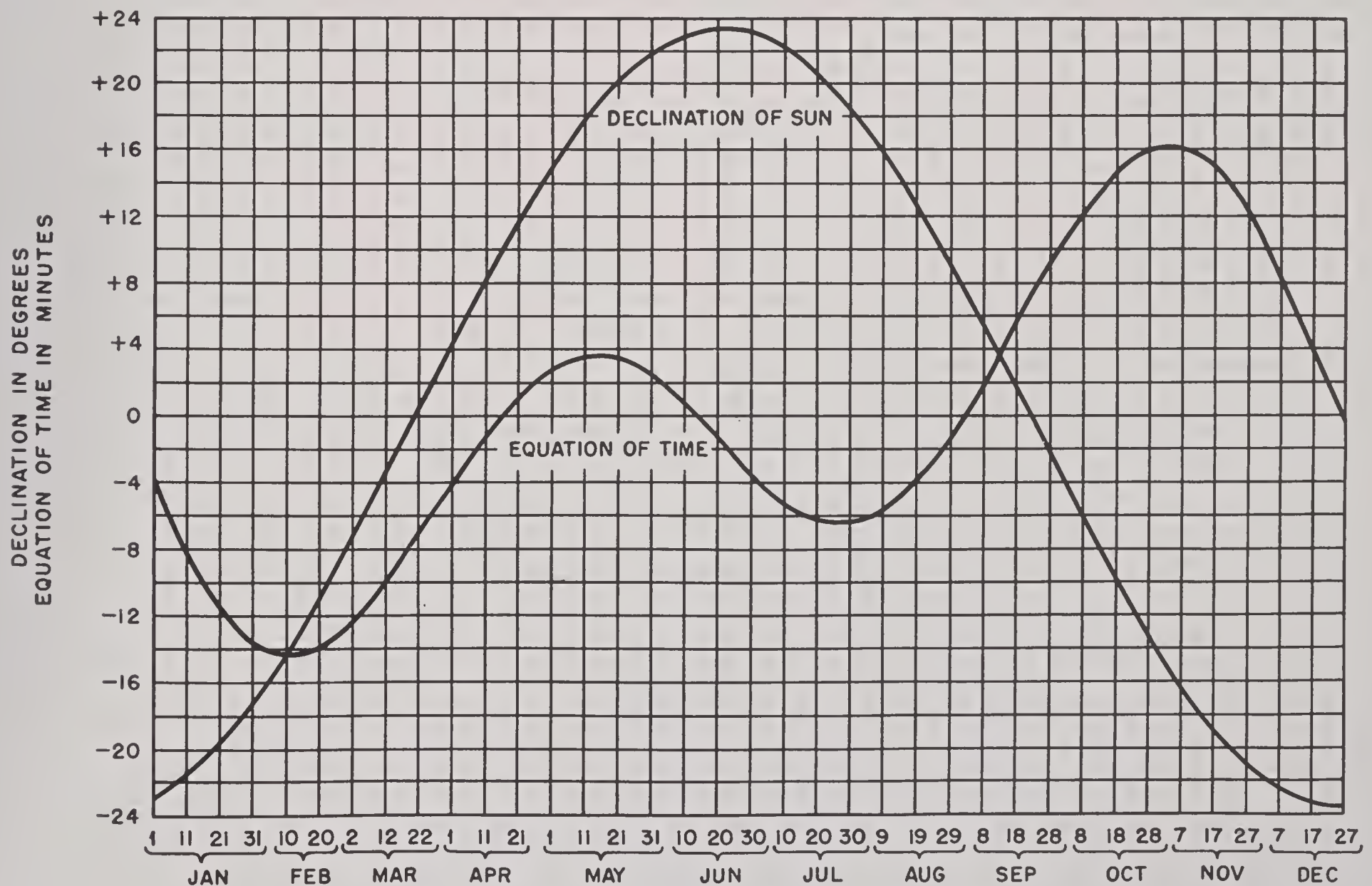
A method that is less convenient but requires no calculation is the equal altitude method. This consists in measuring the horizontal angles between the sun and a mark, when the sun is at the same altitude on both sides of the meridian of the observer. The bisector of the horizontal angle between the two equal altitude positions of the sun during the observations is very close to true south, and the azimuth of the mark may be determined.

A horizontal radiation pattern should be obtained to determine whether the electrical and mechanical axes of the antenna coincide and to discover any abnormalities in the main or secondary lobes. Defective patterns should be corrected by appropriate maintenance.

15.3.5

### Visibility Problems

It is frequently necessary to estimate the effect on rays of intervening obstacles or the curvature of the



SUN DATA FROM NAUTICAL ALMANAC 1945

FIGURE 1. Sun data from nautical almanac, 1945.



earth, or to compute the distance to the horizon, or the amount a ray would have to be diffracted to clear an intervening hill. The methods described here enable one to solve such problems quickly and simply.

#### DISTANCE TO THE HORIZON

The distance  $d$  of the horizon on a spherical earth as seen by an observer at elevation  $h$  is given by the well-known formula:

$$d = \sqrt{\frac{3h}{2}} \quad \text{or} \quad h = \frac{2}{3} d^2, \quad (2)$$

with  $d$  in statute miles and  $h$  in feet. This expression makes no allowance for refraction and is commonly used in visual work.

In radio propagation work the refraction of the standard atmosphere is sufficient to increase the distance of the "radio horizon" to

$$d = \sqrt{2h} \quad \text{or} \quad h = \frac{1}{2} d^2, \quad (3)$$

where  $d$  is expressed in statute miles and  $h$  in feet. This corresponds to the use of an effective radius of the earth equal to  $ka$  where  $k$  is  $\frac{4}{3}$  and  $a$  is 3,960 miles. This value of  $k$  will be used throughout this report. If it is desired to use other values of  $k$ , equation (3) may be written as

$$d = \sqrt{\frac{3kh}{2}} \quad \text{or} \quad h = \frac{2d^2}{3k}.$$

Points at heights  $h_1$  and  $h_2$  which are separated by the sea or smooth earth are visible from each other if the distance between them is less than

$$d_L = \sqrt{2h_1} + \sqrt{2h_2}. \quad (4)$$

#### DIP AND RISE

Over land, visibility is determined by the profile of the path involved. Elevations obtained from map contours may be plotted on a profile so as to take the effective earth curvature into account, and visibility can then be determined by graphical means. However, construction of such profiles on a curved datum line is tedious, and it is easier to compute the earth curvature and the visibility directly from the map by methods given below.

In Figure 2 is shown the relations between various heights on the earth's surface. In considering the reference line (sea level) flat as on a map or ordinary profile diagram, use is made of the line  $H_1TH_2T'$  instead of the curve  $H_1HH_2H'$ . This will be compensated for by using a fictitious ray path  $P_1PP_2P'$  instead of the line  $P_1QP_2Q'$ . The deviation of this fictitious path from  $P_1QP_2Q'$  at  $P$  is  $QP = HT$  and is called the dip. The deviation at  $P'$  is  $Q'P' = H'T'$  and is called the rise.

In the figure on the left the triangles  $HH_2T$  and  $H_1KT$  are similar and

$$\frac{TH_2}{TK} = \frac{HT}{H_1T},$$

or approximately (right-hand figure)

$$HT \times 2ka = d_1d_2.$$

Therefore the dip,

$$QP = \frac{5,280 \times d_1d_2 \times 3}{2 \times 3,960 \times 4} = \frac{d_1d_2}{2}. \quad (5)$$

Similarly for the rise

$$Q'P' = \frac{d_1'd_2'}{2}.$$

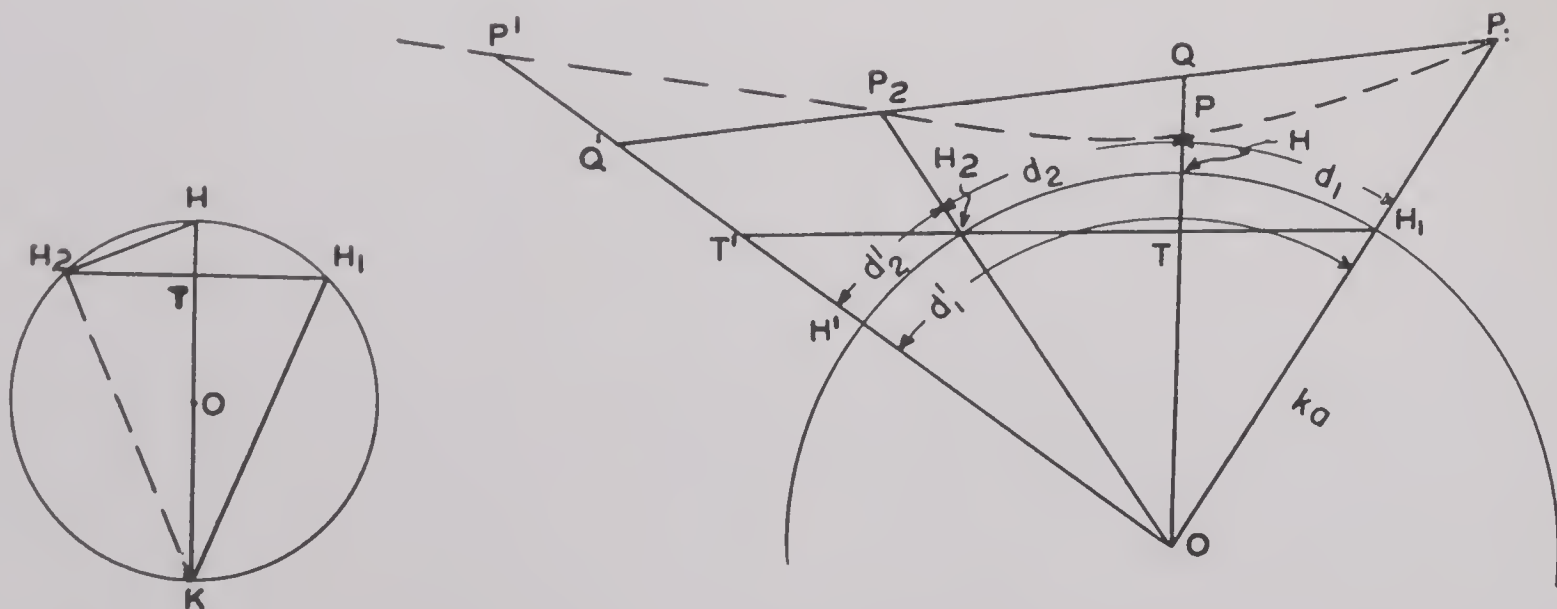


FIGURE 2. Relations between various heights on earth's surface. Dip and rise.



The application of these formulas will be shown by a number of examples.

*Example 2. Intervening Obstructions — Graphical Solution.* In Figure 3 is shown a profile as may be

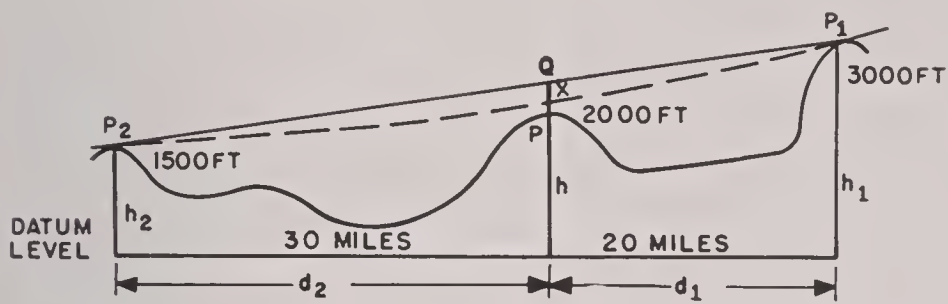


FIGURE 3. Intervening obstruction of radiation between two points.

obtained from a topographical map. It is desired to ascertain whether  $P_2$  will receive radiation from  $P_1$  without being obstructed by the intervening hill  $P$ .

Owing to the curvature of the earth the line marked "datum level" is actually curved instead of being straight as shown. To compensate for this distortion the line of sight of the radar is taken as the parabola  $P_1XP_2$  (shown dashed) instead of the straight line  $P_1QP_2$ . If  $X$  lies above the top of the intervening hill  $P$ , the ray is not obstructed. The distance  $QX$  is from equation (5).

$$QX = \frac{d_1 d_2}{2} = \frac{20 \times 30}{2} = 300 \text{ ft.}$$

Scaling this distance down from  $Q$ , it will be found that  $X$  lies above  $P$  and there is no obstruction to the radiation.

It will be noted that  $QX$  is a maximum midway between  $P_1$  and  $P_2$ .

$$QX_{\max} = \frac{1}{8} (d_1 + d_2)^2. \quad (6)$$

Where there are several obstructions to be considered the work may be speeded by drawing a line  $S_1S_2$  (Figure 4) parallel to  $P_1P_2$  at a vertical distance

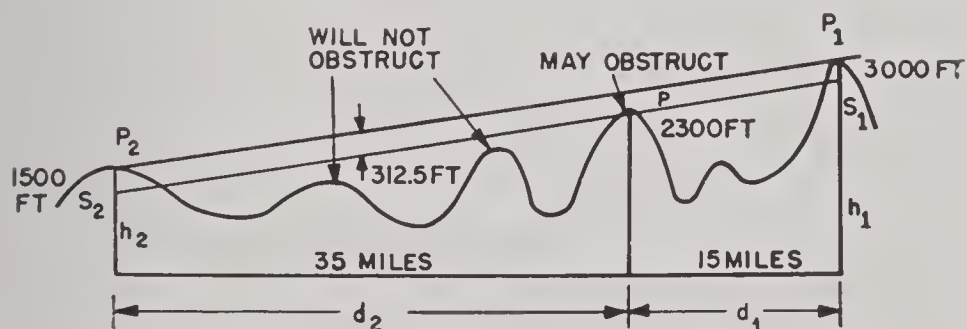


FIGURE 4. Several obstructions of radiation between two points.

below it equal to the maximum dip. Then intervening hills which do not rise above  $S_1S_2$  will not have to be considered, and those that do cut the line may

be checked for obstruction by equation (5) as before.

*Example 3. Remote Shielding—Graphical Solution.* It is frequently desired to know from a position as  $P_1$  what degree of shielding will be obtained from a given profile. In Figure 5 the rise  $Q'X'$  is computed

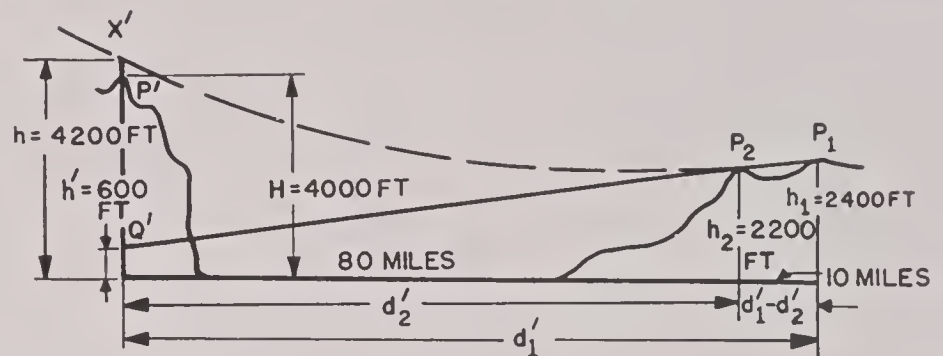


FIGURE 5. Remote shielding obtainable from a given profile.

by equation (5). Since  $P'$  lies below  $X'$  it is shielded from  $P_1$  and the minimum height of radiation is indicated by the dotted lines

$$Q'X' = \frac{d_1' d_2'}{2} = \frac{90 \times 80}{2} = 3,600 \text{ ft.}$$

*Example 4. Visibility Determined by Computation.* In many cases it is not necessary to construct profiles, as visibility may be determined by a simple computation. The critical height,  $h_c$ , which an intervening hill must equal or exceed to obstruct the line of sight, may be computed from Figure 4. Let the height of the line  $P_1P_2$  at  $d_1$  be  $h'$ . Then

$$\frac{h_1 - h'}{d_1} = \frac{h' - h_2}{d_2},$$

or

$$h' = \frac{h_1 d_2 + h_2 d_1}{d_1 + d_2}.$$

But the height  $h'$  exceeds  $h_c$  by the dip  $(d_1 d_2)/2$ ; therefore

$$h_c = \frac{h_1 d_2 + h_2 d_1}{d_1 + d_2} - \frac{d_1 d_2}{2}. \quad (7)$$

For the values given in Figure 4 the critical height at  $d_1$  is

$$\begin{aligned} h_c &= \frac{3,000 \times 35 + 1,500 \times 15}{15 + 35} - \frac{15 \times 35}{2} \\ &= 2,287.5 \text{ ft.} \end{aligned}$$

Since the hill  $P$  is 2,300 ft high it will interfere with radiation to  $P_2$ .

*Example 5. Remote Shielding—Computation.* An important problem is illustrated in Figure 5. A transmitter is located at  $P_1$ , and it is desired to know if the nearby hill  $P_2$  shields the distant mountainous island. The height of the line  $P_1Q'$  at a distance of



$d_1'$  from  $P_1$  is denoted by  $h'$  and may be obtained from the relation:

$$\frac{h_2 - h'}{d_2'} = \frac{h_1 - h'}{d_1'}$$

giving

$$h' = \frac{d_1'h_2 - d_2'h_1}{d_1' - d_2'}$$

For this case the rise  $Q'X'$  due to earth curvature must be added to give the elevation  $X'$  of the line of sight. The height of the lowest ray is therefore

$$h = \frac{d_1'h_2 - d_2'h_1}{d_1' - d_2'} + \frac{d_1'd_2'}{2} \quad (8)$$

For the values given in Figure 5

$$\begin{aligned} h &= \frac{90 \times 2,200 - 80 \times 2,400}{90 - 80} + \frac{90 \times 80}{2} \\ &= 4,200 \text{ ft.} \end{aligned}$$

It is apparent that the hill  $P'$  is shielded from  $P_1$  by the nearby hill  $P_2$  except by diffraction.

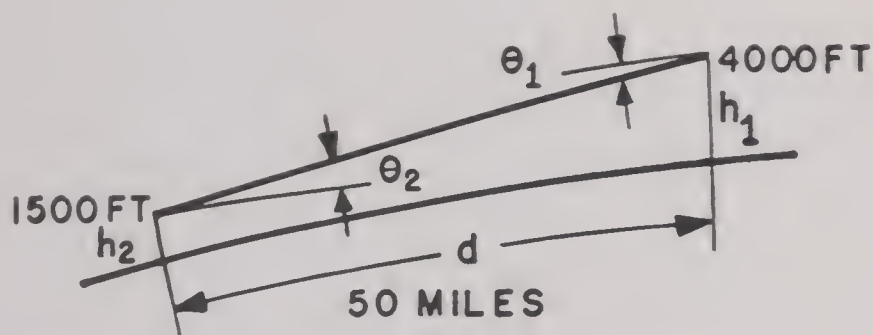


FIGURE 6. Vertical angle computation.

*Example 6. Vertical Angles.* The slope of the line of sight at the near end (Figure 6) is given by

$$\theta_1 = \frac{h_2 - h_1}{5,280d} - \frac{d}{10,560} \quad (9)$$

$\theta_1$  is in radians and is measured from the horizontal at  $h_1$ . The angle with respect to the horizontal at the far end is given by

$$\theta_2 = \frac{h_1 - h_2}{5,280d} - \frac{d}{10,560}$$

Thus for the values shown

$$\theta_1 = \frac{1,500 - 4,000}{5,280 \times 50} - \frac{50}{10,560} = -0.0142 \text{ radian,}$$

$$\text{and } \theta_2 = 0.00474 \text{ radian.}$$

*Example 7. Angle of Diffraction.* One of the principal problems in connection with intervening obstacles is the computation of the angle of diffraction. In Figure 7 the angle of diffraction is  $\theta_d$ . The line  $P_1P$  is the geometrical shadow line;  $h_c$  is the height of the

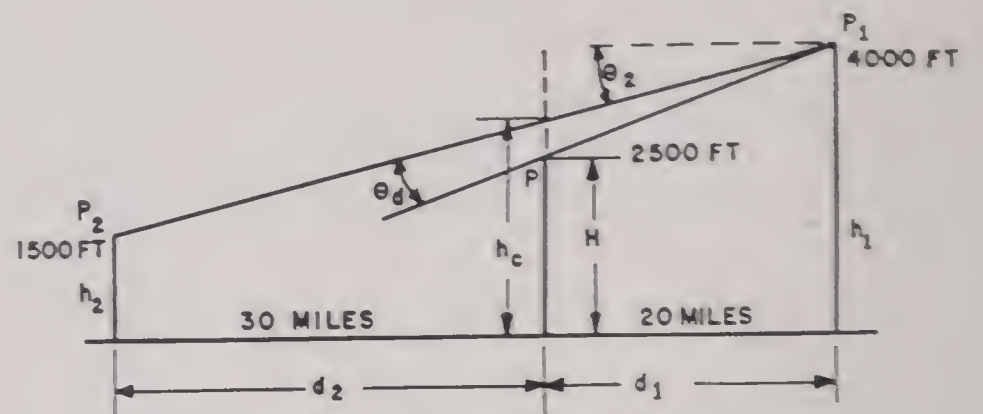


FIGURE 7. Angle of diffraction computation.

direct line  $P_1P_2$  at the distance  $d_1$  and is given by equation (7).

$$\theta_d = \frac{h_c - H}{5,280d_1} \quad (10)$$

For the values shown in Figure 7

$$\begin{aligned} h_c &= \frac{4,000 \times 30 + 1,500 \times 20}{20 + 30} - \frac{20 \times 30}{2} \\ &= 2,700 \text{ ft.} \end{aligned}$$

$$\theta_d = \frac{2,700 - 2,500}{5,280 \times 20} = 0.00189 \text{ radian.}$$

$P_2$  is therefore in the illuminated region. Had  $h_2$  been 100 ft instead of 1,500 ft,  $h_c$  would be 2,140 ft and

$$\theta_d = \frac{2,140 - 2,500}{5,280 \times 20} = -0.00341 \text{ radian,}$$

and  $P_2$  would then have been in the shadow region.

## 15.4 DIFFRACTION OF RADIO WAVES

### 15.4.1

### Introduction

Whenever interference effects are important, the reflecting surface must be examined to determine to what extent the assumption of an ideal plane or spherical surface with uniform values for the ground constants is valid. This uniformity holds when the reflecting surface is the sea; but it is often not true over land areas, and especially at the coastline. More important deviations from the ideal case are roughness of the reflecting surface, such as waves on the sea, or irregularities of the land, such as hilly or broken terrain. This frequently causes diffuse reflection and virtual elimination of useful reinforcement of the direct ray. To deal with these practical terrain problems the methods of physical optics are employed.



## 15.4.2

## Wave Propagation

For most purposes the antenna may be considered as a point source of radiation. Near the antenna the wavefront (the locus of points of constant transit time) is spherical, but at great distances it is practically plane. According to Huyghens' principle each point of a wavefront may be considered as a source emitting wavelets whose envelope at a given time is the new wavefront. In Figure 8A,  $O$  is the source

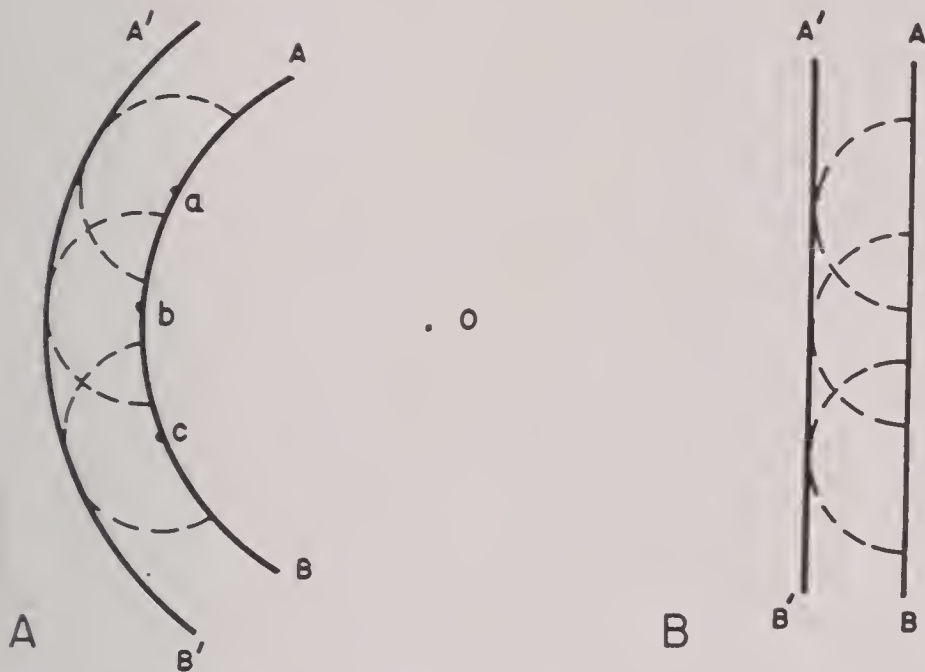


FIGURE 8. Radiation wavefronts. A. Spherical wavefront. B. Plane wavefront.

of radiation, and  $AB$  a portion of the spherical wavefront. From centers  $a$ ,  $b$ , and  $c$ , secondary waves spread out as shown by the dotted lines and are enveloped in the new front  $A'B'$ . A similar construction is made in Figure 8B for a plane wavefront.

Another example showing how waves are reflected from a plane surface is given in Figure 9. A wavefront  $AB$  is descending in an oblique direction on the reflecting surface  $AB'$ . Points  $ACDEB'$  are struck successively and in turn become centers of new wavelets. In the time required for  $B$  to reach  $B'$  the wavelet from  $A$  spreads to a radius  $AA'$ , the distance it would have traveled if there were no reflector. Other wavelets have lesser radii which, in spreading, form a new wavefront. This is the reflected wavefront, and its angle with the reflecting surface is the same as that of the incident wavefront.

The secondary wavelet from a point on a spherical wavefront ( $AB$  in Figure 10) does not produce the same effect in all directions. The field strength in a direction  $ac$  varies in proportion to  $(1 + \cos \theta)$ . The field strength drops from a value 2 in the forward direction to 1 along the line  $xy$  and to zero in the backward direction ( $\theta = 180^\circ$ ). While in Figure 8A an envelope of secondary wavelets can also be drawn

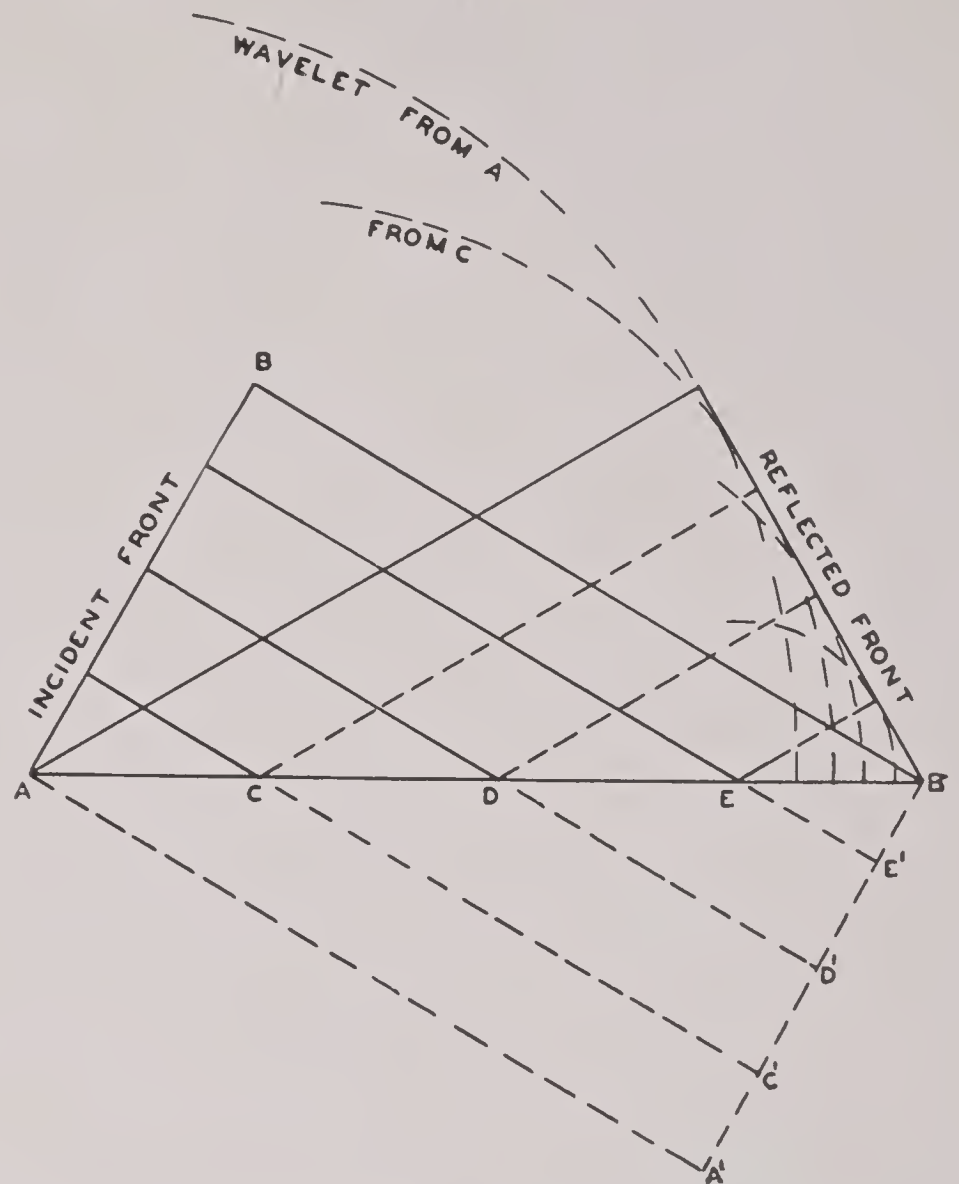


FIGURE 9. Reflection of waves from a plane surface. Huyghens' construction.

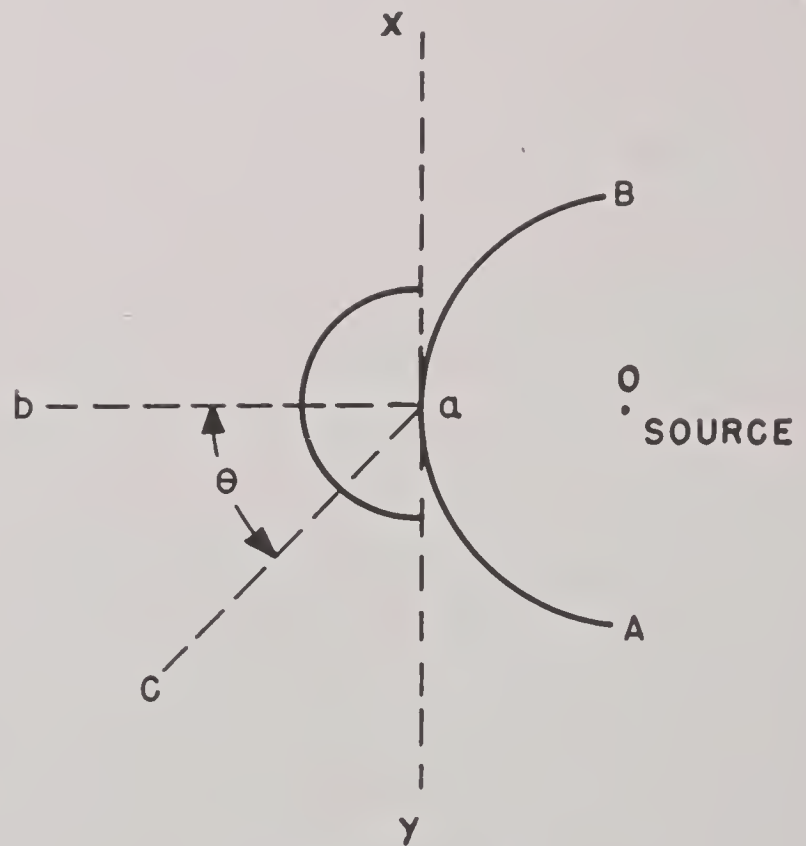


FIGURE 10. The secondary wavelet.

to the right of  $AB$  so as to produce a convergent wave traveling back to zero, it can be shown that this backwave does not exist. Only waves in the forward direction should be considered.

## 15.4.3

## Fresnel Zones

In Figure 11,  $BC$  denotes a plane wavefront moving from a distant source on the right toward



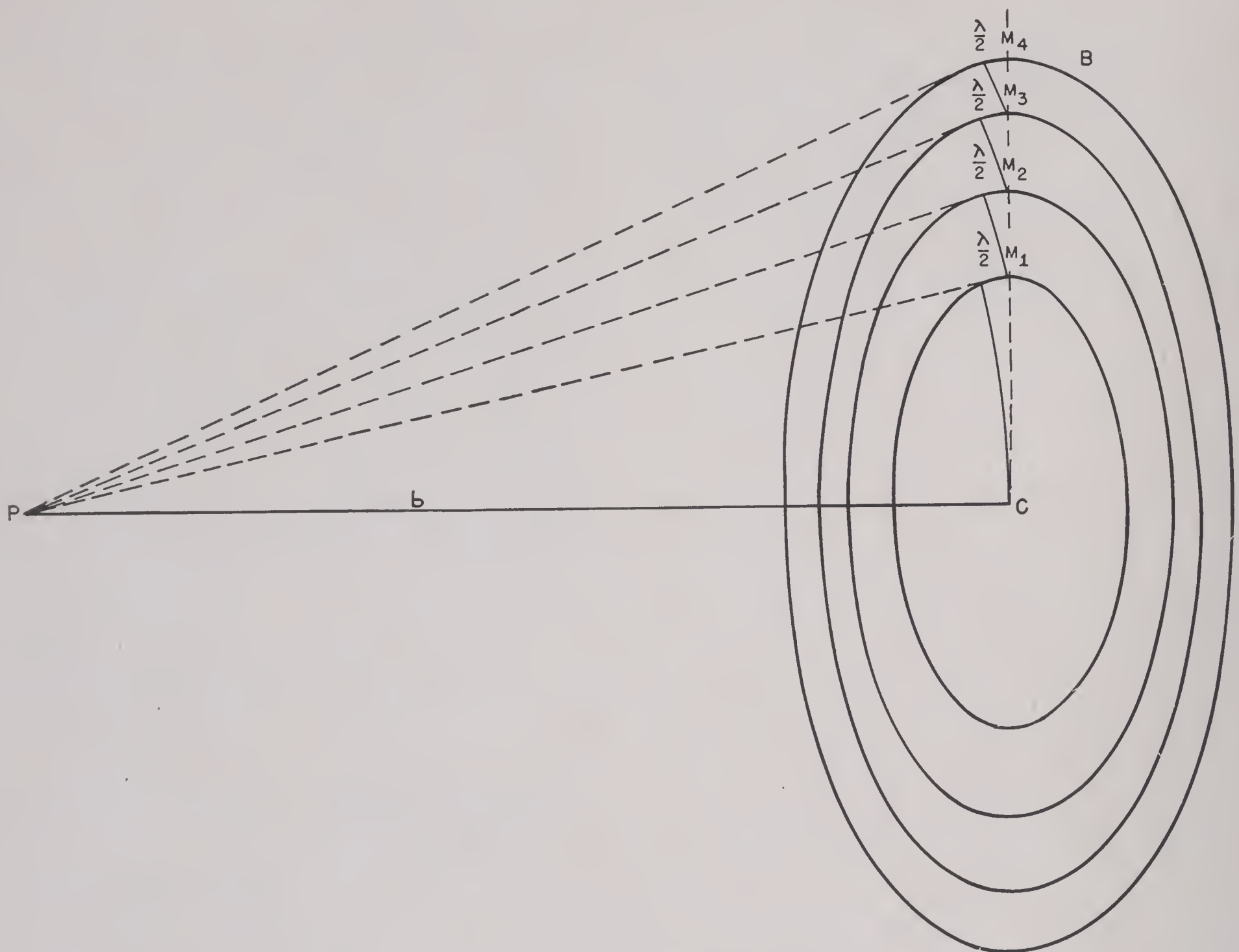


FIGURE 11. Fresnel zones.

a point  $P$  to the left. It is desired to know the effect at  $P$  of the secondary wavelets emanating from the wavefront. A straight line is drawn from the distant source to point  $P$  cutting the wavefront at  $C$ . In the wavefront with  $C$  as a center are drawn circles such that the first is a half wavelength further from  $P$  than  $C$  is, the second is 2 half wavelengths, etc., so that the secondary disturbance from any circle will reach  $P$  half a wavelength ahead of those from the circle enclosing it.

If  $PC = b$ , the radius  $r_1$  of the first zone may be obtained from

$$\left(b + \frac{\lambda}{2}\right)^2 - b^2 = r_1^2.$$

Neglecting  $\lambda^2/4$ , the radius  $r_1 = \sqrt{b\lambda}$  and the radii,  $r_2 = \sqrt{2b\lambda}$ ,  $r_3 = \sqrt{3b\lambda}$ , etc., and in general

$$r_m = \sqrt{mb\lambda}. \quad (11)$$

The corresponding areas are approximately  $\pi b\lambda$ ,  $2\pi b\lambda$ ,  $3\pi b\lambda$ , and  $m\pi b\lambda$ . The area of the central zone

is  $\pi b\lambda$ , and each succeeding ring or zone is slightly greater.

The effect which one of the zones produces at  $P$  is proportional to its area and inversely proportional to its distance from  $P$ . These factors compensate as the radius increases, so that the successive zones may be regarded as producing equal and opposite effects at the point  $P$ . The zones become less effective further from the center owing to the increased obliquity, since the effect at  $P$  is proportional to  $1 + \cos \theta$  (see Figure 10). The resultant effect may be represented by a series of terms of alternate sign which decrease slowly at first and then more rapidly, eventually becoming zero, thus:

$$\begin{aligned} S &= m_1 - m_2 + m_3, \text{ etc.}, \\ &= \frac{1}{2}m_1 + \left(\frac{1}{2}m_1 - m_2 + \frac{1}{2}m_3\right) \\ &\quad + \left(\frac{1}{2}m_3 - m_4 + \frac{1}{2}m_5\right) + \cdots \frac{1}{2}m_n. \end{aligned}$$



It can be shown that all terms except the first cancel so that

$$S = \frac{1}{2}m_1. \quad (12)$$

The resultant effect of the entire wavefront is equal to one-half of that due to the central zone.

The secondary wavelets from the central zone unite into a disturbance whose phase is midway between the center and the rim. This may be shown by dividing the first zone into rings such that the effect of each ring at the point  $P$  is equal in amplitude, and the phases range over half a complete period. The electric vectors corresponding to these subdivisions may be combined to obtain the resultant phase as in Figure 12. The vector for the central

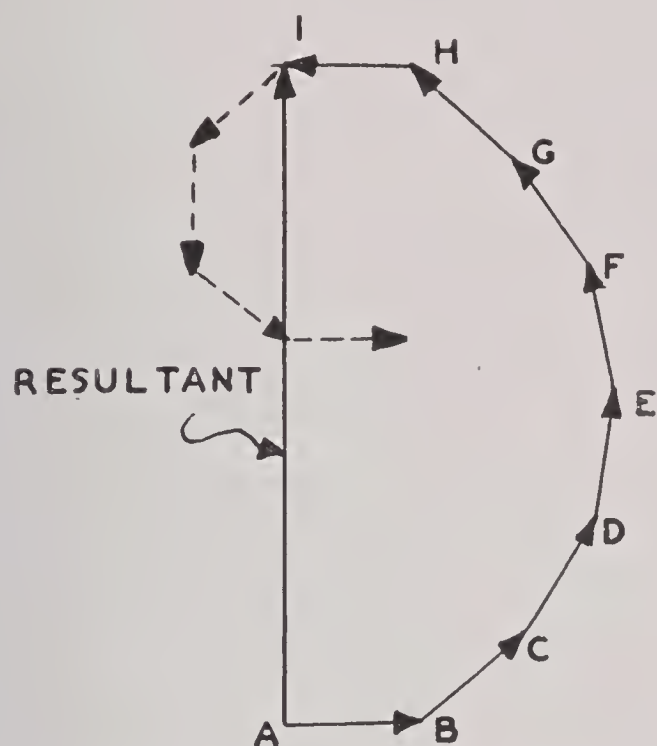


FIGURE 12. Phase of a zone.

area of the first zone is  $AB$  with succeeding surrounding rings represented by  $BC$ ,  $CD$ , etc. These vectors fall along the perimeter of a half circle, as a consequence of which the resultant amplitude is  $2/\pi$  times the sum of the amplitudes of the individual vectors. The vectors for the second zone are shown dotted.

In Figure 13 is shown the first six half-wave zones and the phases relative to the center of the first zone are indicated. A set of alternate black and white zones as shown at the top is known as a zone plate.

If a screen is provided which has an aperture of the same diameter as the first zone, it will be found that the electric intensity of the wave at the point  $P$  is doubled ( $m_1 = 2S$ ) and the power intensity is four times as great as for the unobstructed wave. If the aperture is increased to include the second zone, the intensity at  $P$  will be reduced nearly to zero. The

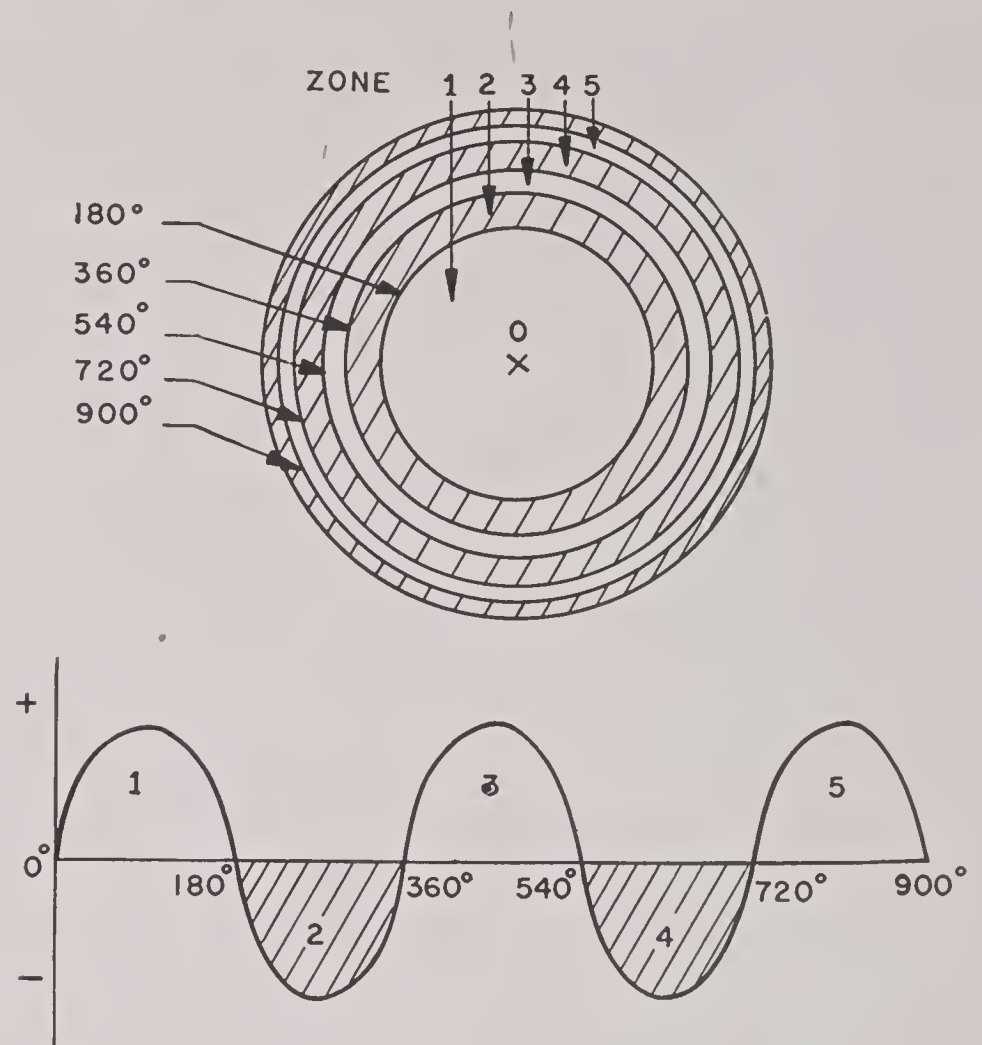


FIGURE 13. Polarity of zones.

disturbances from the second zone are out of phase with those of the first zone and equal in magnitude and therefore cause cancellation.

#### 15.4.4 Reflection from Rough Surfaces—Rayleigh's Criterion

A rough surface may destroy all phase relations between the elements on the wavefront. The secondary wavelets start from the elevated portions of the surface first, since these portions are struck first by the incident wave, and the lower portions send out secondary disturbances at various other times in random phase. It is impossible to arrange any zone system on such a surface for there are all possible phase differences irregularly distributed over the reflected wavefront and each point on the surface acts as an independent source radiating in all directions.

In Figure 14 is shown a plane surface  $xy$  with incident rays  $SB$  and  $SA$  falling on a raised portion and a crevice respectively and being reflected to  $P$ . The path difference is  $SA + AP - (SB + BP)$ . Since  $BP$  and  $AP$  are practically parallel, the path difference may be taken as  $BA - BK$ .

$$BA = \frac{H}{\sin \Psi},$$

$$BK = BA \cdot \cos 2\Psi.$$



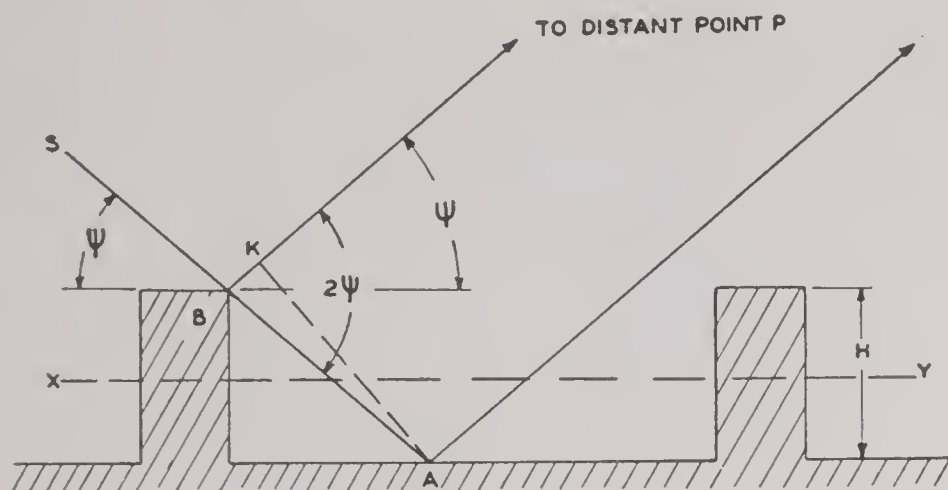


FIGURE 14. Reflection from rough surface.

The path difference

$$\begin{aligned}\Delta &= \frac{H}{\sin \Psi} (1 - \cos 2\Psi) \\ &= 2H \sin \Psi .\end{aligned}\quad (13)$$

The corresponding difference in phase is

$$\Phi = \frac{2\pi\Delta}{\lambda} = \frac{4\pi H}{\lambda} \sin \Psi .\quad (14)$$

Since the path difference increases as the grazing angle increases, the diffusion is greatest when the rays are perpendicular. When the angle is small, near zero, regular reflection may be obtained. It was suggested by Rayleigh to take as an upper limit for the grazing angle, giving regular reflection, the value corresponding to a phase difference of  $\pi/4$ . By equation (14) this angle is given by

$$\frac{\pi}{4} = \frac{4\pi H}{\lambda} \sin \Psi ,$$

or

$$\sin \Psi = \frac{\lambda}{16H} .\quad (15)$$

For a given wavelength and lobe angle the terrain at the reflection point may be examined to determine the limiting height of the roughness for regular reflections. Equation (15) may also be given in a more convenient form using the approximation  $\sin \Psi = \Psi$  radians for small values of  $\Psi$ :

$$H = \frac{3,520}{f\Psi} ,\quad (16)$$

with  $H$  in feet,  $f$  in mc, and  $\Psi$  in degrees. Thus for 100 mc regular reflection may be obtained over ridges as high as 35 ft for a grazing angle of  $1^\circ$ , but for 3,000 mc the roughness could not exceed 1 ft in height at this angle.

15.4.5

## Diffraction at Obstacles

The preceding considerations of Fresnel zones in a wavefront will now be applied to the problem of radio wave diffraction past hills, ridges, or nearby objects. These obstacles will be treated as though they were straight edges, narrow screens, or rectangular slits.

In Figure 15 is shown a distant source of radiation

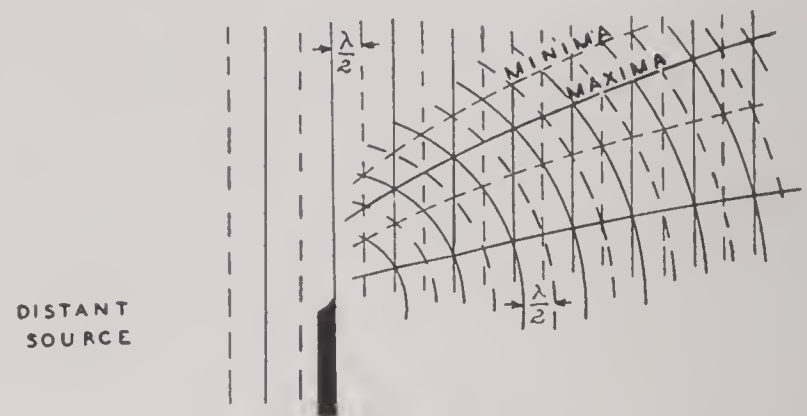


FIGURE 15. Interference of waves at an edge.

and a diffracting edge. The illuminated edge is considered to send out secondary cylindrical wavelets which interfere with the plane waves which are not shielded by the edge. The dotted and solid lines are spaced a half wavelength apart. In the unshaded region the intersection of two dotted or two solid lines indicates reinforcement and the intersection of a dotted and a solid line indicates cancellation. The loci of maxima and minima are parabolas along which the relative intensities are practically constant. In the shadow region, where only the wavelets from the edge are propagated, the relative intensity falls off continuously as the angle of diffraction is increased, since the angle  $\theta$  (see Figure 10) approaches  $90^\circ$ .

In Figure 16 is shown the zone system obtained because of a diffracting edge with the source of radiation at a distance behind the paper and with the edge viewed from a screen on which diffraction fringes are formed. The observer is within the shadow region a distance  $bc$ , and the zone system is largely obscured as indicated by the dotted lines. The radiation received at  $c$  comes from the exposed zones, and its intensity is equal to a series of the form  $m_1 - m_2 + m_3 \dots$ , etc., where  $m_1$  is the electric intensity due to the exposed portion of the first uncovered zone, etc. The sum of this series is a fraction of  $m_1$  since the outer zones tend to cancel. As  $c$  is moved to the right, that is, further into the shadow,  $m_1$  will decrease very rapidly without passing through maxima and minima.



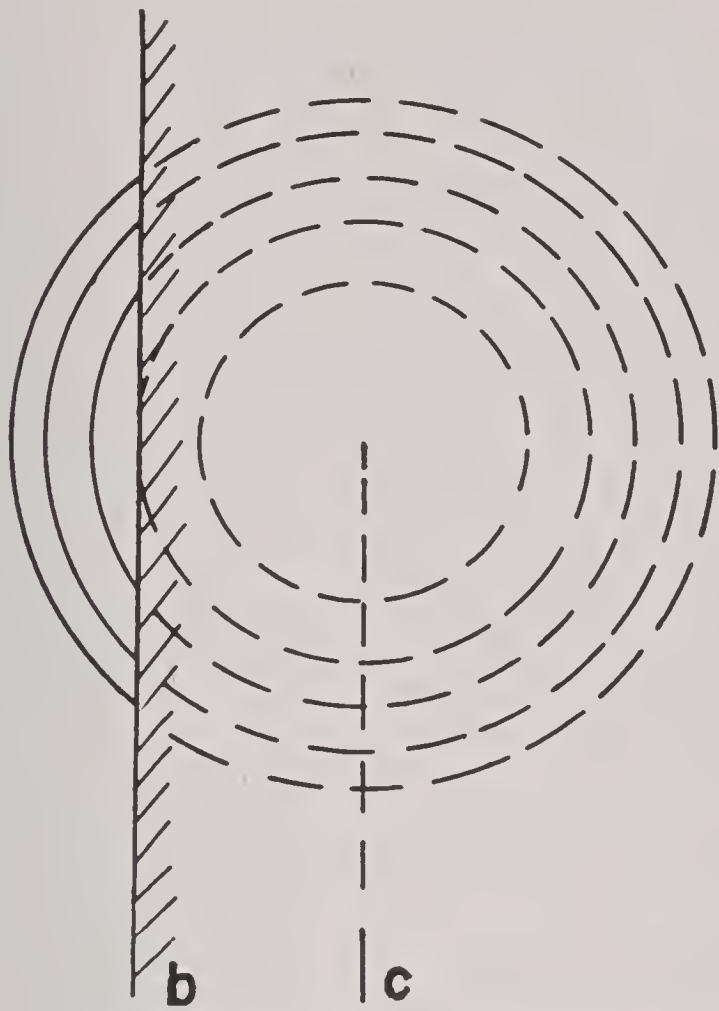


FIGURE 16. Fresnel zones in the shadow region.

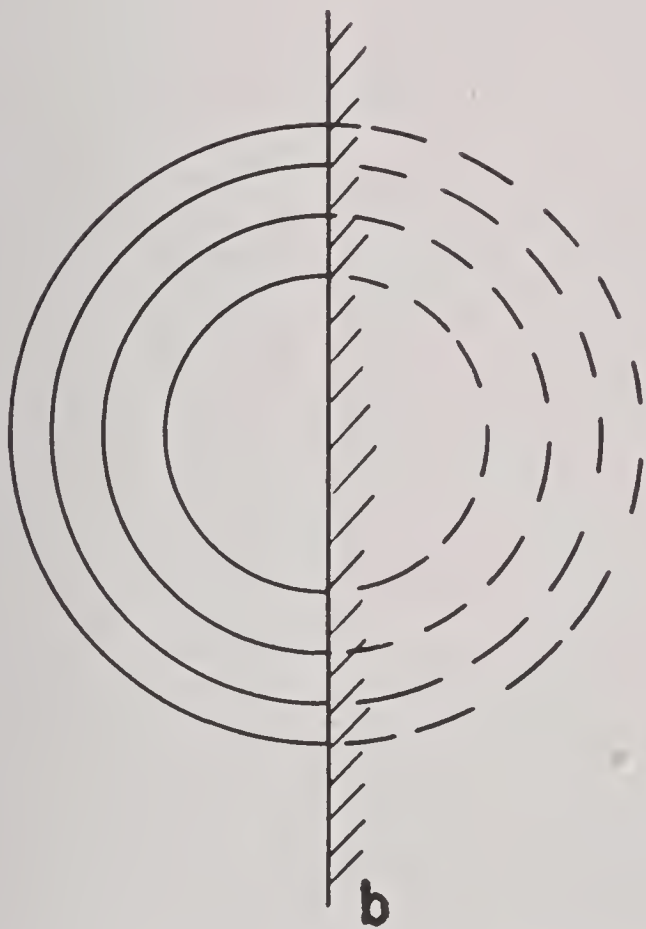


FIGURE 17. Fresnel zones on the shadow line.

In Figure 17 the observer is at the geometrical edge of the shadow. Only one-half of the wave is effective and the electric intensity is reduced to one-half, considering the unobstructed wave as unity. Outside the edge, Figure 18, at a distance  $ab$  the electric intensity is that due to the half of the wave, plus such portions of the zones between  $a$  and  $b$  that are uncovered. If an even number of zones is uncovered there is approximately a minimum of radiation received at the line  $a$ , that is, the half

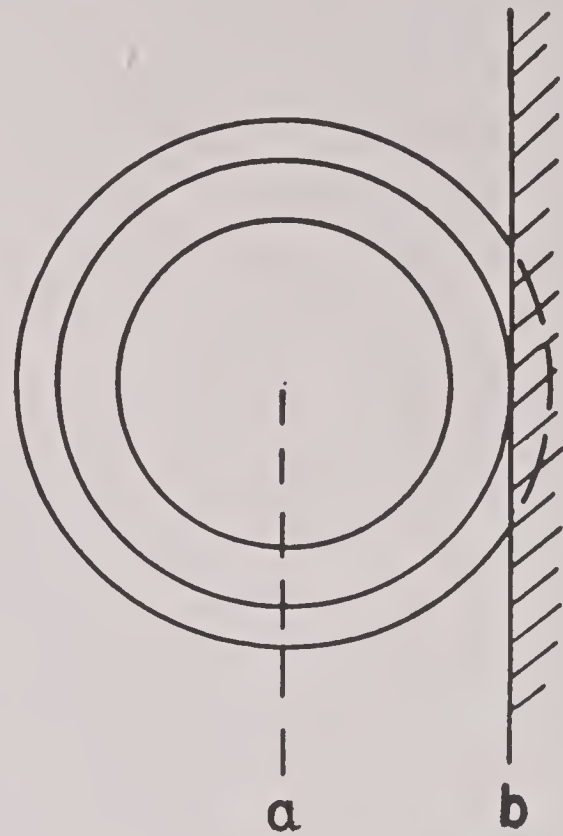


FIGURE 18. Fresnel zones in the illuminated region.

wave plus the effect of the two zones,  $\frac{1}{2} + m_1 - m_2$ , for the case shown. If  $a$  were moved to the right so that slightly less than one zone were uncovered there would be a maximum,  $\frac{1}{2} + m_1$ , in which case  $m_1$  is greater than one-half owing to the partial screening of the other zones, which, if allowed to operate, would reduce the effect due to the right-hand half of the central zone. For this reason the fringes formed outside the shadow may exceed the electric intensity of the unobstructed wave. As  $a$  is moved to the left, more zones are uncovered, and the maxima and minima are spaced approximately according to the radii of the zones; that is, the distances are proportional to the square roots of 1, 2, 3, etc.

## 15.4.6

## Fresnel Integrals

The preceding discussion is approximate and provides a qualitative picture of diffraction phenomena. The problem will now be formulated quantitatively by the method of Fresnel. Since the applications in view all have to do with diffraction by straight edges, slits, etc., the theoretical approach will be limited to diffraction of cylindrical waves by long edges parallel to the axis of the cylinder. The diffraction images of the source will then be bright bands also parallel to this axis, and the whole problem may be reduced to the consideration of rays in a plane perpendicular to the axis. The fact that in the applications to be discussed later the illumination is due to a point source rather than a line source is probably of little importance provided the distance



from the source to the diffracting edge is sufficiently large.

In Figure 19 is shown a cylindrical wavefront  $AB$

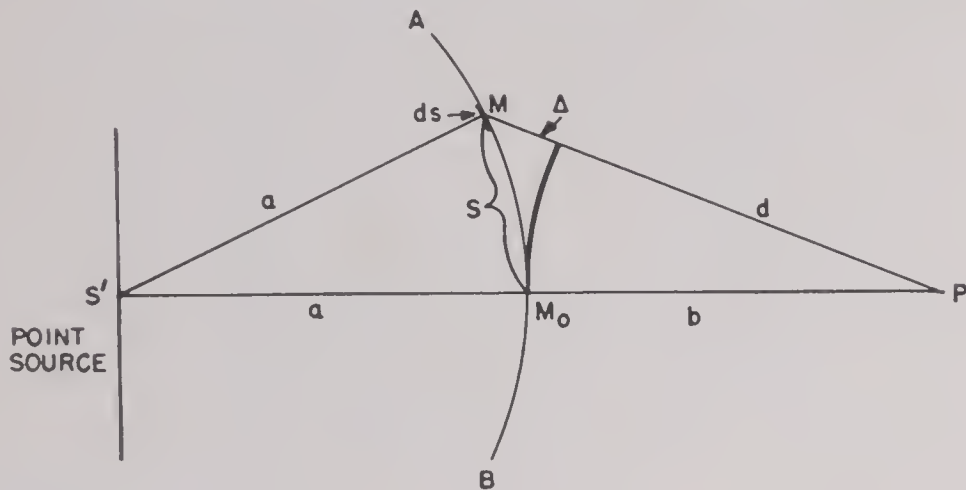


FIGURE 19. Effect at point  $P$  of wavefront  $AB$ .

with its axis at the line source  $S'$  (say an illuminated narrow slit). The secondary wavelets from the various line elements  $ds$  of the wavefront arrive at  $P$  with different phases, having traveled different distances  $MP$ . It is desired to find the resultant field strength  $MP$  due to wavelets from any given finite part of the front.

Let the electric field strength at a point in the wavefront be given by the expression

$$E = E_0 \sin 2\pi ft, \quad (17)$$

where  $t$  is the time,  $f$  the frequency, and  $E_0$  the amplitude of  $E$ . The phase has been adjusted so as to make  $E = 0$  when  $t = 0$ .

Consider next the secondary wavelets spreading from the front in the direction of  $P$ . The field intensity at  $P$  due to the secondary wavelet emanating from the line element  $ds$  at the point  $M$  (see Figure 19) is proportional to  $dsE_0$  and is inversely proportional to the square root of the distance  $MP = d$  (since this is a cylindrical wave). Further, the field intensity must show a phase retardation corresponding to the distance  $d$ , that is  $2\pi d/\lambda$ . Hence the field strength of the wavelet at  $P$  is given by an expression of the form

$$dE = kE_0 ds \sin \left( 2\pi ft - \frac{2\pi d}{\lambda} \right), \quad (18)$$

where  $k$  is a factor of proportionality which depends to some degree on the angle  $MPM_0$  and the distance  $d$ , but which will be considered constant here, as the dependence of the phase on  $d$  is of much greater importance. To obtain the intensity due to wavelets emanating from a finite part of the front, equation (18) must be integrated over the corresponding region of  $s$ . For this purpose we need a relation between  $d$  and  $s$ . This is obtained by applying the

cosine law to the triangle  $MSP$ , which gives at once

$$d^2 = (a + b)^2 + a^2 - 2a(a + b) \cos \frac{s}{a}, \quad (19)$$

or after a simple reduction, using the identity

$$\cos \left( \frac{s}{a} \right) = 1 - 2 \sin^2 \frac{s}{2a}$$

then

$$d^2 = b^2 + 4a(a + b) \sin^2 \frac{s}{2a}. \quad (20)$$

For the present purpose it is sufficient to consider the case when angle  $s/a$  is so small that powers of  $s/a$  above the square may be neglected in comparison with unity. This means that

$$d = \sqrt{b^2 + 4a(a + b) \sin^2 \frac{s}{2a}} \sim b + 2a \frac{(a + b)}{b} \sin^2 \frac{s}{2a} \sim b + \frac{(a + b)}{2ab} s^2, \quad (21)$$

or again, on writing

$$\sqrt{\frac{(a + b)}{2\lambda ab}} s = \frac{1}{2} v, \quad (22)$$

the phase lag  $2\pi d/\lambda$  assumes the form

$$\frac{2\pi d}{\lambda} = \frac{2\pi b}{\lambda} + \frac{\pi}{2} v^2. \quad (23)$$

Using equations (22) and (23), expanding the sine expression of equation (18), it follows that

$$dE = k \sqrt{\frac{ab\lambda}{2(a + b)}} E_0 \left[ \cos \left( \frac{\pi}{2} v^2 \right) \cdot \sin 2\pi \left( ft - \frac{b}{\lambda} \right) - \sin \left( \frac{\pi}{2} v^2 \right) \cdot \cos 2\pi \left( ft - \frac{b}{\lambda} \right) \right] dv. \quad (24)$$

This expression may now be integrated over a certain region of the wavefront, say from  $v = v_0$  to  $v = v$ , corresponding to  $s = s_0$  to  $s = s$ , giving the following expression for the electric field strength at  $P$ :

$$E = k \sqrt{\frac{ab\lambda}{2(a + b)}} E_0 \left[ f(v, v_0) \sin 2\pi \left( ft - \frac{b}{\lambda} \right) - g(v, v_0) \cos 2\pi \left( ft - \frac{b}{\lambda} \right) \right] \quad (25)$$

where

$$f(v, v_0) = \int_{v_0}^v \cos \left( \frac{\pi}{2} v^2 \right) dv, \quad (26)$$

and

$$g(v, v_0) = \int_{v_0}^v \sin \left( \frac{\pi}{2} v^2 \right) dv. \quad (27)$$



Equation (25) may be brought into a more convenient form by writing

$$\tan \theta = \frac{g(v, v_0)}{f(v, v_0)}, \quad (28)$$

$$\text{and} \quad R = \sqrt{f^2(v, v_0) + g^2(v, v_0)}. \quad (29)$$

It then follows that equation (26) assumes the form

$$E = k \sqrt{\frac{ab\lambda}{2(a+b)}} E_0 R \sin \left[ 2\pi \left( ft - \frac{b}{\lambda} \right) - \theta \right]. \quad (30)$$

For tabulation purposes the quantities  $f(v, v_0)$  and  $g(v, v_0)$  are replaced by the Fresnel integrals, defined by:

$$C(v) = \int_0^v \cos \left( \frac{\pi}{2} v^2 \right) dv \quad (31)$$

and

$$S(v) = \int_0^v \sin \left( \frac{\pi}{2} v^2 \right) dv. \quad (32)$$

Evidently

$$f(v, v_0) = C(v) - C(v_0), \quad (33)$$

and

$$g(v, v_0) = S(v) - S(v_0). \quad (34)$$

In the sequel the arguments will be omitted wherever it can be done without causing misunderstandings, and the above symbols will be written simply as  $f$ ,  $g$ ,  $C$ , and  $S$ .

TABLE 1. Fresnel integrals.

$v$	$C$	$S$	$v$	$C$	$S$
0.00	0.0000	0.0000	2.50	0.4574	0.6192
0.10	0.0999	0.0005	2.60	0.3889	0.5500
0.20	0.1999	0.0042	2.70	0.3926	0.4529
0.30	0.2994	0.0141	2.80	0.4675	0.3915
0.40	0.3975	0.0334	2.90	0.5624	0.4102
0.50	0.4923	0.0647	3.00	0.6057	0.4963
0.60	0.5811	0.1105	3.10	0.5616	0.5818
0.70	0.6597	0.1721	3.20	0.4663	0.5933
0.80	0.7230	0.2493	3.30	0.4057	0.5193
0.90	0.7648	0.3398	3.40	0.4385	0.4297
1.00	0.7799	0.4383	3.50	0.5326	0.4153
1.10	0.7648	0.5365	3.60	0.5880	0.4923
1.20	0.7154	0.6234	3.70	0.5419	0.5750
1.30	0.6386	0.6863	3.80	0.4481	0.5656
1.40	0.5431	0.7135	3.90	0.4223	0.4752
1.50	0.4453	0.6975	4.00	0.4984	0.4205
1.60	0.3655	0.6389	4.10	0.5737	0.4758
1.70	0.3238	0.5492	4.20	0.5417	0.5632
1.80	0.3337	0.4509	4.30	0.4494	0.5540
1.90	0.3945	0.3734	4.40	0.4383	0.4623
2.00	0.4883	0.3434	4.50	0.5258	0.4342
2.10	0.5814	0.3743	4.60	0.5672	0.5162
2.20	0.6362	0.4556	4.70	0.4914	0.5669
2.30	0.6268	0.5531	4.80	0.4338	0.4968
2.40	0.5550	0.6197	4.90	0.5002	0.4351

15.4.7

## The Cornu Spiral

In Figure 20 the two Fresnel integrals are plotted against each other,  $S$  being the ordinate and  $C$  the abscissa, for different values of  $v$ . The resulting curve is known as Cornu's spiral. The upper positive branch ( $C$  and  $S$  positive) corresponds to points on the wavefront above the line.  $S'P$  in Figure 19, and the lower or negative branch corresponds to the wavefront below the line  $S'P$ .

By their definition  $f$  and  $g$  signify the coordinate differences between any two given points on the Cornu spiral, and it follows that  $R$ , as defined by equation (29), represents the corresponding distance between these points.

Differentiating equations (31) and (32) for  $C$  and  $S$ , squaring and adding, it follows that

$$(dC)^2 + (dS)^2 = (dv)^2, \quad (35)$$

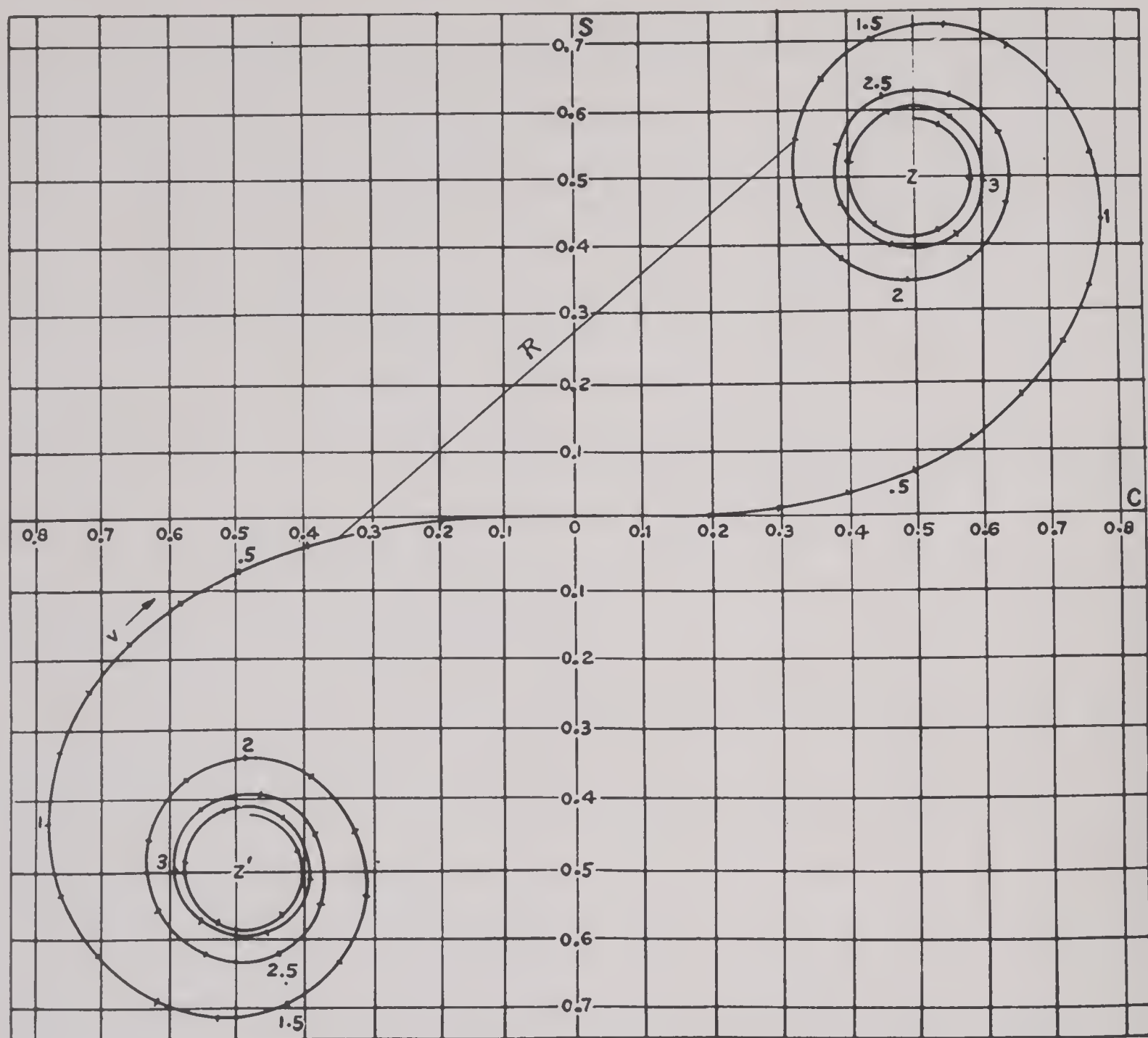
so that  $dv$  is the line element of the spiral, and  $v$  measures length along the curve from the origin.

In order to see more in detail how the Cornu spiral is built up of contributions from different zones we may suppose the half-wave zones on the wavefront to be divided into equal areas and the contributions of these areas to the field strength vectorially combined to obtain the resultant effect as in Figure 22. Then as smaller areas are used and more zones are summed up the vector diagram becomes in the limit the Cornu spiral. This is shown in greater detail in Figures 21 and 22. Here the first half-period zone of Figure 21 is divided into nine parts and the resultant is  $AB$  (Figure 22). The second half-period gives a resultant  $BC$ . The sum of the first two half-periods is  $AC$ . The sum of all half-periods is  $AZ$ , which is thus the resultant effect at  $P$  of the upper half of the wavefront. A similar result is obtained for the lower half.

It may be remarked that the superiority of the dimensionless variable  $v$  over  $s$  shows itself in the fact that one Cornu spiral suffices for all situations of the diffracting edge, while the use of  $s$  would have necessitated the construction of a special spiral for each specific set of values,  $a$ ,  $b$ , and  $\lambda$ . In Figure 20 the values  $v = 1$  and  $v = 2$  are marked and correspond to path differences  $\Delta = \lambda/4$  and  $\Delta = \lambda$ , respectively.

Equation (30) shows that the electric field strength in the diffraction region which is due to a certain section of the wavefront is proportional to the corresponding value of  $R$ . Hence, it follows that the





power per unit area is proportional to  $R^2$ . Let  $W$  denote peak power per unit area at the point  $P$  for a certain arbitrary value of  $R$ . Then

$$W = K \cdot R^2, \quad (36)$$

where  $K$  is a certain constant. When the whole wave is acting, the integration limits extend from  $v = -\infty$  to  $v = +\infty$ , that is, along the full length of the Cornu spiral. The coordinate difference between the foci of the spiral being (1,1) (see Figure 20) it follows that their distance is  $R = \sqrt{2}$ , so that the corresponding peak power per unit area  $W_0$  is, by equation (36),  $W_0 = 2K$  which defines  $K$  as  $\frac{1}{2}W_0$ . Hence it follows that equation (36) may also be written as

$$\frac{W}{W_0} = \frac{1}{2} R^2. \quad (37)$$

15.4.8

### Straight Edge Diffraction

Using Cornu's spiral the diffraction pattern due to a straight edge may be obtained. In Figure 23 is

shown a diffracting edge at  $M_0$ . At  $P$  the upper half of the wave is effective, and on Figure 22 the amplitude is  $AZ$  of length  $1/\sqrt{2}$ . The square of this is one-half, which by equation (37) is multiplied by  $\frac{1}{2}$  to get  $\frac{1}{4}$  for the power intensity at the edge of the shadow. The electric field intensity is  $\frac{1}{2}$ .

Consider next a point such as  $P'$  at a distance  $x$  above  $P$  (see Figure 23). To be specific, the point

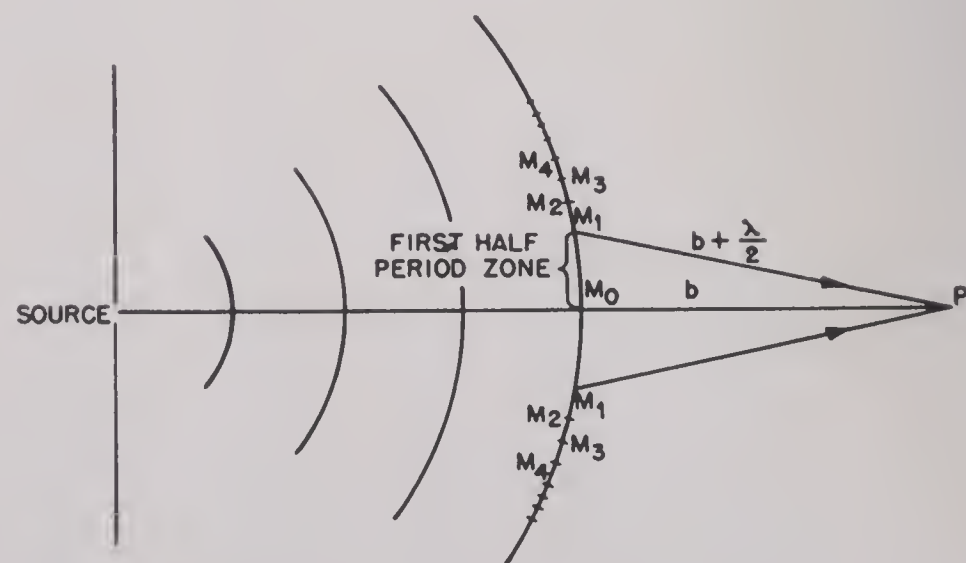


FIGURE 21. Division of wavefront into half-period zones.



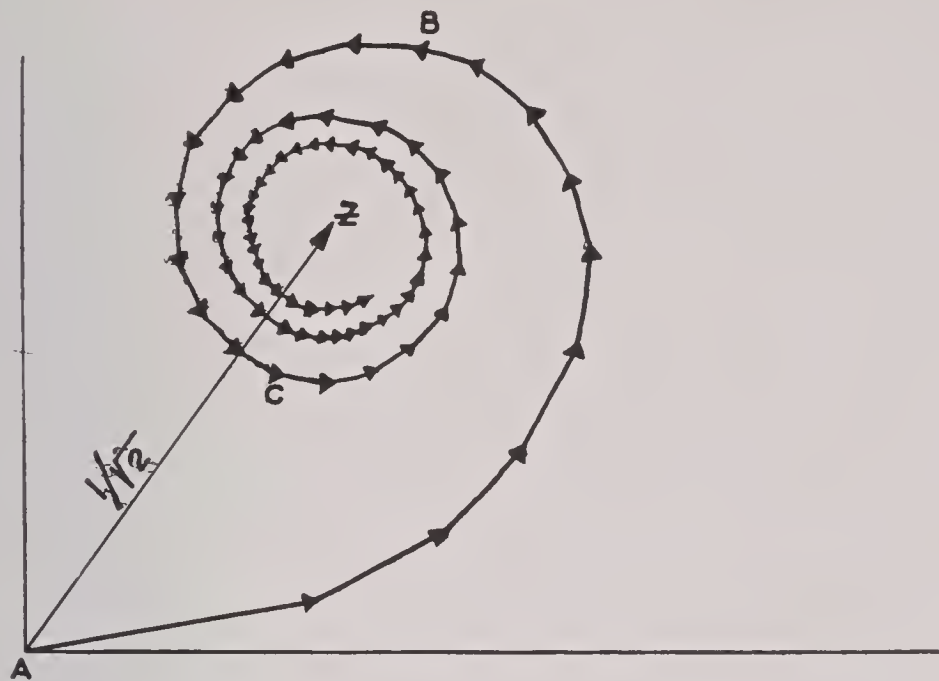


FIGURE 22. Vector sum of subzone contributions.

$P'$  is chosen in the direction of  $SM_1$  of Figure 23, where  $M_1$  is the upper edge of the first half-wavelength zone. The illumination at the point  $P'$  is, firstly, due to all wavelets emanating from the half wavefront above  $P'S$ . In addition, there is the contribution from the lower half of the wavefront extending from  $M_1$  to  $M_0$ . The situation is, in fact, the same as if  $P'$  were brought down to  $P$  and the diffracting edge were lowered from  $M_0$  to  $M'_1$  (see Figure 24). The resultant amplitude  $R$  is represented

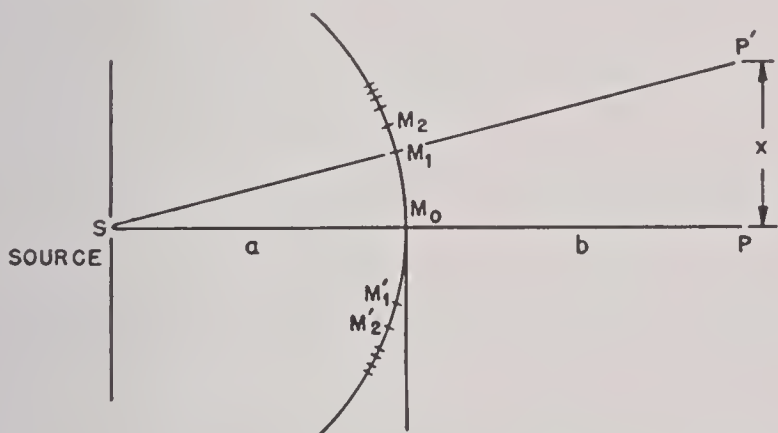


FIGURE 23. Diffraction at shadow line.

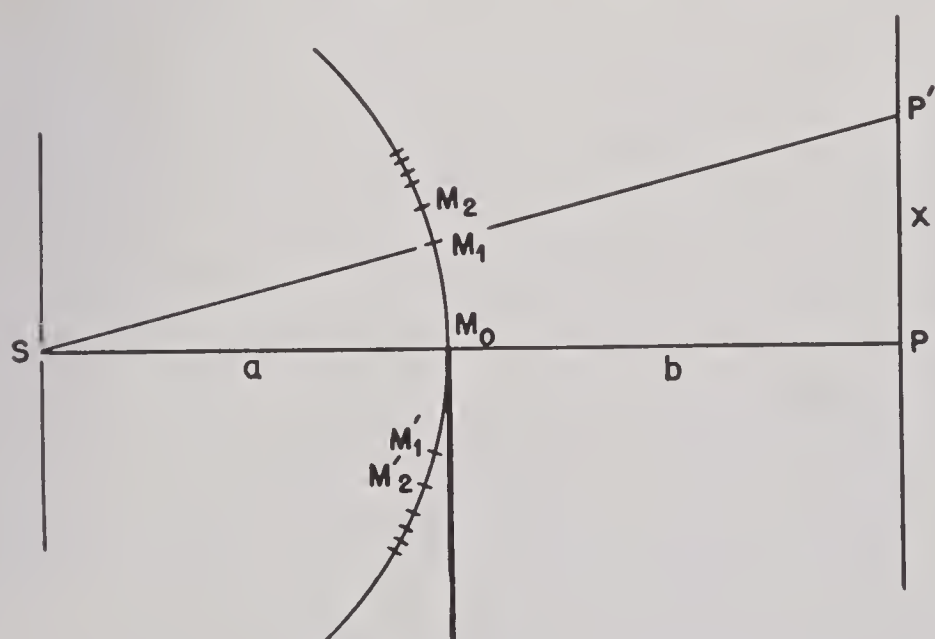


FIGURE 24. Diffraction in illuminated region.

on Figure 25 by  $ZB$ . Starting at the point  $P$  at the edge of the shadow (Figure 23) where the amplitude is  $AZ$ , if the point is moved upward, the tail of the amplitude vector moves to the left along the spiral while its head is fixed at  $Z$ .

The amplitude goes through a maximum at  $b'$ , a minimum at  $c'$ , etc., approaching a value  $ZZ'$  for the unobstructed wave. Moving in the other direction, into the shadow, the vector moves to the right from  $A$ , decreasing steadily to zero.

The power intensity versus  $v$  is plotted in Figure 26, and the points  $B, C, D$ , etc., corresponding to those in Figure 25 represent the exposure of 1, 2, 3, etc., half-period zones below  $M_0$ . The maxima and minima occur a little before these points are reached. This curve may be plotted from the table of Fresnel integrals with the equations

$$\begin{aligned} f &= 0.5 + C, \\ g &= 0.5 + S, \\ z^2 &= \frac{1}{2}(f^2 + g^2), \end{aligned} \quad (38)$$

where  $z^2$  is the relative power intensity compared to the unobstructed wave. The relative electric intensity is

$$z = \sqrt{\frac{f^2 + g^2}{2}}. \quad (39)$$

Equation (39) is plotted in Figure 27. The portion of the curve for  $-v$  has been drawn to the right and is to be used with the right-hand ordinate.

The phase lag  $\zeta$  due to diffraction may be determined from the angular position of the vector  $R$  in Figure 25. In the illuminated region the phase lag oscillates about the reference value,  $Z'Z$ , and is given by

$$\frac{\pi}{4} - \tan^{-1} \frac{g}{f}.$$

At the shadow line the relative value is the same as  $Z'Z$ . In the shadow region the phase lag varies continuously along a parabolic curve and is given by

$$\frac{v^2}{2} + \frac{\pi}{4}.$$

The phase lag relative to that of the shadow line is plotted in Figure 28. The portion of the curve for  $-v$  is drawn to the right, and its ordinate, on the right, has a different scale from that used with the  $+v$  portion of the curve.

#### 15.4.9 Location of Maxima and Minima

When the source is close to the diffracting edge, the positions of the maxima and minima in the



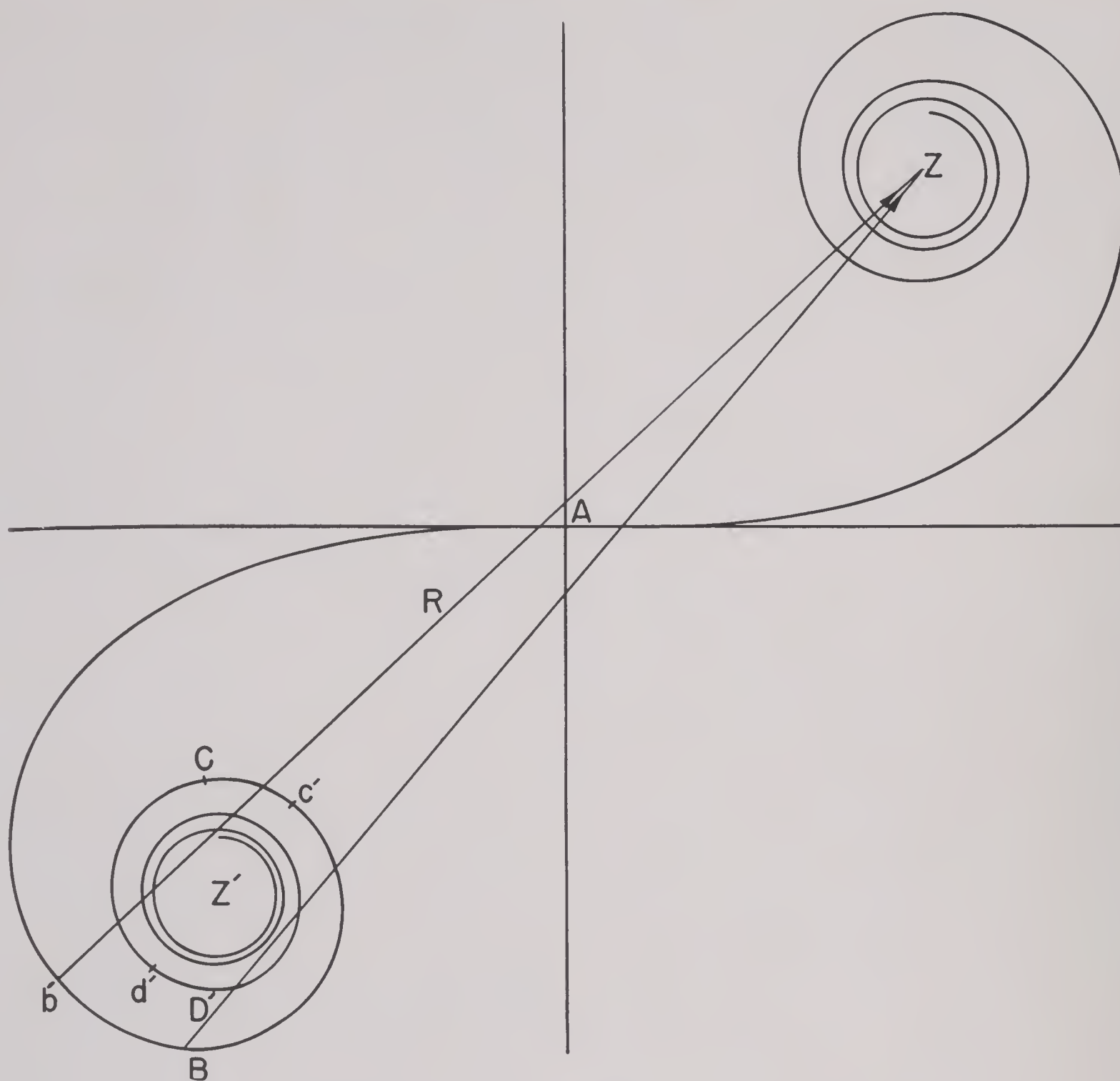


FIGURE 25. Method of using the Cornu spiral.

illuminated region may be determined by the following analysis. The effect of the wave  $RM$  (Figure 29) at  $P'$  may be considered to be due to the upper half of the wave (above  $R$ ), which is unaffected by the edge, and the lower half of the wave (below  $R$ ), which is partly shielded by the edge. If  $RM$  contains an even number of half-period elements the intensity at  $P'$  is a minimum. If the number of half-period

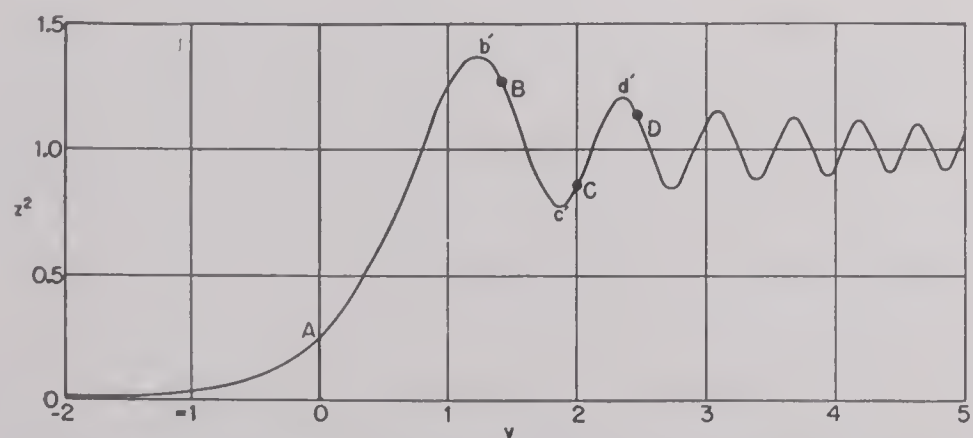


FIGURE 26. Relative power intensity—straight edge diffraction.

elements is odd the intensity is a maximum. That is

$$MP' - RP' = \frac{n\lambda}{2}, \quad (40)$$

where  $n$  is an integer with values 1, 3, 5, etc., for

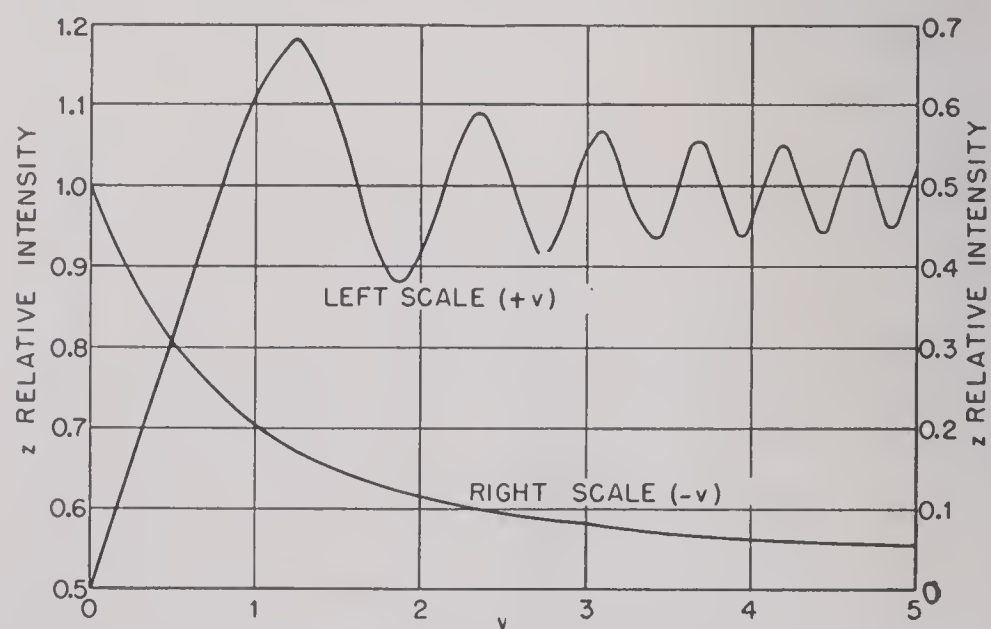


FIGURE 27. Relative electric intensity—straight edge diffraction.



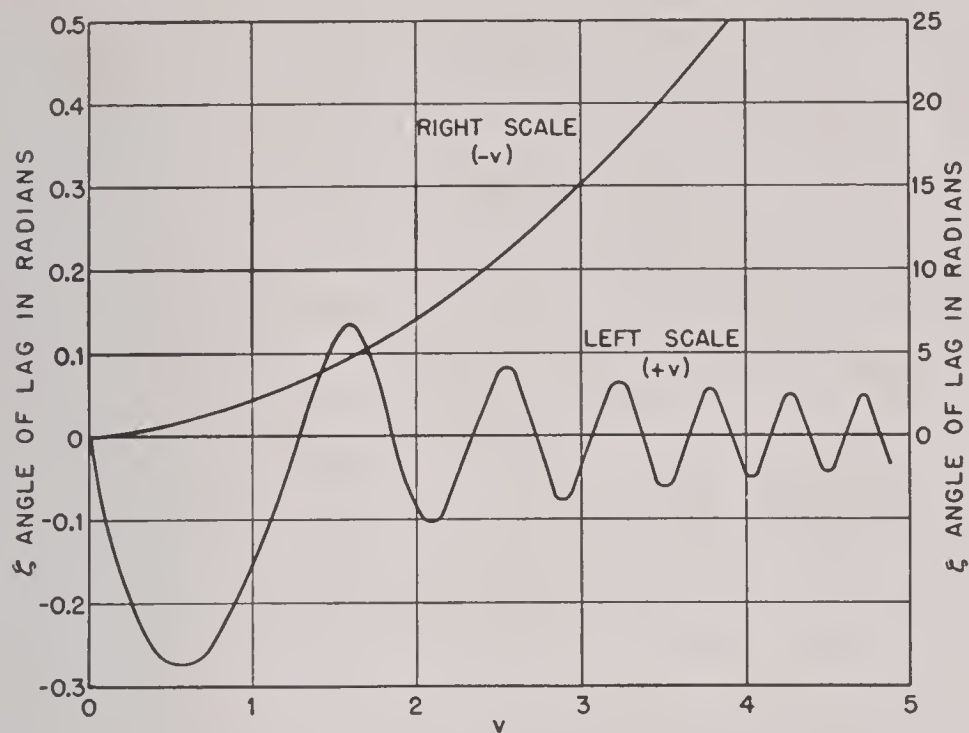


FIGURE 28. Phase lag—straight edge diffraction.

maxima and 2, 4, 6, etc., for minima. The difference  $MP' - RP'$  is a constant, and the locus of the point  $P'$  is a hyperbola having  $M$  and  $S$  for loci. That is,

$$SP' - MP' = SR - (MP' - RP'), \quad (41)$$

and  $SR$  is constant; therefore, the difference of the distances of  $P'$  from the fixed points  $S$  and  $M$  is constant.  $P'$  describes a hyperbola, but its curvature is so small that it almost coincides with its asymptotes.

The distance  $x$  to a maximum or minimum may be computed as follows

$$SP' = (a + b) \left[ 1 + \frac{x^2}{(a + b)^2} \right]^{\frac{1}{2}}.$$

Since  $x$  is small compared to  $a + b$

$$SP' = a + b + \frac{x^2}{2(a + b)}$$

also

$$MP' = b + \frac{x^2}{2b}.$$

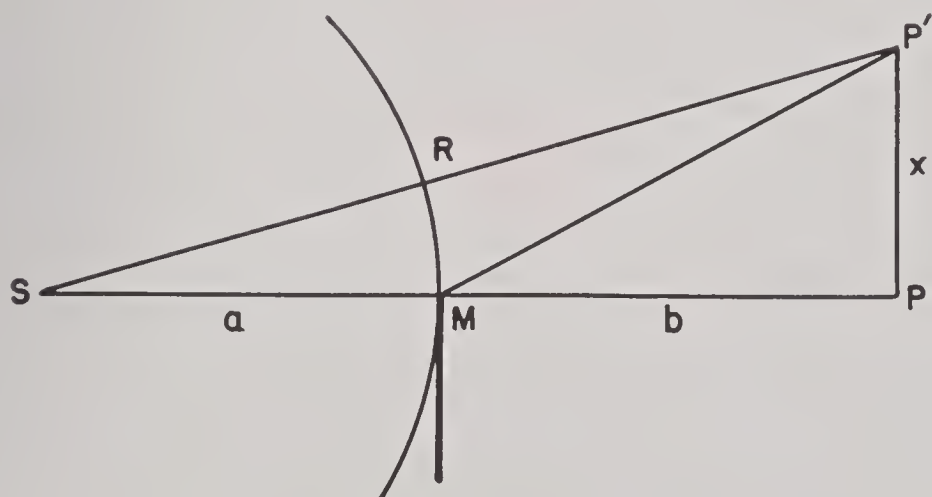


FIGURE 29. Path differences at a straight edge.

Therefore from equations (40) and (41):

$$MP' - RP' = \frac{x^2}{2} \left( \frac{1}{b} - \frac{1}{a + b} \right) = \frac{n\lambda}{2}; \quad (42)$$

hence

$$x = \sqrt{\frac{b(a + b)n\lambda}{a}}, \quad (43)$$

where  $n$  is odd for maxima and even for minima.

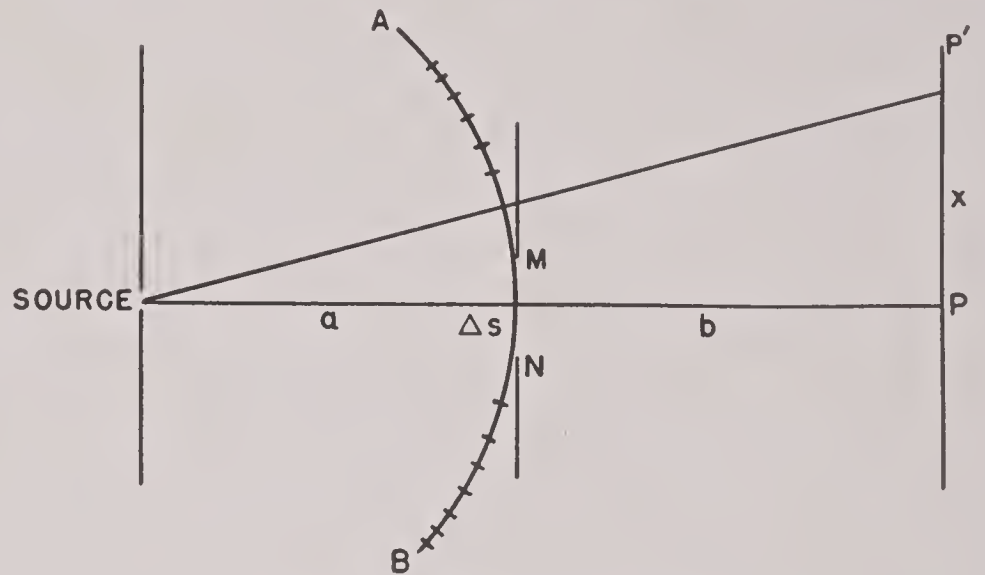


FIGURE 30. Rectangular slit.

15.4.10

### The Rectangular Slit

A problem similar to the straight edge is the rectangular slit (see Figure 30). Cornu's spiral will be used to determine the field intensity along the plane  $PP'$ . With the slit in the central position, the only radiation at the plane is due to the wavefront in the interval  $\Delta s = MN$ . Equation (31) is used to determine what length  $\Delta v$  corresponds to  $\Delta s$ . The resultant field strength at  $P$  is given by the chord of the spiral which has a length  $\Delta v$ . Since the point of observation  $P$  is centrally located, this chord will be centered on the spiral. Thus, if  $\Delta v = 0.5$  the chord (see Figure 20) will extend from approximately  $C = -0.25$  to  $C = +0.25$ . The resultant  $R \cong 0.5$  substituted in equation (37) gives a power intensity of  $\frac{1}{8}$  relative to the unobstructed wave and a field strength of 0.353.

The field intensity at  $P'$  is due to the same length  $\Delta v$  but taken over a different portion of the spiral. For this purpose, it is desired to use distances along the plane  $PP'$ ,  $x$ , instead of  $s$  (Figure 30).

$$x = \frac{a + b}{a} s = v \sqrt{\frac{b\lambda(a + b)}{2a}}. \quad (44)$$

Thus the portion of the spiral  $nO$  in Figure 31 from  $v = 0.9$  to  $v = 1.4$  has an average value of  $v = 1.15$  which multiplied by the radical term of equation (44) gives  $x$ . The chord connecting these points is 0.43,



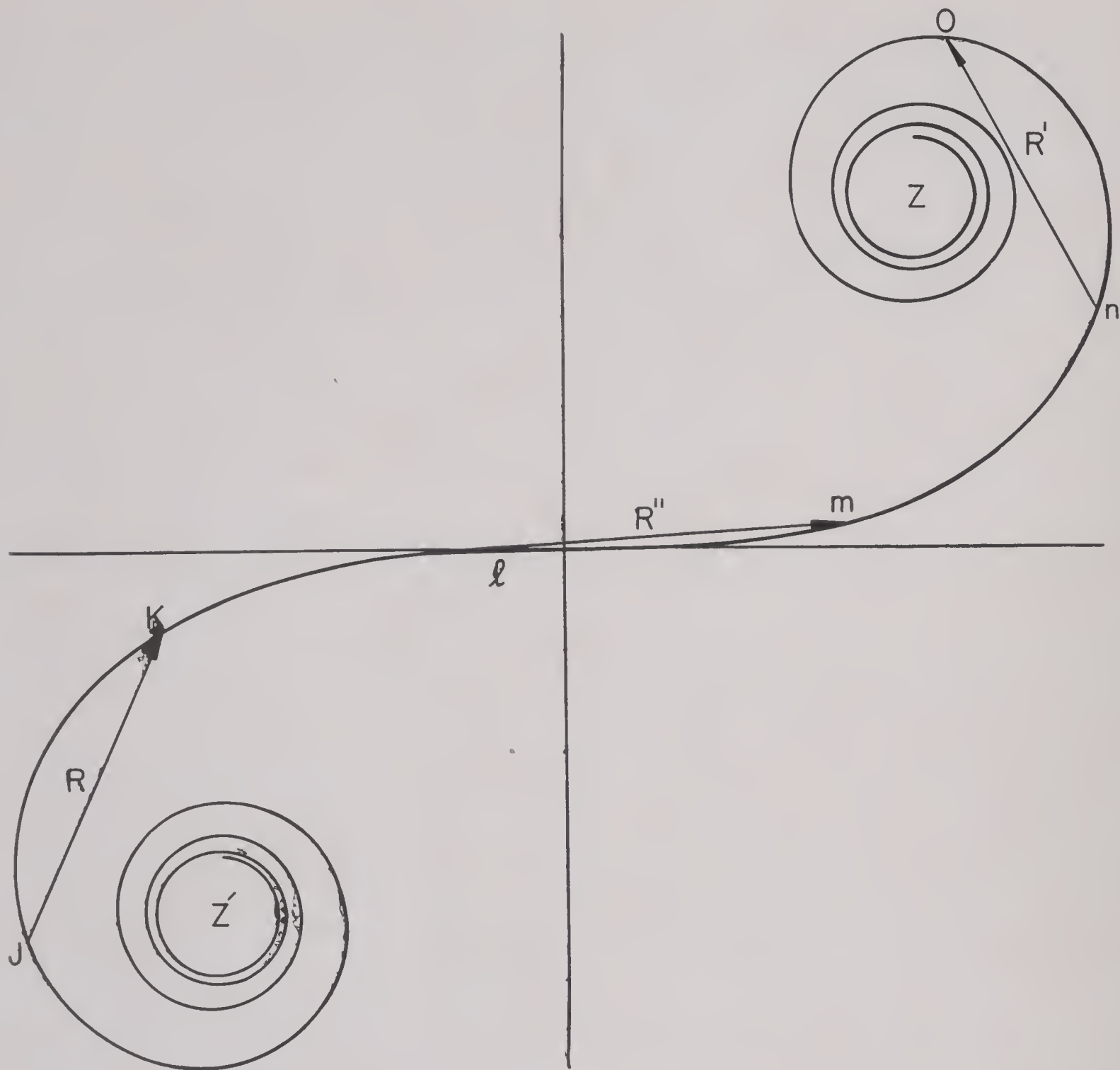


FIGURE 31. The Cornu spiral applied to obstacles and slits.

and the relative power intensity is 0.092. This same result may be computed from the table of Fresnel integrals by obtaining the values of  $\Delta C$  and  $\Delta S$  for  $v = 0.9$  and  $v = 1.4$ . The sum of the squares of  $\Delta C$  and  $\Delta S$  is  $R^2$ . Typical patterns for slits of several widths are shown in Figure 32. It will be noted that there is little radiation outside the slit.

#### 15.4.11 Diffraction by a Narrow Obstacle

The effect of a narrow object with parallel sides may be determined with the Cornu spiral. In the case of the slit only a fixed length slid along the spiral is effective, the remainder being shielded by the edges of the slit. With an obstacle, however, a fixed length slid along the spiral represents the ineffective portion. If the obstacle is of such size that it covers an interval  $\Delta v = 0.5$  on the spiral, Figure 31, the segment  $\Delta v$  may be located as  $JK$ . The radiation at the point considered will be due

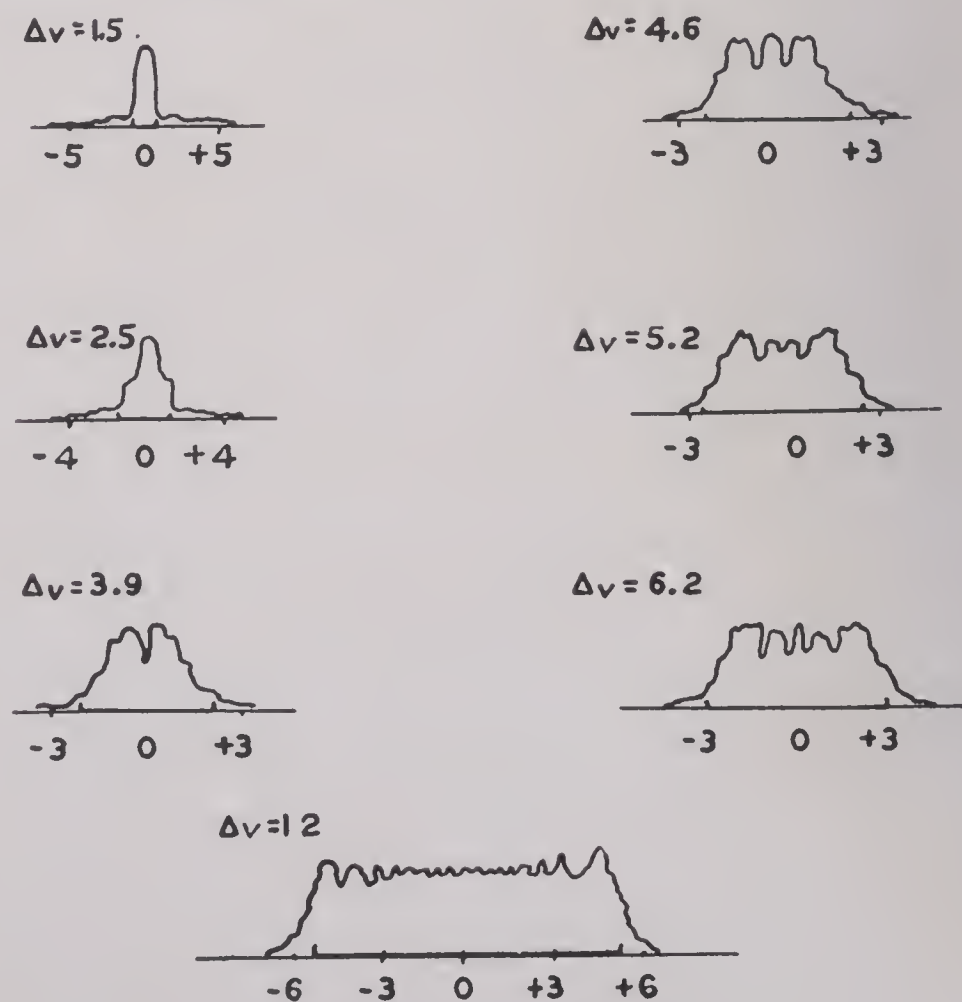


FIGURE 32. Diffraction patterns of slits.



to the two parts of the spiral  $Z'$  to  $J$  and  $K$  to  $Z$ . The resultant amplitude is obtained by adding the two vectors  $Z'J$  and  $KZ$ . The sum is  $R$  for a point midway between  $J$  and  $K$ . The head of the vector is always in the direction  $Z$  along the spiral. Typical patterns for narrow obstacles are shown in Figure 33.

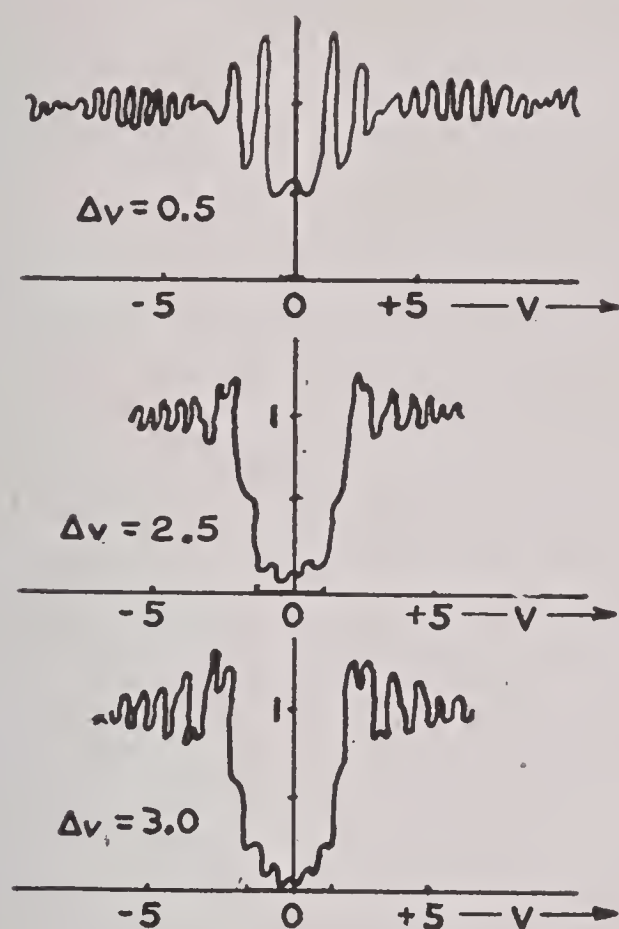


FIGURE 33. Diffraction of narrow obstacles.

15.4.12

### Multiple Slits and Obstacles

Slits or obstacles with parallel sides may be treated by means of the Cornu spiral and the resultant sum of the vectors obtained. Thus, with two slits of a width such that  $\Delta v = 0.5$  and spaced so that  $\Delta v = 0.5$  may be located on the spiral as  $JK$  and  $lm$  in Figure 31. The total  $R$  is the vector sum of  $R$  and  $R''$ . The field strength pattern is then obtained by sliding the two lengths along the spiral holding their spacing fixed.

In similar fashion two narrow obstacles would cause two absent sections such as  $JK$  and  $lm$  and three open sections  $Z'J$ ,  $Kl$ , and  $mZ$ . The three vectors, obtained by joining these three latter pairs of points, are combined to give the resultant amplitude  $R$ .

15.4.13

### Limitations of Fresnel's Theory

Neither Huyghens' principle nor Fresnel's theory, on which the above treatment is based, is rigorous, and their limitations must be kept in mind when making applications to radio and radar problems.

In the development of the theory no mention was

made of the effect of the shape and composition of the edge. Actually within a region of about one wavelength around the edge the wavefront is affected by the presence of the edge. In Figure 34 the region of the edge disturbance is  $DE$ , and first half period of the wave front is  $DF$ . The first half

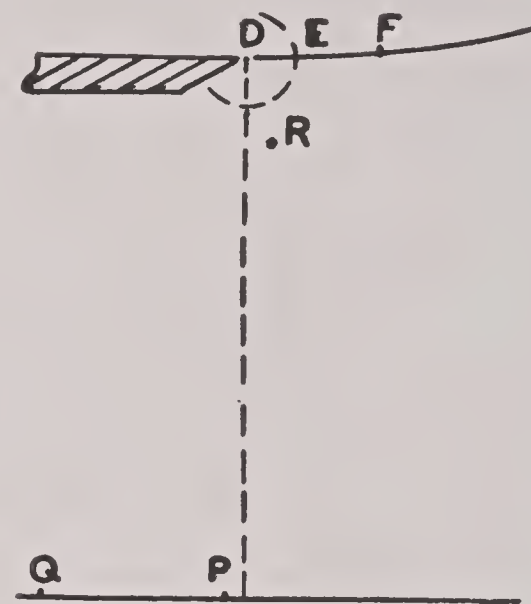


FIGURE 34. Edge effects.

turn of the Cornu spiral is due to  $DF$ . The position of  $F$  depends on the point considered. When  $DE$  is an appreciable part of  $DF$ , the simple Fresnel theory should not be depended upon. This occurs when the field point is at  $Q$ , lying at a large angle of diffraction, or at  $R$ , close to the edge.

Near the diffracting edge, a certain amount of reflection occurs, especially near  $R$ . This reflection is divergent and decreases rapidly in intensity as one recedes from the edge. When the edge is blunt or has a large radius of curvature, the amount reflected is increased and the field is affected over a greater distance. Since the angle is near grazing, the nature of the reflecting surface is not important. If Fresnel's theory is applied to spheres and cylinders, the results may be only approximate.

When the edge and the electric vector are parallel, the theory gives good results. When the electric vector is perpendicular to the edge, the field strength in the shadow region may be several times larger than that obtained with the electric vector parallel, and the theory should then be used only for small angles of diffraction.

Other discrepancies are due to ignoring the obliquity factor and the effect of the inclination of the wavelets with respect to each other. The theory does not give the correct phase angle for the diffracted wave.

The same objections may be raised for apertures and obstacles whose dimensions are of the order of a wavelength.



It should be noted that

1. *Fresnel's theory is valid* when the wavelength is small compared to the dimensions of the diffracting object (as in optics).
2. *Fresnel's theory should not be used:*
  - a. For large angles of diffraction.
  - b. Close to the diffracting edge.
  - c. For apertures or obstacles of the order of a wavelength.
  - d. When the diffracting edge is not parallel to the direction of polarization of the wave.

In spite of these shortcomings the theory is useful because it provides simple solutions for the majority of the diffraction problems encountered in the field, and, considering the difficult nature of the general problem, it is still the most manageable treatment that has been developed.

## 15.5 PERMANENT ECHOES

### 15.5.1 Introduction

Permanent echoes are due to reflection from terrain features such as mountains, islands, or even smooth surfaces near the antenna (ground clutter). Nearby hills and surfaces produce strong echoes which obscure the indicator and widen the main pulse so that the minimum range of detection is increased. More important are the distant hills, especially those in the operating sector which obscure areas of tactical importance. Permanent echoes are a prime consideration in siting, as many otherwise excellent sites are rendered worthless by excessive fixed echoes. A careful analysis of the terrain will enable an approximate prediction of such echoes. In this section is presented a systematic method of preparing permanent echo predictions so that the suitability of sites may be determined *without* actual field tests.

Several factors combine to make permanent echoes more troublesome than might be expected on first thought.

1. Hills and land surfaces are so much greater in extent than the target which the equipment is designed to detect, that strong echoes may be obtained from distances where an ordinary target would give an echo far below normal detection levels.
2. The low elevation of the land surfaces places them in regions most subject to nonstandard propagation effects where extreme ranges and large responses are frequently obtained.
3. Side lobes of the horizontal pattern of the

antenna cause permanent echoes to appear at several other azimuths in addition to that of the main lobe. Although the signal intensity of the side lobes is much reduced, the echoes may still be strong enough to obscure targets.

4. Strong permanent echoes causing considerable trouble may be obtained from distant mountains in the rear as a result of back radiation. Again, the weakness of the radiation and distance of the mountains are often compensated for by the large extent of the reflecting surface.

5. Antennas with wide beams cause permanent echoes to be much wider than the object that produces them.

6. Diffraction over intervening ridges is often sufficient to nullify their screening action so that objects behind the ridge are visible.

### 15.5.2 Permanent Echo Diagrams

The permanent echoes associated with a radar station may be plotted on a chart and their extent, location, and strength represented. Permanent echo diagrams should be prepared for each unit of a radar system using a standard procedure for the taking and presentation of data. These diagrams are very useful for:

1. Indicating blind areas in a station's coverage.
2. Assigning the operating area of a station.
3. Checking the range and azimuth accuracy.
4. Checking the transmitter output and receiver sensitivity.
5. Estimating nonstandard propagation.
6. Planning test flights.

While methods used in different theaters vary as to detail, the typical permanent echo diagram is prepared about as follows. The equipment should be in normal operating condition: that is, the transmitter output and receiver sensitivity should be as recommended by the instruction manual; the range and azimuth calibrations should be accurate; and the weather conditions that affect propagation should be average. The receiver gain should be set to some standard level, usually maximum, or to some definite noise height. The value of the data taken will depend to a considerable extent on the skill and judgment of the operator. The station would normally be taken out of operation for about an hour while data are taken, although it is possible to take observations during normal scanning by stopping momentarily. Where antenna switching is provided, the low-angle,



long-distance beam should receive the most attention although the other combinations should be checked also.

If the beam is highly directive and can be changed in elevation, a low angle such as would be used for distant search should be used for recording permanent echoes. In some situations several elevations should be used. On *plan position indicator* [PPI] scopes it may be more convenient to photograph the screen if proper equipment is available. Care should be taken not to confuse storm and fog echoes with permanent echoes on microwave sets.

A more detailed procedure is required where A-scope presentation is used. After the initial adjustments have been made the next step is to decide on the intervals in azimuth at which readings are to be made. The definition of the echoes will depend in part upon the beam width so that the narrow beam radars should be checked at closer azimuth intervals. Readings may be taken at intervals of  $10^\circ$  or  $5^\circ$  or even less depending upon the detail desired; in general an interval of about a fourth of the beam angle is sufficient. Permanent echo readings should be taken through  $360^\circ$  regardless of the sweep sector used, so that back and side echoes may be investigated also.

At each azimuth the range of all permanent echoes is recorded from zero out to the extreme range. The width of the main pulse and local ground echoes should be noted as well. Echoes one mile or less in width are recorded by a single reading at the center of the echo. Wider echoes are recorded by two readings, one at the left of the echo where the trace leaves the baseline and a second at the right where the trace returns. Adjacent echoes less than 1 mile apart are recorded as a single echo. Where the separation is greater, care should be taken not to lump echoes together.

For most purposes variations in amplitude may be disregarded. Amplitude is, however, sometimes recorded for a few azimuths of special interest such as those used for test flights or in tactically important regions.

To plot the data an overlay of a regional aeronautical map or other chart with a scale of 1 to 1,000,000 may be made showing some of the significant features as coastlines, islands, and cities. On this should be drawn radial azimuth lines every 10 degrees and range circles every 10 miles. The data are then marked on the chart as short lines, and these lines are connected as indicated by inspection.

The enclosed areas may then be shaded lightly. If it is desired to represent amplitudes, a few equal amplitude contours may be shown within an echo area. More detail may be shown by plotting amplitude versus range on a rectangular graph for each azimuth.

The completed permanent echo diagram should be compared with a topographical map to check the degree of shielding obtained and the range and azimuth accuracy of the equipment and back and side lobe radiation effects. Care must be exercised in identifying the cause of an echo, as distant echoes may come in on the second or third sweep on the scope after the main pulse.

In Figure 35 is shown a permanent echo diagram which was selected for purposes of illustration rather than as an example of a good site. A few miles from the coast is an extensive range of mountains which are poorly shielded to the north. The large echo at  $200^\circ$  is due to a mountainous island 260 miles away.

### 15.5.3 Use of Permanent Echoes in Testing

Permanent echoes are useful for tuning the equipment, estimating the output and sensitivity, and checking the range and azimuth accuracy. While such observations may be used as an overall test of performance, care should be used in selecting the test echo and in interpreting the indications.

Careful tests have shown that, even though equipment performance is closely controlled, the strength of permanent echoes varies over a considerable range. It is noted further that indications from aircraft also vary, but there is little correlation with the changes in permanent echoes. Other tests show that, as the performance of the set is reduced, the maximum range for small targets is reduced at a much faster rate than for large targets. Thus a reduction of receiver sensitivity may cause weak echoes to disappear entirely without a noticeable effect on strong permanent echoes.

Permanent echoes vary for the following reasons:

1. Atmospheric changes affect both the direct and reflected rays. This may be due to a change in the amount of refraction from standard or in the degree of trapping. Under some conditions marked absorption may occur. The changes may occur slowly or fluctuate erratically, being most marked in connection with microwaves.

2. If the reflecting surface is the ocean, variation of the reflected ray may occur if the tide changes



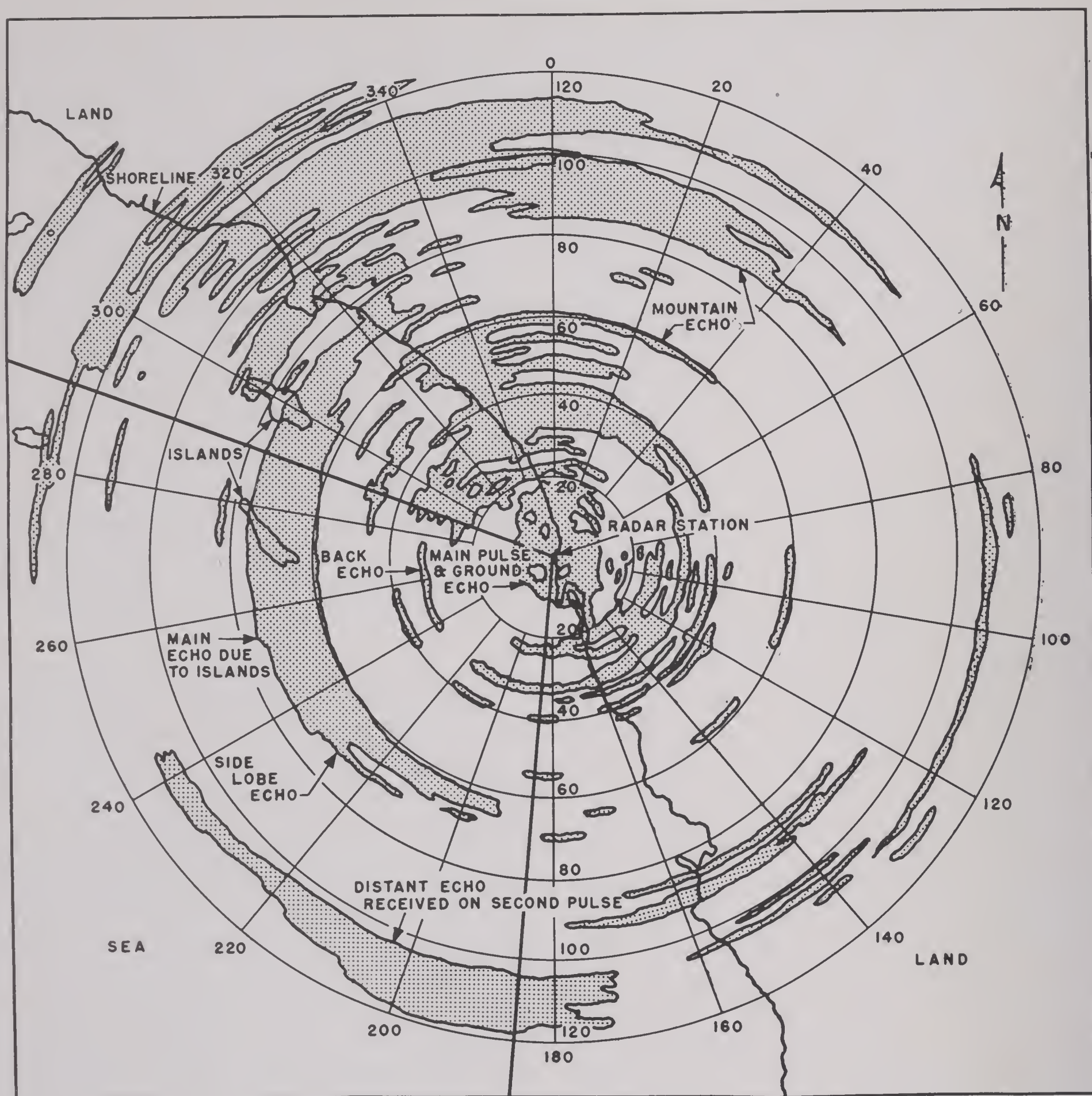


FIGURE 35. Permanent echo diagram.

or the roughness of the surface becomes excessive.

3. Frequency variations will affect the echo from complex reflectors such as rugged terrain. Peaks which are separated in distance such that the returns from a single pulse overlap are said to be frequency sensitive. In the overlap portion the echo strength will depend upon the relative phase of the two returns. Thus if the pulse width is  $10 \mu\text{sec}$  the wave train will be about 2 miles long. If there are peaks at 10 miles and  $10\frac{1}{4}$  miles their echoes will appear as follows on an A scope:

10 to  $10\frac{1}{2}$  miles    near peak echo only

$10\frac{1}{2}$  to 12 miles    combined echo of both peaks  
12 to  $12\frac{1}{2}$  miles    far peak echo only

The combined portion of the echo may have a height from zero to twice that of the individual echoes and usually fluctuates rapidly as the frequency drifts. A change of a half wavelength in the separation of the peaks will change the combined echo from maximum to minimum. This means that a frequency stability of the order of one part in a million is required for a steady combined echo.

Permanent echoes used for testing should therefore be (1) nearby but distinct from ground clutter and



other echoes, (2) separated from the transmitter by rough nonreflecting land, (3) a single distinct target such as a steel tower, (4) weak in response, that is, comparable to that of a distant aircraft.

The range of echoes which come in on the second or third pulse may be estimated by adding one or two times the length of the range scale to the observed range plus an allowance for the return trace time, usually several miles. To determine by test which sweep an echo is associated with, the pulse repetition rate should be changed, and the shift in range of the echo observed. Thus if the range scale is 200 miles long and the pulse rate is reduced 10 per cent, then a target at 250 miles which had been appearing at 48 miles would shift to an indicated range of 23 miles and could thus be distinguished from a 48-mile target that would shift to 43.2 miles.

Frequency-sensitive permanent echoes are not suitable for checking range accuracy. The frequency changes from maximum to minimum return are usually too small to be detected on a frequency meter, so that frequency-sensitive echoes are recognized chiefly by their unsteady appearance.

Azimuths may be determined to best accuracy by "beam splitting." This consists in turning the antenna slightly to one side of the maximum until the signal decreases to a predetermined level. The antenna is then turned past the maximum until the same level is reached and the two azimuths are averaged. When checking azimuth accuracy the possibility of horizontal diffraction due to a nearby hill should be considered.

## 15.5.4

**Shielding**

The principal device for control of fixed echoes is shielding. This means that the antenna is to be sited in such a way that distant hills are screened by a local obstruction. A local echo at say 3 miles, is combined with the main pulse or ground return, and the distant echo is weakened or eliminated entirely. In operating regions the loss of coverage may be more serious than the permanent echo, so shielding should be used with caution.

Rear areas which are not scanned should be well shielded so that back and side echoes do not interfere with targets in important tactical regions. Operation over such shielded sectors would be limited to high targets.

Construction of artificial shields made of poultry

netting has been suggested in some cases, where the back radiation and side lobes were relatively strong. The very large size of such structures ordinarily renders them impractical. Most of the antennas using parabolas have a small back radiation, and permanent echo problems are much simpler.

In special cases it may be desirable to eliminate a particular echo from some obstacle without using shielding. This may be done by constructing a target of sheet metal on the side of the obstacle, spaced so that the target echo and obstacle echo are about  $180^\circ$  out of phase. This requires accurate alignment of the target (so that it is normal to the radiation to within  $5^\circ$  or less) and close control of the frequency. It is also necessary that the area be adjusted so that the response of the target and obstacle are equal.

## 15.5.5

**Prediction of Permanent Echoes**

Permanent echoes may be determined by several methods:

1. Tests with the radar at the site.
2. Profile method.
3. Radar planning device [RPD].
4. Supersonic method.

The feasibility of moving the radar to the site to determine the permanent echoes is dependent on portability, accessibility, etc. Echoes obtained with one type of equipment may be very different from those from another type of radar with different directivity, frequency, and range.

The profile method, which will be described in detail below, involves a study of topographical maps and plotting the echoes according to their visibility and the amount of diffraction. A fairly difficult site may be handled in perhaps 8 man-hours. This method is adapted to long-range, low-frequency radars where diffraction and side and back lobe radiation are important. On microwave equipment fixed echo prediction is simpler and the profile method may be worked out in a few hours.

The RPD technique requires construction of a relief model of the terrain considered. A small light source is used to simulate the radar and the echoes are plotted as a result of a study of the areas illuminated. This method is adapted for short ranges and microwaves where the diffraction and side and back lobe radiation are small. Construction of a fairly difficult model may take a crew of men several days to a week, as a model should be accurate.



Once completed, all possible sites or aspects from a plane or ship may be readily examined. Models of enemy areas may be used to predict the coverage of possible enemy sites, and evasive action may be planned. The RPD is well suited for training and briefing of air personnel. Kits are provided containing the light source, supports, etc. Darkroom facilities are required, and special processing of films is used to secure more realistic pictures.

The supersonic method requires a model made of sand, glass beads, etc., to be used under water. Such models are much easier to construct than the RPD type. Supersonic gear is used to send out pulses which are reflected like radar pulses and the echo is picked up and presented on a PPI scope. Photos may be taken of the scope picture, and the method may also be used for training and briefing. Special equipment is required, but the models may be made easily and the presentation is obtained direct on the PPI scope without further processing. This method is well adapted for training, as flight, changes in altitude, etc., may be simulated readily by movement of the sonar head.

In general the profile method should be used on long waves or on microwaves where only a few sites are being considered. It is well adapted for the estimation of nonstandard atmospheric effects. For air- or ship-borne radar the RPD or supersonic methods are convenient because of the large number of aspects involved. It may be noted that the latter two methods should not be considered more exact than the profile method, as the principle of similitude does not apply unless all elements including the wavelength are changed in proportion. The principal difficulty is to secure a source which has the same radiation characteristics as the antenna system.

#### 15.5.6

### Prediction by Profile Method

The profile method will be described in detail. The discussion will refer chiefly to VHF radars in a mountainous terrain, but the methods have general application. The principal requirements are topographic maps of the surrounding area with a scale of 1 or 2 miles to the inch and a contour interval of 20 ft, although intervals up to 100 ft may be used. Maps with a scale of about 20 miles to the inch are needed for checking distant echoes. Regional aeronautical maps, with a scale of about 1 inch to 16 miles and 1,000-ft contours, are suitable as the height of prominent peaks is indicated.

From the maps, profiles are prepared for various azimuths about the radar station. The first mile or so should be plotted accurately, and at greater distances the critical points such as hills and breaks should receive the most attention. A convenient scale is 2 miles to the inch for range and 500 ft to the inch for elevation. The distances to which the profile should be plotted is a matter of judgment, but it should be extended to perhaps 20 miles, or further if there is doubt.

On each profile is drawn the tangent line from the center of the antenna to the point on the profile which determines the shielding, as in Figure 36.

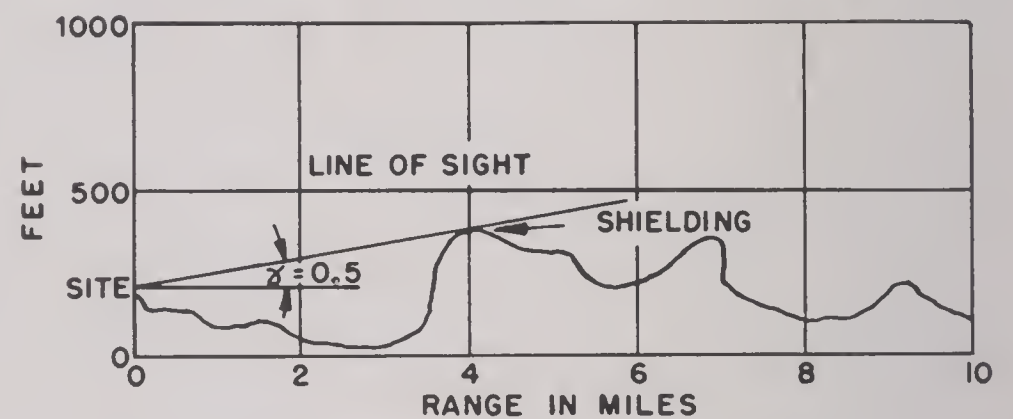


FIGURE 36. Typical profile. (Note:  $\gamma$  in degrees).

This is the line-of-sight curve; it is drawn for each azimuth, and the vertical angle  $\gamma$  is marked on the profile. If the angle is below the horizontal it is negative, and caution must be used on high sites not to exceed the limiting shielding angle of the radar horizon. This is given by the expression

$$\gamma = -0.0108 \sqrt{2h_1}, \quad (45)$$

where  $\gamma$  is the angle between the effective horizon and the horizontal at the antenna in degrees and  $h_1$  is the height of the center of the antenna in feet.

The line of sight is actually curved, as explained in the section on visibility problems, but for ranges up to 10 miles the error in using a straight line is small. For longer distances the dip  $QX$  as computed from equation (5) should be considered. More convenient for this purpose are the curves of the line of sight for various angles which are calculated from Figure 37. Standard refraction is taken into account by use of  $\frac{4}{3}a$  instead of  $a$  for the earth's radius,

$$\frac{4}{3}a = 1.33 \times 3,960 = 5,280, \quad (46)$$

$$h_2 - h_1 = 5,280d \tan \gamma + \frac{d^2}{2},$$

with  $h_1$  and  $h_2$  in feet and  $d$  in miles. Above  $10^\circ$ , or where the shielding is distant, equation (8) should be used.



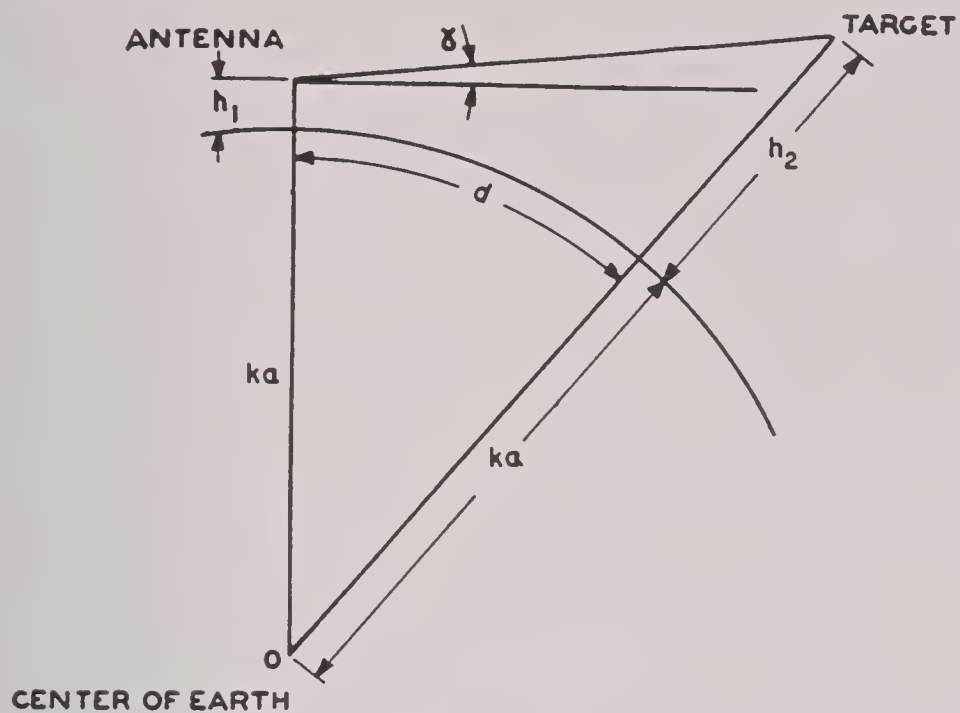


FIGURE 37. Line-of-sight geometry.

These curves are plotted in Figures 38 and 39, and their use is illustrated in Figure 36. The center of the antenna is at 200-ft elevation, and the height of the shielding ridge 4 miles away is 400 ft. For a

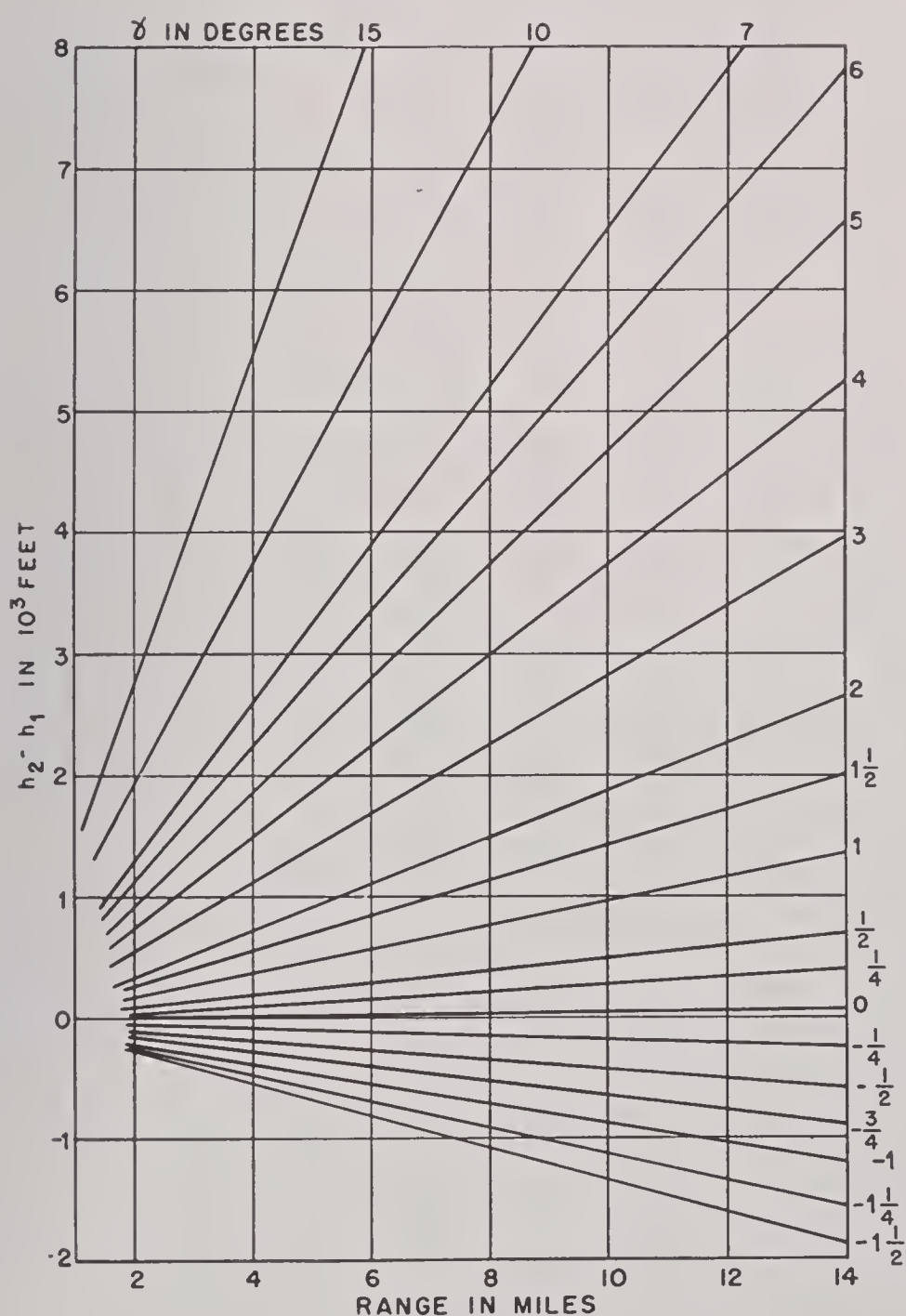


FIGURE 38. Line-of-sight curves.

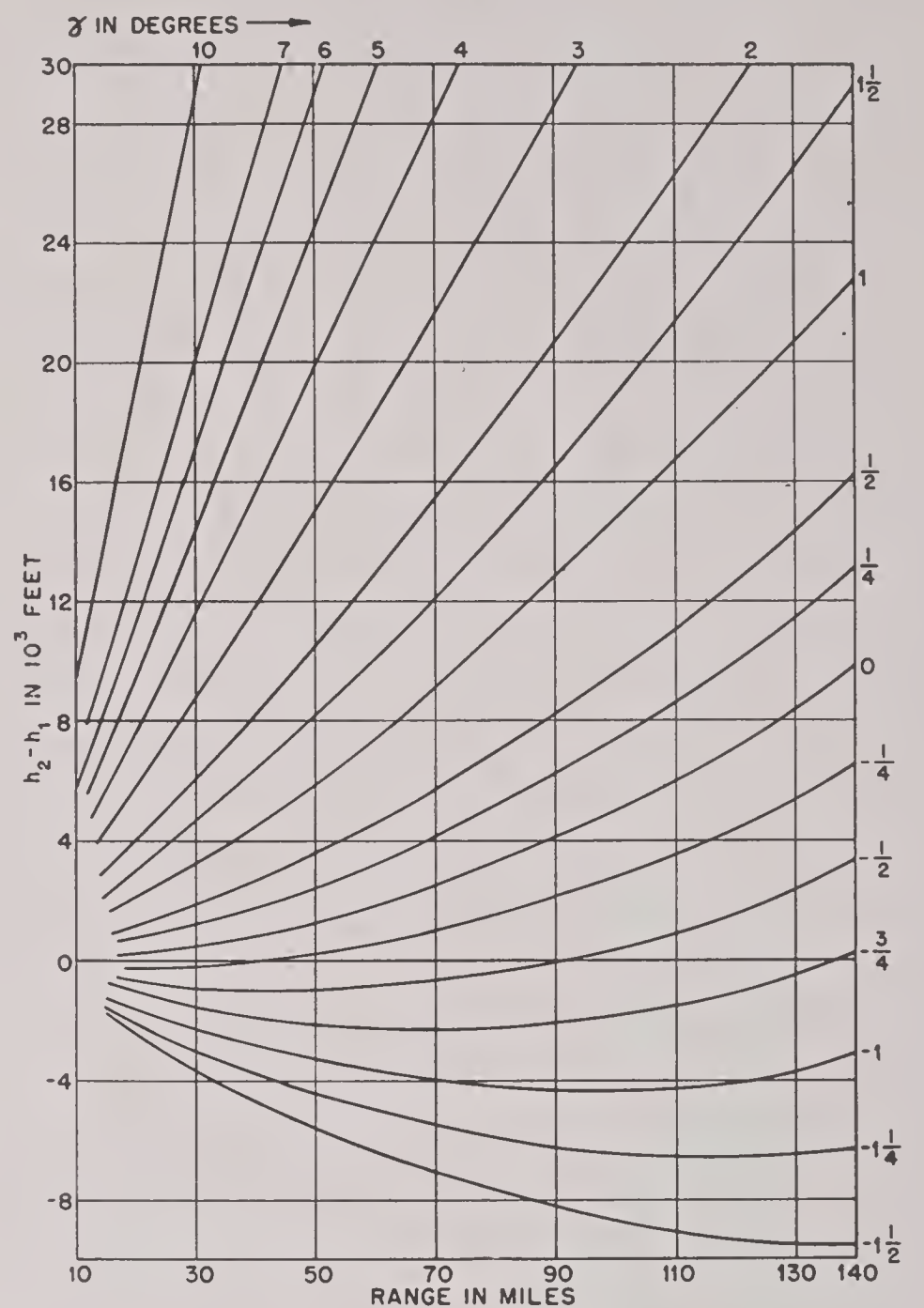


FIGURE 39. Line-of-sight curves.

200-ft rise in 4 miles the angle is found from Figure 38 to be 0.5 degree. This curve can then be used to determine the height of the shielded region at other ranges. Thus the range at which the shielded region is 4,000 ft high for the case considered is found from Figure 39 by using  $h_2 - h_1 = 4,000 - 200 = 3,800$  ft for height and the  $\frac{1}{2}$ -degree curve, giving 53 miles.

It is desirable to be able to estimate diffraction effects in a simple fashion suited to the approximate nature of this kind of work. As shown in Section 15.4.8 the field intensity varies in a rather complicated manner with the diffracting angle  $\theta_d$  and the distance of the shield  $d_1$  [Figure 7 and equation (10)]. In Figure 40 is plotted the relative field intensity compared to that obtained without a shield for shields at several distances. This graph is intended for 200 mc but may be used on other frequencies by changing  $d_1$  in proportion to the change in  $\lambda$ . It enables one to make an estimate of the effectiveness of a shield. Thus if a shield is 1 mile away it may be neglected for values of  $\theta_d$  in excess of  $+3^\circ$ . Likewise



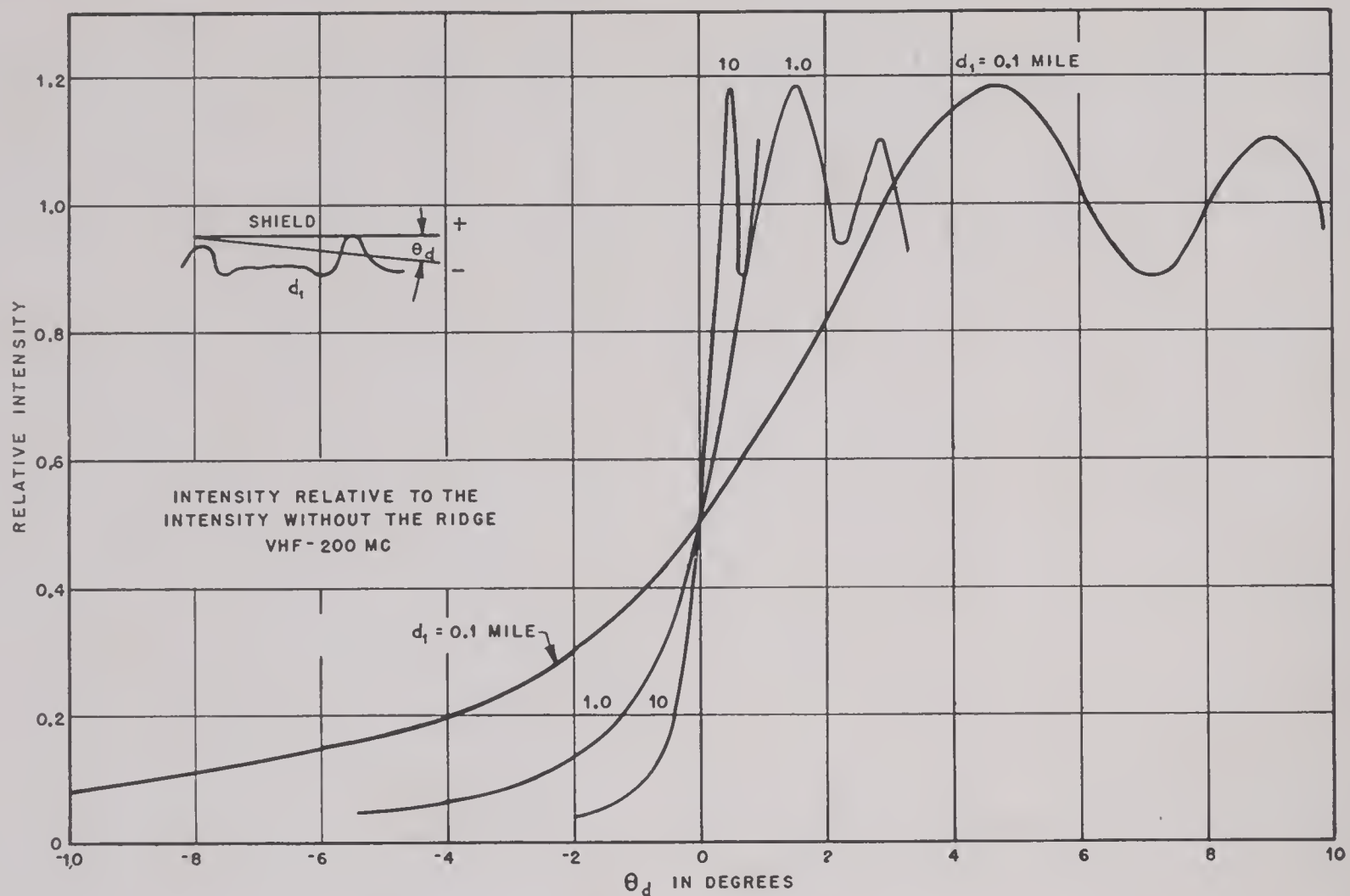


FIGURE 40. Diffraction over a ridge. (200 mc) (For other frequencies change  $d_1$  in proportion to the change in wavelength.)

objects below  $-3^\circ$  in the shadow region would give weak echoes in most cases. For intermediate angles the relative intensity may be read from the curve. For shields closer than 0.1 mile the methods of Section 15.4.8 should be employed.

Figure 15 shows that the relative intensity of a diffracted wave is virtually constant for a given angle when the distance from the edge is large. Equation (22) may then be written in the form

$$v = \frac{\theta_a}{\sqrt{\frac{\lambda}{2d_1}}} \quad (47)$$

where  $\theta_a$  is in radians ( $1 \text{ radian} = 57.3^\circ$ ) measured from the geometrical shadow line (Figure 7) and  $d_1$  is in the same units as  $\lambda$ . This equation is approximate, and the error is of the order of  $a/b$ .

Where the shield consists of several ridges close together, an equivalent shield is used instead of successive shields. The height and distance of the equivalent shield is found by constructing a triangle between the radar and the reflecting object which encloses the shielding ridges. The apex of this triangle is then treated as though it were the diffracting edge. In Figure 41  $H$  and  $d_1$  are the quantities to be used in equations (10) and (47).

The general procedure to be followed in preparing

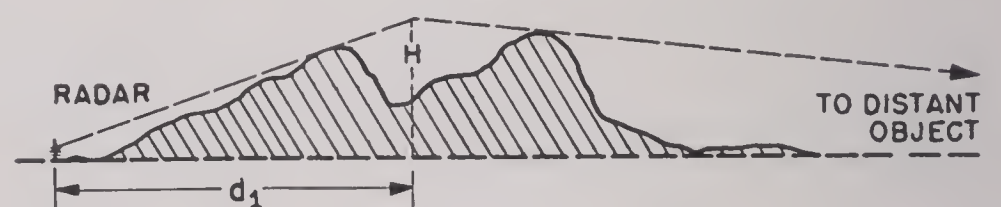


FIGURE 41. The equivalent shield.

a prediction of permanent echoes will now be outlined. By examining a topographical sheet the azimuths are determined at which profiles should be prepared. This will normally be about every 10 degrees. Where the shielding is obviously good the interval may be 20 degrees, but where the terrain is questionable such as a region of low hills the profiles should be taken at 5-degree intervals. The profiles are prepared and the angle of the line of sight determined as described above.

The next step is to make an overlay of a map of scale 1 to 1,000,000. The principal features as coastline, towns, and rivers are sketched in to aid in reading the completed chart. On this is drawn a polar coordinate system with azimuths marked every 10 degrees and range circles every 10 miles out to the full range of the indicator.

On the overlay are now drawn the coverage contour lines. These lines represent the limits of the heights of the shielded regions. Targets or mountains below these coverage contours will not



be visible except by diffraction, and targets above the contours are in line of sight and receive direct radiation. For each azimuth and the corresponding angle of sight (Figure 36) the ranges are plotted for various contour heights as 1,000, 5,000, 10,000, and 15,000 feet. Where these coverage contour lines are close together the shielding is good but the coverage is poor; where the lines are widely separated, the shielding is weak, and toward the sea there is no shielding except by the horizon.

With the coverage contour diagram superimposed on a map, the peaks exposed to radiation may be noted. The extent of the echoes due to these peaks depends on the horizontal radiation pattern and pulse width. The horizontal beam width is only a very rough measure of the width of an echo, and some other angle usually between the half-power points and the nulls will determine the echo width. The angle may be estimated by considering the range and size of the peak. The extension of the echo in range will be at least as great as the pulse width in miles, which as it appears on the indicator is about 0.1 mile per  $\mu\text{sec}$ . Actual echoes are usually much wider than this, as all of the exposed hill sends back an echo.

The echoes are then sketched in, based on inspection of the profiles. The plotter's judgment is a very important factor, but the following rules may be used as a guide.

1. Shade in a circle for the main pulse several miles wide, depending on the pulse width and local return.

2. Consider each profile in turn and for each peak or hillside in front of the shielding plot an echo on the main and all sidelobes.

3. A series of sharp hills within the shielding region should be plotted as a single echo rather than a number of echoes.

4. The inner edge of an echo should be at the same range as the hill, and its extension depends on the slope of the hill and the pulse width, which may be several miles with some sets.

5. In case of doubt plot the echo.

6. Peaks beyond the shield may be in the diffraction region and the relative intensity of the radiation at these peaks will then be obtained from Figure 40 as described above.

7. If the mountain is large enough to intercept several lobes, the interference effects may be ignored. The echo strength may be estimated roughly as proportional to the cross-sectional area of the moun-

tain, the relative intensity of the radiation from Figure 40, and the inverse square of the distance. For side and back lobes an additional factor is required.

8. The 1 to 1,000,000 scale map should be carefully checked to make sure that no peaks are missed in between the azimuth considered or at extreme ranges.

In the above method much is left to the judgment of the plotter but it will be found that with experience a reasonably good estimate of permanent echoes may be made from a map.

*Example 8. Profile Method.* A detailed example of a difficult site will be worked out, and comparison will be made with the actual recorded echoes. The site selected is that of Figure 35. The characteristics of the SCR-270B radar are given in Table 2.

TABLE 2. Type SCR-270B. Characteristics of antenna pattern.

	Horizontal pol.	Vertical pol.
Half-power beam angle	26°	6.5°
First null angle	40°	14°
Secondary lobe angle	45°	....
Secondary null angle	90°	....
Secondary lobe angle	5%	....
Back radiation	4%	....

Other characteristics of this set are as follows:

Pulse width	30 $\mu\text{sec}$ = 3 miles
Nominal range	150 miles
Sweep sector	185° to 290°
Elevation: center of antenna	387 ft

From these data may be calculated the relative echo strengths of mountains at various distances and the relative side and back echoes. A reference value of 1.0 is taken for the main echo from a typical mountain 100 miles distant, and the relative intensity from Figure 40 is taken equal to 1.0. It is estimated that all echoes whose strength compared to the reference value is over 0.25 will be strong enough to obscure targets. Thus the back echo of a mountain 10 miles away in a diffraction region where the relative strength is 0.5 would have an echo value of  $(100/10)^2 \times 0.5 \times 0.04 = 2.0$  and should be plotted since it exceeds 0.25.

A table may be constructed for the main, side, and back lobes ( $M$ ,  $S$ ,  $B$ ) for various distances and degrees of diffraction to show which echoes should be plotted. Table 3 is such a table, corresponding to a reference strength equal to 0.25. This table will apply only for the conditions of this example.



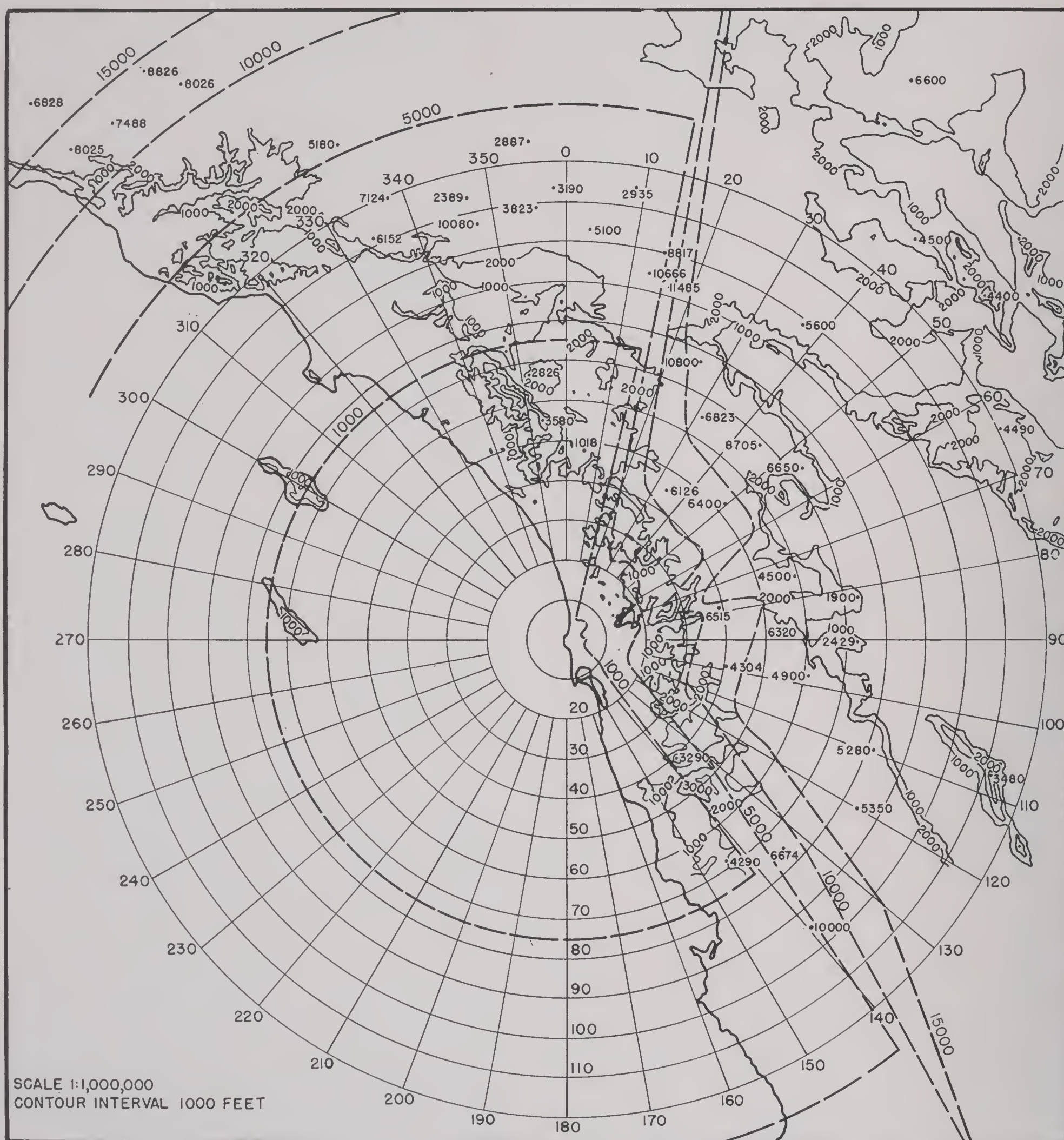


FIGURE 42. Topographical map for Example 8.

TABLE 3. Prediction of permanent echoes.\*

	Relative intensities from Figure 40.						
Distance in miles	1.18	1.00	0.75	0.50	0.25	0.10	0.03
1	<i>MSB</i>	<i>MSB</i>	<i>MSB</i>	<i>MSB</i>	<i>MSB</i>	<i>MSB</i>	<i>MSB</i>
10	<i>MSB</i>	<i>MSB</i>	<i>MSB</i>	<i>MSB</i>	<i>MSB</i>	<i>MSB</i>	<i>M</i>
20	<i>MSB</i>	<i>MSB</i>	<i>MSB</i>	<i>MSB</i>	<i>MSB</i>	<i>M</i>	<i>M</i>
50	<i>M</i>	<i>M</i>	<i>M</i>	<i>M</i>	<i>M</i>	<i>M</i>	..
100	<i>M</i>	<i>M</i>	<i>M</i>	<i>M</i>	<i>M</i>	..	..
200	<i>M</i>	<i>M</i>	..	..	..	..	..

\*This table will apply only for the conditions of Example 8.

In Figure 42 is shown a topographical map of the area. Contours are drawn for the first few thousand feet, and prominent peaks are indicated. From topographical sheets of a 20-ft interval and a scale of 2 in. to the mile the profiles of Figures 43 and 44 are obtained. From the center of the antenna to the "effective" shielding, the line of sight has been drawn and the angle of the line of sight noted. In some cases, as at 20 degrees (Figure 43) a near sharp ridge is not



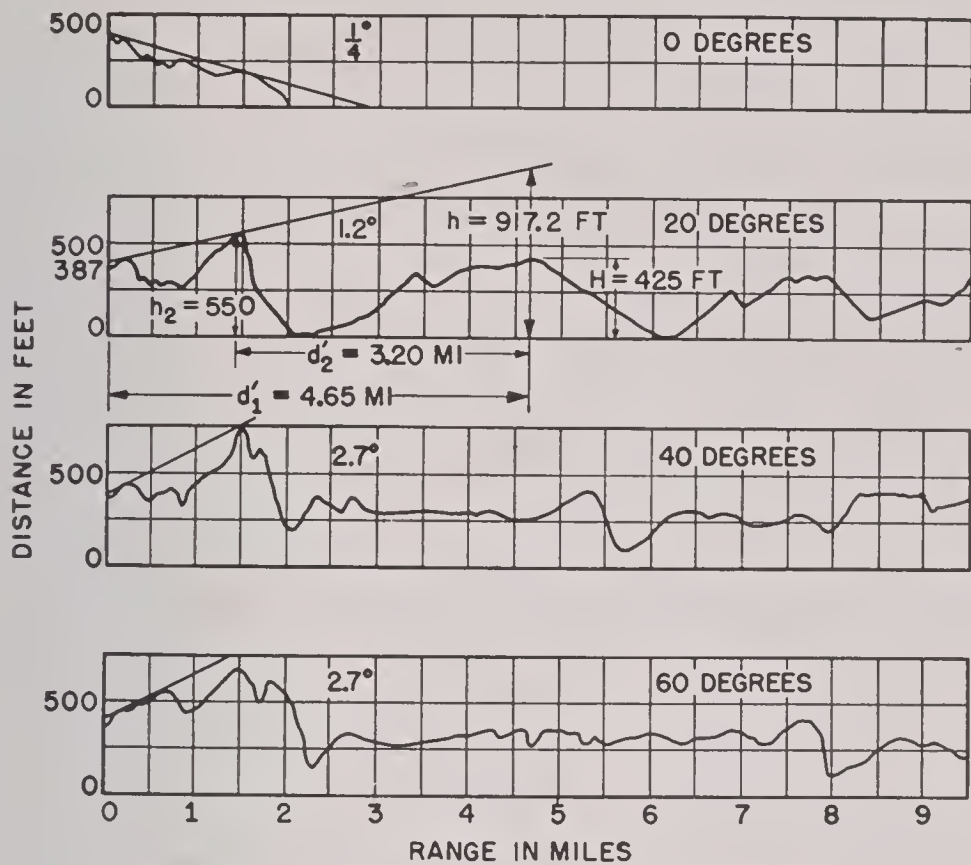


FIGURE 43. Profiles for Example 8.

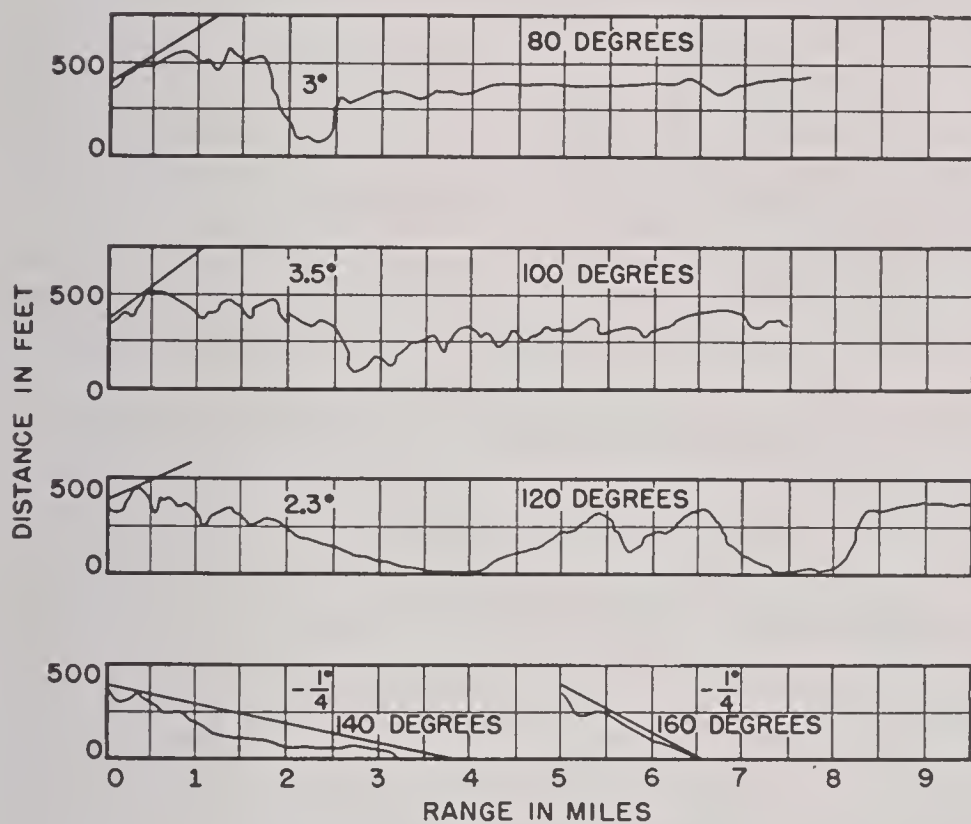


FIGURE 44. Profiles for Example 8.

considered an effective shield because of the large diffraction around such obstacles. The map is inspected between the azimuths used and the horizontal limit of shielding of a ridge noted. Thus the shielding ridge on 120 degrees (Figure 44) is found to drop off at 138 degrees. From the curves of Figures 38 and 39 are read the ranges for  $h_2 - h_1 = 1,000, 5,000, 10,000$ , and  $15,000$  ft for the line-of-sight angles at various azimuths. These points are plotted on Figure 42; they are connected by heavy dashed lines and are the coverage contours.

In Figure 45 are plotted the predicted echoes. It will be noted that the shielding to the east is very good and most of the mountains are not visible. To

the north the numerous mountains are unshielded and give rise to many echoes which extend into the search sector to the west. The islands are inherently bad and cannot be shielded without drastic loss of coverage. In some cases, as along azimuth  $345^\circ$ , ridges which cause large echoes shield more distant ridges. The broken terrain in this region is taken to give one large echo rather than a number of small echoes. In most cases the simple rules for plotting echoes may be applied directly.

Where diffraction is involved the procedure should be more detailed. In Figure 43 azimuth  $20^\circ$  will be examined to determine the visibility of the hill at 4.65 miles. The following data are obtained from the profile.

$$\begin{aligned} h_1 &= 387 \text{ ft}; d'_1 - d'_2 = 1.45 \text{ miles} \\ h_2 &= 550 \text{ ft}; d'_2 = 3.20 \text{ miles} \\ H &= 425 \text{ ft}; d'_1 = 4.65 \text{ miles} \end{aligned}$$

From equation (8):

$$\begin{aligned} h &= \frac{4.65 \times 550 - 3.20 \times 387}{4.65 - 3.20} + \frac{4.65 \times 3.20}{2} \\ &= 917.2 \text{ ft.} \end{aligned}$$

From equation (10):

$$\theta_a = \frac{425 - 917.2}{5,280 \times 4.65} \times 57.3 = -1.15^\circ.$$

From Figure 40 the intensity is found to be 15 per cent. At the very short range of this hill a strong echo would be expected at this intensity, and all lobes would be plotted.

At  $138.5^\circ$  azimuth and 160 miles is a 10,000-ft mountain (not shown in any figure). The data for this case are:

$$\begin{aligned} h_1 &= 387 \text{ ft}; d'_1 - d'_2 = 0.27 \text{ miles} \\ h_2 &= 380 \text{ ft}; d'_2 = 160 \text{ miles approximately} \\ H &= 10,000 \text{ ft}; d'_1 = 160 \text{ miles approximately} \end{aligned}$$

$$\begin{aligned} h &= \frac{160 \times 380 - 160 \times 387}{0.27} + \frac{160 \times 160}{2} \\ &= 16,950 \text{ ft.} \end{aligned}$$

$$\theta_a = \frac{10,000 - 16,950}{5,280 \times 160} \times 57.3 = -0.472^\circ.$$

From Figure 40 the relative intensity is 43 per cent. A main lobe echo is plotted on the second sweep at 10 miles since the first sweep is only 150 miles.

In Figure 35 is shown a large echo at 110 miles from  $175$  to  $242$  degrees. This is received only when



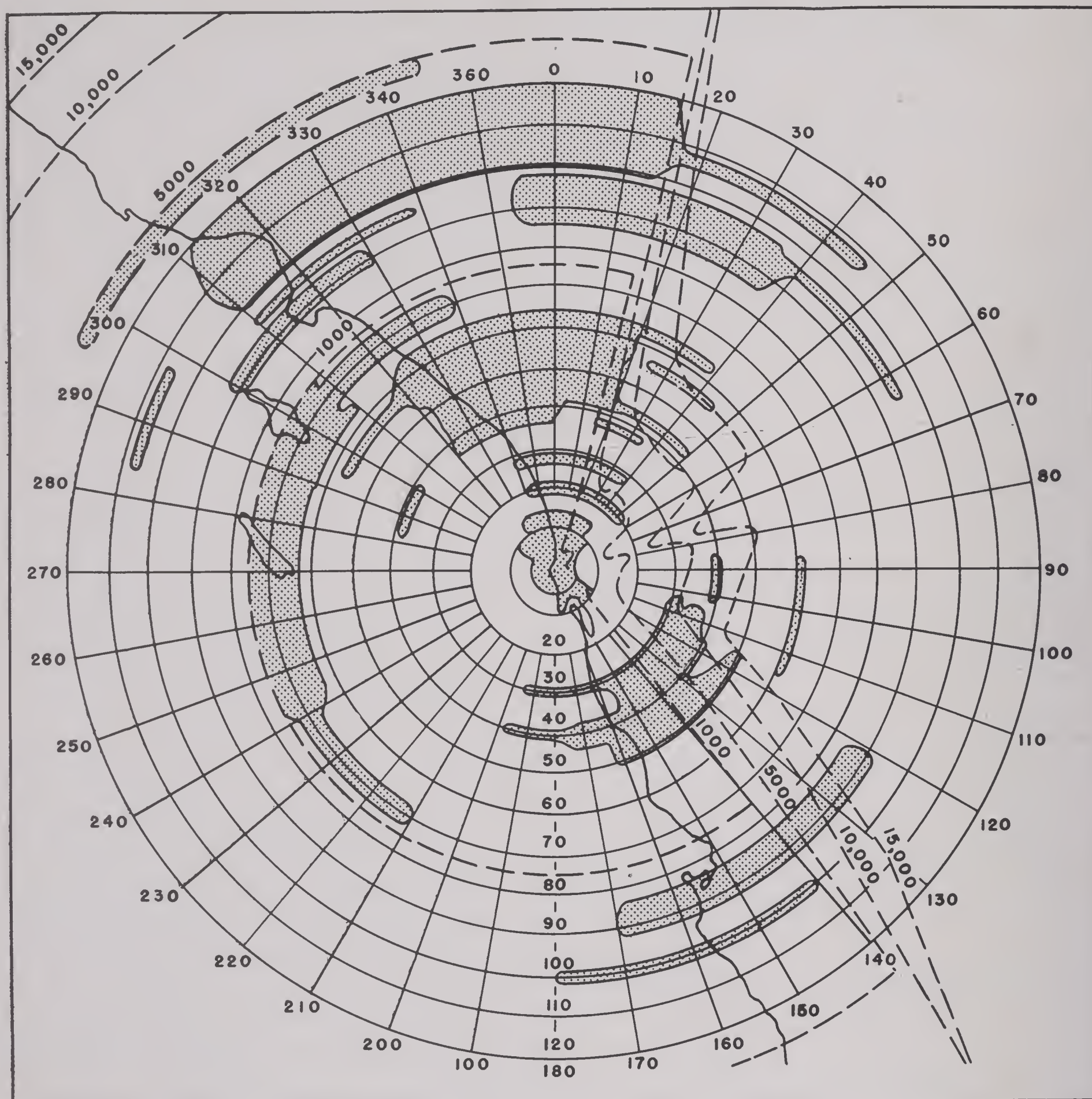


FIGURE 45. Predicted permanent echoes. (Example 8.)

there is trapping, and the size of this echo indicates the unusual weather conditions at the time the data were taken. This echo is due to a mountainous island 260 miles away and about 5,000 ft high. There is no shielding except from the curvature of the earth. The relative intensity compared to the free space intensity computed from the formulas for the diffractive region (not given here) is 0.5 per cent. This echo would not ordinarily be plotted in spite of the large area of the mountain side.

In correlating the predicted and actual fixed echo diagrams, Figures 45 and 35 respectively, it will be

noted that the degree of success achieved depends on the effort expended. Numerous small echoes were not predicted, but these are unimportant from an operating standpoint. "Permanent" echoes vary over wide limits with changes in weather conditions and efficiency of the equipment so that only a fair agreement should be expected in their predictions.

15.5.7

### Microwave Permanent Echoes

With microwave equipment a simple analysis of the terrain is generally sufficient. The beam may



be treated virtually as a searchlight, as the back radiation and diffraction effects are small. Trapping is likely to be severe and in some regions it is the controlling factor. Sea or land clutters are important and the extent of such echoes may be estimated from equation (16).

Microwave sets because of their narrow beamwidth, high resolution, and PPI presentation are well adapted to navigational uses. Coastlines may be readily identified, and ships near land may accurately determine their position. Over land it is frequently difficult to correlate a PPI picture with a map. In many cases it may be very desirable to be able to locate terrain features accurately.

The presence of some distinctive echo is of great assistance in orientation of the picture, but scope distortions and the nature of the echoes cause much confusion. It is therefore desirable to be able to correct the distortions and to be able to prepare a radar map which shows the terrain features likely to contribute to the observed pattern.

The PPI distortions are due to the beamwidth, range marker errors, and nonlinear sweep. The width of the beam causes objects to appear wider than they are, as discussed in preceding sections. The range marker errors may be determined by calibration with a precision-type calibrator. By preparing a cardboard scale to line up with the range pips the correct ranges of echoes may be obtained. Because the sweep usually takes about 15  $\mu$ sec to attain a steady speed the pattern is displaced inward with respect to the map. This may be compensated in part by adjusting the centering control so that at least one of the range markers is moved out radially to its true range. The pattern will then show a central hole, and the first half mile will be displaced from its true position, but the pattern as a whole will be more accurate.

For construction of the radar map it is desirable to have topographic sheets of a scale of 1 to 20,000 which show modern structures. Aerial photographs are also useful. Map matching is done by adjusting the sweep length and centering controls with major changes in scale made photographically. To eliminate detail of little interest it is desirable to ink in only those contours which correspond to equal increments of radar range based on the curved surface of the earth. That is, the retraced contour intervals should form a sequence of squared numbers (1, 4, 9, 16, 25  $\dots n^2$ ), for example, 20, 80, 180, 320, and 500 ft. The amount of distortion to introduce into the radar

map is obtained from the range correction scale and the shift of the PPI center. For each azimuth considered the map is shifted to compensate for the centering error, and the corrected range scale is used to lay off distance.

15.6

## THE CALCULATION OF VERTICAL COVERAGE

15.6.1

### Introduction

The computation of vertical coverage diagrams in the optical region consists essentially of adding two vectors, the contributions of the direct and reflected waves, which have been modified by earth curvature, antenna directivity, etc. The actual computation of the contours of constant field strength tends to be laborious because of the implicit nature of the parameters. The problem may be formulated in a rigorous, general manner, but the solution is likely to be unwieldy.

For field purposes where high accuracy is not required, a method of computing vertical lobe patterns is desired that is direct, does not require excessive calculations, provides a simple physical interpretation of terrain effects, and is flexible. The methods presented here are designed to meet these requirements, and the computer may readily accommodate the labor of calculations to the required accuracy and the complexity of the problem.

The path difference of the direct and reflected rays, the distance of the reflection point, and the vertical angle are functions of each other, while the reflection coefficient, the divergence factor, and other factors depend on the vertical angle. It is therefore desirable to examine the problem in a general way to determine what simplifications may be introduced.

With microwaves the reflecting surface must be quite smooth to be effective. Thus by equation (16) for the S band and an angle of 1 degree the roughness must be less than 15 in. if the reflection is to be of much assistance. The rolling character of sea waves makes a substantial variation in signal strength so that the reliable range is only slightly greater than that of the direct wave alone. Also highly directive antennas are commonly used with microwave radars. These factors reduce the magnitude of the interference effects. The fineness of the structure of a microwave pattern and the relatively weak reflection effects commonly encountered therefore render it a useful approximation to deal with the direct wave pattern only for most purposes.



Fire control and searchlight radars normally operate at high angles so that they also are mainly concerned with the direct wave. The GCI and other low-sited radars have their reflection areas within a mile of the antenna so that earth curvature may be ignored, which means a considerable simplification. The case which requires the most careful consideration is early warning, VHF, high-sited radar which is dependent on the reflected wave for much of its performance. A careful analysis of all factors involved is therefore usually required. Prepared diagrams for various heights and wavelengths must be considered carefully before being used, as local terrain features may radically alter the lobe pattern.

The accuracy and detail desired and the type of site influence the amount of calculation involved. With a low-sited VHF radar only a few lobes are formed so that the shape and location of the lobes is of interest. With a high-sited VHF radar the lobes are numerous and the gaps are small so that there is little likelihood of losing a target in a null area or of being able to associate an echo with a particular lobe. In this case the envelope of the lobes is of particular interest.

The high-power microwave radars are best suited for vital areas with high traffic density. However, for most purposes the basic long-range, early warning

radars used by the ground forces operate in the VHF band. They are normally sited high, that is several hundred feet and up, in order to secure low lobe angles and numerous lobes. The need for good reinforcement and tactical considerations lead to the use of the sea as a reflecting surface where feasible. The general high-sited radar problem will be analyzed in detail, and the use of approximate, simplified methods of calculation will be described where applicable.

#### 15.6.2 The Vertical Coverage Diagram

The object of test flights and field intensity calculations is the construction of the vertical coverage diagram. A typical diagram for a long-range, early warning, VHF radar is shown in Figure 46. The contours or lobes on this diagram represent the locus of all points in space along a particular azimuth where an incoming plane of standard type, usually a twin engine medium bomber, will produce a minimum detectable signal. A minimum detectable signal is ordinarily taken to be one that has a signal-to-noise ratio of unity. This may also be expressed in other terms such as field intensity or voltage at the receiver terminals. For other types of planes, or a number of planes, or different aspects of the same plane, the lobe pattern has a different size.

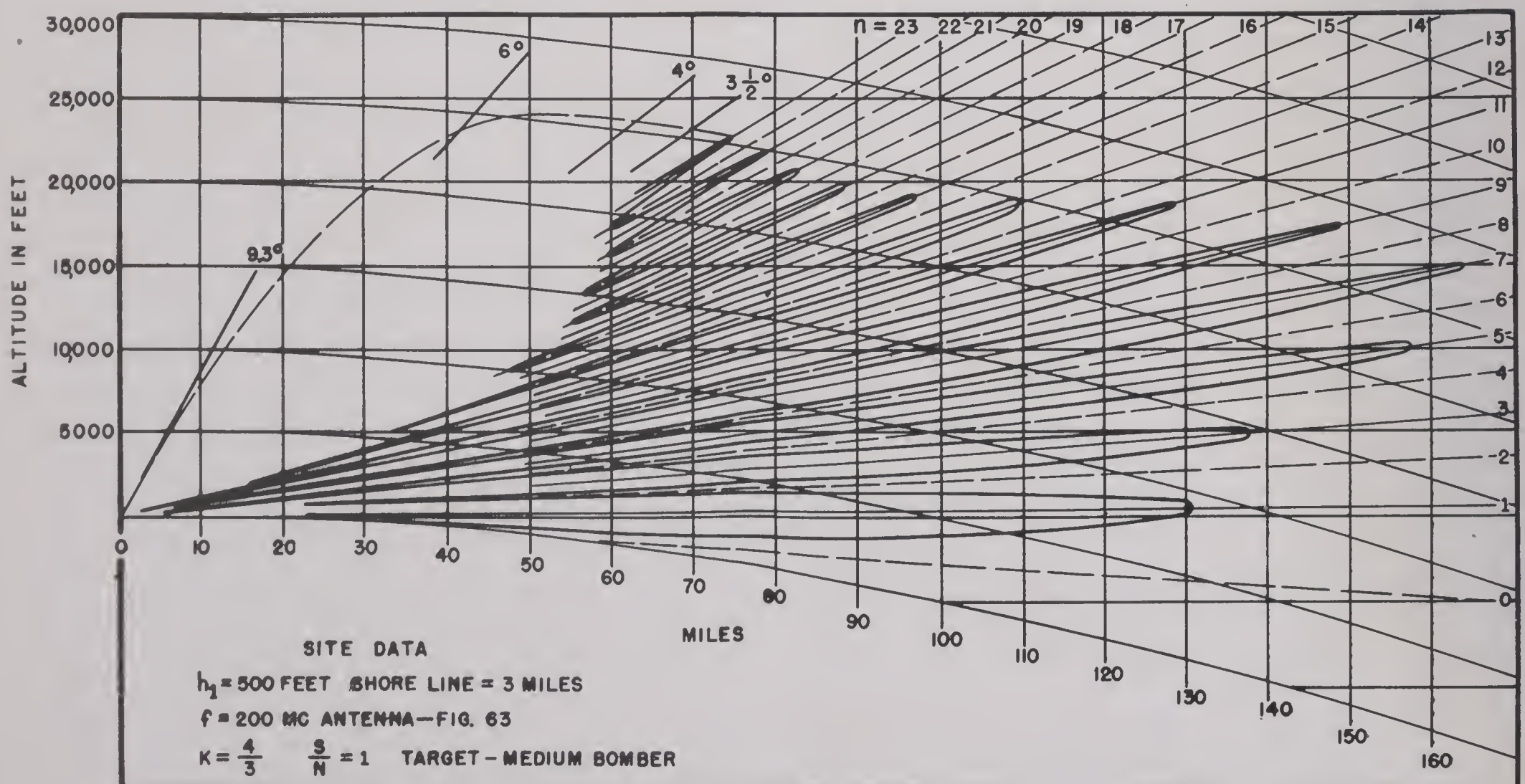


FIGURE 46. Vertical lobe diagram.



It will be noted that the vertical scale is nearly 10 times as great as the horizontal scale, causing a marked distortion in angles and crowding of angles above 10 degrees. The lines of constant altitude are parabolas, owing to the curvature of the earth. Their shape is given by the equation

$$y = h - \frac{d^2 \cdot 5,280}{2ka}. \quad (48)$$

Here  $y$  = the ordinate measured from the horizontal  
line through zero;

$h$  = the height of the curve at zero range, in feet;

$d$  = distance along the earth in miles;

$a$  = radius of the earth in miles;

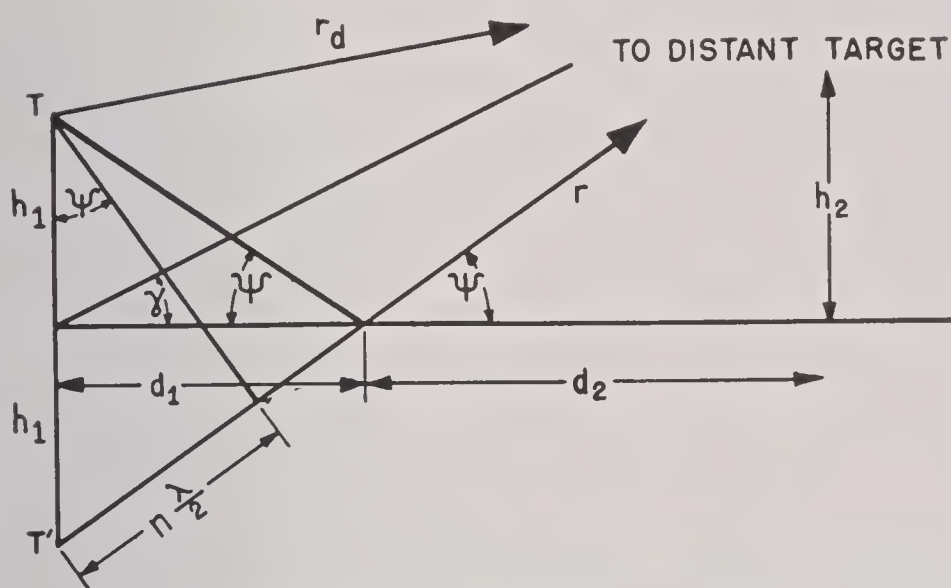
 $ka =$  equivalent earth radius.

FIGURE 47. Flat earth ray diagram.

For standard conditions  $k$  is taken as  $\frac{4}{3}$ . At  $40^\circ$  latitude the radius of the earth is 3,960 miles. Substituting in equation (48) gives the convenient relation:

$$y = h - \frac{d^2}{2}, \quad (49)$$

with  $y$  and  $h$  in feet, and  $d$  in miles.

Thus in Figure 46 a medium bomber coming in at 5,000 ft would first be detected at 108 miles, the signal would increase in strength, reaching a maximum around 96 miles, and then decrease and be lost at 84 miles. In the null region between 84 and 77 miles there would be no detection. Similar regions of detection and nulls would be encountered as the plane came in closer. The nulls do not come into the origin when the direct and reflected rays are unequal. This gap filling is secured at the price of shorter lobes. Above 3 degrees the lobes cannot be distinguished from the nulls.

Only lobes due to the main free space lobe of the antenna pattern are ordinarily plotted, as targets

higher than about 10 degrees are of little interest to an early warning radar. Because most detection occurs at angles under 2 or 3 degrees, no distinction will be made between slant range and horizontal range.

The calculation of the coverage diagram will be approached in successive steps. The first step will consist of calculation of the angular position of the lobe maxima and minima. This will be done in three different degrees of approximation corresponding to different situations encountered in practice. The next step is the calculation of the length and shape of the lobes themselves, which is given in a later section.

### 15.6.3 Flat Earth Lobe Angle Calculations

When the reflection point is so close that earth curvature may be ignored, the rays may be drawn as in Figure 47. The transmitter  $T$  has the center of the antenna at height  $h_1$  above the horizontal reflecting surface. The antenna is assumed to have horizontal polarization; that is, the dipoles are parallel to the reflecting plane and perpendicular to the direct ray  $r_d$ . The target height is  $h_2$ . Both  $h_1$  and  $h_2$  are several wavelengths or more, and  $r_d$  is so large that the field at the target falls off as  $1/r_d$ . The image of the antenna is at  $T'$  at a distance  $h_1$  below the reflector. The length of the ray from  $T'$  is  $r$ .

The coefficient of reflection is  $\rho$ , and the phase lag at reflection is  $\phi$ . The electric field strength due to the combined direct and reflected waves ( $r_d \sim r$ ) may be written as

$$E = \frac{E_1}{r} \sqrt{1 + \rho^2 + 2 \rho \cos (\phi + \delta)} \quad (50)$$

where  $\delta = 2\pi\frac{\Delta}{\lambda}$  = phase lag due to the path difference,

$\Delta = r - r_d =$  path difference of the direct and reflected rays,

$E_1$  = the field strength at unit distance.

For horizontal polarization and small angles  $\rho$  is unity and  $\phi$  is 180 degrees and equation (50) reduces to

$$E = \frac{2E_1}{r} \sin \frac{1}{2} \delta ,$$

$$= \frac{2E_1}{r} \sin \frac{\pi \Delta}{\lambda} . \quad (51)$$



In the construction of a vertical coverage diagram it is important to be able to draw the lines of constant path difference. Of special interest are the lines of maxima in the center of the lobes and the lines of minima or nulls. These lines correspond to

$$\Delta = r - r_d = \text{constant} . \quad (52)$$

For the case of a flat earth these lines are by definition confocal hyperbolae with  $T$  and  $T'$  as foci and  $\Delta$  as the major axis. This is shown in Figure 48 for a target at short range. In a typical case  $\beta$  will be

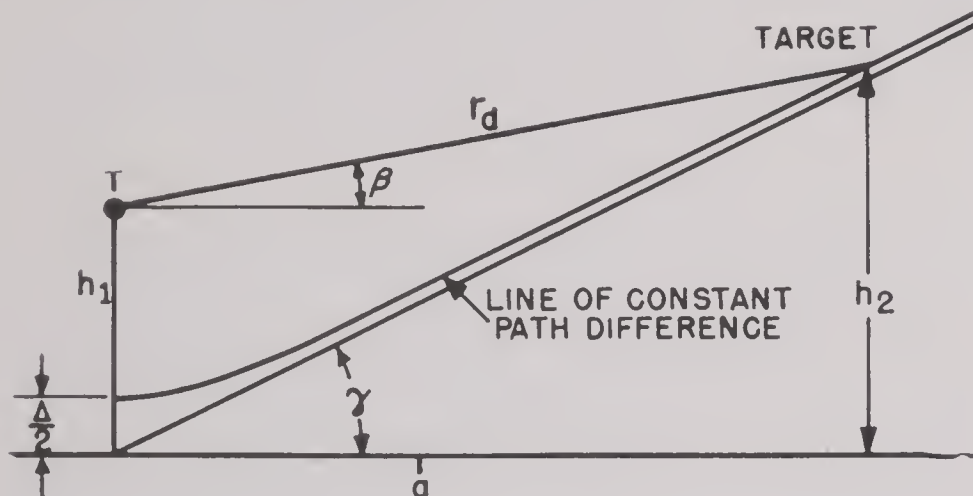


FIGURE 48. Constant path difference hyperbola.

positive and approximately equal to  $\gamma$ . From geometry

$$r_d = \frac{4h_1^2 - \Delta^2}{2\Delta - 4h_1 \sin \beta} . \quad (53)$$

When  $r_d$  is very large compared with  $h_1$  the angle  $\gamma$  is equal to  $\beta$ , and the denominator of equation (53) is practically zero, giving

$$\sin \gamma \cong \frac{\Delta}{2h_1} . \quad (54)$$

Using equation (51) with the  $(\pi\Delta)/\lambda = \pi/2$ , the lobe maxima are given by

$$\Delta = n \frac{\lambda}{2} , \quad (55)$$

where  $n = 1, 3, 5 \dots$ . Minima are given by values of  $n = 0, 2, 4, 6, \dots$ .

Substituting in equation (54)

$$\sin \gamma = \frac{n \lambda}{4h_1} , \quad (56)$$

or to a sufficient approximation

$$\gamma = \frac{n \lambda}{4h_1} . \quad (57)$$

Here  $\gamma$  = the angle of elevation of the target referred to the horizontal at the ground below the antenna, in radians;

$n$  = number of half-wavelengths difference between the direct and indirect paths.  
 $n = 1, 3, 5$ , etc., for maxima of lobe number 1, 2, 3,  $\dots (n+1)/2$  counting from the reflector up.  
 $n = 0, 2, 4, 6$ , etc., for minima of null numbers 1, 2, 3, 4,  $\dots (n+2)/2$ ;

$h_1$  = the height of the center of the antenna above the reflector;

$\lambda$  = wavelength;

with  $h_1$  and  $\lambda$  in the same units.

From Figure 47 it follows that  $d_1$ , the distance to the reflection point, is given by

$$d_1 = \frac{h_1}{\tan \Psi} ,$$

or taking  $\tan \Psi = \sin \Psi = \gamma$  (which may be done provided  $d_1$  is small enough compared to  $d_2$  and large compared to  $h_1$ ) and substituting in equation (57),

$$d_1 = \frac{4h_1^2}{n\lambda} . \quad (58)$$

Here  $d_1$ ,  $h_1$ , and  $\lambda$  must be expressed in the same units.

For high sites and distant targets the angle  $\gamma$  becomes smaller, and the approximation involved in equations (57) and (58) requiring  $d_1$  to be small compared to  $d_2$  becomes worse. In Table 4 are listed the minimum values that  $n\lambda$  may have for an error of 1 per cent or less in equation (57) at different antenna heights. Also is given the minimum value

TABLE 4. One per cent error in  $\gamma$ .

$h_1$ , ft	Minimum $\gamma^\circ$	Minimum $n\lambda$ , ft
400	1.5	43
200	1.1	15
100	0.8	6
50	0.6	2
15	0.3	0.3

of  $\gamma$  corresponding to  $n\lambda$ . Thus equation (57) when used on a 100-ft site at 100 mc ( $\lambda = 9.84$  ft) will give values which are in error by less than 1 per cent for all lobes and for angles above 0.8 degree. If the 100-ft site operated at 1,000 mc ( $\lambda = 0.98$  ft) the minimum value of  $n$  would be 6 corresponding to the fourth null. The error in  $\gamma$  is always positive and increases rapidly with antenna height, and at a height of 1,000 ft and a frequency of 100 mc the formula is incorrect for all angles of interest. At



distances such that the earth curvature drop is comparable to  $h_1$ , equation (57) does not even give the correct order of magnitude for  $\gamma$ .

*Examples 9 and 10. Flat Earth Lobe Angle Computations.* Lobe angles for two cases will be computed, Example 9, a 200-mc set at 15 ft and Example 10, a 500-mc set at 50 ft.

Example 9

Example 10

$$\lambda = \frac{300}{200} \times 3.28 = 4.92 \text{ ft}$$

$$\lambda = 1.97 \text{ ft}$$

For  $n = 1$  (first lobe)

$$\gamma = \frac{1 \times 4.92}{4 \times 15} \times 57.3 = 4.7^\circ \quad \gamma = 0.564^\circ$$

$$d_1 = \frac{4 \times (15)^2}{1 \times 4.92} = 183 \text{ ft} \quad d_1 = 5,080 \text{ ft}$$

TABLE 5. Lobe angle and distance to reflection point.

$n$	Example 9		Example 10	
	$\gamma$ , degrees	$d_1$ , ft	$\gamma$ , degrees	$d_1$ , ft
1 (lobe 1)	4.7	183.0	0.56	5080
2 (null 2)	9.4	91.5	1.13	2540
3 (lobe 2)	14.1	61.0	1.69	1693
4 (null 3)	18.8	45.7	2.26	1270
5 (lobe 3)	23.5	36.6	2.82	1016

In practice some of the lobes listed for Example 9 may be absent because of nulls in the antenna pattern. The angle listed for the first lobe of Example 10 is slightly over 1 per cent too large.

15.6.4

### Lobe Angles Corrected for Standard Earth Curvature

Equation (57) may be modified to include the effect of earth curvature approximately and to give the lobe angles for the majority of sites with acceptable accuracy.

For antennas several hundred or more feet high,  $d_1$  as given by equation (58) may be large enough so that the earth curvature drop is appreciable. In Figure 49 is shown a transmitter of height  $h_1$  above the horizontal plane  $GH$ . The radius of the standard earth is  $ka$ . At  $D$ , the center of the reflection area for the lobe considered, is drawn a tangent plane  $CDE$ , which intersects  $h_1$  at a distance  $h'_1$  below the center of the antenna and which will be considered the equivalent antenna height. This then is the part of  $h_1$  which determines the angle  $\gamma'$  which the lobe center line  $CL$  makes with the tangent plane  $CDE$ . Subtracting from  $\gamma'$  the angle  $\theta$  which

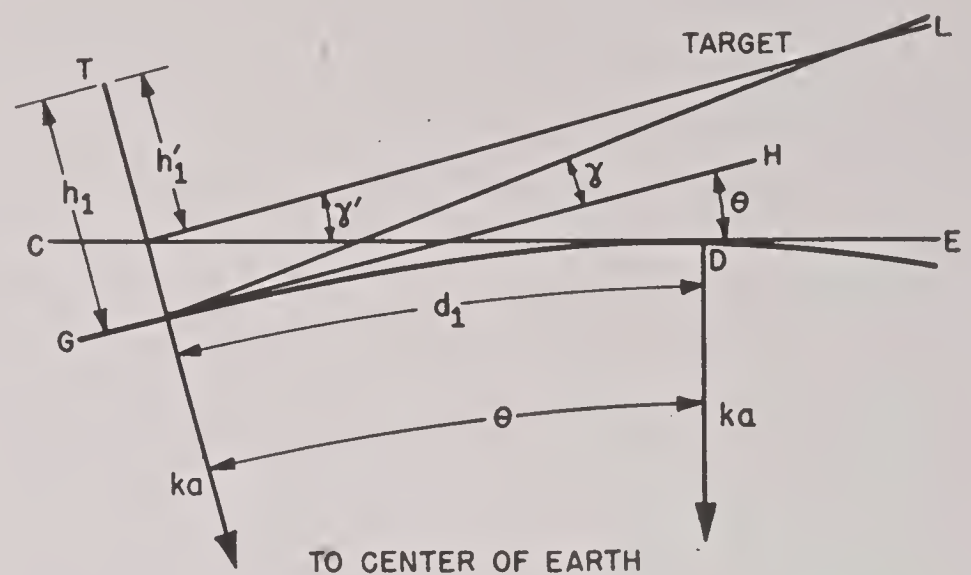


FIGURE 49. Lobe angles corrected for earth curvature.

the tangent plane  $CDE$  makes with the horizontal at the base of the antenna  $GH$ , the lobe angle  $\gamma$  referred to the horizontal at the antenna is obtained. From equation (49) it follows that

$$h'_1 = h_1 - \frac{d_1^2}{2}. \quad (59)$$

Here  $h'_1$  and  $h_1$  are expressed in feet,  $d_1$  in miles, and  $k$  is assumed to be  $\frac{4}{3}$ .

This height  $h'_1$  is the portion of  $h_1$  that is effective in connection with the plane  $CDE$  and when substituted in equation (57) gives the angle  $\gamma'$ .

$$\gamma' = \frac{n\lambda}{4h'_1} = \frac{n\lambda}{4\left(h_1 - \frac{d_1^2}{2}\right)}. \quad (60)$$

Since the earth's radius  $ka$  is perpendicular to  $GH$  and  $CDE$ , the tangent angle is  $\theta$ . It is always negative:

$$\theta = -\frac{d_1}{ka} = -\frac{d_1}{5,280}, \quad (61)$$

$$\gamma = \gamma' + \theta = \frac{n\lambda}{4\left(h_1 - \frac{d_1^2}{2}\right)} - \frac{d_1}{5,280}. \quad (62)$$

$n$  is an odd integer for lobe maxima and an even integer for lobe minima,  $h_1$  in feet,  $d_1$  in miles.

The value of  $d_1$  to substitute in equation (62) must also satisfy equation (58). A convenient method of solving these equations is to plot a curve of equation (59) and also of equation (58) in the form

$$n = \frac{4(h'_1)^2}{5,280d_1\lambda}. \quad (63)$$

Corresponding values of  $h'_1$  and  $d_1$  for the desired value of  $n$  are then substituted in equation (62).

While equation (62) is subject to the same sort of limitation as equation (57), it will be noted that



in the region of greatest interest, that is, small angles,  $h_1'$  is itself small, and this tends to compensate the error. The modifications introduced permit the use of the simple plane earth formulas, since for a particular angle the tangent plane is taken as the reflection surface.

The angle  $\gamma$  given by equation (62) is the transformed angle to be used in constructing the vertical coverage diagram based on a modified earth radius of  $ka = 5,280$  miles. If the true angle is desired, the true earth radius  $a = 3,960$  miles must be used in equation (62) instead of 5,280 miles.

*Examples 11 and 12. Lobe Angles Corrected for Earth Curvature.* Lobe angles will be computed by this method for two radar sites.

*Example 11*

$$h_1 = 500 \text{ ft}$$

$$f = 200 \text{ mc}$$

From equation (59)

$$h_1' = 500 - \frac{d_1^2}{2}$$

*Example 12*

$$h_1 = 3,000 \text{ ft}$$

$$f = 100 \text{ mc}$$

$$h_1' = 3,000 - \frac{d_1^2}{2}$$

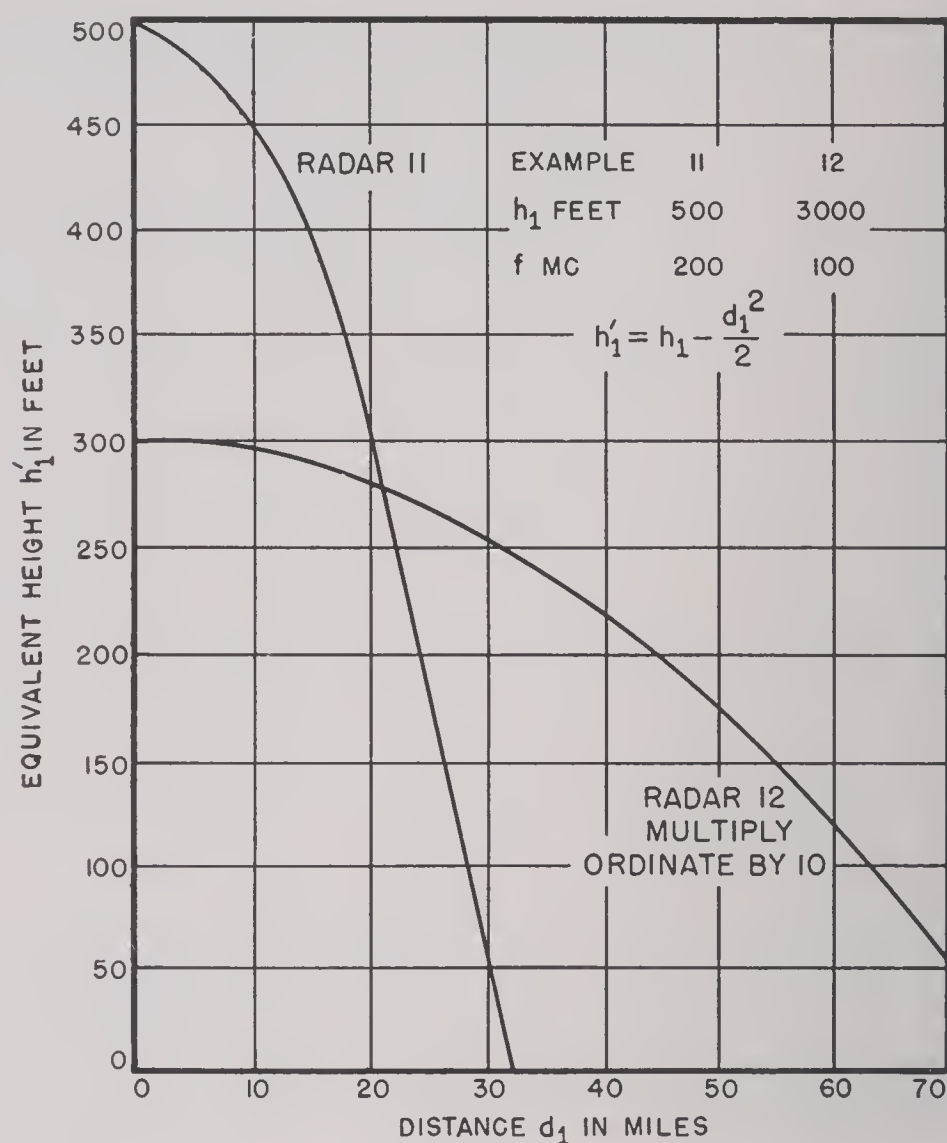


FIGURE 50. Equivalent height graph.

TABLE 6. Lobe angles for radar. (Example 11.)

From Figures 50 and 51.			Equation (60) $\gamma' = 1.23 \frac{n}{h_1'}$	Equation (61) $\theta = -\frac{d_1}{5,280}$	Equation (62) $\gamma = \gamma' + \theta$		Equation (57) $\gamma = \frac{n}{4h_1}$
$n$	$h_1'$	$d_1$	radians	radians	radians	degrees	radians
0	0	31.6	0	-.005983	-.005983	-0°20'22"	0
1	341.5	17.8	.003602	-.003372	+.000230	+0° 0'47"	.00246
2	414.0	13.1	.005943	-.002481	.003462	0°11'54"	.00492
3	448.0	10.2	.008238	-.001932	.006306	0°21'39"	.00739
4	464.6	8.4	.010592	-.001591	.009001	0°30'56"	.00985
5	475.5	7.0	.01294	-.001326	.01161	0°39'54"	.0123
6	481.4	6.1	.01532	-.001155	.01417	0°48'43"	.0148
7	486.0	5.3	.01772	-.001004	.01672	0°57'29"	.0172
8	489.0	4.7	.02011	-.000890	.01922	1° 6' 4"	.0197
9	491.6	4.1	.02252	-.000776	.02174	1°14'45"	.0221
10	493.2	3.7	.02493	-.000701	.02423	1°23'19"	.0246
11	494.6	3.3	.02734	-.000625	.02672	1°31'55"	.0271
12	495.5	3.0	.02978	-.000568	.02921	1°40'26"	.0295
13	496.1	2.8	.03222	-.000530	.03169	1°48'58"	.0320
14	496.6	2.6	.03468	-.000492	.03419	1°57'33"	.0345
15	497.1	2.4	.03720	-.000454	.03675	2° 6'23"	.0369
16	497.4	2.3	.03955	-.000436	.03911	2°14'30"	.0394
17	497.6	2.2	.0420	-.000417	.0416	2°23' 2"	.0418
18	497.8	2.1	.0445	-.000398	.0441	2°31'44"	.0444
19	498.0	2.0	.0469	-.000379	.0465	2°39'54"	.0468
20	498.2	1.9	.0494	-.000360	.0490	2°48'30"	.0492
21	498.4	1.8	.0518	-.000341	.0515	2°57' 8"	.0517
22	498.6	1.7	.0542	-.000322	.0539	3° 5'22"	.0541
23	498.8	1.6	.0567	-.000303	.0564	3°14' 0"	.0567



TABLE 7. Lobe angles for radar. (Example 12.)

From Figures 50 and 51			Equation (60) $\gamma' = 2.46 \frac{n}{h_1'}$	Equation (61) $\theta = - \frac{d_1}{5,280}$	Equation (62) $\gamma = \gamma' + \theta$		Equation (57) $\gamma = \frac{n}{4h_1}$
$n$	$h_1'$	$d_1$	radians	radians	radians	degrees	radians
0	0	77.4	0	-.01466	-.01466	-0°50'24"	0
1	930	64.3	.002645	-.01218	-.00954	-0°32'49"	.00082
2	1245	59.2	.003952	-.01121	-.00726	-0°25' 0"	.00164
3	1458	55.5	.005063	-.01051	-.00545	-0°18'44"	.00246
4	1638	52.2	.006007	-.00989	-.00388	-0°13'20"	.00328
5	1788	49.2	.006880	-.00932	-.00244	-0° 8'22"	.00410
6	1910	46.7	.007730	-.00885	-.00112	-0° 3'52"	.00492
7	2013	44.4	.008550	-.00841	+.00014	+0° 0'29"	.00574
8	2108	42.4	.009335	-.00803	.00130	0° 4'28"	.00656
9	2195	40.6	.01018	-.00769	.00249	0° 8'33"	.00738
10	2246	38.8	.01095	-.00735	.00360	0°12'22"	.00820
11	2308	37.2	.01173	-.00705	.00468	0°16' 6"	.00902
12	2359	35.8	.01251	-.00678	.00573	0°19'41"	.00984
13	2408	34.4	.01328	-.00651	.00677	0°23'16"	.01066
14	2452	33.1	.01404	-.00627	.00777	0°26'44"	.01148
15	2488	32.0	.01484	-.00606	.00878	0°30'10"	.01230
16	2525	30.8	.01558	-.00583	.00975	0°33'31"	.01312
17	2559	29.7	.01635	-.00562	.01073	0°36'50"	.01394
18	2588	28.7	.01712	-.00544	.01168	0°40' 8"	.01476
19	2623	27.8	.01782	-.00526	.01256	0°43'10"	.01558
20	2638	26.9	.01866	-.00509	.01357	0°46'40"	.01640
21	2662	26.0	.01940	-.00492	.01448	0°49'48"	.01722
22	2685	25.1	.02030	-.00475	.01555	0°53'26"	.01804
23	2702	24.4	.02093	-.00462	.01631	0°56' 4"	.01860

These equations are plotted in Figure 50. From equation (63):

$$n = \frac{4(h_1')^2}{5,280 \times 4.92 \times d_1}, \quad n = 0.000077 \frac{(h_1')^2}{d_1}.$$

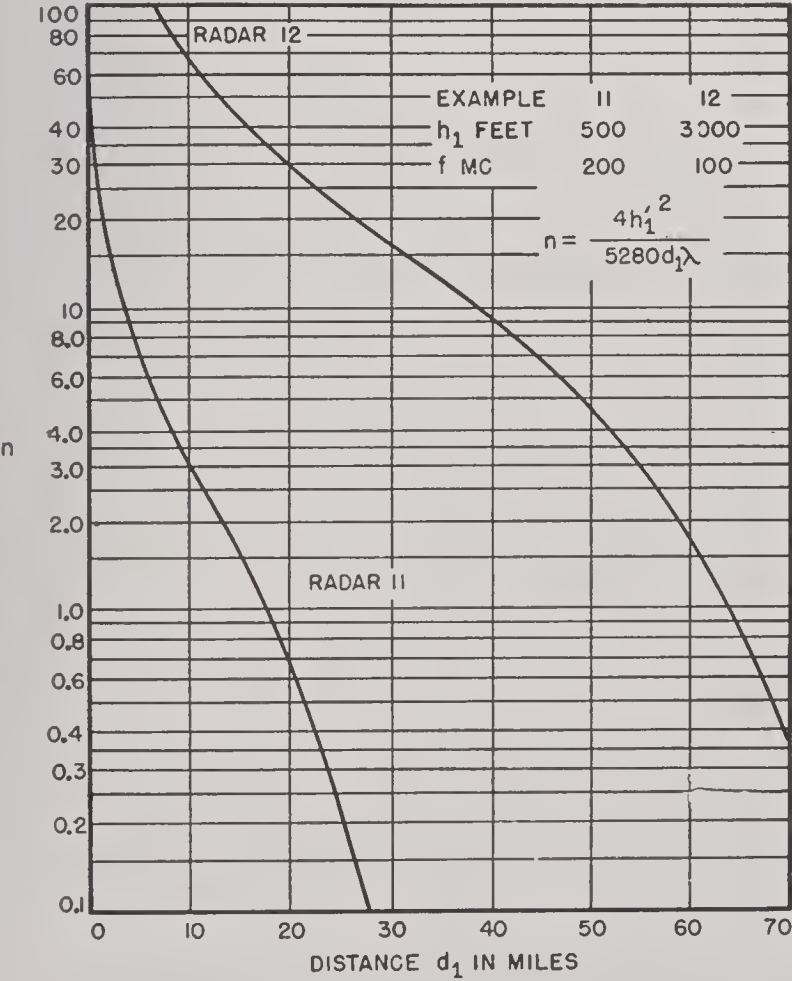


FIGURE 51. Reflection area graph.

Reading values of  $h_1'$  and  $d_1$  from Figure 50 and substituting in the above equations, curves of  $n$  and  $d_1$  are plotted in Figure 51. From these two curves may be read the values of  $h_1'$  and  $d_1$  corresponding to integral values of  $n$ . The calculation of  $\gamma'$  and  $\theta$  from equations (60) and (61) are conveniently performed by arranging columns as shown in Tables 6 and 7.

For purposes of comparison with equation (62) the last column gives values of  $\gamma$  computed by means of equation (57). In Table 6 the error in the figures computed from equation (57) is seen to be considerably below  $n = 10$ ; for higher values of  $n$  the two formulas tend to show fair agreement. In Table 7 the disagreement is marked even at  $n = 23$  indicating that equation (57) is unsuitable for high sites.

The lobe angles are shown in Figures 52 and 53. The lines of constant altitude over the modified earth are plotted from equation (49). The lobe angles are constructed by drawing radial lines from the center of the antenna, while the height in feet at a given distance is obtained by multiplying  $\gamma$  (in radians) by 5,280 times this distance in miles. The lines have not been drawn close in because of the crowding and because they actually start near



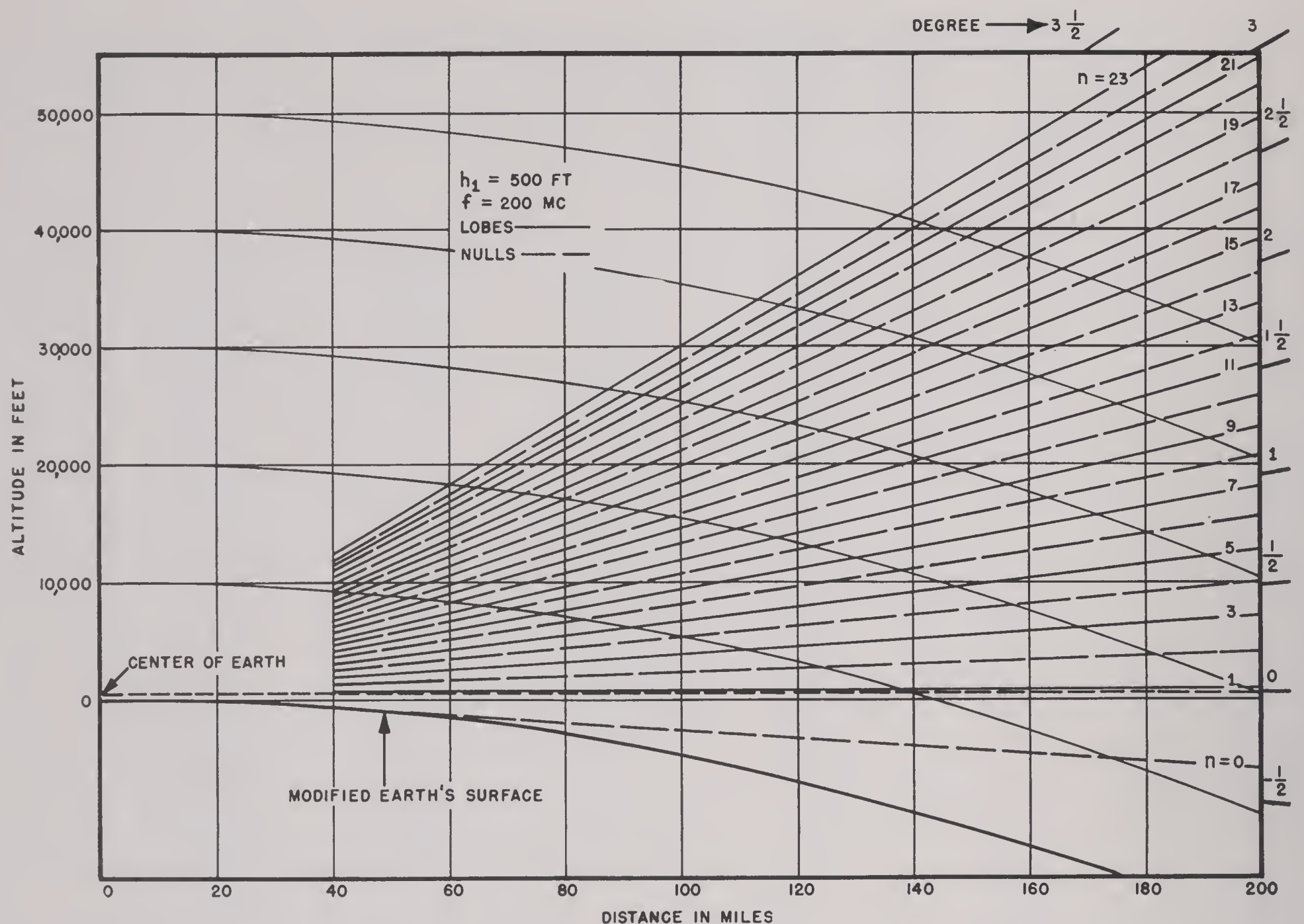


FIGURE 52. Lobe angles for Example 11.

the origin rather than at the center of the antenna.

The error in the position of the center lines of the lobes near the antenna is a limitation on this method; but this occurs in a region which, because of gap filling, has no nulls and is therefore of little concern. Another difficulty is that the lower lobes are actually curved instead of straight; but as long as the site is not too high, say under 100 ft (100 mc), the curvature is small and unimportant. In general the method of equation (62) gives reasonably correct lobe angles for most high sites and with a moderate amount of computation. This is the first step in the preparation of the coverage diagram. Later sections will discuss construction of lobes about these center lines.

#### 15.6.5 The General Lobe Angle Formula

For very high sites (over 1,000 ft) and frequencies over 200 mc, it is desirable to have a more accurate expression for the locus of constant path difference than is afforded by straight lines. This is of especial interest in the first few lobes as these determine the

low coverage which is of great tactical importance. The method described here overcomes the limitations of equation (62) and may be used for the highest sites.

In Figure 54 is shown the antenna above a curved reflecting surface whose radius is taken as  $\frac{4}{3}$  of the earth's radius to allow for atmospheric refraction. The tangent plane  $CE$  makes an angle  $\theta$  with the horizontal at the antenna, and  $\theta$  is given by  $-(d_1/ka)$  as shown in Figure 49.

$h_1$  = height of the center of the antenna above the earth's surface, in feet.

$h_1'$  = equivalent height of the antenna, in feet — equation (59).

$r_d$  = distance from the antenna to the target, in miles.

$A$  = distance from the antenna to the reflection point, in miles.

$B$  = distance from the reflection point to the target, in miles.

$\Delta$  = path difference,  $A + B - r_d$ , in miles.

$\lambda$  = wavelength, in feet.



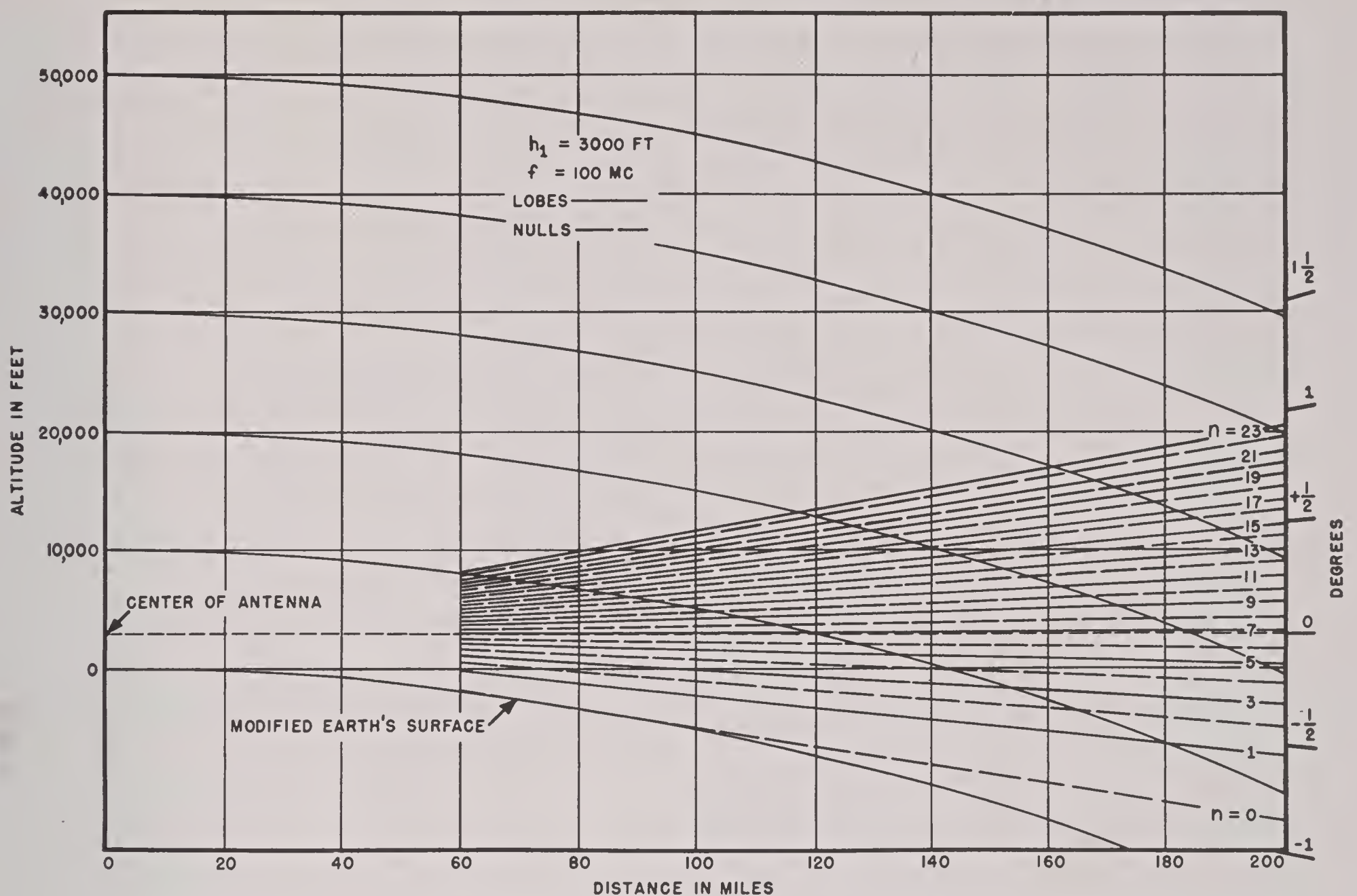


FIGURE 53. Lobe angles for Example 12.

$\theta$  = angle between the tangent plane  $CE$  and the horizontal at the antenna, in radians. This angle is always negative.

$ka$  = radius of the modified earth, 5,280 miles.

$\Psi_d$  = angle between the direct ray  $r_d$  and the horizontal plane  $CE$ , in radians.

$\Psi$  = angle between the reflected ray  $A$  or  $B$  and the horizontal plane  $CE$ , in radians.

$n'$  = number of half-wavelengths path difference.

In the triangle  $ABr_d$  (cosine law)

$$r_d = \sqrt{A^2 + B^2 + 2AB \cos 2\Psi}. \quad (64)$$

From the definition of path difference:

$$\Delta = A + B - r_d = \frac{n\lambda}{2 \times 5,280}, \quad (65)$$

$$A + B - \Delta = \sqrt{A^2 + B^2 + 2AB \cos 2\Psi};$$

squaring and dropping terms that cancel out gives

$$2AB - 2AB \cos 2\Psi - 2B\Delta = 2A\Delta - \Delta^2,$$

or solving with respect to  $B$ ,

$$B = \frac{A\Delta - \frac{1}{2}\Delta^2}{A(1 - \cos 2\Psi) - \Delta}. \quad (66)$$

Substituting

$$\Delta = \frac{n\lambda}{2 \times 5,280},$$

into equation (66) gives

$$B = \frac{\frac{n\lambda}{10,560}A - \frac{1}{2} \left( \frac{n\lambda}{10,560} \right)^2}{A(1 - \cos 2\Psi) - \frac{n\lambda}{10,560}}. \quad (67)$$

Several approximations will be introduced to simplify equation (67):

$A$  will be taken to equal  $d_1$  since  $\Psi$  is of the order of  $3^\circ$  or less.

From Figure 54 it follows that  $\sin \Psi = h_1'/5,280A$ , or for small angles,  $\Psi = h_1'/5,280A$ .

Substituting for  $h_1'$  [equation (59)] it follows that

$$\Psi = \frac{h_1 - \frac{1}{2}d_1^2}{5,280d_1}. \quad (68)$$

Using the approximation

$$\cos 2\Psi = 1 - 2\Psi^2,$$







To use this method it is best to arrange the calculations in a tabular form. Points along the lobe center are selected by using various values of  $d_1$  for the value of  $n$  desired. Next  $\Psi$  is obtained from equation (68) and substituted in equation (69), and  $B$  and  $\Psi$  are substituted in equation (70) yielding  $\Psi_d$ , which is combined with  $\theta$  to obtain  $\gamma$ . The curve of constant path difference is then plotted from  $\gamma$  and  $r_d$ , which are now known.

*Example 13. The General Lobe Angle Formula.* To illustrate this method a radar 3,000 ft high and operating at 100 mc will be used. A trial value of 60 miles is arbitrarily selected for  $d_1$  and substituted in equation (68), giving

$$\Psi = \frac{3,000 - \frac{1}{2} \times (60)^2}{5,280 \times 60} = 0.003788 \text{ radian}.$$

In equation (69) using  $n = 1$  and  $\lambda = 9.84$  ft,

$$B = \frac{\frac{1 \times 9.84}{10,560} \times 60}{2 \times 60(0.003788)^2 - \frac{1 \times 9.84}{10,560}} = 70.85 \text{ miles}.$$

$$\Psi_d = \frac{70.85 - 60}{70.85 + 60} \times 0.003788 = 0.000314 \text{ radian}.$$

$$\theta = -\frac{60}{5,280} = -0.01136 \text{ radian}.$$

$$\gamma = 0.000314 - 0.01136 = -0.01105 \text{ radian}.$$

$$r_d = 60 + 70.85 = 130.85 \text{ miles}.$$

Laying out the angle  $\gamma$  from the antenna and marking off the distance  $r_d$  gives one point on the curve of constant path difference. Enough other

points are computed to enable one to draw a smooth curve. The computations may be arranged as shown in Table 8. The values selected for  $d_1$  should be small enough so that the denominator of equation (69) is positive.

These two curves are plotted in Figure 55. For comparison is shown the first lobe as computed from equation (62), and it can be seen that this equation may lead to appreciable error in estimating low coverage. For most purposes it will suffice to calculate lobes higher than the first one or two by means of equation (62).

15.6.6

### The Calculation of Lobes

Three methods of computing lobe angles were given corresponding to low, medium, and high sites, in order to relate the labor of the computations to the complexity of the problem. A similar procedure will be followed in the calculation of the lobe shapes.

The lobe diagram represents the locus of all points along a particular azimuth of a definite field intensity, usually the threshold of detection. If the site has horizontal symmetry throughout its sector of operation one diagram will suffice. Usually several diagrams are required, and it is common practice to prepare a diagram for the central azimuth of the sector and for 10 degrees inside of each limit of scan.

15.6.7

### Low Site Lobes

The electric field intensity at the target is the resultant of the direct and reflected waves which have the same amplitude and a phase angle which varies continually as the lobe angle  $\gamma$  is increased.

TABLE 8. General lobe angle formula. (Example 13.)

$d_1$ , miles	$\Psi$ , radians	$B$ , miles	$\Psi_d$ , radians	$-\theta$ , radians	$-\gamma$ , radians	$r_d$ , miles
( $n = 1$ ) 65	.002800	696.0	.0023220	.0123105	.00999	761.0
62	.003290	141.2	.0012810	.0117450	.01046	203.2
60	.003788	70.85	.0003140	.0113636	.01105	130.85
58	.004300	44.60	-.0005618	.0109850	.01155	102.60
55	.005118	26.32	-.0018050	.0104166	.01222	81.32
50	.006628	13.45	-.0038380	.0094698	.01331	63.45
30	.016090	1.91	-.0141600	.0056820	.01984	31.91
( $n = 2$ ) 60	.003788	..	..	.0113636	..	..
58	.004300	386.0	.0031770	.0109850	.007808	440.0
56	.004840	137.5	.0020390	.0106060	.008567	193.5
55	.005118	101.0	.0015090	.0104166	.008908	156.0
53	.005700	62.6	.0004733	.0100381	.009565	115.6
50	.006628	36.78	-.0010115	.0094698	.010480	86.78
30	.016090	4.09	-.0122300	.0056820	.017910	34.09



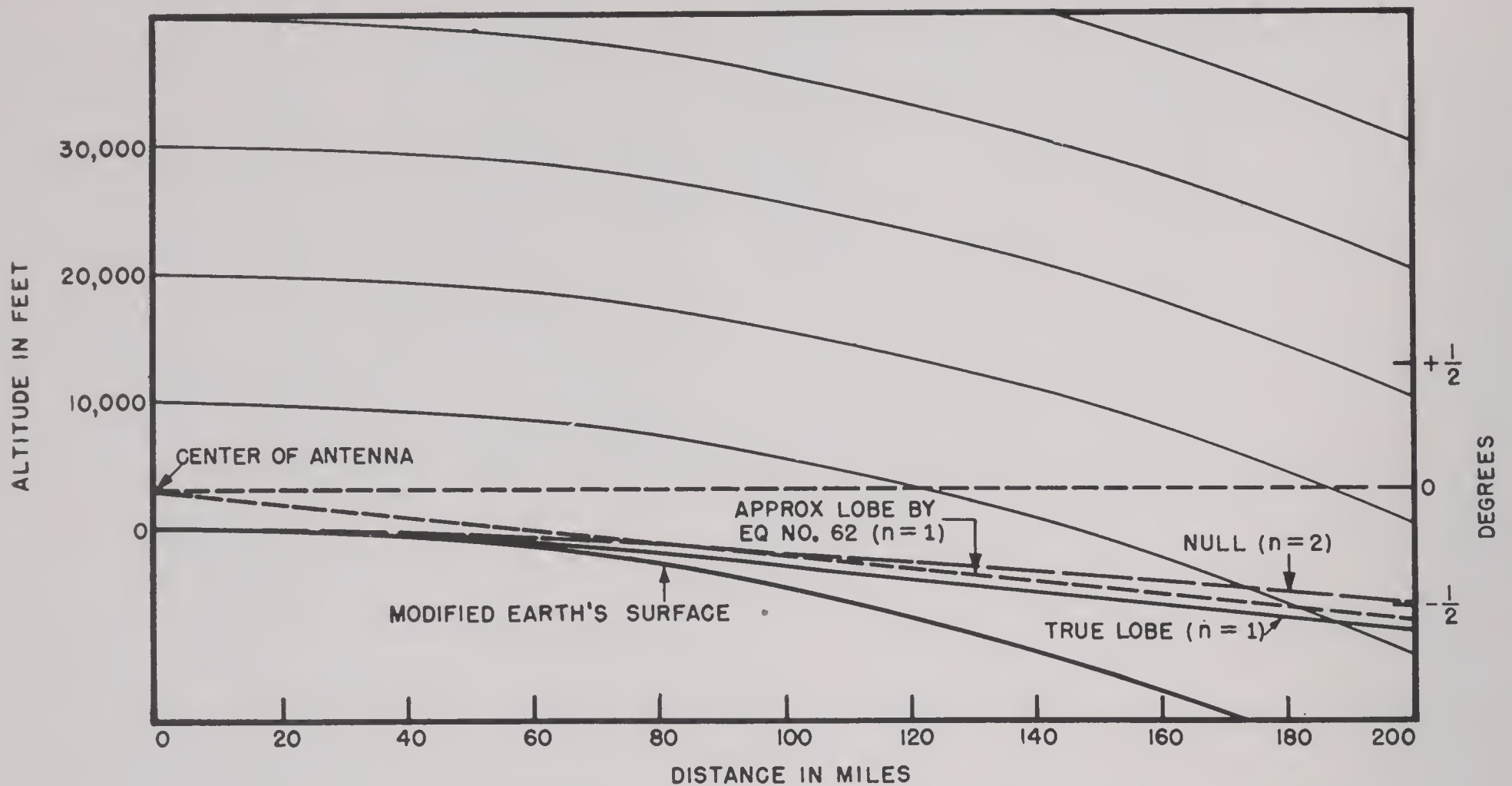


FIGURE 55. Lobe and null lines. (Example 13.)

For a perfect reflector and horizontal polarization the phase lag is equal to  $+\pi + (2\pi/\lambda) \times (n\lambda/2)$  which adds up to  $n\pi + \pi$ . Odd integral values of  $n$  give lobe maxima, and intermediate values give other points on the lobes.

The sum of the two vectors practically parallel and of equal magnitude,  $E_1/d$ , is

$$E = \frac{2E_1}{d} \cos \left[ (n+1) \frac{\pi}{2} \right], \quad (72)$$

where  $E_1$  is the electric intensity (microvolts per meter) in the equatorial plane 1 mile from the antenna in free space, that is, without a reflecting surface.  $E$  is the electric intensity at the point considered in microvolts per meter.  $d$  is the distance to the point, in miles.  $n$  is a number related to the angle of elevation. It is an odd integer for lobe maxima and an even integer for nulls. For a given antenna and radar the electric intensity  $E$  will produce at the input of the receiver a voltage,

$$V_2 = \frac{k_1 E_1}{d} \sin (90^\circ n), \quad (73)$$

where  $k_1$  is a proportionality factor for the voltage applied to the receiver input. If  $V_2$  is set equal to the minimum operating voltage of the receiver equation (73) becomes

$$d = \frac{k_1 E_1}{V_{\min}} \sin (90^\circ n).$$

The term  $k_1 E_1/V_{\min}$  is usually obtained from test

flights on the particular radar or on radars of the same type. The usual form is

$$d = d_{\max} \sin (90^\circ n), \quad (74)$$

where  $d_{\max}$  stands for  $k_1 E_1/V_{\min}$  and is a measure of the performance of the radar set.

The lobes will be polar sinusoids and the minima will go to zero only when the amplitude of the direct and indirect waves are equal. These conditions will not obtain if the vertical directivity of the antenna affects the rays unequally, if the reflected wave suffers imperfect reflection or divergence, or the atmosphere or terrain has unequal effects on the two waves. Low sites are generally free from the above effects and equation (74) may be used with acceptable accuracy.

*Example 14. Low Site Lobes.* A radar operating on 200 mc is 25 ft high and has a maximum range of 60 miles. The lobes occur at  $2.82^\circ$ ,  $8.46^\circ$ , and  $14.1^\circ$  and the nulls at  $0^\circ$ ,  $5.64^\circ$ ,  $11.28^\circ$ . The method of plotting a lobe is shown in Figure 56.  $n$  may be divided into as many parts as desired, and the corresponding range for each obtained from equation (74). Thus at  $n = 0.7$  the angle is

$$\frac{0.7 \times 4.92}{4 \times 25} = 0.0344 \text{ radian},$$

$$d = 60 \sin (90^\circ \times 0.7) = 53.46 \text{ miles}.$$

A line is drawn at this angle, and a point is marked off at a range of 53.46 miles.



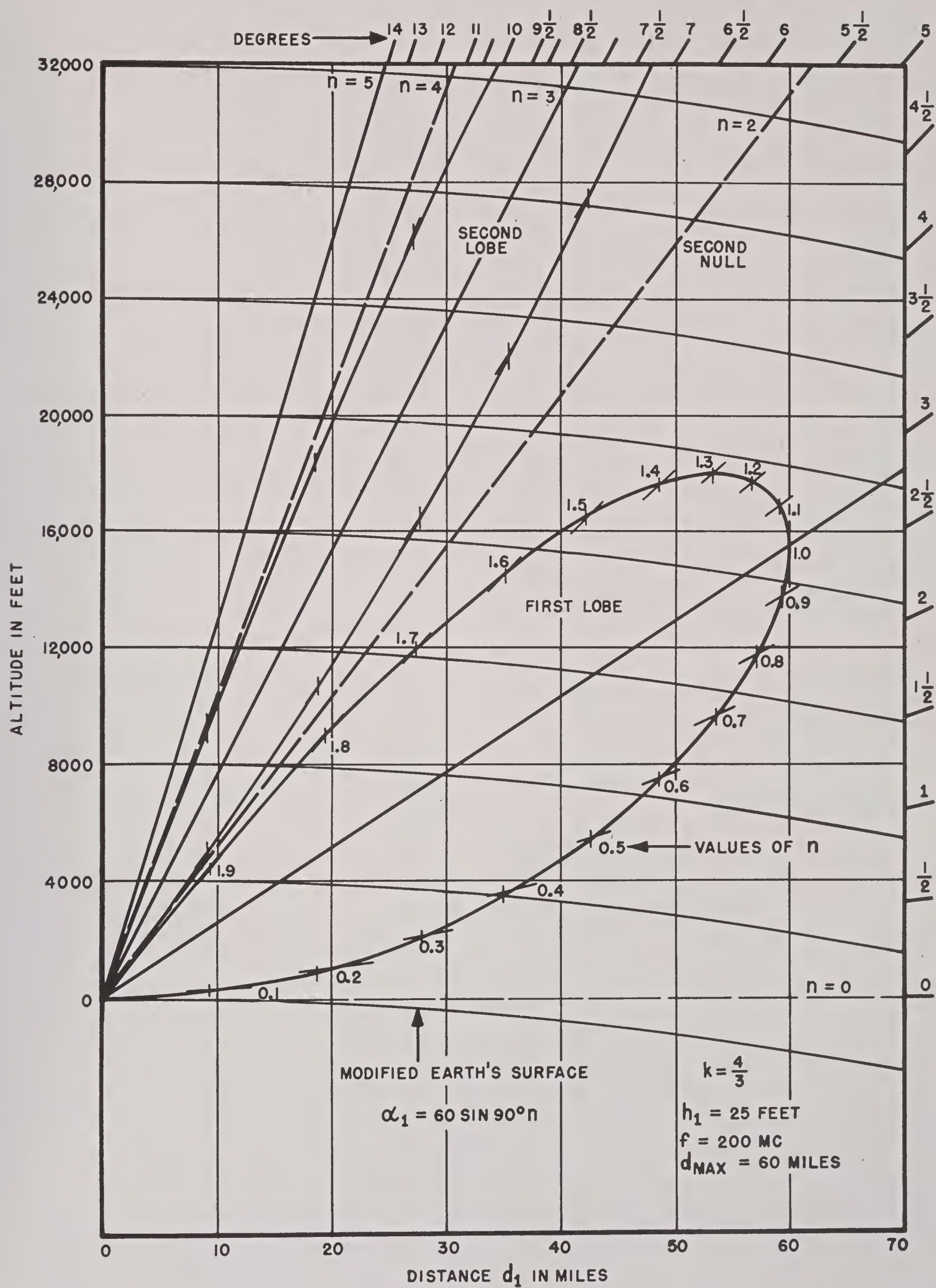


FIGURE 56. Low site lobes. (Example 14.)



### 15.6.8 Lobe Diagrams of Medium Height Sites

In dealing with radars at medium heights, say from 100 to 1,000 ft, a more involved treatment is required, owing to earth curvature effects. The procedure followed in this section is to compute a value of  $d_{\max}$  for each lobe from which a sinusoid is constructed at the angle of the lobe. The envelope of the lobes is considered to be of principal interest, the lobe shape being of secondary importance.

The strength of a wave is measured in miles, that is, the distance at which the standard target must be to give a standard signal response such as a signal-to-noise ratio of one. The distances corresponding to the direct and reflected waves are added to get lobe maxima and subtracted to get minima. The direct and reflected waves will therefore be computed separately. The phase shift due to reflection will be taken as  $180^\circ$ , and the phase shift due to other causes than path difference will be considered negligible. This assumption greatly simplifies calculations and is a good approximation for small angles and horizontal polarization. For vertical polarization, especially in the VHF band, it is a poor approximation.

The direct wave is affected only by the modified antenna pattern. The reflected wave is affected by:

1. Shoreline diffraction.
2. The modified antenna pattern.
3. Earth curvature.
4. Coefficient of reflection.
5. Divergence.

Terrain effects such as reflection areas of limited extent, the shoreline, cliff edges, and obstacles involve diffraction. A simple, flexible method for solving such problems will be developed in the next section.

15.6.9

### Shoreline Diffraction

Unfortunately sites of sufficient height are frequently some distance inland, and a considerable portion of the reflection surface is on land. The poor reflecting qualities of land, especially when rough, causes the high angle lobes due to nearby reflection to be reduced as much as 50 per cent in length. This is a common cause of poor high coverage so often experienced in field installations and the inability to detect high-level bombing attacks except at perhaps 10-mile ranges. In this section will be developed a method of computing the vertical coverage pattern for the typical high site with part land and part sea reflecting surfaces.

In most cases the profile of the land between the transmitter and the shore will be found to be too rough for coherent reflection, as may be determined from equation (16). If substantial regular areas or obstacles occur between the antenna and the shore line they should be treated as described in Section 15.6.12, on the modified antenna pattern.

15.6.10

### Sea Reflection with Diffuse Land Reflection

The problem treated in this section will be that shown in Figure 57. The land in the foreground is so rough as to cause only diffuse reflection, and no regular areas exist which will affect the vertical pattern below  $15^\circ$ .

The diffuse reflection from the land area has a random phase relation, and the field intensity in a particular direction is relatively small. The effect of the land reflection on the interference pattern is

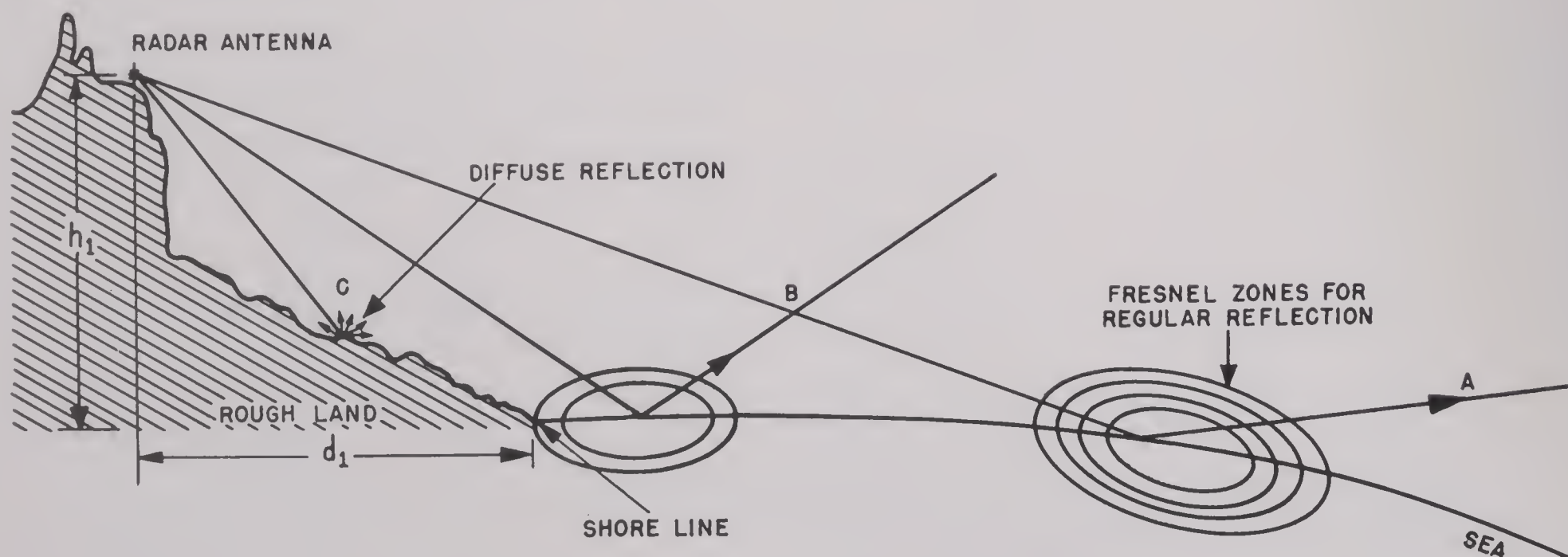


FIGURE 57. Fresnel zones on land and sea areas.



therefore neglected. This is equivalent to termination of the reflecting surface at the shore line.

In order to describe diffraction at a shore line a system of Fresnel zones for each lobe is considered to be formed on the sea with the reflection point of the lobe as their center. The zones will be ellipses because of the inclination of the rays. The influence of the shore line will be determined by the number of zones which are not interfered with by the shore.

Thus a low angle lobe which has its central Fresnel zone far out to sea would be virtually unaffected by the limited reflection area, as numerous zones are formed on the sea. This is indicated by *A* in Figure 57, which represents the reflected wave. At *B*, a higher angle lobe, there are only two zones intact, and the reflected wave is weak. Had only one zone been complete, the reflected wave would have been stronger than *A*. At *C* only portions of outer zones are formed on the sea, and the reflected wave is negligible.

The effect of the reflecting surface may be represented by an image antenna located in the earth under the radar antenna at a depth  $h_1$  below the

surface as in Figure 58. The nonreflecting land surface then acts precisely as a straight diffracting edge for the image antenna and indirect ray. A general formula will be developed which gives the situation of any Fresnel zone of any lobe for a given radar station. From this formula and the distance to the shoreline it may be determined for each lobe which zone is intercepted by the shore. In the graph in Figure 58 is plotted the relative intensity of the reflected ray as a function of  $m$ , the number of the zone touching the shore. In the illuminated region at large angles, as *A*, the relative intensity is close to unity. Approaching the shore it oscillates about unity, reaching a maximum of 1.18. In the shadow region, the intensity drops to low values. Thus, knowing  $m$ , the effect of shoreline diffraction on the reflected ray may be obtained. The derivation will be developed for a plane reflecting surface, since, as it has been shown in Section 15.6.4, for lobe angles corrected for standard earth curvature, the effect of earth curvature may be taken into account by using  $h_1'$  [equation (59)] instead of  $h_1$ . In most cases  $d_1$  will be small and  $h_1$  may be used with little error.

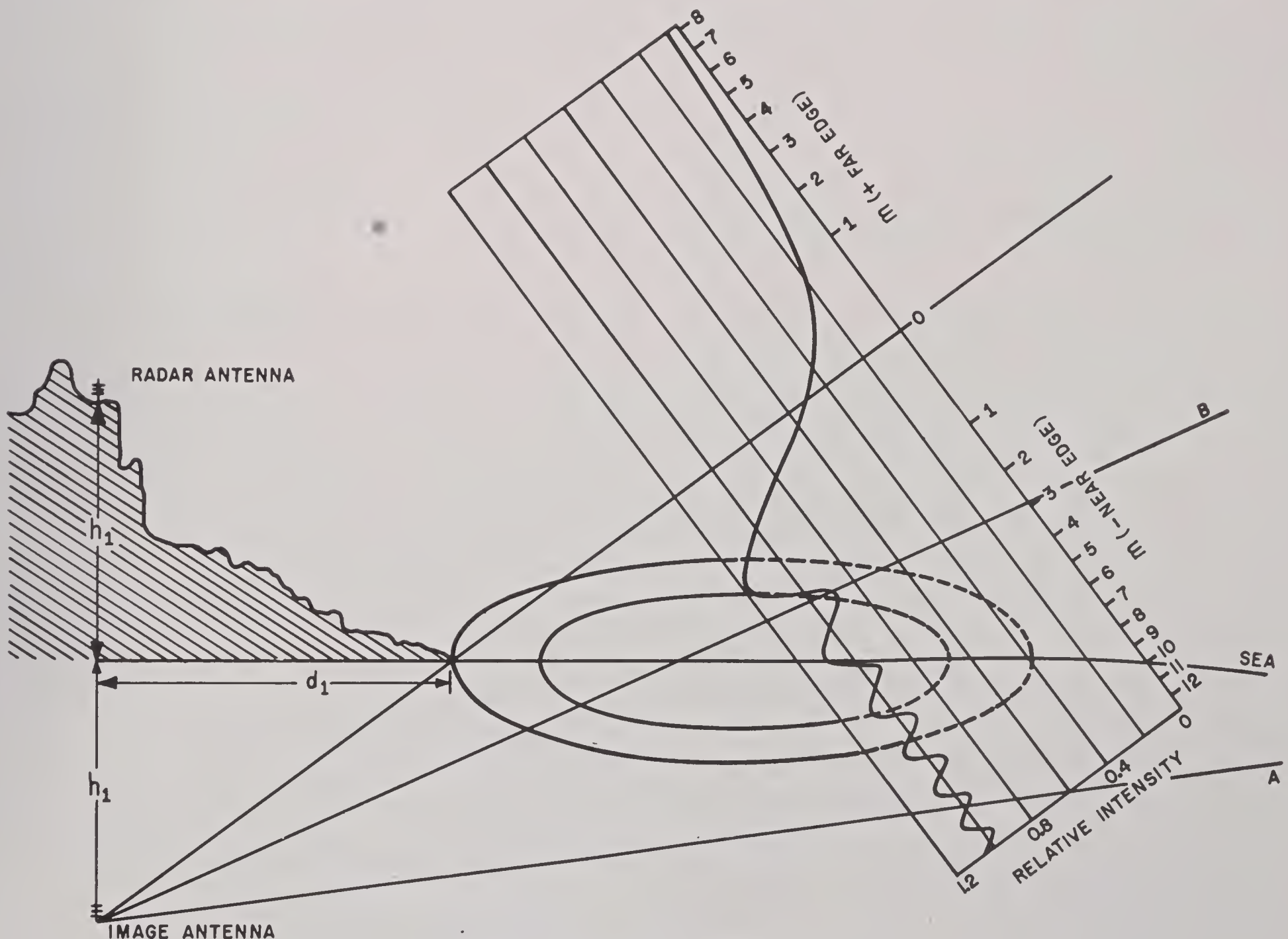


FIGURE 58. Shore line diffraction.



15.6.11

### General Formula for the Reflection Area

In Figure 59 is shown an image antenna  $T'$  sending radiation through a plane of indefinite extent. In

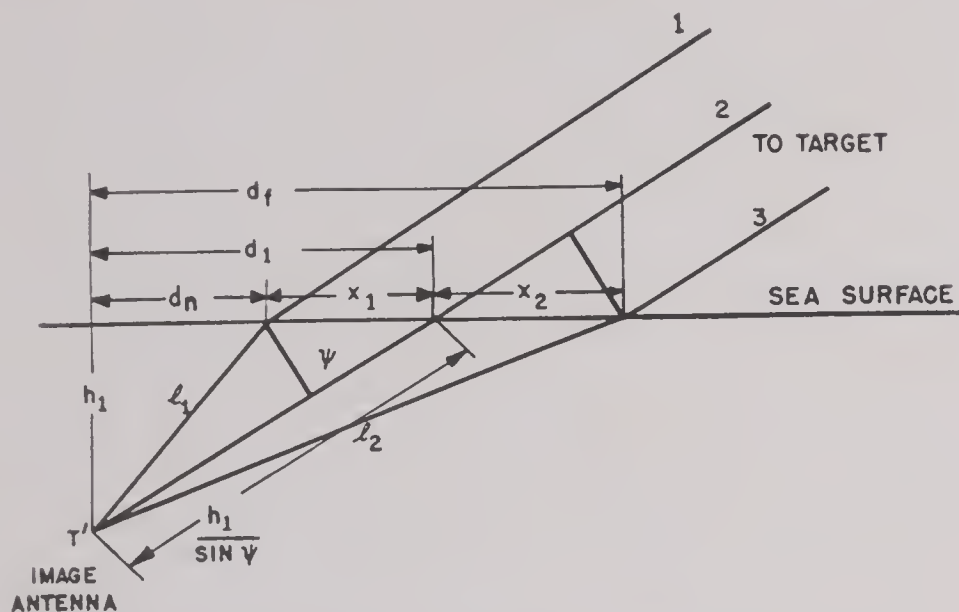


FIGURE 59. Fresnel zones on the reflecting surface.

order to simplify the calculations it will be assumed that the distance from the reflection point to the target is large, so that the rays from the Fresnel zones may be considered parallel. With regard to the transmitter distance, however, no such approximation will be made.

$h_1$  = depth of the image antenna below the reflecting surface, in feet.

$\Psi$  = angle of the lobe considered with reference to the tangent plane at the reflection point, in radians.

$m$  = number of the Fresnel zone.

$m = 0$  for the center of the first zone.

$m = +1$  for the far edge of the first zone.

$m = -1$  for the near edge of the first zone.

$m = +2$  or  $-2$  for the edge between the second and third zones.

$n$  = lobe number. For a given radar station  $n$  is related to the angle  $\Psi$  by the equation  $n = (4h_1/\lambda) \sin \Psi$ .

$\lambda$  = wavelength in feet.

$d_n$  = distance from the transmitter to the near edge for the Fresnel zone and lobe considered, in feet.

$d_f$  = distance from the transmitter to the far edge for the Fresnel zone and lobe considered, in feet.

$d_1$  = distance from the transmitter to the center of the first Fresnel zone for a particular lobe, in feet.

In Figure 59 is shown the first Fresnel zone for an angle  $\Psi$  with a corresponding value of  $n$ . Ray 2 passes through the center of the first zone and rays 1 and 3 pass through the near and far edges respectively. Because of the great distance of the target the rays 1, 2, and 3 are parallel.

For the first zone the path difference between 1 and 2 is  $\lambda/2$ . For zone  $m$  the path difference is  $m\lambda/2$  (where  $m = 1, 2, 3$ , etc.). Since the points  $d_1$  and  $d_n$  are not equidistant from the target, the distance  $x_1 \cos \Psi$  must be subtracted from ray 2 to compensate for the increased path length of ray 1 above the plane.

$$\frac{m\lambda}{2} = l_1 - \left( \frac{h_1}{\sin \Psi} - x_1 \cos \Psi \right).$$

In the right triangle

$$l_1^2 = x_1^2 \sin^2 \Psi + \left( \frac{h_1}{\sin \Psi} - x_1 \cos \Psi \right)^2.$$

Eliminating  $l_1$  from these equations and solving for  $x_1$

$$x_1 = \frac{-m\lambda \cos \Psi + \sqrt{m^2\lambda^2 + 4m\lambda h_1 \sin \Psi}}{2 \sin^2 \Psi}. \quad (75)$$

For the far point of the zone

$$\frac{m\lambda}{2} = l_2 - \left( \frac{h_1}{\sin \Psi} + x_2 \cos \Psi \right),$$

also

$$l_2^2 = x_2^2 \sin^2 \Psi + \left( \frac{h_1}{\sin \Psi} + x_2 \cos \Psi \right)^2.$$

By a similar process of elimination of  $l_2$  and solving for  $x_2$ :

$$x_2 = \frac{m\lambda \cos \Psi + \sqrt{m^2\lambda^2 + 4m\lambda h_1 \sin \Psi}}{2 \sin^2 \Psi}. \quad (76)$$

For the near point of the zone

$$d_n = \frac{h_1}{\tan \Psi} - \frac{-m\lambda \cos \Psi + \sqrt{m^2\lambda^2 + 4m\lambda h_1 \sin \Psi}}{2 \sin^2 \Psi}.$$

Since  $\sin \Psi = n\lambda/4h_1$  and  $\Psi$  is small,  $\cos \Psi$  may be taken as unity with the following error:

up to $2\frac{1}{2}^\circ$	less than 0.1 per cent,
up to $10^\circ$	less than 1.5 per cent,
up to $15^\circ$	less than 4.5 per cent,

$$d_n = \left( \frac{1}{2n} + \frac{m}{n^2} - \frac{\sqrt{m^2 + mn}}{n^2} \right) \frac{8h_1^2}{\lambda}.$$



For the far point

$$d_f = \left( \frac{1}{2n} + \frac{m}{n^2} + \frac{\sqrt{m^2 + mn}}{n^2} \right) \frac{8h_1^2}{\lambda}.$$

These equations may be combined:

$$d = \left( \frac{1}{2n} + \frac{m}{n^2} \pm \frac{\sqrt{m^2 + mn}}{n^2} \right) \frac{8h_1^2}{\lambda}, \quad (77)$$

where the plus sign gives the far point and the minus sign gives the near point. The reflection point is obtained by using  $m = 0$  and equation (77) reduces to:

$$d_1 = \frac{4h_1^2}{n\lambda}. \quad (78)$$

Thus to obtain the range of the near edge of the first Fresnel zone for the first lobe, substitute  $n = 1$ ,  $m = 1$  and use the minus sign in equation (77):

$$d_n = 0.688 \frac{h_1^2}{\lambda}. \quad (79)$$

The far edge of this zone is obtained by using the plus sign

$$d_f = 23.3 \frac{h_1^2}{\lambda}. \quad (80)$$

Equation (77) is in the form

$$d = T \frac{h_1^2}{\lambda}, \quad (81)$$

where

$$T = 8 \left( \frac{1}{2n} + \frac{m}{n^2} \pm \frac{\sqrt{m^2 + mn}}{n^2} \right), \quad (82)$$

or

$$T_1 = \frac{d_1\lambda}{h_1^2}. \quad (83)$$

If  $d_1$  is taken as the distance of the shoreline,  $T_1$  may be considered as a characteristic site or terrain factor at a particular azimuth and combined with the height and wavelength to obtain the range of any zone of any lobe.

In order to read the relative intensity and phase lag of the reflected wave from the diffraction graphs, Figure 27 and Figure 28 respectively, it is necessary to have  $m$  expressed in terms of  $v$ . In Figure 19 the path difference is by definition of  $m$

$$\Delta = m \frac{\lambda}{2}. \quad (84)$$

Equation (23), with  $\Delta = d - b$ , yields

$$\Delta = \frac{\lambda v^2}{4},$$

hence

$$m = \frac{v^2}{2}. \quad (85)$$

It is also desirable to have an expression for  $v$  in terms of  $n$  and  $T$ . This is obtained by substituting  $v^2/2$  for  $m$  in equation (82) and solving

$$v = \sqrt{\frac{Tn^2}{8} - n + \frac{2}{T}} \quad (86)$$

The width of the zones, that is, along a chord at  $d_1$  parallel to the minor axis of the elliptical rings,

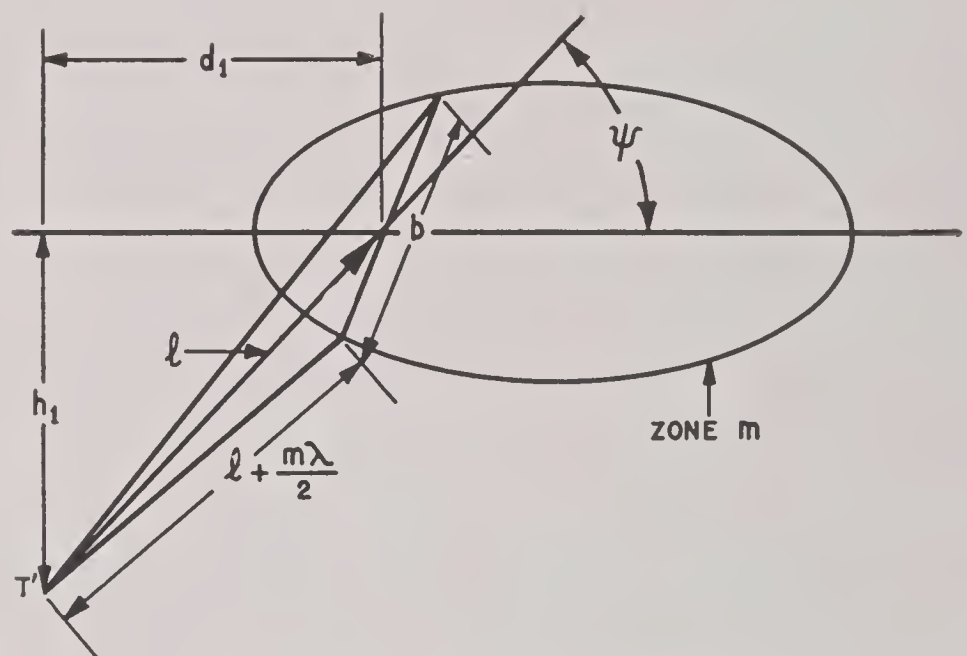


FIGURE 60. Width of Fresnel zones.

may be obtained from Figure 60. Zone  $m$  is shown with a chord length  $b$ . The distance from the image antenna to the intersection of the chord and ring  $m$  is  $l + m\lambda/2$ . From this may be written

$$\left( l + \frac{m\lambda}{2} \right)^2 = l^2 + \left( \frac{b}{2} \right)^2. \quad (87)$$

Neglecting  $m^2\lambda^2/4$  since it is small compared to the other terms,

$$l^2 + m\lambda l = l^2 + \left( \frac{b}{2} \right)^2,$$

$$b = \sqrt{4m\lambda l},$$

$$l = \frac{d_1}{\cos \Psi} = d_1 = \frac{4h_1^2}{n\lambda},$$

from equation (78), since  $\Psi$  is small.

Where earth curvature effects are appreciable the



effective height, from equation (59), should be used.

$$b = 4h_1' \sqrt{\frac{m}{n}}. \quad (88)$$

To apply this method the distance of the shoreline,  $d_1$ , is substituted in equation (81), and the equation is solved for  $T_1$ , the terrain factor. This quantity is a constant for a particular azimuth and is substituted in equation (86) along with the values of  $n$  desired and solved for  $v$ . The values of  $m$  corresponding to these values of  $v$  are the numbers of the zones which intersect the shoreline for each value of  $n$ . These values of  $v$  are entered in Figures 27 and 28 to obtain the intensity and phase lag relative to that which would be obtained if the rough land were replaced by the sea.

*Example 15. Shoreline Diffraction.* A radar station is assumed to have the same height and frequency as in Example 11. The shoreline distance is 3 miles, and the intervening land is occupied by a large city.  $h_1 = 500$  ft;  $f = 200$  mc;  $d_1 = 15,840$  ft. At this distance the effect of earth curvature is less than 1 per cent and may be neglected. The greatest angle at which waves are reflected from the sea is given by

$$\frac{500}{15,840} \times 57.3 = 1.81^\circ.$$

In equation (16) the maximum height of roughness for regular reflection is

$$H = \frac{3,520}{200 \times 1.81} = 9.7 \text{ ft}.$$

The land is evidently a diffuse reflector. From equation (83)

$$T_1 = \frac{d_1 \lambda}{(h_1')^2} = \frac{15,840 \times 4.92}{(500 - 4.5)^2} = 0.317.$$

Substituting in equation (86) for  $n = 2$

$$v = \sqrt{\frac{0.317 \times 4}{8} - 2 + \frac{2}{0.317}} = 2.11,$$

$$m = \frac{v^2}{2} = 2.23.$$

That is, somewhat more than two zones are completely formed on the sea. In order to determine which sign to use in reading Figure 27 it is only necessary to know whether the main reflection point  $d_1$  for this lobe falls on the land or the sea corresponding to shadow or illuminated regions. A more general procedure is to solve equation (63) using the shoreline distance for  $d_1$ :

$$n = \frac{4 \times (500 - 4.5)^2}{15,840 \times 4.92} = 12.6.$$

For all values of  $n$  less than 12.6,  $d_1$  will be on the sea and equation (84) applies to the near edge, and the minus sign is used in equation (82) corresponding to  $+v$  in Figure 27. For  $n$  greater than 12.6 the plus sign is used in equation (82) and  $-v$  in Figure 27. Thus, for  $n = 2$  and  $v = +2.11$ , is read in Figure 27 the relative intensity  $z = 0.980$  and in Figure 28 the phase lag,  $\zeta = -0.103$  radians. Other values are listed in Table 9.

The width of the second zone may be computed from equation (88). The effective height for  $n = 2$  is obtained from Figures 50 and 51 and is 414 ft.

$$b = 4 \times 414 \sqrt{\frac{2}{2}} = 1,656 \text{ ft}.$$

TABLE 9. Shoreline diffraction. (Example 15.)

$n$	$v$	Sign	$z$	$\zeta$	$n$	$v$	Sign	$z$	$\zeta$
0	2.51	+	1.036	+0.080	12	0.14	+	0.582	-0.130
1	2.31	+	1.083	-0.015	13	0.089	-	0.459	+0.2
2	2.11	+	0.980	-0.103	14	0.28	-	0.377	+0.5
3	1.91	+	0.884	-0.038	15	0.49	-	0.308	+0.9
4	1.71	+	0.938	+0.100	16	0.68	-	0.261	+1.4
5	1.51	+	1.082	+0.120	17	0.87	-	0.223	+1.9
6	1.32	+	1.170	+0.030	18	1.08	-	0.192	+2.6
7	1.12	+	1.156	-0.085	19	1.27	-	0.170	+3.3
8	0.92	+	1.073	-0.181	20	1.48	-	0.150	+4.2
9	0.72	+	0.953	-0.255	21	1.67	-	0.135	+5.2
10	0.52	+	0.825	-0.273	22	1.88	-	0.121	+6.4
11	0.32	+	0.696	-0.224	23	2.07	-	0.111	+7.6

## 15.6.12 The Modified Antenna Pattern

The vertical directivity of the antenna is modified by the local terrain. Unless the ground under the antenna is an extension of the reflection plane the modification of the free space directivity characteristics should be taken into consideration in the calculation of radar coverage.

The vertical pattern of the antenna in the absence of a reflecting surface is referred to as the free space pattern,  $f_A$ . This is usually given in the instruction manual for the set. If this pattern is not available or if the antenna has been modified, the vertical directivity may be computed by methods given in the next section. Local terrain effects are treated in some detail as they are in many cases a controlling factor. The resultant effect of the local terrain and free space pattern is called the modified antenna pattern,  $f(\gamma)$ . It does not include the effect of the main reflecting surface.



15.6.13

## Antenna Patterns

To obtain  $f_A$ , the relative amplitude of the radiation from the antenna, as a function of the vertical angle  $\gamma$  it is only necessary to take into account the path differences of the elements of the array. The absolute field intensity and time phase will not be considered. In Figure 61 is shown an array of four

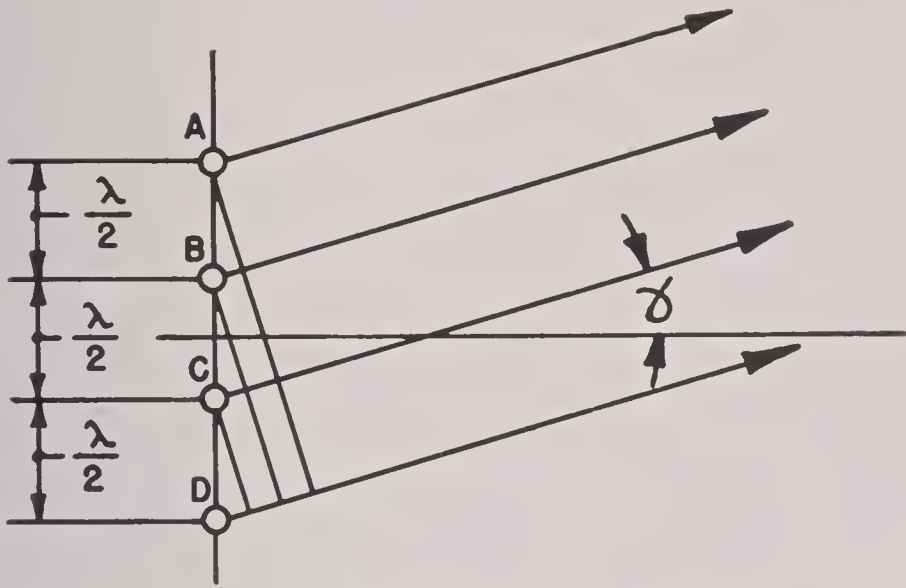


FIGURE 61. The four-element array.

horizontal half-wave dipoles spaced a half wavelength apart. The radiation from A in the direction  $\gamma$  may be taken as proportional to  $\cos \omega t$ . The path difference of radiation from B is  $\lambda/2 \cdot \sin \gamma$ . The corresponding phase difference is

$$-\frac{2\pi}{\lambda} \times \frac{\lambda}{2} \sin \gamma = -\pi \sin \gamma.$$

For C and D the phase is  $-2\pi \sin \gamma$  and  $-3\pi \sin \gamma$  respectively. The total field intensity pattern is

$$\begin{aligned} f_A &= \cos \omega t + \cos (\omega t - \pi \sin \gamma) \\ &+ \cos (\omega t - 2\pi \sin \gamma) + \cos (\omega t - 3\pi \sin \gamma), \end{aligned}$$

grouping

$$\begin{aligned} &[\cos \omega t + \cos (\omega t - 3\pi \sin \gamma)] \\ &+ [\cos (\omega t - \pi \sin \gamma) + \cos (\omega t - 2\pi \sin \gamma)]. \end{aligned} \quad (89)$$

From the identity

$$\cos A + \cos B = 2 \cos \frac{1}{2} (A + B) \cos \frac{1}{2} (A - B)$$

equation (89) may be written

$$\begin{aligned} f_A &= 2 \cos \left( \omega t - \frac{3\pi}{2} \sin \gamma \right) \cos \left( \frac{3\pi}{2} \sin \gamma \right) \\ &+ 2 \cos \left( \omega t - \frac{3\pi}{2} \sin \gamma \right) \cos \left( \frac{\pi}{2} \sin \gamma \right), \\ f_A &= 2 \cos \left( \omega t - \frac{3\pi}{2} \sin \gamma \right) \cdot \end{aligned}$$

$$\left[ \cos \left( \frac{3\pi}{2} \sin \gamma \right) + \cos \left( \frac{\pi}{2} \sin \gamma \right) \right],$$

$$\begin{aligned} f_A &= 4 \cos \left( \omega t - \frac{3\pi}{2} \sin \gamma \right) \cos (\pi \sin \gamma) \cdot \\ &\cos \left( \frac{\pi}{2} \sin \gamma \right). \end{aligned}$$

Since only the rms value of this equation is significant, the terms containing  $\omega t$  may be dropped, and the result for the four-element array is

$$f_A = \cos (\pi \sin \gamma) \cos \left( \frac{\pi}{2} \sin \gamma \right). \quad (90)$$

It is easily verified that this is a special case of the general expression for an  $N$  element array spaced at intervals of  $n\lambda$  and excited in phase (not derived here)

$$f_A = \frac{\sin (Nn \pi \sin \gamma)}{N \sin (n \pi \sin \gamma)}. \quad (91)$$

The effect of a reflecting screen may be computed by treating it as though it were  $\lambda/4$  from the dipole as in Figure 62. In practice the spacing may be

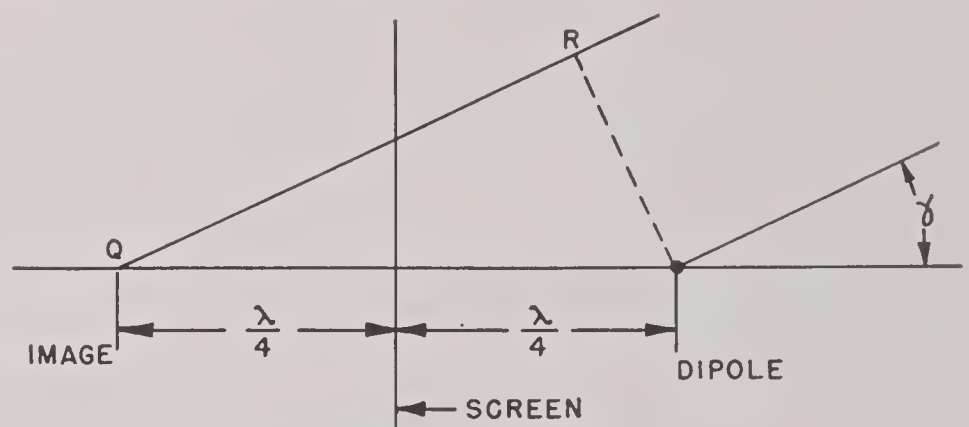


FIGURE 62. The reflecting screen.

more nearly  $\lambda/8$  but for  $\gamma$  less than  $30^\circ$  the method given here is satisfactory and avoids a complicated analysis. The path difference  $QR$  is  $(\lambda/2) \cos \gamma$ , and the phase difference is  $\pi \cos \gamma$ . Then

$$f_A = \cos \omega t - \cos (\omega t - \pi \cos \gamma). \quad (92)$$

From the relation

$$\cos A - \cos B = -2 \sin \frac{1}{2} (A + B) \sin \frac{1}{2} (A - B),$$

it follows that equation (92) may be written in the form

$$f_A = -2 \sin \left( \omega t - \frac{\pi}{2} \cos \gamma \right) \sin \left( \frac{\pi}{2} \cos \gamma \right).$$

Dealing only with the rms value,

$$f_A = \sin \left( \frac{\pi}{2} \cos \gamma \right). \quad (93)$$

For small angles this factor is usually unimportant. Factors are given in Table 10 for some typical arrays with horizontal radiators in a vertical column and a reflector screen.



TABLE 10. Antenna pattern factors.

Array with screen	Vertical pattern $f_A$
Two radiators spaced $\frac{\lambda}{2}$	$\cos \left( \frac{\pi}{2} \sin \gamma \right) \sin \left( \frac{\pi}{2} \cos \gamma \right)$
Four radiators spaced $\frac{\lambda}{2}$	$\cos \left( \frac{\pi}{2} \sin \gamma \right) \cos (\pi \sin \gamma) \sin \left( \frac{\pi}{2} \cos \gamma \right)$
Two sets of four radiators each (Vertical spacing between centers of sets is $3\lambda$ .)	$\cos \left( \frac{\pi}{2} \sin \gamma \right) \cos (\pi \sin \gamma) \times$ $\cos (3\pi \sin \gamma) \sin \left( \frac{\pi}{2} \cos \gamma \right)$

*Example 16. Vertical Pattern of an Antenna.* Using the eight element array in Table 10, the relative intensity at angle of  $5^\circ$  from the horizontal is computed as follows.

$$\begin{aligned}
 f_A &= \cos (90 \sin 5^\circ) \cos (180 \sin 5^\circ) \\
 &\quad \cos (540 \sin 5^\circ) \sin (90 \cos 5^\circ), \\
 &= \cos 7^\circ 51' \times \cos 15^\circ 41' \\
 &\quad \times \cos 47^\circ 4' \times \sin 89^\circ 39', \\
 &= 0.9906 \times 0.9628 \times 0.6809 \times 0.9999, \\
 &= 0.65.
 \end{aligned}$$

The main vertical lobe is plotted in Figure 63. The first null is at  $9^\circ 36'$  and the half-power beam width

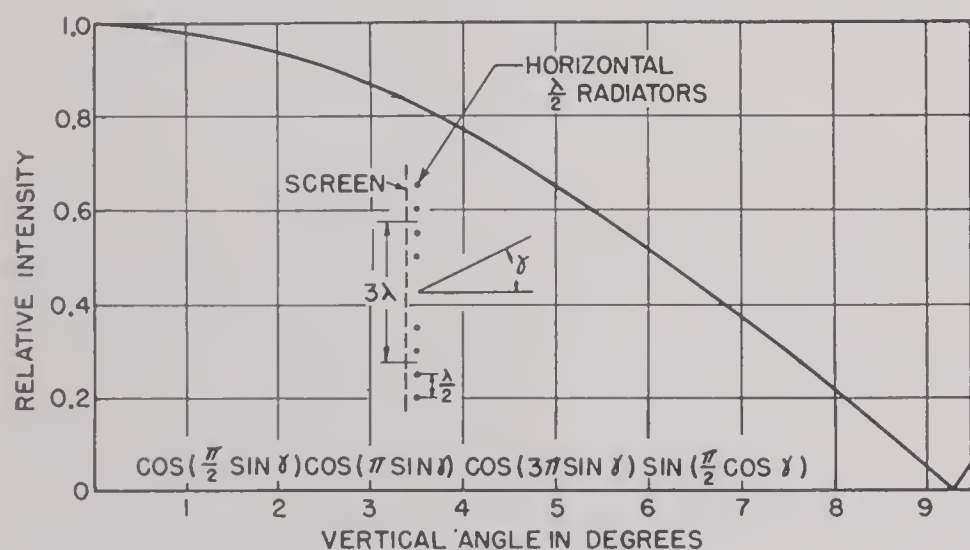


FIGURE 63. Vertical pattern of a typical antenna. (Example 16.)

is  $4.53^\circ$ . It will be noted that the effect of the reflector screen may be neglected for small angles.

The pattern from a parabola is closely dependent on the feed system which controls the uniformity of illumination. To reduce side lobes it is common practice to taper the illumination toward the edge of the dish. This is accompanied by a broadening of the beam and a loss of gain. The half-power beam width for uniform illumination is  $59\lambda/D$  degrees, where  $D$  is the diameter of the aperture. The first

side lobe is then about 2 per cent of the maximum. A typical dish with a tapered feed would have a half-power band width of  $68.8\lambda/D$  degrees. This reduces the first side lobe to 0.5 per cent. Some designs are further modified by deforming the dish, off-center feeds, etc., so that the patterns may not be easily computed. Such patterns are best obtained experimentally and are usually given in the manual for the equipment.

15.6.14

### Local Terrain Effects

The vertical pattern of the antenna may be modified by reflection from local flat areas or by diffraction over hills or other obstacles. To take these effects into account, factors are computed from the diffraction equations which are used to modify the direct and reflected ray patterns.

A detailed method of calculating  $f(\gamma)$  cannot be given because of the great variety of sites encountered. However, the following discussion of the effects of particular terrain features will suggest methods of combining them to analyze a particular site.

A large, flat land area will in general produce lobes and nulls at angles given by equation (57) with an envelope twice as large as the free space pattern. If the land area is not level, the lobe pattern will be tilted by the angle of the land. However, the problem is essentially a matter of diffraction since the land is of limited extent. Equation (16) should be used to determine whether the area is sufficiently flat to act as a regular reflector.

If the land is flat from the antenna out to a distance  $d_1$  the relative intensity of the reflected ray is  $\frac{1}{2}$  when  $d_1 = h_1 \times \cot \gamma$ . This assumes the land beyond  $d_1$  to be nonreflecting and that the distant



boundary acts as a diffracting edge. As  $d_1$  increases further, the relative intensity increases to about 1.18 and then decreases again and oscillates about unity in gradually decreasing swings. This is accompanied by a variation of phase.

Several typical terrain problems will be solved in detail to illustrate the methods.

*Example 17. Limited Reflecting Area.* A 200-mc radar, Figure 64, with an antenna as described in

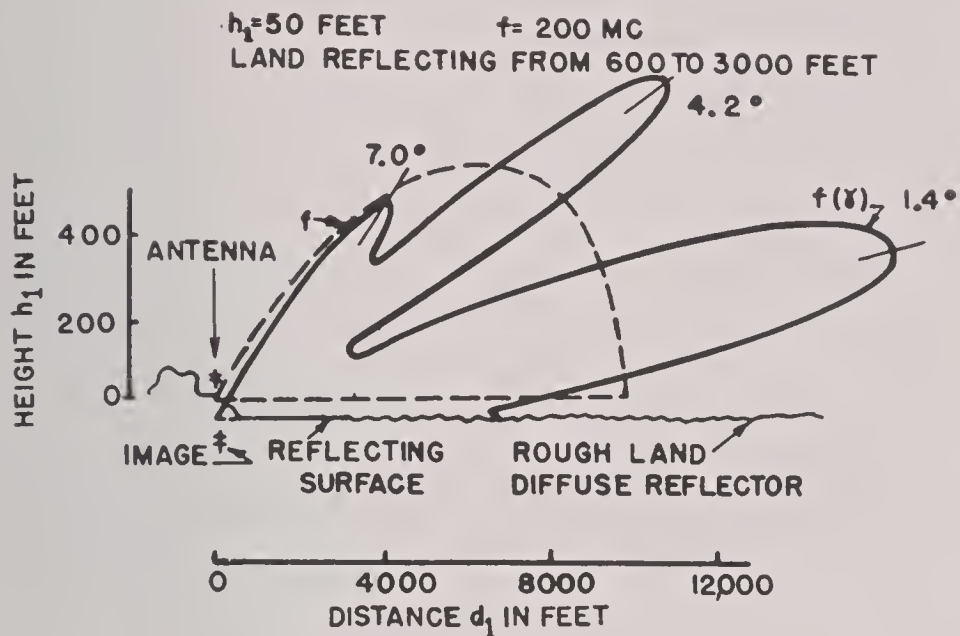


FIGURE 64. Lobes from a limited reflecting area.

Example 16, is 50 ft above a smooth reflecting surface (a lake) which extends from 600 to 3,000 ft. From 0 to 600 ft and from 3,000 ft on is rough land. The shore line diffraction method will be used to determine the effect of the reflection from the limited area upon the antenna pattern  $f_A$ . The vertical pattern is plotted from Figure 63 and shown dotted. To obtain the pattern for the reflected wave the shore at 600 ft is taken as a diffracting edge, and the relative intensity computed as a function of  $\gamma$  as though the surface from 600 ft on were a perfect reflector. This is then repeated using the shore at 3,000 ft. The difference between these two functions is then the effect of the area between 600 and 3,000 ft. From equation (83) for  $n = 1$

$$T_{600} = \frac{600 \times 4.92}{1 \times (50)^2} = 1.18; \quad T_{3,000} = 5.9;$$

$$v_{600} = \sqrt{\frac{1.18}{8} \times 1 - 1 + \frac{2}{1.18}} = 0.918;$$

$$v_{3,000} = 0.279.$$

From equation (78)

$$n_{600} = \frac{4 \times (50)^2}{600 \times 4.92} = 3.39; \quad n_{3,000} = 0.678.$$

From Figure 27, using the plus sign for  $v_{600}$  and the minus sign for  $v_{3,000}$ , is obtained the relative intensity

$$z_{600} = 1.073; \quad z_{3,000} = 0.375.$$

The reflection factor for  $n = 1$  is given by

$$z = 1.073 - 0.375 = 0.698.$$

From equation (57)

$$\gamma = \frac{1 \times 4.92}{4 \times 50} = 0.0246 \text{ radian} = 1.41^\circ.$$

Other values are given in Table 11.

TABLE 11. Limited reflecting area. (Example 17.)

$n$	$\gamma$	$v_{600}$	$v_{3,000}$	$z_{600}$	$z_{3,000}$	$z$	$f_T$	$f(\gamma)$
0	0	+1.30	+0.583	1.177	0.870	0.307	0.693	0.693
0.1	0.14	+1.26	+0.498	1.181	0.810	0.371	0.658	0.658
0.4	0.56	+1.15	+0.241	1.164	0.645	0.519	0.973	0.973
0.5	0.70	+1.11	+0.155	1.153	0.592	0.561	1.147	1.147
0.6	0.85	+1.071	+0.077	1.142	0.544	0.598	1.314	1.314
1.0	1.41	+0.918	-0.279	1.073	0.375	0.698	1.700	1.650
1.5	2.11	+0.727	-0.707	0.960	0.257	0.703	1.223	1.137
2.0	2.82	+0.535	-1.136	0.838	0.186	0.652	0.349	0.314
3.0	4.23	+0.155	-1.995	0.592	0.116	0.476	1.475	1.090
4.0	5.64	-0.237	-2.853	0.393	0.082	0.311	0.689	0.386
5.0	7.05	-0.619	-3.710	0.277	0.067	0.210	1.210	0.436

The values of  $z$  multiplied by  $f_A$  from Figure 63 are plotted in Figure 65 as the reflected pattern. The

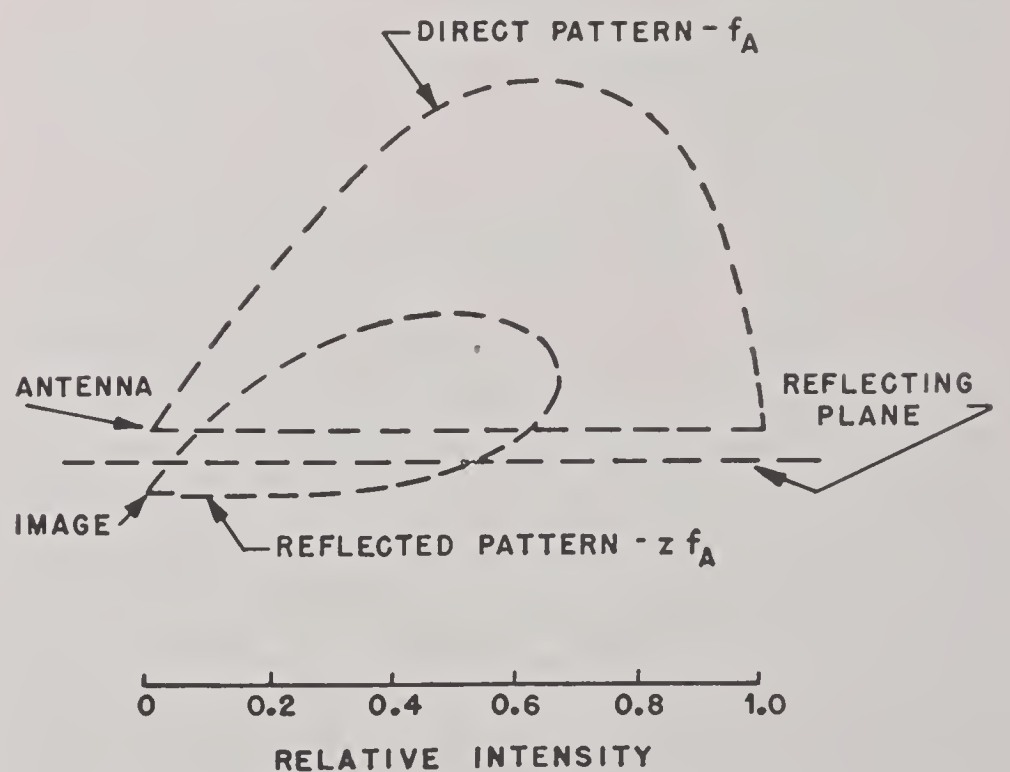


FIGURE 65. Components of the modified antenna for a limited reflecting area.

resultant of the two vectors,  $f_A$  and  $zf_A$ , in terms of  $n$  is given by the cosine law:

$$f_T = \sqrt{1 + z^2 - 2z \cos(n\pi)}. \quad (94)$$

Thus for  $n = 0.1$

$$f_T = \sqrt{1 + (0.371)^2 - 2 \times 0.371 \cos(0.1\pi)} = 0.658$$



The product of  $f_T$  and  $f_A$  is the modified antenna factor  $f(\gamma)$ . This is plotted in Figure 64. With a larger reflecting surface, the length of lobes would approach twice the value of  $f_A$ . Figures 64 and 65 were drawn for purposes of illustration and would not ordinarily be required.

*Example 18. Cliff Edge Diffraction.* A 200-mc radar, Figure 66, with an antenna as described in Example

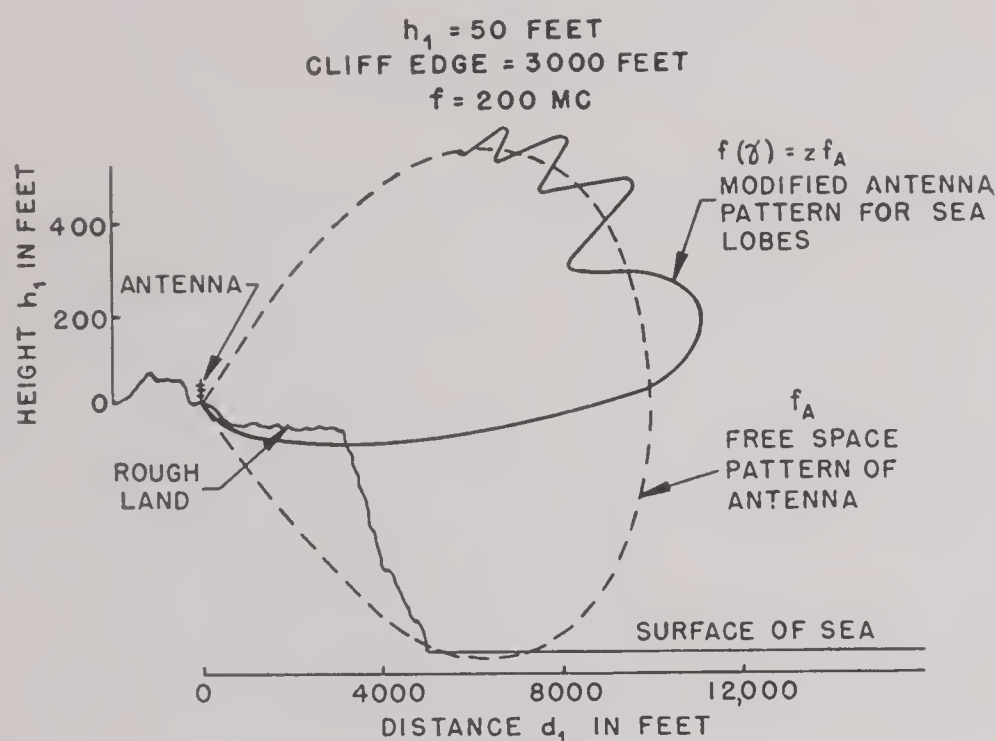


FIGURE 66. Cliff edge diffraction. (Example 18.)

16, is 50 ft above a rough land surface, the top of a cliff whose edge is 3,000 ft away.

The geometrical shadow line makes an angle with the horizontal of

$$\tan^{-1} \left( -\frac{50}{3,000} \right) = -0.955^\circ.$$

At this angle, the relative intensity,  $z = 0.5$ . Other values of  $z$  may be read from Figure 27 after converting the angle of diffraction to  $v$  by means of equation (47).

$$v = \frac{\theta_d^\circ}{\sqrt{\frac{4.92}{2 \times 3,000}} \times 57.3} = 0.61 \theta_d^\circ.$$

At  $0.377^\circ$  in the shadow region  $v = -0.377 \times 0.61 = -0.23$ . From Figure 27,  $z$  is 0.4. This angle, referred to the horizontal at the antenna, is

$$\gamma = \Phi - 0.955 = -1.332^\circ.$$

Some other values are:

$\gamma^\circ$	$z$
+3.535	0.917
+1.060	1.18
-0.955	0.50
-8.335	0.05

The modified antenna pattern  $f(\gamma)$  is the product of  $z$  and  $f_A$  and is plotted in Figure 66. This pattern gives the factors for both the direct and reflected waves for the sea lobes.

*Example 19. Land Reflection and Diffraction.* This site is similar to that of Example 18 except that the cliff top is smooth. This is shown in Figure 67.

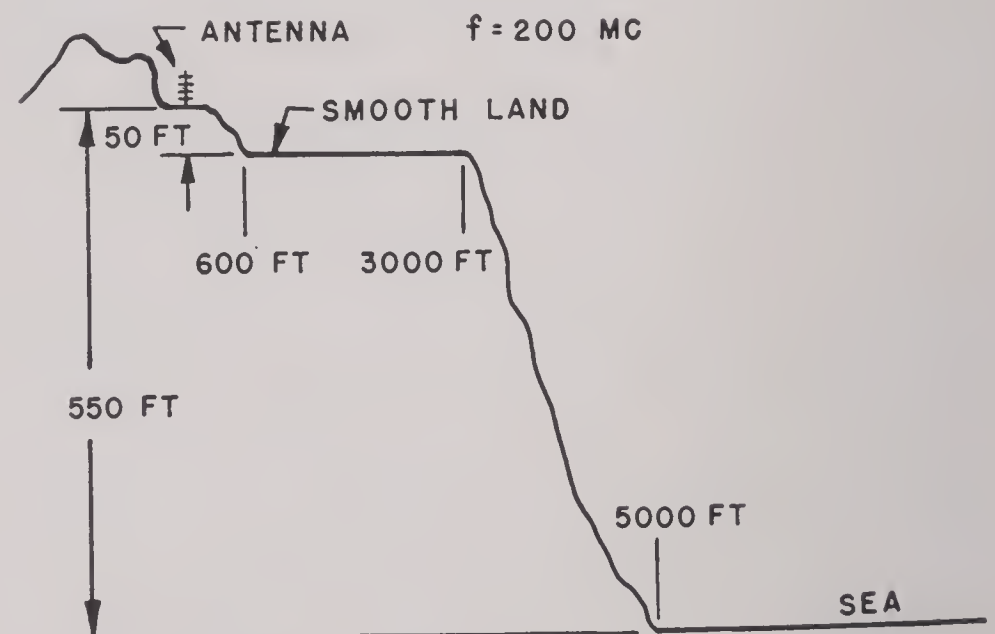


FIGURE 67. Land reflection and diffraction. (Example 19.)

The smooth land causes land lobes to be formed as in Example 17 which furnish high angle coverage. The sea lobes are computed using the method of Example 18 for the direct and reflected rays. If the cliff top were tilted down, the land lobes would be tilted by the angle of the land. Speculation about complex sites yields many unusual patterns, but in practice the results are usually disappointing. Complex sites seldom have horizontal symmetry, and gaps in the coverage pattern may be expected. Attempts to reinforce the pattern in a particular direction by siting back from the cliff edge generally cause poor coverage at other angles. Best all-round CHL operation results from siting on cliff edges and exclusive use of the sea as a reflector.

#### 15.6.15

### Earth Curvature Effect on Lobe Lengths

The effect of earth curvature on lobe angles was described in Section 15.6.4. The angles to be used with the modified antenna pattern of the image antenna are affected by earth curvature, and therefore the strength of the reflected wave is also affected. In Figure 68 is shown a radar antenna at height  $h_1$  above the earth's surface, with the center line of the antenna pattern parallel to  $GH$ , the horizontal at



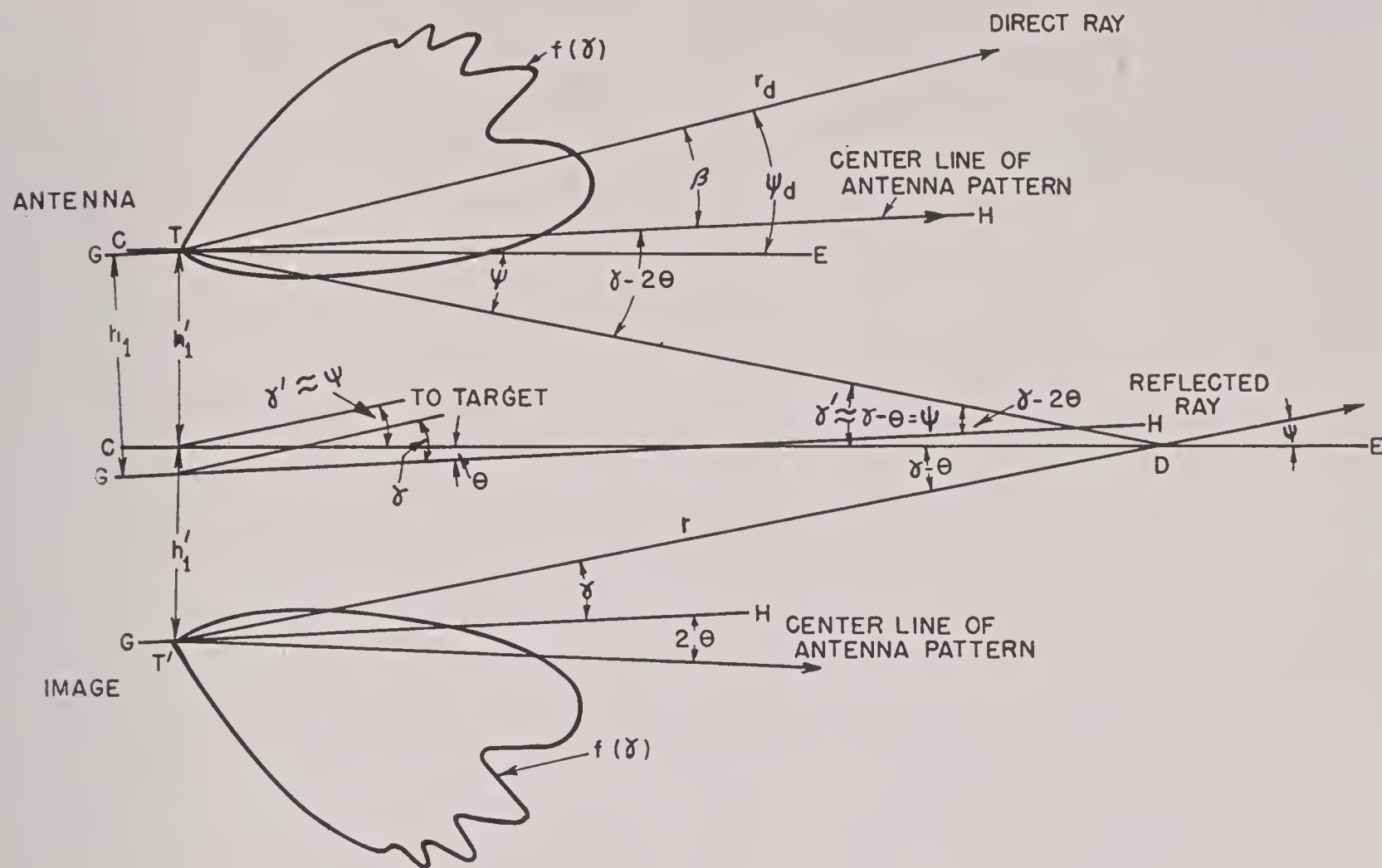


FIGURE 68. Earth curvature effect on direct and image patterns. Note:  $GH$  horizontal at the antenna;  $CE$  horizontal at the reflection point  $\theta = \frac{d_1}{ka}$

the base of the antenna. Because of diffraction at a cliff edge the modified antenna pattern  $f(\gamma)$  is unsymmetrical as in Example 18. The lines  $GH$  are parallel to the horizontal at the antenna. The line  $CE$  is horizontal at the reflection point and makes an angle  $\theta$  with  $GH$ . The target is at an angle  $\gamma$  with respect to  $GH$ . The incident and reflected rays make the angle  $\gamma - \theta$  with  $CE$ . It will be noted that the direct ray makes the angle  $\gamma \approx \beta$  with the centerline of the antenna pattern, and the reflected ray makes the angle  $\gamma - 2\theta$ .

15.6.16

### Coefficient of Reflection

The coefficient of reflection of the reflecting surface is in general complex. That is, both the magnitude and phase of the reflected wave are affected. The reflection coefficient varies with the conductivity and dielectric constant of the reflector and with the frequency, polarization, and angle of incidence. Careful consideration should be given to the roughness of the surface, and a substantial reduction in the coefficient should be made when the height of roughness is comparable to that computed from equation (16). In general the reflection obtained with microwaves is of minor importance.

The magnitude and phase angle of the reflection

coefficient are plotted as functions of the angle of reflection,  $\Psi$  in Figures 69 and 70. Curves are given for horizontal and vertical polarization and for the extreme conditions of sea water and dry soil. For dry soil the reflection coefficient is not sensitive to frequency changes, and the 100-mc curve may also be used for 3,000 mc.

For most purposes the reflection coefficient for horizontal polarization may be taken as unity, and the phase angle as  $180^\circ$ . The use of these values simplifies computations.

The coefficients of reflection and phase angle for vertical polarization vary rapidly with frequency and angle of reflection for sea water and more gradually for dry land. The minimum point of the curves in Figure 69 is known as the pseudo-Brewster angle corresponding to a similar angle in optics.

Cases not covered by Figures 69 and 70 may be computed from the following equations.

*Vertical Polarization:*

$$\rho \exp(-j\phi) = \frac{\epsilon_c \sin \Psi - \sqrt{\epsilon_c - \cos^2 \Psi}}{\epsilon_c \sin \Psi + \sqrt{\epsilon_c - \cos^2 \Psi}}, \quad (95)$$

*Horizontal Polarization:*

$$\rho \exp(-j\phi) = -\frac{\sqrt{\epsilon_c - \cos^2 \Psi} - \sin \Psi}{\sqrt{\epsilon_c - \cos^2 \Psi} + \sin \Psi}, \quad (96)$$



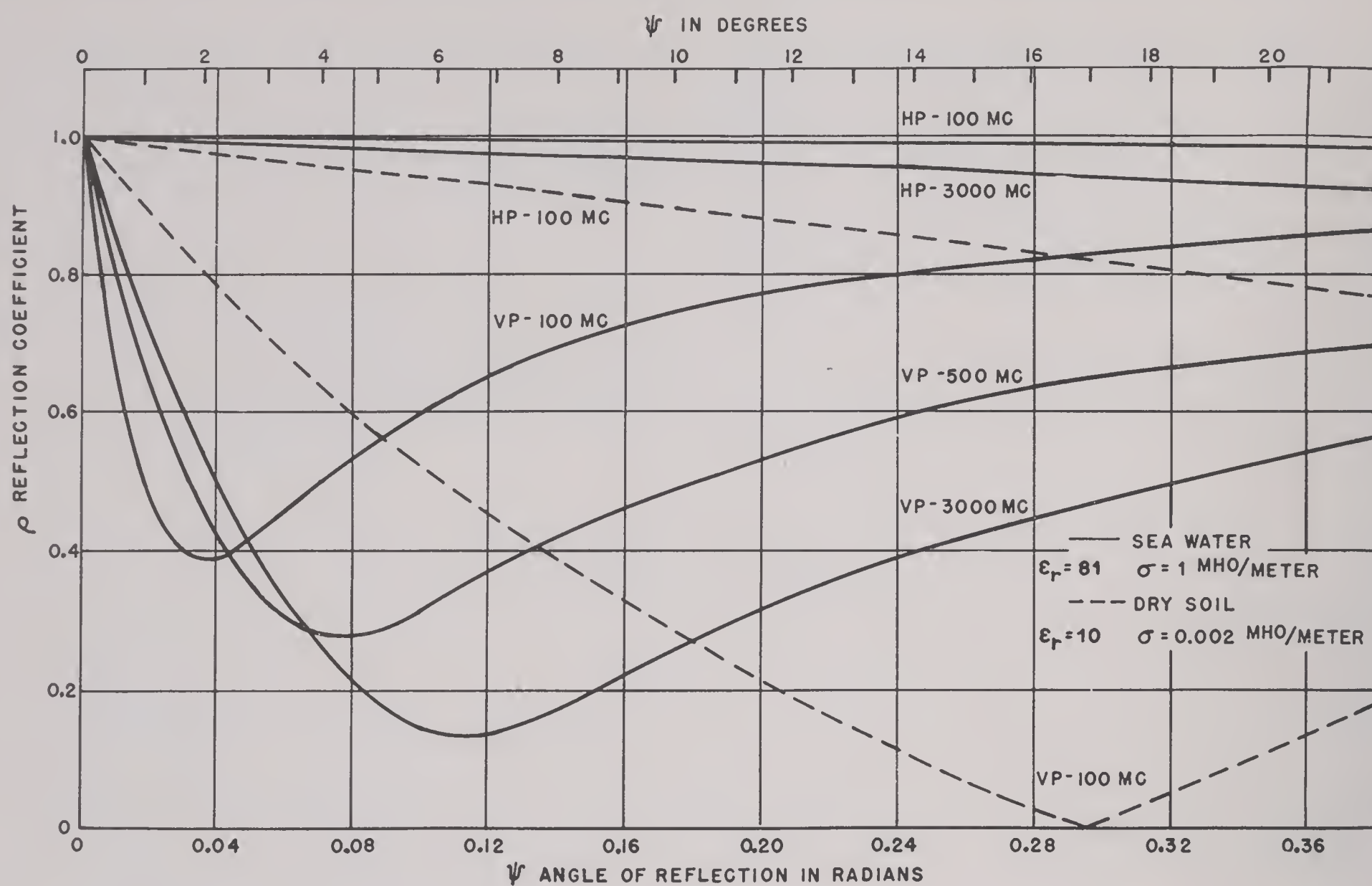


FIGURE 69. Reflecting coefficient curves.

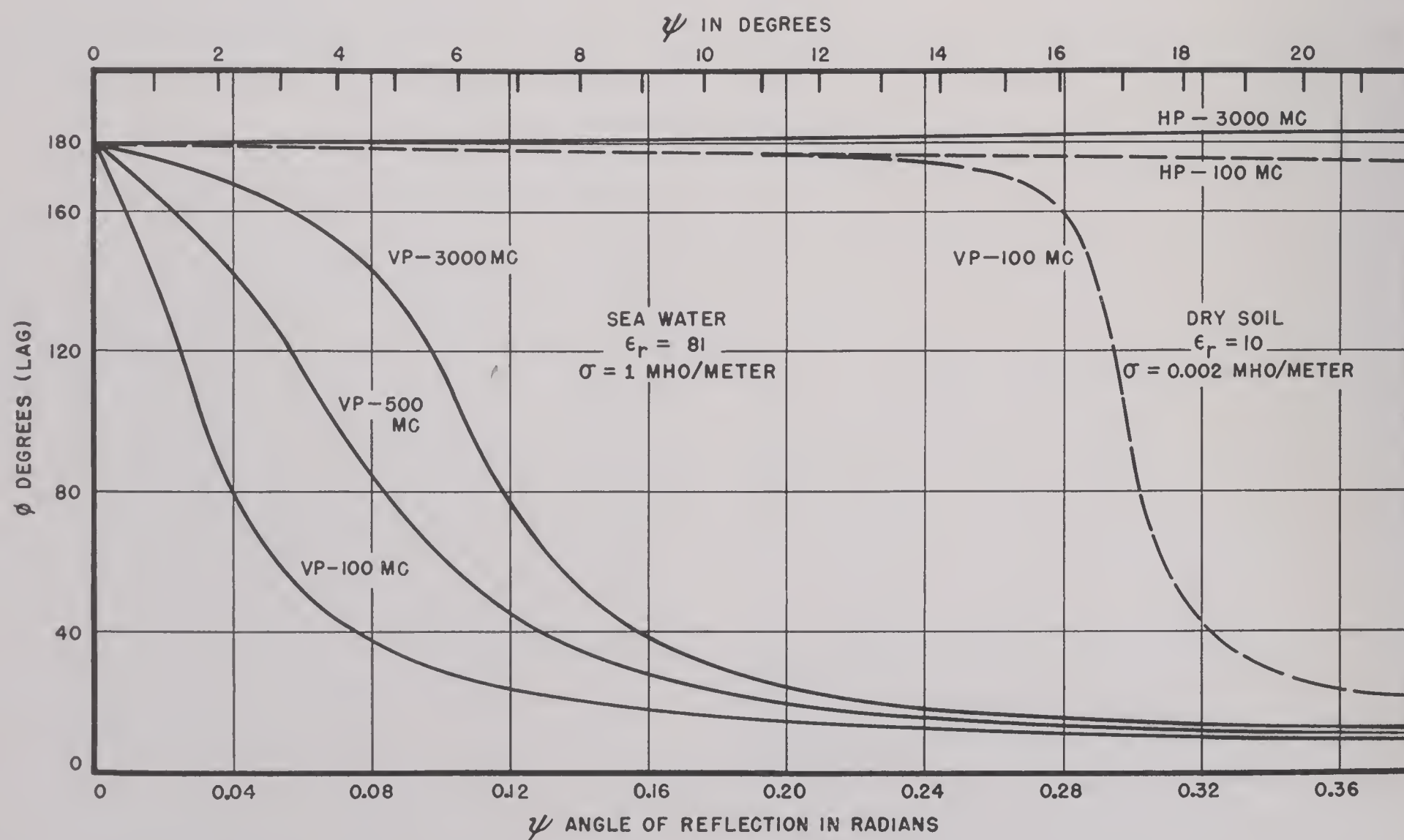


FIGURE 70. Phase of reflection coefficient curves. Note: Solid curve represents seawater. Dotted curve represents dry soil.



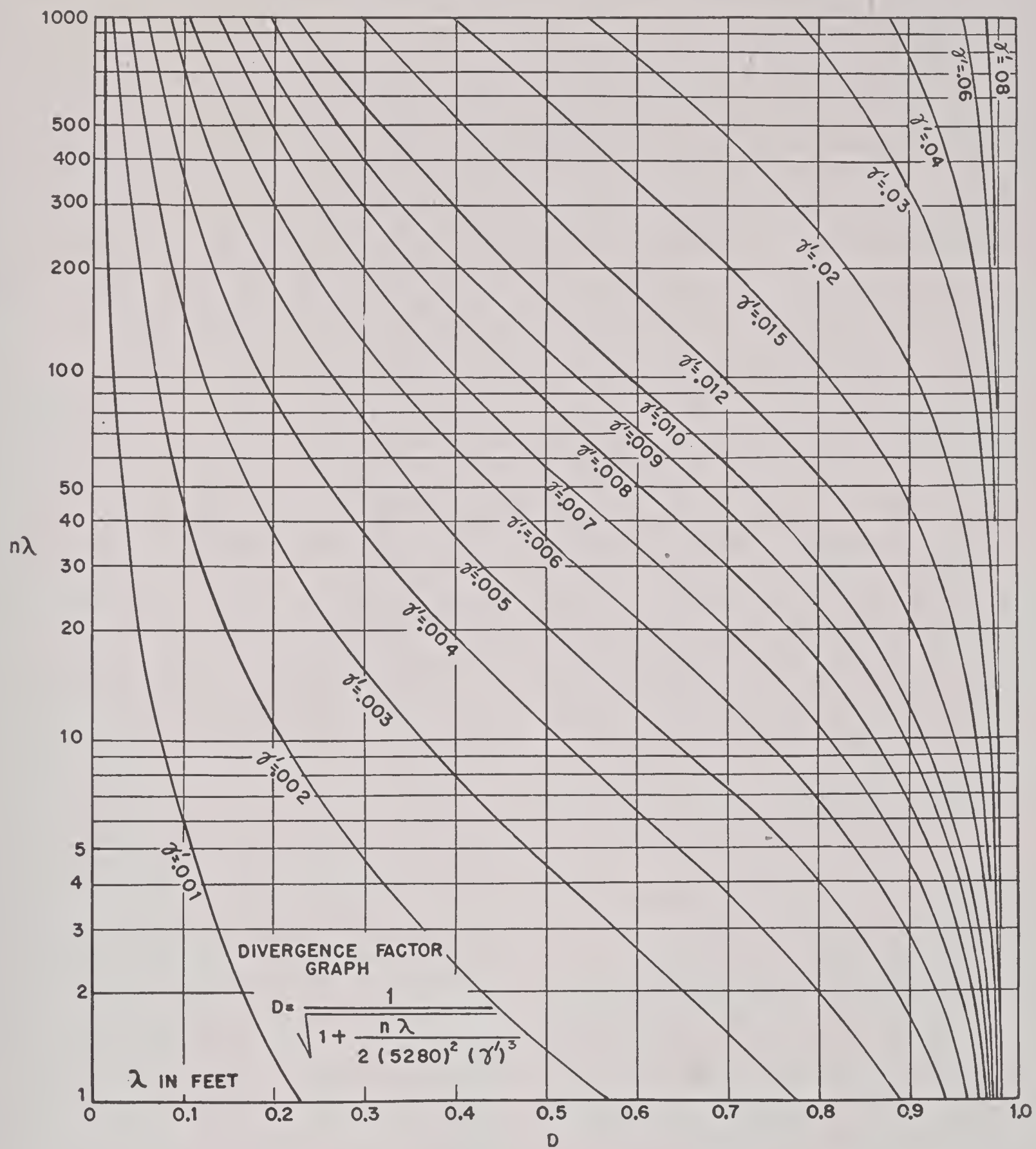


FIGURE 71. Divergence factor graph.

where  $\Psi$  = the angle of reflection measured from the horizontal;

$\epsilon_c = \epsilon_r - j60\sigma\lambda$ ;

$\epsilon_r$  = dielectric constant of the reflector relative to air;

$\sigma$  = conductivity of the reflector, mhos per meter;

$\lambda$  = wavelength, in meters;

$\phi$  = phase angle, lagging.

Some typical ground constants are given in Table 12.

TABLE 12. Terrain reflection characteristics.

Type of terrain	$\epsilon_r$	$\sigma$ , mhos per meter
Fresh water	81	$10^{-3}$
Sea water	81	1
Rich soil	20	$3 \times 10^{-2}$
Heavy clay	13	$4 \times 10^{-3}$
Rocky soil	14	$2 \times 10^{-3}$
Sandy dry soil	10	$2 \times 10^{-3}$
City—industrial area	5	$10^{-3}$



15.6.17

### Divergence

The reflected wave is scattered somewhat by being reflected from the spherical surface of the earth instead of a plane surface, and this reduction of field strength is taken into account by the divergence factor. This is dependent on geometrical considerations and may be expressed as follows (for  $\gamma' < 3^\circ$ ):

$$D = \frac{1}{\sqrt{1 + \frac{n\lambda}{2(5,280)^2 (\gamma')^3}}}, \quad (97)$$

where  $n$  is the lobe number,

$\lambda$  is the wavelength, in feet,

$\gamma'$  is the reflection angle, in radians, obtained from equation 60.

A convenient chart for obtaining  $D$  is given in Figure 71. The parameters are  $\gamma'$  in radians and  $n\lambda$ , with  $\lambda$  expressed in feet.

As  $\gamma'$  approaches zero,  $n$  also approaches zero, and the equation is indeterminate. At the point of tangency of the line of sight and the earth,  $D$  is 0.5773. At low angles the field is modified by diffraction around the curved earth. The lower limit of the angle  $\gamma'$  for which the optical treatment is valid is usually given by

$$\gamma' > \sqrt[3]{\frac{\lambda}{2\pi ka}} > 0.00382 \sqrt[3]{\lambda}, \quad (98)$$

where  $k$  is  $\frac{4}{3}$  and  $\lambda$  is in feet.

For angles below this limit the theory for diffraction of radio waves around the earth is required for a rigorous solution. *However, in practice it is found that angles as low as the first maximum ( $n = 1$ ) may be treated by the ray theory with little error.*

Applying equation (98) to Example 11

$$\gamma' > 0.00382 \sqrt[3]{4.92} = 0.0065 \text{ radian.}$$

In Table 6 this corresponds to  $n = 2.25$ . However using  $n = 1$  and  $\gamma' = 0.0036$  the divergence factor  $D$  is found from Figure 71 to be 0.58. For angles below  $\gamma' = 0.0036$  it is necessary to estimate  $D$ . Experience indicates that a fair minimum value to select for  $D$  is 0.5773. For angles much below the first maximum, the optical treatment gives values of field strength which are too low because it neglects diffraction. This may be compensated in part by using values of  $D$  between 0.5773 and 1.0.

15.6.18

### Lobe Lengths

The contributions of the direct and reflected waves may now be added to obtain the length of the lobes.

$$L = [f(\gamma) \pm f(\gamma - 2\theta) z \rho D] d_0 \quad (99)$$

where  $L$  is the distance to the end of the lobes or the nulls, in miles.  $d_0$  is the maximum range (in miles) at which a given response (usually the minimum detectable signal) would be obtained if the antenna were in free space. If the lobe diagram were plotted for some signal level above the minimum detectable,  $d_0$  and  $L$  would be correspondingly smaller.

*Example 20. Lobes for a Medium Height Radar.* A 200-mc radar using horizontal polarization has an antenna composed of two groups of dipoles spaced three wavelengths between centers, each group having four dipoles spaced  $\lambda/2$ , as in Example 16. The antenna is 500 ft high and 3 miles inland as in Examples 11 and 15. It is desired to compute the vertical coverage pattern.

From previous tests on this type of equipment it is known that the maximum range that would be obtained in free space  $d_0$  is 80 miles. Since the polarization is horizontal,  $\rho$  will be taken as unity. Precision is not required for most of this kind of work, and it will suffice to compute values for equation (99) at each integral value of  $n$  and to consider the values for odd  $n$ 's (with the plus sign) as the average of the lobe. The lobe shape will be taken as sinusoidal and the range at the nulls obtained by using even values of  $n$  and the minus sign;  $f(\gamma)$  and  $f(\gamma - 2\theta)$  are obtained from Figure 63, by using values of  $\gamma$  and  $\gamma - 2\theta$  from Example 11 corresponding to integral values of  $n$ . The values of  $z$  are obtained from Example 15. The computations are shown in Table 13. Had cliff edge diffraction been involved  $f(\gamma)$  and  $f(\gamma - 2\theta)$  would be read from curves as in Example 18 with marked effects on the pattern.

The lobes are plotted in Figure 46 using equation (74) and the value of  $L$  for odd numbered  $n$ 's. For intermediate values of  $n$  the factors are:

Fractional value of $n$	$\sin(90^\circ n)$
0.33	0.500
0.50	0.707
0.70	0.891

Using these three points above and below the lobe line and the maximum and minimum values from Table 13 the lobes may be plotted quickly as explained in Example 14.



TABLE 13. Lobes for a medium-height radar. (Example 20.)

$n$	$f(\gamma)$	$f(\gamma - 2\theta)$	$z$	$D$	$f(\gamma - 2\theta) \times \rho z D$	$f(\gamma) \pm f(\gamma - 2\theta) \rho z D$	$L$
0	0.999	0.999	1.036	0.577	-0.597	0.402	32.2
1	1.000	0.998	1.083	0.580	+0.627	1.627	130.2
2	0.999	0.997	0.980	0.735	-0.718	0.281	22.5
3	0.999	0.994	0.884	0.823	+0.723	1.722	137.8
4	0.997	0.992	0.938	0.890	-0.828	0.169	13.5
5	0.992	0.989	1.082	0.912	+0.976	1.968	157.4
6	0.989	0.987	1.170	0.933	-1.077	0.088	7.0
7	0.985	0.981	1.156	0.942	+1.068	2.053	164.3
8	0.980	0.978	1.073	0.959	-1.006	0.026	2.1
9	0.975	0.972	0.953	0.963	+0.892	1.867	149.4
10	0.970	0.967	0.825	0.968	-0.772	0.198	15.8
11	0.963	0.961	0.696	0.973	+0.651	1.614	129.1
12	0.958	0.952	0.582	0.979	-0.542	0.416	33.3
13	0.950	0.947	0.459	0.981	+0.426	1.376	110.0
14	0.941	0.939	0.377	0.984	-0.348	0.593	47.4
15	0.932	0.929	0.308	0.987	+0.282	1.214	97.2
16	0.923	0.920	0.261	0.989	-0.237	0.686	54.9
17	0.913	0.910	0.223	0.991	+0.201	1.114	89.1
18	0.903	0.900	0.192	0.992	-0.171	0.732	58.6
19	0.893	0.890	0.170	0.992	+0.150	1.043	83.5
20	0.881	0.879	0.150	0.992	-0.131	0.750	60.0
21	0.871	0.869	0.135	0.992	+0.116	0.987	79.0
22	0.857	0.853	0.121	0.992	-0.102	0.755	60.4
23	0.844	0.841	0.111	0.992	+0.093	0.937	75.0

15.6.19

## The General Lobe Formula

The assumption of a sinusoidal lobe shape and the neglect of the phase of reflection and diffraction in the preceding section may in some cases lead to considerable error, especially when the direct and reflected waves are very different in strength. In general a more accurate method is required for sites over 1,000 ft in height, where vertical polarization is used or where it is desired to know the lobe shape in detail. The method given in this section provides a general solution of the coverage problem in the optical region (except along the bottom of the first lobe).

The development of the lobe formula will be reviewed, and equation (99) will be given in a somewhat different form. The expression for the electric vector due to the direct wave is

$$E_d = \frac{E_1}{r_d} f(\gamma) \exp \left( -j2\pi \frac{r_d}{\lambda} \right). \quad (100)$$

For the reflected wave

$$E_r = \frac{E_1}{r} f(\gamma - 2\theta) R \exp \left( -j2\pi \frac{r}{\lambda} \right), \quad (101)$$

where  $E_d$  = electric field intensity at the target due to the direct wave, microvolts per meter;

$E_r$  = electric field intensity at the target due to the reflected wave, microvolts per meter;

$E_1$  = electric field intensity at 1 mile in the equatorial plane of the antenna, microvolts per meter;

$f(\gamma)$  = modified antenna factor for the direct wave (Section 15.6.12);

$f(\gamma - 2\theta)$  = modified antenna factor for the reflected wave (Section 15.6.15);

$R$  = a complex factor for the reflected wave given by

$$R = D \rho z \{ \exp[-j(\phi + \zeta)] \}; \quad (102)$$

where  $D$  = divergence factor (Section 15.6.17);

$\rho \exp(-j\phi)$  = complex reflection factor (Section 15.6.16);

$z \exp(-j\zeta)$  = complex diffraction factor (Section 15.6.11).

The net field at the target is

$$E_T = E_d + E_r,$$

$$\left| E_T \right| = \frac{E_1}{d} \left| f(\gamma) + f(\gamma - 2\theta) \right|$$

$$D \rho z \{ \exp[-j(\phi + \zeta + \delta)] \} \left| \right|, \quad (103)$$

considering only the absolute value of  $E_T$  and taking  $r = r_d = d$  except where the path difference is involved. The path difference phase shift is

$$\delta = \frac{2\pi}{\lambda} (r - r_d). \quad (104)$$

Equation (103) may for convenience be written

$$\left| E_T \right| = \frac{E_1}{d} A. \quad (105)$$

The target is assumed to have a complicated form and to be changing its aspect constantly. The reflected energy is considered to be of random phase and magnitude. The magnitude of the reradiated field (microvolts per meter at a distance of 1 mile from the target) is found by using a coefficient of reradiation,  $\rho_T$ , which varies with the target and aspect.

The received field intensity is by the reciprocity theorem:

$$\left| E \right| = \frac{\rho_T \left| E_T \right|}{d} A. \quad (106)$$

Substituting from equation (105)

$$\left| E \right| = \frac{\rho_T E_1}{d^2} A^2.$$



For a particular coverage contour, such as the threshold of detection, usually taken as a signal-to-noise ratio of unity, a minimum received field intensity  $|E_N|$  may be assumed. This is related to receiver noise voltages, antenna gain, and other factors of design. Using  $|E_N|$  for  $|E|$  and solving for  $d$

$$d = \sqrt{\frac{\rho_T |E_1|}{|E_N|}} A = d_0 A. \quad (107)$$

Because of the way in which  $E_1$  and  $\rho_T$  are defined,  $d_0$ , the maximum free space range, has the dimensions of length (in miles). It depends on the design of the transmitter and receiver and on the target.  $A$  may be considered a coverage factor which depends on  $\gamma$  and terrain effects.

Because of the implicit character of the parameters of  $A$  in equation (103), a general solution of  $A$  as a function of  $\gamma$  is not feasible. However, examination of typical problems discloses that the range of variation of some of the factors is limited, and a method of successive approximations may be readily applied.

In most cases  $\phi$  and  $\zeta$  will vary slowly (about  $\frac{1}{20}$  as fast) compared to  $\delta$  below  $2^\circ$  or  $3^\circ$ . At higher angles the rate of change may be faster, but contribution of the reflected wave at these angles is likely to be unimportant.

The method described here consists in computing the lobe angles, diffraction, and divergence as though the only phase shift involved was that due to path difference as in Sections 15.6.4, 15.6.11 and 15.6.17. The phase shifts from the apparent lobe angles thus computed are then determined. The diffraction phase shift is  $\zeta$ , and the reflection phase shift is

$$\phi' = \phi - 180^\circ, \quad (108)$$

where  $\phi$  is obtained from Figure 70. If horizontal polarization is used  $\phi$  may be taken as  $180^\circ$ , and  $\phi'$  is then zero. With curves of the phase shift  $\phi' + \zeta$  and the product  $f(\gamma - 2\theta)D\rho z$  plotted against  $\gamma$  the apparent lobe angles and lengths computed above may be corrected to obtain the actual values. The details of this method will be given in the example below.

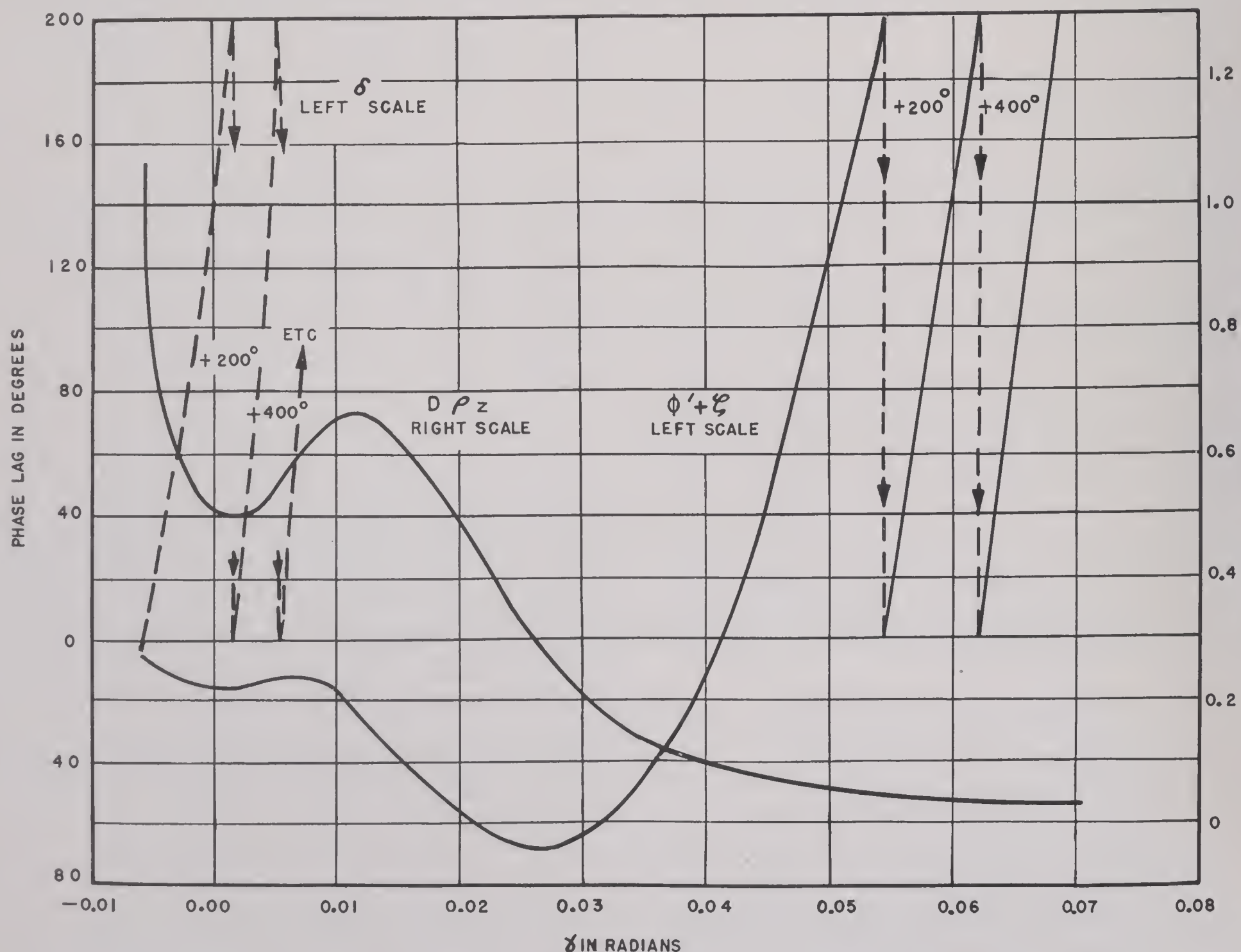


FIGURE 72. Relative magnitude and phase of the reflected ray.



*Example 21. The General Lobe Formula.* An interrogator equipment is used with the radar of Example 20. It operates on 160 mc; the height of the antenna above the sea is 500 ft; and the distance to the shore is 15,840 ft. The intervening land is too rough for coherent reflection. The antenna consists of two vertical radiating elements and parasitic reflectors. The radiators are approximately a half wavelength long and spaced a half wavelength apart. The maximum distance at which reliable interrogation may be obtained in the absence of a reflecting surface has been found to be 110 miles for this particular equipment. It is desired to construct for this site the vertical coverage diagram of the interrogator system.

The vertical pattern of a vertical half-wave dipole is given by

$$f_A = \frac{\cos\left(\frac{\pi}{2} \sin \gamma\right)}{\cos \gamma}$$

Since this factor is over 0.98 for angles up to 10 degrees,  $f(\gamma)$  and  $f(\gamma - 2\theta)$  will be taken as unity. The lobe angles are then computed neglecting  $\phi$  and  $\zeta$ , as in Example 11. Diffraction and divergence are computed as in Example 15 and Section 15.6.17. The results of these calculations are listed in Table 14.

The values of  $\rho$  and  $\phi$  depend on  $\gamma'$  and are read from Figures 69 and 70. Using equation (108),  $\phi'$  is obtained and added to  $\zeta$ . The sum  $\phi' + \zeta$  is the net phase shift of the reflected wave from the values used in computing the lobe angles and is plotted against  $\gamma$  in Figure 72. For purposes of comparison  $\delta$  has also been plotted, but this curve is not required otherwise. The product  $D\rho z$  is the relative strength of the reflected ray and is plotted in Figure 72.

The points on the coverage diagram are obtained in polar form from equation (107).

$$d = 110\sqrt{1 + (D\rho z)^2 - 2D\rho z \cos(\phi' + \zeta + \delta)}.$$

The vector representing the reflected wave is shifted in the lagging direction by  $\phi' + \zeta$  degrees when this sum is positive, and in the leading direction when the sum is negative. The effect of this phase shift on the point on the lobe being considered may be determined by inspection of Figure 72.

Thus, to determine the first maximum point the following procedure may be used. At  $n = 1$  the angle  $\gamma$  is 0.0011 radian and  $\phi' + \zeta$  is  $-14.8$  degrees. This means that for the cosine term to be  $-1$  the path difference must be increased until  $\delta$  is 194.8 degrees. The angle  $\gamma_d$  at which this value of  $\delta$  occurs

is found by interpolating between 0.00110 and 0.00492 since  $\delta$  changes from  $180^\circ$  to  $360^\circ$  in this interval. This angle is then 0.00141 radian. Had the angle  $\phi' + \zeta$  changed appreciably from 0.00110 to 0.00141 the interpolation would be repeated using the new value of  $\phi' + \zeta$ . In most cases the new value of  $\phi' + \zeta$  may be estimated from the curve, and the first approximation will be close enough.

TABLE 14. The general lobe formula. (Example 21.)

$n$	$\gamma'$ radians	$\gamma$ radians	$z$	$\zeta^\circ$	$D$	$\gamma_d$ radians	$d$	
0	0	-.00600	1.061	-	2.86	1.000	-.00589	0
1	.00421	+.00110	0.920	-	5.27	0.640	+.00141	165.0
2	.00712	.00492	0.897	+	3.04	0.792	.00527	48.5
3	.01000	.00835	1.039	+	7.56	0.862	.00858	180.5
4	.01295	.01163	1.158	+	2.75	0.908	.01206	36.3
5	.01595	.01485	1.158	-	5.04	0.938	.01557	178.5
6	.01897	.01802	1.067	-	10.88	0.955	.01894	52.7
7	.02200	.02119	0.930	-	15.00	0.963	.02225	155.6
8	.02500	.02428	0.779	-	15.00	0.969	.02544	66.5
9	.02810	.02744	0.648	-	11.00	0.973	.02860	137.0
10	.03110	.03051	0.500		0.00	0.982	.03161	89.1
11	.03420	.03365	0.408	+	17.18	0.984	.03453	126.4
12	.03720	.03669	0.332	+	43.0	0.987	.03731	96.6
13	.04050	.04005	0.267	+	74.4	0.991	.04024	120.6
14	.04330	.04288	0.222	+	108.9	0.991	.04253	100.7
15	.04640	.04600	0.190	+	154.6	0.992	.04493	117.7
16	.04950	.04912	0.165	+	206.2	0.993	.04894	103.0
17	.05250	.05216	0.143	+	263.3	0.993	.05010	116.5
18	.05560	.05528	0.129	+	326.2	0.994	.05264	104.0
19	.05870	.05840	0.114	+	412.3	0.995	.05479	115.6
20	.06170	.06142	0.104	+	492.6	0.997	.05694	104.5
21	.06480	.06454	0.094	+	590.0	0.998	.05909	114.6
22	.06780	.06755	0.089	+	687.0	0.998	.06127	105.6
23	.07090	.07067	0.081	+	813.0	0.998	.06436	114.2

At 0.00141 radian  $D\rho z$  is 0.501. Substituting this value:

$$d = 110\sqrt{1 + (0.501)^2 - 2 \times 0.501 \times (-1)} \\ = 165.0 \text{ miles,}$$

which is laid off on the coverage diagram at an angle of 0.00141 radian. As many other points as required to sketch the diagram may be computed in a similar fashion. For an intermediate point it is convenient to use the net angle equal to  $90^\circ$  since the equation then reduces to

$$d = 110\sqrt{1 + (D\rho z)^2}.$$

The angles of the lobes have been listed in Table 14 under  $\gamma_d$  and the lobe lengths under  $d$ .

The vertical coverage diagram is shown in Figure 73. The lobe maxima and minima and the 90-degree points have been sufficient for sketching the lobes except on the first lobe where a few additional points have been computed. When the net angle is 60 degrees, the field strength at the bottom of the first



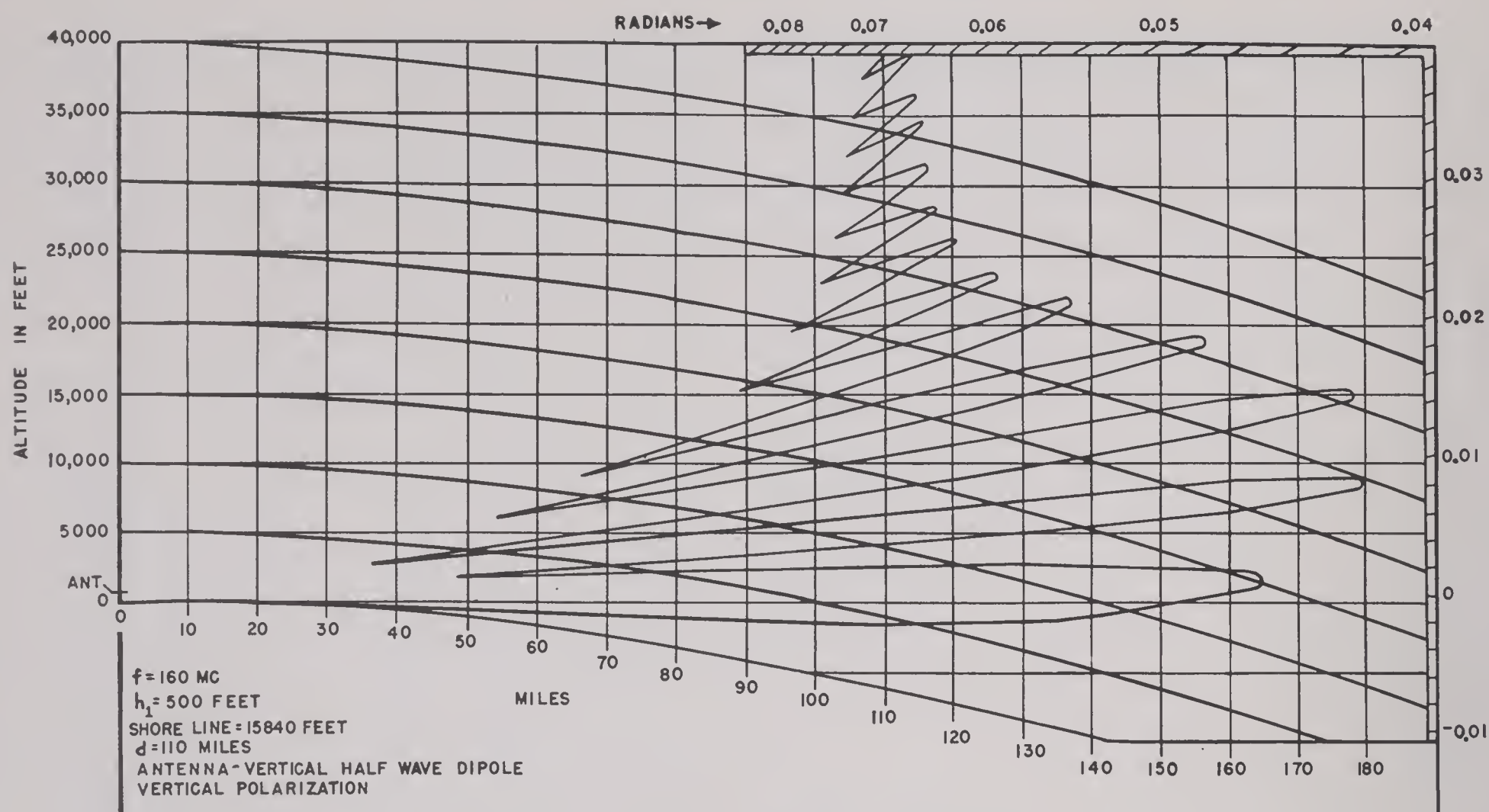


FIGURE 73. Coverage diagram for Example 21.

lobe is equal to the free space field. At ranges shorter than this the reflected wave opposes the direct wave. Directly under the antenna the contour passes near the surface so that the waves are very nearly in opposition. Because of the variation in  $D\rho z$  with  $\gamma$  the maxima will not occur exactly when the cosine is unity, but this effect is generally negligible.

## 15.7 CALIBRATION AND TESTING

### 15.7.1 Introduction

It should not be inferred from Section 15.6 that a reliable coverage diagram can be obtained by calculation alone. Under field conditions it is necessary to make test flights and other checks before equipment can be depended upon to meet a calculated performance. On the other hand it is seldom possible or desirable to obtain a satisfactory coverage diagram from tests alone. Best results are attained when tests and analysis supplement each other.

Test flights are arduous, expensive in personnel and materials, and time consuming. In most theaters a number of agencies become involved, and careful planning and organization are required to achieve a useful result. For these reasons the amount of test flying should be held to a minimum by intensive analysis and equipment tests before and after the test flights. "Calibration and testing" might well be

a book in itself, but only a very brief discussion will be given here for the sake of completeness.

### 15.7.2

## Equipment Tests

It is difficult to overemphasize the importance of proper equipment maintenance. An unfortunate tendency of inexperienced personnel is to maintain on an emergency basis, rather than as a matter of systematic routine. In most cases the need is for a careful check of all elements and restoration to as-good-as-new condition, rather than a brilliant intuitive process known as "trouble shooting." One survey of a large number of systems disclosed an average reduction from optimum performance of 13.5 db. This corresponds to a maximum range of 50 per cent of normal. Careful tests have shown the use of "standard targets" to be very misleading in many cases. Large changes in the maximum ranges of small targets were found without appreciable changes in the strength of the permanent echoes used for checking purposes.

Full use of test instruments available should be made in checking the equipment. Orientation should be completed and the accuracy of range and azimuth indicators checked. Tuning and modifications should be done before the test flights are made, unless the tests indicate poor performance. A great handicap



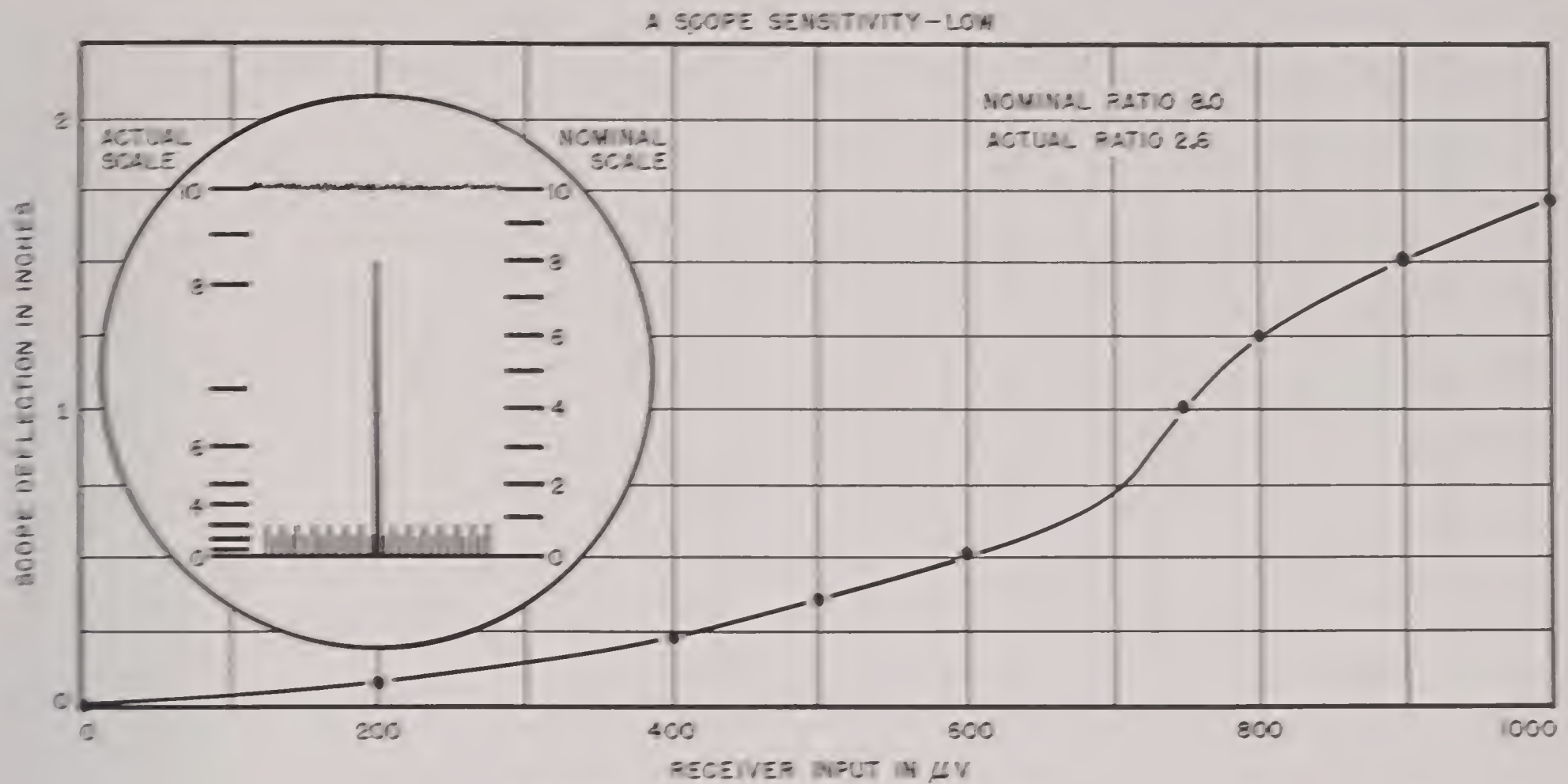


FIGURE 74. Typical receiver characteristics.

in this work is the lack of absolute measures of power output, but much may be done with echo boxes and field intensity meters. Reference is made to service publications and instruction manuals for further details.

#### 147.3

### Signal Measurements

Several methods are used for recording signal strength, and these determine the type of receiver calibration required. Estimation of signal-to-noise ratios by means of scales on the face of the scope requires some means of specifying the gain setting. The means used, such as height of noise, position of gain dial, and so forth, should be calibrated with a signal generator so that there is an assurance of adequate sensitivity and a way of checking the measurements. The saturation line on the scope is assigned a height of 10, and the signal and noise heights are read in proportion. Ratios in excess of 10 are usually read as 10+. This method requires considerable skill on the operator's part and is limited in scope. In Figure 74 is shown a calibration curve on a typical "square law" receiver. In the circle is represented a signal on an A scope which would commonly be read as a signal-to-noise [S/N] ratio of 8. Actually the ratio of receiver inputs corresponding to the signal and noise heights is 8.5/3.25 or 2.6.

A considerable improvement over the above method may be obtained as follows. An index line is drawn on the face of the A scope about an inch

from the baseline. To measure a signal it is brought to the index line by adjustment of the gain control, and the gain control voltage is recorded. The gain voltage required to bring the noise to the index line is also noted occasionally during the test. A calibration curve is made using a pip signal generator or a modulated signal generator connected to the receiver input. The gain voltage required to bring the signal to the index line is measured for various inputs. Gain voltage readings on the test target and noise are converted by means of the curve to equivalent input voltages. Test data may be conveniently plotted as decibels above noise after this conversion. It should be noted that the calibration depends upon the type and percentage of modulation.

A third method involves calibration of the gain control dial by comparison of permanent echoes. Three lines are drawn on the scope face such as  $\frac{1}{2}$ , 1, and  $1\frac{1}{2}$  in. from the baseline. The position of the gain dial with the noise at  $\frac{1}{2}$  in. is marked 0 db. A permanent echo is selected which comes to the 1-in. line at this setting. The gain dial is then turned to bring this echo to the  $\frac{1}{2}$ -in. mark, and this position of the dial is marked 6 db. Another echo is then selected which is 1 in. high, and it is brought down to  $\frac{1}{2}$  in. by further adjustment of the gain dial. This position is marked 12 db. In this manner the gain dial may be calibrated over the full range of adjustment. It may be necessary to change the series resistor on the gain potentiometer to spread the



working part of the scale over a sufficiently wide angle. A common difficulty with this method is lack of suitable permanent echoes (Section 15.5.3).

A fourth method is suitable for microwave gear where search is conducted with a PPI scope. As the beam sweeps past the target a hit or miss is recorded. If desired, additional note may be made such as miss, very weak, weak, or hit. In analyzing the data the percentage of hits in an arbitrary period of 30 sec is plotted against range, counting very weak signals or stronger as a hit, as in Figure 75. The data may be

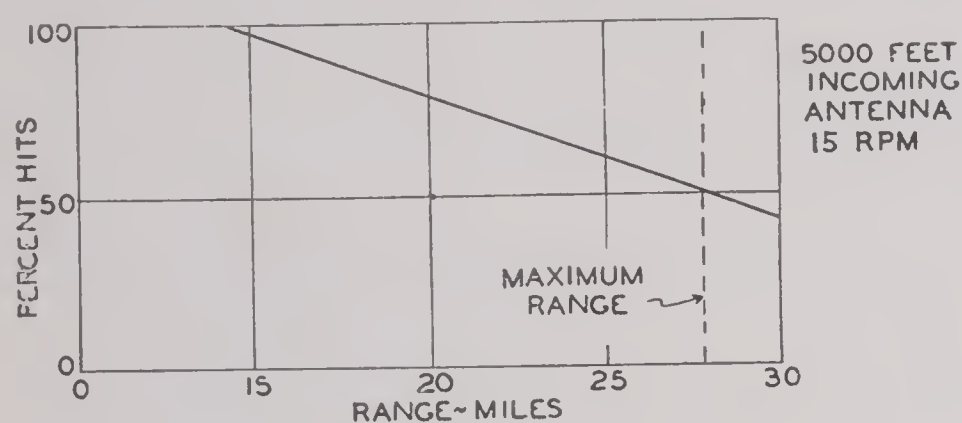


FIGURE 75. Test flight data for PPI scope.

scattered, but it is not difficult to decide the range at which the percentage of hits is 50 per cent. This is taken as the maximum range. At lower altitudes a lobe structure may be detected, indicating ground reflection.

#### 15.7.4

### Conduct of Test Flights

The test planes should have two or more engines. Slow-speed, high-ceiling, long-range planes are most desirable. They should be equipped with navigational aids such as radio compass, DF system, and loran, and full complement of communication sets, transponders, and altimeters. For positive identification in regions of high traffic density, a distinctive IFF (identification friend or foe) response is essential. Mark II transponders may be readily modified in the VHF band to give a double pulse by shifting the condenser rotors.

Tests are conducted by flying out from the station and returning at a specified altitude to a range estimated to be about 10 per cent beyond the maximum of the lobes. Suitable altitudes are from 5,000 to 20,000 ft. Little is learned from tests below 1,000 ft since nonstandard propagation effects are most pronounced in this region.

Data should be taken by specially trained operators as considerable judgment is required. Flights should be carefully planned and full provision made

for various contingencies. Changes from prearranged plans should be held to a minimum. Close liaison should be maintained with the flight section and every effort made to avoid hazardous flying. Where feasible, flights over sea should pass near landmarks, etc., to check navigation. Other radars and agencies should be employed to assist the test plane in holding its course. The permanent echoes should be noted during the test and compared with average conditions so that an estimate of nonstandard propagation may be made. Similar checks should be made at other nearby radars.

#### 15.7.5

### Analysis of Test Data

Test data should be accompanied by a complete description of the conditions of the test. Data should be analyzed promptly, and every effort should be made to extract the full amount of useful information.

In Figure 76 is shown a signal-to-noise graph for

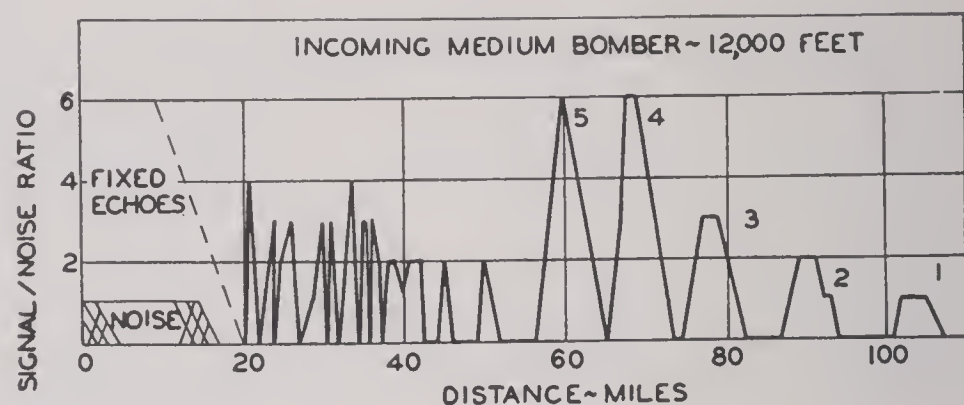


FIGURE 76. Typical signal-to-noise test data.

a station similar to Example 20. The noise is set at a relative height of 1, and the signals are read in proportion as the plane comes in. The weak signals at medium ranges are due to shore line diffraction. The peaks correspond to lobe maxima and ranges at  $S/N = 1$  to the locations of the lobe contour at 12,000 ft. The receiver in this case is of the "linear" type, and the lobe maxima may be obtained by extrapolation. Along a line of constant path difference such as the maxima of the lobes the signal-to-noise ratio varies as the inverse square of distance. Thus the fourth lobe has a peak  $S/N$  ratio of 6 at 68.5 miles, and the lobe length is  $L = 68.5 \sqrt{6} = 167.5$  miles.

In practice the length computed in this manner would be compared to those obtained from tests at other altitudes. Notes made during the test and other factors would be considered and the data weighted accordingly. For example, at 90 miles the  $S/N$  ratio



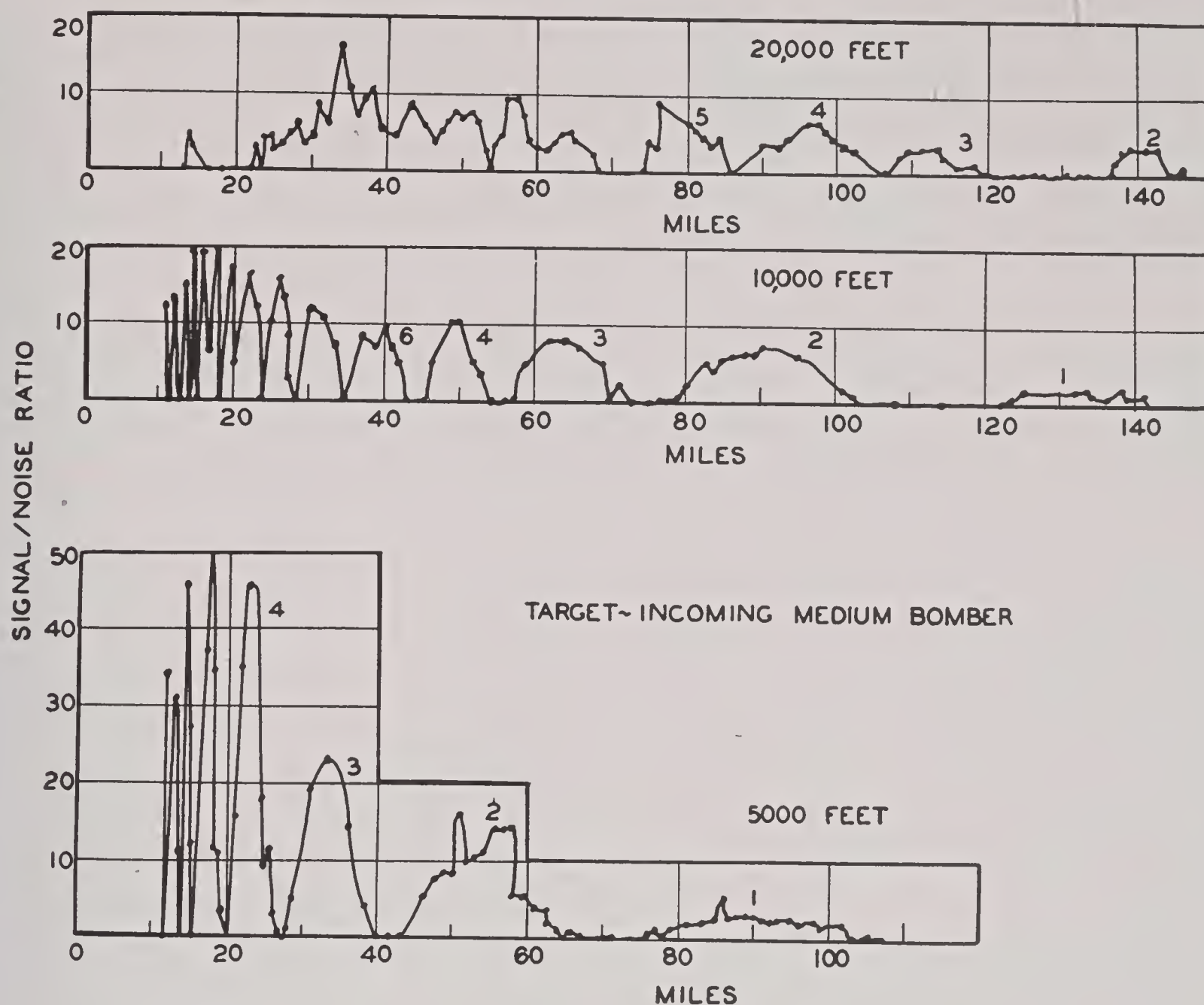


FIGURE 77. Test flight data from a calibrated receiver.

is 2 and the percentage error is probably greater than on the reading at 68.5 miles. The location of points on the lobe cannot be read with accuracy from Figure 76 at  $S/N = 1$  since this is threshold data which may be in considerable error.

To determine the maximum free space range  $F$ , the lengths of the lobes obtained from the test data may be listed along with the site factors from equation (99) or equation (107). A value of  $F$  is then selected which will most nearly fit the test data. Variations in performance of the equipment affects the lobe lengths in proportion. Variations from the standard atmosphere assumed will shift the position of the lobes, particularly at low altitudes.

Where better accuracy is desired or the receiver is nonlinear, the calibrated receiver method is required. Such data are recorded as gain voltage, range, and time. For each gain voltage, the equivalent receiver input voltage is read from a calibration curve such as Figure 74. The equivalent value of the noise voltage of this set is  $30 \mu v$ . Dividing the equivalent receiver signal voltages by 30 gives the  $S/N$  ratio which is plotted against range in Figure 77. The lobes are identified by reference to a lobe angle

diagram. The extrapolated lobe lengths may be listed as follows:

Height, feet	Length of lobes, miles			
	1	2	3	4
20,000	...	243	196	235
10,000	159	212	169	162
5,000	156	216	163	158

The 20,000-ft data were taken last and indicate the effect of certain equipment adjustments. The ability to maintain this performance is one of the questions to be considered in arriving at a weighted average value of lobe lengths. Comparison of these lobe lengths with the computed lobe factors will indicate a fair value to be used for the free space maximum range.

Until suitable instruments are provided for measuring set performance the conduct of successful tests will continue to be a challenge to the ingenuity and diligence of field personnel. However, with a careful analysis of the propagation characteristics of a given site and radar equipment and a well-conducted test with inadequate instrumentation minimized by determined improvisation, it is still practical to obtain a reliable solution to the coverage problem.



VARIATIONS IN RADAR COVERAGE<sup>a</sup>

VARIATIONS IN COVERAGE of radio and radar equipment are caused by atmospheric factors which influence propagation of very short radio waves.

The rapid and accurate evaluation of radar signals is dependent to a great extent upon our knowledge and understanding of the effects produced by the variable conditions of the lower atmosphere.

Evaluation of radar signals influenced by weather introduces problems of identification, actual range determination with second or third sweeps, and radar coverage characteristics, each having a direct bearing on the tactical situation.

Enemy ships far beyond the horizon have been located by radar and sunk by radar-controlled gunfire. United States warships in the Pacific, in several instances, have picked up targets by radar at ranges four to five times those obtained under standard conditions.

Army coastal radars have tracked convoys on some occasions to 20 or 30 miles beyond normal radar ranges. The same radars, a few hours later, may have failed entirely to pick up targets clearly visible to the eye.

Allied forces are employing radar and VHF (very high frequency) equipment with steadily increasing effectiveness. But we are forced to revise and improve our early conceptions of the capabilities and limitations of these useful instruments of World War II. Serious errors and false evaluation of radar presentation may result if we do not take into consideration the effects of weather and atmosphere on radar ranges and VHF coverage.

Complete reports of the variability of radar coverage show that certain weather and atmospheric conditions prevailing along the transmission path may greatly modify the normal range characteristics of radar and VHF radio. The operator, at certain times, can "see" targets or hear messages far beyond the horizon, sometimes at unbelievable distances. At

other times he is unable to contact, by radar or VHF, aircraft or surface craft well within the normal range limit.

These effects of a *nonstandard* atmosphere might leave doubt in our minds as to the effectiveness of radar and the usefulness of VHF radio. But we should adopt the reverse view. We can, by understanding and allowing for these phenomena, make a useful instrument more effective—the weather will work *for*, *instead of against*, radar and microwave equipment.

Unusual ranges are caused by *bending* or refraction of the radio waves by the atmosphere. A most important special case of refraction is the concentration of the wave energy in ducts within the atmosphere. This *bending* and *duct formation* is a direct result of the meteorological factors involved—factors of weather and atmosphere—peculiar, in many cases, to the locality and the season. Such factors are discussed later.

## 16.1

## BENDING

The VHF or radar operator usually assumes that short waves and microwaves, at frequencies above about 30 mc, travel along the line of sight from the transmitter to the receiver and, in the case of radar, to and from the target. Experience has shown that this assumption, nearly true in many instances, may lead to serious errors or false evaluation if applied to radar operation and microwave communication.

Radio waves are bent from a straight line path as a result of refraction by the lower atmosphere. This bending, or refraction, is generally recognized as a property of light. It is equally a property of radio waves. The underlying principles are exactly the same in both cases.

The quantity that determines refraction is called the index of refraction. Refraction occurs whenever there is a change of index of refraction, as at the boundary of two substances. In the interior of a material of constant refractive index, the rays travel in a straight line. The change in angle at the boundary is the larger, the greater the difference in refractive index from one material to the next.

Radio waves are refracted or bent in the atmosphere because the index of refraction of the atmosphere changes with height. The properties of the atmosphere which determine the refractive index and which

<sup>a</sup>This document was published June 1, 1944 and distributed widely to Service personnel under the above title, and under short title JANP 101, by authority of the Joint Communications Board. Originally prepared by the Columbia University Wave Propagation Group, it was amended and improved by representatives of both Services in an effort to prepare a brief, qualitative but authoritative statement of the then known facts concerning the factors contributing to nonstandard propagation.



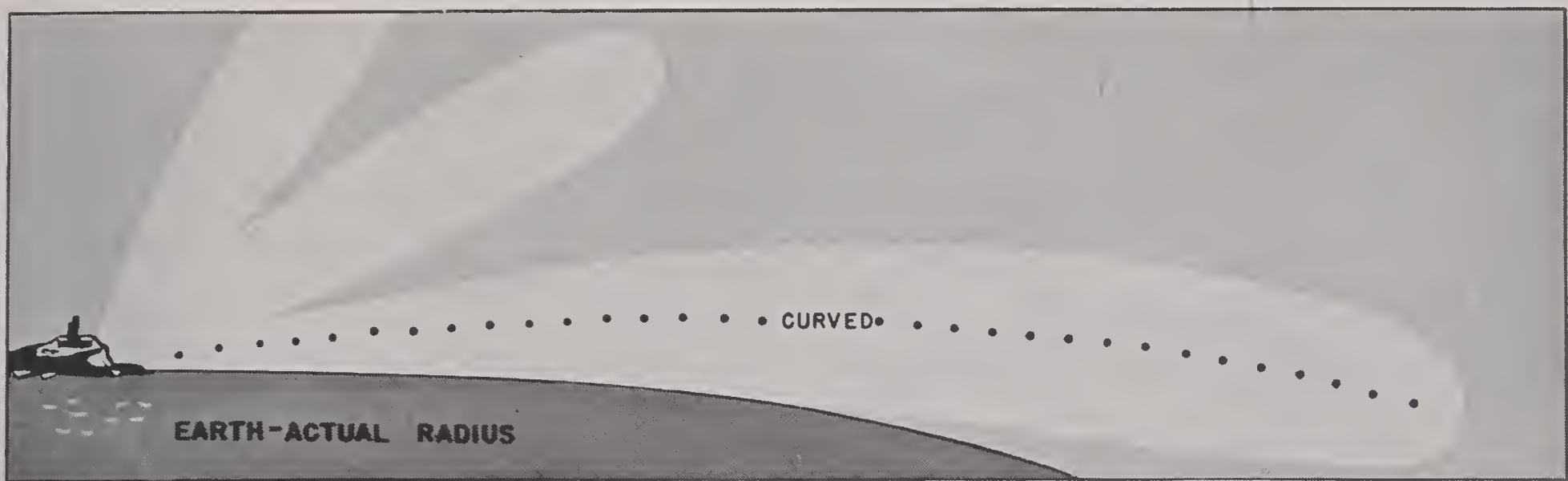


FIGURE 1. Actual pattern showing radar coverage for standard propagation.

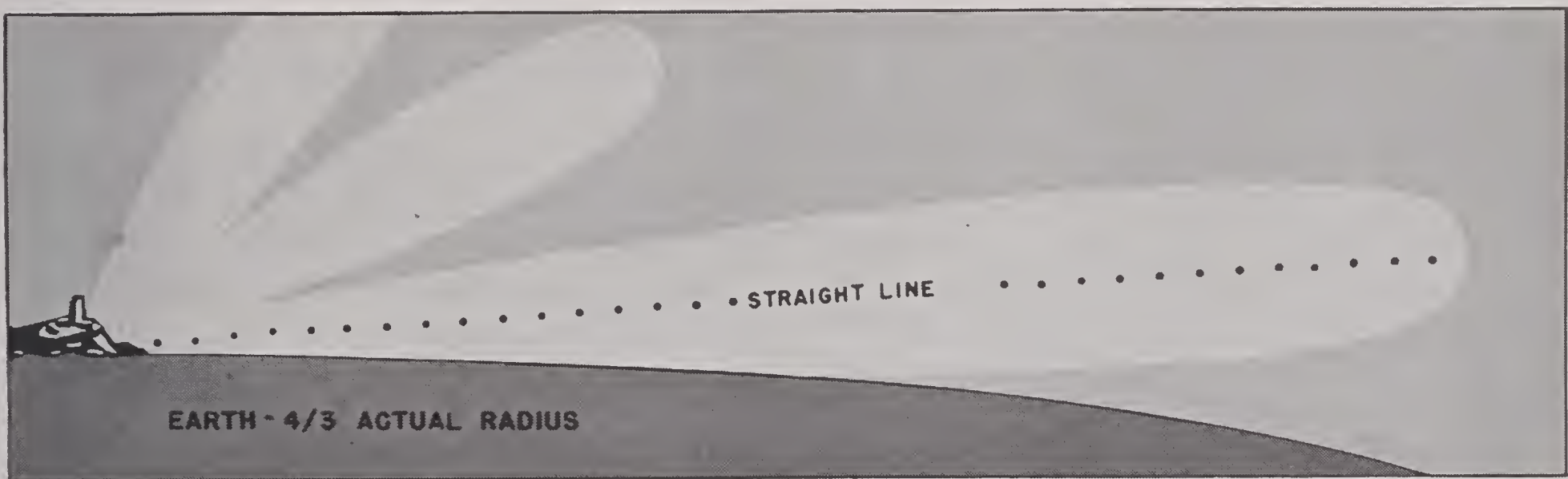


FIGURE 2. Modified presentation of the information shown in Figure 1.

change with height are temperature, pressure, and moisture content. These changes from one level to another are very small compared with that from water to air, and the resulting refraction itself is small. Nevertheless this refraction is of great importance in radar operations and radio communications above 30 mc.

If the atmosphere were composed of a number of successive layers each having a different index of refraction, a wave passing across the successive boundaries of the layers would be abruptly deflected at each surface. The atmosphere does not consist of such distinct layers. Instead, the change in its physical properties and its index of refraction is gradual, continuous. There is, then, no sudden change in direction of the waves; the change in direction becomes gradual and continuous. In other words, a bending of the waves occurs as they pass through the atmosphere. Radio waves passing through the lower atmosphere are usually bent *downwards*.

As can be seen from the illustration of the actual pattern (Figure 1), the bending of the waves, or rays, by the atmosphere permits one to see farther than

he would otherwise. In the figure the vertical dimensions have been strongly exaggerated so that the earth's curvature becomes clearly visible. Under average weather conditions the horizon distance is increased by about 15 per cent, but at an elevation near the first lobe the increase in range is much less than this amount. This is the case of standard refraction, or *standard propagation*.

It is rather inconvenient to draw curved rays in radar coverage and calibration diagrams. This can be avoided by assuming that the earth's radius is  $\frac{4}{3}$  the actual radius. Then in the diagrams the rays appear as straight lines when the propagation is of the standard type. This method often is adopted in radar calibration practice, with coverage diagrams drawn or printed to the  $\frac{4}{3}$  value of the earth's radius (see Figure 2). This corrects for the effect of normal bending in the atmosphere. The radar operator merely plots the position of his target on such a diagram and assumes that the radiation travels along a straight line between the radar and the target. In this way he takes into account the effects of standard refraction while doing his work.



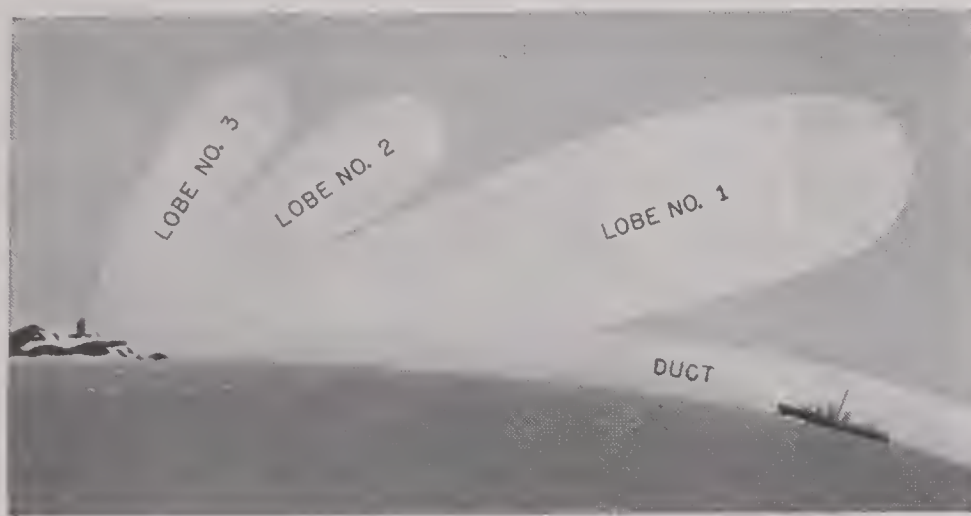


FIGURE 3. Radar lobe pattern in nonstandard atmosphere. A duct has been formed on the surface of the ocean and a ship is detected. Lobe No. 1 is bent downward more than normal, but the other lobes remain substantially unchanged by the duct.

Wave propagation deviating from standard occurs under special weather conditions. The most important type is called “guided propagation,” “trapping,” or “superrefraction”—formerly referred to as anomalous propagation. The main feature of this type of propagation is an excessive bending of the rays due to refraction. This bending occurs principally in the lower layers of the atmosphere and mainly in the lowest few hundred feet. In certain regions, notably in warmer climates, excessive bending is observed as high as 5,000 ft. The amount of bending in regions above this height is almost always that of the standard atmosphere.

As a consequence of the excessive bending in the lower layers the coverage pattern of a radar set is deformed, as illustrated in Figure 3. The fact that atmospheric influences are effective only in the lower layers does not imply that the echo strength from a target will be affected only as it lies in these layers, though the effects will be strongest there. It merely means that excessive bending is suffered by the rays only while passing through the lower layers. However, the deformation of the coverage pattern itself will in general extend to a greater height.

Two factors are operative in producing a rapid change of refractive index with height: variation of moisture with height and variation of temperature with height. Excessive refraction occurs when there is a rapid decrease of moisture with height (“moisture lapse”) and, to a lesser degree, when there is a rapid increase of temperature with height (“temperature inversion”). The most pronounced cases of excessive refraction occur when both these conditions prevail at the same time. These conditions will be discussed later from the meteorological viewpoint.

Since the atmosphere is a very tenuous substance, the amount of refraction, that is, the amount of angular deflection of the rays, is very small and in no case exceeds a fraction of a degree. How then can these small effects influence radar operations? The answer is that they do not influence operations unless the angle between the ray itself and the horizontal is very small. If radar is used for fire control, searchlight control, or fighter intercept control, the targets are usually at medium or short ranges, and the angle between the line of sight and the horizontal is usually larger than one to two degrees. Refraction has practically no effect on such an application of radar.

However, the same equipment may be used for long-range search and then the story is different. With early warning radar the target may be an airplane 50 or 100 miles away, and it may fly at an elevation of only a few thousand feet. In this case the angle of elevation of the target above the horizontal, as seen from the radar, is only a fraction of a degree. This applies still more to seaborne targets. The atmospheric effects then become operationally important. It should always be kept in mind that only low-angle search is affected by meteorological conditions.

As a rule, the operational characteristics of a radar for angles of elevation of the target exceeding 1 degree may be calculated on the assumption of a standard atmosphere, with confidence that all non-standard meteorological effects are negligible.

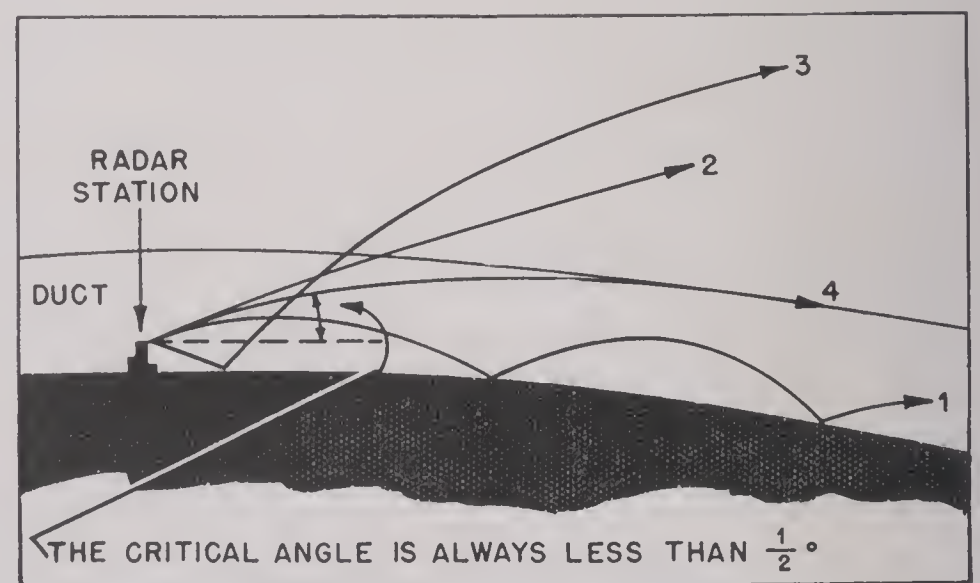


FIGURE 4. Wave paths illustrated as rays in ground-based duct.

16.2

## GUIDED PROPAGATION

It is obvious that excessive bending of the rays in the lower layers of the atmosphere must distort radar coverage patterns. One case of special importance is illustrated in Figure 4. Four rays, out of



many, are shown which leave the transmitter at different angles with the horizontal.

*Ray 1* is bent so much that after some distance it returns to the ground; there it is reflected and then the same course is repeated again. In this way the ray may be reflected a number of times in succession, remaining always in the lowest layer. This super-refraction "traps" the rays in a "duct" and results in guided propagation of the radar waves. Trapping does not occur under standard atmospheric conditions. A ray, under standard conditions, may be reflected by the earth's surface only once before it escapes into space.

*Ray 2* is also bent in the lowest layer but not enough to keep it from escaping into the upper atmosphere whence it does not return to earth.

*Ray 3* is similar to 2 except that it undergoes one reflection by the ground before it escapes into the upper atmosphere.

*Ray 4* separates the two types of rays illustrated by rays 1 and 2. This ray becomes horizontal when it reaches the top of the trapping layer or duct and from there on travels along at the same height. All rays are divided into two groups: those that leave the transmitter at an angle with the horizontal less than the critical angle and are trapped, and those that leave the transmitter at a larger angle and proceed into the upper atmosphere.

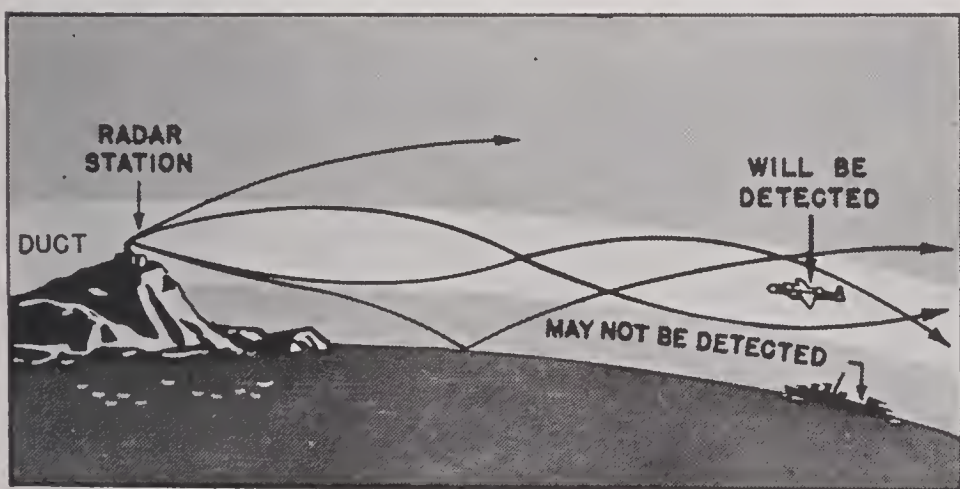


FIGURE 5. Rays in an elevated duct. In this, another common form of duct, the amount of bending may be approximately normal both below and above the duct. The rays oscillate between the upper and lower boundaries; maximum ranges in or near the duct may be even greater than with a ground-based duct.

The critical angle is always small, practically never larger than  $\frac{1}{2}$  degree. Its magnitude may be taken as a measure of the intensity of guided propagation, that is, of the amount of radiant energy trapped within the duct. Rays that leave the transmitter at a somewhat larger angle up to about twice the critical

angle are sufficiently deflected while passing through the lowest layers to distort that part of the radar coverage pattern lying just above the duct. Rays leaving the transmitter at a still larger angle are not appreciably affected.

The ground-based duct or trapping layer guides the wave along the earth's surface in much the same way that hollow metal tubes guide microwaves. Within the duct there is less decrease of signal strength with distance than there is above the duct. Radar ranges on surface craft and low-flying aircraft located within a duct, similar to the one illustrated in Figure 5, are increased—sometimes to two, three, or four times the normal ranges. Ground echoes would be increased at the same time and might, in some cases, obscure partly, or even entirely, the echoes from incoming aircraft.

When the radar is located within the duct, ranges on aircraft flying above the duct will be decreased only slightly, if at all. Often there may be a slight increase in effective ranges. If the angle of elevation of the aircraft is greater than 1 degree, the effects become inappreciable and failure to detect the target cannot be attributed to excessive refraction.

If the duct does not include the radar within its boundaries, as, for example, when a duct forms below a high-sited radar, the effective ranges on surface craft may be either increased or decreased. Similar reasoning may be applied in the case of airborne VHF radio communication. Usually there is no very pronounced effect upon the signal strength when VHF communication is carried on between two aircraft, both flying above the duct.

Interference between the direct rays and the rays reflected from the ground—resulting in the well-known lobe pattern of the coverage diagram—has not been mentioned. Under standard conditions the position of the lobes depends only on the wavelength used and the height of the radar above the ground. When a duct is present the lowest part of the coverage diagram may be strongly distorted.

Coverage depends upon a variety of factors of which the most important are these: height of the top and base of the duct, amount of refraction in the duct, position of the transmitter relative to the duct, frequency (or wavelength) of the radar equipment, and height of the transmitter above ground.

A coverage diagram for standard conditions is shown in Figure 6, diagram 1, with height strongly exaggerated. Only the lowest three lobes are shown, and the higher lobes appear compressed as compared



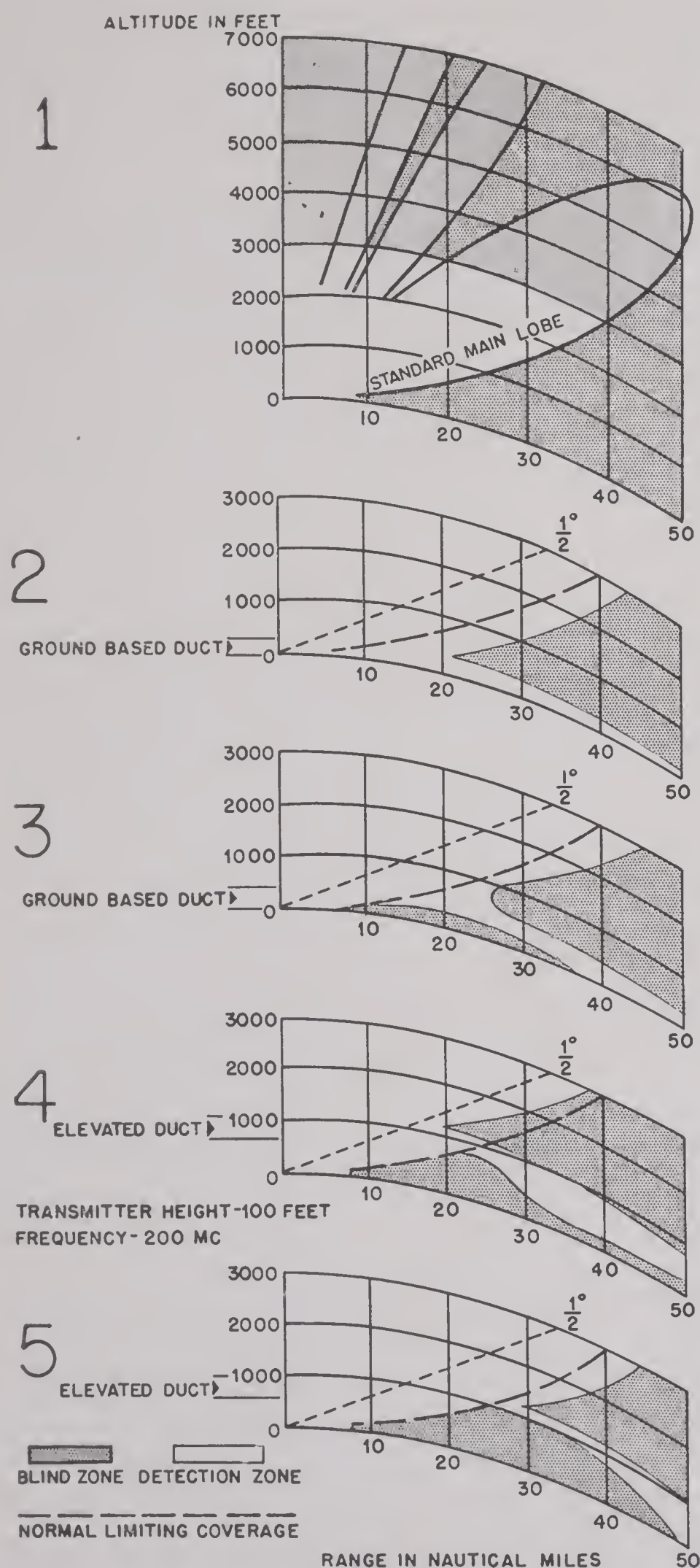


FIGURE 6. Standard and nonstandard coverage diagrams.

to the lowest lobe. In diagrams 2, 3, 4, 5 the lower part of the same diagram is drawn as it appears under various conditions of guided propagation. The bottom part of the "standard" main lobe is shown by a broken line. The lines which separate the "blind zones" from the "detection zones" represent the range at which a medium bomber would just become visible to this particular radar set.

The diagrams clearly indicate the great extension of ranges in the duct and also the moderate change in ranges—sometimes an extension, sometimes a reduction—above the duct. Another feature of some of these diagrams is the appearance of "skip-ranges." A plane flying at an altitude of 500 ft, for instance, would be detected early under the conditions shown in diagrams 4 and 5. As the plane approaches, the echo will disappear from the scope and reappear only at a range less than 20 miles. Similar conditions will prevail for ground clutter. In diagram 3 there would be ground clutter close in and also from beyond 33 miles but not from the space between. For conditions shown in diagram 5, there would be echoes from very remote ground targets but not from targets at intermediate ranges.

A change in echo strength from day to day is not necessarily caused by the weather but might simply be caused by a variation in performance of the set. Cases have occurred where there was extensive trapping, but because of lowered set performance there was no corresponding increase in fixed echo strength. The set then will appear to be in good operating condition, and the operator will be deceived about ranges of detection for craft flying above the duct. Equipment for checking set performance is not usually available in the field. The change in intensity of nearby fixed echoes may be, in some cases, a measure of set performance, but in the absence of more elaborate checks this method can be misleading and should not be relied upon entirely.

Failure of detection of targets is not necessarily due to weather influences. Electrical failure of the set or inadequate adjustment may be the difficulty and may be far more troublesome to identify than meteorological effects which should not be used as a "scapegoat" to be indiscriminately blamed for poor coverage.

## 16.3

## METEOROLOGICAL FACTORS

The atmosphere is responsible for bending and duct formation. To understand the "why" of non-standard ranges of radar and radio with respect to the weather, it is necessary to consider the meteorological factors involved.

The strong refraction which results in guided propagation is caused by a rapid decrease of index of refraction with height within certain layers. The decrease depends upon distribution of moisture and temperature in the atmosphere, particularly in the



lowest few hundred or thousand feet. Normally the temperature decreases with height in the atmosphere (at a rate of about  $2^{\circ}\text{C}$  per 1,000 ft), and the moisture decreases gradually with height. Under these conditions the propagation is of the standard type.

Temperature may sometimes increase with height for a few hundred or thousand feet above ground and then, at greater heights, begin to decrease again. The vertical increase of temperature is called a temperature inversion. Sometimes a layer of moist air is found near the ground, and the air overlying it is very dry. There is then a rapid decrease of moisture over a short vertical distance; in other words there is a pronounced moisture lapse (see Figure 7). A

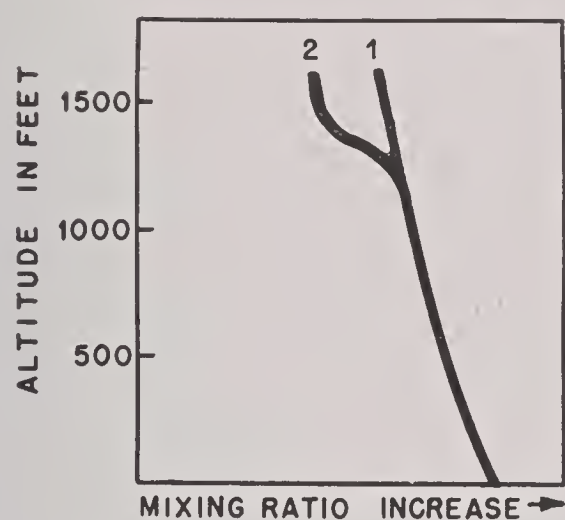


FIGURE 7. Moisture variation aloft. 1. Moisture distribution with height in standard moist atmosphere. 2. Example of sharp moisture lapse (dry air overlying moist air) conducive to guided propagation. Mixing ratio is amount of moisture in a unit weight of dry air expressed as grams of water per kilogram of dry air.

moderate or strong moisture lapse almost always will produce trapping, but a temperature inversion (except at low temperatures) will lead to trapping only if the moisture distribution is favorable. A combination of both effects within the same layer usually will produce trapping.

The meteorological conditions to be found over sea and over land are quite different and must be considered separately.

#### OVER SEA

When warm, dry air flows over colder water, a temperature inversion will be established, and there will be evaporation into the lowest layers of the air, thus creating conditions of pronounced trapping. This weather condition is one of the most common causes of guided propagation. An example in point is the Mediterranean, which to the south, east, and west is surrounded by dry land masses producing a flow of dry, warm air over the water when the winds

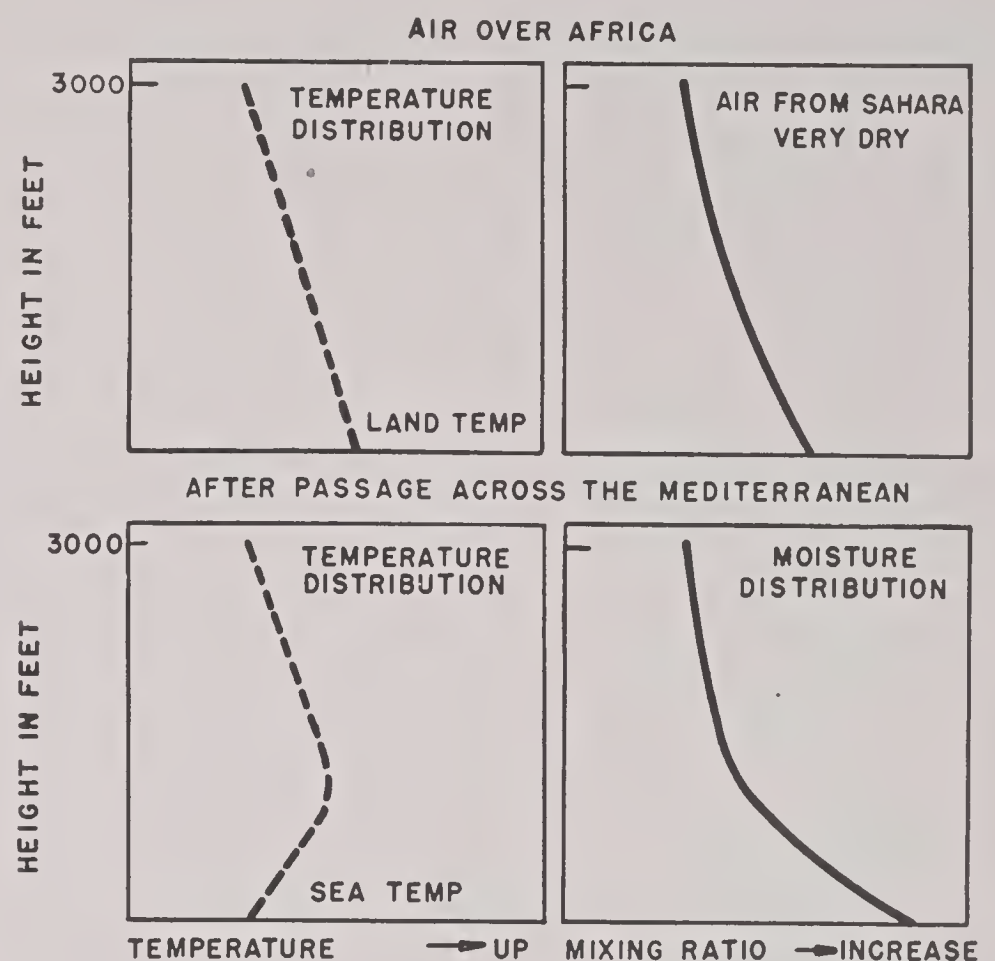


FIGURE 8. Modification of air from Sahara Desert in passing over the Mediterranean.

blow from these directions (see Figure 8). Similar conditions are often caused by westerly winds blowing from land to sea across the eastern boundary of a continent. Land and sea breezes may influence radar operation along a coast line. The wind direction at a coast is often an important factor in determining propagation conditions and should be closely watched. Whenever unusual propagation is observed by coastal radar stations, a record of prevailing winds at the time is very helpful in determination of future expected performance.

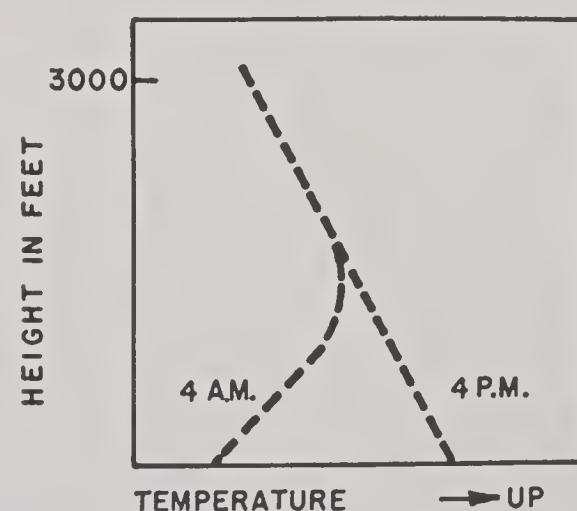


FIGURE 9. Formation of temperature inversion over land due to nocturnal cooling.

#### OVER LAND

Temperature inversions are produced mainly by nocturnal or night cooling of the ground (see Figure 9). Trapping may occur when the moisture distribu-



tion in the lowest layers is such as to reinforce or at least not to counteract the effect of the temperature distribution, that is, when the moisture decreases not too slowly with height. Nocturnal cooling is greatest with clear skies and is quite small under an overcast. Hence guided propagation over land occurs at night almost exclusively with clear skies. This type of temperature inversion is strictly confined to land areas. It does not occur over the ocean because the sea temperature does not show appreciable daily variations. Temperature inversions caused by nocturnal cooling are most pronounced over dry land (desert) but will occur almost anywhere over land with a clear sky and a not too humid atmosphere.

#### SUBSIDENCE

Another weather phenomenon favorable to trapping is subsidence. By subsidence is meant the slow downward motion, combined with horizontal spreading, of air above the lowest layers of the atmosphere. This process, which most frequently occurs in the area of barometric high, will produce temperature inversions; the subsiding air moreover becomes relatively much drier than the unaffected air below. In general the subsidence inversion is quite high (e.g., above 4,000 to 5,000 ft). In the light of present knowledge it appears that high subsidence inversions do not generally affect guided propagation when the sets are situated at low altitudes. It appears, however, that such subsidence inversions might materially affect communications or airborne radar search aloft. Lower subsidence inversions (1,000 to 2,500 ft) along the southwestern coast of the United States are known to produce stable duct layers affecting radar coverage at low angles.

#### TURBULENCE OF THE AIR

This has a distinct normalizing effect in that it tends to smooth out the temperature and moisture variations which are conducive to guided propagation. Moderate to strong winds produce a turbulent layer extending normally to a height of about 4,000 ft. The air is well mixed within this layer, and consequently the standard type of refraction prevails. Regions of a barometric low are characterized by strong to moderate winds and pronounced turbulence in the lower layers. In addition low pressure areas usually have overcast skies. Hence a barometric low will as a rule lead to propagation of the standard type.

#### FREQUENCY OF OCCURRENCE

It is extremely difficult to estimate in general terms the frequency of occurrence of guided propagation, since statistical data are almost nonexistent at present except for very limited regions in Europe such as the North Sea. In the central Mediterranean during the summer months of 1943, ducts have been observed on 9 days out of 10. Frequent trapping has also been observed in some parts of the Pacific. At other times and places guided propagation might be an unusual occurrence, especially if the barometric pressure is generally low and the winds strong. It seems advisable to consult a weather officer with regard to any given locality.

#### MEASUREMENTS

In order to determine weather's influence upon radar in a quantitative way, the variation of refractive index with height must be determined. This requires accurate knowledge of the temperature and moisture distribution in the lowest few hundred or thousand feet of the atmosphere. The ordinary radiosonde is not well adapted to measurements of this type because the measured points on an ascent are usually spaced several hundred feet apart. Among the methods which have been developed for this purpose during the past two years, the one most generally adopted uses a captive balloon (or kite) which carries aloft electrical temperature and moisture—measuring elements. These are connected to a meter on the ground by means of thin wires attached to the cable holding the balloon. This device permits measurements at intervals as closely spaced as desired. A psychrometer held out of the window of a slowly flying plane has been used with good success in the absence of more elaborate equipment.

16.4

#### CLOUD ECHOES IN RADAR

Cloud echoes (more precisely, precipitation echoes) are observed frequently on radar scopes. At times they have caused confusion by blotting out other targets. Their similarity, upon certain occasions, to actual targets have caused some difficulty in the interpretation of the signals.

These echoes are caused by a reflection of the radar pulse from the raindrops in the clouds (or in rain storms). The amount of reflection increases very rapidly with frequency. Cloud echoes are quite exceptional below about 1,000 mc. In microwave



radar they first appeared as a nuisance, but more recently they have been put to practical use. In tropical climates they are very helpful for aerial navigation.

Cloud echoes may be distinguished from other echoes by their fuzzy and diffuse appearance. Not all clouds show up on a scope with equal strength. The strength of the echo seems to depend primarily on the size of the water drops within the cloud or rain storm. Ordinary clouds such as form an even overcast (stratus clouds) are not usually visible on the scopes; the droplets that compose these clouds are so small that they reflect very little energy. Violent showers give intense echoes on the scopes. Storm echoes can be seen much farther than normal land targets, even under standard conditions, because of their great spread in the vertical direction.

In discussing cloud reflections it must be clearly understood that there is no physical relation between cloud echoes and refraction; the mechanics of duct formation is not related to clouds, and with respect to the bending of radio waves a cloud is merely another airborne target.

16.5

### SUMMARY OF BASIC FACTS CONCERNING PROPAGATION AT RADAR FREQUENCIES

1. Standard propagation results in a slight downward bending of the rays throughout the atmosphere, leading to an increase of the horizon distance compared to the geometrical value. It is taken into account operationally by using coverage diagrams with a  $\frac{4}{3}$  earth's radius; on a diagram modified in this way the rays appear as straight lines.

2. Guided propagation occurs almost exclusively in the lowest 2,000 ft above the ground and usually is confined to the lowest few hundred feet (except in warm climates).

3. Superrefraction resulting in guided propagation or trapping is produced:

- a. By a pronounced decrease of moisture with height (moisture lapse), or
- b. By a pronounced increase in temperature with height (temperature inversion), and
- c. Particularly, by a combination of both of the above conditions.

4. Of the meteorological conditions conducive to guided propagation or trapping, the most outstanding are:

- a. Over sea: flow of warm, dry air over colder water producing temperature inversions and evaporation into the lowest layers.
- b. Over land: nocturnal cooling of the ground with clear skies and calm air or light winds (if moisture distribution is favorable).
- c. Over both sea and land: low-level subsidence.

5. Conditions in a barometric high, including calm and clear skies and especially low-level subsidence, favor trapping especially during the night (but do not necessarily produce it). Conditions in a barometric low, including strong winds, intense turbulence in the lowest layers, and overcast skies are conducive to standard propagation.

6. When the transmitter is within the duct, radar range is increased for surface targets (ships) and aircraft flying in the duct. At the same time there is an increase in fixed echo strength and consequently in ground clutter on the scopes. This may be accompanied by a change in the range of detection for craft flying above the duct.

7. When the transmitter is outside the duct, the range may be either increased or decreased from its standard value.

8. Effects of nonstandard propagation are negligible when the angle of elevation of the target is over 1 degree. Failure of detection at such angles must be attributed to other causes.







*PART IV*

*CONFERENCE REPORTS ON NONSTANDARD PROPAGATION*







TROPOSPHERIC PROPAGATION AND RADIO METEOROLOGY<sup>a</sup>

## 17.1 FUNDAMENTALS OF PROPAGATION

## 17.1.1 Significance of Propagation Problems

THE CENTRAL PROBLEM of short and microwave propagation (at frequencies greater than 40 to 60 mc) is the determination of accurate coverage patterns for a given transmitter. These patterns are usually calculated from electromagnetic theory and then may be checked by experiment. For communication work the check is simple, namely, the establishment of satisfactory communication. In the case of radar it is necessary to calibrate by time-consuming airplane flights.

Experience has shown that actual coverage is not constant in time but suffers large variations which are caused by the changeable refraction of the atmosphere. The variations in weather conditions that influence the refraction often are irregular and very rapid, and it is technically impossible to test all these conditions. Coverage diagrams, therefore, must be based on the physical principles of wave propagation, assuming that the characteristics of the atmosphere remain constant for reasonable periods. These principles are outlined here.

At the present stage of technical development it is not always permissible to ascribe an observed variation in coverage to changing atmospheric conditions. Variations in transmitter output or receiver sensitivity are always likely to be present to a degree sufficient to influence results considerably. In practice it is often extremely difficult to tell these causes apart. In fact, investigations carried out with operational radar equipment make it probable that an increase in surface coverage due to favorable conditions of refraction frequently passes unnoticed because of poor set performance. The coverage appears normal, while the set in reality is operating considerably below peak efficiency.

A knowledge and understanding of the effects of weather upon propagation therefore will also be of help in checking set performance in the absence of suitable electrical equipment for measuring output and sensitivity. In dealing with coverage problems this double aspect of propagation phenomena should always be kept in mind. By a suitable analysis of the

various factors determining coverage, and by an intelligent understanding of their interplay, the responsible officer may achieve a better control of the operational performance of his equipment.

In tactical operations and in planning, a knowledge of the nonvariable factors affecting propagation, such as dielectric constant and conductivity of the ground or sea, contours of the terrain, vegetation, etc., is equally important. Many problems concerning these factors cannot be considered in this manual

## 17.1.2 Factors Influencing Propagation

This volume is confined to the propagation of waves within the troposphere and hence is not concerned with ionospheric propagation, which is responsible for the long distance transmission of short waves (high frequency band). The higher the frequency above 30 mc, the less frequently radio waves are returned to the earth by the ionosphere. Consequently very short radio waves are confined to the troposphere, and the treatment given here does not need to be supplemented by a study of the ionosphere. Propagation in the lower atmosphere is called "tropospheric propagation" (see Figure 1).

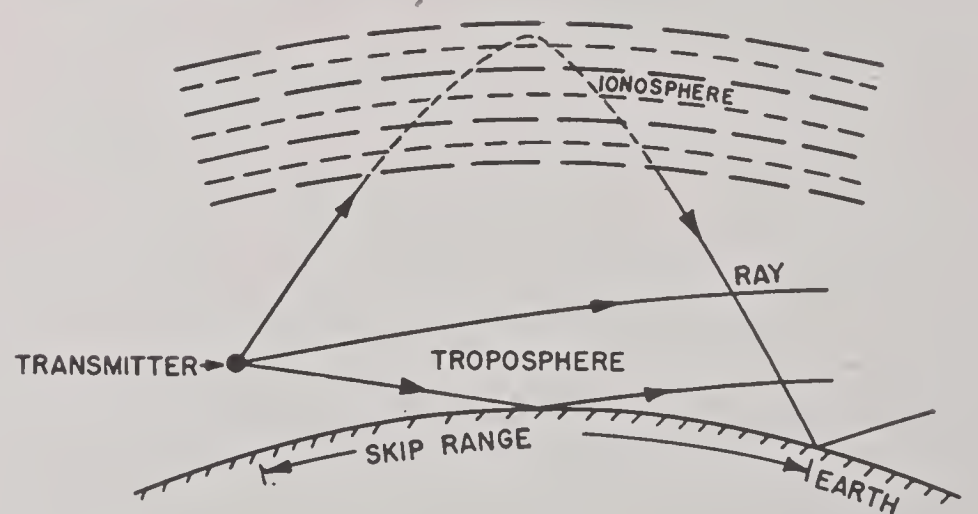


FIGURE 1. Tropospheric versus ionospheric propagation.

The main factors influencing the shape of a coverage diagram under these circumstances are: (1) reflection by the ground, (2) diffraction by the ground contour, (3) refraction by the atmosphere, and (4) guided propagation by superrefraction in the lower atmosphere. The present chapter deals mainly with refraction phenomena, but reflection and diffraction will be briefly considered.

Refraction is influenced by the physical state of the

<sup>a</sup>By Columbia University Wave Propagation Group.



atmosphere, in which the distributions of the temperature, pressure, and humidity are the most important elements. With refraction, rays are bent, and the electromagnetic energy flows along the curved ray paths. A situation frequently realized in practice is that in which the curvature of the rays is independent of height above ground. This is known as *standard refraction*. The term standard propagation is used to designate propagation under conditions where the refraction is of the standard type.

During the war years the increased number of observations, which resulted from the world-wide use of radar, showed that, under certain weather conditions, radio field strengths may depart markedly from the values expected with standard refraction. These deviations are now known to be attributable to a stratification of the atmosphere which is predominantly horizontal and is produced by vertical variations in water-vapor content and temperature. Since these quantities control the index of refraction, and therefore the curvature of the rays, it follows that this curvature varies with the elevation above ground.

Any stratification of the atmosphere tends to produce a distribution of the radiated energy different from that which occurs in the standard atmosphere. Of particular importance is a type of stratification which results in a duct being formed in the atmosphere. In this event, a portion of the wave energy may be guided horizontally along the duct and may be effectively "trapped" within the duct's upper and lower boundaries. This is known as "guided" propagation. The radiation energy may then travel to distances far beyond the geometrical horizon, producing unusually long ranges for short wave receivers or radar targets. The phenomenon which tends to constrain the wave energy to follow the duct is called "superrefraction." When this occurs, the rays in passing through the inversion layer in the upper part of the duct are bent downward with a curvature which exceeds that of the curvature of the earth. The regions covered by the inversion layer and the duct are illustrated in Figures 15, 20, 22, and 23. The distribution of moisture and temperature in the atmosphere, responsible for the formation of ducts, is discussed in Section 17.3.1.

As the stratification of the lower atmosphere that produces superrefraction is part of the weather, the prevailing meteorological conditions become of importance for problems of propagation and coverage. Meteorology as related to wave propagation is treated in Section 17.3.

17.1.3

## Reflection from the Ground

A coverage diagram is a curve, or a set of curves, of constant field strength in a vertical or horizontal plane. The horizontal coverage diagram is determined chiefly by the antenna pattern itself. In the vertical plane, however, the diagram depends primarily upon the interference between the radiation coming directly from the transmitter and that which is reflected from the ground or sea surface. This effect produces the lobe structure of the vertical coverage diagram. At the lobe maxima the two rays reinforce each other, while they cancel each other out, more or less, at the lobe minima.

The propagation problem in its full generality leads to mathematical formulas of forbidding complexity. In order to understand the processes at work it is necessary to proceed in steps and gradually add refinements to the basic features of the problem.

Consider first the field radiated from an antenna which is remote from the earth. This free space field decreases in strength in inverse proportion to the distance,  $R_1$ , from the transmitter and varies with the angular position in accordance with the shape of the radiation pattern of the transmitting antenna. Let this free space field strength at any point at distance  $R_1$  be designated by  $E_0$ .

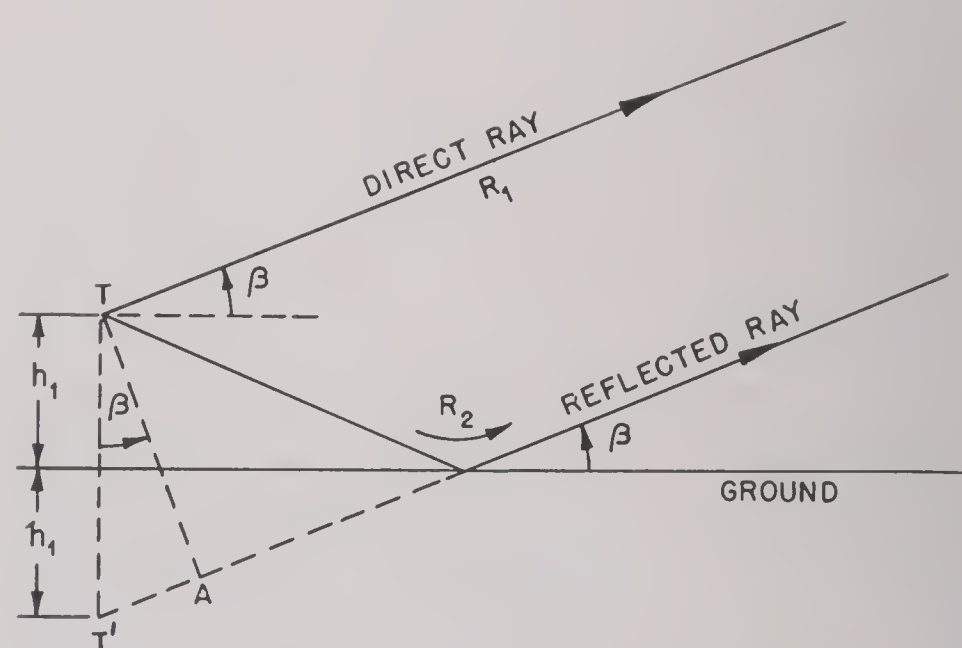


FIGURE 2. Interference of direct and reflected rays.

If, instead, the transmitter is placed near the ground, as at  $T$  in Figure 2, the field at any point in space is produced partly by the direct wave (giving the free space field  $E_0$ ) and partly by the wave which is reflected from the ground. The resultant field is given by the vector sum of the two component fields.

The magnitude of the field strength of the *reflected* beam depends upon:



1. The antenna radiation pattern, which gives the relative strength of the radiation field for different directions.

2. The attenuation, proportional to  $1/R_2$ , resulting from the length of path  $R_2$  of the reflected wave.

3. The attenuation due to increased divergence of nearly parallel rays reflected from the curved earth. This is taken into account by the use of a divergence factor,  $D$ , which depends on range and heights of transmitter and receiver.

4. The magnitude,  $\rho$ , that the coefficient of reflection of the ground would have if the ground were plane. The reflection surface for a spherical surface,  $F$ , is then equal to  $\rho D$ .

5. Irregularities of the earth's surface which affect the reflection coefficient.

If  $E_0$  is the magnitude of the direct wave and  $F$  is the magnitude of the reflection coefficient, then the field strength of the reflected ray is  $FE_0$ .

The phase difference between the direct and reflected fields is given by an angle  $\delta$  which is the sum of:

1. The phase difference,  $\Psi$ , resulting from the difference in path length,  $R_2 - R_1$ ;

2. The phase difference,  $\phi$ , suffered by the reflected wave upon reflection from the ground.

The amplitude of the resultant field for a non-directive antenna is then given by  $GE_0$ , where

$$G = \sqrt{1 + F^2 + 2F \cos \delta} \quad (1)$$

is the earth gain factor which is illustrated in Figure 3.

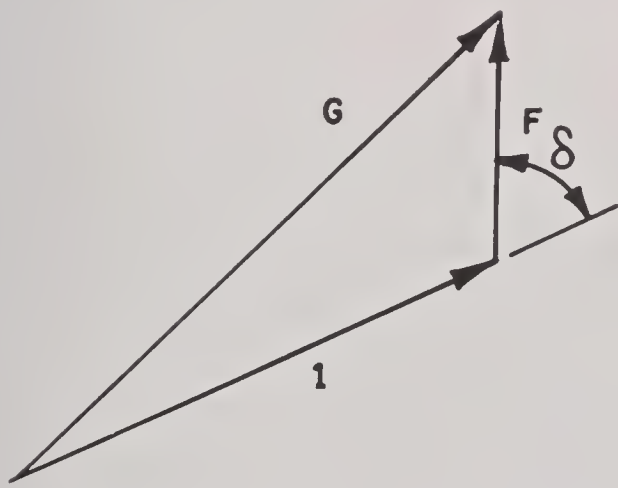


FIGURE 3. Phase addition of direct and reflected rays.

A curve drawn to represent the contour of constant field strength  $E = GE_0$  as a function of the range  $R_1$  and the angle of elevation  $\beta$  gives the vertical coverage diagram for that particular field strength. Calculation of these diagrams usually requires a considerable amount of detailed and laborious work.

Consider the simple case of the vertical coverage

diagram of a horizontal dipole antenna located above a plane earth in a homogeneous atmosphere. If the plane of Figure 2 is perpendicular to the dipole axis, the radiation pattern of the antenna is a circle of unit radius. The ratio,  $F_2$ , of the magnitude of the reflected wave to that of the incident wave is given by the magnitude,  $\rho$ , of the reflection coefficient. For propagation to distances that are great compared with the antenna elevation, the path lengths  $R_2$  and  $R_1$  are not greatly different, and the attenuation due to path length is approximately the same for both direct and reflected waves. For this set of conditions the resultant field is  $E = GE_0$ , and equation (1) reduces to

$$G = \sqrt{1 + \rho^2 + 2\rho \cos \delta} \quad (2)$$

In this form  $G$  is the plane earth gain factor and a plot of the curves  $E = GE_0 = \text{constant}$  as a function of range and angle of elevation gives the coverage diagram. It depends only upon the magnitude of the reflection coefficient, the phase changes related to reflection and to the difference in path length  $R_2 - R_1$ .

Since radar requires two-way transmission the received field strength is proportional to  $G^2/R_1^2$ . Other modifying factors must, however, be introduced if the antenna and the target have directional radiative properties.

Both the magnitude of the reflection coefficient  $+F$  and the phase angle  $\phi$  by which the reflected wave lags behind the incident wave are functions of the frequency, the polarization of the radiation, the angle of grazing with the surface, the conductivity, dielectric constant, and roughness of the ground or sea surface. Figure 4 illustrates the variation of  $F(=\rho)$  and  $\phi$  for reflection from a smooth plane sea surface for frequencies of 100 to 3,000 mc, for both types of polarization, at different grazing angles. It may be noted that for horizontal polarization  $\rho$  is approximately unity and  $\phi$  nearly  $180^\circ$ , irrespective of the frequency and the magnitude of the grazing angle. This is the simplest situation to be encountered and most nearly approximates the idealized case of a perfect reflector with horizontal polarization. For this case  $\rho$  is exactly unity, and  $\phi$  is exactly  $180^\circ$ .

For vertical polarization over the sea or either type of polarization over ground, both  $\rho$  and  $\phi$  depart widely from unity and  $180^\circ$ , respectively. Variations in these quantities greatly complicate the calculation of coverage diagrams.

The reflection coefficient of microwaves is usually found to be small over land. This is essentially due to



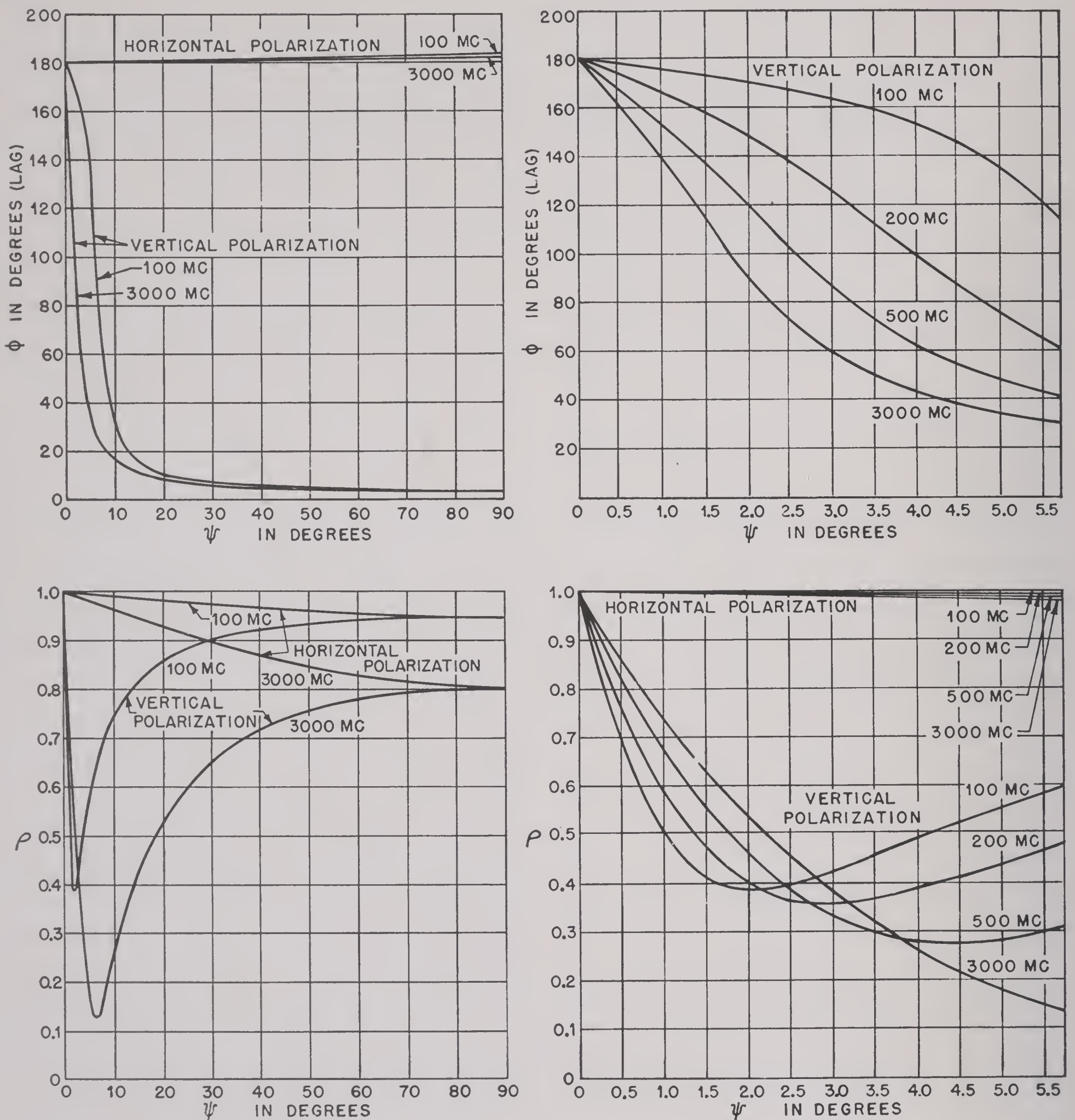


FIGURE 4. Phase and magnitude of reflection coefficient for sea water.

irregularities of the land surface. When these irregularities are sufficiently small, reflection from land is found to be considerable.

Since the receiver, or target, is usually located at a distance from the transmitter which is large in comparison to the height above the ground, the direct and reflected rays are very nearly parallel, making an angle  $\beta$  with the horizontal (Figure 2). The reflected ray may be supposed to issue from an image transmitter  $T'$ , which is as far below the ground as the

true transmitter is above it. The path difference between the direct and reflected rays is equal to the distance  $T'A$ . By the figure this is equal to  $2h_1 \sin \beta$ , where  $h_1$  is transmitter height. For small values of  $\beta$  this is practically equal to  $2h_1\beta$  if  $\beta$  is measured in radians. The corresponding phase shift due to path difference is equal to

$$\Psi = 2h_1\beta \frac{2\pi}{\lambda}.$$

At the point of reflection the phase of a ray changes



discontinuously by the amount  $\phi$ , which is the phase angle of the reflection coefficient. For horizontal polarization, to again take the simplest case, the phase shift  $\phi$  at reflection is practically  $180^\circ$ , or  $\pi$  radians. (For vertical polarization, see Figure 4,  $\phi$  is more complicated.) Adding the phase change  $\Psi$ , corresponding to difference in path length, gives the complete phase change  $\delta$  in the form

$$\delta = \Psi + \phi = 2h_1\beta \frac{2\pi}{\lambda} + \pi \text{ (for horizontal polarization).} \quad (3)$$

Maximum values of the earth gain factor  $G$  occur when  $\delta$  is an integral multiple of  $2\pi$ ; minimum values, for odd integral values of  $\pi$ . The corresponding values of the angle of elevation  $\beta$  are given by

$$\beta = \frac{\lambda}{4h_1} m \quad \begin{cases} m = 1, 3, 5, \dots & \text{(maxima)} \\ m = 0, 2, 4, \dots & \text{(minima)} \end{cases}$$

(for horizontal polarization.)

If the reflection coefficient  $F$  of the surface is assumed to be unity (see Figure 4) the plane earth gain factor  $G$ , from equation (2), reduces to

$$G = 2 \cos \left( \frac{\delta}{2} \right),$$

which fluctuates between the limits of 2 and zero.

The coverage diagram drawn for propagation over a perfectly conducting plane on horizontal polarization is illustrated in Figure 5. As an example, consider

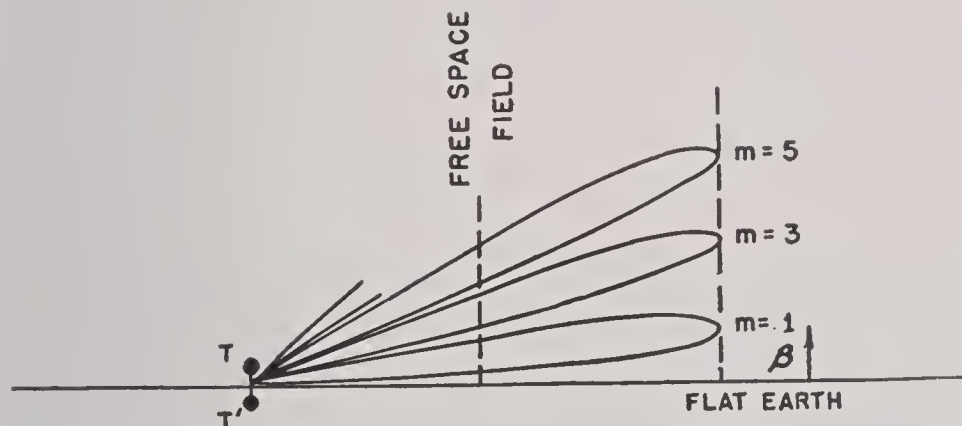


FIGURE 5. Simplified coverage diagram.

$f=200$  mc,  $\lambda=1.5$  m,  $h_1=30.5$  m. The values of  $\beta$  for the first three lobe maxima are  $0.68^\circ$ ,  $1.37^\circ$ , and  $2.05^\circ$ , and the maximum ranges are twice the free space values. The angles at which the minima occur lie half way between. The scale of vertical distances is greatly exaggerated compared with the horizontal scale. Coverage diagrams for the same frequency and transmitter height, but taking account of the earth's curvature, are shown in Figure 24.

Coverage diagrams for more complicated situations must take into account, in addition to the factors already mentioned, the curvature of the

earth, the refraction of the atmosphere, and diffraction into the region below the line of sight.

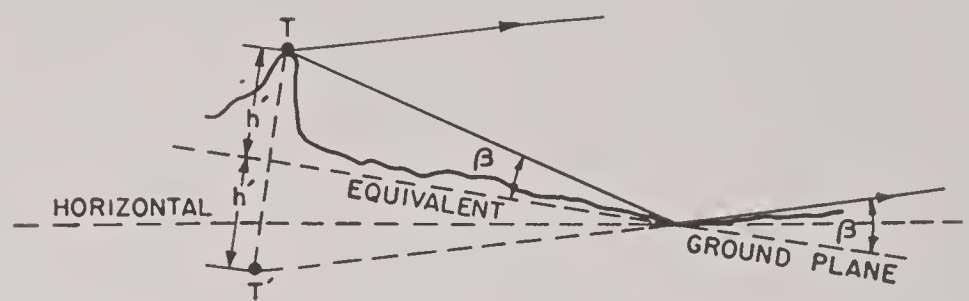


FIGURE 6. Use of equivalent ground plane.

When the ground is sloping, the above construction may be modified as indicated in Figure 6. For any specified lobe, determine approximately the part of the ground where reflection takes place. Draw a tangent to the ground in this region and determine the perpendicular projection of the antenna site on this plane ("equivalent ground"). Use the equivalent height thus determined in equation (3), and let the angle  $\beta$  refer to the plane of the equivalent ground. This procedure is also required when the transmitter and receiver or target are of comparable height so that the reflection point is not near the transmitter.

When the transmitter is set up near a coast, the lobe pattern over the ocean will undergo periodic variations caused by the tides. Since, in equation (3),  $\beta$  is multiplied by  $h_1$ , it follows that the lobes will be low at high tide and high at low tide. This phenomenon may become very important for heightfinding sets.

A more complicated case occurs if ground reflection is not complete. Then  $\rho$  is less than unity, and  $\phi$  differs from  $180^\circ$ . In this event the lobes have max-

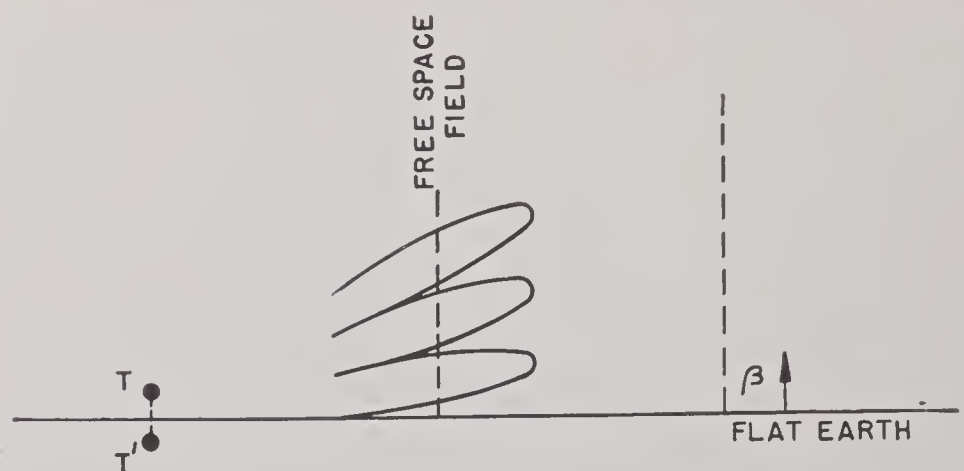


FIGURE 7. Coverage diagram for incomplete reflection.

ima which are less than twice the free space field and minima which never reach zero. The angular positions of the lobes are changed somewhat, but the most noticeable change is found on the lower side of the first lobe. It is likely to lie at a lower elevation and reaches the ground at some distance from the transmitter (compare Figures 5 and 7).



## 17.1.4

## Refraction—Snell's Law

The bending of rays in the atmosphere depends upon the refractive index  $n$  which is a function of the temperature, pressure, and moisture content of the air. The manner in which these quantities control the index of refraction is explained in Section 17.2.1. To a first approximation, assuming horizontal stratification of the atmosphere, the index may be considered to be a function only of height above the ground. The corresponding case, familiar in optics, is that of two media, such as water and air, with different refractive indices  $n_1$  and  $n_2$  (Figure 8A). If  $\alpha_1$  and  $\alpha_2$  are the angles between the rays and the plane of the boundary, Snell's law of refraction states that

$$n_1 \cos \alpha_1 = n_2 \cos \alpha_2 .$$

In the atmosphere the refractive index changes continuously with height. The simplest case, often

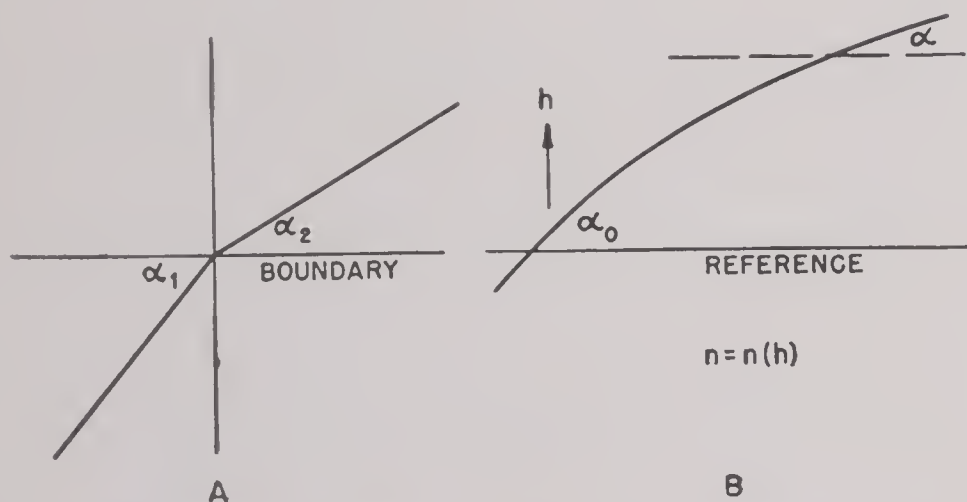


FIGURE 8. A. Refraction at a sharp boundary. B. Refraction through a layer with variable  $n$ .

encountered in practice, is that of a refractive index which decreases linearly with height. This is known as standard refraction. Snell's law applies here also, since the atmosphere may be divided up into an infinity of parallel boundaries, the change of refractive index from one boundary to the next being infinitesimally small. Instead of a sudden change of direction there is then a gradual change or bending of the rays (Figure 8B). Snell's law may then be stated generally as

$$n \cos \alpha = n_0 \cos \alpha_0 ,$$

where now  $n$  and  $\alpha$  are continuous functions of height and the zero subscript on the right-hand side refers to any fixed reference level. The curvature of the refracted rays is downwards or upwards according to whether the refractive index decreases or increases with height.

## 17.1.5

## Refraction over a Curved Earth

In reality the surfaces of constant refractive index are not planes but are concentric spheres about the earth's center. In this case Snell's law assumes a slightly different form. Instead of using angles referred to the plane surfaces it is now necessary to refer the angles to horizontal planes tangent to spheres about the center of the earth (see Figure 9). The new form, as given in Section 17.4, is

$$nr \cos \alpha = an_0 \cos \alpha_0 , \quad (4)$$

where  $r$  and  $a$  are values of the radius vector from the center of the earth to a point in the atmosphere and

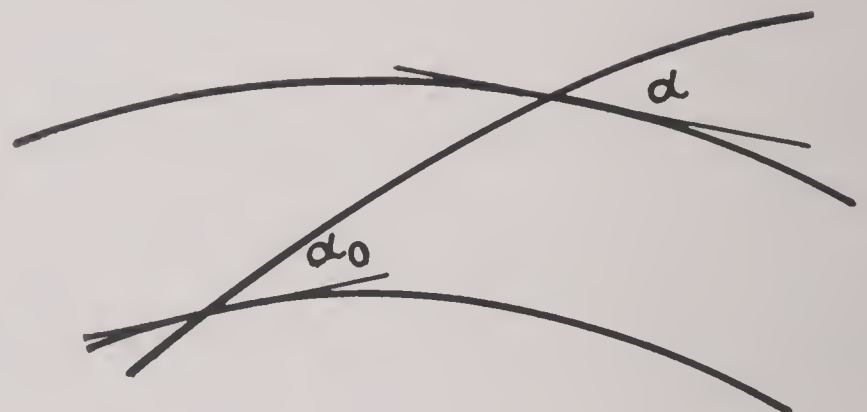


FIGURE 9. Refraction through a curved layer.

to the earth's surface, respectively.  $\alpha$  now stands for the angle formed by the ray with a plane normal to the radius vector.  $\alpha_0$  and  $n_0$  are the values of  $\alpha$  and  $n$  at the ground surface.

If  $h$  is the height above the ground surface, so that  $r = h + a$ , the above equation may also be written in the form

$$n \left( 1 + \frac{h}{a} \right) \cos \alpha = n_0 \cos \alpha_0 . \quad (5)$$

$h/a$  is a very small quantity, and  $n$  differs from unity by only a few parts in 10,000. Under these conditions  $n(1 + h/a)$  may be replaced by  $n + h/a$  with negligible error. The quantity  $n + h/a$  is called the modified refractive index, or the modified index for short. Equation (5) then assumes the form

$$\left( n + \frac{h}{a} \right) \cos \alpha = n_0 \cos \alpha_0 . \quad (6)$$

As a result of general agreement it is customary to use, instead of  $n + h/a$ , the symbol  $M$  defined as follows:

$$M = \left( n + \frac{h}{a} - 1 \right) 10^6 . \quad (7)$$

At the surface of the ground  $M$  reduces to

$$M_0 = (n_0 - 1) 10^6 . \quad (8)$$



Hence  $M$  is the excess of the modified refractive index above unity, measured in units of one millionth. This unit is called an  $M$  unit [MU]. Values of  $M$  for the atmosphere lie in the range of 200 to 500. Customarily  $M$  is referred to simply as the modified index of refraction.

Using the numerical value for the radius of the earth,  $6.37 \times 10^6$  m ( $21 \times 10^6$  ft), the rate of increase of  $M$  with height, owing to the term  $h/a$ , is  $(1/a) 10^6$ , which is equal to 0.157 MU per meter (0.048 MU per foot). As the result of a large number of experiments, carried out chiefly in the northern temperate latitudes, the rate of decrease with height of the refractive index has been found, on the average, to be

$$\begin{aligned} \frac{dn}{dh} 10^6 &= -\frac{1}{4} \frac{1}{a} 10^6 \\ &= -0.039 \text{ MU per meter.} \end{aligned} \quad (9)$$

This is the rate of decrease assumed for the standard atmosphere.

It will be noticed that the average rate of decrease of  $n$  with height is one quarter of the rate of increase of the term  $h/a$  which results from the curvature of the earth. The fact that these quantities are of comparable magnitude is of great importance, as will be seen later.

Consequently the vertical gradient of  $M$  for the standard atmosphere is

$$\begin{aligned} \frac{dM}{dh} &= \left( \frac{dn}{dh} + \frac{1}{a} \right) 10^6 \\ &= \left( \frac{3}{4} \frac{1}{a} \right) 10^6 = \frac{1}{\left( \frac{4}{3} a \right)} 10^6, \end{aligned} \quad (10)$$

which has the value 0.118 MU per meter (0.036 MU per ft). The value of  $M$  at any height, relative to the surface value  $M_0$ , for the standard atmosphere, is equal to

$$\begin{aligned} M - M_0 &= 0.118 h; \quad h \text{ in meters,} \\ M - M_0 &= 0.036 h; \quad h \text{ in feet.} \end{aligned} \quad (11)$$

17.1.6

### Equivalent Earth Radius— Flat Earth Diagram

An important conclusion may be drawn from equation (11). As will be shown in Section 17.2.4,  $dn/dh$  is the negative of the curvature of a ray in the atmosphere, and  $1/a$  is the curvature of the earth. The algebraic sum of these two quantities (their numerical difference) is the curvature of the ray relative to that of the earth. The net result is this: if

the earth is replaced by an equivalent earth with an enlarged radius equal to  $4a/3$  the rays may be drawn as straight lines. To state the result in another way: using the equivalent earth with radius equal to  $4a/3$  corresponds to replacing the actual atmosphere, in which the index  $n$  decreases with height, by a homogeneous atmosphere with an equivalent index  $n'$  which is independent of height (see Figures 10, 11, 13, 14, and 15). This transformation of coordinates greatly facilitates the calculation and interpretation of coverage diagrams for the standard atmosphere.

More generally, if the rate of change of  $n$  with height differs from the value  $-(1/4)(1/a) 10^6$  MU per meter given above, which may be true in certain parts of the world, the equivalent earth radius departs from the value  $4a/3$ . In general the equivalent earth radius is designated by  $ka$ . For a steeper drop of refractive index with height,  $k$  increases and becomes infinite when the curvature of the ray is just equal to the curvature of the earth.

In the general case, when  $k$  is not equal to  $4/3$ , equation (11) must be modified to the form:

$$\begin{aligned} M - M_0 &= \frac{h}{ka} 10^6, \\ &= 0.157 \frac{h}{k}; \quad h \text{ in meters,} \\ &= 0.048 \frac{h}{k}; \quad h \text{ in feet,} \end{aligned} \quad (12)$$

to account for a linear moisture gradient corresponding to a different value of  $k$ .

Since the change of the earth's radius takes care of the variation of refractive index and substitutes a homogeneous atmosphere for the actual atmosphere, it follows that in a diagram in which the earth is given a radius  $ka$ , the radiation propagates along

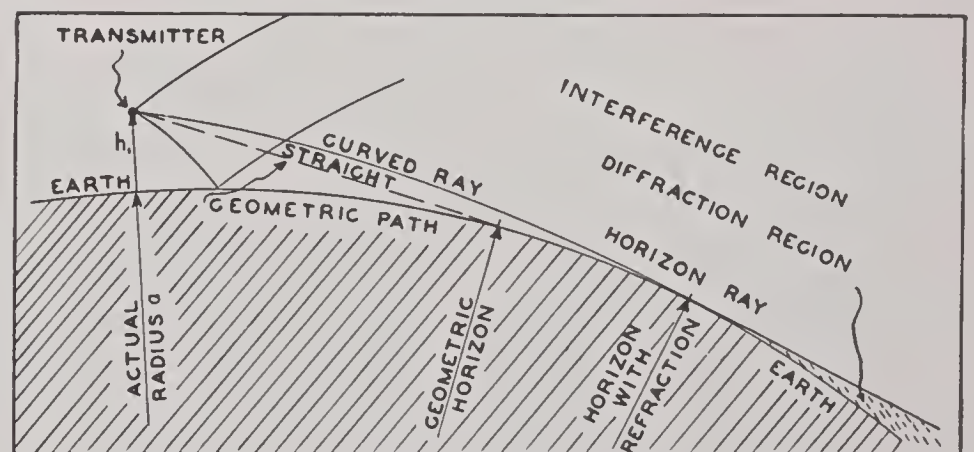


FIGURE 10. Ray curvature over earth of radius  $a$  in an actual atmosphere.

straight lines. The difference is illustrated in Figures 10 and 11. In Figure 10, which shows the true geo-



metrical conditions, the radio horizon appears extended as compared to the geometrical horizon, because of the curvature of the rays. In Figure 11 the rays have been straightened out, but a line that was straight in Figure 10 appears curved in Figure 11.

The value of  $\frac{4}{3}$  for  $k$  is a good average for the atmosphere in the middle latitudes. For particular

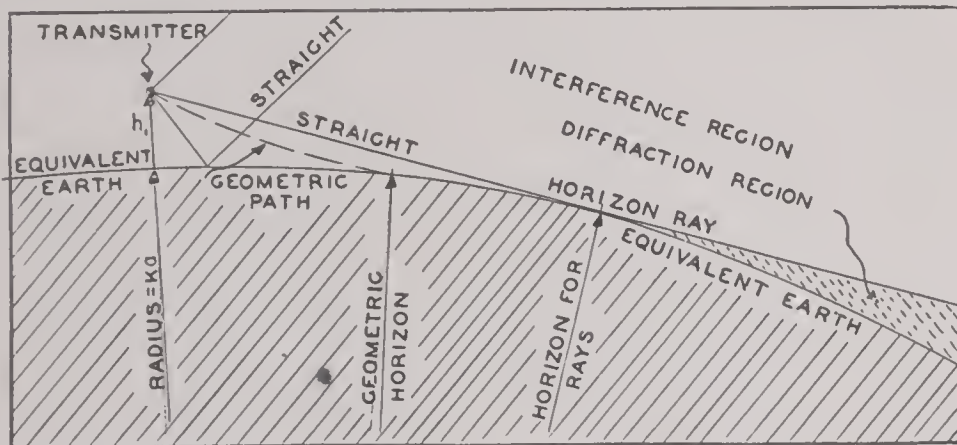


FIGURE 11. Rays in a homogeneous atmosphere. Equivalent radius  $ka$ .

atmospheric conditions the value of  $k$  may be considerably different. The moisture content of the atmosphere is small at the low temperatures of the arctic regions and increases considerably with the higher temperatures of the tropics. However, the

value of  $k$  depends more particularly on the manner in which the moisture content varies with height above the surface of the earth, and to a lesser extent on the distribution of temperature with height. Figure 12 has therefore been constructed to show the dependence of  $k$  on the gradient of relative humidity, measured in per cent per 100 m, for a series of surface temperatures varying between  $T_0 = -30^\circ\text{C}$  and  $T_0 = +40^\circ\text{C}$ . It has been found convenient to plot  $1/k$  rather than  $k$  itself. The lines drawn correspond to the assumption of saturation humidity at the ground; if the humidity at the ground is less than 100 per cent the correction read from the auxiliary table is added to the value of  $1/k$  obtained from the graph. The standard temperature gradient of  $-0.65^\circ\text{C}$  per 100 m is assumed for all the curves.

The curves of Figure 12 indicate that as the temperature increases, smaller and smaller values of relative humidity gradients are required to produce changes in  $k$  of considerable magnitude. This should be of greater importance in the tropics where the moisture content is relatively high.

Changing  $k$  from its standard value of  $\frac{4}{3}$  has an important influence on the strength of the field at any

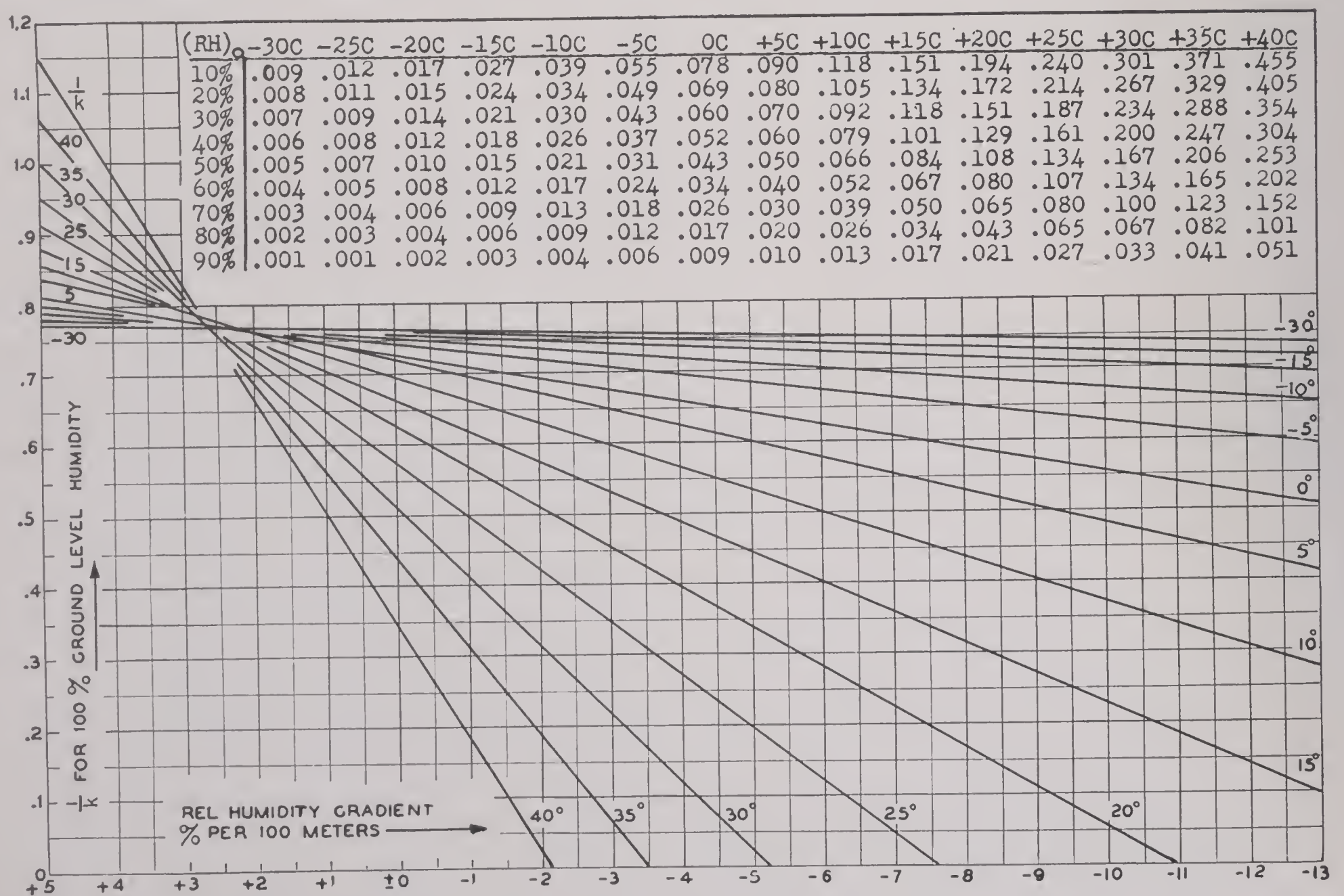


FIGURE 12. Graph:  $1/k$  versus RH gradient and temperature for 100 per cent RH at ground.



point in space. Though it is not easy to state the result in general terms for any position, it is possible to evaluate the change in field strength near the surface (below 60 m altitude for 600 mc and somewhat higher for lower frequencies) and well within the diffraction region, for moderate changes in  $k$ . Here the decibel attenuation below that for the free space field is decreased approximately in the ratio  $k^{\frac{2}{3}}$ . If, for instance,  $k$  changes from  $\frac{4}{3}$  to 8, the original decibel attenuation is to be divided by 3.3. To state the matter another way, the range at which a given field strength is found will be increased approximately in the ratio  $k^{\frac{2}{3}}$ . This has an important bearing on the problem of propagation for communication purposes in this region.

It has been shown above that a linear variation of refractive index can be converted into a change of earth's curvature. The reverse process is equally feasible: to eliminate the earth's curvature by using a modified refractive index curve. This is a general procedure which involves no assumption about the variation of refractive index with height. From the equations in Section 17.1.6 it is seen that the effects of the earth's curvature are equivalent to those of a refractive index increasing linearly with height at the rate of  $1/a$ . Hence one effectively flattens the earth, thus eliminating the curvature effect, by adding to the refractive index the term  $h/a$ . In other words, the angles between a ray and the horizontal over a curved earth are the same as the angles between a ray and the horizontal over a flat earth when the refractive index  $n$  has been replaced by  $n + h/a$ . In practice, the quantity  $M$  defined by equation (7) is used. If  $M$  increases steadily with height, which is the case for the standard atmosphere, the rays appear curved upwards on a flat earth diagram, which is illustrated in Figure 13.

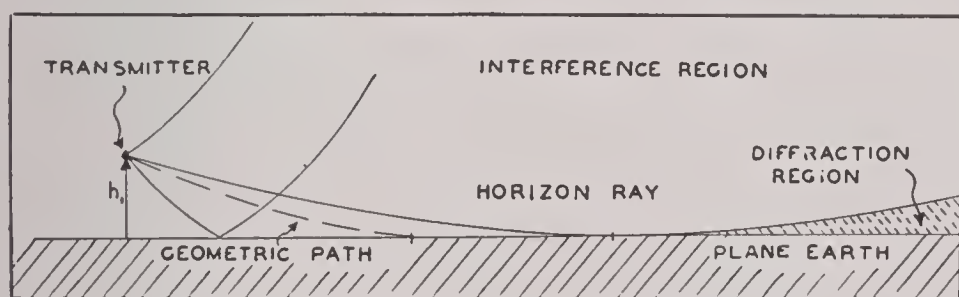


FIGURE 13. Rays in a plane earth diagram.

Summarizing, it is seen that three types of graphical representations of a coverage diagram may be used. (These are illustrated in Figure 14 for the lowest lobe.)

1. The true geometrical representation. With

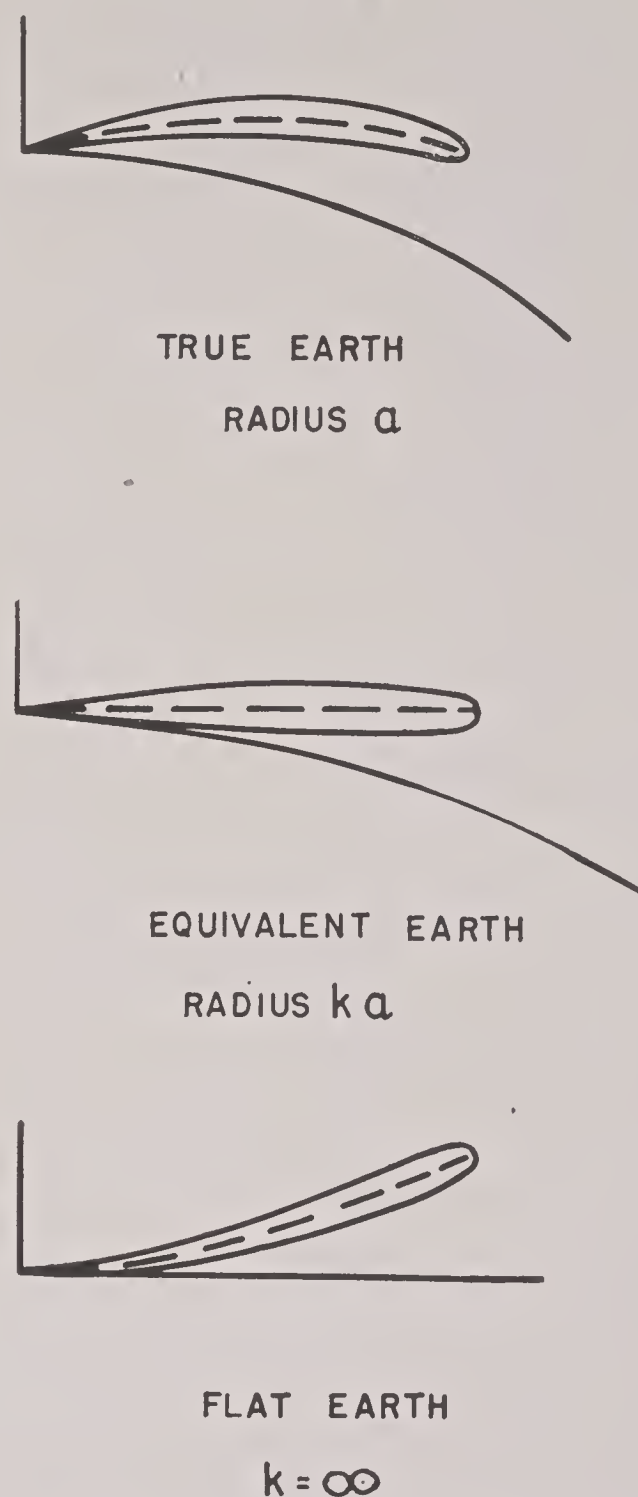


FIGURE 14. Shape of lobes as affected by method of representation.

standard refractive conditions the lobes appear bent downwards. Refractive index  $n$  decreases with height.

2. The equivalent earth radius representation. Earth's radius changed to  $ka$  (normally  $k = \frac{4}{3}$ ). For standard refractive conditions the lobes appear straight. Equivalent refractive index  $n'$  is independent of height since the equivalent atmosphere is homogeneous.

3. The flat earth representation. The earth's surface and other surfaces of constant height have been flattened out. For standard refractive conditions the lobes appear bent upwards. Excess modified index  $M$  increases with height.

The quantities  $n$ ,  $n'$ , and  $M$  for these three cases are illustrated in the left-hand series of diagrams in Figure 15.

17.1.7

### The Horizon—Diffraction

From simple geometrical considerations it can be



shown that two points at elevations  $h_1$  and  $h_2$  are within sight of each other when their distance is less

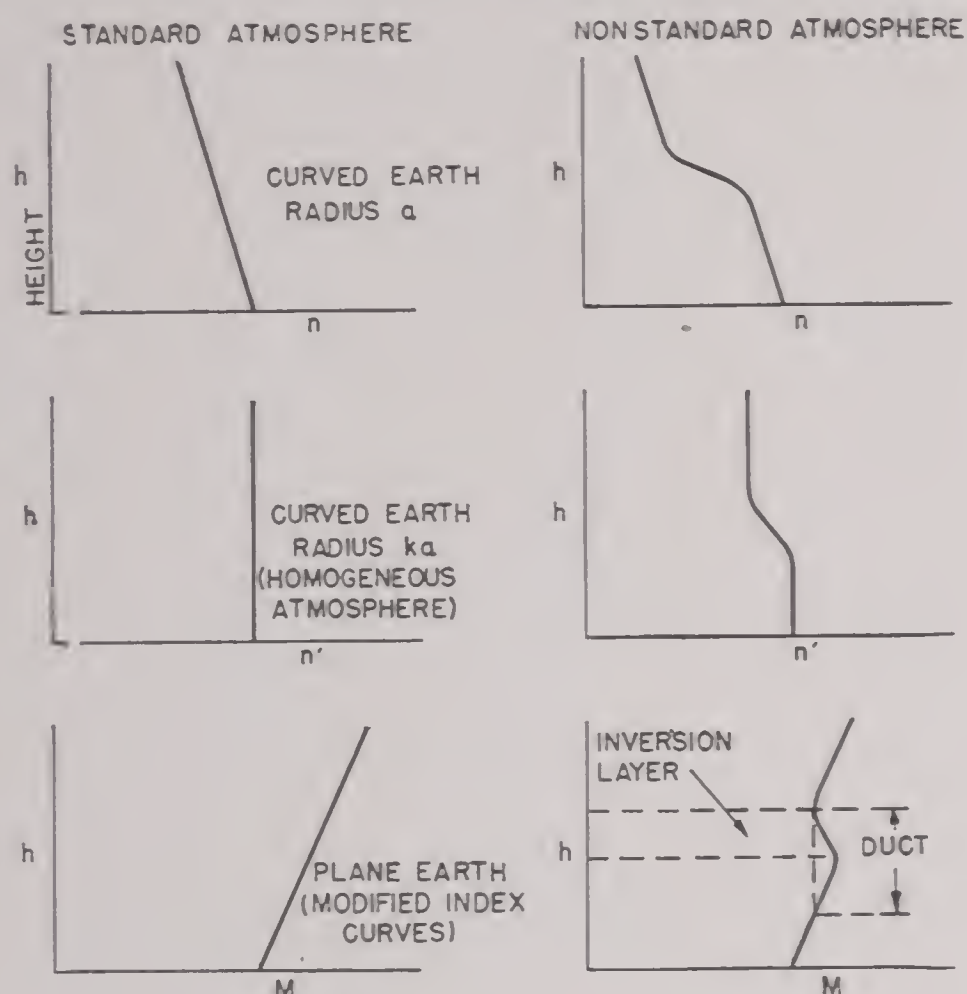


FIGURE 15. Types of index curves.

than the horizon distance  $d_h$  (Figure 16) given by

$$d_h = \sqrt{2ka h_1} + \sqrt{2ka h_2}, \quad (13)$$

where  $d_h$ ,  $a$ , and  $h$  are all expressed in the same units.

For the particular value of  $k = \frac{4}{3}$ ,

$$d_h = \sqrt{17h_1} + \sqrt{17h_2}, \quad (14)$$

where  $d_h$  is measured in kilometers and  $h$  is in meters; and

$$d_h = \sqrt{2h_1} + \sqrt{2h_2}, \quad (15)$$

where  $d_h$  is given in statute miles and  $h$  in feet.

The field strength at different elevations  $h_2$  (Figure 16) for a given range varies in the manner illustrated in Figure 17. The field is given in decibels, relative to the intensity at 1 m from the transmitter, for a range of 50 miles over sea water for frequencies of 100, 200, 500, and 3,000 mc. The horizon elevation for this point is 888 ft. Above point  $P$  in Figure 16, is the interference region where, with increasing height, the

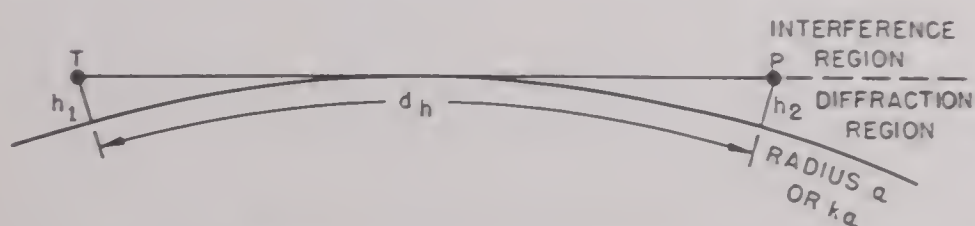


FIGURE 16. Horizon distance.

field strength first increases rapidly and then oscillates between maxima and minima determined by the lobe patterns of the coverage diagrams.

Below point  $P$ , the field strength declines rapidly

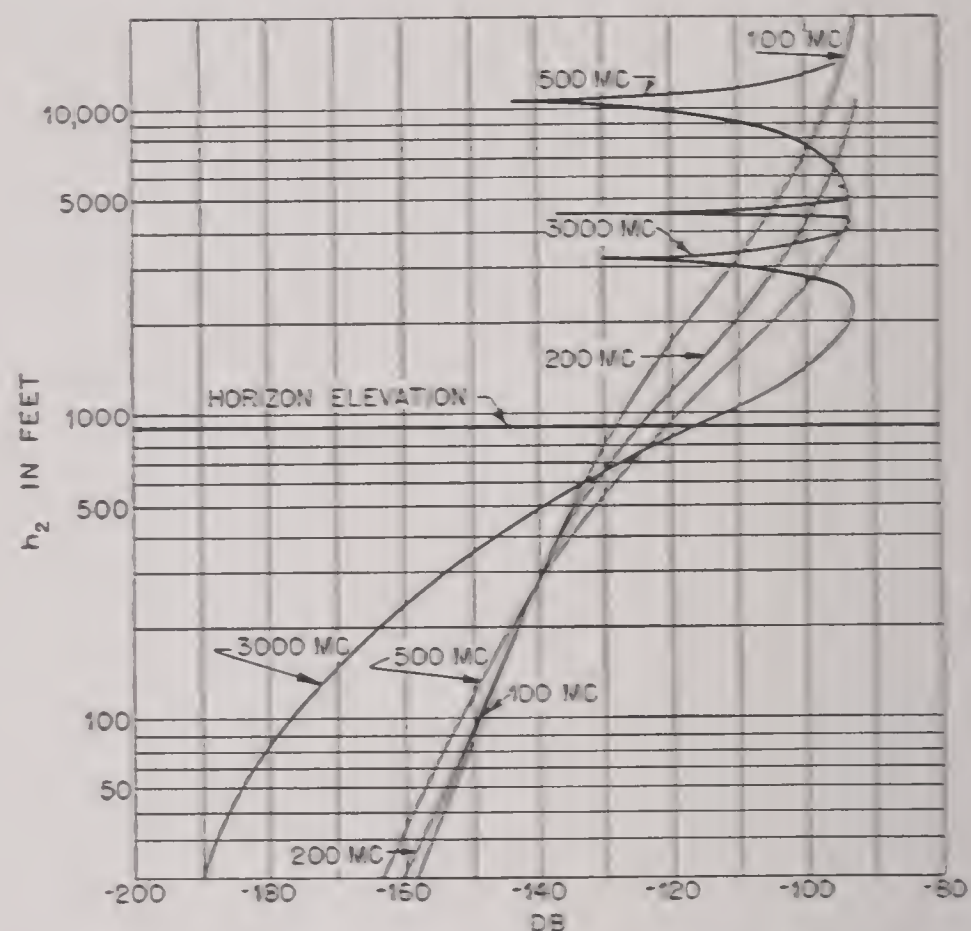


FIGURE 17. Diffraction and interference fields at height  $h_2$ . Field strength at 50 statute miles over sea water in db relative to field at 1 m from transmitter. Horizontal polarization. Transmitter height 30 feet.

with decreasing height to a minimum at ground level; the rate of decrease is larger for the higher frequencies. Neither the direct nor the reflected rays can penetrate into this region, which therefore, receives radiation entirely by diffraction of the energy around the earth's curvature.

Radar targets are rarely visible when they are in the diffraction region. This is certainly true for airplane targets. Very large targets, such as warships or islands, are occasionally visible in this region; but more often the detection of targets is caused by superrefraction. For communication work, on the other hand, the diffraction region is of importance, especially at the longer wavelengths.

## 17.2 ATMOSPHERIC STRATIFICATION AND REFRACTION

### 17.2.1 Origin of Refractive Index Variations

The variation with height of the index of refraction  $n$  controls the curvature of rays in the atmosphere. The value of  $n$  exceeds unity by only a few hundred



parts in a million and may be computed from the following formula:

$$(n - 1) 10^6 = \frac{79p}{T} - \frac{11e}{T} + \frac{3.8 \times 10^5 e}{T^2} \quad (16)$$

in which  $n$  = index of refraction at height  $h$  above ground;

$p$  = barometric pressure of the atmosphere in millibars at height  $h$ . (1 mm Hg pressure = 1.334 mb);

$e$  = partial pressure of the water vapor in millibars (order of 1 per cent of  $p$ );

$T$  = absolute temperature ( $^{\circ}\text{C} + 273$ ) at height  $h$ .

In equation (16) the term  $11e/T$  is very small in comparison with the other terms and may, without serious error, be neglected. This simplification has been used in obtaining the values in the last two columns of Table 1 and in designing the nomogram, Figure 19.

Workers in the field may prefer to use mixing ratio (practically equal to specific humidity) in place of the water vapor pressure. The relation is given by

$$e = 0.00161 ps \quad \text{or} \quad s = \frac{621e}{p}, \quad (17)$$

where  $s$  is in grams of water per kilogram of air.

The variation of  $n$  with temperature and relative humidity for an air pressure of 1,000 mb is illustrated in Figure 18. It is seen that the refractive index depends on humidity more critically than on temperature. The dependence on humidity is greater at the higher temperatures where a given relative humidity represents a larger amount of water vapor.

In practice it is customary to use the modified refractive index given by

$$M = \left( n + \frac{h}{a} - 1 \right) 10^6 \cong \frac{79p}{T} + \frac{3.8 \times 10^5 e}{T^2} + 0.157h \quad (h \text{ in meters}).$$

TABLE 1. Standard atmosphere with 60 per cent relative humidity.

NACA standard atmosphere				Moist standard atmosphere		
Altitude, meters	Temp, $^{\circ}\text{C}$	Dry air pressure, mb	Dry air index, $(n - 1)10^6$	$e(\text{mb})$ for 60% RH	Moist air index, $(n - 1)10^6$	$M = (n + h/a - 1)10^6$
0	15.0	1013	278	10.2	325	325
150	14.0	995	274	9.6	318	342
300	13.0	977	270	9.0	312	359
500	11.7	955	265	8.3	304	382
1000	8.5	894	251	6.7	283	440
1500	5.2	845	240	5.3	266	501

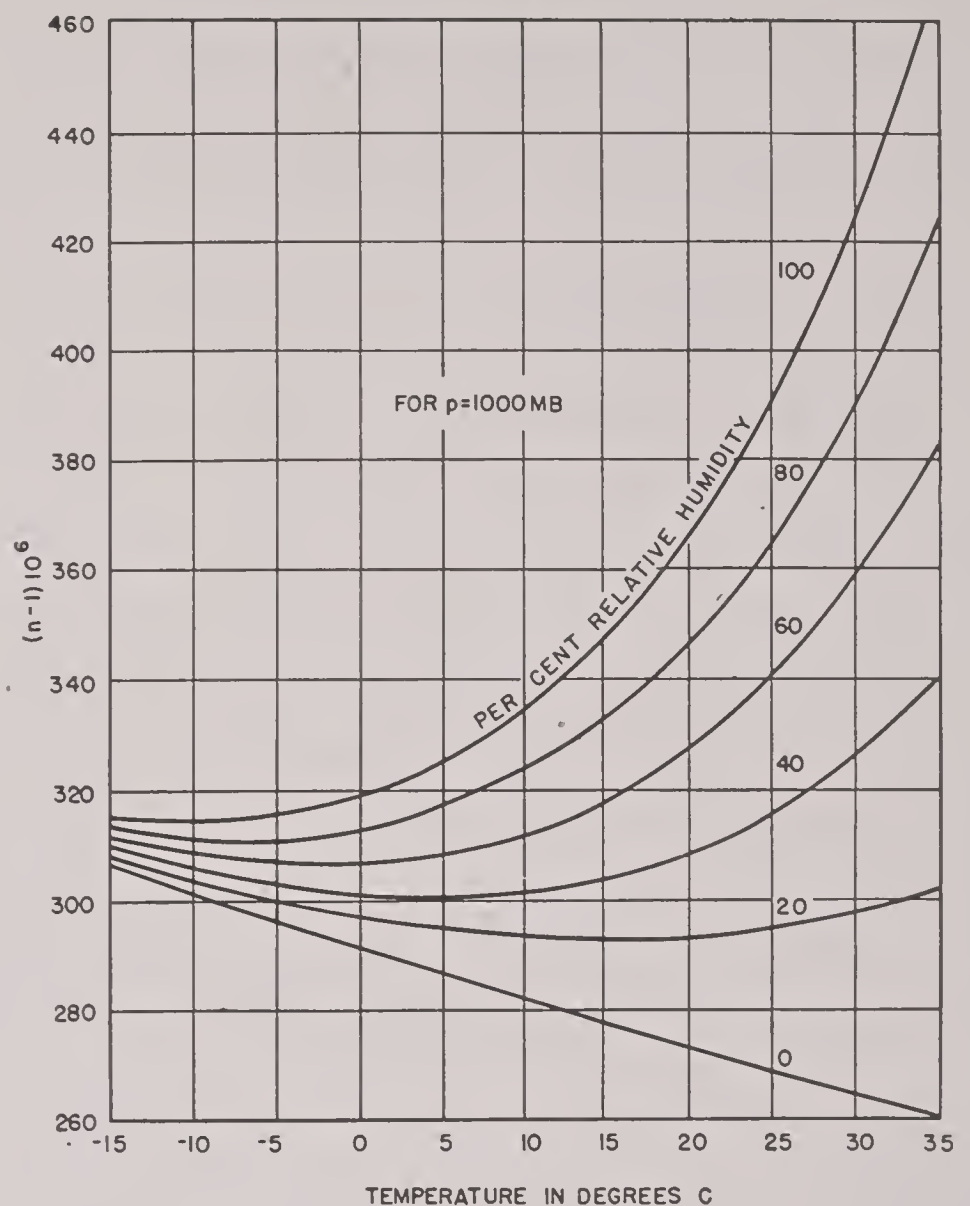


FIGURE 18. Relation of  $n$  to temperature and relative humidity.

In order to compute  $M$  directly from temperature, relative humidity, and height data, the nomogram (Figure 19) has been constructed. Detailed instructions for its use are given.

The National Advisory Committee on Aeronautics [NACA] standard atmosphere commonly used in aeronautics assumes a sea level pressure of 1,013 mb (= 760 mm Hg) and a sea level temperature of  $15^{\circ}\text{C}$ , decreasing at a rate of  $6.5^{\circ}\text{C}$  per kilometer in the lower atmosphere. The NACA standard atmosphere is not concerned with the moisture content. In the actual atmosphere the moisture may vary between extremely wide limits, but as a typical value a relative humidity of 60 per cent may be assumed as the



standard condition. This corresponds to a water vapor pressure of approximately 10 mb at sea level and a rate of decrease of water vapor pressure in the lower levels of about 1 mb per 1,000 ft. At higher levels the rate of decrease of the water vapor pressure is less rapid. These conditions are represented in Table 1 for the atmosphere up to 1,500 m.

Both the dry and the moist standard atmosphere exhibit a very nearly linear increase of  $M$  with height. According to equation (12),

$$M - M_0 = \frac{h}{ka} \cdot 10^6 = 0.157 \frac{h}{k}; \quad h \text{ in meters.}$$

By using this formula in conjunction with Table 1 it is easily shown that  $k = \frac{6}{5}$  for the dry standard atmosphere, and  $k = \frac{4}{3}$  for the standard atmosphere with a 60 per cent relative humidity. This value of  $k$  is the one commonly adopted in coverage diagrams corrected for standard refraction.

Because of the great variability of the moisture content of the atmosphere with season, geographical location, etc., a moist standard atmosphere has a limited physical significance. The standard should rather be defined in terms of a fixed linear slope of the refractive index, and for this purpose the value  $k = \frac{4}{3}$  has been chosen.

### 17.2.2 The Measurement of Refractive Index

The lower atmosphere frequently is stratified by nonstandard distributions of temperature and humidity which vary rapidly and irregularly as functions of the height. The refractive index is then no longer linear but has a more complicated dependence on height, determined from equation (16). The stratification which is of particular importance in tropospheric propagation is found in the lower part of the atmosphere, that is, below about 4,000 to 5,000 ft and frequently in the lowest few hundred feet above ground.

Since the variation in the atmospheric pressure gradient is small, interest is mainly centered in the dependence of the modified refractive index  $M$  on the temperature and humidity distributions. Methods, useful in the field, have been developed for obtaining rapid determinations of temperature and humidity in the lowest levels of the atmosphere. The ordinary radiosonde (radiometeorograph) is not well adapted for this purpose since it is usually designed to give data at levels about 100 m apart, which often is not

close enough to reveal the significant details of the  $M$  curve. Consequently it has proved to be necessary to develop new instruments for this purpose.

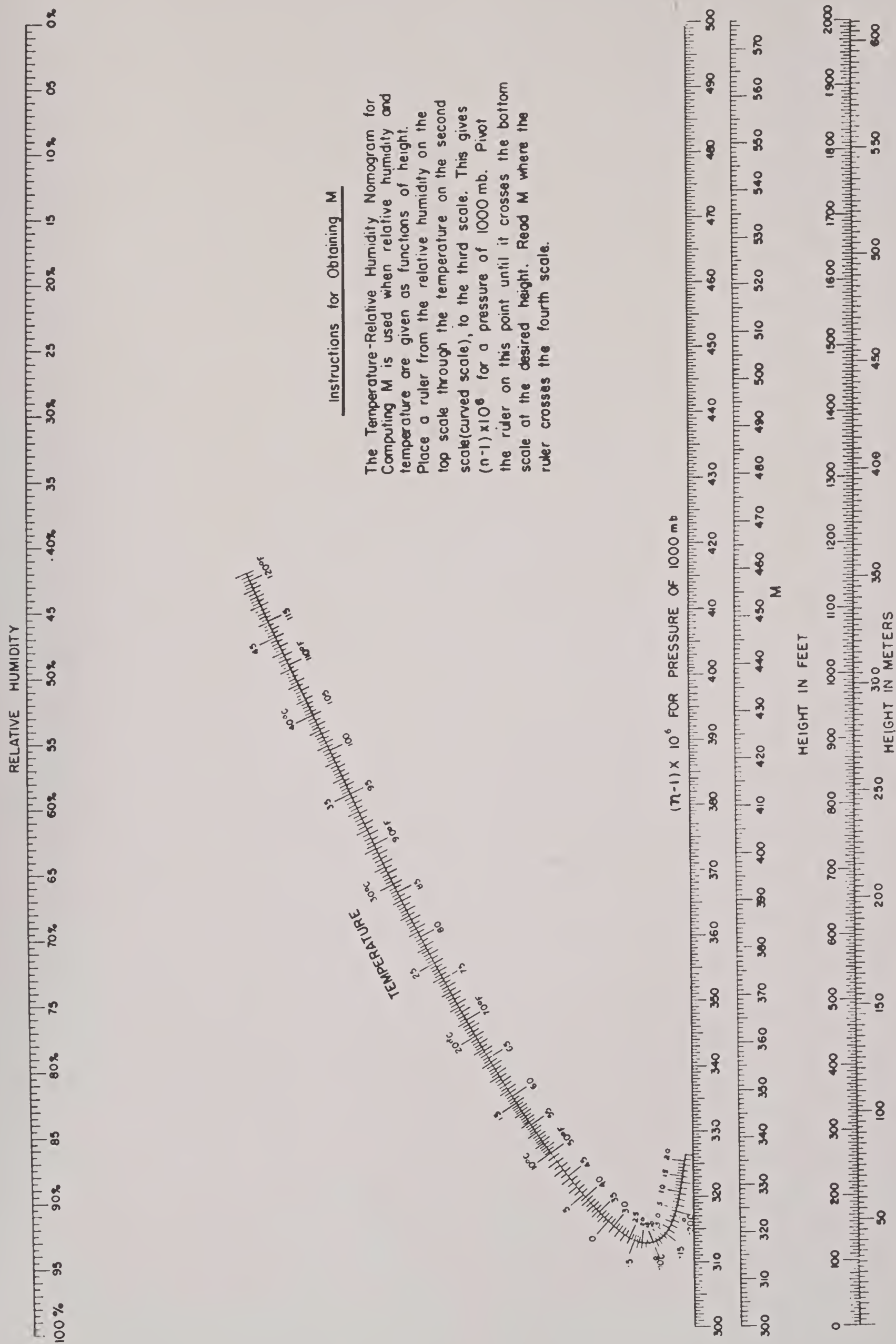
Several types of instruments have been designed which can be placed on towers, or carried by slow-flying airplanes or dirigibles or carried aloft by captive balloons or kites with wires connecting the temperature and humidity elements to measuring or recording equipment located on ground or aboard ship.

Some such measurements have been made with instruments using electrical methods in which dry and wet electrical resistance elements are connected into a circuit to give "dry bulb" and "wet bulb" temperatures. Another electrical method uses the same "dry" temperature element but, in place of the wet bulb, obtains a relative humidity measurement by using an electrolytic humidity element of the type employed in the U. S. Weather Bureau radiosonde. Hair hygrometers are definitely not suitable for this type of work on account of their lag in adjusting themselves to changes in relative humidity (of the order of 3 to 5 min for appreciable changes in humidity).

Measurements made from airplanes have the advantage that it is possible to survey a comparatively large area within a short time. This can be of great importance along coasts where conditions in the lowest levels of the atmosphere sometimes change rather rapidly with increasing distance from the shore. In the absence of suitable special equipment an ordinary psychrometer held out of the window of a plane will give quite satisfactory results in slow-flying planes, providing care is taken to keep the wet bulb sufficiently moist. When measurements are made from an airplane the height above the ground is determined for each measurement by means of the plane's altimeter. Unless carefully done this introduces the possibility of considerable error.

In another method captive balloons, kites, ordinary radiosonde balloons, and, occasionally, barrage balloons have been used to carry the measuring elements aloft. Ordinary captive balloons will work in wind speeds up to about 8 miles per hour; in higher winds kites or, occasionally, barrage balloons are used. Kites can be flown from boats even at low wind speeds or in calm weather. With this type of equipment the electrical measuring elements aloft are connected to an indicating or recording instrument at the ground or aboard ship by means of fine insulated wires that are wound around the cable holding the balloon.



FIGURE 19. Temperature-relative humidity nomogram for computing  $M$ .



### 17.2.3 Types of Modified Index Curves

A large number of meteorological soundings of the lower atmosphere have been carried out by several laboratories and Service units. From these measurements the modified index curves have been calculated as a function of height, and it has been shown that practically all these curves fall into one of the six types illustrated in Figure 20.

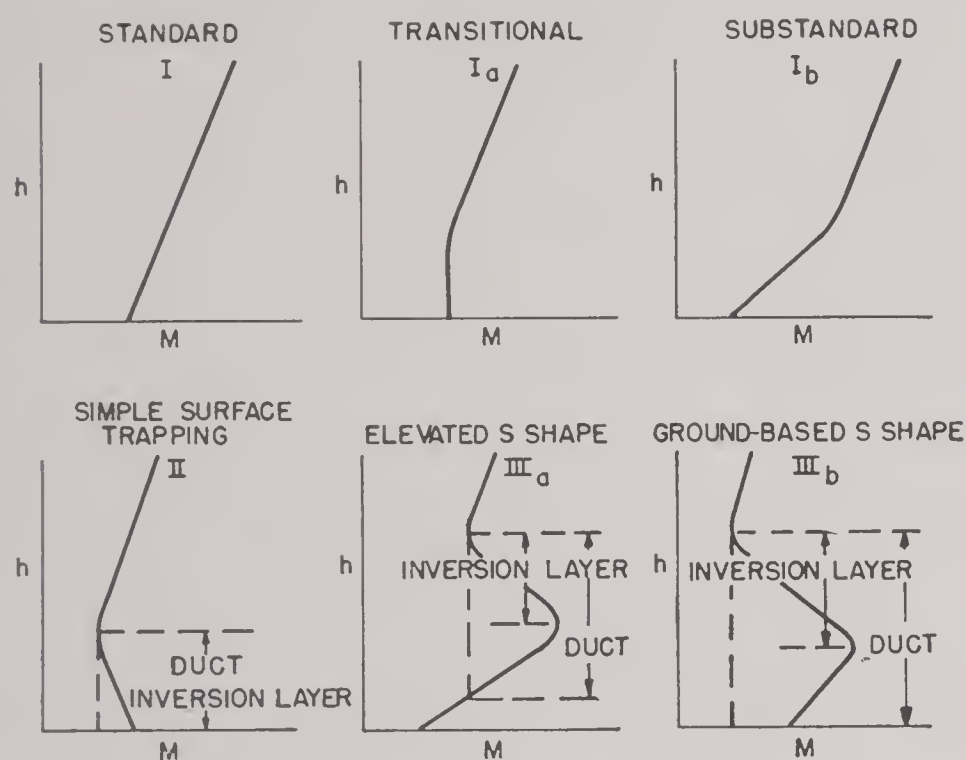


FIGURE 20. Types of  $M$  curves.

For the standard atmosphere the  $M$  curve increases with height as shown in curve I. For nonstandard atmospheres, the  $M$  curves will take one or another of the forms illustrated in curves Ia, Ib, II, IIIa, and IIIb. Of particular interest are those curves in which  $M$  decreases with height for a range of altitudes. (This decrease is the result of a sufficiently sharp decrease in  $n$  with height as illustrated in Figure 15.) In this event an inversion layer is formed in the atmosphere.

Throughout the range of altitudes of decreasing  $M$  the curvature of the rays exceeds the curvature of the earth. Nearly horizontal rays which either originate in, or penetrate into, this layer are trapped, and, if the layer extends far enough, energy may be carried to distances far beyond the geometrical horizon. However, the region in which the waves or rays are trapped may have a thickness or depth exceeding that of the inversion layer. This region is known as a duct. Its precise definition may be taken from Figure 20. It is the strip between an upper minimum of the  $M$  curve and either the ground or the point where the vertical projection from the upper minimum intersects the  $M$  curve. There are two main types of ducts, the ground-based duct,

illustrated by curves II and IIIb, and the elevated duct, illustrated by curve IIIa.

The height in the atmosphere at which the variations in refractive index occur may vary from a few feet to several hundred or even a few thousand feet. These variations are likely to be found at fairly low elevations in cold climates and at the higher elevations in warm climates. The meteorological conditions which yield these various  $M$  curves are described in Section 17.3.

The opposite effect occurs when the  $M$  curve takes the substandard form (curve Ib in Figure 20). Here the lower portion of the  $M$  curve has a slope which is less than standard. In this event the rays in the lower atmosphere are bent downward to a lesser degree than in the standard atmosphere or may even be bent upward. Depending to some extent upon the elevation of the transmitter, the field strength in the substandard region may be reduced considerably below normal, even to the point of producing a radar and communication "blackout." If the  $M$  curve is steeper than average in the lowest layers, the transitional case arises (curve Ia). Here a slight change in the temperature and moisture distribution might lead to a curve of type II and a duct.

### 17.2.4 Rays in a Stratified Atmosphere

Nonstandard vertical variations of refractive index occur frequently in the lower atmosphere. In addition there may be gradual variations in the horizontal direction. So far, the theory of propagation has not reached a stage where such horizontal variations can be taken into account. Unless otherwise stated it is always assumed that the stratification extends horizontally as far as the coverage of the transmitter and that the variation in the  $M$  curve is entirely vertical. Weather conditions often are sufficiently homogeneous horizontally to warrant this assumption, but there are exceptions, mainly near coasts (see Section 17.3).

Only those rays are affected by the vertical variations of refractive index in the lower atmosphere which leave the transmitter at a very small angle. Both theoretically and practically it has been found that the effects of nonstandard refraction are negligible for rays that leave the transmitter at an angle with the horizontal of more than about  $1.5^\circ$ . Rays that leave at an angle with the horizontal of less than  $1.5^\circ$ , and especially those emerging at angles



with the horizontal of  $0.5^\circ$  or less, are strongly affected by nonstandard refraction. This part of the transmitter radiation is of paramount importance in early warning radar and in communications. For such applications of radar as gun-laying or search-light control the effects of nonstandard propagation are usually negligible because the rays which reach the target have emerged from the transmitter at a fairly large angle with the horizontal.

The progress of a ray through the stratified atmosphere is described by Snell's law, discussed in Section 17.1.4. When the angle  $\alpha$  between the ray and the horizontal is small

$$\cos \alpha = 1 - \frac{\alpha^2}{2},$$

provided  $\alpha$  is expressed in radians.

Introducing this into Snell's law for a curved earth, equation (6), noting that  $n + h/a = 1 + M \cdot 10^{-6}$  and neglecting second order quantities, it is seen that

$$\frac{1}{2} (\alpha^2 - \alpha_0^2) = (M - M_0) 10^{-6}. \quad (18)$$

Since  $\alpha$  is the angle which the ray makes with the horizontal it is equal to  $dh/dx$ , the slope of the ray. Solving equation (18) for  $\alpha$ ,

$$\alpha = \frac{dh}{dx} = \sqrt{\alpha_0^2 + 2(M - M_0) 10^{-6}}. \quad (19)$$

These relations apply to *any two* levels provided  $\alpha$  and  $\alpha_0$  are the angles at the levels to which  $M$  and  $M_0$  refer.

variations of the modified index. Although this ray tracing method is only an approximation of the true solution of the wave equation, it can be used, subject to certain limitations, for computing quantitatively the strength of the field. The approximation breaks down when *neighboring* rays cross each other and form caustics.

The method may be illustrated by the case of standard refraction with  $k = 4/3$ . As shown in Figure 21, draw the  $M$  curve with a slope  $ka = 4a/3$ . Let the subscript 1 stand for the transmitter level (of height  $h_1$ ). Pass a vertical line through the corresponding point  $M_1$  of the  $M$  curve. Lay off the distance  $\alpha_1^2/2$  to the left of  $M_1$  for a particular ray, 1, which emerges from the transmitter at angle  $\alpha_1$  with the horizontal. In order to make  $\alpha$  and  $M$  comparable numerically, the factor  $10^{-6}$  should be eliminated from equation (18) above. For this purpose  $\alpha^2$  should be measured in the same unit as  $M$ , that is, in  $10^{-6}$  radian. The distance between  $M$  and 1 at any height  $h$  then is equal to  $(M - M_1) + \alpha_1^2/2$ , and by equation (19) the square root of twice this quantity is equal to the slope of the ray at height  $h$ . Hence, ray 1 starting downward from the transmitter is bent more and more toward the horizontal as  $h$  decreases. At point  $P$  this ray becomes horizontal and from there on increases in slope with increasing height.

Ray 1' starting upward from the transmitter at the same angle  $\alpha_1$  continues to curve upward more and more rapidly as the height increases. Ray 2 is the

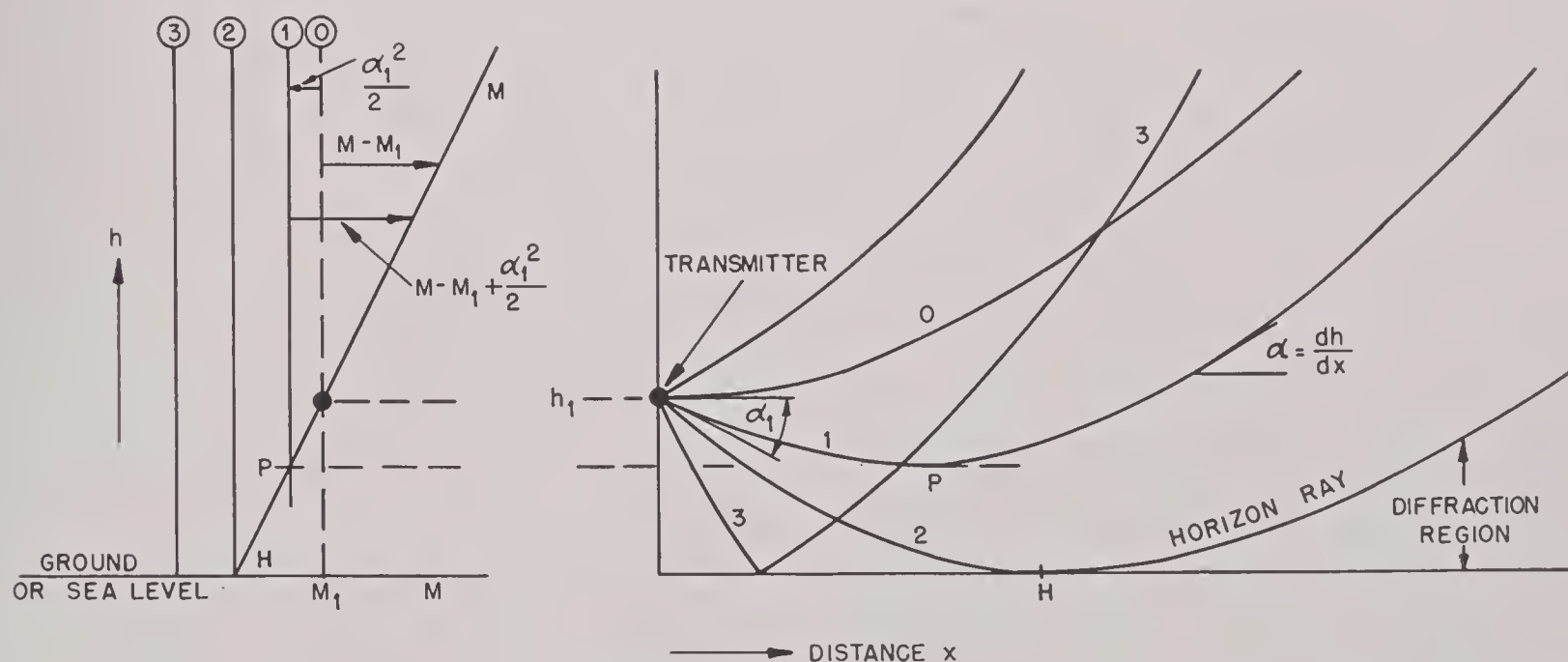


FIGURE 21. Rays in the standard atmosphere.

Equation (19) provides a technique for tracing the paths of rays emitted by a transmitter at various angles with the horizontal, and it indicates how their passage through the atmosphere is controlled by the

horizon ray which represents the limit to which rays can be directed by refraction. Beyond this lies the diffraction region where ray tracing cannot be used. To study the field in the diffraction region the original



wave equation must be used. Ray 3 is reflected from the ground and in crossing some of the other rays produces the phenomenon of interference. In connection with Figure 21 it must be emphasized that the height scale is tremendously exaggerated and that all the rays shown come from a small group which are propagated in a nearly horizontal direction.

Sometimes it is convenient to express the path of the ray in terms of ray *curvature*. The true curvature of a ray as it appears on an undistorted (curved earth) diagram is different from the curvature exhibited by a ray on a plane earth diagram. The true curvature of a ray is given by  $1/\rho$ , where  $\rho$  is the radius of curvature, and it can be shown that, for nearly horizontal rays, this is related to the gradient of  $n$  by

$$\frac{1}{\rho} = -\frac{dn}{dh}. \quad (20)$$

However, the relative curvature of the earth with respect to that of a ray is  $(1/a) - (1/\rho)$ . Now let us set this equal to the curvature  $1/ka$  of an equivalent earth. Then

$$\frac{1}{a} - \frac{1}{\rho} = \frac{1}{ka}, \quad (21)$$

and, introducing equation (20),

$$k = \frac{1}{1 - \frac{a}{\rho}} = \frac{1}{1 + a \frac{dn}{dh}}. \quad (22)$$

This amounts to a definition of  $k$  which is more general than the one introduced in Section 17.1.6 but reduces to the latter when the index curve varies linearly with height.

For a plane-earth diagram,  $M$  is used in place of  $n$ . Since

$$M = \left( n + \frac{h}{a} - 1 \right) 10^6,$$

$$\frac{dM}{dh} = \frac{1}{a} \left( a \frac{dn}{dh} + 1 \right) 10^6.$$

Substituting the last equation into equation (22) gives

$$k = \frac{1}{a} \frac{dh}{dM} 10^6 \quad (23)$$

and shows that  $k$ , in its most general form, is proportional to the slope of the  $M$  curve. Reference to Figure 20 shows that  $k$  assumes negative values for a range of altitudes whenever a duct is formed in the atmosphere.

These relations may also be expressed in terms of  $m$ , where

$$m = \frac{\rho}{a} \quad (24)$$

is the ratio of the radius of curvature of a ray to the radius of the earth. From equation (22) it follows that

$$\frac{1}{k} + \frac{1}{m} = 1. \quad (25)$$

Both  $k$  and  $m$  vary with height except in the special circumstance that the  $M$  curve is linear. Table 2 gives a number of corresponding values of  $k$  and  $m$  and indicates their significance.

TABLE 2. Relation of  $k$  and  $m$ .

$k$	1	$\frac{6}{5}$	$\frac{5}{4}$	$\frac{4}{3}$	2	$\infty$	-2	-1
$m$	$\infty$	6	5	4	2	1	$\frac{2}{3}$	$\frac{1}{2}$
		U.S. Standard		Brit. Standard	Moist standard	Zero relative curvature	Duct formation	

17.2.5

### The Duct—Superrefraction

When the  $M$  curve has a negative slope,  $k$  is negative; the curvature of the rays is concave downward on a plane earth diagram, and the true curvature of the rays is greater than the curvature of the earth. Hence rays which enter the duct under sufficiently small angles are bent until they become horizontal and then are turned downwards. This particular form of refraction is called superrefraction. Such rays will be trapped in the duct, oscillating either between the ground and an upper level, or between two levels in the atmosphere. These conditions are illustrated by Figure 22 for the case of a ground-based duct and by Figure 23 for an elevated duct.

The detailed construction of a ray diagram in the case of an elevated duct is shown in Figure 23. It is assumed, for illustration, that the transmitter is placed at the point which produces the maximum amount of trapping, and this point turns out to be located at the maximum of the bend in the  $M$  curve. The vertical line for  $M_1$  corresponding to  $h_1$  is drawn as shown, and again the line 1 is drawn to the left of  $M_1$  at the distance  $\alpha_1^2/2$ , to represent ray 1 which



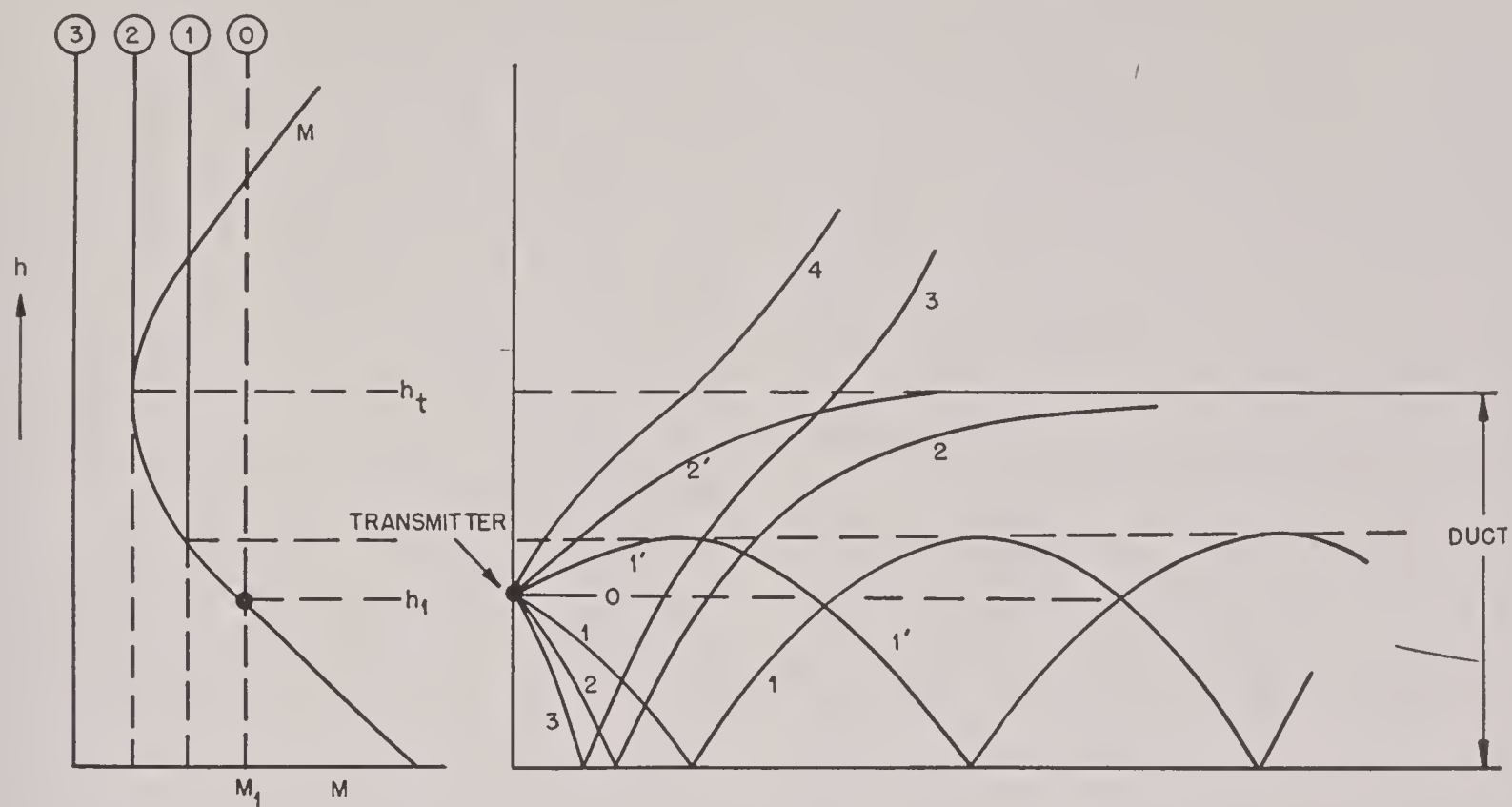


FIGURE 22. Rays with a ground-based duct.

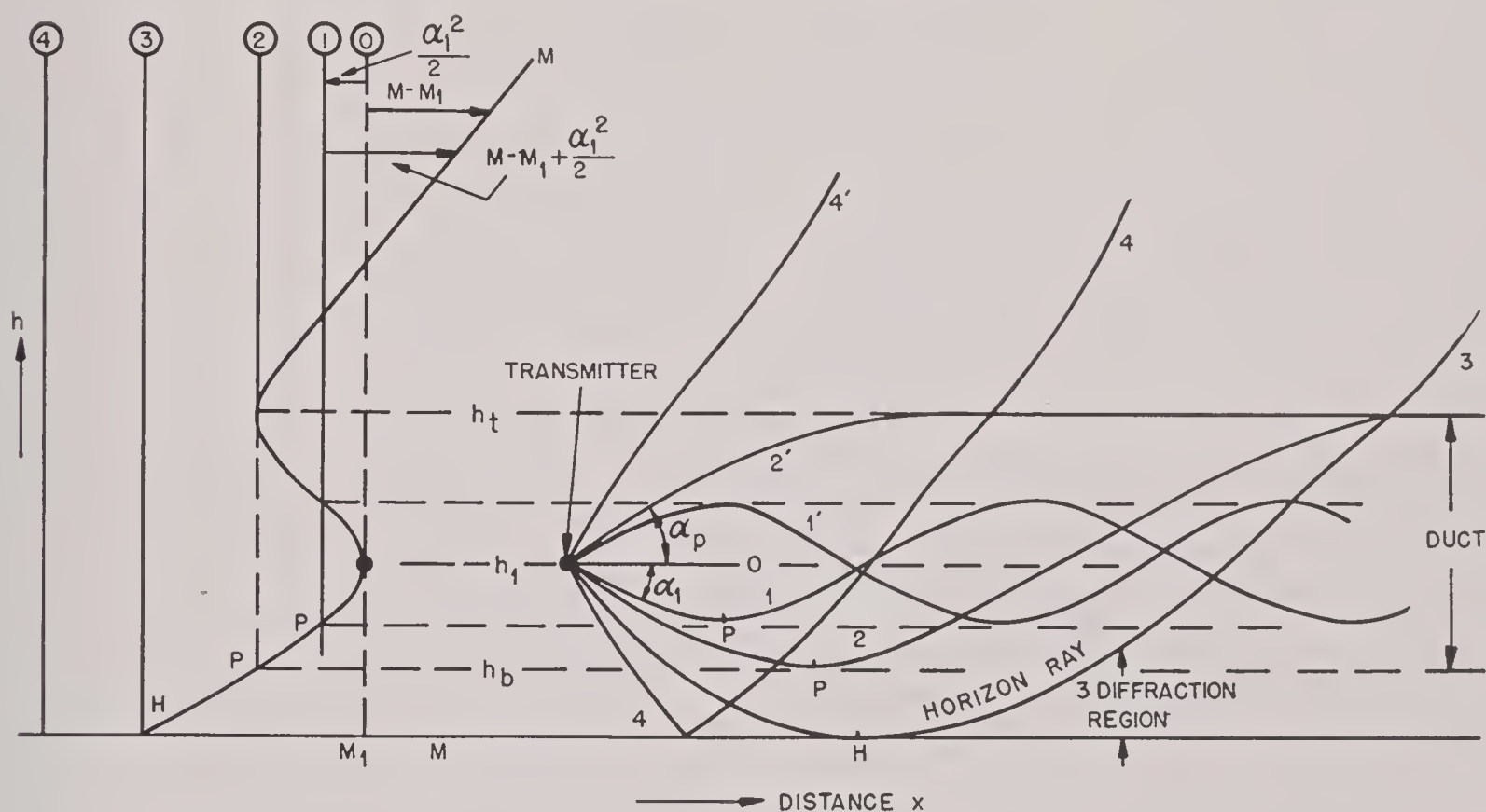


FIGURE 23. Rays with an elevated duct.

departs from the transmitter at angle  $\alpha_1$  measured from the horizontal. As the ray proceeds outward and downward it is bent less and less, corresponding to the decreasing distance between the  $M$  and 1 lines. Finally it reverses and rises to the height indicated. Ray 1 must therefore oscillate between the heights determined by the crossing of the  $M$  and 1 lines. Ray 1' starting upward at the same angle  $\alpha_1$  oscillates between the same height limits as ray 1.

Rays 2 and 2' emerging at angle  $\alpha_p$  are the limiting rays which are trapped in the duct between the heights  $h_t$  and  $h_b$ . Beyond the horizon ray 3 and below the duct lies the diffraction region for this case. Ray 4 emerging at an angle greater than  $\alpha_p$  is

not trapped but after reflection passes entirely through the duct.

Ground-based ducts are likely to be found along coasts where warm, dry air from over land flows out over a colder sea. This situation, for instance, prevails in the summer months along the northeastern coast of the United States. Elevated ducts occur frequently along the southern California coast.

An illustrative series of theoretical coverage diagrams as obtained by the ray tracing method described are collected in reference 448. A few of these diagrams are reproduced in Figure 24, for a frequency of 200 mc and a transmitter elevation of  $h_1 = 100$  ft, corresponding to an  $h_1/\lambda$  ratio of approxi-



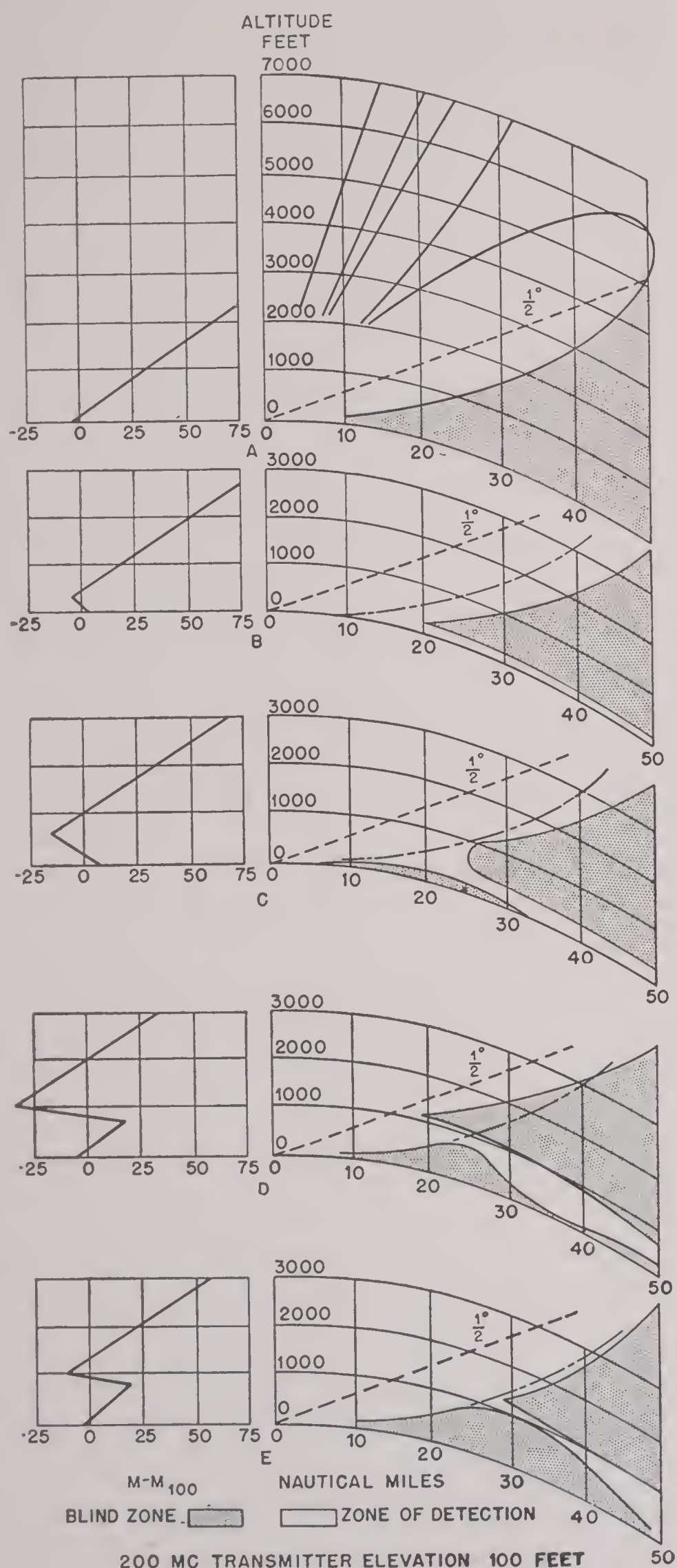


FIGURE 24. Calculated coverage diagram.

mately 20. The height scale is exaggerated in the ratio 40/1. Transmission over sea water is assumed. The coverage range is adjusted to "define the probable low-level zone of detection of a medium bomber with fair aspect by an SC-1 or SC-2 radar at 100-ft elevation. For SK radars and higher alti-

tude installations, the diagrams are conservative. For SC and SA radars or for lower altitude installations, they are optimistic."

Figure 24A shows the lobe structure for the standard atmosphere in which  $M$  increases 36 MU per 1,000 ft. It also shows the value of  $M - M_{100}$ ; that is, the  $M$  curve is drawn so as to pass through zero at the transmitter elevation of 100 ft. On diagrams B through E the lower portion of the standard lower lobe is indicated by a dash-dot line. The blind zones are cross-hatched, and their boundaries represent the calculated limits of detection. An interesting feature of these diagrams is the appearance, in some cases, of blind zones of considerable range and altitude along the surface. These cause "skip ranges" for ground targets that are significant in operational problems. Ray diagrams were used in calculating the field strengths in Figure 24.

The relative heights of the transmitter and the duct have an important bearing on the mechanism of transmission. The duct may develop entirely below the transmitter site or entirely above, or the duct may include the transmitter. With these alternatives a variety of propagation conditions is possible.

One of the important concepts of radiation theory is contained in the principle of reciprocity. This principle states that when a transmitter is at a point in space  $A$ , and the receiver at a point  $B$ , the received intensity is the same when they are interchanged, the transmitter being at  $B$  and the receiver at  $A$ . (It is assumed in making this statement that the transmitter and receiver may be regarded as point sources.) Similarly, for radar the signal intensity remains unaltered if the positions of radar and target are interchanged. It is known that there are serious limitations to the reciprocity principle where ionospheric reflections are involved, but for shorter waves and tropospheric propagation the principle may be applied without restriction. By means of the reciprocity principle any coverage diagram may be used to obtain the field strength when the heights of the target and the radar are interchanged.

From a study of such evidence on coverage diagrams as is available, it appears that (a) the effects of superrefraction are most marked when the transmitter lies in the duct; (b) they exist to a lesser degree if the transmitter lies below the duct: in particular no excessively long ranges for targets are then found above the duct—sometimes the ranges



are extended slightly, other times slightly decreased; (c) for a transmitter above the duct no excessive changes in field strength occur below the duct—this can be deduced from (b) by using the reciprocity principle; (d) there is no appreciable superrefraction when the transmitter lies appreciably above the duct.

For some time after the discovery of superrefraction it was thought that the concentration of radiative energy in the duct might result in a decrease of the amount of radiation above the duct and hence in a reduction of coverage there. The cases illustrated in Figure 24, at least, are not in accord with this presumption. In spite of the great increase in ranges in the duct the amount of energy trapped is small compared to the total energy of the radiation field.

### 17.2.6 Wave Picture of Guided Propagation

It must be realized that while ray treatments give accurate results under certain conditions, there are features of the propagation problem which can be satisfactorily discussed only on the basis of the electromagnetic wave equations. As an aid to understanding the wave treatment the close analogy between the functioning of a duct and a hollow metal waveguide (or dielectric wire) may be used. In both cases the field which is being propagated may be represented as the sum of an infinite number of terms (modes). Each waveguide mode is propagated with a separate phase velocity and an exponential attenuation factor and has a field distribution over the wavefront that is independent of distance in the direction of propagation.

In a metallic waveguide a finite number of modes are propagated with very small attenuation, while the remaining modes, infinite in number, have attenuations so high that they are, practically speaking, not propagated at all. The same division of modes into those that are freely propagated and those that are highly attenuated is found for duct propagation. In the duct, however, the difference between the two types of modes is less pronounced than in a hollow metal tube.

As the frequency is decreased, the number of transmission modes decreases both for the hollow metal tube and the duct until the cutoff frequency is reached, below which neither serves as a waveguide. For the case of simple surface trapping (Section 17.2.3) the following formula gives the approximate maximum value of the wavelength for which guided propagation inside the duct can still take place:

$$\lambda_{\max} = 2.5d \sqrt{\Delta M \cdot 10^{-6}}.$$

Here  $d$  is the height of the top of the duct above the ground in the same units as  $\lambda_{\max}$ , and  $\Delta M$  is the decrease in  $M$  inside the duct. This relationship is represented in Figure 25 where, it should be noted,

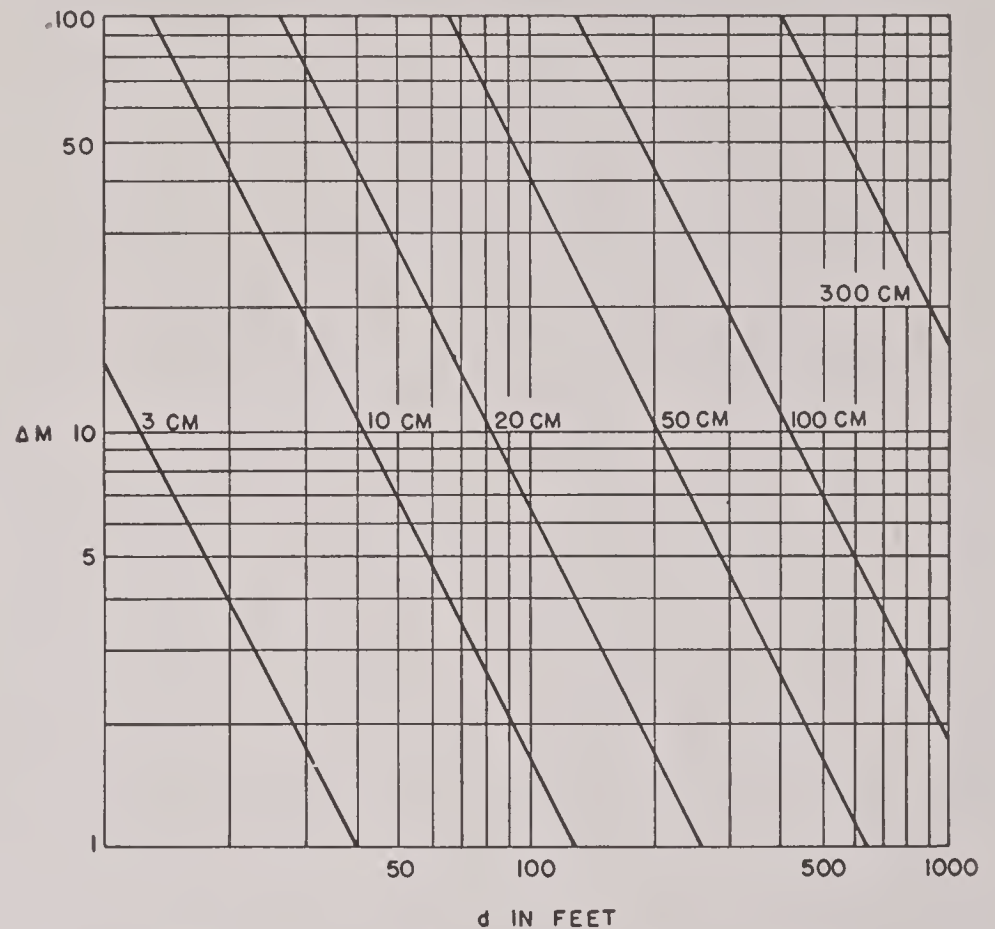


FIGURE 25. Maximum wavelength trapped in simple surface trapping. Duct width  $d$  in feet.  $\Delta M$  is total decrease of  $M$  in duct.

the duct width is given in feet and the wavelength in centimeters. When the wavelength exceeds the critical value obtained from this graph, guided propagation is no longer to be expected.  $M$  curves of different shapes will require slightly different numerical factors in the formula.

The main difference between the modes is found in the vertical distribution of field strength. The first three modes for a simple ground-based duct are illustrated in Figure 26. The lowest mode has

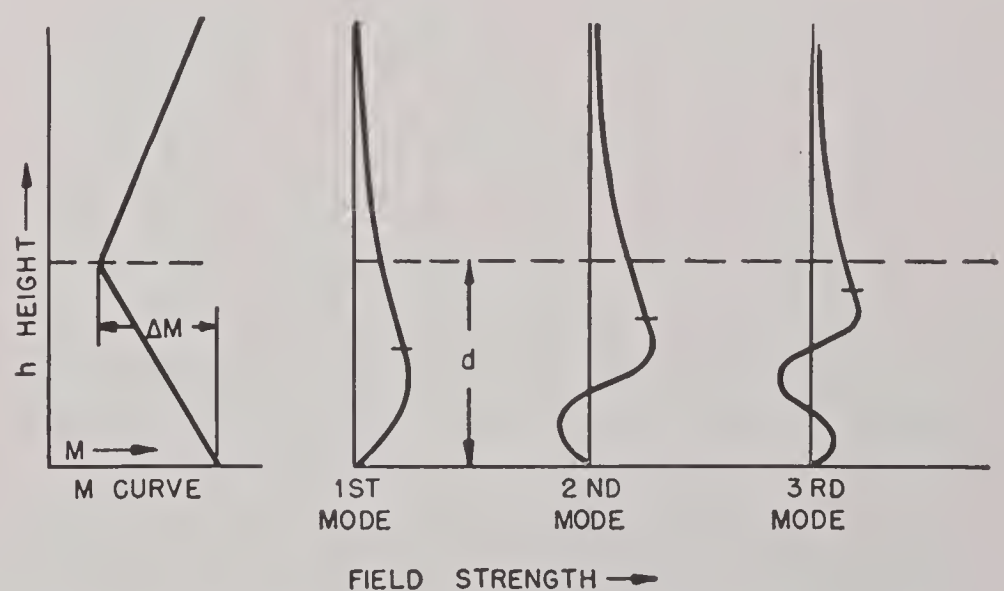


FIGURE 26. Vertical distribution of field strength for first three modes in a duct.



approximately  $\frac{3}{8}$  of a cycle of an approximate sine wave, followed by an exponential decrease. Higher modes have multiples of half cycles added to the sinusoidal part.

How these modes must be combined to give the total field strength and its vertical distribution is a question which depends on the height of transmitter, the distance out to the point where the total field strength is to be obtained, the rate of attenuation of each mode as a function of the distance, and its phase velocity. Since the attenuation and the phase velocity are different for the various modes, the vertical distribution of the total field changes with the distance from the transmitter, and the number of modes composing the total field decreases with increasing distance.

### 17.2.7 Reflection from an Elevated Layer

This phenomenon has been studied extensively at San Diego. The meteorological situation there is rather unique in that the warm and extremely dry upper air overlies a cooler and very moist lower stratum. The transition between the two layers is very sharp. This gives rise to an elevated duct of the type exhibited by the  $M$  curves of Figures 24D and 24E. Often the reversal of the  $M$  curve takes place over an even narrower interval of height than shown in these graphs. In such cases there is a reflection analogous to the reflection of waves at a true discontinuity between two media and which cannot be accounted for by the bending of rays.

At an interface between two media of different refractive indices there is partial reflection of radiation for any angle of incidence, but when the phenomenon (partial reflection and partial transmission) takes place in a layer of finite thickness, the reflected radiation is appreciable only at angles near grazing (less than  $1^\circ$  under the conditions found at San Diego). Furthermore, other things being equal, the reflection coefficient increases with increasing wavelength. This feature distinguishes the reflection by a layer from the duct effects produced by this layer, as the latter generally tend to become less pronounced for longer waves. The reflection gives rise to an additional field strength near the ground, often well beyond the optical horizon.

Transmission experiments carried out at San Diego at frequencies between 50 and 500 mc gave results that are explained satisfactorily on the basis of reflections of the type just described but not on the

duct theory. Thus most of the ducts caused by reversals of the  $M$  curve of the type shown in Figure 24D will be beyond cutoff for a frequency of 50 mc, according to Section 17.2.6. No guided propagation should therefore be expected, whereas the observed field at the receiver, located well beyond the optical horizon, was consistently very high.

At a frequency of 500 mc the reflection is found to be highly critical with respect to the angle of incidence at the reflecting layer. When meteorological conditions are such that the layer is high (3,000 to 4,000 ft), and therefore the angle of incidence large, the intensity of the reflected radiation is found to be very low; when the layer forms at a low level (a few hundred feet only) the reflected radiation becomes very strong. This behavior agrees with the predictions of electromagnetic theory.

So far, the experiment at San Diego is the only instance where a clear-cut case of reflection by an elevated layer has been found, although indications of similar effects have been observed elsewhere. Whether or not this phenomenon will occur at other places in or near the subtropical belt is not conclusively known since our knowledge of meteorological conditions in these climates is far from complete. If it does occur, it will obviously be of great operational significance.

### 17.2.8

## Operational Applications

### RADAR

Ground radars have experienced most of the effects of propagation in nonstandard atmospheres so far observed operationally. Phenomenal ranges on ship and low-flying airplane targets have been observed, especially in the Mediterranean area, the Arabia-India area, in Australia, and the Southwest Pacific theaters. In the United States and Europe ground-based ducts over land have occasionally produced fixed echo clutter seriously interfering with the plotting of aircraft targets over land. This ground clutter interference is especially troublesome with microwave early warning sets plotting targets over land. On ground radars with high pulse repetition rates, echoes from large distances frequently return on the second or later traces. Such echoes interfere with first sweep echoes and sometimes are misinterpreted as having ranges appropriate to the first sweep, with serious tactical consequences.

One of the most serious operational consequences of superrefraction is a secondary effect, that of



misleading operators as to the overall performance of the equipment. Long-range echoes caused by superrefraction have frequently been assumed to indicate good condition of the equipment, when precisely the opposite is actually the case. The phenomenon of superrefraction does not, however, in the same degree invalidate the measurement of signal-to-noise ratio of *nearby* echoes, as a criterion of relative overall set performance. Field strengths from nearby objects well within the optical horizon are far less subject to propagation variations. Echo strengths (signal-to-noise ratio) from nearby objects are still considered a good relative index of overall performance, provided that easily recognized echoes can be measured which are not sensitive to very small changes in the radar frequency. There are other sources of echo fluctuations such as the motion of objects (trees, towers) caused by the wind (important at wind speeds above 15 miles per hour). Great care is needed in the choice of fixed echo "standards" so that they are kept free of the effects enumerated. Sometimes artificial echoing objects are constructed of flat mesh screens perpendicular to the beam in order to secure suitable echoes which are not frequency sensitive. The extreme variability of long-range fixed echoes emphasizes the operational need for reliable test equipment for making quantitative tests on the components as well as on the overall performance of the equipment aspects of radars, as distinct from propagation effects.

In addition to the direct electrical checks on set performance there are a number of ways of making sure indirectly whether any failures of detection by radar may be due to a deformation of the coverage pattern by superrefraction. In the first place, superrefraction rarely affects detection at angles of elevation above about  $1.5^\circ$ . Any irregularity at higher angles must be attributed to other causes. Even between  $0.5^\circ$  and  $1.5^\circ$  failures of detection are exceptional and occur only where there are very strong ducts. A clue to the probability of occurrence of such conditions can be ascertained from a study of the primary meteorological effects which cause them; and even with only a moderate amount of meteorological information it is usually possible to make an estimate of this probability. Such superrefractive conditions almost invariably show up in intensified and extended ground echoes (ground clutter on the scopes) and, in case of an overwater path, in extended ranges of ship detection. A record of meteorological data will be very helpful in deciding, after the fact,

whether any specific failure of aircraft detection might have been ascribed to weather. Even if this is probable, there are, of course, a number of other operational causes that might be responsible rather than the weather.

Experience gained in England indicates that the technique of forecasting whether or not superrefraction occurs is, on the whole, fairly successful, but there are still many occasions when the predictions are not fulfilled. It has been intimated that in England this was due, at least partly, to variations in the sensitivity of the 10-cm set used; when the set is not at peak efficiency, maximum ranges of surface targets appear shortened, and the coverage in the duct may be reduced to a value corresponding to standard conditions.

A major problem in any early warning radar system is that of heightfinding by means of maximum ranges. On this it is difficult to make general statements. The method of heightfinding usually employed in long-range radar work consists in using the boundary of the lowest lobe as a height indicator, assuming that when the target is first sighted it has just entered the lowest lobe. When superrefraction is present, the height estimated in this way can be seriously in error. It may be too high if the enemy is flying in the duct, so that he is discovered earlier than he would be normally; or it may be too low if the enemy is flying in the region above the duct and so he is discovered later than he would be under standard atmospheric conditions. Here, again, it should be possible to find out whether repeated errors in height determination are the result of superrefraction or whether they are due to faulty calibration or to other features not related to the weather. Other methods of heightfinding, such as are used in fighter control and control of antiaircraft fire, are usually carried out at angles of elevation too large to be affected by nonstandard types of atmosphere.

#### VHF COMMUNICATIONS AND NAVIGATIONAL AIDS

The extension of the maximum range of very high frequency [VHF] navigational aids has already been mentioned as an important consequence of superrefraction. Similar extensions of communication ranges of VHF radio sets also occur. Because VHF air-to-ground communications are relied upon only for comparatively short-range communications, this



extension of the normal range by atmospheric conditions is important primarily from a security standpoint. It must always be borne in mind that transmissions on VHF may frequently be propagated hundreds of miles beyond the normal limiting range and are subject to enemy interception. Superrefraction has also been observed to cause very objectionable mutual interference between two control towers attempting to use a common VHF channel, although the distance between the airports was great enough to prevent serious mutual interference under normal conditions. Point-to-point VHF radio links are also affected by refraction, over longer paths than optical.

### RADIO COUNTERMEASURES

The laws of radio propagation enter into the problem of jamming the enemy communication and radar equipment. Since it is rarely possible to locate the jamming transmitter coincident with the enemy transmitter whose signals it is desired to mask, the efficiency of propagation of the signals from the enemy transmitter relative to those of the friendly transmitter enters into the problem. This has been worked out in detail for the standard atmosphere. When conditions are not standard, however, the effectiveness of the enemy transmitter, as determined for standard conditions, no longer applies. A case of special interest occurs when an airborne jamming transmitter is used as a countermeasure against an enemy radio communication link operating between two points on the ground. If the meteorological situation is such as to be favorable to formation of a ground-based duct the enemy signals may be propagated with small attenuation, whereas the signals from the jamming transmitter may be unaffected or even weaker than would normally be expected.

Plans for the employment of ground-based jammers against enemy radio and radar systems should take into consideration the ability of atmospheric refraction to increase, or occasionally to decrease, the signal propagated to the enemy's installation for jamming purposes. However, there has been only limited use of ground-based jamming so far. Unintentional mutual jamming has occurred between the spaced radar sets of a coastal system on the same frequency, where nonstandard propagation conditions caused strong signals to be propagated between normally noninterfering radars.

17.3

## RADIO METEOROLOGY

### 17.3.1 Temperature and Moisture Gradients

Section 17.3 is devoted to a survey of the meteorological conditions which produce the various types of propagation described in the preceding sections. This brief outline is not intended to replace the assistance of a professional meteorologist in analyzing short and microwave propagation problems; but by familiarizing radar or communications personnel with the fundamental physical processes of low-level weather it may open the way toward a more fruitful consultation with the meteorologist.

Duct formation is the most important phenomenon for which a detailed knowledge of the physical state of the lower atmosphere is required. Whenever a duct is formed,  $M$  decreases with height within a certain height interval. Since, according to Sections 17.1.5 and 17.2.1,  $M = (n - 1) \cdot 10^6 + 0.157h$ , the existence of a duct presupposes that the refractive index  $n$  decreases with height over at least a limited range of altitudes at a rate more rapid than 0.157 MU per meter. Such a decrease can be produced by two different meteorological conditions.

1. A rapid increase of temperature with height. This temperature inversion must be very pronounced in order, by itself, to produce a duct. In practice, a temperature inversion contributes to duct formation when accompanied by a sufficiently strong moisture lapse.

2. A rapid decrease of humidity with height designated as a "steep moisture lapse."

When ducts are produced by only one of these causes, they may be designated as "dry ducts" and "wet ducts," respectively. In the general case a temperature inversion and a moisture lapse cooperate in producing a duct, but one of the two factors will be preponderant, thus facilitating the analysis of the meteorological problem.

Whether or not a duct occurs under given meteorological conditions and what the rate of change of  $M$  is inside the duct may be determined by means of the diagram, Figure 27. (This discussion is presented for the purpose of illustrating the importance of temperature and moisture gradients. The technique more readily usable in practice is to compute the values of  $M$  at various altitudes directly from temperature and relative humidity data with the aid of Figure 19.) The abscissa in Figure 27 is the rate of decrease of humidity with height ( $-de/dh$ ), where  $e$  is the water vapor pressure in millibars. ( $e$  can be



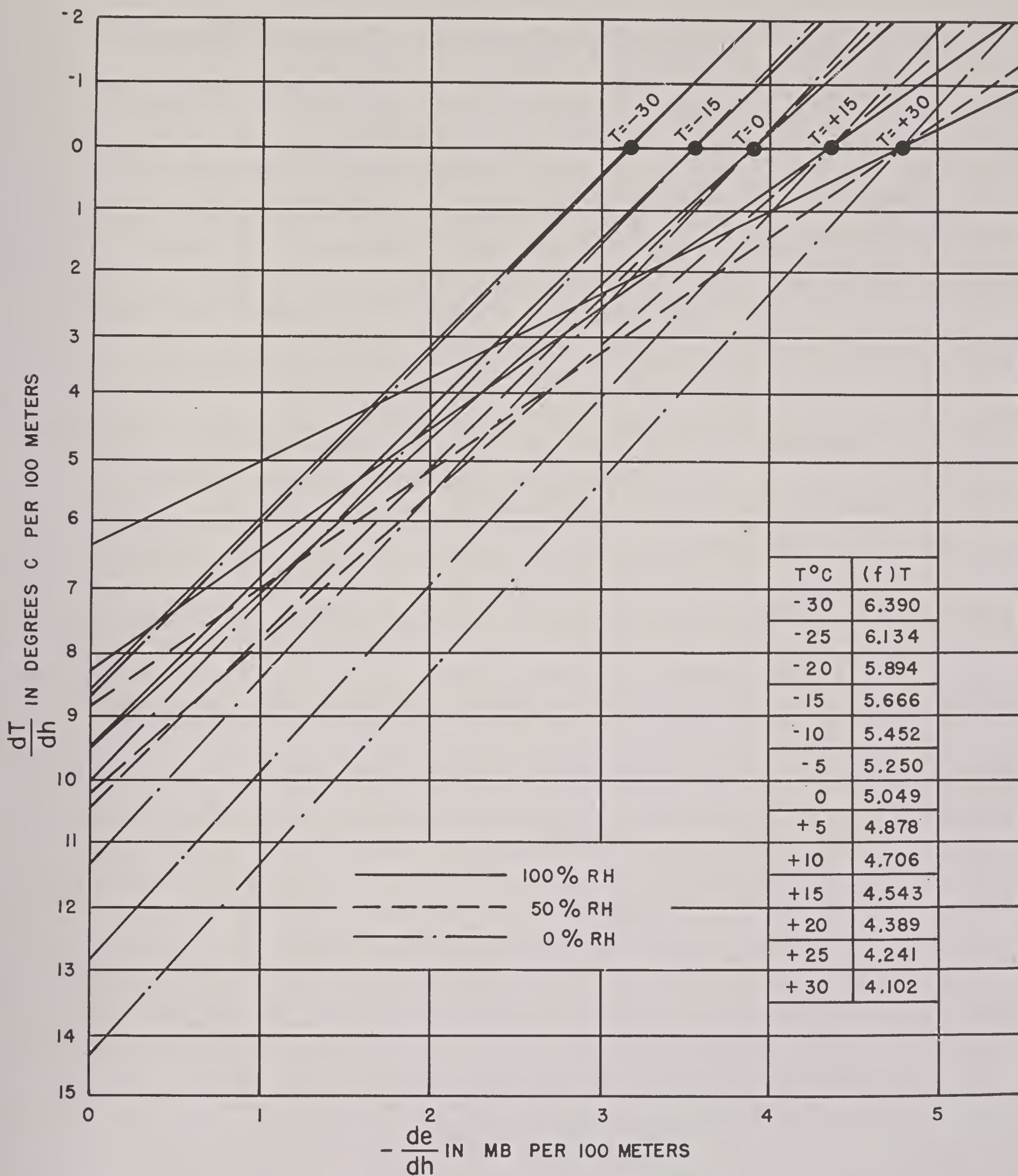


FIGURE 27. Temperature and humidity gradients.

found from meteorological tables when relative humidity and temperature are known.) The ordinate is the rate of *increase* of temperature with height ( $dT/dh$ ). The slanting lines represent various values of temperature and relative humidity at some particular height  $h$ . The lines passing through the same point at the upper right of the diagram correspond to the

same mean temperature; lines of different slopes represent different mean relative humidities.

In order to determine the rate of change of  $M$  at a given level, find the point in the diagram corresponding to the actual rates of change of moisture and temperature. Also pick out the straight line representing the actual mean values of temperature



and humidity in the layer considered. If the point is at the lower right relative to this straight line,  $M$  decreases with height in the layer chosen; that is, a duct exists. If the point is at the upper left of the straight line,  $M$  increases with height and there is no duct.

The rate of change of  $M$ ,  $(dM/dh)$ , may be obtained from the diagram by measuring the horizontal distance from the point to the line and multiplying by the function of the temperature  $f(T)$  given in the table on Figure 27. The result is the value of  $dM/dh$ , the rate of change of  $M$ , in  $M$  units per 100 m. This quantity is negative when the point is to the right of the line and positive when the point is to the left of the line.

It is seen at once from the diagram that for small values of the moisture lapse an extremely steep temperature gradient is required in order to produce a duct (lower left part of the diagram). In cold air such as is found in the arctic the total moisture is small, and hence the moisture gradient will in general be quite small. Ducts will then only occur when a very strong temperature inversion exists.

Strong temperature inversions occur only under special meteorological conditions which will be discussed below. Ordinarily the temperature of the air decreases with height; and this will put our representative point into the upper part of Figure 27. A duct can then exist only when the moisture lapse is large enough, so that the representative point falls to the right of the appropriate slanting line. Such conditions are common in the lower atmosphere. This leads to a wet duct, which is determined almost completely by the moisture lapse.

17.3.2

### Physical Causes of Stratification—Turbulence

There are three basic meteorological factors which tend to modify the temperature and moisture distributions in the lowest layers of the atmosphere. These are: (1) advection, (2) nocturnal cooling (over land), and (3) subsidence.

*Advection* is a meteorological term used to designate the horizontal displacement of air having particular properties. Advection is of great interest in propagation problems particularly because it leads to an exchange of heat and moisture between the air and the underlying ground or sea surface and thus affects the physical structure of the lowest layers.

*Nocturnal cooling* over land is caused by a loss of

heat from the ground by infrared (heat) radiation. The cooling of the ground is communicated to the lower layers of air and leads to the establishment of a low-level temperature inversion.

*Subsidence* means a slow vertical sinking of air over a very large area. It is most likely to be found in regions where barometric Highs are located. Subsidence tends to produce a temperature inversion and also produces very dry air which, spreading out over a humid surface, creates a situation which is favorable for the formation of a duct.

The processes (1) and (2) change the physical characteristics of the air through transfer of heat or moisture between the air and the underlying surface of the ground or sea. The operating factor in this exchange is turbulence. The main features of turbulence in the lower atmosphere are outlined briefly below.

*Convection* occurs spontaneously whenever the decrease of temperature with height exceeds a value of about 1 C per 100 m. This convective condition is usually produced as a result of the heating of the ground by the sun's rays. Even with a cloudy sky the diffuse daylight often is strong enough to produce moderate convection. On a hot summer day convection over land extends to great heights. Convection mixes the air thoroughly and thus causes a uniform distribution of moisture and a uniform decrease of temperature with height of about 1 C per 100 m. Hence even moderate convection tends to produce a smooth  $M$  curve which varies linearly with height. Standard conditions may therefore be assumed to prevail on clear summer days (and not infrequently on clear days in the cooler seasons) from the hours of late morning until late afternoon, during which time convection is most active.

*Frictional turbulence* occurs frequently in the lower atmosphere even in the absence of convective conditions. It is caused by the wind and requires the presence of at least light winds, but with moderate or strong winds the effect is more pronounced. In conditions of calm or with a gentle breeze, frictional turbulence is confined to the lowest strata. Moderate or strong winds develop a layer of intense turbulence, caused by friction of the air at the irregularities of the ground. This layer is usually quite well defined in height and extends to an average elevation of about 1,000 m over land. Over a relatively smooth sea where friction is small the height of the layer is much reduced. In this frictional layer the air becomes thoroughly mixed; the vertical temperature gradient



caused by convection is about  $-1$  C per 100 m, and the moisture lapse is steady and rather small. Standard refraction will therefore prevail when winds are moderate to strong over land, and over the ocean also when the winds are sufficiently strong.

*Temperature inversions* occur when the temperature of the surface (sea or land) is appreciably lower than the temperature of the air. The transition from the ground temperature to the free air temperature takes the form shown in Figure 28. The heat and moisture

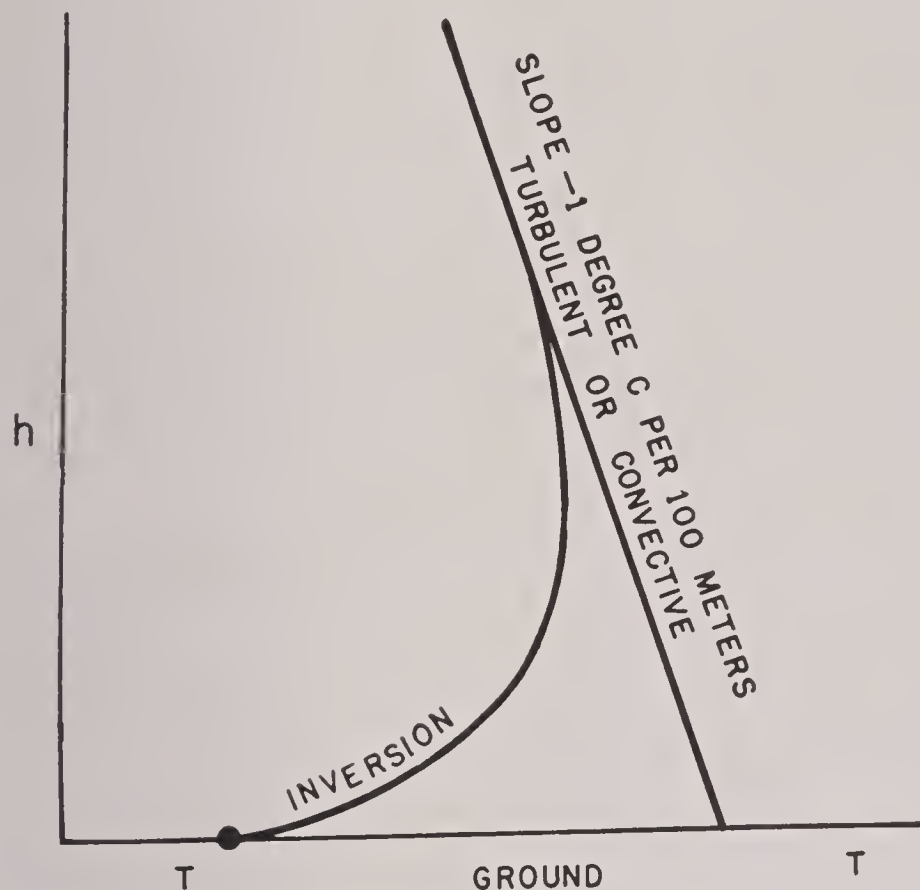


FIGURE 28. Air temperature versus height for an inversion.

transfer caused by turbulence in a temperature inversion is less simple than that in a frictional layer. The turbulent processes active in inversion regions are highly complex and are not yet very well explored. It is known, however, that the intensity of the vertical transfer of heat and moisture is greatly reduced as compared to the rate of transfer with frictional turbulence. The reduction is the more pronounced, the steeper the vertical increase of temperature; in a steep inversion the rate of transfer may be many times less than in a frictional layer. This tends to produce a vertical stabilization of the air layers in the inversion region. As soon, therefore, as a temperature inversion has begun to form, the rapid mixing in the lowest layers, usually effected by frictional turbulence, stops and is replaced by a much more gradual diffusion.

Assume now, for instance, that the rate of diffusion has become so slow that the transfer of moisture over a height of a few hundred feet takes many hours or,

perhaps, a day or two. When the air in the inversion is dry to begin with and flows over ground capable of evaporation (the sea or moist land) there will be established, in such an air mass, a steep moisture lapse, since the water vapor that has been taken up by the air near the ground will only gradually diffuse into the dry air aloft. Conditions are then favorable for the formation of an evaporation duct, in addition to whatever tendency toward duct formation may be caused by the temperature inversion itself.

### 17.3.3 Advective Ducts—Coastal Conditions

Advective formation of ducts may occur both over land and over sea, but this process is most important over the ocean near coasts. The most common illustration is that of air above a warm land surface flowing out over a cooler sea. Over the land the air will usually have acquired a convective or nearly convective temperature gradient of  $-1$  C per 100 m. When this air flows out over the cool water surface, a temperature inversion is rapidly formed which grows in height as the process of turbulent transfer progresses. The temperature inversion does not, in itself, give rise to a pronounced duct because the effect of a temperature gradient upon the  $M$  curve is relatively small; but when the air is dry, evaporation from the sea surface takes place simultaneously with the heat transfer, and a moisture lapse rate is established in the lowest layers. The combination of temperature inversion and moisture lapse rate is most favorable for the formation of a duct off shore.

The gradual formation of this type of duct is illustrated in Figure 29. This shows  $M$  curves, corres-

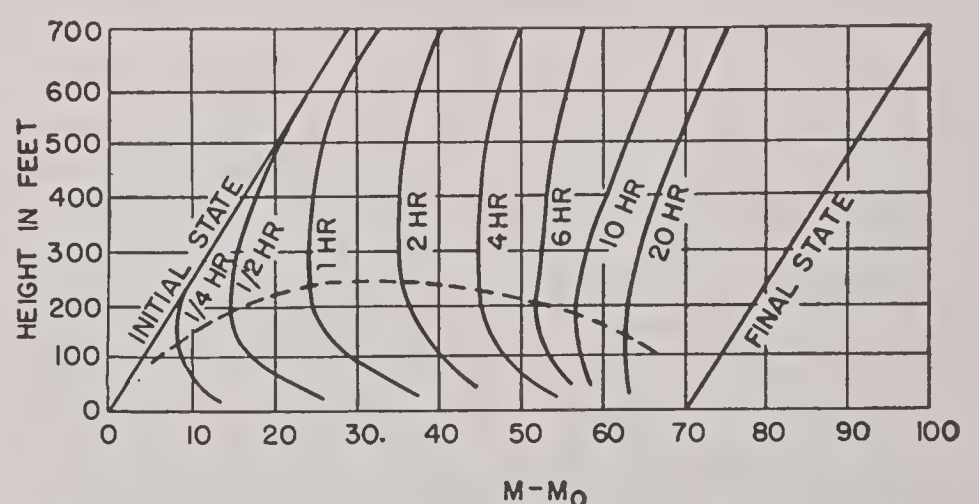


FIGURE 29. Development of duct off coast. Initial state corresponds to air at coast line.  $\frac{1}{4}$  hr,  $\frac{1}{2}$  hr, etc., refer to time air has been over water. Initial conditions for this set of curves: unmodified air  $T_0 = 32$  C,  $e = 12.3$  mb; water  $T_w = 22$  C,  $e_w = 26.5$  mb saturation.

ponding to the simple surface type of trapping (see Figure 20, curve II) for a series of time intervals



(and distances) as the air moves out over the water. The top of the duct is given by the elevation of the minimum value of the  $M$  curve. It will be noticed that the duct acquires a maximum depth some time after the air has touched the cold water surface; thereafter the depth decreases. The cause of this behavior is found in the progressive decrease in moisture and temperature differences which is the final result of the diffusion process. Thus the final stage of this transformation is an air mass whose temperature and moisture distributions are in equilibrium with the underlying water surface and no longer show a rapid variation with height.

Duct formation in such a case depends on two quantities: (1) the excess of the unmodified air temperature above that of the water and (2) the humidity deficit, that is, the difference of the saturation vapor pressure corresponding to the water temperature minus the actual water vapor pressure in the unmodified air. If these quantities are large, especially the humidity deficit, a duct will develop. A great variety of local conditions may, however, be encountered in problems of this type, and empirical rules developed for one locality may not at all apply to others.

Advective processes may also occur over land, but the conditions required for duct formation are likely to be found much less frequently. Evaporation over land need by no means be small unless the land surface is very arid (desert); in fact, evaporation over a moist soil or a ground covered with vegetation may be comparable to, or even larger than, evaporation from a sea surface. A duct may therefore be formed when dry, warm air flows over a colder ground surface capable of evaporation. The temperature excess and humidity deficit may again be defined as above.

*Land and sea breezes* often produce ducts near coastal regions. These winds are of thermal origin and are produced by temperature differences between land and sea. The mechanism is illustrated in Figure 30. During the day, when the land gets warmer than

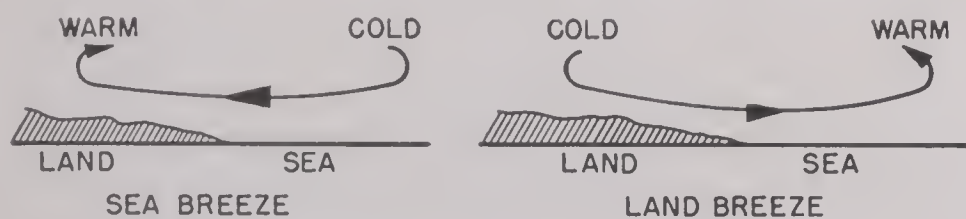


FIGURE 30. Land and sea breezes.

the sea, the air rises over the land and descends over the sea and causes an air circulation in which the wind blows from sea to land (sea breeze) in the lowest

levels. Vice versa, if during the night the land becomes colder than the sea, a circulation in the opposite direction arises. This is the land breeze. As a rule, this type of phenomenon is extremely shallow, and the winds do not extend above a few hundred feet at the most. Often there is a reverse wind in the layer above the land or sea breeze layer. A sea breeze may modify the advective conditions described above in various ways, and extremely strong ducts have been observed repeatedly under sea breeze conditions. The land and sea breezes are of a strictly local nature and in some cases will extend only a few kilometers to both sides of the shore. Nevertheless this region may be an important part of the trajectory of radiation. These breezes develop only under fairly calm conditions; under conditions of moderately strong wind, the sea and land breeze will be perceptible only as a slight modification of the existing wind. Because of their limited extent, forecasting of these breezes requires a study of the local wind and temperature conditions.

Advective ducts caused in the manner described here are often quite limited horizontally. This is especially true if a sea breeze is involved. The assumption made throughout this report, namely that the stratification of the air is of infinite extent horizontally, will no longer be valid, and superrefraction may be restricted to a stretch along the coast.

17.3.4

### Ducts over the Open Ocean

A type of duct that is somewhat similar to the advective duct described above is found over the open ocean where the air has had an extensive over-water trajectory. It has been studied in experiments carried out at the island of Antigua in the West Indies. The subsequent description refers to this particular location, but on the basis of experience gained operationally and in other experiments it may be presumed that similar conditions prevail in numerous other regions of the world, particularly in the trade wind regions.

At Antigua, in winter and early spring when these tests were made, the wind is usually from the northeast since the island is situated at the southeastern fringe of the so-called Bermuda High, a large semi-permanent circulation system over the North Atlantic, extending from about 10° to 30° North latitude. The air at Antigua has thus had an ocean trajectory of thousands of miles. The relative humidity is of the order of 60 to 80 per cent, indicating



that in spite of the long passage over the sea no diffusion equilibrium has been established between the sea surface and the moisture in the lower atmosphere. On the other hand, there is little difference between the air and sea temperature, the latter being rather constant at 25 C and the former varying between 23 and 26 C. The air is, therefore, nearly in convective thermal equilibrium with the sea surface, and no appreciably "dry" duct can develop. The duct is caused by the moisture variation in the lowest layers.

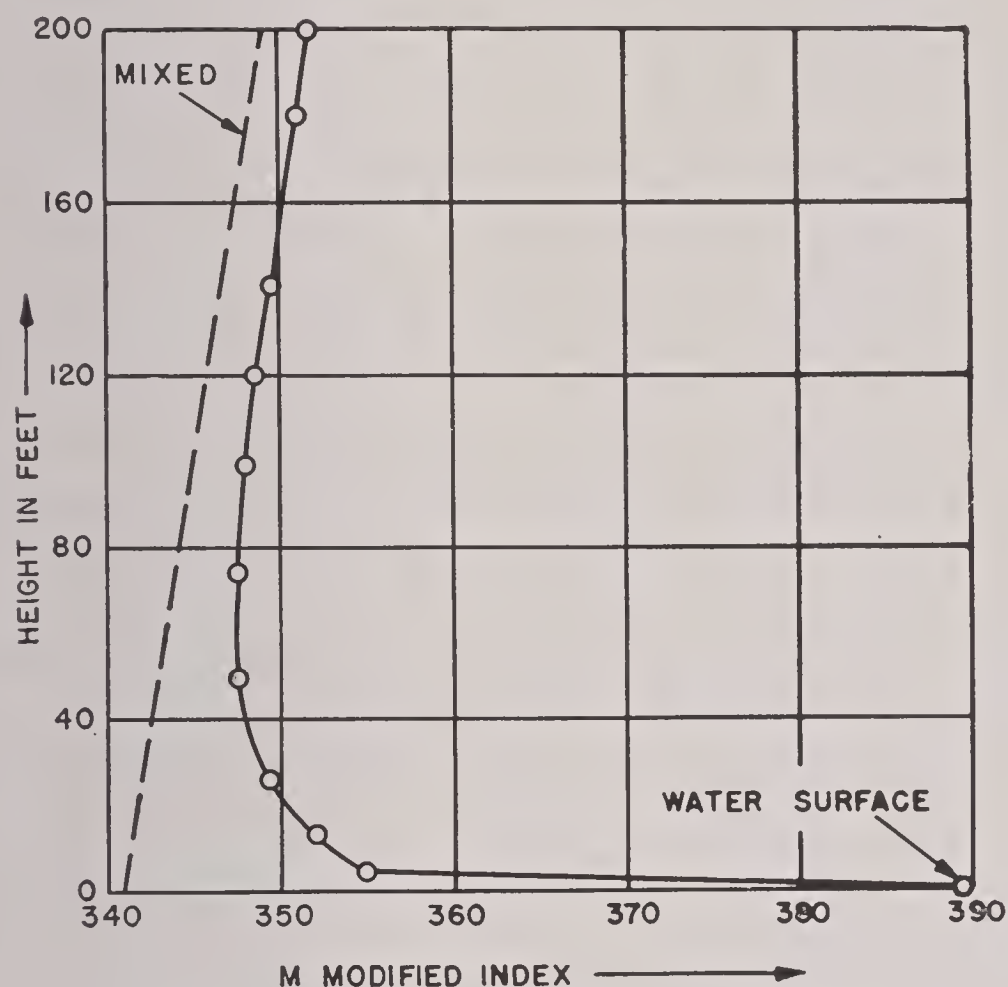


FIGURE 31. *M* curve over West Indian Ocean.

A typical *M* curve is shown in Figure 31. It may be seen that at as small a height as 0.5 m above the sea *M* has a value much lower than at the surface itself. As the surface value of *M* is obtained by the assumption that the air in immediate contact with the water is saturated with moisture, this indicates that 0.5 m above the water the moisture content of the air is still appreciably below saturation. The moisture in the lowest levels is subject to considerable variations caused partly by turbulence, partly by the waviness of the sea surface. *M* curves, such as Figure 31, are obtained by averaging over several measurements.

These ducts are much lower than the advective ducts discussed in the previous section; their height is about 12 to 15 m (around 40 ft). The effective decrease of *M* in the duct (apart from the sharp decrease in the lowest half meter) is of the order of 4 to 8 MU.

The latter figure depends somewhat on the wind speed. There is a maximum decrease of 8 MU at a wind speed of about 8 m per sec (13 miles per hour) and lower values for both lower and higher wind speed. The duct height in turn shows a very slight dependence on wind speed, increasing somewhat with increasing speed.

These ducts are so low that they are not very effective for trapping of waves even as short as S band, presumably on account of strong leakage (see Section 17.2.6), and signal strength is not increased when an S-band transmitter or receiver is placed inside the duct. For K band, on the other hand, the trapping effect is marked; on raising the transmitter or receiver from the ground a maximum of signal strength is observed at about 9 m, but from there on the signal begins to decrease up to about 20 m (overall decrease 5 db); at greater heights the signal gradually rises again.

These ducts appear to be a permanent feature at Antigua, at least during the season these observations were carried on. This is probably true also for many locations in the trade wind belt. The daily variation of weather phenomena and of duct characteristics at such purely maritime locations seems to be insignificant.

### 17.3.5 Nocturnal Cooling—Daily Variations

A daily variation of surface temperature occurs only over land. During the day the heating is caused by the sun's rays, and the cooling of the ground surface during the night is produced by radiation from the ground. The diurnal temperature variation of the sea is extremely small. However, shallow bodies of water sometimes have an appreciable diurnal variation.

The radiation which causes nocturnal cooling of the ground is temperature or heat radiation which is composed of waves in the infrared portion of the spectrum. It is the same kind of radiation that is given off by a hot stove or electric heater, but since the temperature of the earth is less than that of a stove the earth emits comparatively less heat radiation. Nevertheless, radiation is a very powerful agent in cooling the ground. From about sunrise until the late afternoon, the surface of the earth gains more heat from the sun and atmosphere than it loses by radiation to space; in the late afternoon and during the night, the surface loses more heat than it gains. The amount of heat radiated is very nearly inde-



pendent of the physical constitution of the ground but is dependent upon its temperature and increases very rapidly with a rise in ground temperature.

The atmosphere has a "blanketing" effect upon the infrared radiation emitted by the ground. The atmosphere itself absorbs and emits infrared radiation, and the cooling of the ground may be greatly reduced by the action of the atmosphere. The blanketing effect is least with a clear sky and dry, cool air; it is somewhat stronger when, with a clear sky, the atmosphere is very warm and humid, as in the tropics. A cloud will produce a distinct blanketing effect, and with a complete overcast of low cloud the blanketing is so pronounced that the nocturnal cooling of the ground is reduced to only a small fraction of its value with clear skies.

The loss of heat from the ground is distributed by turbulence over the lowest layers of the atmosphere, thus giving rise to a temperature inversion. Inversions of this type are strongest in temperate and cold climates with a clear sky and cold, dry air overhead; they are less pronounced in the tropics with humid air and a clear sky and are practically absent with an overcast sky. A meteorologist, after some experience, can estimate the magnitude of an inversion to be expected with given local weather conditions.

Temperature inversions, by themselves, can at best produce only weak ducts, but strong ducts may result when the inversion is accompanied by a sufficient moisture lapse. This requires that the air be dry enough to allow evaporation into it from the ground. In warmer climates where the transition between night and day is rapid, evaporation may set in in the early hours of the morning before the nocturnal inversion has been completely destroyed by the action of the sun. A strong duct will then be formed for a short period. This condition seems to be frequent during certain seasons in Florida.

It is obvious that the shape of the  $M$  curve, when it deviates from the normal, may undergo rapid variations with the period of a day. One example has just been quoted; another is illustrated by the advective ducts over the North Sea produced by the mechanism described in Section 17.3.3. These ducts usually form in the hours before midnight and last until the early hours of the morning.

17.3.6

### Fog

Contrary to what might perhaps be expected, the formation of fog results, in general, in a decrease of

refractive index. When fog forms, e.g., by nocturnal cooling of the ground, the total amount of water in the air remains substantially unchanged, but part of the water changes from the gaseous to the liquid state. The contribution of a given quantity of water to the refractive index is found to be far less when the water is contained in liquid drops than when it exists in the form of vapor. The formation of fog, therefore, results in a reduction of the amount of water vapor contributing to the value of  $M$ . If there is a temperature inversion in the fog layer, the saturation vapor pressure increases with height, and a substandard  $M$  curve frequently results (see Figure 20, curve Ib). This occurs with radiative fog (caused by nocturnal cooling of the ground) and also with advective fog (caused by the advection of warmer air over a cooler surface). Advective fog is very common in the Aleutian Islands and off Newfoundland.

If fog causes a substandard  $M$  curve, it is to be inferred that the rays will be bent upward, instead of downward as with superrefraction, and lead to a weakening of the field in the lowest layers, even to the point of producing a complete fade-out of radio reception. Appreciable reduction of radar ranges and interruption of microwave transmission have frequently been observed in such cases.

Fog, however, does not always produce a substandard  $M$  curve, though this is the most common case. In certain other less frequent types of fog, the temperature (and thereby the vapor pressure) may be constant or increase with height through the fog layer. In this event near-standard propagation will prevail, or a duct may develop when the temperature inversion is strong enough. An example is steam fog, formed when cold air passes over a warm sea (see also Section 17.3.9).

17.3.7

### Subsidence—Dynamic Effects

The temperature inversions discussed so far owe their existence to the modification of air by contact with the ground, but subsidence inversions are produced by a mechanism of an entirely different nature. By subsidence is meant the sinking of air, that is, a vertical displacement, which must of course be accompanied by a lateral spreading (divergence) in the lower part of the subsiding column of air; otherwise there would be an accumulation of air in the lower levels. The thermodynamic analysis of this complex process shows that if the effect of subsidence



is strong enough a temperature inversion will be created. Since this process does not require the presence of a ground surface, it may occur, and in fact often does occur, aloft in the atmosphere. The effects of subsidence frequently are the most pronounced at an elevation of the order of a kilometer or more.

As a general rule, subsidence occurs in regions of high barometric pressure. In fact, subsidence always does occur in such regions, but it may not always be intense enough to give rise to a strong temperature inversion. The flow of air in a barometric High is shown in Figure 32 as it appears on a weather map

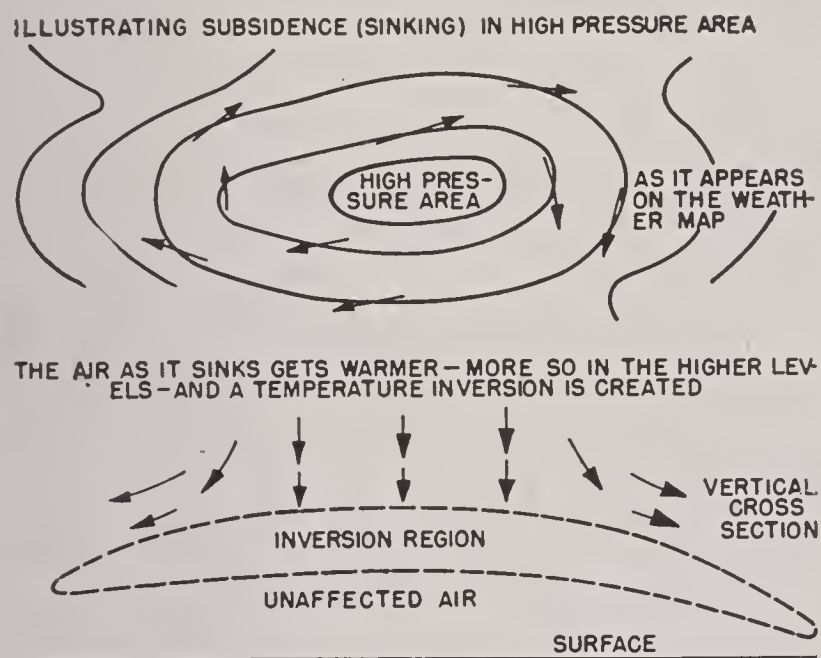


FIGURE 32. Characteristics of subsidence.

in horizontal projection, and also in a vertical cross section.

With subsidence, the air as a rule is very dry, and there is nothing in the process which can change the moisture content or produce moisture gradients. If, however, the dry air finds itself over a surface capable of evaporation, such as the sea surface, a steep moisture gradient may be established and a duct will be created. It is thus seen that subsidence in itself does not produce a duct, except in extreme cases, but it can act as an auxiliary factor and greatly enhance the formation of a duct whenever other conditions are favorable. Thus, forecasts of superrefraction based on a purely advective mechanism, or purely on radiative cooling or evaporation, may have to be modified in the presence of subsidence; an otherwise very weak duct may be converted into a strong duct by the effect of subsidence upon the lower strata.

Strong subsidence effects are of frequent occurrence on the southern California coast where they may continue with little change for days at a time.

At times the duct is elevated, giving an elevated S-shaped  $M$  curve like IIIa in Figure 20. Again the duct may extend practically from the ground up with  $M$  curves similar to curves II or IIIb in Figure 20. The elevation of the top of the duct may vary from 300 to 5,000 ft, and the thickness may lie between a few feet and 1,000 ft. Coverage diagrams and the corresponding  $M$  curves for several typical situations are illustrated in Figure 24.

For a number of reasons the meteorological conditions in a barometric High are favorable for the formation of ducts. Among the favorable factors are: subsidence, creating very dry air into which evaporation from the surface can take place; again subsidence, creating temperature inversions; calm conditions preventing mixing of the lowest layers by frictional turbulence and maintaining the thermal stratification caused by radiative cooling or local breezes; clear skies producing nocturnal cooling over land.

The conditions in a barometric Low, on the other hand, generally favor standard propagation. A lifting of the air, the opposite of subsidence, usually occurs in such regions and is accompanied by strong winds. The combined effect is to destroy any local thermal stratification and to create a deep layer of frictional turbulence. The air is therefore well mixed, and nonstandard vertical temperature and moisture gradients are wiped out in the early stages of their creation. Moreover, the sky is usually overcast in a low-pressure area and nocturnal cooling, therefore, is negligible.

To summarize, high-pressure regions, clear skies, and calm air are conducive to duct formation, while low-pressure areas, cloudy skies, and winds favor standard refraction.

*Fronts* in the atmosphere are possible sources of refractive effects. A front is a surface of discontinuity which separates two air masses of different temperatures. The surface slants at an angle of  $1^\circ$  to  $2^\circ$  with the horizontal, with the colder air forming a wedge under the warmer air. Fronts are a common occurrence in the atmosphere, and it might be thought that they should have a considerable influence on wave propagation. This is, however, not borne out by English radar experience, which shows very little superrefraction connected with fronts. The explanation is probably that fronts are invariably accompanied by low-pressure areas, and turbulence along a front is usually so strong that the transition from the cold air to the overlying warm air takes place



continuously over a vertical distance of about a kilometer. Propagation conditions might, however, be somewhat different with fronts in sub-tropical climates, although our knowledge is still inadequate on this point. In one-way transmission frontal effects have been studied to a limited extent (see Section 17.3.9).

### 17.3.8 Seasonal and Global Aspects of Superrefraction

Although the general picture is still incomplete, enough is now known about the geographical and seasonal aspects of superrefraction to warrant a general summary.

#### ATLANTIC COAST OF THE UNITED STATES

Along the northern part of this coast superrefraction is common in summer, while in the Florida region the seasonal trend is the reverse, with a maximum in the winter season.

#### WESTERN EUROPE

On the eastern side of the Atlantic, around the British Isles and in the North Sea, there is a pronounced maximum in the summer months. Conditions in the Irish Sea, the Channel, and East Anglia have been studied by observing the appearance or non-appearance of fixed echoes (see Figure 33). Additional

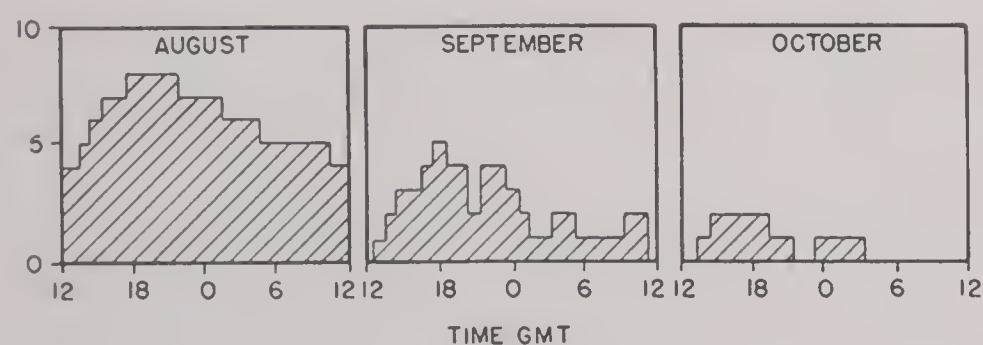


FIGURE 33. Diurnal frequency of long-range fixed echoes at North Foreland, Kent. Wavelength 10 cm.

data based on one-way communication confirmed the radar investigations.

#### MEDITERRANEAN REGION

The campaign in this region provided good opportunities for the study of local propagation conditions. The seasonal variation is very marked, with superrefraction more or less the rule in summer, while

conditions are approximately standard in the winter. An illuminating example is provided by observations from Malta, where the island of Pantelleria was visible 90 per cent of the time during the summer months, although it lies beyond the normal radio range.

Superrefraction in the central Mediterranean area is caused by flow of warm, dry air from the south (sirocco) which moves across the ocean and thus provides an excellent opportunity for the formation of ducts. In the winter time, however, the climate in the central Mediterranean is more or less a reflection of Atlantic conditions and hence is not favorable for duct formation.

#### THE ARABIAN SEA

Observations covering a considerable period are available from stations in India, the inlet to the Persian Gulf, and the Gulf of Aden. The dominating meteorological factor in this region is the southwest monsoon that blows from early June to mid-September and covers the whole Arabian Sea with moist equatorial air up to considerable heights. Where this meteorological situation is fully developed, no occurrence of superrefraction is to be expected. In accordance with this expectation the stations along the west side of the Deccan all report normal conditions during the wet season (middle of June to middle of September). During the dry season, on the other hand, conditions are very different. Superrefraction then is the rule rather than the exception, and on some occasions very long ranges, up to 1,500 miles (Oman, Somaliland), have been observed on 200-mc radar on fixed echoes.

When the southwest monsoon sets in early in June, superrefraction disappears on the Indian side of the Arabian Sea. However, along the western coasts conditions favoring superrefraction may still linger. This has been reported from the Gulf of Aden and the Strait of Hormuz, both of which lie on the outskirts of the main region dominated by the monsoon. The Strait of Hormuz is particularly interesting as the monsoon there has to contest against the shamal from the north. The Strait itself falls at the boundary between the two wind systems, forming a front, with the dry and warm shamal on top, and the colder, humid monsoon underneath. As a consequence, conditions are favorable for the formation of an extensive radio duct, which is of great importance for radar operation in the Strait.



### THE BAY OF BENGAL

Such reports as are available from this region indicate that the seasonal trend is the same as in the Arabian Sea, with normal conditions occurring during the season of the southwest monsoon, while superrefraction is found during the dry season. It appears, however, that superrefraction is much less pronounced than on the northwest side of the peninsula.

### THE PACIFIC OCEAN

This region appears to be the one where, up to the present, least precise knowledge is available. There seems, however, to be definite evidence for the frequent occurrence of superrefraction at some locations; e.g., Guadalcanal, the east coast of Australia, around New Guinea, and on Saipan. Along the Pacific coast of the United States observations indicate frequent occurrence of superrefraction, but no statement as to its seasonal trend seems to be available. The same holds good for the region near Australia.

In the tropics there is found a very strong and persistent seasonal temperature inversion, the so-called trade wind inversion. It has no doubt a very profound influence on the operation of radar and short-wave communication equipment in the Pacific theater.

### 17.3.9 Fluctuations in Signal Strength with Time

A number of different causes tend to produce variations of signal strength with time. These are discussed briefly in the following paragraphs.

#### TARGET MODULATION

Very rapid fluctuations having periods of only a small fraction of a second frequently are encountered in radar observations, especially with centimeter waves. These fluctuations arise as a consequence of the internal motions of the target and are especially noticeable for aircraft. Similar effects have been observed with reflection of microwaves from wooded hills, the fluctuations in signal probably being caused by foliage moving in the wind.

#### EFFECT OF WAVES ON THE SEA

A similar phenomenon is observed when the transmitter and receiver are so situated that reflection

from a water surface contributes to the received signal strength. Owing to irregularities of the water surface and their rapid change with time, variations in signal strength will appear. The fluctuations arising in this way have a time scale of the order of a second, in the case of a lightly ruffled sea (see Figure 34). Evidently rays reflected from different

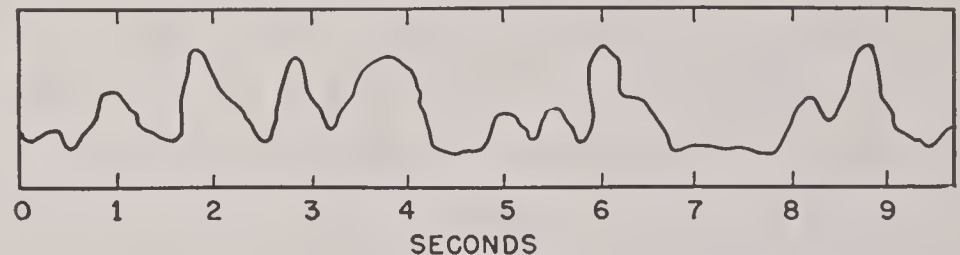


FIGURE 34. Variation in signal strength with time in radiation reflected from the sea (direct radiation cut off).  $\lambda = 9$  cm.

parts of the water surface interfere, and with the changing form of the surface the interference pattern at the place of the receiver changes accordingly. The time scale of these changes must be connected with the speed, wavelength, and amplitude of the waves, but the exact relation is not known thus far.

#### TIDAL EFFECTS

The rise and fall of the tide produces a gradual variation in signal strength by changing the interference between the direct and the reflected rays. The path difference between these rays is  $2h_1h_2/R$ , where  $h_1$ ,  $h_2$  are the heights of the transmitter and receiver relative to the instantaneous water level and  $R$  is the range. The corresponding difference in phase between the two rays is equal to

$$\frac{2h_1h_2}{R} \cdot \frac{2\pi}{\lambda} = \phi, \quad (26)$$

measured in radians. The variation in the signal strength depends upon the variation in  $\phi$ . It is small when the change in  $\phi$  is small and increases to a maximum for a change in  $\phi$  of  $\pi$  radians. It follows from equation (26) that the tidal effect increases with the variation in the water level of the tide and with the heights  $h_1$  and  $h_2$  and decreases with the range and the wavelength.

#### SCINTILLATIONS

The really conspicuous fluctuations in propagation conditions, however, are due to changing meteorological conditions. A characteristic type is an irregular fluctuation in signal strength on a time scale of the order of a minute and with an amplitude rarely



exceeding 2 db. It varies in intensity according to the state of turbulence in the air along the propagation path. In perfectly calm air the fluctuation is practically nonexistent but becomes quite noticeable in turbulent air. This sort of fading is analogous to the scintillation of the fixed stars or the unsteadiness of the telescopic picture of distant objects occurring especially on warm summer days. The physical explanation for the scintillations is found in the fact that the turbulent motion of the air produces irregular variations in refractive index. The consequent irregular bending of rays passing through such a medium produces a patchy distribution of intensity over the wave front. In the case of stellar scintillations the main change in refractive index is caused by fluctuations in air density, and the significant level of turbulence is at an elevation of several thousand feet. For radio waves fluctuations of water vapor density are the chief cause of the scintillations, and the active region is consequently close to the ground. For typical radio scintillations see Figure 35A.

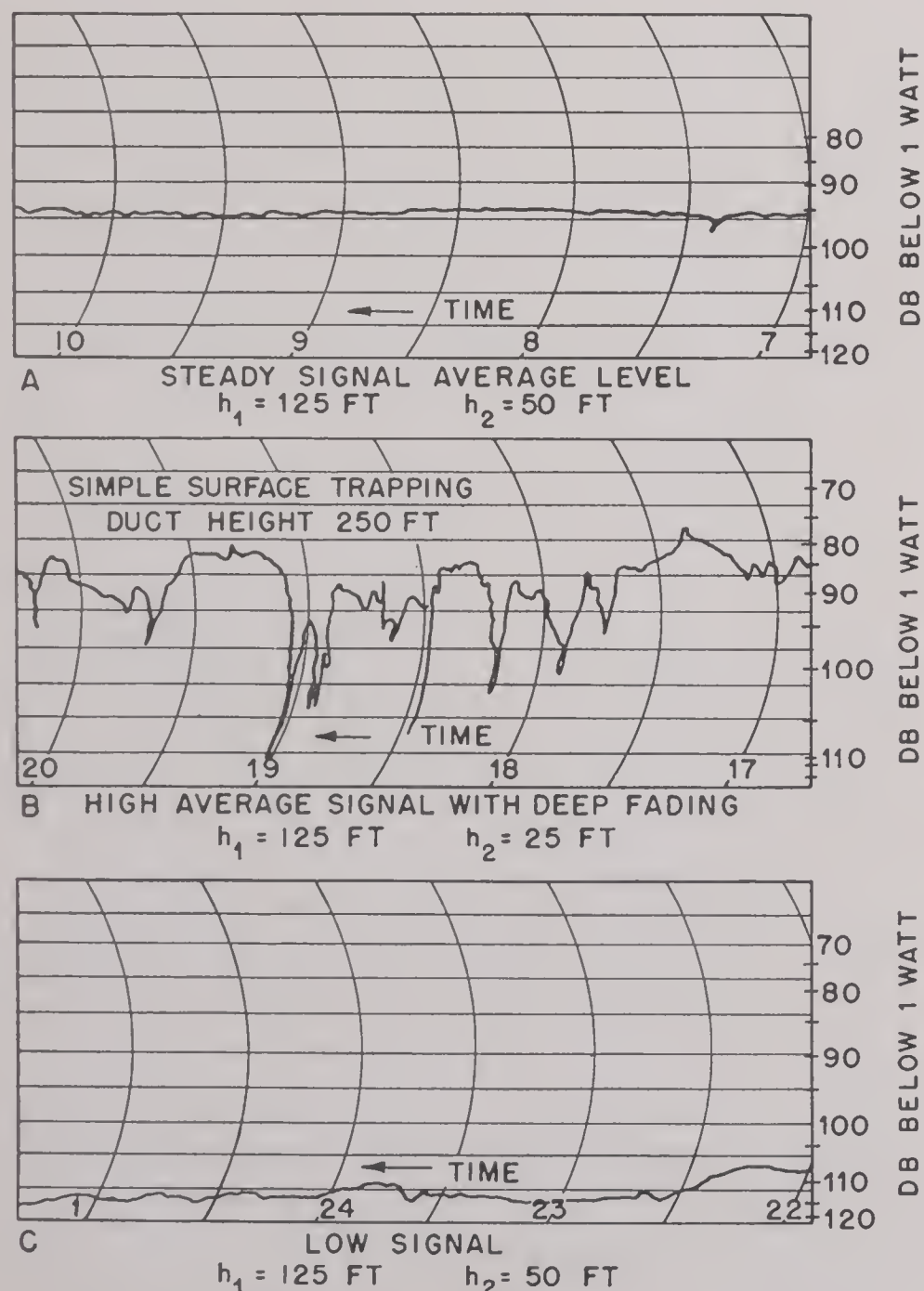


FIGURE 35. Signal strengths for  $\lambda = 10$  cm over sea.

## DUCT FADES

A duct is normally accompanied by fades in the signal strength of large amplitude (up to 30 db) and of moderate periods (of the order of 15 min). A detailed theory of this type of fluctuation in signal strength is not available. When the duct is fully developed, there is a large-scale deviation from standard conditions with regard to mean field strength. If, in particular, both transmitter and receiver are situated inside the duct, there is a great increase in received field strength. Suppose, however, that for some reason the duct does not function according to the simple theory. The field strength at the receiver may then drop to the value corresponding to standard conditions. The observed fades exhibit just this characteristic in that they consist in sharp drops of signal strength *down* from a mean upper level. The conditions are illustrated in Figure 35, which shows three records obtained for a 22-mile path over sea. Figure 35A shows the normal record on a calm day when the only disturbances are due to scintillations. The record shown in Figure 35B, on the other hand, was obtained for a condition of simple surface trapping, with transmitter and receiver inside the duct. It will be noted that the signal strength is considerably above the 95-db average as given in Figure 35A.

Duct-type fades have been observed over land as well as over sea and appear to form a characteristic feature from which the presence of superrefraction may be inferred.

## BLACKOUT

Figure 35C shows a fade in which the signal level is far *below* average and which for this reason is called "blackout." This type is liable to occur when warm, moist air is cooled from below (see the sub-standard *M* curve Ib in Figure 20) and is often correlated with fog. The main irregularities in signal strength are again on a time scale of the order of  $\frac{1}{4}$  hour; the amplitude of variation is smaller than in the preceding case and rarely exceeds 10 db.

## FRONTS AND THUNDERSTORMS

On several occasions marked variations in signal strength have been observed when fronts pass between the transmitter and receiver. The passage of the front itself is marked by very rapid and deep fluctuations, followed by less violent changes on a



longer time scale (see Figure 36). It appears that similar effects are likely to occur during thunderstorms.

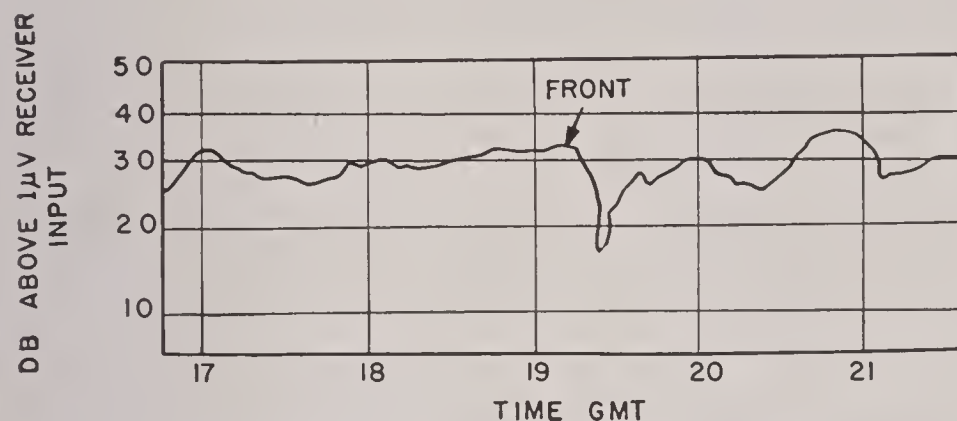


FIGURE 36. Effect of a front on signal strength (Haslemere-Wembley Link, England).

### Fog

Some peculiar effects were observed by transmission through fog over an experimental overland radio link in England. The effect of a shallow layer of radiation fog in the early autumn (September-October) was to produce a nearly complete fade-out of signal strength which lasted for hours and rose to normal as the fog cleared. The explanation of this effect is probably the same as in the case of the "blackout" type fades discussed above, indicating that radiation

fog produces a substandard *M* curve. Later in the autumn (November-December) or winter (January) it was found that the effect of fog was quite different. In this season the signal strength was increased and deep fades appeared which are reminiscent of the duct-type fades described earlier.

### FADING ON DIFFERENT WAVELENGTHS

Several experiments have been performed in which transmitters working on different wavelengths operate simultaneously over the same path and the received field intensities are recorded on the same chart. Figure 37 shows one such record for the 42.5-mile (optical) path from the Empire State Building, New York City, to Hauppauge, Long Island, for May 14 and 15, 1943, at frequencies of 474 mc and 2,800 mc. It will be noticed that on May 14 up to about 5:45 p.m. the two records show a close agreement. At 6:00 p.m. violent fading sets in on both frequencies, but with great diversity in detail. Not infrequently the signal on one frequency increases while on the other frequency it decreases. About 1:00 a.m. on May 16 the disturbance dies down, and the initial harmony in the two records is restored.

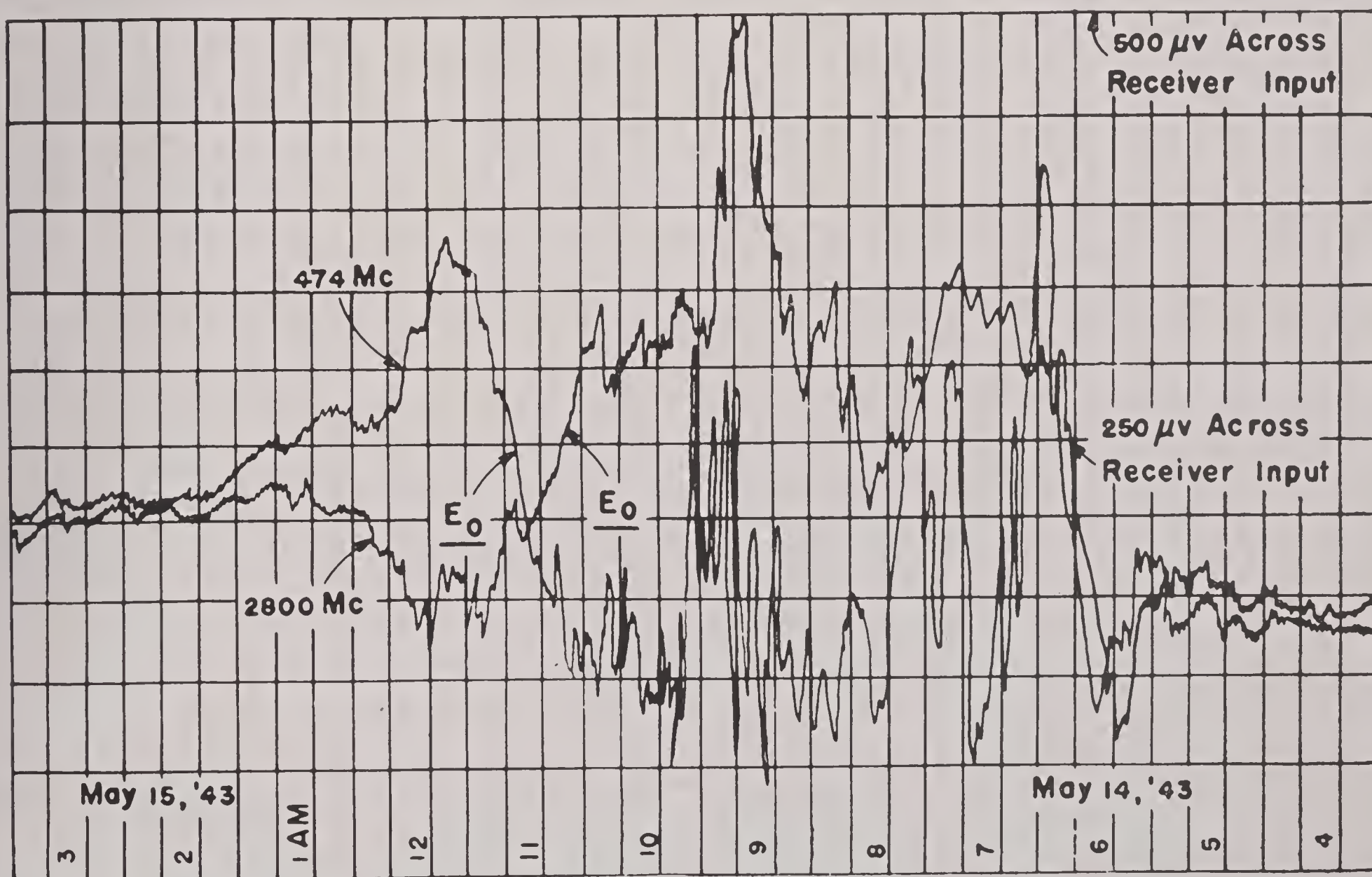


FIGURE 37. Simultaneous variations of signal strength with frequency. (Empire State Bldg. to Hauppauge, L. I., N. Y.)



Experiments over the longer (nonoptical) path from the Empire State Building, New York City, to Riverhead, Long Island (range 70.1 miles), showed much greater diversity in the fading patterns for the different frequencies. On the other hand, observations over the British radio link from Guernsey to Chaldon on 60 mc and 37.5 mc (range 85 miles) showed that if there were marked variations on one frequency similar results were likely to be found on the other frequency.

#### RELIABILITY OF CIRCUITS

The reader must be warned that the amount of the fading in the signal strength is not a measure of the performance of radar and communication circuits. These will operate successfully so long as the periods of low signal are relatively short. Neither the scintillations of Figure 35A nor the larger dips of Figure 35B would seriously affect operation, but a prolonged signal such as in Figure 35C would certainly interfere seriously with communication and radar performance.

Some quantitative data are available from the transmission path referred to in the previous paragraph. On the optical path, New York to Hauppauge, the range of signal fluctuations increased rapidly with increasing frequency. On 45 mc the "undisturbed" level (the observational equivalent of standard) was 21 db below free space with an amplitude of fluctuations that very rarely exceeded  $\pm 4$  db. On the 474-mc circuit the undisturbed level was 3.5 db below free space while the fluctuations varied between 10.5 db above to more than 30 db below free space. The level was 5 db or more below the undisturbed value during 0.01 per cent of the time in January and during 0.4 per cent of the time in July. On the 2,800-mc circuit the undisturbed level was  $-2$  db below free space; the maximum was 12 db above and the minimum more than 25 db below free space. During 0.15 per cent of the time the signal was 5 db or more below the undisturbed level in January; the corresponding figure for July was 3.6 per cent. The conclusion may be drawn from this and similar experiments that over optical paths transmission becomes gradually less reliable as the frequency is raised.

Over the nonoptical path, New York to Riverhead, the margin of fluctuations was much larger. On the 45-mc circuit the undisturbed value was 35 db below free space, the maximum 18 db below, and the minimum more than 50 db below free space. During 1.6 per cent of the time the signal was 5 db or more

below the undisturbed level. On the 474-mc circuit the undisturbed signal was 30 to 35 db below free space, the maximum 10 db above, and the minimum 44 db below free space. During 0.47 per cent of the time the signal was 5 db or more below the undisturbed value. At 2,800 mc the undisturbed signal was 50 to 60 db below free space near the limit of sensitivity; the observed maximum was 13 db above free space, and the minimum could not be observed. In this case the effects of superrefraction were quite pronounced. In January the signal was less than 40 db below free space during 6.5 per cent of the time; the corresponding figure for July is as high as 33 per cent.

The reliability of these transmission circuits is shown in Figure 38. Here, both for the optical and nonoptical paths, the percentage of time during which the signal strength was below specified values is plotted for the various frequencies used. The specified values of signal strength, for each frequency and path, are measured relative to the corresponding undisturbed value. The results, which give averages of the performance during July 1943 and January 1944, indicate that the reliability increases appreciably with decreasing frequency.

It must be said that the New York area where these experiments were made is not particularly affected by blackout situations, and the results are probably not typical for locations where blackouts are a frequent occurrence. The general nature of these data is confirmed by results of extensive experiments in England and in Massachusetts Bay.

17.3.10

#### Scattering and Absorption by Water Drops

As microwave sets have come into general use in recent years the "rain echoes" frequently seen on the scope have attracted attention. The possibility of using microwave radar as an aid to meteorological forecasting and for aerial navigation was early recognized and is now being put to operational use.

At first sight, ground clutter resulting from trapping of radiation in a ground-based duct and rain reflections look somewhat alike on the scope of a radar set. At closer inspection differences appear; the cloud pictures are usually more fuzzy and less sharply defined than the echoes received from ground targets. An experienced operator usually has little difficulty in distinguishing rain echoes from echoes of targets or objects at the ground, but occasional



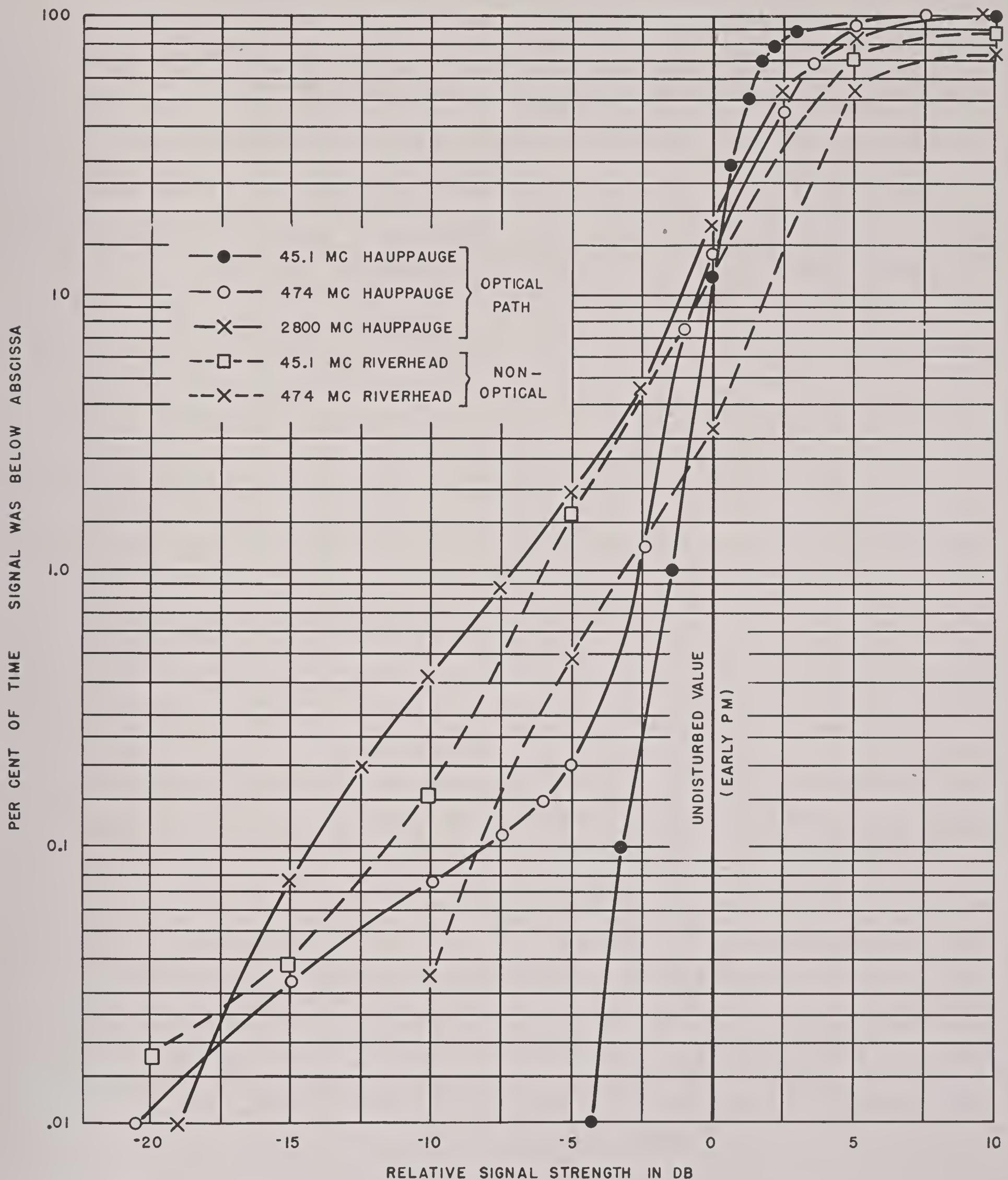


FIGURE 38. Reliability of circuit. Average of July 1943 and January 1944. (Empire State Building to Hauppauge and Riverhead, L. I., N. Y.)

mistakes have been reported, especially from the tropics.

Rain echoes are a result of the scattering of microwaves by the raindrops. Electromagnetic theory

shows that the amount of scattering increases very rapidly as the wavelength is decreased. It also increases rapidly with increasing drop diameter. On account of this sharp variation the scattering effects



become appreciable only when the wavelength is below a certain maximum value and when the drops exceed a certain critical size. Rain echoes are rarely observed at longer waves than S band, but they are common at S band and become very important at the shorter microwaves.

For a time it was thought that clouds could produce microwave echoes, but more thorough investigations have now established the fact that the droplets in clouds are too small to produce appreciable scattering. Only drops that are large enough to constitute genuine rain are seen by a radar, and, especially at S band, light rains will often escape detection. The term "storm echo," invented at a time when the origin of these echoes was not yet clearly understood, should be avoided, and the terms "rain echo" or "precipitation echo" should be used instead. A rain seen by the radar is not necessarily recorded by an observer at the ground, as the rain may be confined to the free atmosphere and never reach the earth. This occurs either when the rain falls in an ascending stratum of air where the air rises more rapidly than the drops fall or when the raindrops evaporate again before reaching the ground. Both cases occur quite commonly in the atmosphere, especially under convective conditions such as are indicated by cumulus clouds and thunderstorms. Snow may also be seen on microwave scopes provided the snowfall is sufficiently heavy.

While clouds themselves do not produce microwave echoes, they may contain falling rain of one of the forms just indicated. Visual appearances are deceiving, and an imposing looking cumulus cloud might be entirely invisible on the scope, whereas a cloud that is inconspicuous to the eye but contains falling raindrops might give a pronounced echo.

The question of "shadow" cast by a storm echo is of some operational interest. A shadow is formed when the absorption that accompanies scattering by the raindrops becomes so strong that the remaining radiation no longer suffices to produce visible echoes from targets behind the rain area. This effect is pronounced on X band, and even more on K band, and is often quite conspicuous with airborne equipment where it may happen that a rain storm blanks out a sector of the sweep. On S band the absorption is usually much weaker and targets can often be seen behind a rain echo.

The usefulness of rain echoes for aerial navigation, particularly in the tropics, is now so generally known that the subject need not be discussed further.

17.4

### SNELL'S LAW

The ordinary law of refraction known as Snell's law may be expressed as

$$n_0 \sin \beta_0 = n_1 \sin \beta_1,$$

where  $\beta_0$  and  $\beta_1$  are the angles which the ray makes with the perpendicular to the boundary. Here it is more convenient to take the angle  $\alpha$  between the ray and the boundary surface. Snell's law then reads

$$n_0 \cos \alpha_0 = n_1 \cos \alpha_1.$$

The refraction at a sharp boundary is shown in Figure 39A. If there are several boundaries it is

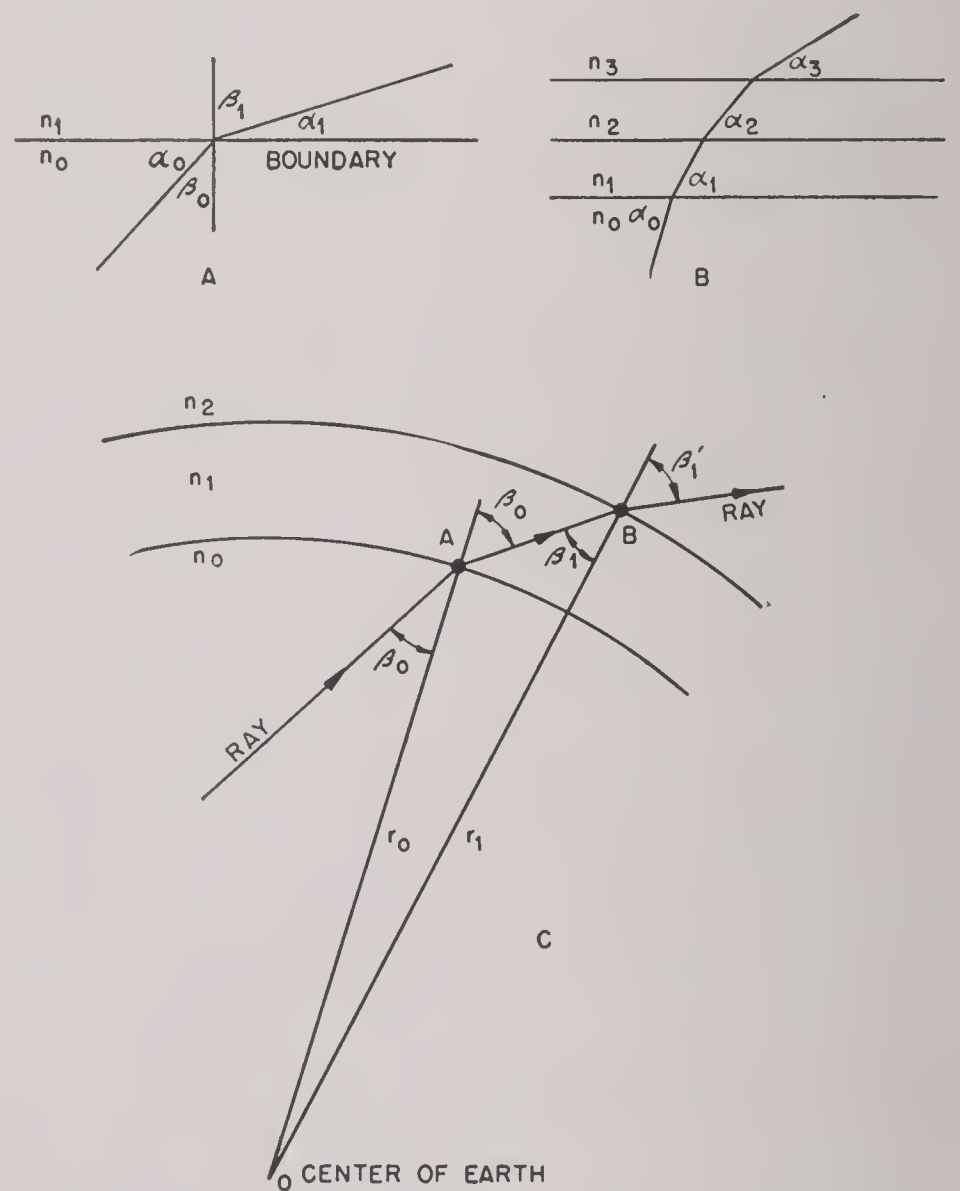


FIGURE 39. Application of Snell's law of refraction.

readily seen that Snell's law generalizes (Figure 39B) to

$$n_0 \cos \alpha_0 = n_1 \cos \alpha_1 = n_2 \cos \alpha_2 = \dots,$$

and for a continuously variable layer it becomes

$$n \cos \alpha = n_0 \cos \alpha_0,$$

where  $n$  and  $\alpha$  are continuous variables which are functions of the height and the index 0 designates an arbitrary reference level.

Snell's law for a curved earth may be derived from Figure 39C. For successive boundaries it is found:



$$\begin{aligned} n_0 \sin \beta_0 &= n_1 \sin \beta'_0, \\ n_1 \sin \beta_1 &= n_2 \sin \beta'_1, \text{ etc.} \end{aligned}$$

Multiply the first equation by  $r_0$ , the second by  $r_1$ , etc. Then

$$\begin{aligned} n_0 r_0 \sin \beta_0 &= n_1 r_0 \sin \beta'_0, \\ n_1 r_1 \sin \beta_1 &= n_2 r_1 \sin \beta'_1, \text{ etc.} \end{aligned}$$

But from the triangle  $OAB$

$$\frac{\sin \beta'_0}{r_1} = \frac{\sin \beta_1}{r_0}, \text{ etc. ,}$$

so that:

$$n_0 r_0 \sin \beta_0 = n_1 r_1 \sin \beta_1 = n_2 r_2 \sin \beta_2 = \cdots .$$

Again introducing the angle  $\alpha$  with the horizontal and making the transition to a continuously variable refractive index gives

$$nr \cos \alpha = n_0 r_0 \cos \alpha_0 ,$$

which is the generalization of Snell's law for a curved earth.  $r_0$  may be chosen as any convenient height, say  $a$  for the surface of the earth or  $a + h_1$  for the height of the transmitter, and  $n_0$  is the corresponding value of  $n$ .



## THEORETICAL TREATMENT OF NONSTANDARD PROPAGATION IN THE DIFFRACTION ZONE<sup>a</sup>

THE ASSUMPTIONS and restrictions underlying this presentation are:

1. We concern ourselves with problems of the *diffraction region* only: the field is calculated at considerable distance from the transmitter and not too great height above the ground.

2. The plane-earth model is used, in which the effect of curvature is simulated by using the modified index  $M$  instead of the index of refraction  $n$ .

3. The earth's surface is assumed smooth, and  $M$  depends on height only (horizontal stratification).

4. Simplified boundary conditions at the earth's surface are used, appropriate to the treatment of the diffraction zone at microwave frequencies. This results in a formula which refers only to a discrete spectrum of modes and makes the calculations independent of polarization.

5. The directional pattern of the transmitter need not be considered, since only the intensity at the azimuth in question and within 1 degree of the horizontal plane is of importance. The problem solved is that of a vertical dipole, electric or magnetic.

6. The field is described in terms of a single quantity  $\Psi$ , the Hertzian vector being  $(0,0,\Psi)$ . Then, at a point in the diffraction region,

$$\text{actual field strength} = |\Psi|^2 \cdot d^2 \cdot E_0, \quad (1)$$

with  $d$  = horizontal distance from source,

$E_0$  = free space field at distance  $d$ .

An expression for  $\Psi$  can then be found in the form

$$\Psi(d,z) = e^{i\omega t - i\pi/4} \sqrt{\frac{2\pi}{kd}} \sum_m e^{-\gamma_m d} U_m(h_1) U_m(z), \quad (2)$$

where  $h_1$  = transmitter height;

$z$  = height at which  $\Psi$  is calculated;

$$\omega = 2\pi f, \quad k = \frac{2\pi}{\lambda}.$$

$\gamma_m$  and  $U_m$  are characteristic values and functions of the boundary value problem

$$\frac{d^2 U}{dz^2} + [k^2 M^2(z) + \gamma^2] U = 0, \quad (3)$$

$$\text{where } \begin{cases} Ue^{i\omega t} & \text{wave moving upward, } z \rightarrow \infty, \\ U(0) = 0. \end{cases} \quad (4) \quad (5)$$

The modified index of refraction  $M$  is supposed to be defined without the factor  $10^6$  usually included.

The functions  $U$  must be normalized in a suitable way. If we had not agreed to use simplified boundary conditions, the last equation (5) would be more complicated and would depend on the type of polarization. Also an integral would appear in addition to the discrete sum in the expression for  $\Psi$ . The actual value for  $\Psi$ , for the diffraction zone and microwave frequencies, would not be affected significantly.

The quantities  $\gamma_m$  are complex:

$$\gamma_m = \alpha_m + i\beta_m. \quad (6)$$

$\alpha_m$  and  $\beta_m$  are positive real quantities. It is convenient to think of the terms of the series as arranged in order of increasing  $\alpha$ :

$$\alpha_1 < \alpha_2 < \alpha_3 < \alpha_4 \cdots$$

These quantities determine the *horizontal attenuations* of the various modes. For large  $d$  only one or at most a few terms of the series are required to give the value of  $\Psi$ . The quantities  $\beta_m$  are all very nearly equal to  $k$ . The slight differences between the  $\beta_m$ 's determine the phase relations and hence the interferences between the various modes.

It is convenient to classify the modes into two types: (1) "Gamow" modes which are strongly trapped, so that  $\alpha$  is very small; (2) "Eckersley" modes which are incompletely trapped or untrapped. The names "Gamow" and "Eckersley" refer to the men who devised the approximate phase integral methods which apply in the two sorts of cases. For practical purposes, when working within the diffraction region, we need consider only the Gamow modes, or at most the Gamow modes and the first Eckersley mode.

In order to be able to use the formula to calculate  $\Psi$  for a given index curve  $M(z)$ , we must obtain the following information about the modes which are to be used:

1. The characteristic values.
2. "Raw" or unnormalized characteristic func-

<sup>a</sup>By W. H. Furry, Radiation Laboratory, MIT.



tions, which satisfy the differential equation and the boundary conditions but still require multiplication by suitable normalization factors.

### 3. The normalization factors.

There are three methods of attack on the problem:

1. Numerical integration of the differential equation, accomplished in practice by the use of a differential analyser.

2. Phase integral methods.

3. Use of known functions and tables, for suitably chosen  $M$  curves.

The method of numerical integration is being used intensively in England by Booker, Hartree, and others. It encounters considerable difficulties in connection with the fitting of the boundary condition at  $z \rightarrow \infty$  and also in the determination of normalization factors. These difficulties have been overcome by special and fairly elaborate procedures. In this country the feeling has been that we should direct our efforts toward the use of the other methods.

If either method (2) or method (3) is to be readily applied to a variety of cases without a prohibitive amount of labor, the  $M$  curves must have a suitable form. The form indicated turns out to be the same in both cases. It consists of portions, each of which is a straight line. If enough such portions are used, any actual  $M$  curve can be accurately represented, but it is impractical to use more than a very few. Present efforts are directed toward dealing with cases where there are just two straight-line portions and there is no prospect of going beyond the cases with three (Figure 1).

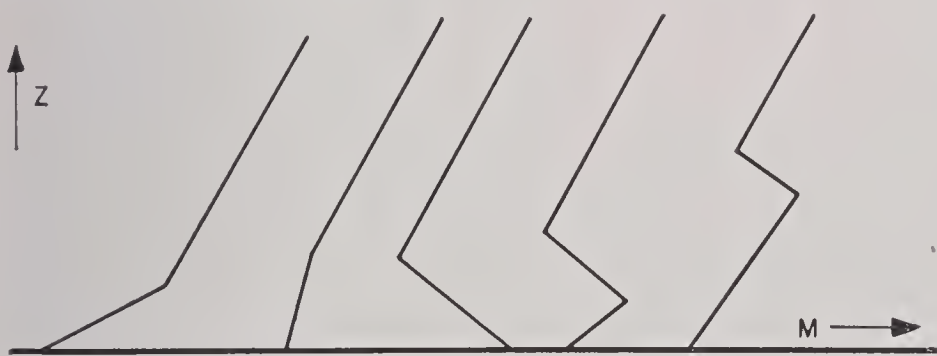


FIGURE 1. Schematic straight-line  $M$  curves.

At first sight these curves look overly artificial, but there are considerations which indicate that they are really an altogether reasonable choice. First, some actually occurring curves have very much this sort of appearance. Second, the sharp breaks in the curves have no really strong effect on the results. Third, practical considerations severely limit the number of parameters which can be used in specifying the curve, so that a meticulous reproduction of every actual curve is out of the question. Fourth,

the assumption of horizontal stratification is usually not well enough justified to make highly precise results really significant.

The use of the jointed-line model for phase integral work was decided on last winter in the Radiation Laboratory.<sup>b</sup>

The phase integral methods were pushed first, because the calculations are quite easy and do not require special tables of functions. Unfortunately the gaps between the regions of validity of the different phase integral approximations turn out to be extremely wide and to cover just the more interesting ranges of slope and duct height. This makes it necessary to resort to the exact solutions to determine characteristic values and normalization factors. The phase integral methods provide limiting cases which can help in guiding the exact computations. Also the phase integral formulas are usually quite adequate for the computation of the "raw" characteristic functions, once the characteristic values are known.

In order to make the exact calculation, we need tables for *complex arguments* of the solutions of the equation

$$\frac{d^2 U}{dz^2} = -zU.$$

These solutions can be expressed in terms of the Airy integrals, but for greater convenience the solutions have been standardized in the form

$$h_j(z) = \left(\frac{2}{3}\right)^{\frac{1}{3}} z^{\frac{1}{3}} H_{\frac{1}{3}}^{(j)}\left(\frac{2}{3}z^{\frac{2}{3}}\right) \quad (j = 1, 2).$$

The tabulation of these functions for  $|z| \leq 6$ , on a square mesh 0.1 unit on a side is being done on the automatic sequence-controlled calculating machine at Harvard University. Work was begun in the latter part of August 1944, under authorization from the Bureau of Ships. Photostats of about one-fourth of the tables were obtained by November 1944.

The present objective is to produce charts from which  $\alpha_1$  and  $\beta_1$  and the normalization factor for the first mode can be obtained for any  $M$  curve made up of two straight portions, the upper one being of standard slope. After this, similar charts for the second mode, and perhaps the third and fourth, will be undertaken. When this has been done, the approximate determination of field strengths and coverage will be possible by a definite routine procedure.

<sup>b</sup>The use of the solutions for this case in terms of Hankel functions was suggested by Lt. Comdr. Menzel.



## CHARACTERISTIC VALUES FOR THE FIRST MODE FOR THE BILINEAR $M$ CURVE<sup>a</sup>

THE MODEL of an  $M$  curve composed of straight-line segments suggested itself to workers at the Radiation Laboratory early in 1944 as one in which phase integral calculations could be carried out very rapidly. At about the same time Lt. Comdr. Menzel suggested the use of this model together with tables of Hankel functions to obtain exact solutions. In the fall of 1944 it became evident that phase integral methods were not of much use with this model. Tables of the required Hankel functions, essentially standard height-gain functions, for complex argument were prepared at the Harvard Computation Laboratory, and considerable effort was directed to the obtaining of exact solutions.

Work at the Radiation Laboratory has been largely confined to the first mode for a curve composed of two segments. This work has progressed largely through the efforts of Miss Dodson and Miss Gill and Howard and Parker. Dr. Pekeris of the Columbia University Wave Propagation Group has been directing work on the second mode.

The units, notation, and model are given by the following formulas and illustrated in Figure 1.

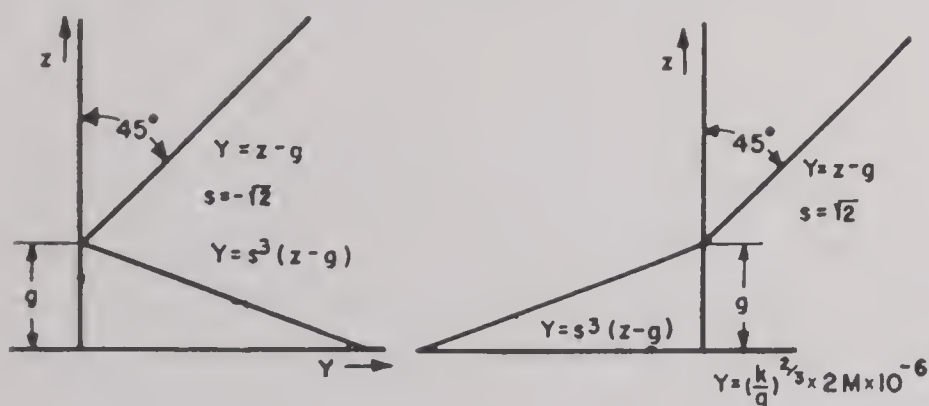


FIGURE 1. Models and units.

$$H = (k^2 q^2)^{-\frac{1}{2}} = \left( \frac{\lambda}{2\pi} \right)^{\frac{2}{3}} \cdot \left( \frac{\frac{4}{3}a}{2} \right)^{\frac{1}{3}}$$

with  $H$  (feet) =  $7.24 [\lambda(\text{cm})]^{\frac{2}{3}}$ ,

$$L = 2(kq^2)^{-\frac{1}{2}} = 2 \left( \frac{\lambda}{2\pi} \right)^{\frac{1}{3}} \cdot \left( \frac{\frac{4}{3}a}{2} \right)^{\frac{2}{3}}$$

with  $L$  (thousand yds) =  $6.69 [\lambda(\text{cm})]^{\frac{1}{3}}$ ,

$$z = \frac{h}{H}; x = \frac{d}{L}; \frac{d^2 U}{dz^2} + (Y + D) U = 0.$$

<sup>a</sup>By W. H. Furry, Radiation Laboratory, MIT.

The natural units of height and distance represent two different compromises between wavelength  $\lambda$  and earth radius  $a$ , so that  $\lambda \div H \div L \div a$  form, very roughly, a geometric progression. It is seen that for microwaves, heights and distances occurring in practice are fairly small numbers of natural units.

The  $M$  curves are plotted in terms of the height  $z$  in natural units and of a quantity  $Y$  which is simply  $M$  multiplied by a suitable wavelength dependent factor. The standard part of the curve then has slope unity. In the bilinear model the anomaly consists of a segment with slope  $s^3$  times standard, or, in these diagrams, simply slope  $s^3$ . For negative  $s$  there is a duct;  $s$  positive but less than 1 gives transitional cases; and  $s$  greater than 1 gives substandard cases.

The essential quantity  $\Psi$  used in calculating the field is given by:

$$\Psi = (e^{i\omega t - 2\pi i d/\lambda - i\pi/4}) \frac{2\sqrt{\pi}}{L} x^{-\frac{1}{2}} \times \sum_m e^{-A_m x + iB_m x} U_m(z_1) U_m(z_2).$$

The power density is equal to the free space power density multiplied by  $\Psi^2 d^2$ . The characteristic values are complex:  $D = B + iA$ . For the standard case:  $D_1 = -1.17 + 2.02i$ . (For  $\lambda = 10$  cm this corresponds to an attenuation of 1.22 db per thousand yards.)  $\Psi$  consists of three factors: one, that for a plane wave, which can ordinarily be omitted; the second, a constant factor which depends on wavelength through  $L$ , the natural unit of distance [this factor can be replaced by just  $2\sqrt{\pi}$  if  $x^2 (= d^2/L^2)$  instead of  $d^2$  is written in the first line]; and finally the critical factor written in terms of natural units only and involving characteristic values and characteristic functions. The imaginary parts of the characteristic values are the coefficients of horizontal attenuation, and the characteristic functions are the height-gain functions.

It is seen that for a typical microwave frequency the horizontal attenuation of the first standard mode ( $g = 0$ ) is rather sizable. The plot of the height-gain curve shows that if both transmitter and receiver are at about 200 ft there is a gain of 50 to 60 db.







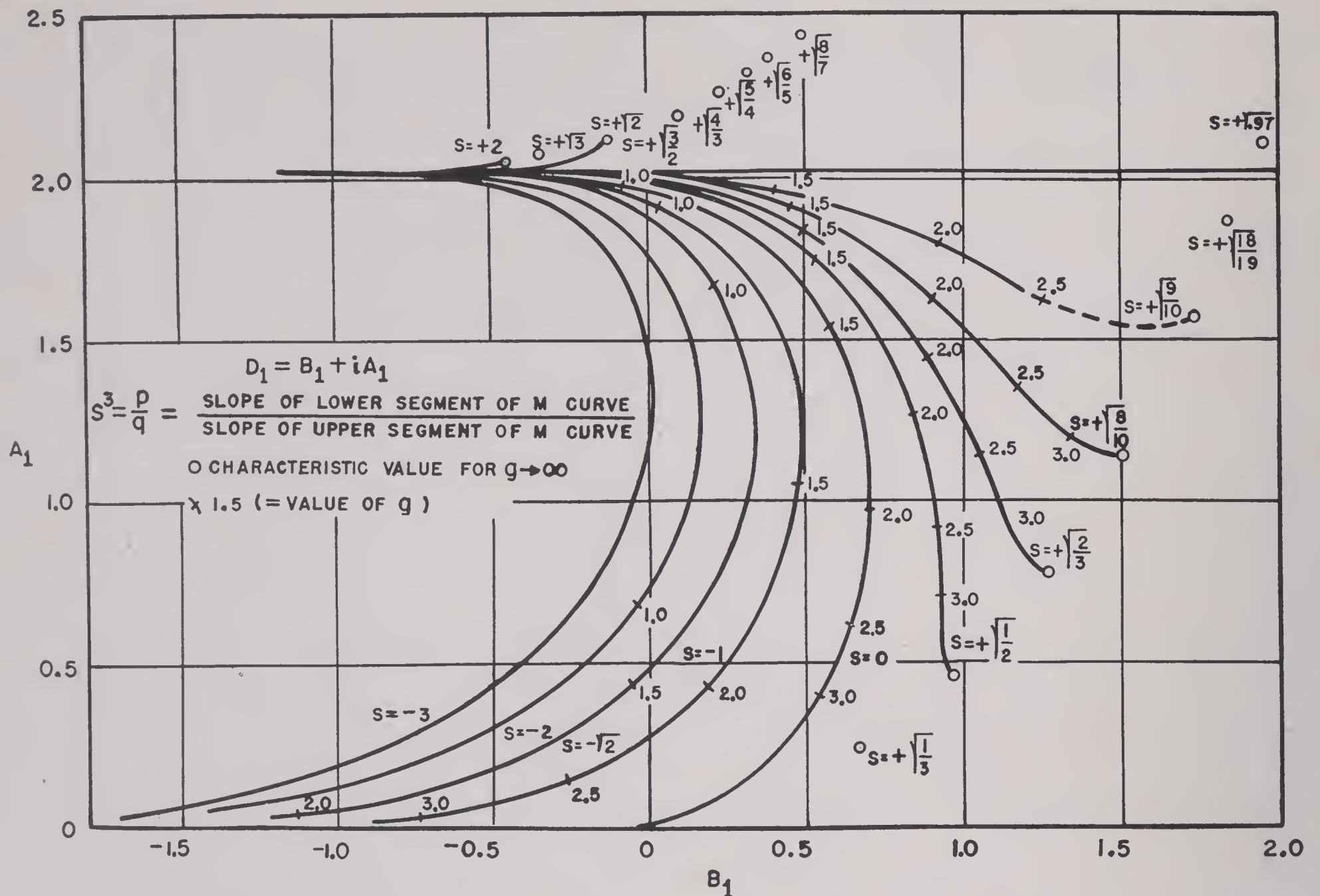


FIGURE 4. Characteristic values for the first mode.

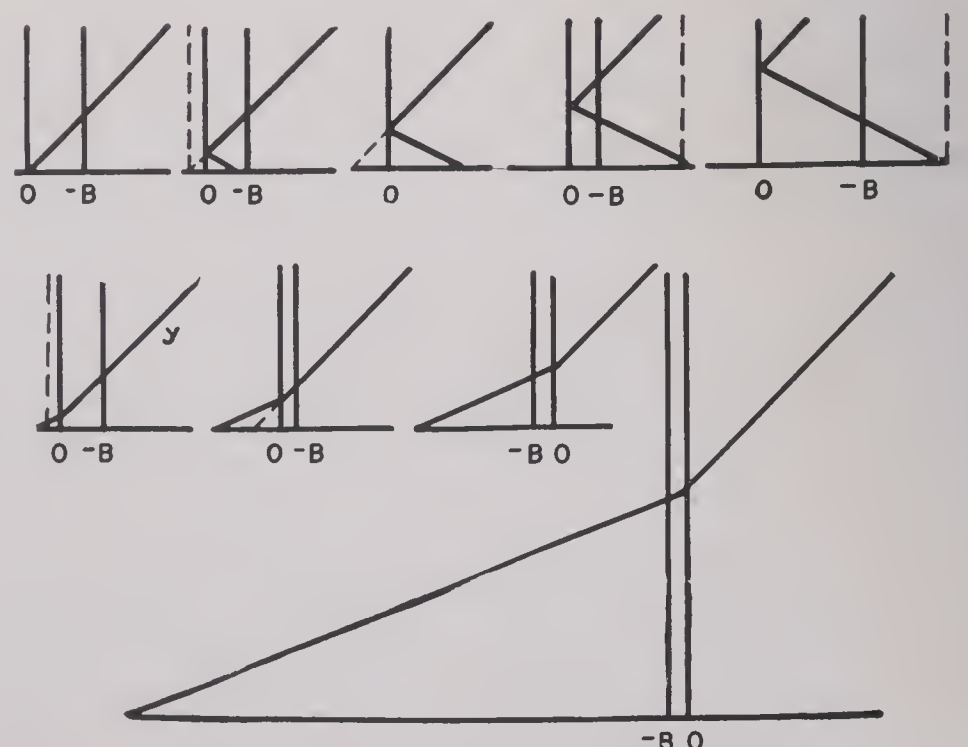
hand, for positive  $s$ , the attenuation constant approaches a finite asymptotic value. It is interesting to note that this is always definitely less than the value  $s^2x$  standard, which corresponds to a single straight line of slope  $s^2x$  standard slope.

It is also useful to know the real part  $B$  of the characteristic value. Figure 4 shows the complex  $D$  plane. For  $g = 0$  the  $Y$  curve is just standard, and as  $g$  increases the value of  $D$  for each value of  $s$  traces out a curve; for *small* values of  $g$  all these curves practically coincide. For negative  $s$  the real part decreases steadily as soon as the imaginary part becomes very small. For positive  $s$ , on the other hand, the real part as well as the imaginary approaches a finite limiting value, so that each curve has an end point.

Some of the consequences of this behavior of the real part can be seen by studying Figure 5. The first row of diagrams shows the situation for fixed negative  $s$  and increasing value of  $g$ . The first diagram shows the standard curve. The next shows a curve with a small superstandard section, but  $-B$  still lies in nearly the same location relative to the dotted line which marks where the origin lay for the stand-

ard curve; thus  $B$  has increased. The first figure of the second line shows how the same thing happens for a small substandard section. Thus for small  $g$  the first order effect is just to add the amount  $g$  to  $D$ , for all values of  $s$ .

In the third diagram of the first row we have a case in which the superstandard has a pronounced

FIGURE 5. Curves for negative and positive  $s$ .



effect, but trapping has not yet set in. In such intermediate cases  $B$  may become positive, but the diagram shows a case in which it happens to be zero. In the fourth diagram trapping is definitely established;  $B$  has become negative, and the line  $-B$  has taken on a definite position relative to  $Y(0)$  (dotted line). This same relation is maintained for larger values of  $g$ , as in the last diagram of the top row. In the last diagram the "barrier" has become much more formidable. This means that the value of  $U$  just above the barrier is extremely small, and thus the attenuation is very small because of the small leakage.

In the second row, as has been remarked, the first diagram shows a small substandard section which has only a small perturbing effect;  $-B$  lies essentially at the standard distance from the intercept of the extrapolated standard curve. The second shows an intermediate case. In the third diagram the limiting value of  $D$  has been reached, and the line at  $-B$  has taken its final position relative to the joint of the  $Y$  curve. In the last, larger, diagram  $g$  has become much larger, but  $-B$  has still the same position relative to the joint.

The difference between the last two diagrams is essentially the increase in the strength of the *surface barrier*. The structure of the height-gain curves near and above the joint is practically the same in the two cases. The very thick barrier in the last case causes the intensity near the earth's surface to be extremely small. This particular kind of height-gain effect can be more suggestively referred to as *depth loss*. The amount of this depth loss is very large: the first 200 ft of the substandard layer produces a loss in the product  $U(z_1)U(z_2)$  of at least 200 db (at 10 cm), which is about four times the gain for a similar height in the standard case. Moreover, this loss proceeds at a rapidly accelerating rate, whereas standard height gain goes at a decreasing rate. The same situation of depth loss in thick nonstandard layers occurs in transitional cases, with  $s$  positive but less than unity.

In general the results for the first mode for positive  $s$  can be summarized as follows:

In nonstandard layers of fairly small thickness, less than 100 ft for 10-cm waves, the propagation is not markedly different from standard for the substandard case and can have attenuation strikingly less than standard for suitable thickness of a transitional layer.

For thick layers there is a strong depth-loss effect

in the first mode in both sorts of cases, and the first mode cannot be expected to be the dominant term in  $\Psi$  except at great distances. Some other mode, which does not suffer from the depth-loss effect, although it may have greater attenuation, will be the important mode at smaller distances.

The conclusions for positive  $s$  cannot be expected to apply unless the lower part of the  $M$  curve is really sensibly straight over a considerable part of its length. For negative  $s$  (trapping) this requirement is not so important.

It was mentioned that other models had been employed by various investigators in calculating field strength in the presence of a duct. The British used an index distribution given essentially by  $Y = (z - z^m/m)$ , where  $m$  lies between zero and unity. When  $m = \frac{1}{2}$  the problem could be treated by a phase integral method, which Booker had done. The differential analyzers at Manchester and Cambridge had been used to obtain the characteristic values for other values of  $m$ . The linear variation of index had been studied by Hartree and Pearcey. In this case of linear exponential variation  $Y = z + Ae^{-Bz}$ , where  $A$  and  $B$  are adjustable parameters. This model offers the advantage that the index is an analytic function of  $z$  and also that the modification term approaches zero with increasing height.

An alternative method (Langer's) for joining the two parts of an otherwise bilinear  $M$  profile was brought up. This method gives a solution in terms of Bessel functions and solves the difficulty perfectly for joining two straight lines.

It was inquired whether, in case of positive  $s$  it had been ascertained that for large  $g$  there were no roots of the secular equation corresponding to a linear  $M$  curve having the slope of the lower segment. There was the possibility that the root found might be one of a possible pair and that there might be another solution of the wave equation for positive  $s$  which had not yet been discovered.

The author replied that the roots varied continuously as  $g$  varied and that the investigation had dealt with the root obtained when starting with the first standard value for  $g = 0$ . What happened with increasing  $g$  when the start was made from some other standard value of  $g = 0$  was not known definitely, but the effects were believed to be peculiar. It is expected that there may be some values lying fairly near the  $s$  squared value for the imaginary part. They are not considered to lie close to the  $s$  squared value for the real part, as they would for



the simple assumption previously mentioned—that when the joint is very high the upper segment can be forgotten and the curve can be assumed to be a single line all the way. This is believed incorrect, because when the result is derived by taking only the first terms in the asymptotic expansions, computing a small correction from the next terms in the asymptotic expansions produces terms which are infinite compared to the first terms. This means that the value  $s$  squared times  $D$  is an impossible one. It may well be that there are results with  $s$  squared times  $A$  plus some different value of  $B$  rather than simply  $s$  squared times  $B$ , but these have not been investigated. This does not occur for the first mode, which is all that this report covers, but it may happen that some other mode goes over to that value. Any mode which does so would probably not suffer from depth-loss effect and would be the important mode close in when there was a thick layer with positive slope.

The need was pointed out for stressing the difference between “completely trapped” modes and “leaky” modes. With completely trapped modes the field decreases exponentially with height, and the power carried by each mode is finite, but with leaky modes the field increases exponentially with height, and the power carried by each mode is infinite. This means that completely trapped modes may exist separately, but leaky modes may not. The expansions of fields in terms of leaky modes are thus essentially mathematical and from physical considerations it is no longer possible to anticipate that these expansions would be convergent; the question of convergence has to be settled formally. The reactions of trapped and leaky modes to small perturbations are quite different. The former are relatively insensitive and the latter are very sensitive. In considering the field at a certain distance from the transmitter, it must be ascertained whether the relevant modes are affected by changes in the dielectric constant at heights large compared with this distance; if this is the case particular care must

be taken in proving the sum to be still the same, since even a perfectly reflecting layer at such great heights can have little effect on the field in the region of interest.

It was noted that these remarks pertained to a phenomenon which had greatly puzzled the investigators for several months. The trouble occasioned by the concept that infinite energy is carried by a mode does exist. This means that the formula in terms of modes is valid only if all those modes are summed that make any appreciable contribution. It becomes extremely difficult to carry out the summation when there are numerous modes, as they begin to cancel each other more and more with progress into that region. This occurs in leaving the diffraction region to which this work is meant to apply and in approaching the optical region. The question of what a small departure from the shape of the curve at great heights does is something which was very troublesome during studies made some months ago. There is no doubt that a small departure from a smooth shape of the  $M$  curve has an enormous effect on the results if it occurs at a great height. If the departure is located high enough it need not amount to more than a millionth of an  $M$  unit to spoil the calculation completely. That is because it is a reflecting layer similar to the Heaviside layer, and if placed high enough it not only can reflect to enormous distances but also becomes extremely effective. It was decided not to give this effect too much concern as all these calculations are made on the basis of horizontal stratification. Doubtless all sorts of small departures from a smooth curve occur at various rather large heights, but they do not occur perfectly stratified over areas of hundreds of square miles, and only such perfectly stratified departures could cause embarrassing results. Accordingly it was decided that such fluctuations as occur probably cause fading or fluctuation but do not cause the particularly troublesome effect mentioned, because they are local disturbances which are not stratified over large areas.



## INCIPIENT LEAKAGE IN A SURFACE DUCT

## 20.1 CALCULATIONS FOR THE FIRST MODE OF THE BILINEAR MODEL

A RECENT INTERCHANGE of ideas on problems of mutual interest with members of the wave propagation group of the Radiation Laboratory prompted the author to investigate the variation of the attenuation constant (or space decrement)  $\alpha(h)$  of the first mode with the duct height  $h$  and negative index gradient  $a$  of a surface duct (see Figure 1).

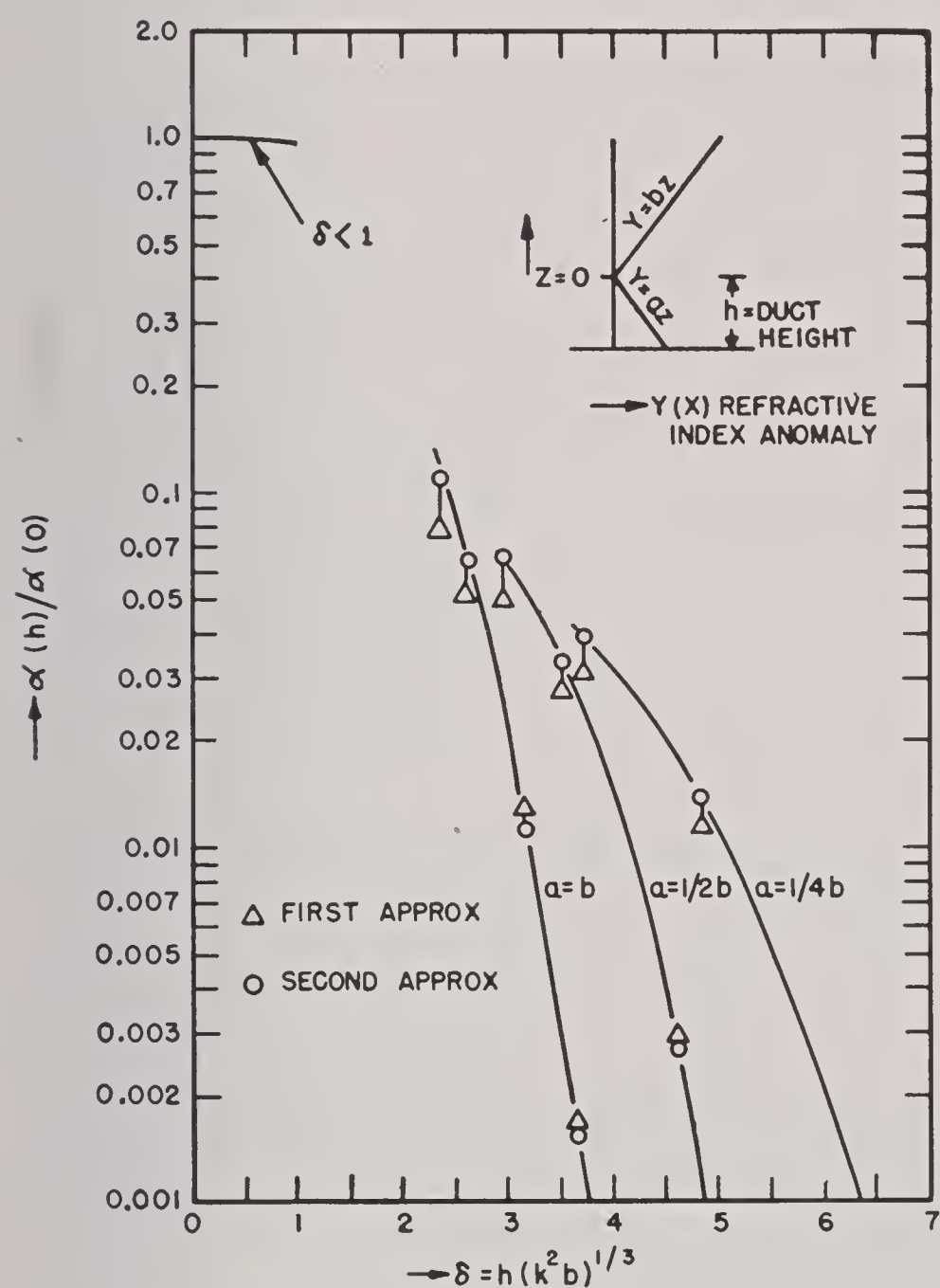


FIGURE 1. Variation of the attenuation constant with duct height.

The attenuation constant is defined as the constant  $\alpha$  which occurs in the factor as:  $(1/\sqrt{d}) e^{-\alpha d}$ , giving the variation of the amplitude with range  $d$ .

The results are shown in Figure 1. In this figure the attenuation constant  $\alpha(h)$  is expressed in terms of the attenuation constant for zero duct height

<sup>a</sup>By C. L. Pekeris, Columbia University Wave Propagation Group.

$\alpha(0)$ . In Figure 1 the curve for  $\delta < 1$  was computed from a formula developed by Freehafer and Furry of the Radiation Laboratory:

$$\frac{\alpha(h)}{\alpha(0)} = 1 - \left(1 + \frac{a}{b}\right) \frac{\delta^6}{90} - \left(1 + \frac{a}{b}\right) \frac{\delta^8}{1,260} - \dots \quad (1)$$

where

$$\delta = h(k^2 b)^{1/3}.$$

Here  $h$  = duct height;  
 $a = -dM/dz$  inside the duct;  
 $b = dM/dz$  above the duct;  
 $k = 2\pi/\lambda$ .

It was felt that this equation could be used up to  $\delta$  equal to about 1.3 but not beyond this value.

The curves on the right for  $\delta > 2$ , for which a condition of nearly complete trapping is approached, were obtained as follows. The secular equation for the proper value of  $\Lambda$  ( $\alpha \sim I_m \Lambda$ ), is

$$\frac{H_{\frac{1}{3}}^{(2)}(p)}{H_{\frac{1}{3}}^{(1)}(p)} - \frac{H_{\frac{1}{3}}^{(2)}(s)H_{-\frac{2}{3}}^{(2)}(q) + H_{-\frac{2}{3}}^{(2)}(s)H_{\frac{1}{3}}^{(2)}(q)}{H_{\frac{1}{3}}^{(2)}(s)H_{-\frac{1}{3}}^{(1)}(q) + H_{-\frac{2}{3}}^{(2)}(s)H_{\frac{1}{3}}^{(1)}(q)} = 0, \quad (2)$$

where

$$q = \frac{2k}{3a} \Lambda^{\frac{3}{2}}, p = \frac{2k}{3a} (\Lambda + ah)^{\frac{3}{2}}, s = \gamma q, \gamma = \frac{a}{b} \quad (3)$$

is transformed by the substitution

$$q = e^{i3\pi/2} x, p = (x^2 + \beta)^{\frac{3}{2}}, \beta = ah \left( \frac{2k}{3a} \right)^{\frac{2}{3}} \quad (4)$$

into

$$f(p) - F(x) = 0, \quad (5)$$

with

$$f(p) = \frac{H_{\frac{1}{3}}^{(2)}(p)}{H_{\frac{1}{3}}^{(1)}(p)} \quad (6)$$

$$F(x) = \frac{U(\gamma x) V(x) + V(\gamma x) U(x)}{e^{i\pi/3} V(\gamma x) \bar{U}(x) - U(\gamma x) \bar{V}(x)}$$

$$U(x) = I_{\frac{1}{3}}(x) + e^{-i\pi/3} I_{-\frac{1}{3}}(x),$$

$$V(x) = I_{\frac{1}{3}}(x) + e^{i\pi/3} I_{-\frac{1}{3}}(x). \quad (7)$$



Assume now that

$$p = p_0 + \Delta, \quad (8)$$

where  $p_0$  is a constant, which is to be chosen in such a manner that  $\Delta$  is small in comparison to  $p_0$  in the region under consideration. Expanding equation (5) in a power series in  $\Delta$ , one obtains as a first approximation for  $\Delta$ :

$$\Delta_1 = \frac{F(x_0) - f(p_0)}{f'(p_0)}, \quad (9)$$

and for a second approximation

$$\Delta_2 = \Delta_1 \left[ 1 - \frac{\Delta_1 f'(p_0)}{2 f(p_0)} + \frac{F(x_0)}{f(p_0)} \frac{dx}{dp} \right]. \quad (10)$$

These expressions can be computed with the aid of the WPA Tables (unpublished) for the  $I$  functions with *real* argument. The curves in Figure 1 were computed down to values of  $\delta$  such that  $\Delta_2$  did not deviate appreciably from  $\Delta_1$ .

*Conclusion.* From the computed attenuation for a surface duct it appears that, for the first mode, when  $\delta (= hk^3 b^{\frac{1}{2}})$  is less than 1, trapping is less than 2 per cent and that when  $\delta = 3$  to 5 (depending on the negative gradient  $a$ ), trapping is 98 per cent complete. (For the meaning of the constants see Figure 1.) There is therefore a rather narrow range of values of the parameter  $\delta$  (1 to 4) within which a rapid transition takes place from a condition of negligible trapping to a condition of nearly complete trapping. This result may have a bearing on the observed fading which is associated with ducts.

## 20.2 CALCULATIONS FOR THE SECOND AND HIGHER MODES OF THE BILINEAR MODEL

The Analysis Section of Columbia University Wave Propagation Group has undertaken the computation of the characteristic values and height-gain functions for the second and higher modes of a bilinear model  $M$  curve. The first mode of the bilinear model is being treated at the Radiation Laboratory. The computations were carried out with the aid of tables of  $h$  functions prepared by the Harvard Computation Laboratory, under the direction of Furry. Our work to date has been mainly on surface ducts, in which the slope of the lower segment of the  $M$  curve is negative. Cases with positive slopes of the lower

segment of the  $M$  curve have been tried but were found to involve  $h$  functions which are beyond the range of existing tables.

Some results on the characteristic values are shown in Figures 2 and 3 (for a definition of natural units see preceding articles). In Figure 2 the slope of the lower segment of the  $M$  curve is the negative of the standard slope, while in Figure 3 the ratio of the slope of the lower segment to the standard slope is

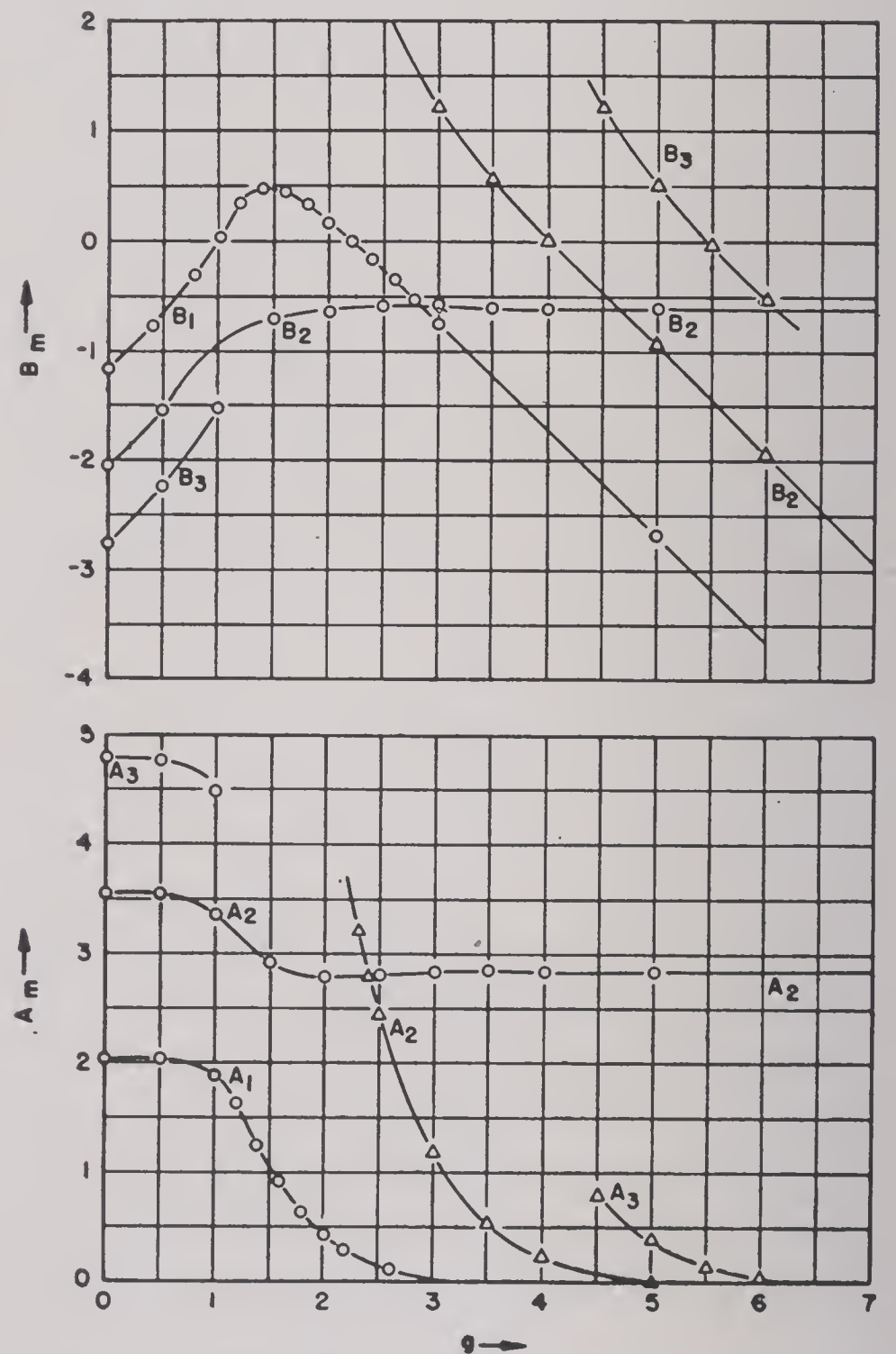


FIGURE 2. Characteristic values of  $D_m$  for a bilinear model.  $s = -1$ .  $D_m = B_m + i A_m$ .  $s^1$  = ratio of slope of lower segment to standard slope =  $s^3$ .  $g$  = height of joint in natural units.

$-\sqrt{8}$ . The curves  $A_1$  and  $B_1$  for the first mode were computed at the Radiation Laboratory. An imaginary part  $A_1$ , which is proportional to the horizontal attenuation (decrement), starts at  $g = 0$  with a value appropriate for a standard atmosphere and decreases continuously as duct height  $g$  increases. Beyond  $g = 3$  the first mode is completely trapped. The curve  $A_2$  for the second mode decreases initially



too but beyond  $g = 2$  is seen to level off to a constant limiting value. The real part of the characteristic value  $B_2$  also approaches a constant limiting value for  $g$  greater than 3. These curves were obtained by solving the secular equation for  $D$  and also determining the slope  $dD/dg$  at each point. The characteristic values curves can also be computed by starting first with Gamow's values appropriate for

TABLE 1. Comparison of exact limiting values of  $D$  with values obtained from the asymptotic formula.\*

$s$	Second mode	Third mode	
-1	$-0.60 + 2.80i$	$-1.06 + 3.60i$	Asymptotic
	$-0.59 + 2.83i$		Exact
$-\sqrt{2}$	$-0.78 + 2.74i$	$-1.22 + 3.40i$	Asymptotic
	$-0.70 + 2.70i$	$-1.42 + 4.08i$	Exact
-2	$-1.00 + 2.60i$	$-1.36 + 3.48i$	Asymptotic
	$-0.80 + 2.44i$		Exact

$$*\exp\left(-\frac{i4}{3}D\right) - \left(1 - s^3\right)/8D^{\frac{3}{2}} = 0.$$

proves that both solutions satisfy the boundary conditions. As a second step in testing the reality of the limiting points, an asymptotic expression was derived for the limiting values, and the values com-

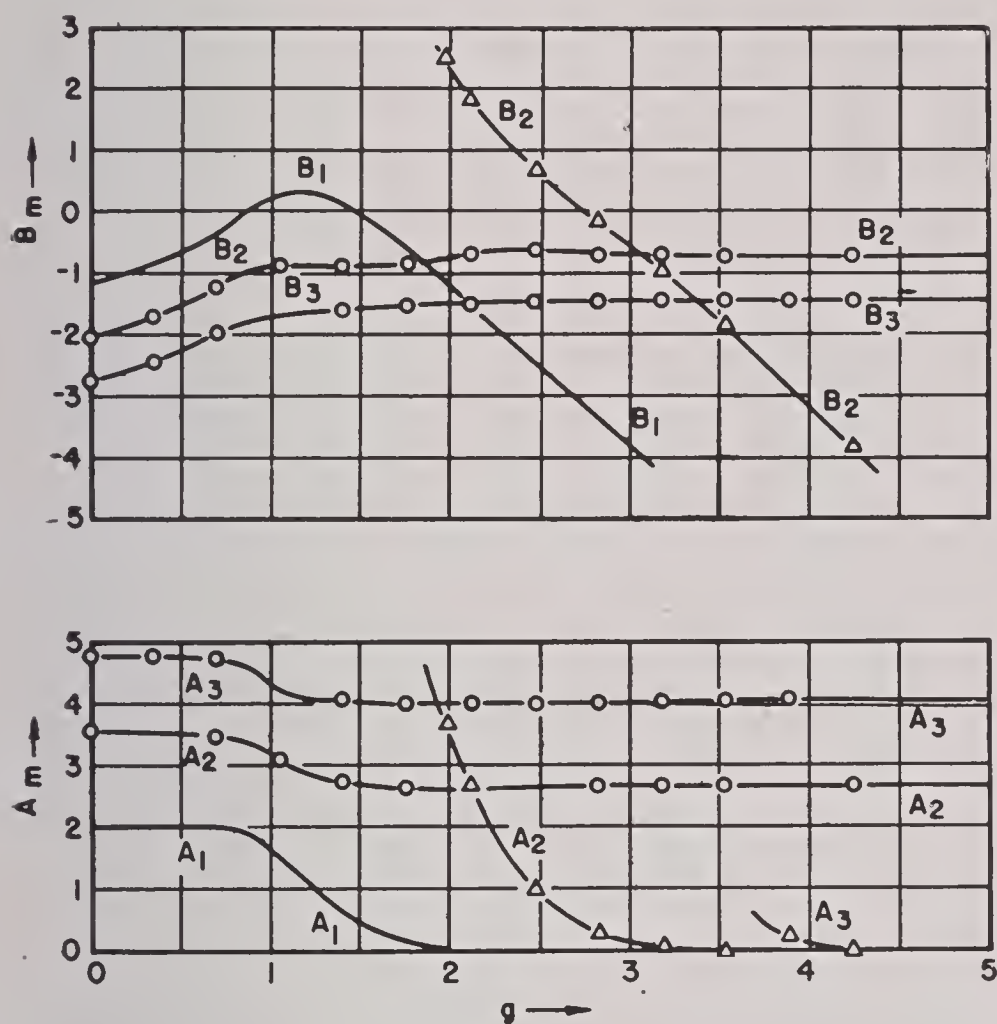


FIGURE 3. Characteristic values  $D_m$  for a bilinear  $M$  curve.  $s = -\sqrt{2}$ .  $g$  = height of joint in natural units.  $s^3$  = ratio of slope of lower segment of  $M$  curve to the standard slope.  $D_m = B_m + iA_m$ .

large  $g$  and continuing backwards toward smaller values of  $g$ , being careful to determine the slope of the curves at each point. It is seen from Figures 2 and 3 that, in contrast to the first mode, these branches of the curves for the second and third modes do not join on smoothly to the other branches which start with standard values at  $g = 0$  and approach limiting values for large  $g$ .

This duplicity of the solutions, which was doubted at first, was substantiated in two ways. The values of  $A_2$  and  $B_2$  at  $g = 3$  and  $g = 5$  in Figure 1 were computed at both branches with increasing accuracy (up to  $10^{-5}$ ), and it was found that the matching of the solutions at the duct height and the degree of vanishing of the height-gain function of the ground improved correspondingly in both branches. This

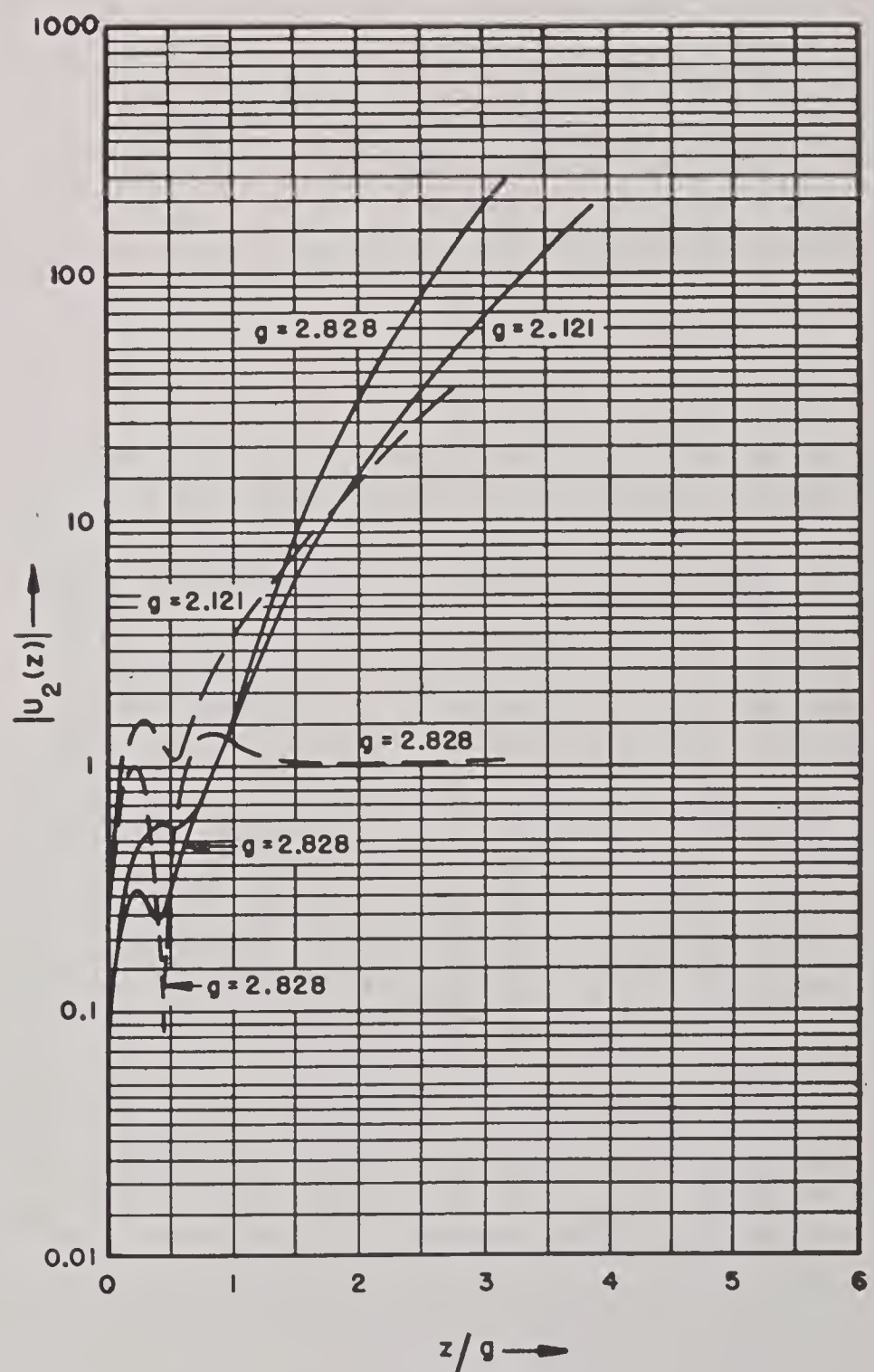


FIGURE 4. Height-gain functions of the second mode for a bilinear  $M$  curve.  $s = -\sqrt{2}$ .  $z$  = height above ground in natural units.  $g$  = height of joint in natural units.  $U_2(z)$  = normalized wave function.



puted therefrom were found to be in fair agreement with the exact values, as is shown in Table 1.

The physical nature of the duplicity of solutions seems to be as follows. The solutions approaching a limiting characteristic value for large duct height  $g$  correspond to the case where the ground sinks to great depths; the other solution corresponds, of course, to the limiting case when the height of joint rises to infinity.

The relative importance of the two types of solution will depend on the ranges and heights considered. At sufficiently great ranges the solutions with the smaller value of  $A_m$  will predominate, but the greater the height considered the farther must one recede from the source before the initial advantage of the limiting solution due to a greater height gain is overcome by the stronger horizontal attenuation. The greater height gain of the limiting solutions at high elevations is illustrated in Figures 4 and 5. In these figures, the height-gain functions for the limiting solutions are drawn in solid lines, those for the Gamow solutions in dashed lines; and the unit of height is the duct height. It should also be pointed out that the normalization condition applied was

$$\int_0 U_m^2(z) dz = g, \quad (13)$$

so that, if a comparison of height-gain functions of solutions of the same class for different values of  $g$  is desired, the plotted values should be divided by  $\sqrt{g}$ .

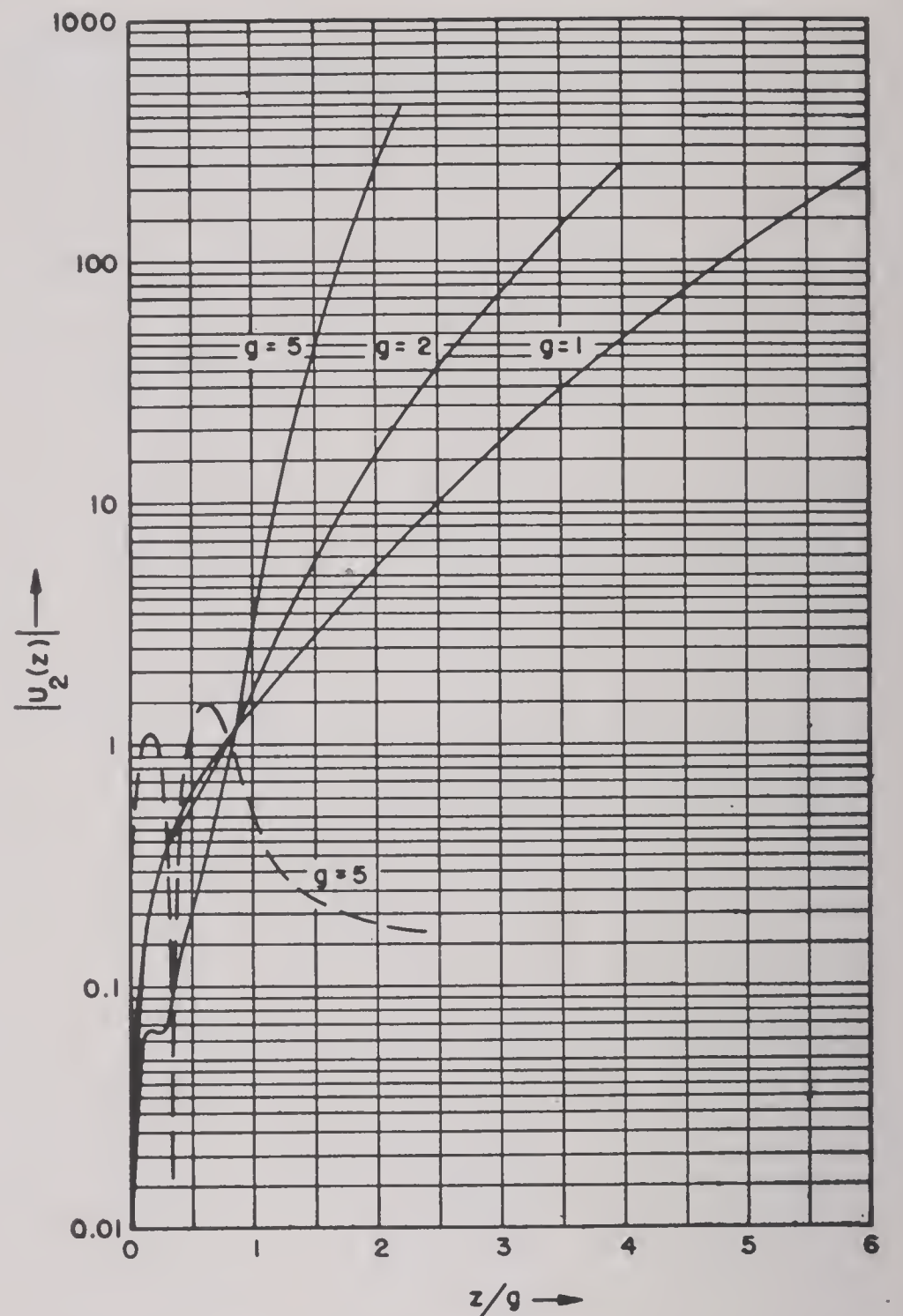


FIGURE 5. Height-gain functions of the second mode for a bilinear  $M$  curve.  $s = -1$ .  $z$  = height above ground in natural units.  $g$  = height of joint in natural units.  $U_2(z)$  = normalized wave function.



## Chapter 21

# THE SOLUTION OF THE PROPAGATION EQUATION IN TERMS OF HANKEL FUNCTIONS<sup>a</sup>

THE CALCULATION of the field strength in the atmosphere depends upon finding a solution of a wave equation incorporating the propagation properties of the atmosphere and satisfying the boundary conditions at the surface of the earth and for large heights. This chapter shows how the wave equation, for certain specified conditions, may be solved in terms of Hankel functions.

Let

- $z$  = height of receiver above earth's surface,
- $h_t$  = height of transmitter,
- $d$  = great circle distance between source and receiver,
- $\lambda$  = wavelength,  $k = 2\pi/\lambda$ ,
- $f$  = frequency,  $\omega = 2\pi f$ ,
- $M$  = modified index of refraction,
- $a$  = radius of the earth.

Under the simplifying assumptions of horizontal stratification, slight variation of refractive index in a wavelength, smooth earth's surface, the plane earth representation, and the use of the simplified boundary condition  $\Psi = 0$  for  $z = 0$ , which eliminates the polarization of the source, the field of a (dipole) source is described by a scalar wave equation:

$$\Delta^2 \Psi + k^2 M^2 \Psi = 0, \quad (1)$$

plus appropriate boundary conditions. Separation of equation (1) in cylindrical coordinates leads to the formal expansion for the field of a dipole source:

$$\Psi = ei\omega t \sum_{n=1}^{\infty} -i\pi H_0^{(2)}(kd \cos \alpha_n) U_n(z) U_n(h_t), \quad (2)$$

where  $\text{Re}(\cos \alpha_n) > 0$ .

Here the characteristic values  $\sin^2 \alpha_n$  and the (normalized) characteristic functions  $U_n(z)$  satisfy the equation

$$\frac{d^2 U}{dz^2} + k^2 [\sin^2 \alpha + M^2] U = 0, \quad (3)$$

plus the boundary and normalization conditions:

$$U(0) = 0 \quad (3a)$$

$ei\omega t U(z)$  represents an outgoing wave for large positive  $z$ . (3b)

$$\lim_{I_m(k) \rightarrow 0} \int_0^{\infty} U^2 dz = 1. \quad (3c)$$

Usually  $\sin^2 \alpha$  is small,  $kd$  is large, and one has

$$\begin{aligned} & \left| H_0^{(2)}(kd \cos \alpha_n) \right| \\ & \cong \left| \left( \frac{2}{\pi kd \cos \alpha_n} \right)^{\frac{1}{2}} \right| \left| e^{-i(kd \cos \alpha_n)} \right| \\ & \cong \left| \frac{2}{dk\pi \cos \alpha_n} \right|^{\frac{1}{2}} \left| e^{-ikd(1 - (1/2) \sin^2 \alpha_n)} \right|. \end{aligned} \quad (4)$$

The exponential decay factor of the horizontal waves thus has the form

$$\exp \left[ -\frac{kd}{2} I_m(\sin^2 \alpha_n) \right],$$

and the  $\sin^2 \alpha_n$  values evidently lie in the upper half of the complex plane.

The problem is then to find the characteristic values and characteristic functions of the system (3) for a given dependence of modified index of refraction upon height. For a ground-based duct of height  $h$  with an  $M$  curve being made up of two line segments, the upper having standard slope, equation (3) becomes

$$\frac{d^2 U}{dz^2} + k^2 [\Lambda + y(z)] U = 0, \quad (3')$$

where

$$y(z) = 2a_1(z - h), \quad 0 \leq z \leq h,$$

$$y(z) = 2a_2(z - h), \quad z \geq h,$$

$$\Lambda = \sin^2 \alpha + 2a_2 h,$$

$$a_2 = \frac{1}{\frac{4}{3}a}.$$

The linear change of variable

$$x_1 = \left( \frac{k}{2} a_1 \right)^{\frac{2}{3}} [\Lambda + 2a_1(z - h)]$$

<sup>a</sup>By Lt. W. F. Eberlein, USNR, Office of the Chief of Naval Operations.



inside the duct, and

$$x_2 = \left(\frac{k}{2} a\right)^{\frac{2}{3}} [\Lambda + 2a_2(z - h)]$$

above the duct reduces equation (3') to

$$\frac{d^2 U}{dx^2} + xU = 0, \quad (3'')$$

whose general solution is

$$U = \begin{cases} A_1 h_1(x_1) + B_1 h_2(x_1) \\ A_2 h_1(x_2) + B_2 h_2(x_2) \end{cases}$$

The " $h_j$ " functions are expressible in terms of Hankel functions of order  $1/3$ :

$$h_j(x) = \left(\frac{2}{3}\right)^{\frac{1}{3}} x^{\frac{1}{3}} H_{\frac{1}{3}}^{(j)}\left(\frac{2}{3} x^{\frac{2}{3}}\right) \quad (j = 1, 2). \quad (5)$$

Condition (3b) is satisfied by setting  $A_2 = 0$ .  $A_1$  and  $B_1$  are determined by the requirement of continuity of  $U$  and  $dU/dz$  at  $z = h$ .

$$\begin{aligned} A_1 &= \frac{i\pi\left(\frac{2}{3}\right)^{\frac{1}{3}}}{4} B_2 \left\{ h_2 \left[ \left(\frac{k}{2a_2}\right)^{\frac{2}{3}} \Lambda \right] h'_2 \left[ \left(\frac{k}{2a_1}\right)^{\frac{2}{3}} \Lambda \right] \right. \\ &\quad \left. - \left(\frac{a_2}{a_1}\right)^{\frac{1}{3}} h'_2 \left[ \left(\frac{k}{2a_2}\right)^{\frac{2}{3}} \Lambda \right] h_2 \left[ \left(\frac{k}{2a_1}\right)^{\frac{2}{3}} \Lambda \right] \right\}, \\ B_1 &= \frac{i\pi\left(\frac{2}{3}\right)^{\frac{1}{3}}}{4} B_2 \left\{ \left(\frac{a_2}{a_1}\right)^{\frac{1}{3}} h'_2 \left[ \left(\frac{k}{2a_2}\right)^{\frac{2}{3}} \Lambda \right] h_1 \left[ \left(\frac{k}{2a_1}\right)^{\frac{2}{3}} \Lambda \right] \right. \\ &\quad \left. - h_2 \left[ \left(\frac{k}{2a_2}\right)^{\frac{2}{3}} \Lambda \right] h'_1 \left[ \left(\frac{k}{2a_1}\right)^{\frac{2}{3}} \Lambda \right] \right\}. \end{aligned} \quad (6)$$

The characteristic values  $\Lambda$  then appear as the roots of the equation

$$\begin{aligned} U(0) &= A_1 h_1 \left[ \left(\frac{k}{2a_1}\right)^{\frac{2}{3}} (\Lambda - 2a_1 h) \right] \\ &\quad + B_1 h_2 \left[ \left(\frac{k}{2a_1}\right)^{\frac{2}{3}} (\Lambda - 2a_1 h) \right] = 0. \end{aligned} \quad (7)$$

The constant factor  $B_2$  appearing throughout is determined by the normalization condition (3c), which takes a peculiarly simple form in this case, since (3'') implies the identity

$$U^2 = \frac{d}{dx} \left[ xU^2 + \left(\frac{dU}{dx}\right)^2 \right]. \quad (8)$$

Owing to the present lack of adequate tables of the  $H_{\frac{1}{3}}^{(j)}$  or  $h_j$  functions for complex arguments and the complicated nature of equation (7), one is forced to employ asymptotic expansions to determine the

$\Lambda$ 's so far as possible. Due care must be exercised in dealing with the branches of the multiple-valued approximations appearing, as well as with the so-called "Stokes phenomenon." For example, in deciding between the two rival asymptotic approximations

$$H_{\frac{1}{3}}^{(2)}(W) \cong \left(\frac{2}{\pi W}\right)^{\frac{1}{2}} e^{-i(W-5\pi/12)}, \quad (9)$$

$$H_{\frac{1}{3}}^{(2)}(W) \cong \left(\frac{2}{\pi W}\right)^{\frac{1}{2}} [e^{-i(W-5\pi/12)} + e^{i(W+11\pi/12)}],$$

both formally valid in the common domain  $0 < \arg W < \pi$ , one employs the first when  $\arg W < \pi/2$ , and the second when  $\arg W > \pi/2$ . The ambiguity on a "Stokes line" ( $\arg W = \pi/2$ ) apparently must be resolved by taking the mean of the two expressions when their difference is important, as it is when strongly trapped modes exist ( $a_1 < 0$ ).

The nature of the results obtained is illustrated in the important case of complete inversion ( $a_1 < 0$ ). For simplicity set

$$\rho = -\frac{\Lambda}{2a_1 h}, \quad (10)$$

$$\sigma = \left(\frac{k}{-3a_1}\right) (-2a_1 h)^{\frac{2}{3}}.$$

Then

$$\text{I} \quad (\rho + 1)^{\frac{3}{2}} - \left(1 - \frac{a_1}{a_2}\right) \rho^{\frac{3}{2}} = \frac{(n - \frac{1}{4})}{\sigma}, \quad \left[ \arg(\rho + 1) > \frac{\pi}{3} \right]$$

$$\begin{aligned} \text{II} \quad 1 + ie^{-2i\sigma(\rho+1)^{\frac{3}{2}}} + e^{-2i\sigma(1-\frac{a_1}{a_2})\rho^{\frac{3}{2}}} \\ = 0, \quad \left(\frac{\pi}{3} < \arg \rho < \pi - \delta\right) \end{aligned} \quad (11)$$

$$\begin{aligned} \text{III} \quad 1 + ie^{-2i\sigma(\rho+1)^{\frac{3}{2}}} + \frac{1}{2}e^{-2i\sigma(1-\frac{a_1}{a_2})\rho^{\frac{3}{2}}} \\ = 0, \quad (\arg \rho \cong \pi). \end{aligned}$$

( $n$  a positive integer)

The corresponding regions of validity are indicated in Figure 1, which also shows the dependence of one characteristic value on  $\sigma$  for a particular ratio  $a_2/a_1$ . If one numbers the characteristic values  $\rho_n$  in order of increasing imaginary part, those for which  $n$  is greater than some integer are defined by equation



I. There is an infinite number of these "Eckersley" or "leaky" modes. Equation II joins on smoothly to

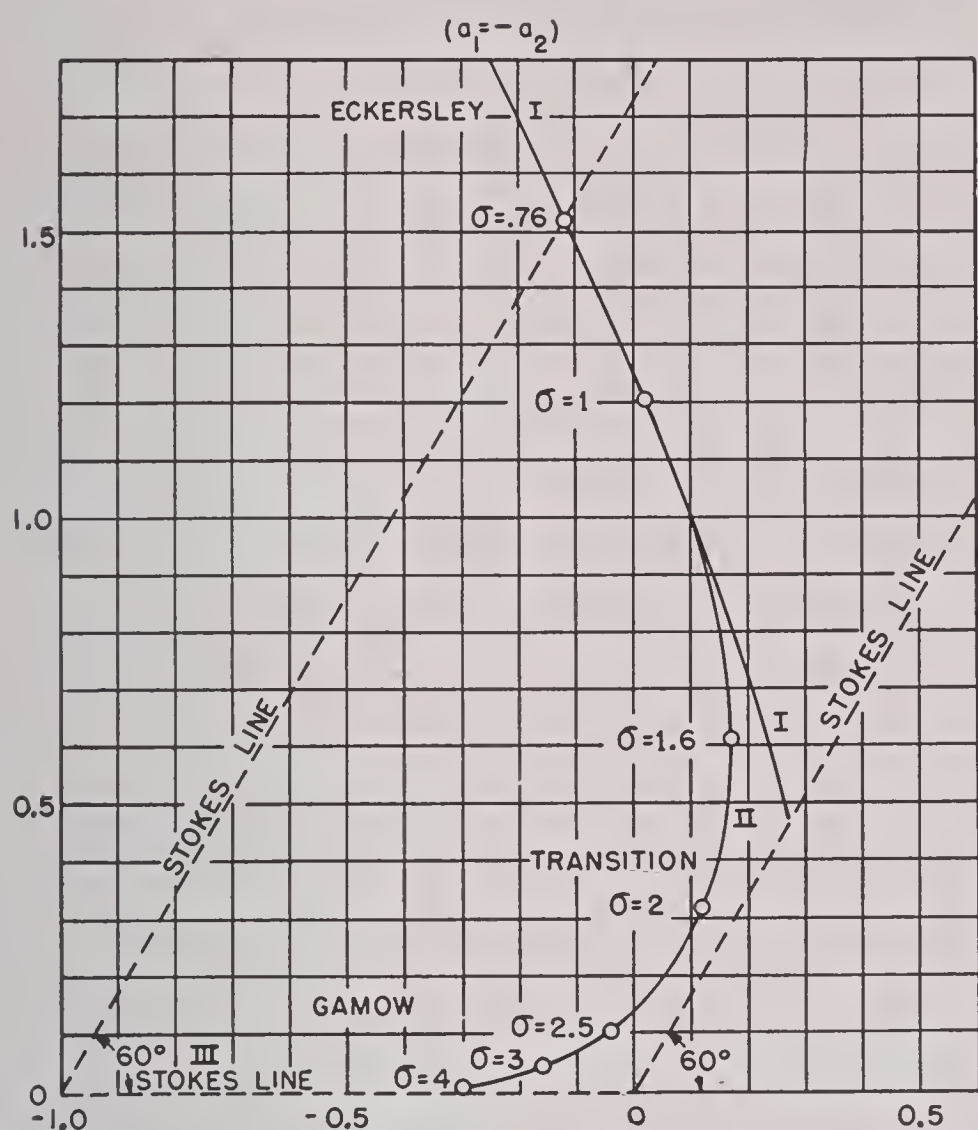


FIGURE 1. Diagram showing the locus of  $\rho$  in the complex plane of  $\sigma$  varies.

I and defines a finite number of "transitional" or "semileaky" modes.

Equation III defines the strongly trapped or Gamow modes for which  $0 < I_m(\rho) \ll -\text{Re}(\rho) < 1$ . In this case the characteristic values lie almost

upon a Stokes line ( $\arg \rho = \pi - \delta$ ). The approximations valid above the line yield II; the ones valid below yield

$$\text{IV} \quad 1 + ie^{-2i\sigma(\rho+1)^{3/2}} = 0, \text{ or}$$

$$(\rho+1)^{3/2} = (n - 1/4) \frac{\pi}{\sigma} < 1 \quad (n = 0, 1, 2, \dots).$$

Thus in the Gamow case IV makes  $I_m(\rho) = 0$  while II yields almost the same real part, but a very small positive imaginary part for  $\rho$ . The mean approximations effectively yield III whose roots are essentially the mean of the roots of II and IV. This averaging process checks closely with an exact calculation based on the (unpublished) WPA tables of Bessel functions of order  $1/3$  for real and pure imaginary arguments. It is to be noted also that IV determines the number of strongly trapped modes as the largest integer  $n$  such that  $(n - 1/4) \pi/\sigma < 1$ .

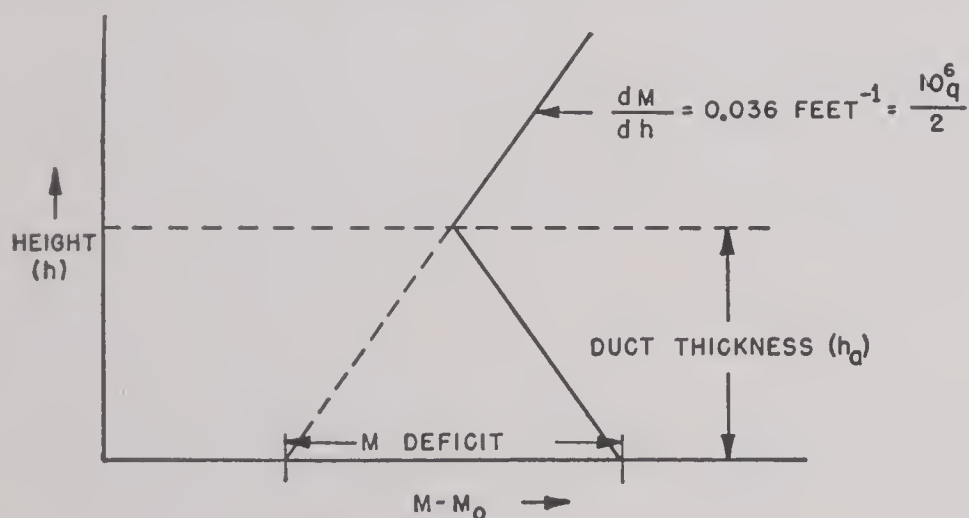
The characteristic value problem may be regarded as essentially solved in the cases of leaky modes (I) and strongly trapped modes (III). In doubt still is the question of the transition between III and II; this uncertainty plus the fact that actual determination of the roots of II is much more complicated than in the other cases, and that in case II the arguments of certain of the Hankel functions lie so close to the origin as to make doubtful the validity of the asymptotic procedure—all these considerations indicate that resolution of the transitional mode question awaits appearance of adequate tables of the Hankel functions for complex arguments.



ATTENUATION DIAGRAMS FOR SURFACE DUCTS<sup>a</sup>

THE HORIZONTAL ATTENUATION (decibels per unit distance) of a signal under assumed propagation conditions not only is of intrinsic interest but is one of the simplest quantities to verify experimentally. In terms of the wave equation formulation this attenuation is proportional to the imaginary part of the characteristic value associated with the mode dominant in the region of space in question. No one mode may necessarily be dominant, and in certain regions a weakly attenuated mode may be outweighed by a mode more strongly attenuated but with a stronger initial excitation. Well inside the shadow zone, however, the "first" or least attenuated mode is frequently dominant. The results presented apply primarily to this situation.

The type of  $M$  curve considered is the bilinear model in which the  $M$  curve consists of two straight-line segments, the upper being assumed to possess standard slope. This model  $M$  curve is completely characterized by two parameters: duct thickness and  $M$  deficit. Figures 2, 3 and 4 refer to three frequencies (200, 3,000, and 10,000 mc) and super-

FIGURE 1.  $M$ -curve model.

standard conditions corresponding to ranges of 1 to 100  $M$  units in  $M$  deficit and 10 to 1,000 ft in duct thickness.

<sup>a</sup>By Lt. William F. Eberlein, USNR, Office of the Chief of Naval Operations.

The solid curves are contours of constant decibel attenuation (of the first mode) per thousand yards. One enters the diagram with given values of duct thickness and  $M$  deficit and interpolates between these contours to obtain the corresponding attenuation.

The dashed curves are contours of constant "trapping index" (number of classically trapped modes). In terms of the standard notation their equation is

$$M \text{ deficit} = \frac{10^6}{2} \left[ qh_a + \frac{9\lambda^2}{16h_a^2} \left( m - \frac{1}{4} \right)^2 \right].$$

Their significance lies in that they furnish an indication of the number of modes other than the first that must be taken into account. If, for example, the bilinear  $M$  curve in question corresponds to a point midway between the  $m = 1$  and  $m = 2$  contours, the first mode is strongly trapped and the second mode attenuation is reduced considerably below standard. Which mode is dominant then depends critically upon the heights of transmitter and receiver, and the simple first mode picture becomes incomplete except at great distances and small heights.

If one attempts to apply these results to simple surface ducts differing from the idealized bilinear model one should first approximate the actual  $M$  curve by a bilinear curve and then enter the diagram with the values of  $M$  deficit and duct thickness corresponding to the *idealized curve*. How to make the best bilinear approximation to a given  $M$  curve is an important but still open question.

Except for the 0.01- and 0.001-db contours, which were computed by an asymptotic method, the attenuation contours were cross-faired from preliminary Radiation Laboratory calculations. The author wishes to thank the Radiation Laboratory group, and Doctors Freehafer and Furry in particular, for permission to use their data.



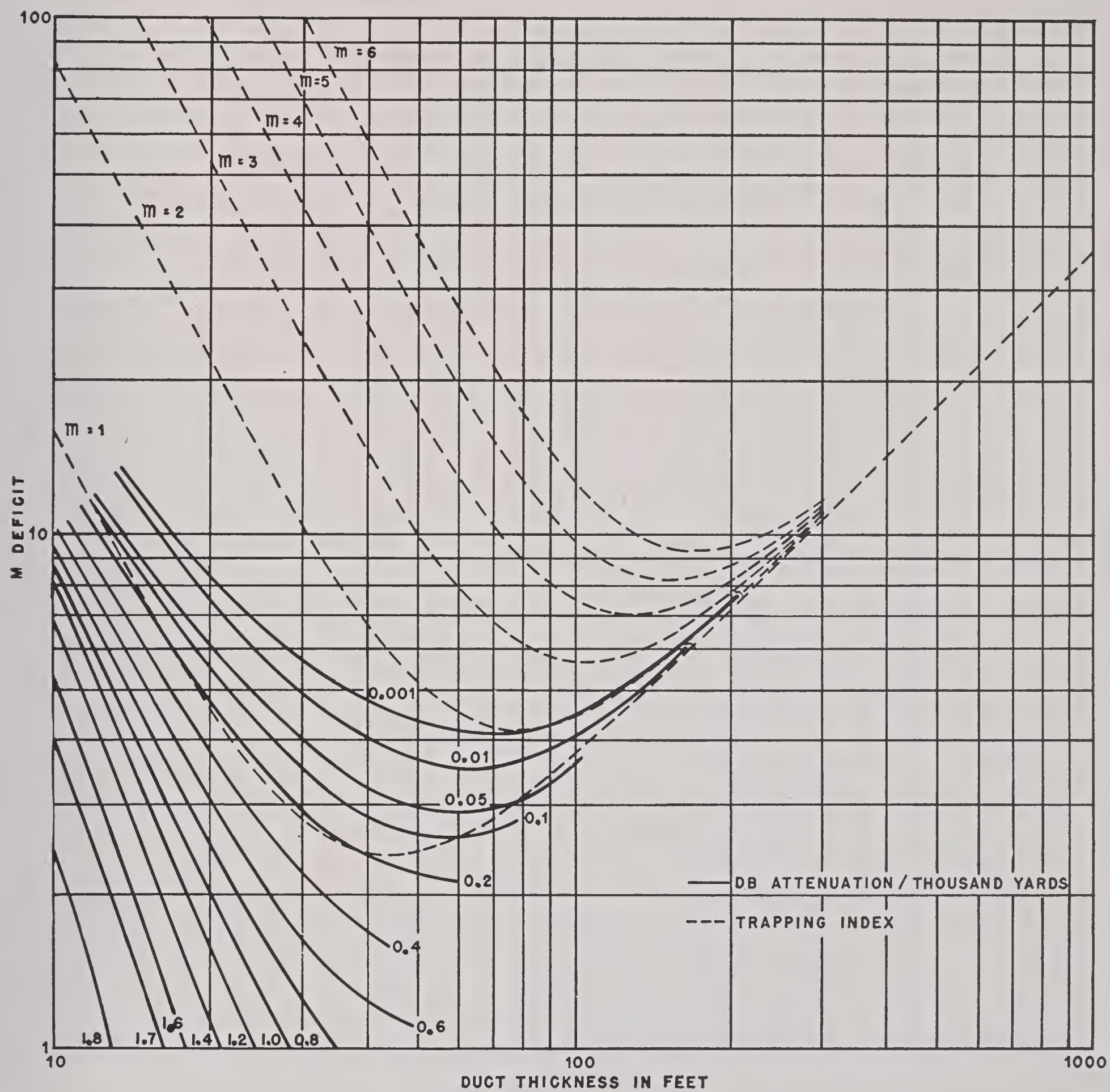


FIGURE 2. Horizontal attenuation of first mode and trapping index, 10,000 mc, standard attenuation (0  $M$  deficit): 1.83 db per 1,000 yd.



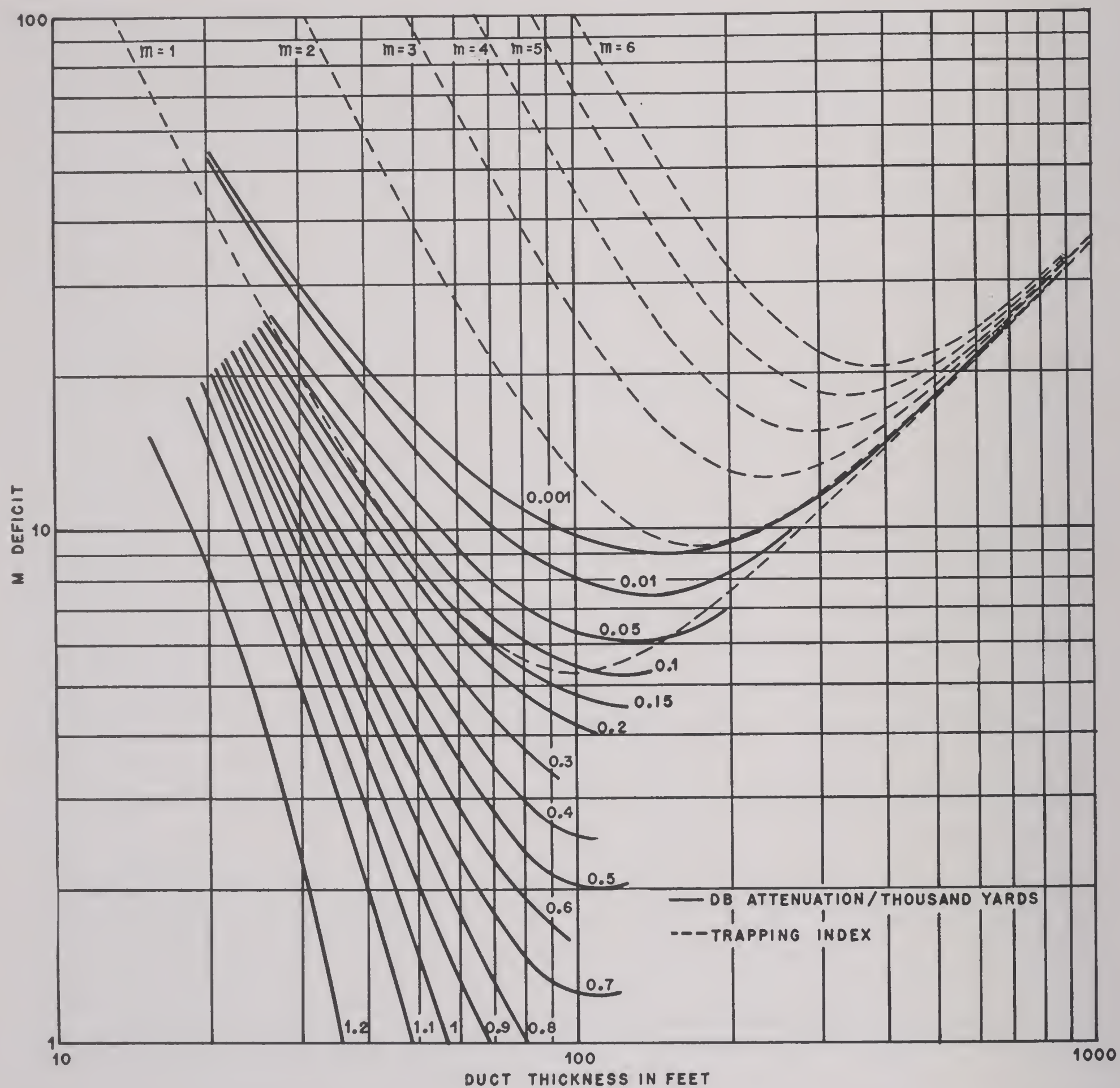


FIGURE 3. Horizontal attenuation of first mode and trapping index, 3,000 mc, standard attenuation (0  $M$  deficit): 1.23 db per 1,000 yd.



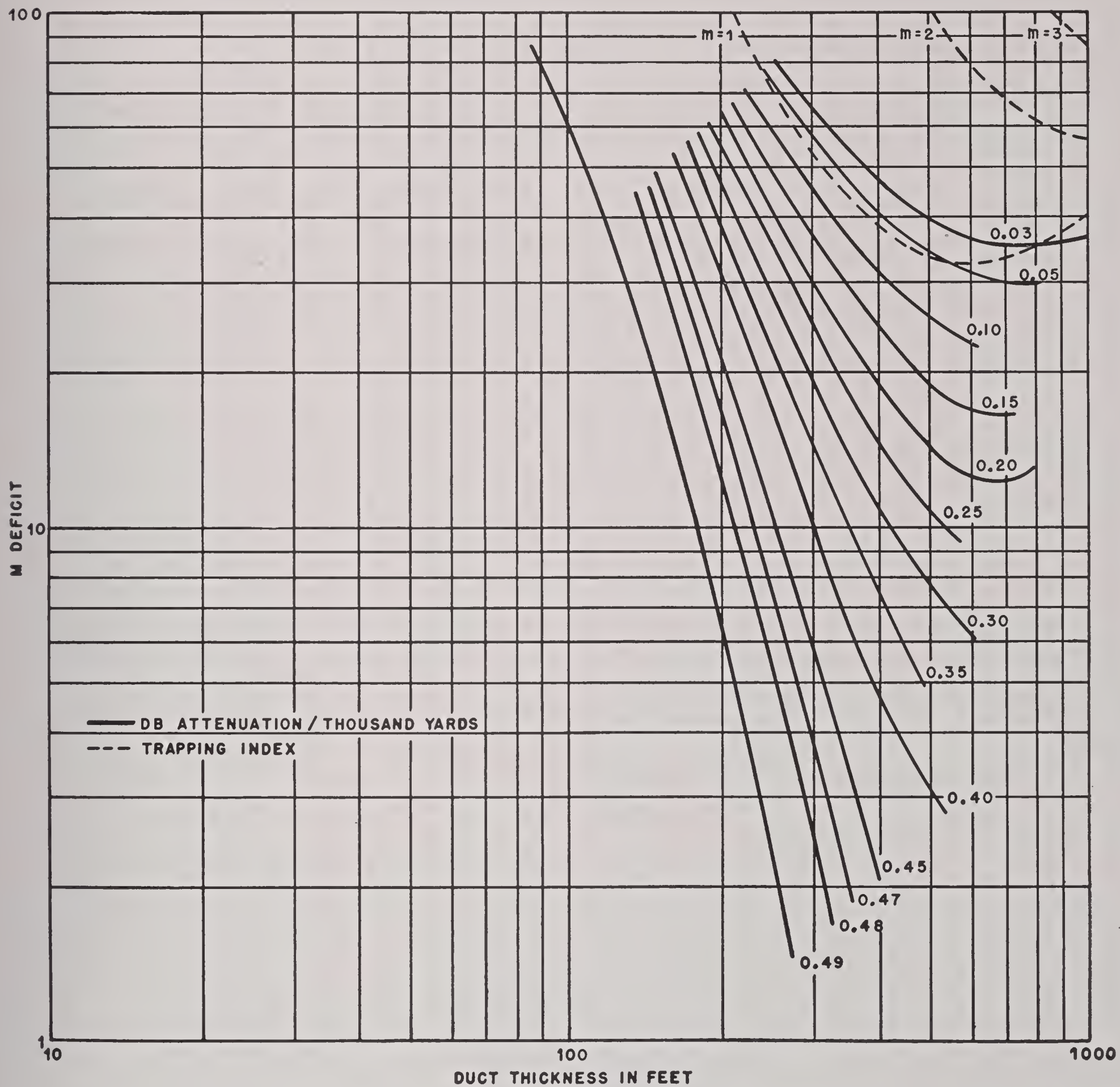


FIGURE 4. Horizontal attenuation of first mode and trapping index, 200 mc, standard attenuation (0  $M$  deficit): 0.498 db per 1,000 yd.



## APPROXIMATE ANALYSIS OF GUIDED PROPAGATION IN A NONHOMOGENEOUS ATMOSPHERE<sup>a</sup>

THE MILITARY IMPORTANCE of guided or “anomalous” propagation in a stratified atmosphere is now well known. Unfortunately, or perhaps fortunately, the problem cannot be treated with the aid of known and tabulated functions except in some special cases because the exact field distribution with height is a function of a function, namely a function of the distribution of the modified index of refraction. For each distribution of this index with height we should have a curve for the field distribution. These curves will look similar in a general way and yet they will differ in detail; but in this particular problem we are not much concerned with details. Even if we had exact solutions we should still want some generalized way of expressing pertinent information.

An approximate analysis of field distribution in terms of master curves, depending on one, or at most, two parameters, will be discussed. For example, if we have atmospheric conditions favoring formation of a guiding layer immediately above the ground or sea level, then we can try to represent the field distribution with height with the aid of the master curve shown in Figure 1. This curve depends on only one parameter,  $H$ , so chosen that in the layer between  $(1/3)H$  and  $H$ , the field intensity does not deviate by more than 6 db from the maximum.

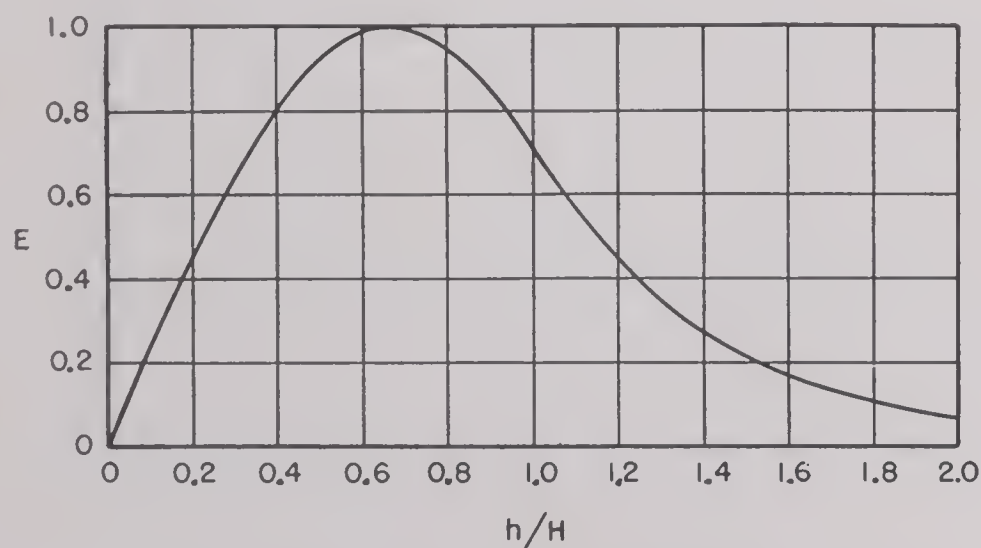


FIGURE 1. Master curve for field distribution with height inside a duct.

This particular curve is chosen for the *first transmission mode*, and it has been suggested by the exact

<sup>a</sup>By S. A. Schelkunoff, Bell Telephone Laboratories.

analysis of guided waves in a homogeneous layer. In this case of sharp discontinuity in the index of refraction the field distribution curves are sinusoidal in the layer and exponential outside. The position of the maximum of the sinusoidal portion of the curve and the relative rate of decay of the exponential part depend on the ratio of the wavelength to the thickness of the layer and on the amount of discontinuity in the index of refraction. In Figure 2, curve 1 is identical with the curve in Figure 1; curve 2 shows what happens if the wavelength is doubled;

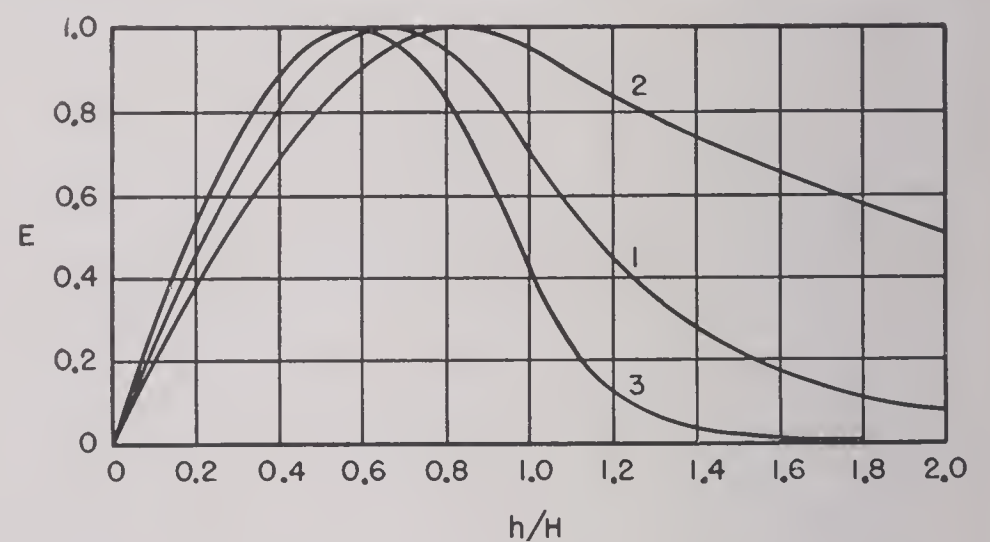


FIGURE 2. Master curves for wavelength  $\lambda$  (1),  $2\lambda$  (2), and  $\frac{1}{2}\lambda$  (3).

and curve 3 corresponds to the case in which the wavelength is halved. If the wavelength is  $(3\pi\sqrt{2})/4 \cong 3.3$  times as large as the wavelength corresponding to curve 1 or larger, no guided waves are possible with the field intensity vanishing at the ground or sea level.

The situation is different if the index of refraction is allowed to vary continuously and to diminish indefinitely. Suppose, for instance, that the lapse rate of the index of refraction is constant. We don't expect any critical wavelength in this case; as the wavelength increases we expect the field to spread out more and more. In fact, we expect the shape of the field distribution curve to remain the same, namely to be determined by that solution of

$$\frac{d^2 E}{dh^2} = [\hat{\beta}^2 - \omega^2 \mu \epsilon(h)] E \quad (1)$$

which vanishes at  $h = 0$ . In this equation



$E$  = the electric intensity;  
 $h$  = the height;  
 $\epsilon$  = the modified dielectric constant;  
 $\omega$  = the radian frequency;  
 $\hat{\beta}$  = the phase constant in the direction parallel to the stratification.

We can try to approximate this solution by a curve of the type shown in Figure 1 in which case the problem is to select a proper value for  $H$ . The question may be raised regarding our preference for this particular curve rather than for curve 2 or 3 in Figure 2. We shall return to this point later; for the present we shall merely point out that curve 1 occupies a "mean" position among other curves of this type.

There are two methods for selecting  $H$ . In one method  $H$  is defined as that value of  $h$  for which the coefficient  $\hat{\beta}^2 - \omega^2 \mu \epsilon(h)$  in equation (1) vanishes. This value of  $h$  separates the region in which the solution of equation (1) is "more" or less sinusoidal from the region in which the solution is "more or less exponential." This definition leads to one equation connecting  $H$  and  $\hat{\beta}$ . Next, the stratified region  $0 < h < H$  is replaced by a homogeneous region in which the dielectric constant is equal to the average value of  $\epsilon(h)$  in the interval  $(0, h)$ . If we impose the requirement that curve 1 represents the exact field distribution under the new conditions, we obtain the second equation for  $H$  and  $\hat{\beta}$ . Eliminating  $\hat{\beta}$  and expressing the result in symbols approved by the wave propagation committee, we have

$$H \int_0^H M(h) dh - H^2 M(H) = \frac{9 \times 10^6}{128} \lambda^2. \quad (2)$$

If the lapse rate of  $M$  is constant, this equation gives

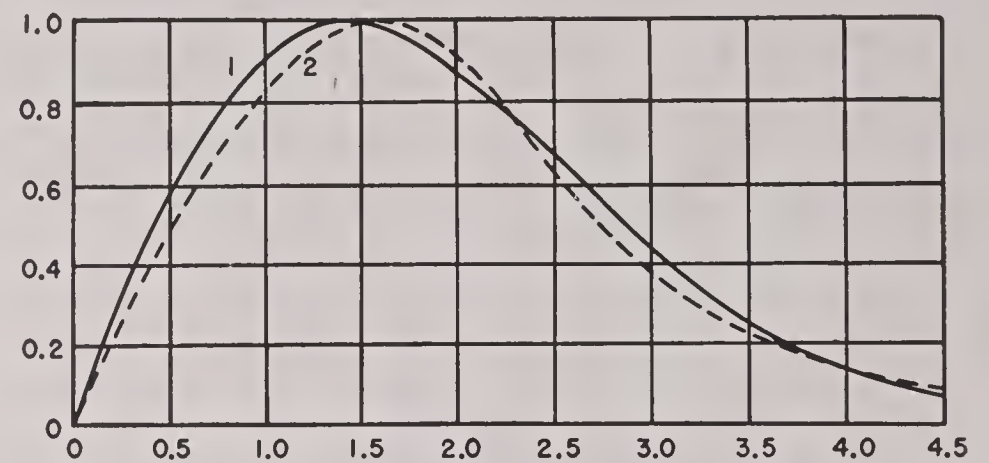
$$H = 65 \lambda^{\frac{2}{3}} \left( -2 \frac{dM}{dh} \right)^{-\frac{1}{3}}. \quad (3)$$

If  $M(h)$  is proportional to  $h^2$ , then

$$H = 18 \lambda^{\frac{1}{2}} \left[ \frac{-M(h)}{h^2} \right]^{-\frac{1}{2}}. \quad (4)$$

If the lapse rate of  $M$  is constant, the exact solution may be expressed in terms of Bessel functions. Figure 3 shows the exact and approximate solutions. For this comparison I am indebted to J. E. Freehafer of the Radiation Laboratory.

The second method is based on the fact that the



$$\begin{aligned}
 Ey &= (\text{const}) U^{\frac{1}{2}} [J_{\frac{1}{2}}(U) + J_{-\frac{1}{2}}(U)] & Ey &= \sin \rho \quad \rho \leq \frac{3\pi}{4} \\
 U &= \frac{3\pi}{4} \left\{ 1 - \frac{8}{3^{5/3}\pi} \right\}^{\frac{3}{2}} & Ey &= \frac{\sqrt{2}}{2} e^{3\pi/4} e^{-\rho} \quad \rho > \frac{3\pi}{4}
 \end{aligned}$$

FIGURE 3. (1) Exact solution normalized to have minimum value of unity. (2) Approximation.

solutions of equation (1) minimize and reduce to zero the following function:

$$\begin{aligned}
 I &= \hat{\beta}^2 \int_0^\infty E^2 dh - \omega^2 \mu \epsilon(o) \int_0^\infty \frac{\epsilon(h)}{\epsilon(o)} E^2 dh \\
 &\quad + \int_0^\infty \left( \frac{dE}{dh} \right)^2 dh. \quad (5)
 \end{aligned}$$

In deriving this equation we should remember that we are concerned with solutions which vanish at  $h = 0$  and  $h = \infty$ . Hence, if we wish to approximate this solution by a function of one parameter  $H$ , we eliminate  $H$  from the following two equations

$$I = 0, \quad \frac{\partial I}{\partial H} = 0. \quad (6)$$

If, for instance, we wish to approximate the field distribution by the master curve in Figure 1, we solve

$$H^2 \frac{\partial P}{\partial H} - HP = \frac{9 \times 10^5}{128} \lambda^2, \quad (7)$$

where

$$\begin{aligned}
 P &= - \int_0^H M \sin^2 \frac{3\pi h}{4H} dh \\
 &\quad - 55.5 \int_H^\infty M \exp \frac{-3\pi h}{2H} dh. \quad (8)
 \end{aligned}$$

By this variational method the numerical coefficient



in equation (3) is found to be 64 rather than 65.

The great advantage of the variational method lies in the fact that, if we wish, we can increase the number of parameters in the approximating function. For example, we can assume

$$E(h) = \sin\left(\frac{\theta h}{H}\right), 0 \leq h \leq H$$

$$= \sin \theta \exp\left[-\psi \frac{h - H}{H}\right], h > H, \quad (9)$$

without specifying that  $\theta = \psi = 3\pi/4$  as we did in obtaining the curve in Figure 1. We should then calculate  $H$ ,  $\theta$ , and  $\psi$  from

$$I = 0, \frac{\partial I}{\partial \theta} = 0, \frac{\partial I}{\partial \psi} = 0. \quad (10)$$

However, aside from the labor of solving these equations and having to deal with more complicated

results, we shall lose the advantage inherent in a description of the field in terms of only one easily understood parameter. The most we could hope for from an analysis of these equations is a somewhat better choice of the master curve for the type of atmospheric conditions which are the most likely to occur.

The obvious general conclusion from equations (7) and (8) is this: if  $M(h)$  is multiplied by a constant factor, the effect on  $H$  is the same as that obtained if we divide  $\lambda$  by the square root of this factor. If  $M$  is proportional to  $h^n$ , then  $H$  is proportional to  $\lambda^{2/(n+2)}$ . Since the gain of the guided wave over a free space wave is proportional to  $\lambda\rho/H^2$ , where  $\rho$  is the distance from the transmitter, the gain is independent of the wavelength when  $M(h)$  is proportional to  $h^2$ . For a uniform lapse rate the gain varies inversely as one-third power of the wavelength.



SOME THEORETICAL RESULTS ON NONSTANDARD PROPAGATION<sup>a</sup>

## 24.1 PROPAGATION IN THE OCEANIC SURFACE DUCT

THE ANALYSIS SECTION of Columbia University Wave Propagation Group undertook a theoretical study of propagation in case of surface ducts, which have recently been reported to be of common occurrence in oceanic areas. The  $M$  curve chosen was

$$M(h) = 346.4 + 0.036h + 43e^{-0.1h}, \quad (1)$$

where the height  $h$  is expressed in feet. This curve has an  $M$  deficit of 43 units and a duct height of 48 ft and is considered to be representative of conditions prevailing around Saipan when the wind is of the order of 10 to 20 mph.

The analysis was based on the phase integral method. The standard W.K.B. (Wentzel-Kramers-Brillouin) version of the asymptotic solutions of the wave equation<sup>107</sup> had to be extended in two ways. One was in the adoption of Langer's form of the asymptotic solutions,<sup>449</sup> which enables one to bridge the "gaps" around the turning points. The other, and more important, development was in the extension of Langer's method to handle a case with *two* turning points. This was accomplished by joining the solutions from each turning point at the duct height. The resulting solution agrees with Gamow's for completely trapped modes but deviates from it when leakage begins. For leaky modes the standard Langer solution is adequate.

Coverage diagrams were computed for the S and X bands and for transmitter heights of 16 and 46 ft. In case of the S band, it was found that the first mode was nearly trapped, while the second mode was considerably leaky with a decrement of about 3 db per nautical mile. The two modes were combined, and coverage diagrams were computed over ranges and heights such that the second mode contributed no more than 25 per cent to the total field.

In the case of the X band, it was found that the first two modes were completely trapped, the third mode nearly trapped, while the fourth mode was leaky with a decrement of over 3 db per nautical mile. In computing the coverage diagrams for the X

band, the four modes were combined over such ranges and heights that the fourth mode did not contribute more than 25 per cent to the total field.

## 24.2 CHARACTERISTIC VALUES FOR A CONTINUOUSLY VARYING MODIFIED INDEX

In the theoretical treatment of nonstandard propagation by the method of normal modes, one is confronted with the task of solving the differential equation for the height-gain function  $U(h)$  given by equation (2), which, it will be noted, is identical with equation (8) in Chapter 25.

$$\ddot{U}_m(h) + k^2 [y(h) + \Lambda_m] U_m(h) = 0, \quad (2)$$

$$k = \frac{2\pi}{\lambda}, \quad y(h) = 2 \times 10^{-6} M(h),$$

by asymptotic methods, the characteristic value  $\Lambda_m$  is determined, to a first approximation, by the condition that

$$k \int_0^{h_1} \sqrt{y(h) - y(h_1)} dh = v_m \cong \pi \left( m - \frac{1}{4} \right), \quad (3)$$

$$\Lambda_m = -y(h_1). \quad (4)$$

In order to solve equation (3) one has to find a value  $h_1$ , which is generally complex, such that when  $y(h_1)$  is substituted in the radicand and the integral

$$\int_0^{h_1} \sqrt{y(h) - y(h_1)} dh \equiv F(h_1) \quad (5)$$

evaluated, the result should be purely real, and equal to  $v_m/k$ . In case of a surface duct,  $F(h_1)$  is real and is a continuously increasing function of its argument for real values of  $h_1$  ranging from zero up to the duct height  $h_0$ . In order for  $F(h_1)$  to increase beyond the value  $F(h_0)$  and still to remain real it is found that  $h_1$  must be complex; i.e., the path in the complex  $h_1$ -plane along which  $F(h_1)$  is real consists of the portion of real axis  $0 \leq h_1 \leq h_0$  followed by a curve in the fourth quadrant.

In case of substandard refraction,  $F(h_1)$  is real only for complex values of  $h_1$ , and the method of solving equation (3) to be explained presently is

<sup>a</sup>By C. L. Pekeris, Columbia University Wave Propagation Group, Analysis Section.



particularly helpful in this case.

Let

$$y(h) = y(0) + b_1 h + b_2 h^2 + \dots + b_n h^n + \dots,$$

$$\dot{h} \equiv \frac{dh}{dy} (h = 0) = \frac{1}{b_1}, \quad \ddot{h} = \frac{-2b_2}{b_1^3},$$

$$\ddot{\ddot{h}} = \frac{(-6b_3 b_1 + 12b_2^2)}{b_1^5},$$

$$h = \frac{(120b_1 b_2 b_3 - 24b_1^2 b_4 - 120b_2^3)}{b_1^7}, \text{ etc.}$$

$$\theta = e^{i\pi/3} \left( \frac{3v_m}{2kh} \right)^{1/3}, \quad w = \Lambda_m + y(0), \quad (6)$$

then

$$\begin{aligned} \Lambda_m = -y(h_1) = -y(0) + \theta^2 + \left( \frac{4}{15} \right) (h_2) \theta^4 \\ + \theta^6 \left[ \frac{4}{25} (h_2)^2 - \frac{8}{105} (h_3) \right] \\ + \frac{16}{27} \theta^8 \left[ \frac{77}{375} (h_2)^3 - \frac{33}{175} (h_2) (h_3) + \frac{1}{35} (h_4) \right] + \dots, \end{aligned} \quad (7)$$

$$h_1 = -\dot{h}w + \frac{\ddot{h}}{2!} w^2 - \frac{\ddot{\ddot{h}}}{3!} w^3 + \dots, \quad (8)$$

where

$$h_2 \equiv \frac{\ddot{h}}{\dot{h}}, \quad h_3 \equiv \frac{\ddot{\ddot{h}}}{\dot{h}}, \dots$$

Equations (7) and (8) are of the nature of asymptotic formulas; they should be terminated when the individual terms begin to increase, and the error in  $\Lambda_m$  or  $h_1$  is then of the order of magnitude of the last term retained.

The following examples in Table 1 illustrate the degree of accuracy obtainable from equation (7).

TABLE 1. Approximate determination of  $\Lambda_1$  from equation (7) and the verification that  $\int_0^{h_1} \sqrt{y(h) + \Lambda_1} dh = 2.383^*$

$\alpha$	$\lambda$	$\Lambda_1$ from equation (7)	$h_1$ from $y(h_1) = -\Lambda_1$	$\int_0^{h_1} \sqrt{y(h) + \Lambda_1} dh$	$v_1$
-20	0.6356	12.360 + 9.775 <i>i</i>	0.3997 - 0.9518 <i>i</i>	2.370 + 0.004 <i>i</i>	2.383
-10	0.6356	4.878 + 6.302 <i>i</i>	0.4745 - 1.1982 <i>i</i>	2.397 + 0.010 <i>i</i>	2.383
-5	0.6356	1.499 + 4.257 <i>i</i>	0.5691 - 1.4692 <i>i</i>	2.393 + 0.009 <i>i</i>	2.383
-2	0.6356	-0.246 + 2.902 <i>i</i>	-0.764 - 1.787 <i>i</i>	2.363 - 0.008 <i>i</i>	2.383

\*  $y(h) = h + c e^{-\lambda h}$ .

As a further check, we treated the case  $\alpha = +20$ ,  $\lambda = 0.6356$ , for which Pearcey and Whitehead<sup>156</sup> give a value  $\Lambda_1 = -10.21 + 1.07 \times 10^{-13}i$ . Equation (7) yields  $\Lambda_1 = -10.22$ , while the imaginary part obtainable from Gamow's formula is  $1.24 \times 10^{-13}i$ .

It must be emphasized that the value obtained from equation (7) should be verified by carrying out the integration of  $F(h_1) = \int_0^{h_1} \sqrt{y(h) + \Lambda_m} dh$ . While doing so, one may as well compute

$$\frac{dF}{dh_1} = -\frac{1}{2} y(h_1) \int_0^{h_1} \frac{dh}{\sqrt{y(h) - y(h_1)}}, \quad (10)$$

and then obtain a correction to  $h_1$  by Newton's method.

The method of solving equation (3) explained above has been found especially useful in the treatment of substandard refraction, and to a lesser extent in the treatment of the trapped modes in case of a surface duct. In the latter case one can, of course, solve for  $\Lambda_m$  directly by computing  $F(h_1)$  by numerical integration. The method is not applicable for the leaky modes in case of a surface duct.

So far the discussion has centered on the solution of equation (3), which in itself is only an approximate asymptotic formula valid for large values of  $k$ . Let the value of  $\Lambda_m$  which satisfies equation (3) be denoted by  $\Lambda_m^{(0)}$ ; then an improved value for  $\Lambda_m$  can be obtained from

$$\begin{aligned} \Lambda_m = \Lambda_m^{(0)} \\ + \frac{3e^{i\pi/3}(v_m)^{1/3}}{\theta' k^{7/3}} \left( \frac{3}{2} \right)^{4/3} (\dot{y})^{-3} \left[ \frac{1}{35} \left( \frac{\ddot{y}}{\dot{y}} \right)^2 - \frac{2}{63} \left( \frac{\ddot{\ddot{y}}}{\dot{y}} \right) \right] \end{aligned} \quad (11)$$

where

$$\theta' = \int_0^{h_1} \frac{dh}{\sqrt{y(h) + \Lambda_m^{(0)}}}, \quad \dot{y} = \frac{dy}{dh_1}, \text{ etc.}, \quad (12)$$

and the derivatives of  $y$  are to be evaluated at  $h = h_1$ .



# PERTURBATION THEORY FOR AN EXPONENTIAL $M$ CURVE IN NONSTANDARD PROPAGATION<sup>a</sup>

25.1

## ABSTRACT

IN THIS chapter a perturbation method is developed for treating nonstandard propagation in the case when the deviation of the  $M$  curve from the standard ( $\equiv$  the  $M$  anomaly) can be represented by a term  $\alpha e^{-\lambda z}$ , where  $z$  denotes height in natural units. The method is also applicable to other forms of the  $M$  anomaly which can be derived from an exponential term by differentiation with respect to  $\lambda$ ; in fact, in its region of convergence, it is formally applicable to the most general type of  $M$  curve, including elevated ducts. The region of practical convergence of the method ranges from standard down to cases where the decrement is a small fraction of the standard value.

The procedure followed is to express the height-gain function  $U_k(z)$  of the  $k$ -th mode in the nonstandard case as a linear combination of the height-gain functions  $U_m^0(z)$  of all the modes in the standard case.

$$U_k(z) = \sum_{m=1}^{\infty} A_{km} U_m^0(z). \quad (1)$$

The execution of this plan hinges on the possibility of evaluating the quantities

$$\beta_{nm}(\lambda) = \int_0^{\infty} U_n^0(z) U_m^0(z) e^{-\lambda z} dz. \quad (2)$$

It is shown that  $\beta_{nm}(\lambda)$  satisfies the differential equation

$$\frac{d\beta_{nm}}{d\lambda} = \frac{1}{2\lambda} + \beta_{nm}(\lambda).$$

$$\left[ -\frac{1}{2\lambda} + \frac{1}{2}(D_m^0 + D_n^0) + \frac{\lambda^2}{4} + \frac{1}{4\lambda^2}(D_m^0 - D_n^0)^2 \right], \quad (3)$$

whose solution is

$$\beta_{nm}(\lambda) = \frac{1}{2\sqrt{\lambda}} e^{\frac{\lambda}{2}(D_n^0 + D_m^0) + \frac{\lambda^3}{12} - \frac{1}{4\lambda}(D_m^0 - D_n^0)^2} \int_0^{\lambda} \frac{dx}{\sqrt{x}} e^{-\frac{x}{2}(D_m^0 + D_n^0) - \frac{x^3}{12} + \frac{1}{4x}(D_n^0 - D_m^0)^2}. \quad (4)$$

Here  $D_m^0$  denotes the characteristic value of the  $m$ -th mode in the standard case. For large  $\lambda$  the following asymptotic formula holds

$$\beta_{nm} = \frac{2}{\left[ \lambda^3 + 2\lambda(D_m^0 + D_n^0) - 2 + \frac{1}{\lambda}(D_m^0 - D_n^0)^2 \right]} + \frac{8 \left[ 3\lambda^3 + 2\lambda(D_m^0 + D_n^0) - \frac{1}{\lambda}(D_m^0 - D_n^0)^2 \right]}{\left[ \lambda^3 + 2\lambda(D_m^0 + D_n^0) - 2 + \frac{1}{\lambda}(D_m^0 - D_n^0)^2 \right]^3}. \quad (5)$$

Having determined the  $\beta_{nm}(\lambda)$  from equation (4), or by a numerical solution of equation (3), the characteristic values  $D_k$  and the coefficients  $A_{km}$  are to be solved from the infinite system of equations

$$\sum_{m=1}^{\infty} A_{km} \left[ (D_k - D_m^0) \delta_{nm} + \alpha \beta_{nm}(\lambda) \right] = 0, \quad n = 1, 2, 3, \dots \quad (6)^b$$

For this purpose a simple iterative procedure has been developed, which has been found to be rapidly convergent. The  $A_{km}$  are normalized by the condition

$$\int_0^{\infty} U_k^2(z) dz = 1 = \sum_{m=1}^{\infty} A_{km}^2. \quad (7)^c$$

One can also expand  $D_k$  as a power series in  $\alpha$

$$D_k = D_k^0 + \alpha D_k^1 + \alpha^2 D_k^2 + \dots,$$

$$D_k^{(1)} = -\beta_{kk}; \quad D_k^{(2)} = e^{i\pi/3} \sum_m \frac{\beta_{mk}^2}{(\tau_m - \tau_k)}, \quad m \neq k.$$

An alternative expression for  $D_k^{(2)}$  is given in equation (65).

<sup>a</sup>By C. L. Pekeris, Columbia University Wave Propagation Group.

<sup>b</sup> $\delta_{nm} = 1, \quad n = m$   
 $\delta_{nm} = 0, \quad n \neq m.$

<sup>c</sup>The integral  $\int_0^{\infty} U_k^2(z) dz$  diverges when taken along the real axis; it converges, however, and to the same limit, when the path is a radial line in the fourth quadrant of the  $z$  plane. In the sequel, whenever an integral is divergent it will be understood that the path is suitably modified.



25.2

## INTRODUCTION

In the theoretical treatment of nonstandard propagation by the method of normal modes, one is confronted with the task of solving the equation

$$\frac{d^2 U_m}{dh^2} + k^2 \left[ y(h) + \Lambda_m \right] U_m = 0, \quad (8)$$

subject to the condition that  $U_m(0) = 0$  and that at  $h \rightarrow \infty$ ,  $U_m$  should represent an upgoing wave only. Here  $h$  denotes height in feet.

$$y(h) = N^2(h) - 1 = 2 \times 10^{-6} M(h), \quad k = \frac{2\pi}{\lambda}, \quad (9)$$

and  $\Lambda_m$  is the characteristic value which is generally complex. It is convenient to introduce natural units of height

$$z = \frac{h}{H}, \quad H = (k^2 q)^{-\frac{1}{2}}, \quad q = \frac{dN^2}{dh} = 2.36 \times 10^{-9} \text{ cm}^{-1},$$

$$D_m = \Lambda_m \left( \frac{k}{q} \right)^{\frac{2}{3}}, \quad (10)$$

whereby equation (8) is transformed into

$$\frac{d^2 U_m}{dz^2} + \left[ z + f(z) + D_m \right] U_m(z) = 0. \quad (11)$$

The term  $f(z)$  in equation (11) represents the refraction anomaly and is equal to zero for a standard atmosphere. In the first instance we shall be treating the case where

$$f(z) = \alpha e^{-\lambda z}, \quad (12)^d$$

and we shall later generalize the treatment to deal with any  $M$  curve represented as a series of Laguerre functions. If the original  $M$  curve is represented by the expression

$$M(h) = bh + ae^{-ch}, \quad b = 0.036 \text{ ft}^{-1}, \quad (13)$$

then  $\alpha$  and  $\lambda$  are obtained as follows:

$$\alpha = 2 \times 10^{-6} \left( \frac{k}{q} \right)^{\frac{2}{3}} a, \quad \lambda = cH. \quad (14)$$

It is to be noted that in contrast to the constants  $a$  and  $c$  in equation (13), which are independent of frequency, the constants  $\alpha$  and  $\lambda$  in equation (12) are frequency dependent. For a given observed  $M$  curve the constants  $\alpha$  and  $\lambda$  will therefore differ with

<sup>d</sup>No confusion should arise from the use of  $\lambda$  in equation (12) and the standard usage of  $\lambda$  to denote wavelength.

the frequency band used, as will also the height represented by one unit of  $z$ .

## 25.3 FORMAL SOLUTION OF THE PROBLEM BY THE PERTURBATION METHOD

In order to solve the equation

$$\frac{d^2 U_k(z)}{dz^2} + \left[ z + \alpha e^{-\lambda z} + D_k \right] U_k(z) = 0, \quad (15)$$

we seek a solution in the form

$$U_k = \sum_{m=1}^{\infty} A_{km} U_m^0(z), \quad (16)$$

where  $U_m^0(z)$  are the height-gain functions of the  $m$ -th mode in the standard case, which satisfy the equation

$$\frac{d^2 U_m^0(z)}{dz^2} + \left[ z + D_m^0 \right] U_m^0(z) = 0. \quad (17)$$

$$\int_0^{\infty} \left[ U_m^0(z) \right]^2 dz = 1. \quad (18)$$

The solutions of equations (17) and (18) are well known:

$$U_m^0(z) = C_m u^{\frac{1}{3}} H_{\frac{2}{3}}^{(2)}(u), \quad u = \frac{2}{3} (z + D_m^0)^{\frac{3}{2}}, \quad (19)$$

$$C_m = \left\{ e^{i\pi/3} \frac{2}{\sqrt{3}} \left( \frac{3}{2} \right)^{\frac{1}{3}} v_m^{\frac{2}{3}} \left[ J_{\frac{2}{3}}(v_m) - J_{-\frac{2}{3}}(v_m) \right] \right\}^{-1}, \quad (20)$$

$$D_m^0 = \tau_m e^{i2\pi/3}, \quad \tau_m = \left( \frac{3v_m}{2} \right)^{\frac{2}{3}}, \quad (21)$$

where

$$J_{\frac{1}{3}}(v_m) + J_{-\frac{1}{3}}(v_m) = 0. \quad (22)$$

For small  $z$  the power series development of  $U_m^0(z)$  is useful:

$$U_m^0(z) = i \sum_{k=1}^{\infty} A_k z^k, \quad (23)$$

$$A_k = -\frac{1}{k(k-1)} \left[ D_m^0 A_{k-2} + A_{k-3} \right], \quad (24)$$

$$U_m^0(z) = i \left[ z - \left( \frac{D_m^0}{6} \right) z^3 - \frac{z^4}{12} + \left( \frac{D_m^0}{120} \right)^2 z^5 + \left( \frac{D_m^0}{120} \right) z^6 + \dots \right], \quad (25)$$



while for large  $z$  one may use asymptotic expansion of equation (19)

$$H_{\frac{1}{2}}^{(2)}(u) \rightarrow \sqrt{\frac{2}{\pi u}} e^{i(-u + 5\pi/12)} .$$

$$\left[ 1 + \frac{5i}{72u} - \frac{385}{10,368u^2} + \dots \right] . \quad (26)$$

If now the expansion (16) be substituted into equation (15), we obtain, on making use of equation (17), the condition

$$\sum_{m=1}^{\infty} A_{km} \left[ (D_k - D_m^0) + \alpha e^{-\lambda z} \right] U_m^0(z) = 0 . \quad (27)$$

On multiplying this equation by  $U_n^0(z)$ , where  $n$  is any integer, and integrating from 0 to  $\infty$  we get a system of equations for the determination of  $D_k$  and the  $A_{km}$ :

$$\sum_{m=1}^{\infty} A_{km} \left[ (D_k - D_m^0) \delta_{nm} + \alpha \beta_{nm}(\lambda) \right] = 0 , \quad n = 1, 2, 3, \dots \quad (28)$$

$$\beta_{nm}(\lambda) = \int_0^{\infty} U_m^0(z) U_n^0(z) e^{-\lambda z} dz . \quad (29)$$

The characteristic values  $D_k$  are then obtained as the roots of the infinite determinant.

$$\begin{vmatrix} D_k - D_1^0 + \alpha\beta_{11}, & \alpha\beta_{12}, & \alpha\beta_{13}, & \dots \\ \alpha\beta_{21}, & D_k - D_2^0 + \alpha\beta_{22}, & \alpha\beta_{23}, & \dots \\ \alpha\beta_{31}, & \alpha\beta_{32}, & D_k - D_3^0 + \alpha\beta_{33}, & \dots \\ \dots, & \dots, & \dots, & \dots \end{vmatrix} = 0 . \quad (30)$$

Having determined  $D_k$  from equation (30), the  $A_{km}$  are obtained by solving the system of linear equations (28).

#### 25.4 EVALUATION OF $\beta_{nm}(\lambda)$ AS AN INDEFINITE INTEGRAL

The primary task in the perturbation method is the evaluation of the exchange integrals  $\beta_{nm}(\lambda)$  defined in equation (29). We shall accomplish this by proving that  $\beta_{nm}(\lambda)$ , as a function of  $\lambda$ , satisfies a differential equation of the first order for which an explicit solution can be given. For this purpose

we shall study the function

$$F(z) \equiv U_n^0(z) U_m^0(z) , \quad (31)$$

where

$$\ddot{U}_m^0(z) + [z + D_m^0] U_m^0(z) = 0 , \quad (32)$$

$$\ddot{U}_n^0(z) + [z + D_n^0] U_n^0(z) = 0 . \quad (33)$$

By multiplying equation (32) by  $U_n^0(z)$ , equation (33) by  $U_m^0(z)$  and subtracting, we obtain

$$\frac{d}{dz} (\dot{U}_m^0 U_n^0 - U_m^0 \dot{U}_n^0) = - (D_m^0 - D_n^0) U_m^0 U_n^0 , \quad (34)$$

$$\begin{aligned} \dot{U}_m^0 U_n^0 - U_m^0 \dot{U}_n^0 \\ = - (D_m^0 - D_n^0) \int_0^z U_m^0(x) U_n^0(x) dx . \end{aligned} \quad (35)$$

Now it can be verified by direct substitution that

$$\begin{aligned} \ddot{F} + 2\dot{F} (D_n + D_m + 2z) + 2F \\ = (D_m^0 - D_n^0) (\dot{U}_m^0 U_n^0 - U_m^0 \dot{U}_n^0) \\ = - (D_m^0 - D_n^0)^2 \int_0^z F(x) dx . \end{aligned} \quad (36)^e$$

From equation (36) it follows that

$$\begin{aligned} F = \frac{d}{dz} \left[ (2z + D_m^0 + D_n^0) F + \frac{1}{2} \ddot{F} \right] \\ + \frac{1}{2} (D_m^0 - D_n^0)^2 \int_0^z F(x) dx . \end{aligned} \quad (37)$$

We may also note that

$$\ddot{F}(0) = 2\dot{U}_m^0(0) \dot{U}_n^0(0) = -2 , \quad (38)$$

$$\begin{aligned} \int_0^{\infty} e^{-\lambda z} \ddot{F} dz = e^{-\lambda z} (\dot{F} + \lambda F) \Big|_0^{\infty} + \lambda^2 \int_0^{\infty} e^{-\lambda z} F dz \\ = \lambda^2 \int_0^{\infty} e^{-\lambda z} F dz . \end{aligned} \quad (39)$$

$$\begin{aligned} \int_0^{\infty} e^{-\lambda z} dz \int_0^z F(x) dx = - \frac{1}{\lambda} e^{-\lambda z} \int_0^z F(x) dx \Big|_0^{\infty} \\ + \frac{1}{\lambda} \int_0^{\infty} e^{-\lambda z} F(z) dz = \frac{1}{\lambda} \int_0^{\infty} e^{-\lambda z} F(z) dz . \end{aligned} \quad (40)$$

$$\int_0^{\infty} e^{-\lambda z} F(z) dz = - \frac{d}{d\lambda} \int_0^{\infty} e^{-\lambda z} F(z) dz . \quad (41)$$

<sup>e</sup>This is the first occasion in the author's experience where use is made of the fact that the product of two functions, each of which is a solution of a distinct second order ordinary linear differential equation, satisfies a fourth order linear differential equation.<sup>450</sup>



We now substitute equation (37) in the integrand of equation (29) and obtain

$$\begin{aligned}\beta_{nm}(\lambda) &= \int_0^\infty F(z) e^{-\lambda z} dz = \int_0^\infty e^{-\lambda z} dz \times \\ &\quad \left\{ \frac{d}{dz} \left[ (2z + D_m^0 + D_n^0) F + \frac{1}{2} \ddot{F} \right] \right. \\ &\quad \left. + \frac{1}{2} (D_m^0 - D_n^0)^2 \int_0^z F(x) dx \right\} \\ &= \frac{1}{2\lambda} (D_m^0 - D_n^0)^2 \int_0^\infty e^{-\lambda z} F(z) dz \\ &\quad + \left[ (2z + D_n^0 + D_m^0) F + \frac{1}{2} \ddot{F} \right] e^{-\lambda z} \Big|_0^\infty \\ &\quad + \lambda \int_0^\infty e^{-\lambda z} \left[ (2z + D_n^0 + D_m^0) F + \frac{1}{2} \ddot{F} \right] dz \\ &= 1 + \int_0^\infty e^{-\lambda z} F(z) dz \\ &\quad \left[ 2\lambda z + \lambda(D_m^0 + D_n^0) + \frac{1}{2} \lambda^3 + \frac{1}{2\lambda} (D_m^0 - D_n^0)^2 \right] dz \\ &= 1 - 2\lambda \frac{d\beta_{nm}(\lambda)}{d\lambda} \\ &\quad + \beta_{nm}(\lambda) \left[ \lambda(D_m^0 + D_n^0) + \frac{\lambda^3}{2} + \frac{1}{2\lambda} (D_m^0 - D_n^0)^2 \right].\end{aligned}\quad (42)$$

It follows that the exchange integral  $\beta_{nm}(\lambda)$  satisfies the first order differential equation

$$\frac{d\beta_{nm}(\lambda)}{d\lambda} = \frac{1}{2\lambda} + \beta_{nm}(\lambda) \cdot \left[ -\frac{1}{2\lambda} + \frac{1}{2} (D_m^0 + D_n^0) + \frac{\lambda^2}{4} + \frac{1}{4\lambda^2} (D_m^0 - D_n^0)^2 \right]. \quad (43)$$

The solution of equation (43) is

$$\begin{aligned}\beta_{nm}(\lambda) &= \frac{1}{2\sqrt{\lambda}} e^{\frac{\lambda}{2} (D_m^0 + D_n^0) + \frac{\lambda^3}{12} - \frac{1}{4\lambda} (D_m^0 - D_n^0)^2} \\ &\quad \int_0^\lambda \frac{dx}{\sqrt{x}} e^{-\frac{x}{2} (D_m^0 + D_n^0) - \frac{x^3}{12} + \frac{1}{4x} (D_m^0 - D_n^0)^2}.\end{aligned}\quad (44)$$

25.5

#### PROPERTIES OF $\beta_{nm}(\lambda)$

For small  $\lambda$  the solution of the differential equation (43) can be started with a power series in  $\lambda$ .

1.  $n \neq m$

$$\beta_{nm}(\lambda) = - \frac{2\lambda e^{i2\pi/3}}{(\tau_m - \tau_n)^2} \sum_{k=0}^{\infty} C_k e^{i2\pi k/3} \lambda^k, \quad (45)$$

$$C_0 = 1, \quad C_1 = \frac{6}{(\tau_m - \tau_n)^2},$$

$$C_2 = \frac{10C_1 - 2(\tau_m + \tau_n)}{(\tau_m - \tau_n)^2},$$

$$C_3 = \frac{14C_2 - 2C_1(\tau_m + \tau_n)}{(\tau_m - \tau_n)^2},$$

$$C_n = \frac{(4n+2)C_{n-1} - 2(\tau_m + \tau_n)C_{n-2} - C_{n-4}}{(\tau_m - \tau_n)^2}. \quad (46)$$

2.  $n = m$

$$\beta_{nm} = 1 + B_1 \lambda + B_2 \lambda^2 + \dots, \quad (47)$$

$$B_1 = \frac{2}{3} D_m^0, \quad B_2 = \frac{4}{15} D_m^{2(0)},$$

$$B_3 = \frac{1}{14} + \frac{8}{105} D_m^{3(0)},$$

$$B_n = \frac{1}{(2n+1)} \left[ 2D_m^0 B_{n-1} + \frac{1}{2} B_{n-3} \right]. \quad (48)$$

For intermediate values of  $\lambda$  one may either use the integral in equation (44) or integrate numerically the differential equation (43). The latter procedure was advocated by Hartree.

For large values of  $\lambda$  an asymptotic expansion can be obtained directly from equation (43) by writing it in the form

$$\begin{aligned}\beta_{nm}(\lambda) &= \frac{-2 + 4\lambda \frac{d\beta_{nm}(\lambda)}{d\lambda}}{\lambda^3 + 2\lambda (D_m^0 + D_n^0) - 2 + \frac{1}{\lambda} (D_m^0 - D_n^0)^2} \\ &\quad - \frac{2}{\lambda^3 + 2\lambda (D_m^0 + D_n^0) - 2 + \frac{1}{\lambda} (D_m^0 - D_n^0)^2} \\ &\quad + \frac{8 \left[ 3\lambda^3 + 2\lambda (D_m^0 + D_n^0) - \frac{1}{\lambda} (D_m^0 - D_n^0)^2 \right]}{\left[ \lambda^3 + 2\lambda (D_m^0 + D_n^0) - 2 + \frac{1}{\lambda} (D_m^0 - D_n^0)^2 \right]^3}.\end{aligned}\quad (49)$$



An alternative asymptotic expansion can be derived from equation (44) by partial integration

$$\beta_{mn} \rightarrow - \frac{2}{\left[ \lambda^3 + 2\lambda (D_m^0 + D_n^0) + \frac{1}{\lambda} (D_m^0 - D_n^0)^2 \right]} + \frac{4 \left[ 5\lambda^3 + 2\lambda (D_m^0 + D_n^0) - \frac{3}{\lambda} (D_m^0 - D_n^0)^2 \right]}{\left[ \lambda^3 + 2\lambda (D_m^0 + D_n^0) + \frac{1}{\lambda} (D_m^0 - D_n^0)^2 \right]^3}. \quad (50)$$

In doing so one needs to prove that

$$\int_0^\infty \frac{dx}{\sqrt{x}} e^{-\frac{x}{2}(D_m^0 + D_n^0) - \frac{x^3}{12} + \frac{1}{4x}(D_m^0 - D_n^0)^2} \equiv \Psi_{nm} = 0. \quad (51)$$

We shall state here without proof that

$$\begin{aligned} \Psi_{mm} &= \int_0^\infty \frac{dx}{\sqrt{x}} e^{-xD_m^0 - \frac{x^3}{12}} \\ &= \frac{\pi\sqrt{\pi}}{2} \left(\frac{2}{3}\right)^{\frac{1}{3}} h_1(D_m^0) h_2(D_m^0), \end{aligned} \quad (52)$$

where  $h_1$  and  $h_2$  are Furry's functions of the first and second kind defined as

$$h_1(x) = \left(\frac{2}{3}\right)^{\frac{1}{3}} \sqrt{x} H_{\frac{1}{3}}^{(1)}\left(\frac{2}{3}x^{\frac{3}{2}}\right). \quad (53)$$

$$h_2(x) = \left(\frac{2}{3}\right)^{\frac{1}{3}} \sqrt{x} H_{\frac{1}{3}}^{(2)}\left(\frac{2}{3}x^{\frac{3}{2}}\right). \quad (54)$$

Since by definition of  $D_m^0$ ,  $h_2(D_m^0) = 0$ , it follows that  $\Psi_{mm} = 0$ . The proof of equation (51) for  $n \neq m$  is left as an exercise to the interested reader.

## 25.6 ITERATION METHOD OF SOLVING FOR THE CHARACTERISTIC VALUES $D_k$ AND THE COEFFICIENTS $A_{km}$

In solving equations (28) and (30), which are of infinite order, one proceeds by first assuming that  $A_{km} = 0$  for  $m > p$ , where  $p$  is a convenient integer, and then evaluating  $D_k$  and  $A_{km}$ ,  $m = 1, 2 \dots p$ . Next, one assumes that  $A_{km} = 0$  for  $m > p + 1$ , resolves for  $D_k$  and the  $A_{km}$ , and the accuracy of the results is judged by the agreement between the values in successive approximations. The direct solu-

tion of equations (30) and (28) is, however, a laborious process which rapidly increases in complexity as  $p$  exceeds about 4. The following iterative procedure has been found effective and of the same intrinsic simplicity for any value of  $p$ .

To begin with, the  $p$  equations in equation (28), being homogeneous, do not determine the absolute values of all the  $A_{km}$  but merely the ratios of  $(p - 1)$  of them to a  $p$ -th one. The absolute values are then determined from the normalization condition

$$\int_0^\infty U_k^2(z) dz = 1 = \sum_{m=1}^\infty A_{km}^2. \quad (7)$$

Let therefore

$$C_{km} = \frac{A_{km}}{A_{kk}}, \quad C_{kk} = 1, \quad (55)$$

and the  $p$  equations in equation (24) are just sufficient to determine the  $(p - 1)$  constants  $C_{km}$  and  $D_k$ . We divide the equations in (28) by  $A_{kk}$  and pick the  $k$ -th equation ( $n = k$ ) to solve for  $D_k$ , while the other equations are used to solve for the  $C_{km}$ , as is illustrated in the scheme below for the particular case of  $k = 1$ .

$$\frac{D_1}{\alpha} = \frac{D_1^0}{\alpha} - \beta_{11} - C_{12}\beta_{12} - C_{13}\beta_{13} - \dots, \quad (56)$$

$$\begin{aligned} &\left(\frac{D_1}{\alpha} - \frac{D_2^0}{\alpha} + \beta_{22}\right) C_{12} \\ &= -\beta_{12} - C_{13}\beta_{23} - C_{14}\beta_{24} - \dots, \end{aligned} \quad (57)$$

$$\begin{aligned} &\left(\frac{D_1}{\alpha} - \frac{D_3^0}{\alpha} + \beta_{33}\right) C_{13} \\ &= -\beta_{13} - C_{12}\beta_{23} - C_{14}\beta_{34} - \dots, \end{aligned} \quad (58)$$

$$\begin{aligned} &\left(\frac{D_1}{\alpha} - \frac{D_4^0}{\alpha} + \beta_{44}\right) C_{14} \\ &= -\beta_{14} - C_{12}\beta_{24} - C_{13}\beta_{34} - \dots \end{aligned} \quad (59)$$

As a first approximation one puts

$$\frac{D_1}{\alpha} = \frac{D_1^0}{\alpha} - \beta_{11}; \quad (60)$$

$$C_{12} = - \frac{\beta_{12}}{\left(\frac{D_1}{\alpha} - \frac{D_2^0}{\alpha} + \beta_{22}\right)}, \quad (61)$$



$$C_{13} = - \frac{\beta_{13}}{\left(\frac{D_1}{\alpha} - \frac{D_3^0}{\alpha} + \beta_{33}\right)}, \text{ etc. , } (62)$$

where the value of  $D_1/\alpha$  obtained from equation (60) is used in equations (61) and (62). Next, one substitutes these values of the  $C$ 's in the right-hand sides of equations (56) to (59) and resolves for  $D_1/\alpha$  and the  $C$ 's. This procedure has been found to be rapidly convergent and is, furthermore, self-correcting in case of arithmetical errors.

### 25.7 EXPANSION OF $D_k$ INTO A POWER SERIES IN $\alpha$

When  $\alpha$  is small, it is convenient to expand  $D_k$  into the series

$$D_k = D_k^{(0)} + \alpha D_k^{(1)} + \alpha^2 D_k^{(2)} + \dots (63)$$

It is known from standard perturbation theory that

$$D_k^{(1)} = -\beta_{kk}; D_k^{(2)} = e^{i\pi/3} \sum_m \frac{\beta_{mk}^2}{(\tau_m - \tau_k)}, \quad m \neq k. \quad (64)$$

It is possible also to derive an alternative expression for  $D_k^{(2)}$ :

$$\begin{aligned} D_k^{(2)}(\lambda) &= \frac{1}{2} \lambda D_k^{(1)}(\lambda)^2 + \frac{1}{2\sqrt{\lambda}} e^{D_k^{(0)}\lambda + \frac{\lambda^3}{12}} \\ &\quad \int_0^\lambda e^{-D_k^{(0)}x - (x^3/12)} \\ &\quad \left[ \left(1 + \frac{\lambda}{2x}\right) D_k^{(1)}(\lambda + x) + D_k^{(1)}(\lambda) D_k^{(1)}(x) \right] \sqrt{x} dx \\ &= \lambda D_k^{(1)}(\lambda)^2 + \frac{1}{4\sqrt{\lambda}} e^{D_k^{(0)}\lambda + (\lambda^3/12)}. \end{aligned}$$

$$\int_0^\lambda \left[ D_k^{(1)}(\lambda) + \left(2 + \frac{\lambda}{x}\right) D_k^{(1)}(\lambda + x) \right] \sqrt{x} dx. \quad (65)$$

Since the former expression is simpler for computational purposes, we shall not give here the derivation of equation (65).

### 25.8 APPLICABILITY OF PERTURBATION METHOD TO A MORE GENERAL CLASS OF $M$ ANOMALIES

It is possible to apply the results obtained for the case when the  $M$  anomaly is of the form  $f(z) = \alpha e^{-\lambda z}$

to more general types of  $M$  anomalies. To begin with, if

$$f(z) = \alpha e^{-\lambda z} + \gamma e^{-\mu z}, \quad (66)$$

then we merely write in equation (28) in place of  $\alpha\beta_{nm}(\lambda)$ ,  $[\alpha\beta_{nm}(\lambda) + \gamma\beta_{nm}(\mu)]$ . Once the  $\beta_{nm}(\lambda)$  are computed as functions of  $\lambda$ , there is no additional labor required to deal with an  $f(z)$  which consists of a sum of any number of exponential terms. If instead of  $f(z) = \alpha e^{-\lambda z}$  we had  $f(z) = \alpha z e^{-\lambda z}$ , then the corresponding  $\beta'_{nm}(\lambda)$  would be

$$\beta'_{nm}(\lambda) = \int_0^\infty U_m^0(z) U_n^0(z) z e^{-\lambda z} dz = -\frac{d\beta_{nm}(\lambda)}{d\lambda}. \quad (67)$$

If  $\beta_{nm}(\lambda)$  is known,  $d\beta_{nm}(\lambda)/d\lambda$  can be computed directly from equation (43). When equation (43) is integrated numerically, the derivative  $d\beta_{nm}(\lambda)/d\lambda$  is computed at each point in any case. Evidently, for  $f(z) = \alpha z^k e^{-\lambda z}$ , where  $k$  is a positive integer.

$$\begin{aligned} \beta'_{nm}(\lambda) &= \int_0^\infty U_m^0(z) U_n^0(z) z^k e^{-\lambda z} dz \\ &= (-)^k \frac{d^k \beta_{nm}(\lambda)}{d\lambda^k}. \end{aligned} \quad (68)$$

By successive differentiation of equation (43), it is possible to express any high order derivative of  $\beta_{nm}(\lambda)$  in terms of  $\beta_{nm}(\lambda)$ . From a purely formal point of view we can say therefore that by our method we can treat any  $M$  anomaly by expanding it into a series of Laguerre functions, since these functions involve only terms of the form  $z^k e^{-\lambda z}$ . It may be pointed out that a single term  $z^k e^{-\lambda z}$  vanishes both at the ground and at great height and reaches a maximum at  $z = k/\lambda$ . Such a single term is therefore suitable to represent an elevated duct.

### 25.9 COMPUTATIONAL PROGRAM FOR THE EXPONENTIAL MODEL

The Analysis Section of the Columbia University Wave Propagation Group has undertaken the computation of  $\beta_{nm}(\lambda)$  for  $\lambda = 0(0.1)4.0$  and  $n, m = 1, 2, 3, 4, 5$ . With these functions tabulated, it is planned to compute the characteristic values  $D_k$  for such values of  $\alpha$  and  $\lambda$  that the difference between the values of  $D_k$  obtained from the fourth order determinant and from the fifth order determinant will be only about 0.01. The program also calls for the computation of the height-gain functions from equa-



tion (2), since the coefficients  $A_{km}$  will be obtained simultaneously with the  $D_k$  when the iteration procedure is used. This will be possible only in a limited region of low altitudes, since at great heights the  $U_m^0(z)$  increase rapidly in magnitude as  $m$  is increased. However, near the ground the  $U_m^0(z)$  are all of the same order of magnitude ( $= iz$ ) and

$$\frac{dU_k(0)}{dz} = i \sum_{m=1} A_{km} . \quad (69)$$

If this derivative of  $U_k(z)$  at the ground can be obtained with sufficient accuracy, then one may use it to integrate numerically the original equation (11). It is well known that, for a given order of the determinant used, the characteristic values  $D_k$  are obtained with higher accuracy than the height-gain functions.

It may be added here that  $\beta_{11}(\lambda)$  computed from equation (44) agrees up to  $\lambda = 5.0$  with the values given by Pearcey and Tomlin.<sup>106</sup>

The perturbation method will of course become inefficient when trapping conditions are approached. For such values of  $\alpha$  and  $\lambda$ , asymptotic methods may provide approximate values for the  $D_k$ , provided care is taken at each stage to estimate the order of magnitude of the error involved. It is planned to map out by a combination of these methods the real and imaginary parts of  $D_k$  in the operationally relevant region of the  $\alpha, \lambda$  plane.

#### Symbols for Use in Theory of Nonstandard Propagation

$q$  = standard slope of  $N^2$  curve =  $2.38 \cdot 10^{-7} m^{-1}$  .

$p$  = slope of lower section of  $N^2$  curve in bilinear model .

$$\frac{p}{q} = s^3 .$$

$$y = N^2 - 1 = 2M \cdot 10^{-6} .$$

$$z = (k^2 q)^{\frac{1}{2}} h = h/H \text{ height in natural units} \\ (k = 2\pi/\lambda) .$$

$$H = (k^2 q)^{-\frac{1}{2}} = 7.24 \lambda_{cm}^{\frac{2}{3}} (\text{feet}) \text{ natural unit of height} .$$

$$x = 1/2 (kq^2)^{\frac{1}{2}} d = d/L \text{ distance in natural units} .$$

$$L = 2 (kq^2)^{-\frac{1}{2}} = 6.69 \lambda_{cm}^{\frac{1}{3}} (\text{thousands of yards}) = \\ \text{natural unit of distance} .$$

$$h_a = \text{anomaly height (height of joint in bilinear model)} .$$

$$g = h_a/H \text{ anomaly height in natural units} .$$

$$\Lambda_m = \text{characteristic value (for } y = 0 \text{ at } h = h_a) .$$

$$D_m = (k/q)^{\frac{2}{3}} \Lambda_m = B_m + iA_m \text{ characteristic value in natural units} .$$

$$X = s^{-2} D \text{ (abbreviation for use in computing)} .$$

$$\Psi = e^{\underbrace{et\omega t - 2\pi id/\lambda - i\pi/4}_{\text{plane wave}}} \cdot \underbrace{\frac{2\pi^{\frac{1}{2}}}{L}}_{\text{depends on } \lambda} .$$

$$\underbrace{x^{-\frac{1}{2}} \sum_1^{\infty} e^{-A_m x + iB_m x} \cdot U_m(z_1) U_m(z_2)}_{\text{natural units only}}$$

$$\int_0^{\infty} U^2 dz = 1 .$$

$$R = \text{slant range} .$$

$$d = \text{horizontal range} .$$



# FIRST ORDER ESTIMATION OF RADAR RANGES OVER THE OPEN OCEAN<sup>a</sup>

THE MOST STRIKING nonstandard propagation conditions are for the most part associated with meteorological conditions which can exist only over those portions of the sea which are contiguous to extensive land masses. At large distances from the coasts, however, low ducts exist which, though they never produce strongly locked modes at the usual radar frequencies, nevertheless modify radar ranges. The problem of the low duct has the great advantage that conditions are sufficiently near standard that numerical solutions can be found in convenient form by an extension of the perturbation methods of wave mechanics.

At appreciable distances from land the temperature of the air is essentially that of the sea, and the air is in neutral equilibrium. Montgomery has pointed out that under these conditions there is much evidence to support a logarithmic distribution of specific humidity.

The logarithmic distribution of water vapor leads to an  $M$  curve given by

$$M - M_0 = \frac{3}{4} \cdot 10^6 \left( \frac{d}{a} \right) \left[ \frac{z}{d} - \ln \frac{z}{d} \right]$$

where  $d$  is the duct thickness,  $z$  is the height coordinate, and  $a$  is the radius of the earth. If we plot the function in the brackets, we obtain the dashed curve of Figure 1.

This type of  $M$  distribution is inconvenient because (a) the logarithmic term which represents the modification does not approach zero as the height increases as a modification term should; and (b)  $\ln(z/d)$  becomes infinite when  $z = 0$ . Accordingly it is proposed to replace the function in the brackets by the first two terms of its series expansion about the minimum. This amounts to substituting for the logarithmic curve a parabolic curve which has the same minimum point and the same radius of curvature at the minimum point as the original distribution. At twice the duct height the parabola has a standard slope, and it is continued from that point upward as a straight line of this slope ( $AB$  in Figure 1).

The modification term is now represented entirely

<sup>a</sup>By J. E. Freehafer, Radiation Laboratory, MIT.

by the departure of the parabola from the line  $AB$ , i.e.,

$$M - M_0 = \frac{3}{4} 10^6 \frac{d}{a} \left[ 1 + \frac{1}{2} \left( \frac{z}{d} - 1 \right)^2 \right], \quad 0 \leq \frac{z}{d} \leq 2$$

$$M - M_0 = \frac{3}{4} 10^6 \frac{d}{a} \frac{z}{d}, \quad 2 \leq \frac{z}{d}.$$

When the duct is low, the modes leak and are not far different from the standard ones. Thus it seems

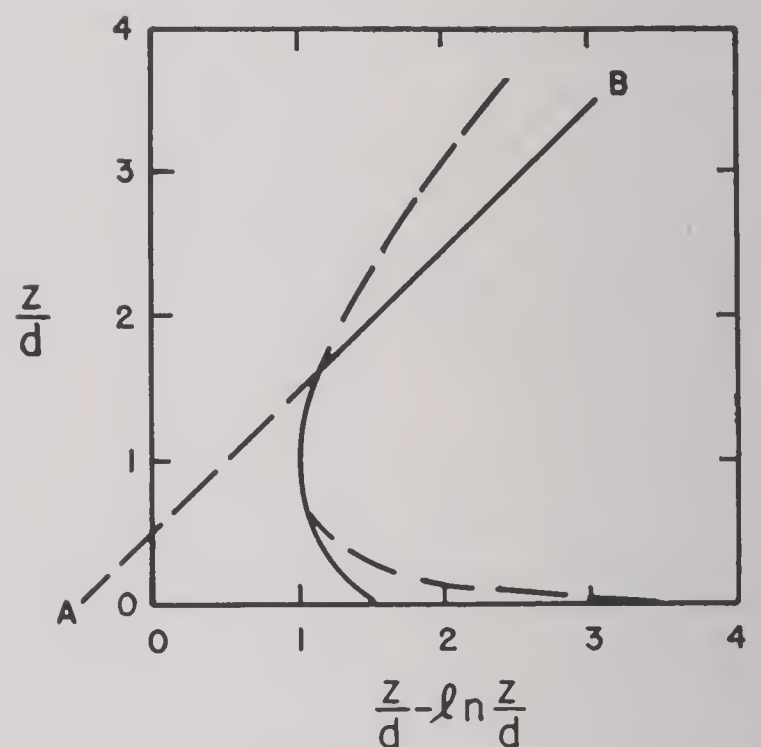


FIGURE 1. Schematic  $M$  curve for ground-based duct.

reasonable to employ the well-known methods of perturbation theory for calculating the characteristic values and functions of the parabolic atmosphere in terms of departures from standard.

If we brush aside mathematical questions of a delicate nature, it is possible to obtain an approximation for the characteristic values which leads to the following expression for the fractional change in the attenuation constant (i.e., the real part of  $\gamma_m$ )

$$\begin{aligned} & \frac{\text{Re}(\bar{\gamma}_m) - \text{Re}(\gamma_m)}{\text{Re}(\bar{\gamma}_m)} \\ &= \frac{- \int_0^\delta (\zeta - \delta) \text{Im}[h_2^2(\zeta + e_m)] d\zeta}{\delta [h_2'(e_m)]^2 \text{Im}(e_m)} = \frac{\delta^6}{315} + \dots \end{aligned}$$

Here,  $\text{Re}$  and  $\text{Im}$  designate the real and imaginary parts, and



$$\delta = \frac{2d}{L}.$$

$L$  is an abbreviation for  $(a\lambda^2/6\pi^2)^{1/2}$  and is equal to 33 ft for  $\lambda = 10$  cm,

$\bar{\gamma}_m$  is the characteristic value for the standard case,

$\gamma_m$  is the characteristic value for the parabolic case,

$h_2(z)$  is  $\left(\frac{2}{3}\right)^{1/2} z^{1/2} H_{1/2}^{(2)}\left(\frac{2}{3}z^{3/2}\right)$ ,

$H_{1/2}^{(2)}$  is the Hankel function of second kind, order  $1/2$ , of the argument  $\left(\frac{2}{3}z^{3/2}\right)$ ,

$e_m$ 's are roots of  $h_2(\zeta) = 0$ .

The expression above has been evaluated for the first mode by summing the series for  $h_2$  and performing the integration numerically. This curve is remarkable for the considerable interval in which the ordinate is practically zero. The attenuation constant differs by less than 1 per cent from the standard for ducts below  $\delta = 1.2$ . Beyond this value the effect of the duct increases rapidly, and when  $\delta = 1.7$  the attenuation constant is 10 per cent different from standard, and at  $\delta = 2$  it is 20 per cent different.

It seems that at least for radar purposes the condition  $\delta \leq 1$  is a reasonable and convenient condition for defining a negligible duct. This is equivalent to saying that  $L/2$  is the thickness below which a duct may for practical purposes be disregarded. For instance, at  $\lambda = 10$  cm,  $L = 33$  ft, and hence we conclude that the effect of ducts less than 16 ft in thickness on 10-cm radars may be neglected. On the other hand, if the wavelength is 3 m,  $L = 300$  ft, and ducts below 150 ft in thickness are negligible.

If in the interest of simplicity we neglect the effect of small variations in the characteristic values on the characteristic functions, the fractional change in attenuation constant is also equal to the fractional change in the range against surface targets. It follows that the estimation of range can be reduced to a measurement of sea temperature and specific humidity at masthead level; for the duct thickness  $d$  under conditions of neutral equilibrium is given by

$$d = - \frac{(q_s - q_a) \Gamma}{\left(\frac{dq}{dz}\right)_0}.$$

$q_s$  is the saturation specific humidity at sea temperature and  $q_a$  the specific humidity at masthead.  $\Gamma$  is a parameter for which a representative value is 0.08, and  $(dq/dz)_0$  is the gradient of specific humidity required to give zero  $M$  gradient under conditions

of constant potential temperature. It is taken as  $1/2$  g per kg.

Thus it turns out that

$$\delta = 0.32 \frac{q_s - q_a}{L}$$

where  $\frac{q_s - q_a}{L}$  is in grams per kg per 100 ft.

If  $L$  is given the appropriate value for  $\lambda = 10$  cm

$$\delta \cong q_s - q_a \text{ (g per kg)}.$$

For illustrative purposes, scales of  $(q_s - q_a)/L$  and  $q_s - q_a$  for  $\lambda = 10$  cm have been added in Figure 2.

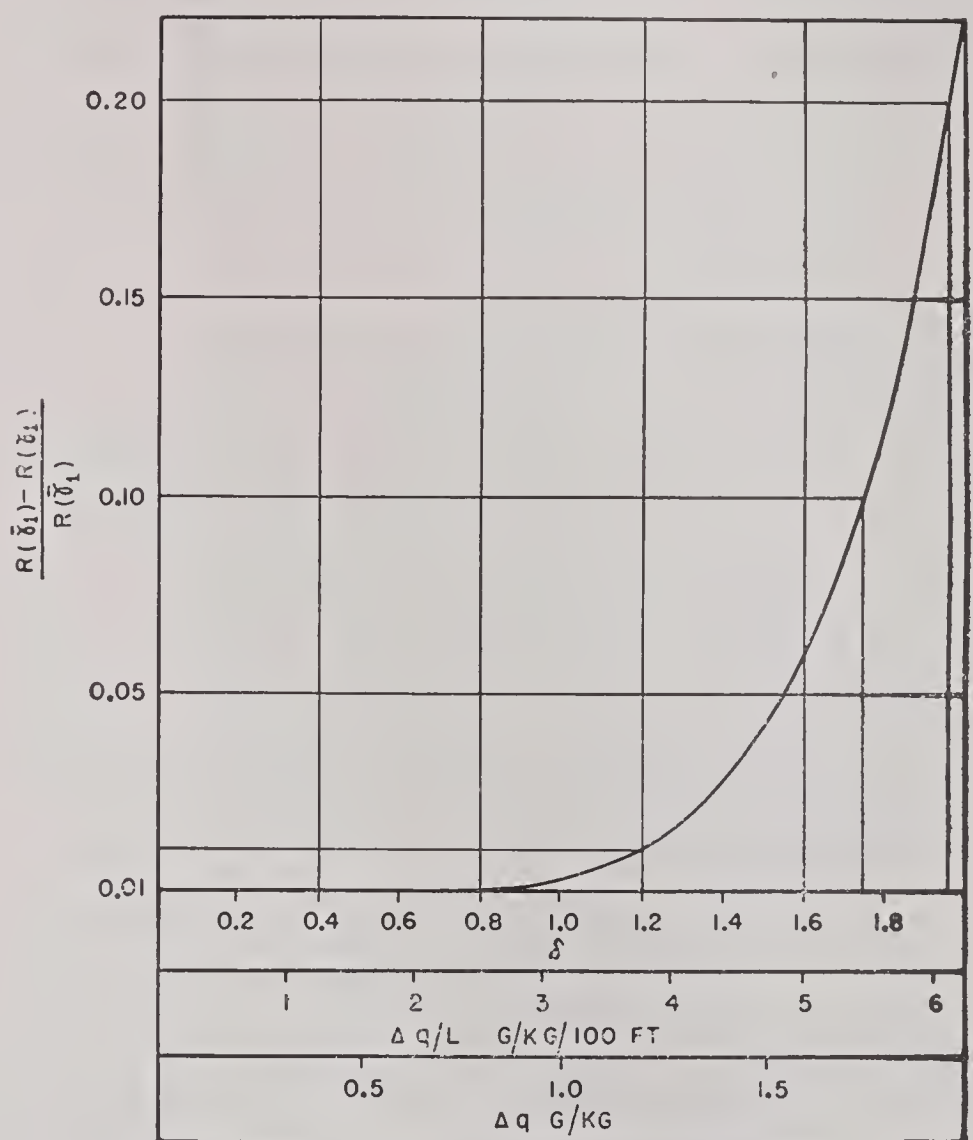


FIGURE 2. Fractional drop in attenuation constant of the first mode versus duct thickness. Bottom scale for  $\Delta q$  and  $\Delta q/L$  corresponds to  $\lambda = 10$  cm.

It is emphasized that the calculations are rough and are presented only in the belief that some sort of simple guiding principle may be more useful than a highly accurate and cumbersome formula. The results given are accurate out to variations in range of 1 per cent, and the determination of threshold thickness is completely reliable. Extension beyond  $\delta = 1.2$  is a definite extrapolation. The trend indicating that the increase in range goes up at least as fast as the sixth power of the duct thickness for  $\delta > 1$  is, we believe, real.



## Chapter 27

# CONVERGENCE EFFECTS IN REFLECTIONS FROM TROPOSPHERIC LAYERS<sup>a</sup>

**A**N ELEVATED DUCT may be treated as a concave spherical mirror whose radius of curvature is  $a$ , the *effective* earth radius. This includes any layer that can act as a reflector to radiation incident at a sufficiently small angle. The problem is here considered as one of geometrical optics only. Ray tracing methods are used, and the phases are assumed to add randomly. This assumption may introduce an error as large as 3 db in the result but is necessary to simplify the solution of the problem. If the reflection coefficient is other than unity, it must be multiplied into the general relation which will be given for  $C = KLM$  the net convergence factor.

27.1

### CONVERGENCE FACTOR

A bundle of rays leaving a transmitter below the reflecting layer is converged on reflection from a concave surface. The convergence factor  $K$  is the ratio of the power density at the receiving antenna after convergence to the power density at the receiver that would be expected after reflection from a plane surface (essentially free space condition). Referring to Figure 1, the convergence factor can be expressed as

$$K = \frac{(x + y) \delta \theta_1}{x \delta \theta_1 + y \delta \theta_2}, \quad (1)$$

or

$$K = \left(1 - \frac{2xy}{aK \sin \phi}\right)^{-1}, \quad (2)$$

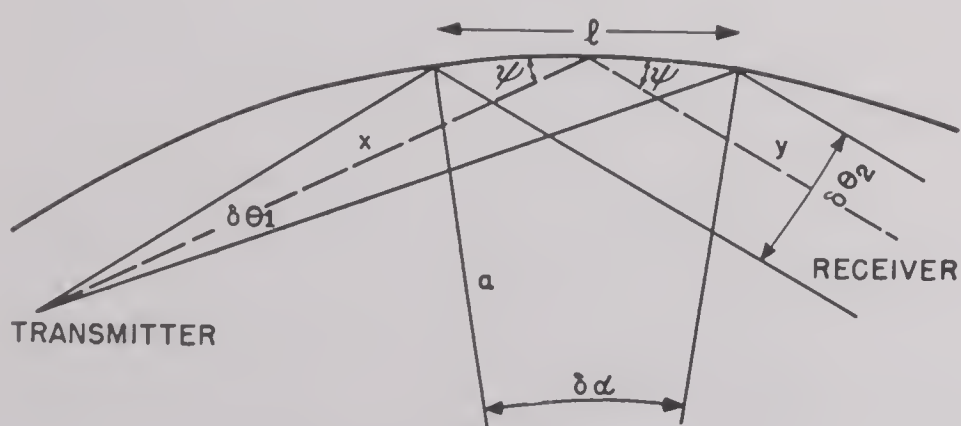


FIGURE 1. Convergence factor  $K$ .

where  $x$  = distance from transmitter to point of reflection,

<sup>a</sup>By Ensign W. W. Carter, USNR Radio Division, Consultant Group.

$y$  = distance from receiver to point of reflection,

$R = x + y$  = total range,

$a$  = *effective* earth's radius (usually 4,590 nautical miles),

$\phi$  = angle of incidence of radiation at reflection,

other angles as shown on Figure 1.

Equation (2) can be deduced from equation (1) by remembering that

$$l = a d\alpha = \frac{x \delta \theta_1}{\sin \phi}, \quad (3)$$

and

$$\delta \theta_1 - \delta \theta_2 = 2d\alpha = \frac{2x \delta \theta_1}{a \sin \phi}.$$

The form shown in equation (2) is the more useful and is similar to the divergence factor for reflection at a convex surface that has been in use for some time. Equation (2) shows that  $K$  can grow quite large and even become infinite for certain conditions. Curve 1, Figure 2, shows a plot of the absolute value

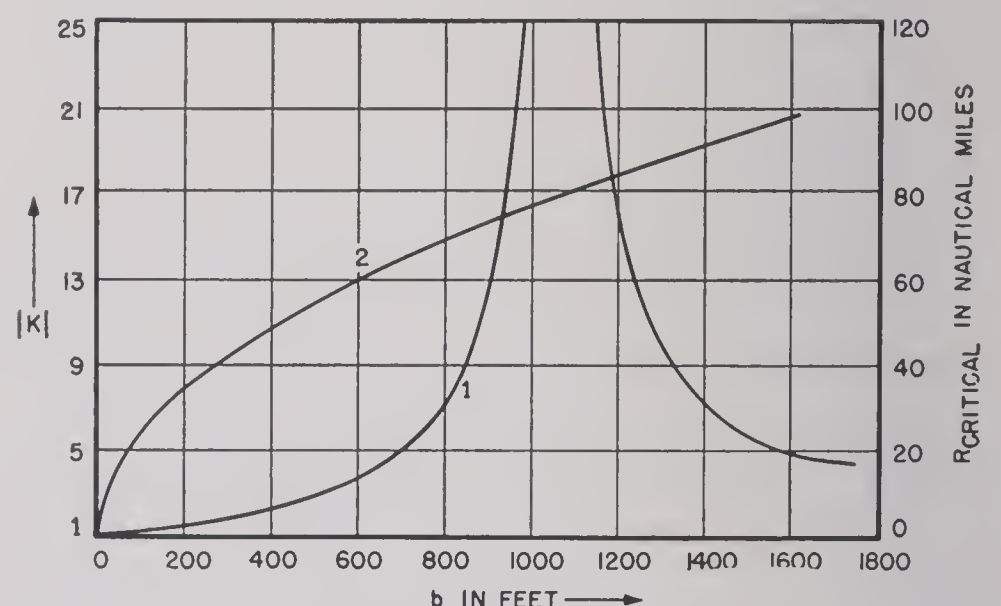


FIGURE 2. Value of  $K$  for height of layer ( $b$  in ft) versus range (nautical miles).

of  $K$  as a function of  $b$ , the height of the layer above the antennas, for a total range of 80 nautical miles. This plot also assumes  $x = y = 40$  miles, which is a necessary condition for a smooth reflector. In this case,  $K$  becomes infinite for a layer 1,100 ft above the antennas. Curve 2, Figure 2, shows a plot of



the layer height  $b$  necessary to give infinite convergence as a function of the range (plotted on right-hand scale).

27.2

### ROUGHNESS EFFECT

The most apparent difficulty with the picture presented so far is that the layers actually are not perfectly smooth. In order to take that fact into consideration, it was assumed that the layer was composed of a large number of plates set at various small angles about the horizontal according to a Gaussian distribution. As in other parts of this problem, variations are considered only in the plane of transmission, since the effect of sideways deviation would cancel out. This reduces the problem to one of two dimensions only. Each plate is further assumed to retain its original curvature.

A beam falling on a patch of these plates would be reflected in such a way as to spread the energy at the receiver in a vertical pattern similar to the Gaussian distribution of the plates. It is only necessary to integrate this curve over the width of the antenna to find the fraction,  $L$ , of the total energy that will be useful.  $L$  will be a function of the probable value of the deviation of the plates, the range, and the antenna width.

With the rough layer assumption, there will be some plates correctly oriented at each part of the layer to reflect energy into the receiver. Therefore, a third factor,  $M$ , must be included that is the ratio of  $\gamma/\beta$ , where  $\gamma$  is the total angle subtended by the layer that can reflect rays to the receiver.  $\gamma$  would be limited by the optical horizons.  $\beta$  is the angle subtended by the receiving antenna when reflection is from a plane surface; i.e., essentially, free space conditions.

The net convergence factor  $C$  must be the product of these three quantities  $K$ ,  $L$ ,  $M$ . In this case,  $K$

must be the mean value of  $K$  averaged for various points of reflection. In order to integrate the expression for the mean value of  $K$ , it is necessary to substitute for  $\sin \phi$  in equation (2).

$$\sin \phi = \left( \frac{b}{x} + \frac{x}{2a} + \frac{b}{y} + \frac{y}{2a} \right), \quad (5)$$

which gives

$$K = \left[ 1 - \frac{8(xy)^2}{R^2(2ab + xy)} \right]^{-1}. \quad (6)$$

This expression is easily integrated if the product  $xy$  is used for the variable and  $x_1y_1 = x_1(R - x_1)$ .

*Example.* The preceding developments have been applied to the one-way link of the U. S. Navy Radio and Sound Laboratory at San Diego, which has been extensively studied. High subsidence layers are common for this region. The probable value of the deviation of a reflecting plate from horizontal was taken as  $0.1^\circ$  as an engineering approximation. In this case,  $C$  equals 43, assuming a reflection coefficient of 1. If the reflection coefficient is not unity, its value as a function of angle of incidence must be multiplied into the equation.

Since  $K$ ,  $L$ , and  $M$  can each vary through considerable limits,  $C$  can vary through a very wide range of values.

27.3

### CONCLUSIONS

The statistical treatment of the roughness is not always applicable, since a finite number of plates would actually be engaged in reflecting energy. Hence, the received signal would vary almost randomly with time as the orientation of the plates changed slightly. This could produce marked fading and peaks of large amplitude. Primarily, however, it would explain signals of the magnitude of free space signals or higher.







# BIBLIOGRAPHY

## VOLUME I

Numbers such as CP-100-M1 indicate that the document listed has been microfilmed and that its title appears in the microfilm index printed in a separate volume. For access to the index volume and to the microfilm, consult the Army or Navy agency listed on the reverse of the half-title page.

1. *Notes on Microwave Propagation Conference at MIT, Radiation Laboratory, Division 14 Report 42, RL, Sept. 24, 1943.* CP-100-M1
2. *International Radio Propagation Conference* [held at Inter-service Radio Propagation Laboratory, from April 17 to May 5, 1944], Report IRPL-C61, National Bureau of Standards, June 1944. CP-100-M3
3. *Report of Second Propagation Conference, February 10 to 11, 1944 at the Empire State Building, New York, OEMsr-1207, NDRC CUDWR-WPG, February 1944.* CP-100-M2
4. *Scientific Investigations on Propagation Problems in the Southwest Pacific Area, F.W.G. White, OSRD II-5-6124(S), ATP [Australian Radio Propagation Committee], July 24, 1944.* CP-110-M1
5. *The Air Defense System of the Near Islands, Thomas J. Carroll, Report OAD-55, U.S. Army Air Forces, Eleventh Air Force, OCSO, Operational Analysis Division, Aug. 30, 1944.* CP-202.1-M5
6. *Reviews of Progress of Ultra Short Wave Propagation Work, [USWP]:*
  - 6a. [Part] I, *The Evaluation of Solutions of the Wave Equation for a Stratified Medium, D. R. Hartree, OSRD WA-2961-2, JEIA 5934, RDF 239, Report AC-7017, Sept. 26, 1944.* CP-110-M2
  - 6b. [Part] II, *Statement of Work in Progress Relevant to Investigations of the Propagation of Radio Waves Through the Troposphere, R. L. Smith-Rose, OSRD WA-3005-2, Report AC-7018, NPL, Sept. 25, 1944.* CP-110-M3
  - 6c. [Part] III, *Microwave Propagation Research at the Signals Research and Development Establishment, OSRD WA-3156-7, JEIA 6464, Report AC-7019, SRDE, Sept. 26, 1944.* CP-110-M4
  - 6d. [Part] IV, *Correlation of Radar Operational Data with Meteorological Conditions, OSRD WA-3156-8, JEIA 6463, Report AC-7020, AORG, Sept. 28, 1944.* CP-110-M5
  - 6e. [Part] V, *Progress Report on Forecasting of Radar Conditions, OSRD WA-3156-9, JEIA 6462, Report AC-7021, DMO, Oct. 2, 1944.* CP-110-M6
  - 6f. [Part] VI, *Vertical Temperature and Humidity Gradients at Rye, OSRD WA-3156-10, JEIA 6461, Report AC-7022, DMO, Oct. 2, 1944.* CP-110-M7
  - 6g. [Part] VII, *The Use of Radar for the Detection of Storms, OSRD WA-3156-11, JEIA 6460, Report AC-7023, DMO, Oct. 2, 1944.* CP-110-M8
  - 6h. [Part] VIII, *Present States of Theoretical Study of Radio Propagation, Through the Troposphere by the Mathematics Group, TRE, OSRD WA-3156-12, JEIA 6459, Report AC-7024, TRE, Oct. 2, 1944.* CP-110-M9
  - 6i. [Part] IX, *Review of Short-Period Experimental Studies of Centimetre Wave Propagation, Carried Out Jointly by ASE, SRDE, and GEC, E. C. S. Megaw, OSRD WA-3156-13, JEIA 6458, Report AC-7025, Oct. 16, 1944.* CP-110-M10
  - 6j. [Part] X, *Study of Centimetre Wave Propagation over Cardigan Bay to Mount Snowden, F. Hoyle, OSRD WA-3157-1, Report AC-7026, Oct. 14, 1944.* CP-110-M11
  - 6k. [Part] XI, *Study of Reflection Coefficient of the Sea at Centimetre Wavelengths, F. Hoyle, OSRD WA-3157-2, Report AC-7027, Oct. 14, 1944.* CP-110-M12
  - 6l. [Part] XII, *Some K-, X-, and S-Band (Llandudno) Trials, General Summary of the Experimental Results Obtained which are Concerned with the Dependence of Radio Propagation on Meteorological Conditions, OSRD WA-3157-3, Report AC-7028, TRE and RRDE, Oct. 14, 1944.* CP-110-M13
  - 6m. [Part] XIII, *Progress Report on 369 Trials by Director, Naval Meteorological Service, OSRD WA-3156-1, JEIA 6466, RDF 240, Report AC-7029, Oct. 14, 1944.* CP-110-M14
  - 6n. [Part] XIV, *Survey of Progress in the United Kingdom on the Electromagnetic Theory of Tropospheric Propagation, OSRD WA-3157-4, Report AC-7030, RRDE, Oct. 16, 1944.* CP-110-M15
  - 6o. [Part] XV, *Study of Meteorological Factors Responsible for the Refractive Structure of the Troposphere, OSRD WA-3157-5, Report AC-7031, RRDE, Oct. 16, 1944.* CP-110-M16
7. *Report No. 1 of Project SWP-3.2 of the Office of Field Service, Paul A. Anderson and P. Squires, OEMsr-728, Research Project PDRC-647, Washington State College, Nov. 2, 1944.* CP-335-M3
8. *Data on Super Refraction Supplied by Australian Radar Stations, J. W. Reed, Report RP-229/1, CSIR-RL, Dec. 6, 1944.* CP-223-M11
9. *Report No. 2 of Project SWP-3.2 of the Office of Field Service, Paul A. Anderson and P. Squires, OEMsr-728, Research Project PDRC-647, Washington State College, Jan. 7, 1945.* CP-335-M3
10. *Third Conference on Propagation, Washington, D. C. [on] November 16 to 18, 1944, NDRC CUDWR-WPG, 1945.* CP-100-M4
11. *Survey of Field of Radio Propagation and Noise with Special Reference to Australia, F. J. Kerr, OSRD II-5-6572(S), JEIA 8641, Report RP-231, CSIR, Nov. 27, 1944.* CP-110-M17
12. *Fourth Conference on Propagation, Washington, D. C. [on] May 7 [to] 8, 1945, NDRC CUDWR-WPG, 1945.*
13. *Notes on Microwaves based upon a Series of Lectures by W. W. Hansen, Samuel Seely and Ernest C. Pollard, Division 14 Report T-2, RL, Oct. 20, 1941, Chaps. 1 to 3.* CP-201.1-M1



14. *An Introduction to Microwave Propagation*, Donald E. Kerr and Pearl J. Rubenstein, Division 14 Report 406, RL, Sept. 16, 1943. CP-201.1-M2
15. *Electrical Communication Systems Engineering, General Information*, Technical Manual TM-11-486, U. S. War Department, Feb. 25, 1944. CP-204-M1  
Superseded by TM-11-486, Apr. 25, 1945 and *Electrical Communication Systems Equipment*, TM-11-487, Oct. 2, 1944.
16. *Anomalous Propagation and the Army*, Thomas J. Carroll, Report ORB-P-18-1, OCSO, Mar. 4, 1944. CP-221-M12
17. *Principles of Radar*, Staff of MIT Radar School, June 15, 1944. CP-202-M1
18. *Radar Performance Testing Manual*, Manual 28, USAAF, Second Edition, July 1944. CP-202.31-M1
19. *Effects of Site Conditions on Operation of Ground Radar Installations on Aerodromes*, J. L. Putnam, OSRD WA-4172-12, Report T-1805, TRE. CP-202.31-M2
20. "The Diffraction of Electro-magnetic Waves from an Electrical Point Source Round a Finitely Conducting Sphere, with Applications to Radiotelegraphy and the Theory of the Rainbow," H. Bremmer and Balth. Van Der Pol, *The London, Edinburgh, and Dublin Philosophical Magazine and Journal of Science*, **24**, July 1937, Part I, pp. 141-176; Supplement, **24**, November 1937, Part II, pp. 825-864; **25**, June 1938, Part III, pp. 817-837; **27**, March 1939, Part IV, pp. 261-275.
21. *Ultra Short Wave Propagation Curves, 0.1 to 10 Meters*, OSRD WA-1502-1a, Marconi Handbook, Marconi, Ltd., Mar. 28, 1940. CP-211-M1
22. *Report on Signal Strength Curves Within the Visual Range*, OSRD WA-1463-1, Pamphlet RD-456, Marconi, Ltd., November 1940. CP-211-M2
23. "The Effect of the Earth's Curvature on Ground-Wave Propagation," Chas. R. Burrows and Marion C. Gray, *Proceedings of the Institute of Radio Engineers*, **29**, January 1941, pp. 16-24. CP-231.12-M5
24. "Ultra Short Wave Propagation," I. C. Schelling, Chas. R. Burrows, and E. B. Ferrell, *Proceedings of the Institute of Radio Engineers*, **21**, March 1933, pp. 427-463. (See reference 447.)
25. *Propagation Curves for Wavelengths of 13 Meters, Supplement to U. S. W. Propagation Curves RD-456*, Appendix RD-456A, Marconi, Ltd., November 1941. (See reference 22.)
26. "The Calculation of Ground-Wave Field Intensity over a Finitely Conducting Spherical Earth," K. A. Norton, *Proceedings of the Institute of Radio Engineers*, **29**, December 1941, pp. 623-639.
27. *Siting of Stations for Maximum Range*, H. G. Booker, OSRD II-5-1183, Report M/36, TRE, Feb. 9, 1942. CP-231.11-M2
28. *Microwave Interference Patterns*, J. A. Stratton, Division 14 Report C-1, RL, Mar. 7, 1942. CP-232.1-M1
29. *Theoretical Field Strength of Ten-Centimeter Equipment over a Spherical Earth*, H. G. Booker, OSRD WA-210-3j, Report M/45/HGB, TRE, July 1, 1942. CP-231.12-M1
30. *Atmospheric Refraction and Height Determination by RDF*, E. Eastwood, OSRD II-5-6511, JEIA 7773, Calibration Memorandum 54, RAF, July 6, 1942. (See reference 63.) CP-211-M3
31. *Dependence of Range of Submarine Radar Equipment on Wave Length, Case 20564*, Chas. R. Burrows, Technical Memorandum MM-42-160-70, BTL, July 9, 1942. CP-212-M1
32. *Transmission on 3000 Mc. over Sea Water*, J. A. Stratton, Division 14 Report C-2, RL, July 14, 1942. CP-232.1-M2
33. *Transmission on 100 Mc. over Sea Water*, J. A. Stratton, Division 14 Report C-3, RL, July 14, 1942. CP-232.1-M3
34. *Transmission on 200 Mc. over Sea Water*, J. A. Stratton, Division 14 Report C-4, RL, July 14, 1942. CP-232.1-M4
35. *Transmission on 500 Mc. over Sea Water*, J. A. Stratton, Division 14 Report C-5, RL, July 14, 1942. CP-232.1-M5
36. *Interim Report on Propagation Within and Beyond the Optical Range*, C. Domb and M. H. L. Pryce, Report M-448, ASE, September 1942.
37. *Theoretical Ground Ray Field Strengths and Height Gain Curves for Wavelengths of 2 to 2000 Megacycles*, OSRD II-5-5274, Technical Report 383, Section E, BRL, September 1942. CP-211-M4
38. *Siting for Long Range Aircraft Detection*, Thomas J. Carroll, Technical Report T-13, CESL, Revised Oct. 17, 1942. CP-202.11-M1
39. *V.H.F. Field Strength Curves for Propagation within the Line of Sight*, G. J. Camfield, OSRD WA-570-3, Report Radio/279, Radio/s.2111/OPE 16, RAE, October 1942. CP-211-M5
40. *Relation of Radar Range to Frequency and Polarization*, J. A. Stratton and Richard A. Hutner, Division 14 Report C-6, RL, Nov. 3, 1942. CP-212-M2
41. *Propagation Curves [of] 1 to 10 Cm*, G. Millington, OSRD WA-1502-1c, Report TR-460, Marconi, Ltd., January 1943. CP-211-M6
42. *Properties of the Diffracted Wave Field Intensity*, Richard A. Hutner and Elizabeth M. Lyman, Division 14 Report C-8, RL, Feb. 12, 1943. CP-233-M7
43. *The Effect of Earth Curvature on the Performance Diagram of an RDF Station*, Report 29/R102/LGHH, TRE, Feb. 25, 1943.
44. *Radar Height Finding*, Richard A. Hutner, Helen Dodson, Jocelyn Gill, Bernard Howard, Francis Parker, and J. A. Stratton, Division 14 Report C-9, RL, Apr. 6, 1943. CP-202.311-M1
45. *Technical Requirements of Ground Communications Interceptor Search Systems, Technical Requirements for Early Warning Radar Systems*, L. J. Chu and N. H. Frank, Division 14 Report TCAW-1 and -2, RL, May 10, 1943. CP-202.1-M1
46. *Low-Angle Coverage of Early Warning Radar Systems*, N. H. Frank, Division 14 Report TCAW-3, RL, July 26, 1943. CP-202.1-M2
47. *Factors Relating to the Design of an RDF Air Warning Set*, F. J. Kerr, OSRD II-5-5721, Report RP-187, CSIR-RL, Aug. 11, 1943. CP-202.1-M3



48. *A Graphical Method of Computing the Bending of Radio Beams by the Effective Earth Radius Method*, Harry Raymond, Technical Report T-14, CESL, Aug. 27, 1943.  
CP-231.12-M2
49. *Transmission at Low Altitudes over Sea Water*, Richard A. Hutner, Francis Parker, Bernard Howard, Helen Dodson, and Jocelyn Gill, Division 14 Report C-10, RL, Sept. 1, 1943.  
CP-232.1-M6
50. *Radio-Frequency Propagation Above the Earth's Surface*, Paul F. Godley, Jr., OEMsr-895, Division 15 Report 895-5, RCA, Sept. 11, 1943.  
CP-231.12-M3
51. *Field Intensity Formulas*, Richard A. Hutner, Helen Dodson, Jocelyn Gill, Francis Parker, and Bernard Howard, Division 14 Report C-11, RL, Sept. 28, 1943.  
Div. 14-111-M8
52. *Note on Field Intensity Computations for Elevated Antennas, Case 20878*, Marion C. Gray, OSRD WA-1463-23, Technical Memorandum MM-43-110-28, BTL, Oct. 9, 1943.  
CP-211-M7
53. *The Calculation of Expected Vertical Coverage Diagrams by Max Sherman, February 19, 1943*, revised by Walter S. McAfee, Technical Report T-17, CESL, Oct. 15, 1943.  
CP-211-M8
54. *Charts for Use in Field Intensity Computations*, K. Bullington, OEMsr-1018, Research Project C-79, NDRC Division 13 Preliminary Report 3460-KB-NF, Western Electric Company, Inc., Nov. 2, 1943.  
CP-211-M9
55. *Notes on Visibility Problems, Taking Account of the Curvature of the Earth*, OSRD WA-1368-19, Report 152, AORG, Dec. 1, 1943.  
CP-231.12-M4
56. *Simplified Methods of Field Intensity Calculations in the Interference Region*, William T. Fishback, Division 14 Report 461, RL, Dec. 8, 1943.  
CP-211-M10
57. *Field Strength Near and Beyond the Horizon for Wavelengths of Ten and Thirty Cms.*, M/Report 53/WW, TRE, Dec. 24, 1943.
58. *Theoretical Field Strength Near and Beyond Horizon for Orthodox Propagation of Fifty Centimeter Waves*, OSRD WA-1976-5, Report T-1635/WW, TRE, Feb. 24, 1944.  
CP-211-M11
59. *The Propagation Functions for an Atmosphere with Uniform Lapse-Rate of Refractive Index*, T. Pearcey, OSRD WA-2985-1, Research Report 256, RRDE, Sept. 1, 1944.  
CP-211-M12
60. *Propagation Curves* (third edition), NDRC Division 15 Report 966-6C, October 1944.  
CP-211-M13
61. *Field Strength Calculator for Vertical Coverage Patterns and Propagation Curves*, Clarence R. White, Technical Memorandum 154-E, CESL, Dec. 20, 1944.  
CP-211-M14
62. *Theory of the Vertical Field Patterns for RDF Stations*, J. C. Jaeger, OSRD II-5-4297, Report RP-174, CSIR-RL, Mar. 17, 1943.  
CP-213-M1
63. *Height, Range [and] Alpha Tables, Tables Relating to the Height, Range and Angle of Elevation of an Aircraft*, OSRD II-5-6512, JEIA 7766, Radar Memorandum 50, ORS-ADGB, Aug. 10, 1944. (See reference 30.)  
CP-213-M2
64. *The Calculation of Field Strength for Vertical Polarization over Land and Sea on 20 to 80 Megacycles per Second*, A. M. Woodward, OSRD WA-4395-11, Report T-1704, TRE.  
CP-211-M15
65. *Field Intensity Contours in Generalized Coordinates*, Helen Dodson, Jocelyn Gill, and Bernard Howard, OEMsr-262, Division 14 Report 702, RL, May 2, 1945.  
CP-211-M16
66. *The Limiting Ranges of RDF Sets over the Sea*, F. Hoyle and M. H. L. Pryce, OSRD WA-1514-17, Report M-395, ASE, 1943.  
CP-232.2-M2
67. *The Theory of Anomalous Propagation in the Troposphere and Its Relation to Waveguides and Diffraction*, H. G. Booker, OSRD WA-599-10, Report T-1447, M/60/HGB, TRE, Apr. 12, 1943.  
CP-221-M2
68. *The Tracing of Rays in the Refracting Atmosphere*, T. Pearcey, OSRD WA-645-42, Report AC-3878, ADRDE-USW, Apr. 21, 1943.  
CP-222-M2
69. *Graphical Construction of a Radar Radiation Pattern in a Stratified Atmosphere*, Lloyd J. Anderson and F. R. Abbott, BuShips Problem X4-49CD, Report WP-4 [for the period from] March 1, 1943 to May 1, 1943, NRSL, May 1, 1943.  
CP-232.2-M3
70. *Improved Tropospheric Propagation, Curves Embracing Anomalous Propagation*, H. G. Booker, OSRD II-5-4950, Report T-1482, M/65/HGB, TRE, July 6, 1943.  
CP-221-M3
71. *Radiation Patterns under Cases of Anomalous Propagation*, T. Pearcey, OSRD WA-830-8, Report R-35/TP, ADRDE, July 19, 1943.  
CP-221-M5
72. *Effect of Humidity Gradients in the Atmosphere on Propagation at RDF Frequencies*, Operational Research Report 22, AORG, July 28, 1943.  
CP-222.1-M2
73. *The Calculation of Field Strength Near the Surface of the Earth under Particular Conditions of Anomalous Propagation*, T. Pearcey, OSRD WA-931-6, Research Report 203, ADRDE, Oct. 28, 1943.  
CP-221-M6
74. *Anomalous Propagation over the Earth, Case 23703*, S. A. Schelkunoff, OSRD WA-1463-50, Report MM-43-110-33, BTL, Oct. 30, 1943.  
CP-221-M7
75. *The Effect of Atmospheric Refraction on Short Radio Waves*, John E. Freehafer, Division 14 Report 447, RL, Nov. 29, 1943.  
CP-222-M5
76. *Radar Ray Patterns Associated with Normal and Anomalous Propagation Conditions*, F. P. Dane, R. U. F. Hopkins, and Lloyd J. Anderson, BuShips Problem X4-49CD Report WP-6 [for the period from] November 1 to December 6, 1943, NRSL, Dec. 10, 1943.  
CP-221-M8
77. *Transmission of Plane Waves Through a Single Stratum Separating Two Media*, John B. Smyth, BuShips Problem X4-49CD, Report WP-9, NRSL, Dec. 22, 1943.  
CP-221-M9
78. *Notes on Theoretical Coverage Diagrams for Anomalous Propagation*, Donald E. Kerr, OSRD WA-1464-9, TM/Memorandum/14/AMW, TRE, Jan. 1, 1944.  
CP-221-M11
79. *The Dependence of Microwave Propagation over Sea on the Structure of the Atmosphere*, J. M. C. Scott and T. Pearcey, OSRD WA-1591-9, Memorandum 40, ADRDE, Feb. 4, 1944.  
CP-232.2-M8
80. *Improved Tropospheric Propagation, Curves Embracing Superrefraction* (revised edition), OSRD WA-1666-27, Report T-1625/WW, TRE, Feb. 18, 1944.  
CP-223-M1



81. *TRE Requirements for Propagation, Curves Embracing Superrefraction*, OSRD WA-1666-26, Report M/Memo-16/HAB, TRE, Feb. 25, 1944. CP-223-M2
82. *The Mechanical Determination of the Path Difference of Rays Subject to Discontinuities in the Vertical Gradient of Refractive Index*, F. R. Abbott, BuShips Problem X4-49CD, Report WP-10, NRSL, Mar. 10, 1944. CP-222.1-M3
83. *Improved Tropospheric Propagation, Curves Embracing Superrefraction*, OSRD WA-2026-2, Report T-1626/WW, TRE, Mar. 28, 1944. CP-223-M3
84. *Interservice Propagation, Curves Embracing Superrefraction, Dependence of Mathematical Parameter L on Physical Entities*, Report M/Memo-18/WW, TRE, Apr. 3, 1944. CP-223-M4
85. *Theoretical Coverage-Diagrams for 10 Cm. Radars Embracing Superrefraction*, JEIA 3229, Report T-1634, TRE, Apr. 14, 1944. CP-223-M5
86. *Theoretical Coverage-Diagrams for 50 Cm. Radars Embracing Superrefraction*, OSRD WA-1992-4, JEIA 3230, Report T-1659, TRE, Apr. 14, 1944. CP-223-M6
87. *Theoretical Coverage of Navigational Aids Embracing Superrefraction*, OSRD WA-1992-6A, Report T-1660, TRE, Apr. 14, 1944. CP-223-M7
88. *The Theory of Propagation of Radio Waves in an Inhomogeneous Atmosphere (Part I)*, T. Pearcey, OSRD WA-2251-5, Research Report 245, ADRDE, April 1944. CP-221-M10
89. *Reflection Coefficient of Layers of Varying Refractive Index*, G. Millington, OSRD WA-2562-13, JEIA 4644, Report TR-483, BRL, April 1944. CP-222.1-M4
90. *Evaluation of the Solution of the Wave Equation for a Stratified Medium*, D. R. Hartree, P. Nicholson, N. Eyres, J. Howlett, and T. Pearcey, OSRD WA-2341-4, Memorandum 47, ADRDE, May 24, 1944. (See reference 108.) CP-221-M13
91. *Transmission of Plane Waves Through a Single Stratum Separating Two Media (Part II)*, John B. Smyth, BuShips Problem X4-49CD, Report WP-13, NRSL, June 23, 1944. CP-221-M9
92. *Waves Guided by Dielectric Layers*, S. A. Schelkunoff, Report MM-44-110-52, BTL, July 5, 1944. CP-221-M14
93. *Microwave Transmission in Nonhomogeneous Atmosphere*, S. A. Schelkunoff, Report MM-44-110-53, BTL, July 5, 1944. CP-221-M15
94. *Contour Diagrams of the Radiated Field of a Dipole under Various Conditions of Anomalous Propagation*, T. Pearcey and F. Whitehead, OSRD WA-2985-2, Research Report 257, RRDE, July 15, 1944. (See reference 110.) CP-221-M16
95. *Theoretical Coverage-Diagrams for 1½-Meter Radars Embracing Super-refraction*, A. M. W. Woodward, OSRD WA-2854-2, Report T-1708, TRE, July 23, 1944. CP-223-M9
96. *Propagation Curves Embracing Super-refraction: SS Duct, Profile-Index 0.2 (Preliminary Edition)*, H. G. Booker, M/Memo-23/WW, TRE, Sept. 7, 1944. CP-223-M10
97. *A Note on the Reflection Coefficient of an Isotropic Layer of Varying Refractive Index*, G. Millington, OSRD WA-3172-1, JEIA 6481, Report TR-497, BRL, Oct. 5, 1944. CP-222.1-M5
98. *Predicted Low Level Coverage of S-Band Shipborne Radars as Affected by Weather*, F. R. Abbott, L. L. Whittemore, L. W. Cross, and E. J. Wyrostek, BuShips Problem X4-49CD, Report WP-14, NRSL, Nov. 1, 1944. CP-232.2-M9
99. *Predicted Low Level Coverage of 200 MCS Band Shipborne Radars as Affected by Weather*, F. R. Abbott, L. L. Whittemore, L. W. Cross, and E. J. Wyrostek, BuShips Problem X4-49CD, Report WP-15, NRSL, Nov. 4, 1944. CP-232.2-M10
100. *Variational Method for Determining Eigenvalues of Wave Equation of Anomalous Propagation*, G. G. Macfarlane, Report T-1756, TRE, Nov. 13, 1944.
101. *Wave Propagation Analysis with the Aid of Non-Euclidian Spaces*, Benjamin Liebowitz, OEMsr-1207, Report WPG-7, CUDWR, December 1944. CP-221-M18
102. *Atmospheric Waves, Fluctuations in High Frequency Radio Waves*, L. G. Trolese and John B. Smyth, BuShips Problem X4-49CD, Report WP-18, NRSL, Feb. 1, 1945. CP-225-M1
103. *The Relation Between the Wave Equation and the Non-Linear First Order Equation of the Riccati Type*, T. L. Eckersley, OSRD WA-4223-7, JEIA 9104, Report TR-501, BRL, January 1945. (See reference 111.) CP-221.1-M1
104. *A Report on Transmission of Waves over the Earth*, T. L. Eckersley, OSRD WA-4002-13, Report TR-504, BRL, January 1945. CP-221.1-M2
105. *New Convergent Integrals*, T. L. Eckersley, OSRD, WA-4002-11, Report TR-509, BRL, February 1945. CP-221.1-M3
106. *The Effect of a Subrefracting Layer of Atmosphere upon the Propagation of Radio Waves*, T. Pearcey and M. Tomlin, OSRD WA-4016-28, JEIA 8371, Memorandum 83, RRDE, Feb. 12, 1945. CP-223-M13
107. *Theory of Characteristic Functions in Problems of Anomalous Propagation*, W. H. Furry, OEMsr-262, Division 14 Report 680, RL, Feb. 28, 1945. CP-221-M19
108. *The Evaluation of the Solution of the Wave Equation for a Stratified Medium ([Part] II)*, D. R. Hartree, OSRD WA-4424-11, Research Report 279, RRDE, Mar. 12, 1945. (See reference 90.) CP-221-M20
109. *Theoretical Coverage Diagrams for 3-Meter Radars Embracing Super-refraction*, W. Walkinshaw and R. Hensman, OSRD WA-4320-7, JEIA 9198, Report T-1815, TRE, Mar. 18, 1945. CP-223-M12
110. *The Radiation Field of a Dipole under Various Conditions of Anomalous Propagation*, T. Pearcey, M. Tomlin, and F. Whitehead, OSRD WA-4392-7, Research Report 275, RRDE, Apr. 13, 1945. (See reference 94.) CP-221-M21
111. *Notes on the Solution of a Non-Linear First Order Equation of the Riccati Type*, T. L. Eckersley, OSRD WA-4428-7, JEIA 9725, Report TR-502, BRL, May 1945. (See reference 103.) CP-222.1-M6
112. *Perturbation Theory for an Exponential M-Curve in Non-Standard Propagation*, C. L. Pekeris, OEMsr-1207, Report WPG-12, CUDWR, July 1945. CP-221.1-M4
113. *Graphs for Computing the Diffraction Field with Standard and Superstandard Refraction*, Pearl J. Rubenstein and William T. Fishback, OEMsr-262, Division 14, Report 799, RL, Aug. 13, 1945. CP-222-M11



114. *Radio Interpretation of Meteorological Observations in the First Two Meters of Atmosphere Above Grass at Harlington, Middlesex, January to June, 1940*, OSRD WA-861-3, Report T-1471, M/63, TRE, June 1940. CP-222.1-M1
115. *Anomalous Echoes Observed with 10 Cm C.D. Set*, A. E. Kempton, OSRD II-5-564, Research Report 119, ADRDE, Oct. 8, 1941. CP-623-M1
116. *Centimeter Wave Propagation over Sea Between High Sites just within Optical Range*, F. Hoyle and E. C. S. Megaw, OSRD WA-171-12, ASE-GEC, June 12, 1942. CP-232.2-M1
117. *Centimeter Wave Propagation over Land (Part II), Measurements within and beyond Optical Range*, G. W. N. Cobbold, H. Archer-Thomson, and E. C. S. Megaw, Report AC-2917, Com. 136, SRDE-GEC, Oct. 16, 1942.
118. *Radar Wave Propagation*, Lloyd J. Anderson, John B. Smyth, F. R. Abbott, and R. Revelle, BuShips Problem X4-49CD, Report WP-2, NRSL, Nov. 30, 1942. CP-623-M2
119. *Very Short Wave Interception and D.F.*, T. L. Eckersley, OSRD II-5-5276, Report TR-438, BRL, 1943. CP-224-M2
120. *Anomalous Propagation of 10 Cm R.D.F. Waves over the Sea* (February 6, 1943); *First Supplement to Report 87* (July 26, 1943), OSRD WA-909-21, Report 87, AORG, July 26, 1943. CP-232.2-M5
121. *Investigation of Propagation Characteristics of A.W. Stations*, Report 17, AORG, Mar. 9, 1943. CP-332-M1
122. "A Study of Propagation over the Ultra-Short-Wave Radio Link between Guernsey and England on Wavelengths of 5 and 8 Meters (60 and 37.5 Mc/s)," R. L. Smith-Rose and A. C. Stickland, *The Journal of the Institution of Electrical Engineers*, OSRD WA-1463-31, NPL, Vol. 90, No. 9, March 1943, Part III. CP-224-M3
123. *The Effect of Atmospheric Refraction on the Propagation of Radio Waves*, A. C. Stickland, OSRD WA-623-19, Report RRB/S-10, NPL-RRB, Mar. 20, 1943. CP-222-M1
124. *Propagation of Ultra-Short Waves*, H. C. Webster, OSRD II-5-4575(S), Report 354, Australia, Apr. 17, 1943. CP-224-M4
125. *Report on Radar Wave Propagation, Atmospheric Refraction, A Qualitative Investigation*, Lloyd J. Anderson and John B. Smyth, BuShips Problem X4-49CD, Report WP-5, NRSL, May 7, 1943. CP-222-M4
126. *Radio Interpretation of Meteorological Observations in the First 400 Feet Above Cardington, 1942*, OSRD WA-861-1, Report T-1413, M/61, TRE, May 14, 1943. CP-321-M1
127. *Centimeter Wave Propagation over Sea (Part II), Measurements from Shore Sites Near and Beyond Optical Range*, G. W. N. Cobbold, A. J. Jones, H. A. Bonnett, E. C. S. Megaw, H. Archer-Thomson, and E. M. Hickin, OSRD WA-792-10, Report 8180, GEC, May 27, 1943. CP-232.2-M4
128. *Preliminary Observations on Radio Propagation at 6 Centimeters Between Beer's Hill, New Jersey, and New York, Case 37003-4, File 36691-1*, G. W. Gilman, Report MM-43-160-87, BTL, June 12, 1943. CP-224-M6
129. *Some Observations of Anomalous Propagation*, Report T-1483, M/64, TRE, July 6, 1943.
130. *Application of Anomalous Propagation to Operational Problems at Home and Abroad*, H. G. Booker, JMRP 3, Report T-1484, M/66/HGB, TRE, July 7, 1943. CP-221-M4
131. *Propagation of Signals on 45.1, 474 and 2800 Mc from Empire State Building to Hauppauge and Riverhead, L.I., New York*. G. S. Wickizer and A. M. Braaten, OEMsr-691, NDRC Research Project 423, Division 14 Report 179, Report 1, RCA, July 20, 1943. CP-631-M1
132. *Propagation of Ultra Short Waves*, T. L. Eckersley, OSRD WA-1463-3, Report TR/476, Marconi, Ltd., August 1943. CP-224-M7
133. *The "K" Effect in Anomalous Propagation of Ultra-Short Waves*, F. Syer (RAAF), JMRP 11, Australian Paper 266, Report AC-4496, Australia, Aug. 10, 1943. CP-224-M15
134. *The Propagation of 10 Cm Waves over Land Paths of 14, 52, and 112 Miles*, Paul A. Anderson, C. L. Barker, K. E. Fitzsimmons, and S. T. Stephenson, OEMsr-728, Research Project PDRC-647, Division 14 Report 202, Report 4, Washington State College, Oct. 26, 1943. CP-224-M8
135. *The Propagation of 1-Cm Waves over the Sea as Deduced from Meteorological Measurements*, J. M. C. Scott and T. Pearcey, OSRD WA-1339-6, JMRP 4, Research Report 227, ADRDE, Nov. 11, 1943. CP-232.2-M6
136. *Centimeter Wave Propagation over Land, A Preliminary Study of the Field Strength Records between March and September 1943*, R. L. Smith-Rose and A. C. Stickland, OSRD WA-1514-6, JMRP 10, Paper RRB/S-13, DSIR-NPL, Nov. 15, 1943. CP-333-M1
137. *The Propagation of 10 Cm Waves over an Inland Lake, Correlation with Meteorological Soundings*, Paul A. Anderson, K. E. Fitzsimmons, and S. T. Stephenson, OEMsr-728, Research Project PDRC-647, Division 14 Report 212, Report 5, Washington State College, Nov. 12, 1943. CP-232.2-M7
138. *Measurements of Radar Wave Refraction and Associated Meteorological Conditions*, Lloyd J. Anderson and L. G. Trolese, Report WP-7, NRSL, Dec. 10, 1943. CP-222-M6
139. *Anomalous Propagation in India, Preliminary Report on Overland Transmission in Bengal*, H. G. Booker, OSRD II-5-6555(S), Report S-5, ORS-SEA, Dec. 30, 1943. CP-334-M1
140. *Atmospheric Physics, Summary of Investigations on Anomalous Propagation of Radar Signals Carried Out by the Australian Operational Research Group During 1942-43*, D. F. Martyn, AORG, 1943. CP-221-M1
141. *The Cause of Short Period Fluctuations in Centimeter Wave Communication*, J. M. C. Scott, OSRD WA-1962-7 Memorandum 42, ADRDE, Mar. 8, 1944. CP-224-M10
142. *Anomalous Propagation in the Persian Gulf*, Naval Officer in Charge, Hormuz, OSRD WA-2146-23, Report AC-5975, USW, Received Mar. 20, 1944. CP-331-M4
143. *Effect of Super-refraction on Surface Coverage on Enemy 50-Cm and 80-Cm Radar Sets*, OSRD WA-2284-3, Report M/Memo-19 GGM, TRE, April 1944. CP-223-M8
144. *K-X-S Experiments, News Letter No. 1*, T. Gold, MK. 12201, ASE, May 3, 1944. CP-333.2-M1



145. *Abnormal Radar Propagation in the South Pacific, An Investigation into Conditions in New Zealand and Norfolk Island on 200 Mc/s. with Notes on Fiji, New Caledonia and Solomon Islands*, Air Department Wellington, File 135/14/10, Report 119, ORS-RNZAF, May 4, 1944. CP-335-M1
146. *Procedure and Charts for Estimating the Low Level Coverage of Shipborne 200-Mc Radars under Conditions of Pronounced Refraction*, F. R. Abbott, Lloyd J. Anderson, F. P. Dane, J. P. Day, R. U. F. Hopkins, John B. Smyth, L. G. Trolese, and A. P. D. Stokes, BuShips Problem, X4-49CD, Report WP-11, NRSL, Revised May 10, 1944. CP-202.32-M1
147. *Centimeter Propagation over Land, A Study of the Field Strength Records Obtained During the Year 1943-1944*, A. C. Stickland and R. W. Hatcher, JEIA 4789, Report RRB/S-18, NPL-MO, DSIR, May 11, 1944. CP-224-M11
148. *K-X-S Experiments*, News Letter No. 2, T. Gold, MK. 12201, ASE, May 13, 1944. CP-333.2-M1
149. *Atmospheric Propagation Effects and Relay Equipment*, Thomas J. Carroll, Report ORB-PP-12-1, OCSO, May 18, 1944. CP-311-M2
150. *Low-Level Coverage of Radars as Affected by Weather, Procedures and Charts*, Report IRPL-T2a, NRSL, May 25, 1944. (Reference 146 reprinted.)
151. *Variations in Radar Coverage*, Report JANP-101, Joint Communications Board, June 1, 1944. CP-202.4-M4  
Earlier edition: IRPL T-1, CUDWR-WPG, May, 1944. CP-202.5-M1
152. *Effect of Atmospheric Refraction on Range Measurements*, G. G. Macfarlane, OSRD I-A-320, Report T-1688, TRE, June 12, 1944. CP-222-M7
153. *Microwave Transmission over Water and Land under Various Meteorological Conditions*, Pearl J. Rubenstein, I. Katz, L. J. Neelands, and R. M. Mitchell, OEMsr-262, Division 14 Report 547, RL, June 13, 1944. CP-311-M4
154. *Abnormal Propagation in W. A. C. for May and June, 1944*. Report 10, Canadian ORS-WAC, July 27, 1944.
155. *Propagation of Signals on 45.1, 474 and 2800 Mc from Empire State Building, N.Y.C. to Hauppauge and Riverhead, L.I., N.Y.*, G. S. Wickizer and A. M. Braaten, OEMsr-691, NDRC, Research Project 423, Division 14 Report 298, Report 2, RCA, July 31, 1944. CP-631-M1
156. *The Structure of the Electromagnetic Field During Conditions of Anomalous Propagation*, T. Pearcey and F. Whitehead, OSRD WA-3070-1, Research Report 258, RRDE, Sept. 19, 1944. CP-221-M17
157. *Tropospheric Propagation and Radio-Meteorology*, Report WPG-5, CUDWR-WPG, September 1944.
158. "Some Factors Causing Super-refraction on Ultra High Frequencies on South West Pacific," (Daily Report on Abnormal Echoes, RAAF Form 146 included in ATP 821), D. F. Martyn and P. Squires, Australian Ionosphere Bulletin, October 1944, Section 1.2. CP-224-M14
159. *Atmospheric Refraction, A Preliminary Qualitative Investigation*, Lloyd J. Anderson, F. P. Dane, J. P. Day, R. U. F. Hopkins, L. G. Trolese, and A. P. D. Stokes, BuShips Problem X4-49CD, Report WP-17, NRSL, Dec. 28, 1944. CP-222-M9
160. *Anomalous Propagation with High and Low Sited 3 Cm Ship Watching Radar Sets*, G. C. Varley, OSRD WA-4238-2, Report 250, AORG, Mar. 20, 1945. CP-232.2-M12
161. *Anomalous Propagation at English Coastal Radar Stations, March to September, 1944*, D. Lack, OSRD WA-4491-12, JEIA 9946, Report 258, AORG, May 30, 1945. (See also reference 6d.) CP-232.2-M13
162. *Lebanon-Beer's Hill Transmission on Wavelengths of 2.0 Meters, and 30 Centimeters, Case 20564*, A. B. Crawford, Report MM-39-326-98, BTL, Dec. 5, 1939. CP-224-M1
163. *Centimeter Wave Propagation over Land; Preliminary Trials*, G. W. N. Cobbold, H. A. Bonnett, A. J. Jones, E. C. S. Megaw, H. Archer-Thomson, A. S. Gladwin, and E. M. Hickin, Report 8045, GEC, Aug. 21, 1942.
164. *The Propagation of 10-Cm Waves on a 52-Mile Optical Path over Land, The Correlation of Signal Patterns and Radiosonde Data*, Paul A. Anderson, C. L. Barker, S. T. Stephenson, and K. E. Fitzsimmons, OEMsr-728, NDRC Research Project PDRC-647, Division 14 Report 151, Report 1, Washington State College, June 10, 1943. CP-224-M5
165. *Centimeter Wave Propagation over Sea Within and Beyond the Optical Range*, E. C. S. Megaw, H. Archer-Thomson, E. M. Hickin, and F. Hoyle, Report M-532, ASE, July 1943.
166. *Aden-Berbera V.H.F. Experiments, Final Report on Propagation Aspects*, E. W. Walker and S. R. Bickerdike, OSRD WA-2187-14, Report MS-4, SRDE, December 1942 and July 1943. CP-331-M1
167. [Ultra Short Wave Communication], *Investigation No. 369, Irish Sea Experiment*, OSRD WA-2146-18, -19, -20, -21, and -22; WA-2379-2, WA-2797-36, WA-3158-13; WA-3822-30; and -31. Or, as identified in Progress Reports AC-5970 Sept. 1, 1943, AC-5971 Dec. 14, 1943, AC-5972 Jan. 15, 1944, AC-5973 Feb. 9, 1944, AC-5974 Mar. 20, 1944, AC-6334 May 14, 1944, AC-6828 Aug. 12, 1944, AC-7206 Oct. 19, 1944, AC-7465 Nov. 10, 1944, and AC-7668 Jan. 4, 1945, British Ministry of Supply. CP-224-M9
168. *Experience with Space and Frequency Diversity Fading on New York-Neshanic Microwave Circuit, Case 37003-4*, G. W. Gilman and F. H. Willis, Report MM-43-160-152, BTL, Sept. 18, 1943. CP-240-M1
169. *Investigation of Changes in Direction of Transmission during Periods of Fading in the Microwave Range, Case 37003-4, File 36691-1*, A. C. Peterson, Report MM-43-160-183, BTL, Oct. 30, 1943. CP-240-M2
170. *Radar Calibration Report, New York Region*, R. C. L. Timpson, Mitchell Field, N.Y., Nov. 30, 1943. CP-202.1-M4
171. *Aden-Berbera VHF Experiments, Meteorological Conditions and Possible Correlations*, E. W. Walker, OSRD WA-1614-1, JMRP 14, Report AC-5493, USW-SRDE, Dec. 20, 1943. CP-331-M3
172. *Propagation over Short Paths and Rough Terrain at 200 Mc/s*, A. B. Vane and D. G. Wilson, OEMsr-262, Division 14 Report 468, RL, Jan. 18, 1944. CP-231.2-M1
173. *Propagation and Reflection Characteristics of Radio Waves as Affecting Radar*, William G. Michels and



- William C. Pomeroy, Service Project (M-3) 11a, U.S. Army Air Forces Board, Jan. 31, 1944. CP-531-M1
174. *Microwave Propagation Measurements (Conference of February, 1944)*, F. H. Willis, Report MM-44-160-55, BTL, Mar. 10, 1944. (See reference 3.)
  175. *An Estimation of the Incidence of Anomalous Propagation in the Cook Strait Area of New Zealand from January 1943 to January 1944*, F. E. S. Alexander, OSRD II-5-5849(S), Report RD-1/373, RDL-DSIR, NZ, May 2, 1944. CP-332-M2
  176. *K-Band Radar Transmission, A Preliminary Report of Tests Made Near Atlantic Highlands, N.J. between December 1943 and April 1944*, G. C. Southworth, A. P. King, and S. D. Robertson, Report MM-44-160-115, BTL, May 19, 1944. CP-202.2-M1
  177. *Report on Cross Channel Propagation of British No. 10 Set*, K. R. Spangenberg, Report OAB-2, OCSO, Aug. 26, 1944. CP-224-M12
  178. *Radar Range and Signal Strength*, L. Jofey and A. C. Cossor, Report MR-142, Research Department, Myra Works, London E10, August 1944.
  179. *Results of Microwave Propagation, Tests on the New York-Neshanic Path, Case 37003-4, File 36691-1*, A. L. Durkee, Report MM-44-160-190, BTL, Aug. 28, 1944. CP-224-M13
  180. *Height-Gain Tests in the Troposphere*, G. A. Isted, JEIA 5560, JMRP 36, Report TR-488, BRL, September, 1944. CP-312-M1
  181. *Interim Report on Investigation of 120 Mc/s and 50-Cm Propagation Across the English Channel*, W. R. Piggott, OSRD WA-3157-6, Report AC-7081, USW, Oct. 4, 1944. CP-333-M5
  182. *Measurements of the Angle of Arrival of Microwaves in the X-Band, Case 20564*, W. M. Sharpless, Report MM-44-160-249, BTL, Nov. 7, 1944.
  183. *Overwater Transmission Measurements, 1944-Part I: Preliminary Analysis of Radio and Radar Measurements*, Pearl J. Rubenstein, OEMsr-262, Division 14 Report 649, RL, Dec. 15, 1944. CP-222-M8
  184. *The Vertical Distribution of Field Strength over the Sea Under Conditions of Normal and Anomalous Propagation*, J. A. Ramsay and P. B. Blow, OSRD WA-3870-1, Research Report 267, CAEE-RRDE, Jan. 5, 1945. CP-232-M1
  185. *Centimetre Wave Propagation over Sea, A Study of Signal Strength Records Taken in Cardigan Bay, Wales Between February and September, 1944*, R. L. Smith-Rose and A. C. Stickland, OSRD WA-4297-9, JMRP 50, Paper RRB/C-114, NPL-DSIR, Feb. 28, 1945. CP-333-M3
  186. *Over-Water Tests of S-Band Early Warning for Ships, Vertical Coverage of the CXHR (SCI) Search System*, Walter O. Gordey, Donald T. Drake, and M. Kessler, OEMsr-262, Service Project NS-194, Division 14 Report 703, RL, Mar. 5, 1945. CP-232.2-M11
  187. *Preliminary Report on S- and X- Band Propagation in Low Ducts Formed in Oceanic Air*, Martin Katzin, Problem S411.2R-S, Report R-2493, NRL, Mar. 24, 1945. CP-222.2-M2
  188. *Atmospheric Refraction under Conditions of a Radiation Inversion*, Lloyd J. Anderson, J. P. Day, C. H. Freres, R. U. F. Hopkins, John B. Smyth, and A. P. D. Stokes, BuShips Problem X4-49CD, Report WP-19, NRSL, Apr. 21, 1945. CP-222-M10
  189. *Radio-Meteorological Relationships*, E. C. S. Megaw and F. L. Westwater, OSRD WA-4594-15, Report AC-8140, USW-138, May 4, 1945. CP-222.2-M3
  190. *Calculated Relationship Between Signal Level and Uniform Gradient of Refractive Index for the Irish Sea Paths*, E. C. S. Megaw, OSRD WA-4594-13, GEC Report 8656, AC-8225, USW-141, GEC-USW, Apr. 19, 1945. CP-222.1-M8
  191. *Radio-Meteorological Relationships, General Summary of Papers AC-8140/USW.138 and AC-8225/USW.141*, E. C. S. Megaw and F. L. Westwater, OSRD WA-4618-1, Report AC-8336, USW-149, USW, 1945. (See references 189 and 190.) CP-222.2-M4
  192. *General Summary Covering the Work of the KXS Inter-Service Trials, Llandudno, 1944*, J. R. Atkinson, JMRP 64, Report T-1770, TRE, May 1945. CP-333.2-M2
  193. *X-Band Trials at Rosehearty*, J. R. Atkinson, OSRD WA-4596-11, JEIA 10401, Report AC-8228, USW-142, May 28, 1945. CP-222.3-M1
  194. *S- and X- Band Propagation in Low Ocean Ducts (Fourth Conference)*, R. W. Bauchman and W. Binnian, Report R-2565, NRL, July 5, 1945. (See reference 12 and 187.)
  195. *KXS Llandudno Interservice Trials, Summer 1944*, JMRP 68, Report T-1865, TRE, 1944.
  196. *Survey of Radio Meteorological Information Available at TRE*, JMRP 67, Report M/98 (T-1888)/JWH, TRE, August 1945.
  197. *The Diffusive Properties of the Lower Atmosphere*, O. G. Sutton, OSRD WA-670-9a, Report MRP-59, Chemical Defense Experimental Station, Air Ministry Meteorological Research Committee, Dec. 29, 1942. CP-323-M1
  198. *A Study of the Effect of the Meteorology on the Refraction of Radio Beams*, H. Raymond, Technical Report T-2, CESL, May 4, 1943. CP-222-M3
  199. *The Rapid Reduction of Meteorological Data to Index of Refraction*, Lloyd J. Anderson and F. R. Abbott, Report WP-8, NRSL, Dec. 10, 1943.
  200. *Application of Diffusion Theory to Radio Refraction Caused by Advection*, P. M. Woodward, OSRD, WA-2047-4, Report T-1647, TRE, Apr. 6, 1944. CP-323-M2
  201. *Qualitative Survey of Meteorological Factors Affecting Microwave Propagation*, I. Katz and J. M. Austin, OEMsr-262, Division 14 Report 488, RL, June 1, 1944. CP-311-M3
  202. *The Influence of Ground Contour on Air Flow (Translation)*, P. Queney, Translated by Walter M. Elsasser, OEMsr-1207, Report WPG-4, CUDWR, September 1944. CP-322-M1
  203. *Radio-Meteorological Tables*, P. M. Woodward and J. W. Head, OSRD WA-3401-1, JMRP 30, Report T-1724, TRE. CP-222.1-M9
  204. *Modified Index Distribution Close to the Ocean Surface*, R. B. Montgomery and Robert H. Burgoyne, OEMsr-262, Division 14 Report 651, RL, Feb. 16, 1945. CP-222.2-M1



205. *Tables for Computing the Modified Index of Refraction* M, E. R. Wicher, Report WPG-8, CUDWR, March 1945.
206. *Nomograms for Computation of Modified Index of Refraction*, Robert H. Burgoyne, OEMsr-262, Division 14 Report 551, RL, Apr. 6, 1945. CP-222.1-M7
207. *Meteorological Report in Connection with V.H.F. Wireless Experiment Between Aden and Berbera, 1943*, Ronald Frith, OSRD WA-1746-2, JMRP 13, Report AC-5492, USW, Oct. 30, 1943. CP-331-M2
208. *Meteorological Measurements, Irish Sea Experiments: Meteorological Observations [taken] on [Board] the Ship Glen Strathallan in the Irish Sea for the Period November 1, 1943 to October 23, 1944*, OSRD WA-1759-14, WA-1935-1, WA-1951-1, WA-2131-5, WA-2131-C5, WA-2152-13, WA-2131-5A, WA-3180-1, WA-2242-4, WA-2315-1, WA-2364-13, WA-2587-5, WA-2623-13, WA-2843-13, WA-4079-1, WA-2905-4, WA-3029-2, WA-3180-1A, WA-3180-1D, WA-3322-1, and WA-3584-3, NMS. CP-333.1-M1  
*Meteorological Observations [taken] on [Board] the Ship Coila in the Irish Sea for the Period December 15, 1943 to October 26, 1944*, OSRD WA-2131-5B, WA-2843-11, WA-2743-12, WA-4079-2, WA-3305-5, WA-3322-2, and WA-3584-2, NMS. CP-333.1-M2  
*Meteorological Measurements [taken] on [Board] the Ship St. Dominica in the Irish Sea for the Period May 19, 1944 to August 29, 1944*, OSRD WA-2587-6, WA-2645-4, WA-3143-9, WA-3991-2, WA-3180-1B, and WA-3180-1C, Inter-Service Cm. Wave Prop. Research NMS. CP-333.1-M3
209. *Tables of Temperature and Humidity Observations at Rye*, OSRD WA-1463-13A, Report JMRP-5, MO, November 1943. CP-333.3-M1
210. *Low Altitude Measurements in New England to Determine Refractive Index, 1943*, Robert H. Burgoyne and I. Katz, Division 14 Report 42, RL, Feb. 22, 1944. CP-336.2-M1
211. *Climate in Relation to Microwave Radar Propagation in Panama*, Arthur E. Bent, Division 14, Report 476, RL, Feb. 25, 1944. CP-336.1-M1
212. *The Vertical Distribution of Temperature and Humidity at Rye on the Night of January 14-15, 1944*, JEIA 10318, Report JMRP 6, MO, Feb. 26, 1944. CP-333.3-M2
213. *Analysis of Temperature and Humidity Records at Rye*, JEIA 10319, Report JMRP-7, MO, February 1944. CP-333.3-M3
214. *Radio Climatology of the Persian Gulf and Gulf of Oman with Radar Confirmation*, H. G. Booker, Report T-1642, TRE, Mar. 15, 1944. CP-331-M5
215. *Stations in the Western Hemisphere with Conditions in the Lower Layers of the Atmosphere Similar to Those at Selected Stations in the Eastern Hemisphere*, Report 729, U.S. Army Air Forces, Weather Division, March 1944. CP-337-M1
216. *Some Values of the Refractive Index of the Atmosphere at Rye*, S.100958, JEIA 10322, Report JMRP 23, MO 8, June 1-6, 1944.
217. *Low-Level Meteorological Soundings and Radar Correlation for the Panama Canal Zone*, K. E. Fitzsimmons, S. T. Stephenson, and Robert W. Bauchman, OEMsr-728, NDRC Research Project PDRC-647, Report 6, Washington State College, June 12, 1944. CP-336.1-M2
218. *Wave Propagation Report No. 3*, Report 413.44/R113, Naval Research Group, Intel. Br. OCSO Canal Zone, July 1, 1944.
219. *Preliminary Analysis of Height-Gain Tests in the Troposphere*, R. F. C. McDowell, OSRD WA-2930-2, JEIA 5777, Report TR-494, BRL, September 1944. CP-333-M2
220. *Diurnal Variation of Temperature and Humidity at Various Heights at Rye*, S.100958, JEIA 10323, Report JMRP 26, MO 8, Oct. 21, 1944. CP-333.3-M4
221. *Report on General Climatic and Meteorological Conditions in Banda Sea, 4°-7° S., 126°-131° E.*, Report List 2, Section II, Series 7, No. 18, RAAF, Directorate of Meteorological Services, November 1944. CP-335-M2
222. *Hourly Values of Modified Refractive Index M for Meteorological Office [at] Rye, May, 1944*, JEIA 10325, Report JMRP-31, MO, Dec. 28, 1944. CP-333.3-M5
223. *Temperature and Humidity Measurements Made with the Washington State College Wired Sonde Equipment at Kaikoura, New Zealand, Between Sept. 22, 1944 and Oct. 19, 1944*, F. E. S. Alexander, Report RD-1/482, RDL-DSIR, NZ, Jan. 15, 1945. CP-332-M3
224. *Highlights of the December, 1944 Typhoon Including Photographic Radar Observations (Part I), A Distant Observation of a Warm Front Including a Photograph of Cloud Forms and Slope of Front (Part II)*, George F. Kosco, Fleet Weather Central Paper 10, U.S. Navy, Third Fleet, Feb. 10, 1944. CP-336.3-M1
225. *Results of Low Level Atmospheric Soundings in the Southwest and Central Pacific Oceanic Areas*, Paul A. Anderson, K. E. Fitzsimmons, G. M. Grover, and S. T. Stephenson, OEMsr-728, NDRC Research Project PDRC-647, Report 9, Washington State College, Feb. 27, 1945. CP-335-M4
226. *Centimeter Wave Propagation over Sea, Correlation of Radio Field Strength Transmitted Across Cardigan Bay, Wales with Gradient of Refractive Index Obtained from Aircraft Observations*, R. L. Smith-Rose and A. C. Stickland, OSRD WA-4459-9, JEIA 9813, Paper RRB/C-121, DSIR, May 10, 1945. CP-333-M4
227. *Balloon Psychrometer for the Measurement of the Relative Humidity of the Atmosphere at Various Heights (and Addendum)*, S. M. Doble and S. Inglefield, OSRD II-5-5079(S) and OSRD II-5-5080(S), ICI, Apr. 1, 1943; Addendum Sept. 25, 1943. CP-344-M1
228. *The Captive Radiosonde and Wired Sonde Techniques for Detailed Low-Level Meteorological Sounding*, Paul A. Anderson, C. L. Barker, K. E. Fitzsimmons, and S. T. Stephenson, OEMsr-728, NDRC Research Project PDRC-647, Division 14 Report 192, Report 3, Washington State College, Oct. 4, 1943. CP-341-M1
229. *Instruments and Methods for Measuring Temperature and Humidity in the Lower Atmosphere*, I. Katz, OEMsr-262, Service Project SC-8, Division 14 Report 487, RL, Apr. 12, 1944. CP-344-M2
230. *Anomalous Propagation, Adaptation of Model RAU-2 Radio Sonde Receiving and Recording Equipment for Use as Low Level Sounding Device*, Navy Dev. Project Unit 1,



- Friez Instrument Division, Bendix Aviation Corporation, May 31, 1944. CP-342-M1
231. *Meteorological Investigation at Rye, Instrumental Layout for Recording Gradients of Temperature and Relative Humidity (Part I)*, Report JMRP-17, Instruments Branch, MO 4, May 1944. CP-344-M3
232. *Notes on Operational Use of Low-Level Meteorological Sounding Equipment*, K. E. Fitzsimmons, S. T. Stephenson, and Robert W. Bauchman, OEMsr-728, NDRC Research Project PDRC-647, Report 7, Washington State College, June 15, 1944. CP-342-M2
233. *Microwave Propagation Studies, Detection of Troposphere Stratification by Means of Sound Echoes, Preliminary Trial, Case 37003*, H. B. Coxhead and F. H. Willis, Report MM-44-160-143, BTL, June 21, 1944. CP-344-M4
234. *Operating Instructions for the WSC Low-Level Atmospheric Sounding Equipment*, Paul A. Anderson, OEMsr-728, NDRC Research Project PDRC-647, Report 8, Washington State College, July 10, 1944. CP-342-M3
235. *Meteorological Equipment for Short Wave Propagation Studies*, Walter M. Elsasser, Report WPG-3, CUDWR August 1944.
236. *Wired Sonde Equipment for High Altitude Soundings*, Lloyd J. Anderson, BuShips Problem X4-49CD, Report WP-16, NRSL, Nov. 17, 1944. (See reference 238.) CP-341-M2
237. *A Note on the Resistance of Electric Hygrometer Elements*, Lloyd J. Anderson and S. T. Stephenson, Report AERO-1, NRSL, May 8, 1945. CP-343-M1
238. *Improvements in USNRSL Meteorological Sounding Equipment*, Lloyd J. Anderson, S. T. Stephenson, and A. P. D. Stokes, BuShips Problem X4-49CD, Report WP-21, NRSL, July 3, 1945. (See reference 236.) CP-341-M3
239. *Forecasting of R. D. F. Conditions*, JMRP 2, Memorandum 103, AORG, May 31, 1943. CP-410-M1
240. *The Meteorological Aspects of Anomalous Propagation, Short Wave Radio*, R. W. Hatcher, Report JMRP 1, [Great Britain] June 1943. CP-410-M2
241. *Oboe Propagation, August-October, 1943*, H. G. Booker, OSRD WA-1464-5, Report T-1605, TRE, 1943. CP-422-M1
242. "Naviprop" *Forecasts*, E. Gold, OSRD WA-2255-1Q, Report SIS 45, MO, Nov. 8, 1943. CP-422-M2
243. *Issue of Anoprop Forecasts, Synoptic Instruction Special No. 39*, OSRD WA-2255-1R, Report SIS 39, MO, Feb. 11, 1944. CP-422-M3
244. *Elements of Radio Meteorological Forecasting*, H. G. Booker, Report T-1621, Mathematics Group, TRE, Malvern, Feb. 14, 1944. CP-410-M3
245. *Preliminary Instruction Manual, Weather Forecasting for Radar Operations*, Report 614, U. S. Army Air Forces, Weather Division, March 1944. CP-410-M4
246. *Tropospheric Weather Factors Likely to Affect Superrefraction of VHF-SHF Radio Propagation as Applied to the Tropical West Pacific*, E. Dillon Smith and R. D. Fletcher, Report RP-1, U. S. Department of Commerce, Weather Bureau, July 1, 1944. CP-424-M1
247. *Preliminary Instruction Manual of Weather Forecasting for Radar Operations in South West Pacific Area*, D. F. Martyn and P. Squires, Report RP-220, CSIR-RL, Sept. 4, 1944. CP-424-M2
248. *Outline of Radio Climatology in India and Vicinity*, H. G. Booker, JEIA 6061, Report JMRP-25, Report T-1727 (M/85), TRE, Sept. 12, 1944. CP-423-M1
249. *Notes on TRE Report T-1727, JMRP No. 25, Radio Climatology in India and Vicinity*, C. S. Durst, JEIA 10324, Report JMRP-27, MO, Nov. 7, 1944. (See reference 248.) CP-423-M2
250. *A Rough Sketch of World Radio Climatology over Sea*, H. G. Booker, Report T-1730, TRE, Oct. 31, 1944. CP-424-M3
251. *American Continents Meteorological Counterparts of Western Pacific and Indian Ocean Areas as Applied to Tropospheric Radio Propagation*, J. H. Brown, J. L. Paulhus, and E. Dillon Smith, Report RP-2, U. S. Weather Bureau, Nov. 15, 1944.
252. *The Possibility of Investigating the Föhn Wind and Sea Breeze Phenomena in N. Z. with a View to Elucidating Certain Problems of Radio-Meteorological Forecasting in Other Parts of the World*, M. A. F. Barnett and F. E. S. Alexander, JEIA 7469, Report RD-1/471, RDL-DSIR-NZ, Dec. 1, 1944. CP-421-M1
253. *Determination of a Suitable Method of Forecasting Radar Propagation Variations over Water, Tests Conducted by 26th Weather Region, Orlando, Florida*, J. R. Gerhardt and William E. Gordon, Service Project 4252R000.77, U. S. Army Air Forces, Mar. 10, 1945. CP-425-M1
254. *A Qualitative Outline of the Radio Climatology of Australasia*, H. G. Booker, JMRP-53, Report T-1820 (M/95), TRE, Apr. 19, 1945. CP-421-M2
255. *Determination of the Practicability of Forecasting Meteorological Effects on Radar Propagation, Tests Conducted by AAF Tactical Center, Orlando, Florida*, John R. Gerhardt and William E. Gordon, Service Project 3767B000.93, U. S. Army Air Forces, June 13, 1945. CP-425-M2
256. *Absorption of 1-Cm Radiation by Rain*, M. G. Adam, R. A. Hull, and C. Hurst, Misc. Report 3, CVD-CL.
257. *The Absorption of Ultra-Short Wireless Waves in the Water Vapour of the Earth's Atmosphere*, J. A. Saxton, OSRD II-5-210, Paper RRB/C-18, NPL, Feb. 14, 1941. CP-510-M1
258. *Echo Intensities and Attenuation Due to Clouds, Rain, Hail, Sand and Duststorms at Centimeter Wavelengths*, J. W. Ryde, OSRD WA-81-25, Report 7831, GEC, Oct. 13, 1941. CP-511-M1
259. *The Atmospheric Absorption of Microwaves* (in Third Conference Report of CP), J. H. Van Vleck, Report 175 (43-2), RL, Apr. 27, 1942. (See reference 10.) Div. 14-121.1-M4
260. *The Effect of Rain Upon the Propagation of 1-Cm Electro-Magnetic Waves, Case 22098*, S. D. Robertson, Report MM-42-160-87, BTL, Aug. 1, 1942. CP-511-M2
261. *The Effect of Rain on the Propagation of Microwaves, Case 22098*, A. P. King and S. D. Robertson, Report MM-42-160-93, BTL, Aug. 26, 1942. CP-511-M3



262. *Comparison of Theoretical and Experimental Values for the Attenuation of 1-Centimeter Waves in Rain, Case 22098*, S. D. Robertson, Report MM-43-160-2, BTL, Jan. 5, 1943. CP-511-M4
263. *An Investigation on the Number and Size Distribution of Water Particles in Nature*, Josef Mazur, F/Lt. Polish Air Force, OSRD II-5-6306(S), Report MRP-109, Meteorological Research Committee, Great Britain, June 1943. CP-511-M5
264. *Report on the Absorption and Refraction of Electro-Magnetic Waves by the Liquid Water, Water Vapour and Fog or Rain*, N. F. Mott, OSRD II-5-4936, Reference 43/2881, CRB, Sept. 2, 1943. CP-510-M2
265. *Report on the Absorption of Electromagnetic Waves in the Wavelength Range 1-100 Cm by Water in the Atmosphere*, N. F. Mott, OSRD II-5-4937, Reference 43/2882, CRB, Sept. 2, 1943. CP-510-M3
266. *Verification of Mie Theory, Calculations and Measurements of Light Scattering by Dielectric Spherical Particles (Progress Report)*, Victor K. LaMer, OSRD 1857, OEMsr-148, Service Project CWS-1, Division 10, NDRC, Columbia University, Sept. 29, 1943. CP-512-M1
267. *The Absorption of Centimetric Radiation by Atmospheric Gases*, J. M. Hough, ADRDE, USWP-WC, Apr. 27, 1944. CP-510-M4
268. *Attenuation Due to Water Drops in the Atmosphere*, J. M. Hough, ADRDE, USWP-WC, Apr. 28, 1944. CP-511-M6
269. *Propagation of K/2 Band Waves*, G. E. Mueller, Report MM-44-160-150, BTL, July 3, 1944. CP-511-M7
270. *Preliminary Note on Secure Communications on Millimetre Waves*, OSRD WA-2868-3, JEIA 5597, Report L/M40/WBL, TRE, Sept. 11, 1944. CP-510-M5
271. *Rotational Line Width in the Absorption Spectrum of Atmospheric Water Vapor and Supplement*, Arthur Adel, OEMsr-1361, NDRC Division 14 Report 320, University of Michigan, Oct. 10, 1944; Supplement Feb. 1, 1945. CP-510-M6
272. *The Absorption of One-Half Centimeter Electromagnetic Waves in Oxygen*, E. R. Beringer, OEMsr-262, Service Project AN-25, Division 14 Report 684, RL, Jan. 26, 1945. CP-510-M7
273. *The Effect of Rain on Radar Performance*, S. C. Hight, Report MM-44-170-50, BTL, Oct. 17, 1944. CP-511-M8
274. *Measurements of Wave Propagation*, G. E. Mueller, Report MM-45-160-17, BTL, Feb. 5, 1945. CP-511-M9
275. *Further Theoretical Investigations on the Atmospheric Absorption of Microwaves*, John H. Van Vleck, OEMsr-262, Service Project AN-25, Division 14 Report 664, RL, Mar. 1, 1945. CP-510-M8
276. *Measurements of the Attenuation of K-Band Waves by Rain*, G. T. Rado, OEMsr-262, Service Project AN-25, Division 14 Report 603, RL, Mar. 7, 1945. CP-511-M10
277. *Attenuation of Centimetre and Millimetre Waves by Rain, Hail, Fogs, and Clouds (Draft)*, J. W. Ryde and D. Ryde, OSRD WA-5181-10, Report 8670, GEC, May 18, 1945. CP-511-M11
278. *The Relation Between Absorption and the Frequency Dependence of Refraction (Fourth Conference)*, John H. Van Vleck, OEMsr-262, Division 14 Report 735, RL, May 28, 1945. (See reference 12.) Div. 14-122.24-M4
279. *Absorption and Scattering of Microwaves by the Atmosphere (Fourth Conference)*, Louis Goldstein, Report WPG-11, CUDWR, May 1945. (See reference 12.)
280. *C.V.D. Progress Report for May, 1945. The Absorption of K-Band Radiation in Gaseous Ammonia (Part I)*, Progress Report, CVD-CL, May 1945.
281. *K-Band Attenuation Due to Rainfall*, Lloyd J. Anderson, J. P. Day, C. H. Freres, John B. Smyth, A. P. D. Stokes and L. G. Trolese, Report WP-20, NRS�, June 8, 1945. CP-511-M12
282. *A New Method for Measuring Dielectric Constant and Loss in the Range of Centimeter Waves*, S. Roberts and Arthur R. von Hippel; *Wave Guides with Dielectric Sections*, L. J. Chu, Report 102, MIT, March 1941. CP-521-M1
283. *The Electrical Properties of Ice*, T. A. Taylor and Willis Jackson, OSRD W-126-42, Report AC-1516, RDF 110, Com. 78, RDF, Dec. 22, 1941. CP-522.13-M1
284. *The Dielectric Constant and Loss Factor of Water Vapor at a Wavelength of 9 Cm, Frequency 3330 Mc/s*, J. A. Saxton, OSRD W-203-2, Paper RRB/S-1, NPL-DSIR, Mar. 31, 1942. CP-522.12-M1
285. *The Dielectric Constant of Water Vapour and its Effect upon the Propagation of Very Short Waves*, A. C. Stickland, OSRD WA-175-7, Paper RRB/S-2, NPL-DSIR, May 11, 1942. CP-522.12-M2
286. *Progress Report on Ultrahigh Frequency Dielectrics*, Arthur R. von Hippel, OEMsr-191, Division 14 Report 121, MIT, Laboratory for Insulation Research, January 1943. CP-521-M2
287. *Conductivities of Sea, Tap and Distilled Water at  $\lambda=10$  Cm.*, L. B. Turner, OSRD WA-649-1, Report M-496, ASE, April 1943. CP-522.11-M1
288. *The Measurement of Dielectric Constant and Loss with Standing Waves in Coaxial Wave Guides*, Arthur R. von Hippel, D. G. Jelatis, and W. B. Westphal, OEMsr-191, Division 14, Report 142, MIT, Laboratory for Insulation Research, April 1943. CP-521-M4
289. *The Dielectric Constant and Absorption Coefficient of Water Vapour for Wavelengths of 9 Cm and 3.2 Cm, Frequencies 3,330 and 9,350 Mc/s.*, J. A. Saxton, Paper RRB/S-11, NPL-DSIR, June 14, 1943. CP-522.12-M3
290. "Electrical Measurements on Soil with Alternating Currents," R. L. Smith-Rose, *Journal of the Institution of Electrical Engineers* (London), NPL, Vol. 75, August 1943, pp. 221-237. CP-522.3-M1
291. *Memorandum on an Electrical Method of Measuring the Dielectric Constant of Atmospheric Air, and Recording it Continuously*, OSRD WA-1464-7, Report JMRP-8, Report M/Memo-15/PEC, TRE, Jan. 6, 1944. CP-522.2-M1
292. *The Dielectric Constant and Absorption Coefficient of Water Vapour for Radiation of Wavelength 1.6 Cm, Frequency 18,800 Mc/s.*, J. A. Saxton, Paper RRB/S.17, NPL-DSIR, Apr. 22, 1944.
293. *The Dielectric Constant of Water and Ice at Centimetre Wavelengths (Working Committee)*, J. M. Hough, ADRDE, USWP-WC, Apr. 28, 1944. CP-522.1-M1



294. *Preliminary Report on the Dielectric Properties of Water in the K-Band*, C. H. Collie, Report CL Misc. 25, CVD, May 1944.
295. *Recent Dielectric Constant and Loss Tangent Measurements on X-Band (Radome Bulletin No. 5)*, Elizabeth M. Everhart, OEMsr-262, Division 14 Report 483-5, RL, July 14, 1944. CP-522.4-M1  
Div. 14-234.5-M5
296. *Dielectric Properties of Water and Ice at K-Band*, E. L. Younker, OEMsr-262, Service Project AN-25, Division 14 Report 644, RL, Dec. 4, 1944. CP-522.1-M2
297. *The Interaction Between Electromagnetic Fields and Dielectric Materials*, Arthur R. von Hippel and R. G. Breckenridge, OEMsr-191 Division 14 Report 122, MIT, Laboratory for Insulation Research, January, 1943. CP-521-M3
298. *The Dielectric Properties of Water at Wavelengths from 2 Cm to 10 Cm and over the Temperature Range 0° to 40° C*, J. A. Saxton, OSRD WA-4340-5, Paper RRB/C-115, NPL-DSIR, Mar. 20, 1945. CP-522.11-M2
299. *The Dielectric Properties of Water in the Temperature Range 0° C to 40° C for Wavelengths of 1.24 Cm and 1.58 Cm*, J. A. Saxton and J. A. Lane, JEIA 9811, Paper RRB/C.116, NPL-DSIR, Mar. 7, 1945.
300. *The Anomalous Dispersion of Water at Very High Radio Frequencies in the Temperature Range 0° to 40° C*, J. A. Saxton, OSRD WA-4459-8, JEIA 9812, Paper RRB/C-118, NPL-DSIR, Apr. 6, 1945. CP-522.11-M3
301. *Centimeter Wave Propagation over Sea Within the Optical Range*, H. Archer-Thomson, J. C. Dix, F. Hoyle, E. C. S. Megaw, and M. H. L. Pryce, OSRD W-157-16, Report M-398, ASE, January 1942. CP-532.2-M1
302. *Preliminary Report on the Reflection of 9-Cm Radiation at the Surface of the Sea*, H. Archer-Thomson, N. Brooke, T. Gold, and F. Hoyle, OSRD WA-1131-2, Report M-542, ASE, September 1943. CP-532.2-M2
303. *Comment on the Reflection of Microwaves from the Surface of the Ocean (Part II)*, S. O. Rice, Report MM-43-210-6, BTL, Oct. 13, 1943. CP-532.2-M3
304. *S-Band Measurements of Reflection Coefficients for Various Types of Earth*, E. M. Sherwood, Report 5220.129, Sperry Gyroscope Company, Oct. 29, 1943. CP-532.1-M1
305. *Special Report on the Determination of the Coefficient of Reflection of Radio Waves at the Ground by Means of Radar Observations*, W. Sterling Ament, Report RA-3A-212A, NRL, Nov. 10, 1943. CP-532.1-M2
306. *Scattering*, T. L. Eckersley, OSRD WA-2255-1F, JEIA 3904, Report TR-481, BRL, November 1943. CP-512-M3
307. *Preliminary Measurements of 10 Cm Reflection Coefficients of Land and Sea at Small Grazing Angles*, Pearl J. Rubenstein and William T. Fishback, Division 14 Report 478, RL, Dec. 11, 1943. CP-532-M1
308. *Further Measurements of 3- and 10-Cm Reflection Coefficients of Sea Water at Small Grazing Angles*, William T. Fishback and Pearl J. Rubenstein, OEMsr-262, Division 14 Report 568, RL, May 17, 1944. CP-532.2-M4
309. *Microwave Propagation Studies, The Reflection of Sound Signals in the Atmosphere, Case 37003, File 36691-1*, F. H. Willis, Report MM-44-160-156, BTL, July 3 1944.
310. *Interim Report on Experiments on Ground Reflection at a Wavelength of 9 Cm*, L. H. Ford, JEIA 4899, Paper RRB/C.101, DSIR, July 7, 1944.
311. *An Experimental Investigation of the Reflection and Absorption of Radiation of 9-Cm Wavelength*, L. H. Ford and R. Oliver, OSRD WA-3386-2, Paper RRB/C-107, DSIR, Oct. 27, 1944. CP-532-M2
312. *The Measurement of High Reflections at Low Power (Radome Bulletin No. 7)*, Raymond M. Redheffer, OEMsr-262, Division 14 Report RL-483-7, RL, Nov. 20, 1944. CP-531-M3
313. *Ground Reflection Coefficient Experiments on X-Band, Case 20564*, W. M. Sharpless, Report MM-44-160-250, BTL, Dec. 15, 1944. CP-532.1-M3
314. *The Reflection Coefficient of a Linearly Graded Layer*, OSRD WA-3438-5, Report TR-492, BRL, December 1942. CP-531-M2
315. *Reflection and Scattering*, T. L. Eckersley, OSRD WA-4002-12, Report TR-506, BRL, January 1945. CP-532.2-M5
316. *Reflection from an Inversion*, L. E. Beglian and F. J. Northover, OSRD WA-4494-14, JEIA 9997, Report AC-8210, USW-140, USW, May 24, 1945. CP-531-M5
317. *Notes on the Comparison of Vertical and Horizontal Polarization in Ground Wave Propagation*, G. Millington, OSRD WA-1463-5, Report TR/442, BRL, January 1940. CP-540-M1
318. *Horizontal and Vertical Polarization*, T. L. Eckersley, OSRD II-5-5280, Report TR-441, BRL, July 1942. CP-540-M2
319. *The Investigation of Horizontally and Vertically Polarized Direction Finding on Frequencies of the Order of 20 to 70 Megacycles per Second*, T. L. Eckersley, OSRD II-5-5284, Report TR-451, BRL, September 1942. CP-540-M3
320. *Polarization Effects and Aerial System Geometry at Centimeter Wavelengths*, E. C. S. Megaw, H. Archer-Thomson, and E. M. Hickin, Report 8101, GEC, Nov. 26, 1942.
321. *Change of Polarization as a Means of Gap Filling*, Richard A. Hutner, Francis Parker, Bernard Howard, and Jocelyn Gill, Division 14 Report C-7, RL, Dec. 28, 1942. CP-540-M4
322. *Vertical Polarization vs Horizontal Polarization*, Ralph C. Loring, Tentative Technical Report T-1, CESL, Oct. 22, 1943. CP-540-M5
323. *The Depolarization of Microwaves*, M. Kessler, C. E. Mandeville and E. L. Hudspeth, Division 14 Report 458, RL, Nov. 1, 1943. CP-540-M6
324. *Polarization Studies at S and X Frequencies*, O. J. Baltzer, W. M. Fairbank, and J. D. Fairbank, OEMsr-262, Division 14 Report 536, RL, Mar. 14, 1944. CP-540-M7
325. *Screening by Hills*, H. G. Booker, OSRD WA-1105-3C, Report T-1015, TRE, May 1941. CP-231.222-M1
326. *Diffraction Round a Sphere or Cylinder*, G. Millington, OSRD II-5-5703, Report TR-433, BRL, March 1942. CP-231.21-M1



327. *Centimeter Wave Transmission Measurements from an Urban Site*, H. Archer-Thomson, E. M. Hickin, and E. C. S. Megaw, Report 8034, GEC, July 28, 1942.
328. *Report on an Investigation of the Propagation of Centimeter Waves over Ridges and Through Trees*, R. L. Smith-Rose, OSRD WA-772-19, Report AC-4345, Com. 181, NPL, June 2, 1943. CP-231.22-M1
329. *A Note on the Propagation of K-Band Waves Through Trees, Case 22098*, S. D. Robertson, Report MM-43-160-129, BTL, Aug. 13, 1943. CP-231.221-M1
330. *Report on Further Experiments on the Propagation of Centimeter Waves Through Trees in Leaf and over Level Ground*, OSRD WA-1337-3, Report AC-5059, Com. 197, NPL, Sept. 6, 1943. CP-231.221-M2
331. *Centimeter Wave Propagation, Notes on the Effect of Obstruction by a Single Tree*, R. E. Jennings, E. C. S. Megaw, H. Archer-Thomson, and E. M. Hickin, OSRD WA-1356-6, Report M-565, ASE, October 1943. CP-231.221-M3
332. *An Experimental Investigation on the Propagation of Radio Waves over Bare Ridges in the Wavelength Range 10 Centimetres to 10 Metres, Frequencies 30 to 3000 Mc/s*, J. S. McPetrie and L. H. Ford, OSRD WA-1463-17, Paper RRB/S-12, NPL-DSIR, Oct. 1, 1943. CP-231.222-M2
333. *Some Observed Effects of Trees upon Microwave Propagation, Case 37003, File 36691-1*, A. C. Peterson, Report MM-43-160-150, Sept. 17, 1943, Revised Oct. 15, 1943. CP-231.221-M4
334. *Effect of Hills and Trees as Obstructions to Radio Propagation*, Delmer C. Ports, OSRD 3070, OEMsr-1010, Jansky and Bailey, November 1943. CP-231.22-M2
335. *Report on Some Further Experiments on the Effect of Obstacles on the Propagation of Centimetre Waves*, L. H. Ford, A. C. Grace, and J. A. Lane, JEIA 3157, Report AC-5876, NPL-RD, USW, Jan. 20, 1944. Addendum, R. L. Smith-Rose, OSRD WA-3822-12, Report AC-5876a, NPL, Jan. 1, 1945. CP-231.223-M1
336. *The Propagation of Ultra Short Waves Round Hills and Other Obstacles*, T. L. Eckersley, OSRD WA-2884-3, JEIA 5674, Report TR-479, BRL, May 1944. CP-231.222-M3
337. *Scattering of Radio Waves by Metal Wires and Sheets*, F. Horner, JEIA 7793, Paper RRB/C-110, DSIR, Jan. 1, 1945.
338. *Some Experiments on the Propagation over Land of Radiation of 9.2-Cm Wavelength*, L. H. Ford, OSRD WA-4297-8, Paper RRB/C-113, NPL-DSIR, Feb. 15, 1945. CP-231.22-M3
339. *A Preliminary Study of Ground Reflection and Diffraction Effects with Centimetric Radar Equipment*, J. S. Hey, F. Jackson, and S. J. Parsons, OSRD WA-5062-2, Report 274, AORG, June 28, 1945. CP-231.21-M2
340. *Diffraction at Coast Line, Sloping Site*, H. G. Booker, OSRD WA-986-6c, Report 10, TRE, May 1, 1941. CP-233-M2
341. *Mixed Land and Sea Transmissions*, T. L. Eckersley, OSRD II-5-5515, Report E-16, BRL, October 1941. CP-233-M3
342. *Diffraction at Coast Line, Further Numerical Examples*, H. G. Booker, OSRD WA-92-5d, Report M-35, TRE, Feb. 5, 1942. CP-233-M4
343. *Coastal Refraction*, OSRD II-5-5281, Report TR-436, BRL, May 1942. CP-233-M5
344. *Propagation of Wireless Waves over Ground of Varying Earth Constants (Part Land and Part Sea)*, G. Millington, OSRD II-5-5277, Report TR-440, BRL-Marconi, Ltd., July 1942. CP-233-M6
345. *Transmission over Ground of Varying Earth Constants*, OSRD II-5-5457, Report TR-473, BRL, July 1943. CP-233-M8
346. *Diffraction at Coast Line (Appendix to Report on Siting of RDF Stations)*, H. G. Booker, OSRD WA-986-6b, Report 6, TRE, Jan. 27, 1944. CP-233-M1
347. *Siting and Coverage of Ground Radars*, E. J. Emmerling OEMsr-1207, Report WPG-10, CUDWR, May 1945. (See reference 12.) CP-202.4-M6
348. *Scattering and Spurious Echoes*, T. L. Eckersley, OSRD II-5-5275, Report TR-437, BRL, April 1942. CP-621.7-M1
349. *Reflection of 10-Cm Radiation by Model Aircraft*, A. F. Phillips, Christchurch Report 174, ADRDE, Sept. 8, 1942.
350. *Elementary Survey of Scattering and Echoing by Elevated Targets*, H. G. Booker, Report M/48/HGB, TRE, December 1942.
351. *The Resolution of Composite Echoes with Centimeter Wave R.D.F.*, J. R. Benson, J. A. Ramsay, and P. B. Blow, OSRD WA-1789-2, Report 4070/C/104, CAEE, Feb. 10, 1943. CP-623-M3
352. *Microwave Radar Reflection*, J. F. Carlson and S. A. Goudsmit, Division 14 Report 43-23, RL, Feb. 20, 1943. CP-623-M4
353. *Reflection of Radar Waves from Targets of Simple Geometric Form*, Lloyd J. Anderson, John B. Smyth, and F. R. Abbott, BuShips Problem X4-49CD, Report WP-3, NRSL, Feb. 24, 1943. CP-612.4-M1
354. *Radar Echoes from Periscopes*, John E. Freehafer, Division 14 Report 42-1, RL, Mar. 1, 1943. CP-622.1-M1
355. *Radar Echoes from Atmospheric Phenomena*, Arthur E. Bent, Division 14 Report 42-2, RL, Mar. 13, 1943. CP-621.1-M1
356. *Echoes Produced by Perfectly Conducting Objects of Certain Simple Shapes in Free Space*, R. E. B. Makinson OSRD II-5-5691, Report RP-173, CSIR, Mar. 25, 1943. CP-622.5-M1
357. *Gratings and Screens as Microwave Reflectors*, Division 14 Report 54-20, RL, Apr. 1, 1943. CP-611-M1
358. *Report on an Investigation into the Nature of Sea Echoes*, OSRD WA-1142-3, Report T-1497, TRE, May 12, 1943. CP-621.6-M1
359. *The Application of Corner Reflectors to Radar (Theoretical)*, R. D. O'Neil, F. S. Holt, and Prescott D. Crout, Division 14 Report 43-31, RL, May 14, 1943. CP-611.1-M1
360. *The Application of Corner Reflectors to Radar (Experimental)*, R. D. O'Neil, Division 14 Report 55-4, RL, July 1, 1943. CP-611.1-M2



361. *Measurement of the Effective Echoing Areas of Various Aircraft*, Ross Bateman, Report ORG-P-8-1, OCSO, July 2, 1943. CP-622.3-M1
362. *Overwater Observations at X and S Frequencies on Surface Targets*, O. J. Baltzer, V. A. Counter, W. M. Fairbank, W. O. Gordy, and E. L. Hudspeth, Division 14 Report 401, RL, July 26, 1943. CP-612.3-M1
363. *Towed Radar Targets*, G. A. Armstrong and G. H. Beeching, OSRD WA-1012-2, Research Report 212, ADRDE, Aug. 6, 1943. CP-612.2-M1
364. *Corner Reflector Tests at Langley Field*, C. M. Gilbert, Division 14 Report 402, RL, Aug. 6, 1943. CP-611.1-M3
365. *Properties of Corner Reflectors, Case 22098*, S. D. Robertson, Report MM-43-160-130, BTL, Aug. 12, 1943. CP-611.1-M4
366. *Use of Corner Reflectors as IFF on Ships*, OSRD II-5-5680, Operational Research Report 24, Australian ORS and CSIR-RL, Aug. 30, 1943. CP-611.1-M5
367. *An Investigation into the Nature of Sea Echoes*, A. C. Cossor, Ltd., JEIA 1221, Report MR-109, Research Department Myra Works, London E10, Sept. 8, 1943.
368. *The Scattering of Radiation from Rectangular Planes, Half-Cylinders, Hemispheres, and Airplanes*, Contract W-2279sc-551, Item 3, Moore School of Engineering, University of Pennsylvania, Oct. 12, 1943. CP-512-M2
369. *On the Appearance of the A-Scope when the Pulse Travels Through a Homogeneous Distribution of Scatterers*, A. J. F. Siegert, Division 14, Report 466, RL, Nov. 9, 1943. Div. 14-124.2-M2
370. *On the Fluctuations in Signals Returned by Many Independently Moving Scatterers*, A. J. F. Siegert, Division 14 Report 465, RL, Nov. 12, 1943. Div. 14-122.113-M7
371. *The Use of Permanent Echo Amplitudes for Monitoring S-Band Radar Equipment*, F. J. Kerr and J. F. McConnell, OSRD II-5-5750, Report RP-177/2, CSIR-RL, Dec. 7, 1943. CP-623-M5
372. *The Range Calculator*, S. J. Mason, Division 14 Report 497, RL, Dec. 20, 1943. CP-202.4-M2
373. *The Performance of 10-Cm Radar on Surface Craft*, B. F. Schonland, OSRD WA-1570-39, Report 155, AORG, Jan. 3, 1944. CP-202.312-M1
374. *Special Report on Radar Cross Section of Ship Targets*, Martin Katzin, Report RA-3A-213A, NRL, Jan. 24, 1944. CP-612.1-M1
375. *Observations of Life Rafts Equipped with Corner Reflectors*, Emmett L. Hudspeth and John P. Nash, Division 14 Report 533, RL, Feb. 15, 1944. CP-611.1-M6
376. *Radar Cross Section of Ship Targets (Part II)*, W. Sterling Ament, Martin Katzin, and F. C. MacDonald, Report R-2232, NRL, Feb. 18, 1944. CP-612.1-M1
377. *Optical Theory of the Corner Reflector*, R. C. Spencer, OEMsr-262, Division 14 Report 433, RL, Mar. 2, 1944. CP-611.1-M7
378. *Observations on Signal Stability at S and X Frequencies*, Otto J. Baltzer, Jr., William M. Fairbank, and J. D. Fairbank, OEMsr-262, Division 14 Report 537, RL, Mar. 14, 1944. CP-632-M1
379. *Interim Report on the Recognition of Radar Echoes*, F. E. S. Alexander, OSRD II-5-5796(S), JEIA 3401, Report RD-1/353, RDL-DSIR, NZ, Mar. 20, 1944. CP-623-M6
380. *Screened and Unscreened Radar Coverage for Surface Targets*, W. Walkinshaw and J. E. Curran, OSRD WA-2284-2, Report T-1666, TRE, March 1944. CP-612.3-M2
381. *The Performance of Naval Radar Systems Against Aircraft*, F. Hoyle, OSRD WA-2255-10, Report JEIA-3902, ASE, Apr. 3, 1944. CP-202.11-M2
382. *Preliminary Report on the Fluctuations of Radar Signals*, H. Goldstein and Paul D. Bales, OEMsr-262, Division 14 Report 569, RL, May 16, 1944. CP-632-M2
383. *Radar Ranging on Land Targets*, OSRD II-5-6178(S), Memorandum 101/G-36/ALH, TRE, May 18, 1944. CP-202.4-M3
384. *The Radar Echoing Power of Conducting Spheres*, T. Pearcey, and J. M. C. Scott, OSRD WA-2334-6, Report CR-228, ADRDE, May 24, 1944. CP-623-M7
385. *Use of Corner Reflectors in Beaconry*, F. J. Kerr, OSRD II-5-6145(S), JEIA 5180, Report RP-200, CSIR-RL, June 8, 1944. CP-611.1-M8
386. *Calibration and Standardization of Land Based Radars by the Use of Small Plane Targets*, F. R. Abbott, BuShips Problem X4-49CD, Report WP-12, NRSL, June 10, 1944. CP-612.5-M1
387. *Test of the Pre-Production Model Corner Reflector, Final Report of Project E-44-37*, Alvin E. Hebert and C. B. Overacker, AAF Board Project (M-3) 69-Eglin Field, Fla., Report 413.44/R387.1, Intel. Br. OCSO-USA, June 17, 1944. CP-611.1-M9
388. *Radar Cross Section of Ship Targets (Part III)*, W. Sterling Ament, Martin Katzin, and F. C. MacDonald, Report R-2295, NRL, June 27, 1944. CP-612.1-M1
389. *Notes on Echoes and Atmospherics from Lightning Flashes on P Band*, J. L. Pawsey, OSRD II-5-6144(S), JEIA 5177, Report RP-49-2, CSIR-RL, July 11, 1944. CP-621.3-M1
390. *Theory of Ship Echoes as Applied to Naval RCM Operations*, T. S. Kuhn and Peter J. Sutro, OEMsr-411, Research Project RP-186, Report 411-93, Harvard University, RRL, July 14, 1944. Div. 15-221.11-M2
391. *Radar Echoes from the Nearby Atmosphere, Case 37003-4*, Millard W. Baldwin, Jr., Report MM-44-150-2, BTL, July 18, 1944. CP-621-M1
392. *Radar Cross Section of Ship Targets (Part IV)*, W. Sterling Ament, Martin Katzin, and F. C. MacDonald, Report R-2332, NRL, July 21, 1944. CP-612.1-M1
393. *Radar Echoes from the Nearby Atmosphere, Second Report, Case 37003-4*, Millard W. Baldwin, Jr., Report MM-44-150-3, BTL, July 31, 1944. CP-621-M1
394. *Reflecting Properties of Metal Gratings*, J. S. Gooden, OSRD II-5-6230(S), Report RP-215, CSIR-RL, July 31, 1944. CP-611-M2
395. *Theory of the Performance of Radar on Ship Targets (ADRDE and CAEE Joint Report)*, M. V. Wilkes, J. A. Ramsay, and P. B. Blow, OSRD WA-2843-10, ADRDE Reference R04/2/CR252, CAEE Reference 69/C/149, July 1944. CP-612.1-M2
396. *Corner Reflectors for Life Rafts*, Emmett L. Hudspeth and John P. Nash, OEMsr-262, Division 14 Report 608, RL, Aug. 1, 1944. CP-611.1-M10



397. *The Characteristics of S-Band Aircraft Echoes with Particular Reference to Radar A.A. No. 3 MK. II.* G. H. Beeching and N. Corcoran, OSRD WA-2812-13, Research Report 253, ADRDE, Aug. 4, 1944. CP-622.3-M2
398. *Radar Echoes from the Nearby Atmosphere, Third Report, Case 37003-4,* Millard W. Baldwin, Jr., Report MM-44-150-4, BTL, Aug. 11, 1944. CP-621-M1
399. *Considerations Concerning Radar Coverage Diagrams,* J. L. Pawsey, OSRD II-5-6229(S), Report RP-217, CSIR-RL, Aug. 14, 1944. CP-202.4-M5
400. *RDF Echoes to be Expected from Objects of Various Shapes,* OSRD WA-6-21, Extra Mural Res. F.72/80, Report 26, Ministry of Supply, DSR. CP-622.5-M2
401. *Radar Echoes from Shells Bursts at 4 Meters and 50-Cm Wavelengths,* S. M. Taylor and F. E. W. Bugler, Research Report 260, RRDE, Oct. 9, 1944. CP-622.4-M1
402. *Summer Storm Echoes on Radar MEW,* J. S. Marshall, R. C. Langille, William M. Palmer, R. A. Rodgers, G. P. Adamson, and F. F. Knowles, Report 18, CAORG, Nov. 27, 1944. CP-621.1-M2
403. *The Cancellation of Permanent Echoes by the Use of Coherent Pulses (Interim Report),* H. Grayson, OSRD WA-3482-7C, Technical Note RAD-253, RAE, November 1944. CP-623-M8
404. *The Fading of S-Band Echoes from Ships in the Optical Zone,* R. I. B. Cooper, OSRD WA-3677-8, Research Report 265, Dec. 12, 1944. CP-622.2-M3
405. *Rotating Corner-Reflectors for Ship Identification,* Julian M. Sturtevant, OEMsr-262, Division 14 Report 654, RL, Jan. 1, 1945. CP-611.1-M11
406. *Reflection from Smooth Curved Surfaces,* R. C. Spencer, OEMsr-262, Division 14, Report 661, RL, Jan. 26, 1945. CP-531-M4
407. *Analysis of Over-Water Tracking,* Elizabeth J. Campbell, OEMsr-262, Service Project NO-166, Division 14 Report 695, RL, Feb. 12, 1945. CP-202.12-M1
408. *Technical Report on the Maximum Range of Detection of the German Early Warning Radar Equipment, Especially when Viewing Large, Tight Formations of Bomber Aircraft,* W. E. Bales and K. A. Norton, Report OAD-13, ORS, VIII Bomber Command OCSO, Sept. 13, 1943. CP-202.4-M1
409. *Performance Checks and Estimation of Vessel Size on Short-Based 10-Cm Radar Sets,* D. Lack, OSRD WA-1992-3, JEIA 3124, AORG, Mar. 30, 1944. CP-622.2-M1
410. *Report of Trials to Determine the Variations of the Apparent Reflecting Point of Plain 10-Cm Waves from a Destroyer,* J. F. Coales and M. Hopkins, OSRD WA-3702-1, Report M-627, ASE, July 1944. CP-622.2-M2
411. *The Reflection of Electromagnetic Waves by Long Wires and Non-Resonant Cylindrical Conductors,* J. M. C. Scott and T. Pearcey, JEIA 7286, Research Report 259, RRDE, Nov. 13, 1944.
412. *Theory of Radar Return from the Schnorkel,* P. M. Marcus, OEMsr-262, Division 14 Report 671, RL, Jan. 15, 1945. CP-622.1-M2
413. *Sea Returns and the Detection of Schnorkel,* G. G. Macfarlane, OSRD WA-4196-8, JEIA 8643, Report T-1787, TRE, Feb. 13, 1945. (See reference 418.) CP-622.1-M3
414. *Interservice KXS-Band Radar Trials; Over Water Performance Against Surface Targets,* J. A. Ramsay, P. B. Blow, and H. J. Worsdall, JEIA 8820, Report M-688, ASE, February 1945. CP-612.3-M3
415. *An Observation of Diffuse Cloud-Like Echoes,* J. L. Pawsey and F. J. Kerr, OSRD II-5-7007(S), Report RP-246, CSIR-RL, Mar. 6, 1945. CP-621.4-M1
416. *The So-Called Standard Target,* A. H. Brown, OEMsr-262, Division 14 Report S-43, RL, Mar. 10, 1945. CP-612.6-M1
417. *Radar Cross Section of Ship Targets (Part V),* F. C. MacDonald, Report R-2466, NRL, Mar. 12, 1945. CP-612.1-M1
418. *Radar Results Against Schnorkels: A Commentary on TRE T-1787, Sea Returns and the Detection of Schnorkel,* OSRD WA-4276-5, JEIA 9111, Report 338, ORS/CC, Mar. 16, 1945. (See reference 413.) CP-622.1-M4
419. *Radar Echoes from Clouds of Water Droplets,* F. Hoyle, Report AC-7930, Report 128, USW, Mar. 16, 1945.
420. *Comments on Radar Echoes from Water Droplets, (Paper AC-7930, USW Report 128),* R. G. Ross, OSRD WA-4149-10, Paper AC-7931, Report 129, USW, Mar. 16, 1945. CP-621.2-M1
421. *Radar Cross Section of Ship Targets (Part VI)* W. J. Barr, Report R-2467, NRL, Apr. 10, 1945. CP-612.1-M1
422. *S-Band Radar Echoes from Snow,* R. C. Langille, J. S. Marshall, William M. Palmer, and L. G. Tibbles, Report 26, CAORG, June 14, 1945. CP-621.5-M1
423. *Surface Coverage of Some Shipborne Radar Sets on S, X, and K Bands,* J. D. Fairbank and W. M. Fairbank, OEMsr-262, Service Projects NS-234 and NS-175, Division 14 Report 720, RL, June 15, 1945. CP-202.4-M7
424. *Echoes from Tropical Rain on X-Band Airborne Radar,* Arthur E. Bent, OEMsr-262, Division 14 Report 728, RL, June 15, 1945. CP-621.2-M2
425. *Analysis of Storm Echoes in Height Using MHF,* J. S. Marshall, L. G. Eon, and L. G. Tibbles, Report 30, CAORG, June 25, 1945. CP-621.1-M3  
See also: *Radar Camouflage,* Division 14 Report 766, RL, July 16, 1945. CP-633-M1
426. *3000-Megacycle Communication,* H. H. Beverage, OEMsr-32, NDRC Projects SC-13 and PDRC-90, RCA, Mar. 10, 1942. CP-203.1-M1
427. *Microwave Telephone, Part I Omnidirectional, Part II, Directional,* OEMsr-442, NDRC Projects C-42 and SC-13, RCA, Mar. 22, 1943. CP-203.1-M2
428. *Factors Determining the Range of Radio Communications in the Various Theaters of Operation,* Jack W. Herbstreit, Report ORG-P-14-1, OCSO, June 3, 1943. CP-732-M1
429. *Radiotelephone Communication on 3000 Megacycles,* Paul A. Anderson, K. E. Fitzsimmons, C. L. Barker, and S. T. Stephenson, OEMsr-728, NDRC Research Project PDRC-647, Division 14 Report 152, Report 2, Washington State College, June 12, 1943. CP-203.1-M3
430. *An Analysis of the Effect of Frequency on Short Distance Radio Communications,* Ross Bateman and William Q. Crichlow, Report ORB-P-15-1, OCSO, Aug. 18, 1943. CP-732.1-M1
431. *Use of the 25- to 50-Mc/s Band for Short Range Wireless Communication,* OSRD WA-1022-3, Report 130, AORG, Aug. 27, 1943. CP-732.1-M2



432. *Trials with a 250-Watt Frequency-Modulated VHF Sender Across a Sea Water Path Beyond the Optical Range*, G. W. Higgins and W. H. Hill, OSRD WA-1352-5, Report 878, SRDE, September 1943. CP-712-M1
433. *Radio Communication in Jungles*, Arthur C. Omberg, Report ORG-2-1, OCSO, Sept. 1, 1943. CP-711-M1
434. *Measurement of Factors Affecting Jungle Radio Communication*, Jack W. Herbstreit and William Q. Crichlow, Report ORB-2-3, OCSO, Nov. 10, 1943. CP-711-M2
435. *Methods for Improving the Effectiveness of Jungle Radio Communication*, Technical Bulletin Sig. 4, U.S. War Department, Jan. 14, 1944. CP-711-M3
436. *Survey of Existing Information and Data on Atmospheric Noise Level over the Frequency Range 1-30 Mc/s*, H. A. Thomas and R. E. Burgess, OSRD WA-3201-2, JEIA 2815, Paper RRB/C-90, DSIR, Feb. 21, 1944. CP-732-M2
437. *Methods of Reducing Radar Interference to Communication*, Arthur C. Omberg, Joseph B. Epperson, and William Q. Crichlow, Report ORB-E-27-2, OCSO, Apr. 19, 1944. CP-731-M1
438. *The Application of Passive Repeaters to Point to Point Communication at VHF and UHF*, Ross Bateman, Report ORB-P-20-1, OCSO, Apr. 29, 1944. CP-721-M1
- 439a. *Summary of Radio Propagation Problems in Southwest Pacific Area*, W. C. Babcock, JEIA 6298, Report US/413.44/R113, Intel. Br. OCSO, Sept. 6, 1944. CP-713-M1
- 439b. *Point to Point Communication in MF and Via Ground Wave Propagation*, W. C. Babcock, JEIA 6770, Report 413.44/R423.4, Intel. Br. OCSO-SWPA, Aug. 15, 1944.
440. *Measurements of Factors Affecting Radio Communication & Loran Navigation in SWPA*, Ross Bateman, Jack W. Herbstreit, and Robert B. Zechiel, Report ORB-2-4, OCSO, Dec. 16, 1944. CP-713-M2
441. *Field Trials of Ultra Short Wave Frequency and Amplitude Modulated Multichannel Radio Telephone Systems*, A. W. Pearson, W. J. Bray, J. H. H. Merriman, R. W. White, J. G. Hobbs, C. H. Gibbs, and H. Prain, Radio Report 1115, POED, Mar. 27, 1944.
442. *Physics of the Air*, W. J. Humphreys, McGraw-Hill Book Co., 1940, p. 457.
443. *Ergebnisse der Exakten Naturwissenschaften*, H. Plendl and G. Eckart, Berlin, 17, 1938, p. 334.
444. "Reflection of Waves in an Inhomogeneous Absorbing Medium," P. S. Epstein, *Proceedings of the National Academy of Sciences*, 16, 1930, p. 627.
445. "Penetration of a Potential Barrier by Electrons," Carl Eckart, *The Physical Review*, 35, 1930, p. 1303.
446. "The Relation of Drop Size to Intensity," J. O. Laws and D. A. Parsons, *Transactions of the American Geophysical Union*, 1943, p. 452.
447. "Ultra Short Wave Propagation," I. C. Schelleng, Chas. R. Burrows, and E. B. Ferrell, *Bell System Technical Journal*, April 1933. (See reference 24.)
448. Report JANP 102, Joint Communications Board.
449. "On the Connection Formulas and the Solutions of the Wave Equation," R. E. Langer, *The Physical Review*, 51, 1937, p. 670.
450. *Treatise on Theory of Bessel Functions*, George Neville Watson, Cambridge University Press, Second Edition, 1944.







# GENERAL BIBLIOGRAPHY OF REPORTS ON TROPOSPHERIC PROPAGATION REPORT WPG-14

This Bibliography is a comprehensive tabulation of the body of scientific reports pertaining to wave propagation through the troposphere, compiled by the Columbia University Wave Propagation Group to about October 31, 1945. For convenience and clarity it has been divided into twenty sections, each dealing with a particular phase of propagation phenomena. The various headings are self-explanatory, and the list of sources and their abbreviated designations which precede the Bibliography proper will be found helpful.

In preparing the Bibliography, about 560 papers were considered. Of these, 115 were excluded as obsolete, or because their contents were included in other reports retained. An additional 46 papers dealing with doppler effect and the transmission of sound in water were also excluded as not directly relevant. It is believed that the approximately 400 titles included form a fairly exhaustive compilation of present knowledge of electromagnetic wave propagation through the troposphere.

The reports are grouped and a Bibliography number has been assigned to each report. The letter to the right of the Bibliography number designates the present United States security classification.

Requests for copies of the reports listed herein may be made by Bibliography number referring to this edition, but should be made through the proper channels. The Central Radio Bureau is the distributing agent for American reports in Great Britain and for propagation reports originating in Great Baddow, Chelmsford, England. All other British reports may be obtained from the British government department controlling the sources.

The OSRD Liaison Office will, upon request, supply readers in the United States who are not in the Armed Services with all reports originating outside of the United States. They will supply Army and Navy units with all except JEIA-numbered reports. Requests for the latter should be directed to the Joint Electronics Information Agency, Munitions Building, Washington, D.C.

In general, application should be made to the NDRC Chairman's Office for reports written by NDRC Divisions, Committees, or contractors, NDRC Section 6.1 being the present exception; to the Bureau of Ships for reports from Naval Research Laboratory, Navy Radio and Sound Laboratory, and all reports appearing in Section 20 of the Bibliography (Under-Water Sound Propagation); to the Office of the Chief Signal Officer for Signal Corps reports; to Inter-Service Radio Propagation Laboratory, Bureau of Standards for IRPL reports. Requests for case-numbered BTL reports should be sent to the Director of Research, Bell Telephone Laboratories, 463 West Street, New York, N. Y.

## CLASSIFICATION OF REPORTS

1.000	Conferences and Progress Reports	10.000	Radar Forecasting
2.000	General Discussions	11.000	Atmospheric Absorption and Scattering
3.000	Standard Atmosphere Propagation	12.000	Dielectric Constant and Loss Factor
4.000	Non-Standard Atmosphere Propagation—Pure Theory	13.000	Reflection Coefficient
5.000	Non-Standard Atmosphere Propagation — Experiment and Theory	14.000	Horizontal and Vertical Polarization
6.000	Propagation Experiments	15.000	Effect of Hills, Trees, Obstacles, etc.
7.000	Meteorological Theory	16.000	Transmission over Part Land-Part Sea
8.000	Meteorological Experiments	17.000	Targets and Echoes
9.000	Meteorological Equipment	18.000	Doppler Effect
		19.000	Communication (Tropospheric)
		20.000	Under-Water Sound Propagation

## LIST OF ABBREVIATIONS

### AMERICAN

AMG-C.	Applied Mathematics Group, Columbia University	MIT.	Massachusetts Institute of Technology
BTL.	Bell Telephone Laboratories	NATC.	Naval Air Training Center, Corpus Christi, Texas
CBS.	Columbia Broadcasting System	NDRC.	National Defense Research Committee
CESL.	Camp Evans Signal Laboratory	NRL.	Naval Research Laboratory
CP.	Committee on Propagation	NRSL.	Navy Radio and Sound Laboratory
CUDWR.	Columbia University, Division of War Research	OCSO.	Office of the Chief Signal Officer
IRPL.	Inter Service Radio Propagation Laboratory; National Bureau of Standards	OFS.	Office of Field Service
JEIA.	Joint Electronics Information Agency	ORB.	Operational Research Branch; Office of the Chief Signal Officer



ORG.	Operational Research Group; Office of the Chief Signal Officer	GEC.	General Electric Company
RCA.	Radio Corporation of America	ICI.	Imperial Chemical Industries
RL.	Radiation Laboratory, M.I.T.	JIEE.	Journal of the Institution of Electrical Engineers
RRL.	Radio Research Laboratory, Harvard University	JMRP.	Joint Meteorological Radio Propagation Sub-Committee
SWP.	South West Pacific	MAP.	Ministry of Aircraft Production
TCAW.	Technical Committee on Air Warning, Office of the Sec'y of War; Reports distributed by Radiation Laboratory	MO.	Meteorological Office, Air Ministry
UCDWR.	University of California, Division of War Research	MetResCom.	Meteorological Research Committee
WD., HQAAF.	Weather Division, Headquarters Army Air Forces	NMS.	Naval Meteorological Service
WPG	Wave Propagation Group	NPL.	National Physical Laboratory
AUSTRALIAN		ORS-ADGB.	Operational Research Section, Air Defense of Great Britain
AORG.	Australian Operational Research Group	POED.	Post Office Engineering Department
ATP.	Australian Technical Paper	RAE.	Royal Aircraft Establishment
CSIR-RL.	Council for Scientific and Industrial Research, Radiophysics Laboratory	RRB.	Radio Research Board
RAAF.	Royal Australian Air Force	RRDE.	Radar Research and Development Establishment
BRITISH		SDTM.	Synoptic Divisions Technical Memorandum
A& AEE.	Aircraft and Armament Experimental Establishment	SRDE.	Signal Research and Development Establishment
AC.	Advisory Council on Scientific Research and Technical Development	TRE.	Telecommunications Research Establishment
ADRDE.	Air Defense Research and Development Establishment	USWP.	Ultra Short Wave Propagation Panel of the RDF Application Committee
AORG.	Army Operational Research Group	USWP-WC.	Ultra Short Wave Propagation Panel, Working Committee
ASE.	Admiralty Signal Establishment	CANADIAN	
BAD.	British Admiralty Delegation	ORS-WAC.	Operational Research Section, Western Air Command, Royal Canadian Air Force
BCSO.	British Central Scientific Office	CAORG.	Canadian Army Operational Research Group
BRL.	Baddow Research Laboratory	NEW ZEALAND	
CAEE.	Coast Artillery Experimental Establishment	ORS-RNZAF.	Operational Research Station, Royal N.Z. Air Force
CRB.	Central Radio Bureau	RDL-DSIR-NZ.	Radio Development Laboratory, Department of Scientific and Industrial Research—New Zealand
CVD-CL.	Coordination of Valve Development Committee, Clarendon Laboratory	SOUTH EAST ASIA	
DMO.	Director of Meteorological Office	ORS-SEA.	Operational Research Section, South East Asia
DSIR.	Department of Scientific and Industrial Research		

<i>Bib. No.</i>	<i>Title</i>	<i>Author or Source</i>	<i>Number</i>	<i>Date</i>
1.000 CONFERENCES AND PROGRESS REPORTS				
1.001 S	The Effect of the Atmosphere on the Propagation of Radio Waves. First Report on American Investigations.	H. G. Hopkins	BCSO No. 201	June 16 1943
1.002 S	The Effect of the Atmosphere on the Propagation of Radio Waves. Second Report on American Investigations.	H. G. Hopkins	BCSO No. 218	Aug. 6 1943
1.003 C	Notes on Microwave Propagation Conference at MIT Radiation Laboratory.	RL	RL 42-	Sept. 24 1943
1.004 S	Report on K-Band Work in U.S.A.	B. Bleaney	RL 475	Oct. 20 1943
1.005 S	Monthly Progress Report for the Month of March, 1944 (New Zealand).	RDL-DSIR NZ	RD 1/363	Apr. 14 1944



<i>Bib. No.</i>	<i>Title</i>	<i>Author or Source</i>	<i>Number</i>	<i>Date</i>
1.000 CONFERENCES AND PROGRESS REPORTS ( <i>continued</i> )				
1.006 C	Report of International Radio Propagation Conference.	IRPL	IRPL-C61	June 1944
1.007 C	Conference on Propagation—February 10-11, 1944—Empire State Building, New York.	CUDWR WPG	CP NDRC	1944
1.008 S	TRE Progress Report for the Period 16th June to 15th July, 1944.	TRE	MAP File Ref. No. SB 30917	June- July 1944
1.009 S	Progress Report, Radio Development Laboratory, DSIR, New Zealand for Months of June and July, 1944.	RDL-DSIR NZ	RD 1/439 or JEIA 5491	June- July 1944
1.010 S	Scientific Investigations on Propagation Problems in the South West Pacific Area.	F. W. G. White	Australia	July 25 1944
1.011 S	The Air Defense System of the Near Islands.	T. J. Carroll	OCSO OAD-55	Aug. 30 1944
1.012 S	Reviews of Progress of USW Propagation Work, I The Evaluation of Solutions of the Wave Equation for a Stratified Medium.	USWP D. R. Hartree	AC 7017/ RDF 239 or JEIA 593 <sup>4</sup>	Sept. 26 1944
	II Statement of Work in Progress Relevant to Investigations of the Propagation of Radio Waves Through the Troposphere.	R. L. Smith-Rose (NPL)	AC 7018/ USW	Sept. 25 1944
	III Microwave Propagation Research at Signal Research & Development Establishment.	SRDE	AC 7019/ USW or JEIA 6464	Sept. 26 1944
	IV Correlation of Radar Operational Data with Meteorological Conditions.	AORG	AC 7020/ USW or JEIA 6463	Sept. 28 1944
	V Progress Report on Forecasting of Radar Conditions.	DMO	AC 7021/ USW or JEIA 6462	Oct. 2 1944
	VI Vertical Temperature and Humidity Gradients at Rye.	DMO	AC 7022/ USW or JEIA 6461	Oct. 2 1944
	VII The Use of Radar for the Detection of Storms.	DMO	AC 7023/ USW or JEIA 6460	Oct. 2 1944
	VIII Present States of Theoretical Study of Radio Propagation Through the Troposphere by the Mathematics Group.	TRE	AC 7024/ USW or JEIA 6459	Oct. 2 1944
	IX Review of Short-Period Experimental Studies of Centimetre Wave Propagation, Carried out Jointly by ASE, SRDE and GEC.	E. C. S. Megaw (GEC)	AC 7025/ USW or JEIA 6458	Oct. 16 1944
	X Study of Cm. Wave Propagation over Cardigan Bay to Mount Snowden.	F. Hoyle	AC 7026/ USW	Oct. 14 1944
	XI Study of Reflection Coefficient of the Sea at Centimetre Wavelengths.	F. Hoyle	AC 7027/ USW	Oct. 14 1944
	XII K, X, and S (LLANDUDNO) Trials—General Summary of the Experimental Results Obtained which are Concerned with the Dependence of Radio Propagation on Meteorological Conditions.	TRE & RRDE	AC 7028/ USW	Oct. 14 1944
	XIII Progress Report on 369 Trials by DNMS.	DNMS	AC 7029/ RDF 240 USW or JEIA 6466	Oct. 14 1944
	XIV Survey of Progress in the United Kingdom on the Electromagnetic Theory of Tropospheric Propagation.	RRDE	AC 7030/ USW	Oct. 16 1944



<i>Bib. No.</i>	<i>Title</i>	<i>Author or Source</i>	<i>Number</i>	<i>Date</i>
1.000 CONFERENCES AND PROGRESS REPORTS ( <i>continued</i> )				
	XV Study of Meteorological Factors Responsible for the Refractive Structure of the Troposphere.	RRDE	AC 7031/ USW	Oct 16 1944
1.013 S	Report No. 1 of Project SWP—3.2 of the OFS.	P. A. Anderson	Washington State Coll.	Nov. 2 1944
1.014 C	Data on Super Refraction Supplied by Australian Radar Stations. (Progress Report on Analysis of Data from 200 Mc/s. Radar Stations Mar.-Aug., 1944).	J. W. Reed	CSIR-RL RP 229/1	Dec. 6 1944
1.015 S	Report No. 2 of Project SWP—3.2 of the OFS.	P. A. Anderson	Washington State Coll.	Jan. 7 1945
1.016 S	Third Conference on Propagation—Washington, D.C.—Nov. 16-18, 1944.	CUDWR-WPG	CP NDRC	1945
1.017 R	Survey of Field of Radio Propagation and Noise with Special Reference to Australia.	F. J. Kerr	CSIR RP 231 or JEIA 8641	Nov. 27 1944
2.000 GENERAL DISCUSSIONS				
2.001 S	Considerations Affecting Choice of Wavelength.	K. T. Bainbridge	RL- V-7S	Sept. 24 1941
2.002 S	Notes on Microwaves.	W. W. Hansen	RL- T-2	Oct. 20 1941
2.003 S	Fundamentals of Early Warning Radar.	ORG	OCSO ORG-E-5-1	Mar. 5 1943
2.004 S	RDF Propagation at Centimeter Wavelengths.	F. J. Kerr	Australia No. 284 RP 177	Apr. 27 1943
2.005 C	Notes on Ultra Short Wave Propagation in the United States.	H. G. Booker	TRE S 4457	Aug. 9 1943
2.006 C	An Introduction to Microwave Propagation.	D. E. Kerr P. Rubenstein	RL 406	Sept. 16 1943
2.007 R	Electrical Communication Systems Engineering.	War Dept.	TM 11-486 <sup>a</sup>	Feb. 25 1944 2nd Edition Apr. 25 1945
2.008 C	Anomalous Propagation and the Army.	T. J. Carroll	OCSO Rep. No. ORB-P-18-1	Mar. 4 1944
2.009 C	Radar System Fundamentals.	War Dept.	TM 11-467	Apr. 28 1944
2.010 R	Radio Fundamentals.	War Dept.	TM 11-455	May 22 1944
2.011 R	Radar Electronic Fundamentals.	War Dept.	TM 11-466	June 29 1944
2.012 C	Principles of Radar.	Staff of MIT Radar School		1944
2.013 C	Fundamentals of Radar.	Staff of Radar Fund. Sec.- NATC	NAVAER 08- 5S-108	Nov. 10 1944
2.014	General Lecture Series on Radar Components.	RL	RL T-18	Dec. 1, 1944
2.015 C	Radar Performance Testing Manual.	HQ, AAF	Air Forces Manual No. 28	July 1944 2nd Edition
2.016 R	Effects of Site Conditions on Operation of Ground Radar Installation on Aerodromes. See also 10.007.	J. L. Putman	TRE T 1805	
3.000 STANDARD ATMOSPHERE PROPAGATION				
3.001	The Diffraction of Electro-magnetic Waves from an Electrical Point Source Round a Finitely Conducting	H. Bremmer Balth. Van Der Pol	Phil. Mag. Vol. 24,	July 1937



<i>Bib. No.</i>	<i>Title</i>	<i>Author or Source</i>	<i>Number</i>	<i>Date</i>
3.000 STANDARD ATMOSPHERE PROPAGATION ( <i>continued</i> )				
	Sphere, with Applications to Radiotelegraphy and the Theory of the Rainbow. Part I		pp 141-176	
	The Diffraction of Electro-magnetic Waves from an Electrical Point Source Round a Finitely Conducting Sphere, with Applications to Radiotelegraphy and the Theory of the Rainbow. Part II	H. Bremmer Balth. Van Der Pol	Phil. Mag. Vol. 24 pp 825-864	Supp. Nov. 1937
	The Propagation of Radio Waves over a Finitely Conducting Spherical Earth. Part III	H. Bremmer Balth. Van Der Pol	Phil. Mag. Vol. 25 pp 817-837	June 1938
	Further Note on the Propagation of Radio Waves over a Finitely Conducting Spherical Earth. Part IV	H. Bremmer Balth. Van Der Pol	Phil. Mag. Vol. 27 pp 261-275	March 1939
3.002	Ultra Short Wave Propagation Curves (0.1 to 10 Meters).	Marconi	Marconi Handbook	March 28 1940
3.003	Report on Signal Strength Curves Within the Visual Range.	Marconi	Marconi RD 456	Nov. 1940
3.004	The Effect of the Earth's Curvature on Ground-Wave Propagation.	C. R. Burrows M. C. Gray	Proc. IRE Vol. 29 pp 16-24	Jan. 1941
3.005 C	The Siting of RDF Stations. Appendix: Screening of RDF Sets from Fixed Echoes.	TRE	TRE T 1430	July 19 1941
3.006 R	Propagation Curves for Wavelengths of 13 Meters. Supplement to USW Propagation Curves RD 456.	Marconi	Marconi Appendix RD 456A	Nov. 1941
3.007	The Calculation of Ground-Wave Field Intensity over a Finitely Conducting Spherical Earth.	K. A. Norton	Proc. IRE Vol. 29 pp 623-639	Dec. 1941
3.008 S	Siting of Stations for Maximum Range.	H. G. Booker	TRE M/36	Feb. 9 1942
3.009 S	Microwave Interference Patterns.	J. A. Stratton	RL- C-1	Mar. 7 1942
3.010 S	Dependence of Range of Radar Equipment on Wavelength for ASV—Case 23815 and 23817.	C. R. Burrows	BTL MM-42- 160-54	June 1 1942
3.011 S	Theoretical Field Strength of Ten Centimeter Equipment over a Spherical Earth.	H. G. Booker	TRE M/45/HGB	July 1 1942
3.012 C	Atmospheric Refraction and Height Determination by RDF. (Details and Results of a Numerical Method of First Order Correction.) (See 3.050)	E. Eastwood, F/O (RAF)	Calibration Memo No. 54 or JEIA 7773	July 6 1942
3.013 S	Dependence of Range of Submarine Radar Equipment on Wavelength—Case 20564.	C. R. Burrows	BTL MM-42- 160-70	July 9 1942
3.014 S	Transmission on 3000 Mc. over Sea Water.	J. A. Stratton	RL- C-2	July 14 1942
3.015 S	Transmission on 100 Mc. over Sea Water.	J. A. Stratton	RL- C-3	July 14 1942
3.016 S	Transmission on 200 Mc. over Sea Water.	J. A. Stratton	RL- C-4	July 14 1942
3.017 S	Transmission on 500 Mc. over Sea Water.	J. A. Stratton	RL- C-5	July 14 1942
3.018 C	Interim Report on Propagation Within and Beyond the Optical Range.	C. Domb M. H. L. Pryce	ASE M 448	Sept. 1942
3.019 C	Theoretical Ground Ray Field Strengths and Height Gain Curves for Wavelengths of 2—2000 M.	BRL	BRL Section E Tech. Rep. 383	Sept 1942
3.020 C	Siting for Long Range Aircraft Detection.	T. J. Carroll	CESL No. T-13	Oct. 17 1942 (Rev.)



<i>Bib. No.</i>	<i>Title</i>	<i>Author or Source</i>	<i>Number</i>	<i>Date</i>
3.000 STANDARD ATMOSPHERE PROPAGATION ( <i>continued</i> )				
3.021 C	VHF Field Strength Curves for Propagation within the Line of Sight.	G. J. Camfield RAE	Radio/279 RAE Ref: Radio/s. 2111/ OPE 16	Oct. 1942
3.022 S	Relation of Radar Range to Frequency and Polarization.	J. A. Stratton R. A. Hutner	RL- C-6	Nov. 3 1942
3.023	1 to 10 Cm. Propagation Curves.	G. Millington	Marconi TR 460	Jan. 1943
3.024 S	Properties of the Diffracted Wave Field Intensity.	R. A. Hutner E. Lyman	RL- C-8	Feb. 12 1943
3.025 S	The Effect of Earth Curvature on the Performance Diagram of an RDF Station.	TRE	TRE 29/R102/ LGHH	Feb. 25 1943
3.026 S	Radar Height Finding.	R. A. Hutner H. Dodson J. Gill B. Howard F. Parker J. A. Stratton	RL- C-9	Apr. 6 1943
3.027 S	Technical Requirements for GCI Search Systems. Technical Requirements for Early Warning Radar Systems.	L. J. Chu N. H. Frank RL	TCAW 1 and 2	May 10 1943
3.028 S	Low-Angle Coverage of Early Warning Radar Systems.	N. H. Frank RL	TCAW-3	July 26 1943
3.029 S	Factors Relating to the Design of an RDF Air Warning Set.	F. J. Kerr	CSIR-RL RP 187	Aug. 11 1943
3.030 C	A Graphical Method of Computing the Bending of Radio Beams by the Effective Earth Radius Method.	H. Raymond	CESL No. T-14	Aug. 27 1943
3.031 S	Transmission at Low Altitudes over Sea Water.	R. A. Hutner F. Parker B. Howard H. Dodson J. Gill	RL C-10	Sept. 1 1943
3.032 S	Radio-Frequency Propagation Above the Earth's Surface.	P. F. Godley, Jr.	RCA Lab. Rep. No. 895-5 Div. 15 OEMsr-895	Sept. 11 1943
3.033 S	Field Intensity Formulas.	R. A. Hutner H. Dodson J. Gill F. Parker B. Howard	RL- C-11	Sept. 28 1943
3.034 R	Propagation Curves. (See 3.046)	BTL	NDRC Div. 15 966-6A	Oct. 5 1943
3.035	Note on Field Intensity Computations for Elevated Antennas. Case 20878.	M. C. Gray	BTL MM-43- 110-28	Oct. 9 1943
3.036 C	The Calculation of Expected Vertical Coverage Diagrams.	M. Sherman Revised by W. S. McAfee	CESL T-17	2/19/43 Revision 10/15/43
3.037 R	Charts for Use in Field Intensity Computations.	K. Bullington	NDRC Proj. C-79	Nov. 2 1943
3.038 S	Notes on Visibility Problems, Taking Account of the Curvature of the Earth.	English AORG	AORG No. 152	Dec. 1 1943
3.039 C	Simplified Methods of Field Intensity Calculations in the Interference Region.	W. T. Fishback	RL 461	Dec. 8 1943



<i>Bib. No.</i>	<i>Title</i>	<i>Author or Source</i>	<i>Number</i>	<i>Date</i>
3.000 STANDARD ATMOSPHERE PROPAGATION ( <i>continued</i> )				
3.040 C	Field Strength Near and Beyond the Horizon for Wavelengths of Ten and Thirty Cms.	TRE	TRE-M/ Rep. 53/WW	Dec. 24 1943
3.041 S	Theoretical Field Strength Near and Beyond Horizon for Orthodox Propagation of Fifty Centimeter Waves.	TRE	TRE T 1635	Feb. 24 1944
3.042 C	Location of Signal Strength Maxima, Nulls, and Reflection Areas for Standard U.S. Early Warning Radar Equipment.	R. C. L. Timpson, Major	First Air Force	Apr. 7 1944
3.043 S	Cover by German Coastal Radar on Low Flying Aircraft.	R. C. Raymond I. H. Crowne	OCSO OAD-25	Apr. 15 1944
3.044 C	The Propagation Functions for an Atmosphere with Uniform Lapse-Rate of Refractive Index.	T. Pearcey	RRDE Research Rep. No. 256	Sept. 1 1944
3.045 S	Ideal Field Intensity Distribution in the Vertical Plane for Transmitting or Receiving Antennas when Each has the Same Pattern.	J. W. Herbstreit	OCSO ORG-PP-5	1944
3.046 R	Propagation Curves. (Issue 3—Replacing Previous Issues.)	BTL	NDRC Div. 15- Report 966-6C	Oct. 1944
3.047 C	Field Strength Calculator for Vertical Coverage Patterns and Propagation Curves.	C. R. White	CESL Tech. Memo No. 154-E	Dec. 20 1944
3.048 C	<sup>b</sup> Theoretische Resultaten over de Voorplanting Van Radiogolven.	Balth. Van Der Pol	Natuurkundig Laboratorium N. V. Philips Gloeilampen Fabrieken, Eindhoven, Holland	Aug. 1941 Trans. Apr. 14 1945
3.049 S	Theory of the Vertical Field Patterns for RDF Stations.	J. C. Jaeger	CSIR-RL RP 174	Mar. 17 1943
3.050	Height/Range/Alpha Tables (Tables Relating to the Height, Range and Angle of Elevation of an Aircraft.) (See 3.012.)	ORS ADGB	ORS(ADGB) Radar Memo No. 50 or JEIA-7766	Aug. 10 1944
3.051 R	The Calculation of Field Strength for Vertical Polarization over Land and Sea on 20 to 80 Megacycles per Second.	A. M. Woodward	TRE T 1704	
3.052 C	Field Intensity Contours in Generalized Coordinates.	H. Dodson J. Gill B. Howard	RL 702	May 2 1945
4.000 NON-STANDARD ATMOSPHERE PROPAGATION—PURE THEORY				
4.001 S	The Limiting Ranges of RDF Sets over the Sea.	F. Hoyle M. H. L. Pryce	ASE M 395	1943
4.002 S	The Theory of Anomalous Propagation in the Troposphere and Its Relation to Waveguides and Diffraction.	H. G. Booker	TRE M/60/HGB or T 1447	Apr. 12 1943
4.003 C	The Tracing of Rays in the Refracting Atmosphere.	T. Pearcey	ADRDE AC 3878 USW	Apr. 21 1943
4.004 C	Graphical Construction of a Radar Radiation Pattern in a Stratified Atmosphere.	L. Anderson F. R. Abbott	NRSL WP-4	May 1 1943
4.005 S	Improved Tropospheric Propagation—Curves Embracing Anomalous Propagation.	H. G. Booker	TRE M/65/HGB	July 6 1943
4.006 C	Radiation Patterns under Cases of Anomalous Propagation.	T. Pearcey	ADRDE R 35	July 19 1943



<i>Bib. No.</i>	<i>Title</i>	<i>Author or Source</i>	<i>Number</i>	<i>Date</i>
	4.000 NON-STANDARD ATMOSPHERE PROPAGATION—PURE THEORY ( <i>continued</i> )			
4.007 S	Effect of Humidity Gradients in the Atmosphere on Propagation at RDF Frequencies.	Australian Operational Research Group	Oper. Res. Rep. No. 22	July 28 1943
4.008 C	The Calculation of Field Strength Near the Surface of the Earth under Particular Conditions of Anomalous Propagation.	T. Pearcey	ADRDE Research Rep. No. 203	Oct. 28 1943
4.009 C	Anomalous Propagation over the Earth, Case 23703.	S. A. Schelkunoff	BTL MM-43-110 33	Oct. 30 1943
4.010 C	The Effect of Atmospheric Refraction on Short Radio Waves.	J. E. Freehafer	RL 447	Nov. 29 1943
4.011 C	Radar Ray Patterns Associated with Normal and Anomalous Propagation Conditions.	F. P. Dane R. U. F. Hopkins L. J. Anderson	NRSL WP-6	Dec. 10 1943
4.012 C	Transmission of Plane Waves Through a Single Stratum Separating Two Media.	J. B. Smyth	NRSL WP-9	Dec. 22 1943
4.013 S	Notes on Theoretical Coverage Diagrams for Anomalous Propagation.	TRE	TRE TM/Memo/14/AMW	Jan. 1 1944
4.014 C	The Dependence of Microwave Propagation over Sea on the Structure of the Atmosphere.	J. M. C. Scott T. Pearcey	ADRDE Memo No. 40	Feb. 4 1944
4.015 S	Improved Tropospheric Propagation—Curves Embracing Superrefraction.	TRE	TRE T 1625	Feb. 18 1944
4.016 S	TRE Requirements for Propagation—Curves Embracing Superrefraction.	TRE	TRE M/Memo 16/HAB	Feb. 25 1944
4.017 C	The Mechanical Determination of the Path Difference of Rays Subject to Discontinuities in the Vertical Gradient of Refractive Index.	F. R. Abbott NRSL	NRSL Rep. No. WP-10	Mar. 10 1944
4.018 S	Improved Tropospheric Propagation—Curves Embracing Superrefraction.	TRE	TRE T 1626	Mar. 28 1944
4.019 S	Interservice Propagation—Curves Embracing Superrefraction. Dependence of Mathematical Parameter L on Physical Entities.	TRE	TRE M/Memo 18/WW	Apr. 3 1944
4.020 S	Theoretical Coverage-Diagrams for 10 Cm. Radars Embracing Superrefraction.	TRE	TRE T 1634 or JEIA 3229	Apr. 14 1944
4.021 S	Theoretical Coverage-Diagrams for 50 Cm. Radars Embracing Superrefraction.	TRE	TRE T 1659 or JEIA 3230	Apr. 14 1944
4.022 S	Theoretical Coverage of Navigational Aids Embracing Superrefraction.	TRE	TRE T 1660	Apr. 14 1944
4.023 C	The Theory of Propagation of Radio Waves in an Inhomogeneous Atmosphere (I).	T. Pearcey	ADRDE Research Rep. No. 245	April 1944
4.024 C	Reflection Coefficient of Layers of Varying Refractive Index.	G. Millington BRL	BRL TR 483 or JEIA 4644	April 1944
4.025	Evaluation of the Solution of the Wave Equation for a Stratified Medium. (See 4.043.)	D. R. Hartree P. Nicholson N. Eyres J. Howlett T. Pearcey	ADRDE MR 47	May 24 1944
4.026 C	Transmission of Plane Waves Through a Single Stratum Separating Two Media (II).	J. B. Smyth	NRSL WP-13	June 23 1944
4.027	Waves Guided by Dielectric Layers.	S. A. Schelkunoff	BTL MM-44-110-52	July 5 1944



<i>Bib. No.</i>	<i>Title</i>	<i>Author or Source</i>	<i>Number</i>	<i>Date</i>
	4.000 NON-STANDARD ATMOSPHERE PROPAGATION—PURE THEORY ( <i>continued</i> )			
4.028 C	Microwave Transmission in Nonhomogeneous Atmosphere.	S. A. Schelkunoff	BTL MM-44- 110-53	July 5 1944
4.029 C	Contour Diagrams of the Radiated Field of a Dipole under Various Conditions of Anomalous Propagation. (See 4.045.)	T. Pearcey F. Whitehead	RRDE Research Report No. 257	July 15 1944
4.030 R	Theoretical Coverage-Diagrams for 1½ Metre Radars Embracing Superrefraction.	A. M. W. Woodward	TRE T 1708	July 23 1944
4.031 R	Propagation Curves Embracing Superrefraction: SS Duct, Profile-Index 0.2 (Preliminary Edition).	H. G. Booker	TRE M/Memo 23/WW	Sept. 7 1944
4.032 C	A Note on the Reflection Coefficient of an Isotropic Layer of Varying Refractive Index.	G. Millington BRL	BRL TR 497 or JEIA 6481	Oct. 5 1944
4.033 R	Predicted Low Level Coverage of S-Band Shipborne Radars as Affected by Weather. (Horizontal Polarization—Antenna Height 100 Ft.)	F. R. Abbott L. L. Whittemore L. W. Cross E. J. Wyrostek	NRSL WP-14	Nov. 1 1944
4.034 R	Predicted Low Level Coverage of 200 Mcs Band Shipborne Radars as Affected by Weather. (Horizontal Polarization—Antenna Height 100 Feet.)	F. R. Abbott L. L. Whittemore L. W. Cross E. J. Wyrostek	NRSL WP-15	Nov. 4 1944
4.035 R	Variational Method for Determining Eigenvalues of Wave Equation of Anomalous Propagation.	G. G. Macfarlane	TRE T 1756	Nov. 13 1944
4.036 C	Wave Propagation Analysis with the Aid of Non-Euclidian Spaces.	B. Liebowitz	CUDWR WPG-7	Dec. 1944
4.037 C	Atmospheric Waves—Fluctuations in High Frequency Radio Waves.	L. G. Trolese J. B. Smyth	NRSL WP-18	Feb. 1 1945
4.038 C	The Relation Between the Wave Equation and the Non-Linear First Order Equation of the Riccati Type.	T. L. Eckersley	BRL TR-501 or JEIA 9104	Jan. 1945
4.039 C	A Report on Transmission of Waves over the Earth.	T. L. Eckersley	BRL TR 504	Jan. 1945
4.040 C	New Convergent Integrals.	T. L. Eckersley	BRL TR 509	Feb. 1945
4.041 C	The Effect of a Subrefracting Layer of Atmosphere upon the Propagation of Radio Waves.	T. Pearcey M. Tomlin	RRDE Memo No. 83 or JEIA-8371	Feb. 12 1945
4.042 C	Theory of Characteristic Functions in Problems of Anomalous Propagation.	W. H. Furry	RL 680	Feb. 28 1945
4.043 C	The Evaluation of the Solution of the Wave Equation for a Stratified Medium (II). (See 4.025.)	D. R. Hartree	RRDE Res. Rep. No. 279	Mar. 12 1945
4.044 R	Theoretical Coverage Diagrams for 3 Metre Radars Embracing Superrefraction.	W. Walkinshaw R. Hensman	TRE T 1815 or JEIA 9198	Mar. 18 1945
4.045 C	The Radiation Field of a Dipole under Various Conditions of Anomalous Propagation. (See 4.029.)	T. Pearcey M. Tomlin F. Whitehead	RRDE Res. Rep. No. 275	Apr. 13 1945
4.046 C	Notes on the Solution of a Non-Linear First Order Equation of the Riccati Type. (See 4.038.)	T. L. Eckersley	BRL TR 502 or JEIA-9725	May 1945
4.047 C	Perturbation Theory for an Exponential M-curve in Non-Standard Propagation.	C. L. Pekeris	CUDWR WPG-12	July 1945
4.048 C	Graphs for Computing the Diffraction Field with Standard and Superstandard Refraction.	P. J. Rubenstein W. T. Fishback	RL 799	Aug. 13 1945
	5.000 NON-STANDARD ATMOSPHERE PROPAGATION—EXPERIMENT AND THEORY			
5.001 C	Radio Interpretation of Meteorological Observations in the First Two Meters of Atmosphere Above Grass at Harlington, Middlesex, January to June, 1940.	TRE	T 1471 TRE M/63	1940



<i>Bib. No.</i>	<i>Title</i>	<i>Author or Source</i>	<i>Number</i>	<i>Date</i>
5.000	NON-STANDARD ATMOSPHERE PROPAGATION—EXPERIMENT AND THEORY ( <i>continued</i> )			
5.002 S	Anomalous Echoes Observed with 10 Cms. CD Set.	A. E. Kempton	ADRDE Research Rep. No. 119	Oct. 8 1941
5.003 C	Centimeter Wave Propagation over Sea Between High Sites just within Optical Range.	F. Hoyle E. C. S. Megaw	ASE GEC	June 12 1942
5.004 C	Centimeter Wave Propagation over Land, II. Measurements within and beyond Optical Range.	G. W. N. Cobbold H. Archer-Thomson E. C. S. Megaw	SRDE GEC AC 2917/ Com. 136	Oct. 16 1942
5.005 C	Radar Wave Propagation.	L. Anderson J. B. Smyth F. R. Abbott R. Revelle	NRSL WP-2	Nov. 30 1942
5.006 C	Very Short Wave Interception and DF	T. L. Eckersley	BRL TR 438	1943
5.007 C	Anomalous Propagation of 10 Cm. RDF Waves over the Sea, Also: First Supplement.	AORG	AORG No. 87	2/6/43 Supplement 7/26/43
5.008 S	Investigation of Propagation Characteristics of AW Stations.	Australian ORG	Oper. Res. Rep. No. 17	Mar. 9 1943
5.009	A Study of Propagation over the Ultra-Short-Wave Radio Link between Guernsey and England on Wavelengths of 5 and 8 Meters (60 and 37.5 Mc/s.).	R. L. Smith-Rose A. C. Stickland NPL	JIEE 90	Mar. 1943
5.010 C	The Effect of Atmospheric Refraction on the Propagation of Radio Waves.	A. C. Stickland NPL	RRB /S 10	Mar. 20 1943
5.011 S	Propagation of Ultra-Short Waves.	H. C. Webster	Australia Rep. No. 354	Apr. 17 1943
5.012 C	Report on Radar Wave Propagation. Atmospheric Refraction—A Qualitative Investigation.	L. Anderson J. B. Smyth	NRSL WP-5	May 7 1943
5.013 C	Radio Interpretation of Meteorological Observations in the First 400 Feet Above Cardington, 1942.	TRE	TRE M/61 or T 1413	May 14 1943
5.014 S	Centimeter Wave Propagation over Sea, II. Measurements from Shore Sites Near and Beyond Optical Range.	G. W. N. Cobbold A. J. Jones H. A. Bonnett E. C. S. Megaw H. Archer-Thompson E. M. Hickin	GEC No. 8180	May 27 1943
5.015 S	Preliminary Observations on Radio Propagation at 6 Centimeters Between Beer's Hill, New Jersey, and New York—Case 37003-4, File 36691-1.	G. W. Gilman	BTL MM-43- 160-87	June 12 1943
5.016 C	Some Observations of Anomalous Propagation.	TRE	TRE M/64 or T 1483	July 6 1943
5.017 S	Application of Anomalous Propagation to Operational Problems at Home and Abroad.	H. G. Booker	TRE M/66/HGB or T 1484 or JMRP No. 3	July 7 1943
5.018 C	Propagation of Signals on 45.1, 474 and 2800 Mc. from Empire State Building to Hauppauge and Riverhead, L.I., New York.	G. S. Wickizer A. M. Braaten RCA	NDRC Proj. 423 Rep. No. 1	July 20 1943
5.019	Propagation of Ultra Short Waves.	T. L. Eckersley	Marconi TR/476	Aug. 1 1943
5.020 S	The "K" Effect in Anomalous Propagation of Ultra-Short Waves.	F. Syer, Flying Officer, RAAF	Australia No. 266 or JMRP No. 11	Aug. 10 1943
5.021 C	The Propagation of 10 Cm. Waves over Land Paths of 14, 52, and 112 Miles.	P. A. Anderson C. L. Barker K. E. Fitzsimmons S. T. Stephenson	Wash. State Coll. Rep. No. 4 NDRC PDRC-647	Oct. 26 1943
5.022 S	The Propagation of 1-Cm. Waves over the Sea as Deduced from Meteorological Measurements.	J. M. C. Scott T. Pearcey	ADRDE Res. Rep. No. 227 or JMRP No. 4	Nov. 11 1943



<i>Bib. No.</i>	<i>Title</i>	<i>Author or Source</i>	<i>Number</i>	<i>Date</i>
5.000	NON-STANDARD ATMOSPHERE PROPAGATION—EXPERIMENT AND THEORY ( <i>continued</i> )			
5.023 S	Centimeter Wave Propagation over Land. A Preliminary Study of the Field Strength Records between March and Sept., 1943.	R. L. Smith-Rose A. C. Stickland NPL	DSIR RRB/S 13 or JMRP No. 10	Nov. 15 1943
5.024 C	The Propagation of 10 Cm. Waves over an Inland Lake. Correlation with Meteorological Soundings.	P. A. Anderson K. E. Fitzsimmons S. T. Stephenson	Wash. State Coll. Rep. No. 5 NDRC PDRC-647	Nov. 16 1943
5.025 C	Measurements of Radar Wave Refraction and Associated Meteorological Conditions.	L. J. Anderson L. G. Trolese	NRSL WP-7	Dec. 10 1943
5.026 C	Anomalous Propagation in India—Preliminary Report on Overland Transmission in Bengal.	South East Asia	ORS-SEA Rep. No. S 5	Dec. 30 1943
5.027 S	Atmospheric Physics—Summary of Investigations on Anomalous Propagation of Radar Signals Carried out by the Australian Operational Research Group During 1942-43.	D. F. Martyn	Aust. Oper. Research Group	1942- 1943 Summary
5.028 S	The Cause of Short Period Fluctuations in Centimetre Wave Communication.	J. M. C. Scott	ADRDE Memo 42	Mar. 8 1944
5.029 S	Anomalous Propagation in the Persian Gulf.	Naval Officer in Charge, Hormuz	AC 5975/ USW	Rec'd Mar. 20 1944
5.030 S	Effect of Super-refraction on Surface Coverage on Enemy 50 Cm. and 80 Cm. Radar Sets.	TRE	TRE M/Memo 19	April 1944
5.031 S	K-X-S Experiments, News Letter No. 1.	T. Gold ASE	MK 12201	May 3 1944
5.032 S	Abnormal Radar Propagation in the South Pacific. An Investigation into Conditions in New Zealand and Norfolk Island on 200 Mc/s. with Notes on Fiji, New Caledonia and Solomon Islands.	ORS-RNZAF Air Dept. Wellington	RNAZAF Rep. No. 119 File 135/ 14/10	May 4 1944
5.033 C	Procedure and Charts for Estimating the Low Level Coverage of Shipborne 200 Mcs. Radars under Conditions of Pronounced Refraction.	F. R. Abbott L. J. Anderson F. P. Dane J. P. Day R. U. F. Hopkins J. B. Smyth L. G. Trolese Ens. A. P. D. Stokes	NRSL WP-11 (Rev.) BuShips Prob. No. X4-49CD	May 10 1944 Revised
5.034 S	Centimeter Propagation over Land. A Study of the Field Strength Records Obtained During the Year 1943-1944.	A. C. Stickland (NPL) Flt. Lt. R. W. Hatcher (MO)	DSIR RRB/ S 18 or JEIA 4789	May 11 1944
5.035 S	K-X-S Experiments, News Letter No. 2.	T. Gold ASE	MK 12201	May 13 1944
5.036 C	Atmospheric Propagation Effects and Relay Equipment.	T. J. Carroll OCSO	ORB-PP- 12-1	May 18 1944
5.037 C	Low-Level Coverage of Radars as Affected by Weather. Procedures and Charts. (5.033 Reprinted.)	NRSL	IRPL T2a	May 25 1944
5.038 R	Variations in Radar Coverage.	Joint Communi- cations Board	JANP 101	June 1 1944
	Earlier Editions have Appeared As:			
R	Radar Operation and Weather.	CUDWR- WPG	IRPL T-1	May 1944
C	Weather Influences in Radar Wave Propagation.	CUDWR- WPG	NAVAER 50-IT-16	May 1944
5.039 S	Effect of Atmospheric Refraction on Range Measurements.	G. G. Macfarlane	TRE T 1688	June 12 1944



<i>Bib. No.</i>	<i>Title</i>	<i>Author or Source</i>	<i>Number</i>	<i>Date</i>
5.000	NON-STANDARD ATMOSPHERE PROPAGATION—EXPERIMENT AND THEORY ( <i>continued</i> )			
5.040 C	Microwave Transmission over Water and Land under Various Meteorological Conditions.	P. J. Rubenstein I. Katz L. J. Neelands R. M. Mitchell	RL 547	June 13 1944
5.041 S	Abnormal Propagation in WAC for May and June, 1944.	Canadian	ORS-WAC Rep. 10	July 27 1944
5.042 C	Propagation of Signals on 45.1, 474 and 2800 Mc. From Empire State Building, N. Y. C. to Hauppauge and Riverhead, L. I., N. Y.	G. S. Wickizer A. M. Braaten (RCA)	NDRC Proj. 423 Rep. No. 2	July 31 1944
5.043 C	The Structure of the Electromagnetic Field During Conditions of Anomalous Propagation.	T. Pearcey F. Whitehead	RRDE Res. Rep. No. 258	Sept. 19 1944
5.044 C	Tropospheric Propagation and Radio-Meteorology.	CUDWR- WPG	CUDWR WPG-5	Sept. 1944
5.045 C	Some Factors Causing "Superrefraction" on Ultra High Frequencies in South West Pacific. (Daily Report on Abnormal Echoes—RAAF. Form No. 146 Included in ATP 821.)	D. F. Martyn F/Lt. P. Squires	Australian Ionosphere Bul. Sect. 1.2 or ATP 821	Oct. 1944
5.046	Aeroplane Tests.	BRL	JMRP No. 35 or BRL TR 488-A	Dec. 21 1944
5.047 C	Atmospheric Refraction—A Preliminary Qualitative Investigation.	L. J. Anderson F. P. Dane J. P. Day R. F. Hopkins L. G. Trolese Lt. A. P. D. Stokes	NRSL WP-17	Dec. 28 1944
5.048 S	Anomalous Propagation with High and Low Sited 3 cm. Ship Watching Radar Sets.	G. C. Varley	AORG Rep. No. 250	Mar. 20 1945
5.049 S	<sup>a</sup> Anomalous Propagation at English Coastal Radar Stations, March-September, 1944.	D. Lack	AORG Rep. No. 258 or JEIA 9946	May 30 1945
6.000 PROPAGATION EXPERIMENTS				
6.001	Lebanon-Beer's Hill Transmission on Wavelengths of 2.0 Meters and 30 Centimeters—Case 20564.	A. B. Crawford	BTL MM-39- 326-98	Dec. 5 1939
6.002 C	Centimeter Wave Propagation over Land: Preliminary Trials.	G. W. N. Cobbold H. A. Bonnett A. J. Jones E. C. S. Megaw H. Archer-Thomson A. S. Gladwin E. M. Hickin	GEC No. 8045	Aug. 21 1942
6.003 C	The Propagation of 10 Cm. Waves on a 52-Mile Optical Path over Land. The Correlation of Signal Patterns and Radiosonde Data.	P. A. Anderson C. L. Barker S. T. Stephenson K. E. Fitzsimmons	Washington State Coll. Rep. No. 1 NDRC-PDRC- 647	June 10 1943
6.004 C	Centimeter Wave Propagation over Sea Within and Beyond the Optical Range.	E. C. S. Megaw H. Archer-Thomson E. M. Hickin F. Hoyle	ASE M 532	July 1943
6.005 S	Aden-Berbera VHF Experiments—Final Report on Propagation Aspects.	Lt. E. W. Walker Lt. S. R. Bickerdike	SRDE MS 4	Dec. '42 July '43



<i>Bib. No.</i>	<i>Title</i>	<i>Author or Source</i>	<i>Number</i>	<i>Date</i>
6.000 PROPAGATION EXPERIMENTS <i>(continued)</i>				
6.006 S	Investigation No. 369 (Irish Sea Experiment).	British Min. of Supply	AC 5970 AC 5971 AC 5972 AC 5973 AC 5974 AC 6334 AC 6828 AC 7206 AC 7465 AC 7668	9/1/43 12/14/43 1/15/44 2/9/44 3/20/44 5/14/44 8/12/44 10/19/44 11/10/44 1/4/45
6.007 S	Experience with Space and Frequency Diversity Fading on New York-Neshanic Microwave Circuit—Case 37003-4.	G. W. Gilman F. H. Willis	BTL MM-43-160-152	Sept. 18 1943
6.008 C	Investigation of Changes in Direction of Transmission during Periods of Fading in the Microwave Range—Case 37003-4, File 36691-1.	A. C. Peterson	BTL MM-43-160-183	Oct. 30 1943
6.009 C	Radar Calibration Report—New York Region.	Maj. R. C. L. Timpson	Mitchell Field, N. Y.	Nov. 30 1943
6.010 S	Aden-Berbera VHF Experiments—Meteorological Conditions and Possible Correlations.	Lt. E. W. Walker	SRDE AC 5493/ USW or JMRP No. 14	Dec. 20 1943
6.011 S	Propagation Measurements on Polo Pony R/T Equipment.	TRE	TRE T 1609	Dec. 31 1943
6.012 C	Propagation over Short Paths and Rough Terrain at 200 Mc/s.	A. B. Vane D. G. Wilson	RL 468	Jan. 18 1944
6.013 S	Propagation and Reflection Characteristics of Radio Waves as Affecting Radar.	Lt. W. G. Michels Lt. W. C. Pomeroy	Army Air Forces Board Proj. No. (M-3) 11a	Jan. 31 1944
6.014 S	Microwave Propagation Measurements—Report Presented at NDRC Conference of Feb. 10-11, 1944.	F. H. Willis	BTL MM-44-160-55	Mar. 10 1944
6.015 S	Army Air Force Cold Weather Tests, Fairbanks, Alaska, Winter 1943-1944.	R. W. Griffiths	Western Elec. Co.	Apr. 20 1944
6.016 S	An Ultra-Short-Wave Field, Array Polar Diagram, and DF Survey (North Devon and Cornwall—Sept.-Oct., 1943).	D. A. Thorn W. J. Bray J. H. H. Merriman R. J. Harris S. D. Whiddett H. Prain	POED RR No. 1141	Apr. 29 1944
6.017 C	An Estimation of the Incidence of Anomalous Propagation in the Cook Strait Area of New Zealand from Jan., 1943 to Jan., 1944.	F. E. S. Alexander	RDL-DSIR NZ RD 1/373	May 2 1944
6.018 S	K-Band Radar Transmission—A Preliminary Report of Tests Made Near Atlantic Highlands, N. J., between December, 1943 and April, 1944.	G. C. Southworth A. P. King S. D. Robertson	BTL MM-44-160-115	May 19 1944
6.019 S	Effect of Pulse Length on System Performance and Operation.	R. Rollefson A. H. Nelson L. A. Hartman	RL 571	May 30 1944
6.020 S	Report on Cross Channel Propagation of British No. 10 Set.	K. R. Spangenberg	OCSO OAB-2	Aug. 26 1944



<i>Bib. No.</i>	<i>Title</i>	<i>Author or Source</i>	<i>Number</i>	<i>Date</i>
6.000 PROPAGATION EXPERIMENTS ( <i>continued</i> )				
6.021 C	Radar Range and Signal Strength.	L. Jofey A. C. Cossor, Ltd. Res. Dept., Myra Works London E10	MR 142	Aug. 1944
6.022 C	Results of Microwave Propagation Tests on the New York-Neshanic Path—Case 37003-4, File 36691-1.	A. L. Durkee	BTL MM-44- 160-190	Aug. 28 1944
6.023 C	Height-Gain Tests in the Troposphere	G. A. Isted (BRL)	BRL TR 488 or JEIA 5560 or JMRP No. 36	Sept. 1944
6.024 S	Interim Report on Investigation of 120 Mc/s. and 50 cm. Propagation Across the English Channel.	W. R. Piggott	AC 7081/ USW	Oct. 4 1944
6.025 C	Measurements of the Angle of Arrival of Microwaves in the X-Band (Case 20564).	W. M. Sharpless	BTL-MM- 44-160-249	Nov. 7 1944
6.026 C	Over-Water Transmission Measurements, 1944—Part I: Preliminary Analysis of Radio and Radar Measurements.	P. J. Rubenstein	RL 649	Dec. 15 1944
6.027 S	The Vertical Distribution of Field Strength over the Sea Under Conditions of Normal and Anomalous Propagation.	Maj. J. A. Ramsay CAEE & RRDE P. B. Blow (CAEE)	RRDE Res. Rep. No. 267	Jan. 5 1945
6.028 C	Centimetre Wave Propagation over Sea. A Study of Signal Strength Records Taken in Cardigan Bay, Wales, between February and September, 1944.	R. L. Smith-Rose A. C. Stickland (NPL)	DSIR RRB/ C 114 or JMRP No. 50	Feb. 28 1945
6.029 S	Over-Water Tests on S-Band Early Warning for Ships. Vertical Coverage of the CXHR (SCI) Search System.	W. O. Gordey D. T. Drake M. Kessler	RL 703	Mar. 5 1945
6.030 S	Preliminary Report on S- and X-Band Propagation in Low Ducts Formed in Oceanic Air.	M. Katzin	NRL R-2493	Mar. 24 1945
6.031 C	Atmospheric Refraction under Conditions of a Radiation Inversion.	L. J. Anderson J. P. Day C. H. Freres R. U. F. Hopkins J. B. Smyth Lt. A. P. D. Stokes	NRSL WP-19	Apr. 21 1945
6.032 R	Radio-Meteorological Relationships.	E. C. S. Megaw F. L. Westwater	AC 8140/ USW138	May 4 1945
6.033 S	Calculated Relationship Between Signal Level and Uniform Gradient of Refractive Index for the Irish Sea Paths.	E. C. S. Megaw (GEC)	GEC No. 8656 AC 8225/ USW 141	Apr. 19 1945
6.034 R	Radio-Meteorological Relationships. General Summary of Papers AC 8140/USW 138 and AC 8225/USW 141.	E. C. S. Megaw F. L. Westwater	AC 8336/ USW 149	1945
6.035 C	General Summary Covering the Work of the KXS Inter-Service Trials, LLANDUDNO, 1944.	J. R. Atkinson	TRE T1770 JMRP No. 64	May 1945
6.036 S	X-Band Trials at Rosehearty.	J. R. Atkinson	AC 8228/ USW 142 JEIA 10401	May 28 1945
6.037 C	S- and X-Band Propagation in Low Ocean Ducts. (See 6.030.)	R. W. Bauchman, Lt. W. Binnian, Lt.	NRL R-2565	July 5 1945
7.000 METEOROLOGICAL THEORY				
7.001 C	The Diffusive Properties of the Lower Atmosphere.	O. G. Sutton Chemical Defense Experimental Station	MRP 59 Air Min. Met. Res. Com.	Dec. 29 1942



<i>Bib. No.</i>	<i>Title</i>	<i>Author or Source</i>	<i>Number</i>	<i>Date</i>
7.000 METEOROLOGICAL THEORY ( <i>continued</i> )				
7.002	Meteorology for Pilots.	B. C. Haynes	U.S. Dept. Commerce— Civil Aero. Bul. No. 25	Jan. 1943
7.003 R	A Study of the Effect of the Meteorology on the Refraction of Radio Beams.	H. Raymond	CESL T-2	May 4 1943
7.004 R	The Rapid Reduction of Meteorological Data to Index of Refraction.	L. J. Anderson F. R. Abbott	NRSL WP-8	Dec. 10 1943
7.005 S	Application of Diffusion Theory to Radio Refraction Caused by Advection.	P. M. Woodward	TRE T 1647	Apr. 6 1944
7.006 C	Qualitative Survey of Meteorological Factors Affecting Microwave Propagation.	I. Katz J. M. Austin	RL 488	June 1 1944
7.007	Suggested Programme of Observational Investigation into Profiles in the Lower Atmosphere (HQ Air Command, SE Asia, New Delhi).	H. G. Booker (TRE)	TRE S No. 9831	July 29 1944
7.008 R	Analysis of Meteorological Ascents off New England.	TRE  R. A. Finlayson	Preliminary TRE M/Memo 22/ RAF Revised TRE T 1774 or JMRP No. 54	Sept. 7 1944  1945
7.009 C	The Influence of Ground Contour on Air Flow (Translation).	P. Queney Translated by W. M. Elsasser	CUDWR WPG-4	Sept. 1944
7.010 R	Radio-Meteorological Tables.	TRE	TRE T 1724 or JMRP No. 30	
7.011 C	Modified Index Distribution Close to the Ocean Surface.	R. B. Montgomery R. H. Burgoyne	RL 651	Feb. 16 1945
7.012 R	Report of an Investigation of Subsidence in the Free Atmosphere.	Sverre Petterssen P. A. Sheppard C. H. B. Priestley K. R. Johanssen	SDTM 94 or JMRP No. 49	Sept. 29 1944
7.013 R	The Influence of Atmospheric Stability on Air Flow.	Lt. Commander F. L. Westwater	AC 7892/ USW 126 or JMRP No. 57 or JEIA 10395	Mar. 7 1945
7.014	The Slopes of Isopycnic Surfaces in the Lower Atmosphere.	Met. Office Air Ministry	JMRP No. 48	Mar. 29 1945
7.015 C	Tables for Computing the Modified Index of Refraction M.	E. R. Wicher	CUDWR WPG-8	March 1945
7.016 R	Nomograms for Computation of Modified Index of Refraction.	R. H. Burgoyne	NDRC Div. 14 RL 551	Apr. 6 1945
7.017	Note on Errors in Measurement of the Refractive Index of the Air for High Frequency Radio Waves Consequent upon Errors in Meteorological Measurements. Addendum: Note on Errors in Evaluation of Refractive Index of the Air for Ultra-Short Radio Waves from the Data Obtained on the Rye Tower.	G. A. Bull  K. Stormonth	JMRP No. 51  Addendum JMRP No. 51	April 1945



<i>Bib. No.</i>	<i>Title</i>	<i>Author or Source</i>	<i>Number</i>	<i>Date</i>
8.000 METEOROLOGICAL EXPERIMENTS				
8.001	Weather in the Indian Ocean to Latitude 30° S. and Longitude 95° E. including the Red Sea and Persian Gulf.	MO	MO 451b (7)	1940
8.002	Weather on the Australia Station.		RAAF Publication No. 252 Vol. II	July '42 Reprinted Sept. '43
8.003 S	Note on the Hydrolapse in the First 1000 Ft. of the Atmosphere.	W. C. Swinbank	MO SDTM No. 52	July 12 1943
8.004 S	Meteorological Report in Connection with VHF Wireless Experiment Between Aden and Berbera (1943).	Squadron Leader Frith	AC 5492/ USW or JMRP No. 13	Oct. 30 1943
8.005	Meteorological Measurements (Irish Sea Experiments).	Inter-Service Cm. Wave Prop. Research NMS		
	Ship Glen Strathallan.		S JEIA-2778 S HM 3/44 S JEIA-3059 C JEIA-3522 C JEIA-3520 S JEIA-3607 C JEIA-3523 S HM 3/44 S JEIA-3864 C JEIA-4123 C JEIA-4284 C JEIA-4729 C HM 3/44 C JEIA-5533 C HM 3/44 C JEIA-6185 C HM 3/44 C HM 3/44 C JEIA-6875 C JEIA-7309 C JEIA-8522 C JEIA-3521 C JEIA-5207 C JEIA-5525 C JEIA-6850 C JEIA-6874 C JEIA-7307 C*JEIA-8521 C JEIA-4730 C JEIA-4915 C JEIA-6438 C HM 3/44 C HM 3/44 C*JEIA-8257	11/1-5/43 1/14-17/44 3/5-8/44 3/14-16/44 3/17-18/44 3/22-25/44 3/27-29/44 4/3-4/44 4/10-13/44 4/21-23/44 4/27-30/44 5/6-10/44 5/28-31/44 6/21-7/7/44 7/17-22/44 7/24-28/44 8/10-13/44 8/26-30/44 10/6-10/44 10/22-23/44 7/11-14/44 12/15/43 6/17-20/44 6/9-27/44 7/11-20/44 10/10-11/44 10/25-26/44 7/3-6/44 5/19-30/44 6/1-5/44 7/24-27/44 8/19-21/44 8/26-29/44 7/30-8/2/44
	Ship Coila.			
	Ship St. Dominica.			
8.006	Tables of Temperature and Humidity Observations at Rye.	MO	JMRP No. 5	Nov. 1943
8.007 S	Meteorological Information from Radar Stations being Circular Issued to RDF Stations and Fighter Sectors.	Australian	Australia No. 405 or JMRP No. 12	Dec. 7 1943



<i>Bib. No.</i>	<i>Title</i>	<i>Author or Source</i>	<i>Number</i>	<i>Date</i>
8.000 METEOROLOGICAL EXPERIMENTS ( <i>continued</i> )				
8.008 R	Low Altitude Measurements in New England to Determine Refractive Index—1943.	R. H. Burgoyne I. Katz	RL Rep. 42-2/22/44	Feb. 22 1944
8.009 S	Climate in Relation to Microwave Radar Propagation in Panama.	A. E. Bent	RL 476	Feb. 25 1944
8.010 S	The Vertical Distribution of Temperature and Humidity at Rye on the Night of January 14-15, 1944.	MO	JMRP No. 6 or JEIA 10318	Feb. 26 1944
8.011 S	Analysis of Temperature and Humidity Records at Rye.	MO	JMRP No. 7 or JEIA 10319	Feb. 1944
8.012 S	Radio Climatology of the Persian Gulf and Gulf of Oman with Radar Confirmation.	H. G. Booker	TRE T 1642	Mar. 15 1944
8.013 R	Stations in the Western Hemisphere with Conditions in the Lower Layers of the Atmosphere Similar to Those at Selected Stations in the Eastern Hemisphere.	Weather Div. HQ, AAF	Rep. No. 729	March 1944
8.014 C	Rain Cloud Weather Reports Associated with the Frontal Passage of 17-20 December, 1943.	A. J. Oliver, Sergeant, AC	6th Weather Region Res. Section APO No. 825	April 1944
8.015	Some Extracts from Rye Records during April-May, 1944.	MO	JMRP No. 20 or JEIA 10321	Apr.-May 1944
8.016	Extract from Rye Records of Temperature and Humidity Gradients during Selected Radiation Nights, March, 1944.	MO	JMRP No. 18 or JEIA 10320	May 4 1944
8.017	Some Values of the Refractive Index of the Atmosphere at Rye.	MO 8	S 100958 or JMRP No. 23 or JEIA 10322	June 1-6 1944
8.018 C	Low-Level Meteorological Soundings and Radar Correlation for the Panama Canal Zone.	K. E. Fitzsimmons S. T. Stephenson R. W. Bauchman	Wash. State Coll. Rep. No. 6 NDRC PDRC-647	June 12 1944
8.019 C	Wave Propagation Report No. 3.	Naval Res. Group Canal Zone	Intel. Br. OCSO Canal Zone 413.44/ R113	July 1 1944
8.020 S	KXS Inter-Service Trials at LLANDUDNO Report of Colloquium held on June 27 & 28 at ADRDE, LLANDUDNO to Discuss the Results of the Trials up till that Date and to Define the Future Programme.	ADRDE	Part I	Aug. 31 1944
	Minutes of a Meeting of the Radar Section of an Inter-Service Conference held at LLANDUDNO on June 28, 1944—Appendix with Figures. Appendix I, II, III.	ADRDE	Part II	Aug. 31 1944
	Minutes of a Meeting of the Meteorological Section of an Inter-Service Conference held at ADRDE, LLANDUDNO, June 28, 1944.	ADRDE	Part III	July 10 1944
8.021 C	Preliminary Analysis of Height-Gain Tests in the Troposphere.	R. F. C. McDowell	BRL TR 494 or JEIA 5777	Sept. 1944
8.022	Diurnal Variation of Temperature and Humidity at Various Heights at Rye.	MO 8	S 100958 or JMRP No. 26 or JEIA 10323	Oct. 21 1944
8.023 C	Report on General Climatic & Meteorological Conditions in Banda Sea. (4°—7° S., 126°—131° E.)	Directorate of Meteorological Services	RAAF Met. Res. Rep. List No. 2 Sect. II Series 7 No. 18	Nov. 1944



<i>Bib. No.</i>	<i>Title</i>	<i>Author or Source</i>	<i>Number</i>	<i>Date</i>
8.000 METEOROLOGICAL EXPERIMENTS ( <i>continued</i> )				
8.024	Hourly Values of Modified Refractive Index (M) for Meteorological Office, Rye, May, 1944.	MO	JMRP No. 31 or JEIA 10325	Dec. 28 1944
8.025 C	Temperature and Humidity Measurements Made with the Washington State College Wired Sonde Equipment at Kaikoura, New Zealand, Between Sept. 22, 1944 and Oct. 19, 1944.	F. E. S. Alexander	RDL-DSIR NZ RD 1/482	Jan. 15 1945
8.026 C	Fleet Weather Central Paper No. 10. Part I: Highlights of the December, 1944 Typhoon Including Photographic Radar Observations. Part II: A Distant Observation of a Warm Front Including a Photograph of Cloud Forms and Slope of Front.	G. F. Kosco, Cmdr., USN	Fleet Weather Central Paper No. 10	Feb. 10 1944
8.027 C	Results of Low Level Atmospheric Soundings in the Southwest and Central Pacific Oceanic Areas.	P. A. Anderson K. E. Fitzsimmons G. M. Grover S. T. Stephenson	Wash. State Coll. Rep. No. 9 NDRC PDRC-647	Feb. 27 1945
8.028 C	<sup>1</sup> Centimetre Wave Propagation over Sea. Correlation of Radio Field Strength Transmitted Across Cardigan Bay, Wales with Gradient of Refractive Index Obtained from Aircraft Observations.	R. L. Smith-Rose A. C. Stickland	DSIR RRB/ C121 or JEIA 9813	May 10 1945
9.000 METEOROLOGICAL EQUIPMENT				
9.001	Brief Comparison of Air Temperature Thermometers Used and Tested at A & AEE For Meteorological Work.	R. M. Goody	A & AEE MRP 117	
9.002 C	Project for Making Gee Meteorological Observations on Certain CH Towers.	TRE	TRE M/Memo/2	Jan. 3 1943
9.003 S	Balloon Psychrometer for the Measurement of the Relative Humidity of the Atmosphere at Various Heights. Also Addendum.	S. M. Doble Addendum: S. M. Doble S. Inglefield	ICI	Apr. 1, '43 Addendum Sept. 25, '43
9.004	A Distant Reading Electrical Air Temperature Thermometer Employing a Balanced Bridge Suitable for Use in Aircraft.	A. W. Brewer	MO MRP 112	June 21 1943
9.005	The Cambridge Aircraft Electrical Resistance Thermometer—Notes on Its Use.	A. W. Brewer	MO MRP 113	June 21 1943
9.006 S	Measurement of Atmospheric Humidity in Aircraft by Dew-Point Hygrometer.	G. M. B. Dobson A. W. Brewer B. Cwilog	MO MRP 126	Aug. 12 1943
9.007 C	The Captive Radiosonde and Wired Sonde Techniques for Detailed Low-Level Meteorological Sounding.	P. A. Anderson C. L. Barker K. E. Fitzsimmons S. T. Stephenson	Washington State Coll. Rep. No. 3 NDRC- PDRC-647	Oct. 4 1943
9.008 C	A Comparison of Three Types of Cup Anemometer at Low Velocities.	R. G. Dickinson H. S. Johnston	NDRC-Div. 10 Informal Rep. No. 10.3A-38	Oct. 26 1943
9.009 C	A Remote Indicating Cup Anemometer with Magnetic Coupling.	R. G. Dickinson D. L. Kraus	NDRC-Div. 10 OSRD Rep. No. 3714	Apr. 10 1944
9.010 C	An Apparatus for Temperature Profile Measurement.	R. G. Dickinson R. L. Mills H. S. Johnston	NDRC Div. 10 Informal Rep. No. 10.3A- 45	Apr. 11 1944



<i>Bib. No.</i>	<i>Title</i>	<i>Author or Source</i>	<i>Number</i>	<i>Date</i>
9.000 METEOROLOGICAL EQUIPMENT ( <i>continued</i> )				
9.011 R	Instruments and Methods for Measuring Temperature and Humidity in the Lower Atmosphere.	I. Katz	RL 487	Apr. 12 1944
9.012 C	Anomalous Propagation—Adaptation of Model RAU-2 Radio Sonde Receiving and Recording Equipment for Use as Low Level Sounding Device.	Friez Instrument Div.—Bendix Aviation Corp.	Navy Dev. Project Unit No. 1	May 31 1944
9.013 R	Meteorological Investigation at Rye—Part I—Instrumental Layout for Recording Gradients of Temperature and Relative Humidity.	Instruments Branch MO 4	JMRP No. 17	May 1944
9.014 C	Notes on Operational Use of Low-Level Meteorological Sounding Equipment.	K. E. Fitzsimmons S. T. Stephenson R. W. Bauchman	Washington State Coll. Rep. No. 7 NDRC-PDRC-647	June 15 1944
9.015 C	Microwave Propagation Studies—Detection of Troposphere Stratification by Means of Sound Echoes—Preliminary Trial—Case 37003.	H. B. Coxhead F. H. Willis BTL	BTL MM-44-160-143	June 21 1944
9.016 C	Operating Instructions for the WSC Low-Level Atmospheric Sounding Equipment.	P. A. Anderson	Washington State Coll. Rep. No. 8 NDRC-PDRC-647	July 10 1944
9.017 C	Meteorological Equipment for Short Wave Propagation Studies.	W. M. Elsasser	CUDWR WPG-3	August 1944
9.018 R	Wired Sonde Equipment for High Altitude Soundings. (See 9.022.)	L. J. Anderson	NRSL WP-16	Nov. 17 1944
9.019 C	Airborne Radiosonde Recorder.	A. E. Bennett	Intel. Br. OCSO USA 413.6	Mar. 10 1945
9.020	KXS Trials—LLANDUDNO June to Sept., 1944. Lower Atmosphere Radio-Meteorological Flight Technique.	F/Lt. J. Cocheme (RAF)	JMRP No. 55	
9.021 R	A Note on the Resistance of Electric Hygrometer Elements.	L. J. Anderson S. T. Stephenson	NRSL AERO-1	May 8 1945
9.022 R	Improvements in USNRSL Meteorological Sounding Equipment. (See 9.018.)	L. J. Anderson S. T. Stephenson Lt. A. P. D. Stokes	NRSL WP-21	July 3 1945
10.000 RADAR FORECASTING				
10.001 S	Forecasting of RDF Conditions.	AORG	AORG Memo No. 103 or JMRP No. 2	May 31 1943
10.002	The Meteorological Aspects of Anomalous Propagation—Short Wave Radio.	F/Lt. R. W. Hatcher	JMRP No. 1	June 1943
10.003 S	Oboe Propagation, Aug.- Oct., 1943.	H. G. Booker	TRE T1605	1943
10.004	“Naviprop” Forecasts.	E. Gold (MO)	SIS No. 45	Nov. 8 1943
10.005 S	Issue of ANOPROP Forecasts—Synoptic Instruction Special No. 39.	MO	SIS No. 39	Feb. 11 1944
10.006 S	Elements of Radio Meteorological Forecasting (Mathematics Group, TRE, Malvern).	H. G. Booker	TRE T 1621	Feb. 14 1944
10.007 C	Preliminary Instruction Manual—Weather Forecasting for Radar Operations.	Weather Div. HQ, AAF	Rep. No. 614	March 1944
10.008 R	Tropospheric Weather Factors Likely to Affect Superrefraction of VHF-SHF Radio Propagation as Applied to the Tropical West Pacific.	E. Dillon Smith R. D. Fletcher	U.S. Weather Bureau RP-1	July 1 1944



<i>Bib. No.</i>	<i>Title</i>	<i>Author or Source</i>	<i>Number</i>	<i>Date</i>
10.009 C	Preliminary Instruction Manual of Weather Forecasting for Radar Operations in South West Pacific Area.	D. F. Martyn P. Squires	CSIR- RL RP 220	Sept. 4 1944
10.010 C	Outline of Radio Climatology in India and Vicinity.	H. G. Booker	TRE T1727 or JEIA 6061 or JMRP No. 25	Sept. 12 1944
10.011	Notes on TRE Report T.1727—JMRP No. 25 (Radio Climatology in India and Vicinity).	C. S. Durst (MO)	JMRP No. 27 JEIA 10324	Nov. 7 1944
10.012	A Note on the Forecasting of AP (Provisional Draft).	TRE		Sept. 1944
10.013 R	A Rough Sketch of World Radio Climatology over Sea.	H. G. Booker	TRE T1730	Oct. 31 1944
10.014 C	American Continents Meteorological Counterparts of Western Pacific and Indian Ocean Areas as Applied to Tropospheric Radio Propagation.	J. H. Brown J. L. Paulhus E. Dillon Smith	U.S. Weather Bureau RP-2	Nov. 15 1944
10.015 R	The Possibility of Investigating the Föhn Wind and Sea Breeze Phenomena in N.Z. with A View to Elucidating Certain Problems of Radio-Meteorological Forecasting in Other Parts of the World.	M. A. F. Barnett F. E. S. Alexander	RDL-DSIR-NZ RD 1/471 or JEIA 7469	Dec. 1 1944
10.016 C	Determination of a Suitable Method of Forecasting Radar Propagation Variations over Water.	Lt. J. R. Gerhardt Lt. W. E. Gordon	AAF Bd. Proj. #4252R000.77	Mar. 10 1945
10.017 C	A Qualitative Outline of the Radio Climatology of Australasia.	H. G. Booker	TRE T1820 or JMRP No. 53	Apr. 19 1945
10.018 C	<sup>b</sup> Determination of the Practicability of Forecasting Meteorological Effects on Radar Propagation.	Lt. J. R. Gerhardt Lt. W. E. Gordon	AAF Bd. Proj. 3767B000.93	June 13 1945

## 11.000 ATMOSPHERIC ABSORPTION AND SCATTERING

11.001 S	Absorption of 1 Cm. Radiation by Rain.	M. G. Adam R. A. Hull C. Hurst	CVD-CL Misc. 3	
11.002 C	The Absorption of Ultra-Short Wireless Waves in the Water Vapour of the Earth's Atmosphere.	J. A. Saxton (NPL)	RRB/ C 18	Feb. 14 1941
11.003 S	Echo Intensities and Attenuation Due to Clouds, Rain, Hail, Sand and Duststorms at Centimeter Wavelengths.	J. W. Ryde (GEC)	GEC No. 7831	Oct. 13 1941
11.004 C	The Atmospheric Absorption of Microwaves.	J. H. Van Vleck	RL 43-2	Apr. 27 1942
11.005 S	The Effect of Rain upon the Propagation of 1 Cm. Electro-magnetic Waves—Case 22098.	S. D. Robertson (BTL)	MM-42- 160-87	Aug. 1 1942
11.006 S	The Effect of Rain on the Propagation of Microwaves—Case 22098.	A. P. King S. D. Robertson	MM-42- 160-93	Aug. 26 1942
11.007 S	Comparison of Theoretical and Experimental Values for the Attenuation of 1 Centimeter Waves in Rain—Case 22098.	S. D. Robertson (BTL)	MM-43- 160-2	Jan. 5 1943
11.008 S	An Investigation on the Number and Size Distribution of Water Particles in Nature.	Josef Mazur F/Lt. Polish Air Force	Met. Res. Com. MRP 109	June 1943
11.009	Report on the Absorption and Refraction of Electromagnetic Waves by the Liquid Water, Water Vapour and Fog or Rain.	N. F. Mott	CRB 43/2881	Sept. 2 1943
11.010	Report on the Absorption of Electromagnetic Waves in the Wavelength Range 1-100 Cm. by Water in the Atmosphere.	N. F. Mott	CRB 43/2882	Sept. 2 1943
11.011 C	Progress Report on "Verification of Mie Theory-Calculations and Measurements of Light Scattering by Dielectric Spherical Particles.	V. K. LaMer	OSRD 1857 Div. 10 NDRC	Sept. 29 1943



<i>Bib. No.</i>	<i>Title</i>	<i>Author or Source</i>	<i>Number</i>	<i>Date</i>
11.000    ATMOSPHERIC ABSORPTION AND SCATTERING ( <i>continued</i> )				
11.012 S	The Absorption of Centimetric Radiation by Atmospheric Gases.	J. M. Hough (ADRDE)	USWP WC	Apr. 27 1944
11.013 S	Attenuation Due to Water Drops in the Atmosphere.	J. M. Hough (ADRDE)	USWP WC	Apr. 28 1944
11.014 S	Propagation of K/2 Band Waves.	G. E. Mueller BTL	MM-44- 160-150	July 3 1944
11.015 S	Interim Report of the USW Panel Working Committee.	USWP WC	AC 7375/ USW or JEIA-7607	Aug. 14 1944
	Part I Water in the Atmosphere.	A. C. Best MO		July 18 1944
	Part II The Attenuation of Centimetre Waves by Atmospheric Gases.	J. M. Hough RRDE		July 1944
	Part III Attenuation of Centimetre Waves by Rain, Hail and Clouds.	J. W. Ryde D. Ryde GEC	GEC 8516	Aug. 3 1944
	Part IV The Attenuation of Centimetre Waves by Rain.	J. M. Hough RRDE		Aug. 1944
11.016 S	Preliminary Note on Secure Communications on Millimetre Waves.	TRE	L/M40/WBL or JEIA 5597	Sept. 11 1944
11.017 C	Rotational Line Width in the Absorption Spectrum of Atmospheric Water Vapor and Supplement.	Arthur Adel	NDRC Div. 14 No. 320 Univ. of Michigan	Oct. 10 1944 Supp. Feb. 1 1945
11.018 C	The Absorption of One-Half Centimeter Electromagnetic Waves in Oxygen.	E. R. Beringer	RL 684	Jan. 26 1945
11.019 S	The Effect of Rain on Radar Performance.	S. C. Hight	BTL MM-44-170-50	Oct. 17 1944
11.020 S	Measurements of Wave Propagation.	G. E. Mueller	BTL MM-45-160-17	Feb. 5 1945
11.021 C	Further Theoretical Investigations on the Atmospheric Absorption of Microwaves.	J. H. Van Vleck	RL 664	Mar. 1 1945
11.022 S	Measurements of the Attenuation of K-Band Waves by Rain.	G. T. Rado	RL 603	Mar. 7 1945
11.023 S	Attenuation of Centimetre and Millimetre Waves by Rain, Hail, Fogs and Clouds. (Draft.)	J. W. Ryde D. Ryde	GEC 8670	May 18 1945
11.024 C	The Relation Between Absorption and the Frequency Dependence of Refraction.	J. H. Van Vleck	RL 735	May 28 1945
11.025 S	Absorption and Scattering of Microwaves by the Atmosphere.	L. Goldstein	CUDWR WPG-11	May 1945
11.026 S	CVD Progress Report for May, 1945. Part I The Absorption of K-Band Radiation in Gaseous Ammonia.		CVD CL Prog. Rep. 5/45	May 1945
11.027 S	<sup>1</sup> K-Band Attenuation Due to Rainfall.	L. J. Anderson J. P. Day C. H. Freres J. B. Smyth Lt. A. P. D. Stokes L. G. Trolese	NRSL WP-20	June 8 1945
12.000    DIELECTRIC CONSTANT AND LOSS FACTOR				
12.001 R	A New Method for Measuring Dielectric Constant and Loss in the Range of Centimeter Waves. Wave Guides with Dielectric Sections.	S. Roberts A. von Hippel L. J. Chu	MIT 102	March 1941



<i>Bib. No.</i>	<i>Title</i>	<i>Author or Source</i>	<i>Number</i>	<i>Date</i>
12.000 DIELECTRIC CONSTANT AND LOSS FACTOR ( <i>continued</i> )				
12.002 C	The Electrical Properties of Ice.	T. A. Taylor W. Jackson	AC 1516/ RDF 110 Com. 78	Dec. 22 1941
12.003 C	The Dielectric Constant and Loss Factor of Water Vapour at a Wavelength of 9 Cms. (Frequency—3330 Mc/s.)	J. A. Saxton (NPL)	DSIR RRB/S.1	Mar. 31 1942
12.004 C	The Dielectric Constant of Water Vapour and its Effect upon the Propagation of Very Short Waves.	A. C. Stickland (NPL)	DSIR RRB/S.2	May 11 1942
12.005 C	Progress Report on Ultrahigh Frequency Dielectrics.	A. von Hippel	Div. 14 NDRC Rep. No. 121	January 1943
12.006 S	Conductivities of Sea, Tap and Distilled Water at $\lambda=10$ cm.	L. B. Turner	ASE M.496	April 1943
12.007 C	The Measurement of Dielectric Constant and Loss with Standing Waves in Coaxial Wave Guides.	A. von Hippel D. G. Jelatis W. B. Westphal	Div. 14 NDRC Rep. No. 142	April 1943
12.008 S	The Dielectric Constant and Absorption Coefficient of Water Vapour for Wavelengths of 9 cm. and 3.2 cm. (Frequencies 3,330 and 9,350 Mc/s.)	J. A. Saxton (NPL)	DSIR RRB/S.11	June 14 1943
12.009	Electrical Measurements on Soil with Alternating Currents.	R. L. Smith-Rose	JIEE (London) 75, 221-237	Aug. 1943
12.010 C	Auxiliary Equipment for the MIT CO-AX Instrument and Its Use.	A. von Hippel D. G. Jelatis W. B. Westphal M. G. Haugen R. E. Charles	Div. 14 NDRC Rep. No. 210	Nov. 1943
12.011 S	Memorandum on an Electrical Method of Measuring the Dielectric Constant of Atmospheric Air, and Recording it Continuously.	TRE	TRE M/Memo 15/ PEC or JMRP No. 8	Jan. 6 1944
12.012 S	The Dielectric Constant and Absorption Coefficient of Water Vapour for Radiation of Wavelength 1.6 cm. (Frequency 18,800 Mc/s.)	J. A. Saxton (NPL)	DSIR RRB/S.17	Apr. 22 1944
12.013 S	The Dielectric Constant of Water and Ice at Centimetre Wavelengths (Working Committee).	J. M. Hough (ADRDE)	USWP WC	Apr. 28 1944
12.014 S	Preliminary Report on the Dielectric Properties of Water in the K-Band.	C. H. Collie	CVD Rep. CL Misc. 25	May 1944
12.015 C	Transmission and Reflection of Single Plane Sheets. (Radome Bulletin No. 4.)	R. M. Redheffer	RL- 483-4	July 12 1944
12.016 C	Recent Dielectric Constant and Loss Tangent Measurements (on X-Band). (Radome Bulletin No. 5.)	E. M. Everhart	RL- 483-5	July 14 1944
12.017 S	Dielectric Properties of Water and Ice at K-Band.	E. L. Younker	RL 644	Dec. 4 1944
12.018 R	The Interaction Between Electromagnetic Fields and Dielectric Materials.	A. von Hippel R. G. Breckenridge	Div. 14 NDRC Rep. No. 122	Jan. 1943
12.019 C	The Dielectric Properties of Water at Wavelengths from 2 mm. to 10 cm. and over the Temperature Range 0° to 40° C.	J. A. Saxton (NPL)	DSIR RRB/C115	Mar. 20 1945
12.020 C	The Dielectric Properties of Water in the Temperature Range 0° C. to 40° C. for Wavelengths of 1.24 cm. and 1.58 cm.	J. A. Saxton J. A. Lane (NPL)	DSIR RRB/ C.116 or JEIA 9811	Mar. 7 1945
12.021	<sup>1</sup> The Anomalous Dispersion of Water at Very High Radio Frequencies in the Temperature Range 0° to 40° C.	J. A. Saxton (NLP)	DSIR RRB/ C.118 or JEIA 9812	Apr. 6 1945



<i>Bib. No.</i>	<i>Title</i>	<i>Author or Source</i>	<i>Number</i>	<i>Date</i>
13.000 REFLECTION COEFFICIENT				
13.001 C	Centimeter Wave Propagation over Sea Within the Optical Range.	H. Archer-Thomson J. C. Dix F. Hoyle E. C. S. Megaw M. H. L. Pryce	ASE M398	January 1942
13.002 S	Preliminary Report on the Reflection of 9 Cm. Radiation at the Surface of the Sea.	H. Archer-Thomson N. Brooke T. Gold F. Hoyle	ASE M542	Sept. 1943
13.003 C	Comment on the Reflection of Microwaves from the Surface of the Ocean—II.	S. O. Rice	BTL MM-43- 210-6	Oct. 13 1943
13.004 S	S-Band Measurements of Reflection Coefficients for Various Types of Earth.	E. M. Sherwood Sperry Gyroscope Co.	5220.129	Oct. 29 1943
13.005 C	Special Report on the Determination of the Coefficient of Reflection of Radio Waves at the Ground by Means of Radar Observations.	W. S. Ament	NRL RA 3A 212A	Nov. 10 1943
13.006	Scattering.	T. L. Eckersley BRL	JEIA 3904	November 1943
13.007 C	Preliminary Measurements of 10-Cm. Reflection Coefficients of Land and Sea at Small Grazing Angles.	P. J. Rubenstein W. T. Fishback	RL- 478	Dec. 11 1943
13.008 C	Further Measurements of 3 and 10-Cm. Reflection Coefficients of Sea Water at Small Grazing Angles.	W. T. Fishback P. J. Rubenstein	RL- 568	May 17 1944
13.009 C	Microwave Propagation Studies—The Reflection of Sound Signals in the Atmosphere—Case 37003—File 36691-1.	F. H. Willis	BTL MM-44- 160-156	July 3 1944
13.010 C	Interim Report on Experiments on Ground Reflection at a Wavelength of 9 cms.	L. H. Ford	DSIR RRB/C101 or JEIA 4899	July 7 1944
13.011 C	An Experimental Investigation of the Reflection and Absorption of Radiation of 9 cm. Wavelength.	L. H. Ford R. Oliver	DSIR RRB/C.107	Oct. 27 1944
13.012 R	The Measurement of High Reflections at Low Power (Radome Bulletin No. 7.)	R. M. Redheffer	RL- 483-7	Nov. 20 1944
13.013 C	Ground Reflection Coefficient Experiments on X-Band. (Case 20564.)	W. M. Sharpless BTL	BTL MM-44- 160-250	Dec. 15 1944
13.014 C	The Reflection Coefficient of a Linearly Graded Layer.	BRL	BRL TR 492	Dec. 1942
13.015 C	Reflection and Scattering.	T. L. Eckersley	BRL TR 506	Jan. 1945
13.016 S	Reflection from an Inversion.	L. E. Beglian F. J. Northover	AC 8210/ USW 140 or JEIA 9997	May 24 1945
14.000 HORIZONTAL AND VERTICAL POLARIZATION				
14.001	Notes on the Comparison of Vertical and Horizontal Polarization in Ground Wave Propagation.	G. Millington	BRL TR/442	January 1940
14.002 C	Horizontal and Vertical Polarization.	T. L. Eckersley	BRL TR/441	July 1942
14.003 S	The Investigation of Horizontally and Vertically Polarized Direction Finding on Frequencies of the Order of 20 to 70 Megacycles per Second.	T. L. Eckersley	BRL TR/451	Sept. 1942
14.004 S	Polarization Effects and Aerial System Geometry at Centimeter Wavelengths.	E. C. S. Megaw H. Archer-Thomson E. M. Hickin	GEC No. 8101	Nov. 26 1942



<i>Bib. No.</i>	<i>Title</i>	<i>Author or Source</i>	<i>Number</i>	<i>Date</i>
14.005 S	Change of Polarization as a Means of Gap Filling.	R. A. Hutner F. Parker B. Howard J. Gill	RL- C-7	Dec. 28 1942
14.006 S	Photographic Polarization Tests.	G. A. Garrett K. L. Mealey	RL- 93-3	May 7 1943
14.007 R	Vertical Polarization vs Horizontal Polarization (Tentative Report).	R. C. Loring	CESL No. T-1	Oct. 22 1943
14.008 S	The Depolarization of Microwaves.	M. Kessler C. E. Mandeville E. L. Hudspeth	RL 458	Nov. 1 1943
14.009 S	Polarization Studies at S and X Frequencies.	O. J. Baltzer W. M. Fairbank J. D. Fairbank	RL 536	Mar. 14 1944
14.010 S	Alexandria Palace Tests.	T. L. Eckersley	BRL TR/498	October 1944
15.000 EFFECT OF HILLS, TREES, OBSTACLES, ETC.				
15.001 C	Screening by Hills.	H. G. Booker	TRE T1015	May 1941
15.002	Diffraction Round a Sphere or Cylinder.	BRL	TR/433	March 1942
15.003 C	Centimeter Wave Transmission Measurements from an Urban Site.	H. Archer-Thomson E. M. Hickin E. C. S. Megaw	GEC No. 8034	July 28 1942
15.004 C	Report on an Investigation of the Propagation of Centimeter Waves over Ridges and Through Trees.	NPL	NPL AC 4345/ Com. 181	June 2 1943
15.005 S	A Note on the Propagation of K Band Waves Through Trees. Case 22098.	S. D. Robertson	BTL MM-43- 160-129	Aug. 13 1943
15.006 S	Report on Further Experiments on the Propagation of Centimeter Waves Through Trees in Leaf and over Level Ground.	NPL	NPL AC 5059/ Com. 197	Sept. 6 1943
15.007 S	Centimeter Wave Propagation. Notes on the Effect of Obstruction by a Single Tree.	R. E. Jennings E. C. S. Megaw H. Archer-Thomson E. M. Hickin	ASE M.565	Oct. 1943
15.008 S	An Experimental Investigation on the Propagation of Radio Waves over Bare Ridges in the Wavelength Range 10 Centimetres to 10 Metres (Frequencies 30 to 3000 Mc/s.).	J. S. McPetrie L. H. Ford NPL	DSIR RRB/ S.12	Oct. 1 1943
15.009 S	Some Observed Effects of Trees upon Microwave Propagation—Case 37003—File 36691-1.	A. C. Peterson	BTL MM-43- 160-150	9/17/43 Revised 10/15/43
15.010 R	Effect of Hills and Trees as Obstructions to Radio Propagation.	Jansky and Bailey	Cont. OEMsr- 1010: OSRD Rep. 3070	Nov. 1943
15.011 C	On Light Scattering by Spheres I.	L. Brillouin	AMG-C No. 100 NDRC-AMP No. 87.1	December 1943



<i>Bib. No.</i>	<i>Title</i>	<i>Author or Source</i>	<i>Number</i>	<i>Date</i>
15.000 EFFECT OF HILLS, TREES, OBSTACLES, ETC. ( <i>continued</i> )				
15.012	Report on Some Further Experiments on the Effect of Obstacles on the Propagation of Centimetre Waves.	L. H. Ford A. C. Grace J. A. Lane (NPL-RD)	AC 5876/ Com. 213 USW or JEIA 3157	Jan. 20 1944
	Addendum to Paper dated 20th January, 1944 entitled, "Report on Some Further Experiments on the Effect of Obstacles on the Propagation of Centimetre Waves."	L. H. Ford R. Oliver (NPL-RD)	AC 5876a/ Com. 213a USWa or JEIA 7911	Jan. 1 1945
15.013 C	On Light Scattering by Spheres II.	L. Brillouin	AMG-C No. 132 NDRC-AMP No. 87.2	April 1944
15.014 C	The Propagation of Ultra Short Waves Round Hills and Other Obstacles.	T. L. Eckersley	BRL TR.479 or JEIA-5674	May 1944
15.015 R	Scattering of Radio Waves by Metal Wires and Sheets.	F. Horner	DSIR RRB/ C.110 or JEIA 7793	Jan. 1 1945
15.016 R	Some Experiments on the Propagation over Land of Radiation of 9.2 cm. Wavelength.	L. H. Ford NPL	DSIR RRB/ C.113	Feb. 15 1945
15.017 C	A Method of Calculating the Polar Diagram of a Radio Equipment Standing on Flat Ground Looking over a Screen.	N. Corcoran J. M. Hough	RRDE Res. Rep. No. 280 or JEIA- 9113	Mar. 21 1945
15.018 C	A Preliminary Study of Ground Reflection and Diffraction Effects with Centimetric Radar Equipment.	J. S. Hey F. Jackson, Capt. S. J. Parsons, Maj.	AORG No. 274	June 28 1945
16.000 TRANSMISSION OVER PART LAND-PART SEA				
16.001 C	Diffraction at Coast Line: Sloping Site.	H. G. Booker	TRE Rep. No. 10	May 1 1941
16.002	Mixed Land and Sea Transmissions.	T. L. Eckersley	BRL E.16	October 1941
16.003 S	Diffraction at Coast Line: Further Numerical Examples.	H. G. Booker	TRE Rep. M/35	Feb. 5 1942
16.004 C	Coastal Refraction.	BRL	BRL TR/436	May 1942
16.005 C	Propagation of Wireless Waves over Ground of Varying Earth Constants (Part Land and Part Sea).	G. Millington	BRL Marconi TR/440	July 1942
16.006	Transmission over Ground of Varying Earth Constants.	BRL	BRL TR/473	July 1943
16.007 C	Diffraction at Coast Line. (Appendix to Report on Siting of RDF Stations).	H. G. Booker	TRE Rep. No. 6	Jan. 27 1944
16.008 C	Siting and Coverage of Ground Radars.	E. J. Emmerling, Capt., Signal Corps	CUDWR WPG-10	May 1945
17.000 TARGETS AND ECHOES				
17.001 C	Scattering and Spurious Echoes.	T. L. Eckersley	BRL TR 437	April 1942
17.002 C	Reflection of 10 Cm. Radiation by Model Aircraft.	A. F. Phillips	ADRDE Christchurch Rep. No. 174	Sept. 8 1942
17.003 S	Elementary Survey of Scattering and Echoing by Elevated Targets.	H. G. Booker	TRE M/48/HGB	Dec. 1942
17.004 S	The Resolution of Composite Echoes with Centimeter Wave RDF.	Maj. J. R. Benson Capt. J. A. Ramsay P. B. Blow (CAEE)	CAEE 4070/ C/104	Feb. 10 1943



<i>Bib. No.</i>	<i>Title</i>	<i>Author or Source</i>	<i>Number</i>	<i>Date</i>
17.000 TARGETS AND ECHOES ( <i>continued</i> )				
17.005 C	Microwave Radar Reflection.	J. F. Carlson S. A. Goudsmit	RL- 43-23	Feb. 20 1943
17.006 C	Reflection of Radar Waves from Targets of Simple Geometric Form.	L. J. Anderson J. B. Smyth F. R. Abbott	NRSL WP-3	Feb. 24 1943
17.007 S	Radar Echoes from Periscopes.	J. E. Freehafer	RL- 42-1	Mar. 1 1943
17.008 S	Possible Measurement of Radar Echoes by Use of Model Targets.	S. A. Goudsmit P. R. Weiss	RL- 43-24	Mar. 4 1943
17.009 S	Radar Echoes from Atmospheric Phenomena.	A. E. Bent	RL- 42-2	Mar. 13 1943
17.010 S	Echoes Produced by Perfectly Conducting Objects of Certain Simple Shapes in Free Space.	R. E. B. Makinson	DSIR RL 173	Mar. 25 1943
17.011 S	Gratings and Screens as Microwave Reflectors.	RL	RL- 54-20	Apr. 1 1943
17.012 S	Optimum Wavelength for Long Range CW Radar Systems.	W. W. Hansen	Sperry Gyroscope Co., Inc. Rep. No. 5220- 126	May 1 1943
17.013 S	Report on an Investigation into the Nature of Sea Echoes.	TRE	TRE T.1497	May 12 1943
17.014 S	The Application of Corner Reflectors to Radar (Theoretical).	R. D. O'Neil F. S. Holt P. D. Crout	RL- 43-31	May 14 1943
17.015 S	The Application of Corner Reflectors to Radar (Experimental).	R. D. O'Neil	RL- 55-4	July 1 1943
17.016 C	Measurement of the "Effective Echoing Areas" of Various Aircraft.	R. Bateman	OCSO ORG-P-8-1	July 2 1943
17.017 S	Overwater Observations at X and S Frequencies on Surface Targets.	O. J. Baltzer V. A. Counter W. M. Fairbank W. O. Gordy E. L. Hudspeth	RL- 401	July 26 1943
17.018 C	Towed Radar Targets.	G. A. Armstrong G. H. Beeching	ADRDE Res. Rep. No. 212	Aug. 6 1943
17.019 C	Corner Reflector Tests at Langley Field.	C. M. Gilbert	RL 402	Aug. 6 1943
17.020 S	Properties of Corner Reflectors—Case 22098.	S. D. Robertson	BTL MM-43- 160-130	Aug. 12 1943
17.021 S	Use of Corner Reflectors as IFF on Ships.	Australian ORS & CSIR-RL	Oper. Res. Rep. No. 24	Aug. 30 1943
17.022 C	An Investigation into the Nature of Sea Echoes.	A.C.Cossor, Ltd. Research Dept. Myra Works London E10	MR 109 or JEIA 1221	Sept. 8 1943
17.023 S	Bearing Markers for CA No. 1 Sets Provisional Instruction.	J. A. Ramsay	CAEE 70/ C/157 or JEIA 2771	Sept. 24 1943
17.024 S	Probability of Detection of Aircraft by RDF.	T. M. Cherry	CSIR-RL MUM.2 or JEIA 3954	Sept. 30 1943
17.025 S	The Scattering of Radiation from Rectangular Planes, Half-Cylinders, Hemispheres, and Airplanes.	Moore School of Engineering U. of Pa.	Contract W-2279 sc-551 Item 3	Oct. 12 1943



<i>Bib. No.</i>	<i>Title</i>	<i>Author or Source</i>	<i>Number</i>	<i>Date</i>
17.000 TARGETS AND ECHOES ( <i>continued</i> )				
17.026 R	The Theory of Random Processes.	G. E. Uhlenbeck	RL 454	Oct. 15 1943
17.027 C	On the Appearance of the A-Scope when the Pulse Travels Through a Homogeneous Distribution of Scatterers.	A. J. F. Siegert	RL- 466	Nov. 9 1943
17.028 C	On the Fluctuations in Signals Returned by Many Independently Moving Scatterers.	A. J. F. Siegert	RL- 465	Nov. 12 1943
17.029 S	The Use of Permanent Echo Amplitudes for Monitoring S Band Radar Equipment.	F. J. Kerr J. F. McConnell	CSIR-RL #RP 177/2	Dec. 7 1943
17.030 C	The Range Calculator.	S. J. Mason	RL- 497	Dec. 20 1943
17.031 S	The Performance of 10 Cm. Radar on Surface Craft.	B. F. Schonland	AORG Rep. No. 155	Jan. 3 1944
17.032 S	Special Report on Radar Cross Section of Ship Targets.	M. Katzin	NRL RA 3A 213A	Jan. 24 1944
17.033 S	Observations of Life Rafts Equipped with Corner Reflectors.	E. L. Hudspeth J. P. Nash	RL 533	Feb. 15 1944
17.034 S	Radar Cross Section of Ship Targets, II.	W. S. Ament M. Katzin F. C. MacDonald	NRL Rep. No. R-2232	Feb. 18 1944
17.035 S	Optical Theory of the Corner Reflector.	R. C. Spencer	RL- 433	Mar. 2 1944
17.036 S	Observations on Signal Stability at S and X Frequencies.	O. J. Baltzer W. M. Fairbank J. D. Fairbank	RL- 537	Mar. 14 1944
17.037 C	Interim Report on the Recognition of Radar Echoes.	F. E. S. Alexander	RDL-DSIR NZ RD 1/353 or JEIA 3401	Mar. 20 1944
17.038 S	Screened and Unscreened Radar Coverage for Surface Targets.	W. Walkinshaw J. E. Curran	TRE T.1666	March 1944
17.039 S	The Performance of Naval Radar Systems Against Aircraft.	F. Hoyle ASE	JEIA 3902	Apr. 3 1944
17.040 S	Preliminary Report on the Fluctuations of Radar Signals.	H. Goldstein P. D. Bales	RL- 569	May 16 1944
17.041 S	Radar Ranging on Land Targets.	TRE	TRE Memo No. 101/G 36/ ALH	May 18 1944
17.042 R	The Radar Echoing Power of Conducting Spheres.	T. Pearcey J. M. C. Scott	ADRDE CR 228	May 24 1944
17.043 S	Use of Corner Reflectors in Beaconry.	F. J. Kerr	CSIR-RL No. RP.200 or JEIA 5180	June 8 1944
17.044 C	Calibration and Standardization of Land Based Radars by the Use of Small Plane Targets.	F. R. Abbott	NRSL WP-12	June 10 1944
17.045 S	Test of the Pre-Production Model Corner Reflector Final Report Project No. E-44-37 AAF Board Project No. (M-3) 69, Eglin Field, Florida.		Intel. Br. OCSO USA 413.44/R387.1	June 17 1944
17.046 S	Radar Cross Section of Ship Targets, III.	W. S. Ament M. Katzin F. C. MacDonald	NRL Rep. No. R-2295	June 27 1944
17.047 S	Notes on Echoes and Atmospherics From Lightning Flashes on P-Band.	J. L. Pawsey	CSIR-RL No. RP 49.2 or JEIA 5177	July 11 1944
17.048 S	Theory of Ship Echoes as Applied to Naval RCM Operations.	T. S. Kuhn P. J. Sutro	RRL 411-93	July 14 1944



<i>Bib. No.</i>	<i>Title</i>	<i>Author or Source</i>	<i>Number</i>	<i>Date</i>
17.000 TARGETS AND ECHOES ( <i>continued</i> )				
17.049 S	Radar Echoes from the Nearby Atmosphere. Case No. 37003-4.	M. W. Baldwin, Jr.	BTL MM-44- 150-2	July 18 1944
17.050 S	Radar Cross Section of Ship Targets IV.	W. S. Ament M. Katzin F. C. MacDonald	NRL Rep. No. R-2332	July 21 1944
17.051 S	Radar Echoes from the Nearby Atmosphere—Second Report. Case No. 37003-4.	M. W. Baldwin, Jr.	BTL MM-44- 150-3	July 31 1944
17.052 C	Reflecting Properties of Metal Gratings.	J. S. Gooden	CSIR- RL No. RP 215	July 31 1944
17.053 S	Theory of the Performance of Radar on Ship Targets (ADRDE & CAEE Joint Report).	M. V. Wilkes (ADRDE) J. A. Ramsay P. B. Blow (CAEE)	ADRDE Ref. R04/2/CR252 or CAEE Ref. 69/C/149	July 1944
17.054 C	Corner Reflectors for Life Rafts.	E. L. Hudspeth J. P. Nash	RL- 608	Aug. 1 1944
17.055 C	The Characteristics of S-Band Aircraft Echoes with Particular Reference to Radar AA No. 3 MK II.	G. H. Beeching N. Corcoran	ADRDE Res. Rep. No. 253	Aug. 4 1944
17.056 S	Radar Echoes from the Nearby Atmosphere—Third Report. Case No. 37003-4.	M. W. Baldwin, Jr.	BTL MM-44- 150-4	Aug. 11 1944
17.057 C	Considerations Concerning Radar Coverage Diagrams.	J. L. Pawsey	CSIR RL RP-217	Aug. 14 1944
17.058 C	RDF Echoes to be Expected from Objects of Various Shapes.	Min. of Supply DSR	Extra Mural Res. F.72/80 Rep. No. 26	
17.060 S	Radar Echoes from Shell Bursts at 4 Meters and 50 cms. Wavelengths.	S. M. Taylor F. E. W. Bugler	RRDE Res. Rep. No. 260	Oct. 9 1944
17.061 S	Summer Storm Echoes on Radar MEW	J. S. Marshall R. C. Langille W. J. Palmer Capt. R. A. Rodgers Capt. G. P. Adamson Lt. F. F. Knowles	CAORG Rep. No. 18	Nov. 27 1944
17.062 S	The Cancellation of Permanent Echoes by the Use of Coherent Pulses (Interim Report).	H. Grayson	RAE Tech. Note No. RAD 253	Nov. 1944
17.063 C	The Fading of S-Band Echoes from Ships in the Optical Zone.	R. I. B. Cooper	RRDE Res. Rep. No. 265	Dec. 12 1944
17.064 S	Rotating Corner-Reflectors for Ship Identification.	J. M. Sturtevant	RL 654 NDRC Div. 14 OEMsr-262	Jan. 1 1945
17.065 R	Reflection from Smooth Curved Surfaces.	R. C. Spencer	RL 661	Jan. 26 1945
17.066 S	Analysis of Over-Water Tracking.	E. J. Campbell	RL 695	Feb. 12 1945
17.067 S	Technical Report on the Maximum Range of Detection of the German Early Warning Radar Equipment, Especially when Viewing Large, Tight Formations of Bomber Aircraft.	Lt. W. E. Bales K. A. Norton	ORS VIII Bomber Comm. OCSO OAD-13	Sept. 13 1943
17.068 S	Performance Checks and Estimation of Vessel Size on Shore Based 10 cm. Radar Sets.	D. Lack AORG	JEIA No. 3124	Mar. 30 1944



<i>Bib. No.</i>	<i>Title</i>	<i>Author or Source</i>	<i>Number</i>	<i>Date</i>
17.000 TARGETS AND ECHOES ( <i>continued</i> )				
17.069 S	Report of Trials to Determine the Variations of the Apparent Reflecting Point of Plain 10 Cm. Waves from a Destroyer.	J. F. Coales M. Hopkins	ASE M 627	July 1944
17.070 C	The Reflection of Electromagnetic Waves by Long Wires and Non-Resonant Cylindrical Conductors.	J. M. C. Scott T. Pearcey	RRDE Res. Rep. No. 259 or JEIA 7286	Nov. 13 1944
17.071 C	Theory of Radar Return from the Schnorkel.	P. M. Marcus	RL 671	Jan. 15 1945
17.072 S	Sea Returns and the Detection of Schnorkel. (See 17.077.)	G. G. Macfarlane	TRE T 1787 or JEIA 8643	Feb. 13 1945
17.073 S	Interservice KXS Band Radar Trials. Over Water Performance Against Surface Targets.	J. A. Ramsay, Maj., RA (CAEE & RRDE) P. B. Blow, WO II H. J. Worsdall (ASE)	ASE M 688 or JEIA 8820	February 1945
17.074 C	An Observation of Diffuse Cloud-Like Echoes.	L. J. Pawsey F. J. Kerr	CSIR RL RP 246	Mar. 6 1945
17.075 C	The So-Called Standard Target.	A. H. Brown	RL S-43	Mar. 10 1945
17.076 S	Radar Cross Section of Ship Targets V.	F. C. MacDonald	NRL R-2466	Mar. 12 1945
17.077 S	Radar Results Against Schnorkels: A Commentary on TRE T. 1787, "Sea Returns and the Detection of Schnorkel." (See 17.072.)	Coastal Command	ORS/CC Rep. No. 338 JEIA 9111	Mar. 16 1945
17.078 C	Radar Echoes from Clouds of Water Droplets.	F. Hoyle	AC 7930/ USW 128	Mar. 16 1945
17.079 C	Comments on "Radar Echoes from Water Droplets." (Paper AC 7930) USW 128	Lt. R. G. Ross	AC 7931/ USW 129	Mar. 16 1945
17.080 S	Radar Cross Section of Ship Targets VI.	W. J. Barr	NRL R-2467	Apr. 10 1945
17.081 C	S-Band Radar Echoes From Snow.	J. S. Marshall R. C. Langille W. M. Palmer (CAORG) L. G. Tibbles (Met. Ser.)	CAORG Rep. No. 26	June 14 1945
17.082 S	Surface Coverage of Some Shipborne Radar Sets on S, X, and K Bands.	J. D. Fairbank W. M. Fairbank	RL 720	June 15 1945
17.083 C	Echoes from Tropical Rain on X-Band Airborne Radar.	A. E. Bent	RL 728	June 15 1945
17.084 S	Analysis of Storm Echoes in Height Using MHF.	J. S. Marshall Lt. Col. L. G. Eon (CAORG) L. G. Tibbles (Met. Ser.)	CAORG Rep. No. 30	June 25 1945
17.085 S	<sup>k</sup> Radar Camouflage.	M. M. Andrew O. J. Baltzer E. L. Hudspeth (Project Chairman) C. E. Mandeville	RL 766	July 16 1945



<i>Bib. No.</i>	<i>Title</i>	<i>Author or Source</i>	<i>Number</i>	<i>Date</i>
18.000 DOPPLER EFFECT				
18.001 S	Flutter. A Method of Rapidly and Accurately Obtaining the Velocity of A Ship or Aircraft by RDF Using Doppler's Principle.	Australian Operational Research Group	Australia No. 296 Oper. Res. Rep. 21	
18.002 S	"S" Band Doppler Experiment—Case 20564.	W. M. Goodall C. F. P. Rose	BTL MM-43-160-173	Oct. 20 1943
18.003 S	The Detection of Moving Targets Among Ground Clutter by Coherent Pulse Methods.	R. A. McConnell	RL 480	Dec. 14 1943
18.004 S	The Elimination of Ground Clutter.	E. C. Pollard	RL 526	Mar. 13 1944
18.005 C	Pulse Doppler with Reference to Ground Speed Indication.	D. Sayre	RL 63-3/20/44	Mar. 20 1944
18.006 S	Pulse Doppler for Detection of Moving Ground Targets.	R. F. Thomson	RL 553	Apr. 21 1944
18.007 S	Anti-Clutter in North America (Report on A Visit to U.S. and Canada).	W. S. Elliot	Intel. Br. GB 413.44/ R170	August 1944
18.008 S	Tests on the Doppler B-scope Presentation of Moving Targets.	A. E. Bailey W. S. Elliot H. Pursey	RRDE Memo 82 or JEIA 8250	Feb. 12 1945
19.000 COMMUNICATION (TROPOSPHERIC)				
19.001	Data on Wave Propagation (10 Kilocycles to 60 Megacycles).	R. S. Baldwin L. C. Young	NRL Rep. No. R-1300	Aug. 20 1936
19.002 S	Study of Field Strength Records Obtained on the Post Office Ultra-Short-Wave Radio Telephone Link Between Guernsey and England. (Wavelength 5 m and 8 m).	R. L. Smith-Rose A. C. Stickland	DSIR RRB/C.39	Sept. 1 1941
19.003 C	3000 Megacycle Communication.	H. H. Beverage RCA	NDRC- PDRC-90	Mar. 10 1942
19.004 C	Microwave Telephone. Part I: Omnidirectional. Part II: Directional.	H. H. Beverage RCA	NDRC- SC-13	Mar. 22 1943
19.005 S	Trials of WS No. X 20. A.	British Min. of Supply	AC 4139/ Com. 176	June 2 1943
19.006 R	Factors Determining the Range of Radio Communications in the Various Theaters of Operation.	J. W. Herbstreit	OCSO ORG-P-14-1	June 3 1943
19.007 C	Radiotelephone Communication on 3000 Megacycles.	P. A. Anderson K. E. Fitzsimmons C. L. Barker S. T. Stephenson	Wash. State Coll. Rep. No. 2 NDRC-PDRC 647	June 12 1943
19.008 S	An Analysis of the Effect of Frequency on Short Distance Radio Communications.	R. Bateman W. Q. Crichlow	OCSO ORB-P-15-1	Aug. 18 1943
19.009 C	Use of the 25 to 50 Mc/s Band for Short Range Wireless Communication.	English AORG	AORG No. 130	Aug. 27 1943
19.010 S	Trials with a 250-Watt Frequency-Modulated VHF Sender Across a Sea Water Path Beyond the Optical Range.	G. W. Higgins Capt. W. H. Hill	SRDE No. 878	Sept. 1943
19.011 S	Radio Communication in Jungles.	A. C. Omberg	OCSO ORG-2-1	Sept. 1 1943
19.012 C	Measurement of Factors Affecting Jungle Radio Communication.	J. W. Herbstreit W. Q. Crichlow	OCSO ORB-2-3	Nov. 10 1943
19.013 R	Methods for Improving the Effectiveness of Jungle Radio Communication.	War Dept.	War Dept. TB Sig 4	Jan. 14 1944



<i>Bib. No.</i>	<i>Title</i>	<i>Author or Source</i>	<i>Number</i>	<i>Date</i>
19.000 COMMUNICATION (TROPOSPHERIC) (continued)				
19.014 R	Survey of Existing Information and Data on Atmospheric Noise Level over the Frequency Range 1-30 Mc/s.	H. A. Thomas R. E. Burgess NPL	DSIR RRB/C.90 or JEIA 2815	Feb. 21 1944
19.015 S	Proposals for Provision and Application of Propagation Data for Operational & Field Use with Wireless Equipment in the Centimetre Band.	Lt. E. W. Walker	SRDE No. 908	Feb.-Mar. 1944
19.016 C	Methods of Reducing Radar Interference to Communication.	ORB	OCSO ORB-E-27-2	Apr. 19 1944
19.017 C	The Application of Passive Repeaters to Point to Point Communication at VHF and UHF.	R. Bateman	OCSO ORB-P-20-1	Apr. 29 1944
19.018 R	Point to Point Communication in VHF Band Via Ground Wave Propagation. (Southwest Pacific Area.)	W. C. Babcock	JEIA 6768 or Intel. Br. OCSO SWPA 413.44/ R423.5	July 24 1944
19.019 R	Ground Wave Radio Propagation Report. (Southwest Pacific Area.)	W. C. Babcock	JEIA 6769 or Intel. Br. OCSO SWPA 413.44/ R113	Aug. 15 1944
19.020 S	Summary of Radio Propagation Problems in Southwest Pacific Area.	W. C. Babcock	JEIA 6298 or Intel. Br. OCSO US/413.44/ R113	Sept. 6 1944
	And Point to Point Communication in MF Band Via Ground Wave Propagation.	W. C. Babcock	JEIA 6770 or Intel. Br. OCSO SWPA 413.44/ R423.4	Aug. 15 1944
19.021 C	Measurements of Factors Affecting Radio Communication & Loran Navigation in SWPA.	R. Bateman J. W. Herbstreit R. B. Zechiel	OCSO ORB-2-4	Dec. 16 1944
19.022 S	Field Trials of Ultra Short Wave Frequency and Amplitude Modulated Multichannel Radio Telephone Systems.	A. W. Pearson W. J. Bray J. H. H. Merriman R. W. White J. G. Hobbs C. H. Gibbs H. Prain	POED Radio Rep. No. 1115	Mar. 27 1944

## 20.000 UNDER-WATER SOUND PROPAGATION

Included in this Bibliography because of the similarity of problems.

20.001 R	Sound Transmission in Sea Water. (A Preliminary Report.)	Woods Hole Oceanographic Institution for NDRC		Feb. 1 1941
20.002 C	Some Characteristics of the Sound Field in the Sea.	Oceanographic Division. U.C.	NDRC C4-sr30-083	Mar. 13 1942
20.003 C	Theoretical Discussion of Reverberation.	C. L. Pekeris Columbia Univ.	NDRC C4-sr20-097	May 29 1942
20.004 C	Sound Ranges under the Sea.	T. H. Osgood Columbia Univ.	NDRC C4-sr20-100	June 5 1942
20.005 C	Reverberation in Echo Ranging, Part I, General Principles.	W. V. Houston T. H. Osgood Columbia Univ.	NDRC C4-sr20-140	July 28 1942



<i>Bib. No.</i>	<i>Title</i>	<i>Author or Source</i>	<i>Number</i>	<i>Date</i>
20.000 UNDER-WATER SOUND PROPAGATION ( <i>continued</i> )				
20.006 C	Attenuation of Underwater Sound.	F. A. Everest H. T. O'Neil	UCDWR- NDRC C4-sr30-494	2/16/42 Revised 7/30/42
20.007 C	Reverberation Studies at 24 KC.	Reverberation Group, Univ. of California	UCDWR-U7 NDRC-Sec. 6.1 sr30-401	Nov. 23 1942
20.008 C	Transmission of Explosive Impulses in the Sea.	T. F. Johnston R. W. Raitt	UCDWR-U8 NDRC C4-sr30-403	Dec. 2 1942
20.009 C	Variation of the Sound Field Near the Surface in Deep Water.	H. T. O'Neil T. F. Johnston	UCDWR-U49 NDRC-Sec. 6.1 sr30	Mar. 16 1943
20.010 C	Reverberation in Echo Ranging, Part II. Reverberation Found in Practice.	T. H. Osgood	CUDWR NDRC-Sec. 6.1 sr20-840	Apr. 14 1943
20.011 C	Theory of Diffraction of Sound in the Shadow Zone.	C. L. Pekeris	CUDWR NDRC-Sec. 6.1 sr20-846	May 5 1943
20.012 C	Reflection of Sound in the Ocean from Temperature Changes.	R. R. Carhart	UCDWR-U74 NDRC-Sec. 6.1- sr30-960	May 17 1943
20.013 C	The Discrimination of Transducers Against Reverberation.	Reverberation Group, Univ. of California	UCDWR-U75 NDRC Sec. 6.1 sr30-968	May 31 1943
20.014 C	The Propagation of Sound in Shallow Water.	G. M. Roe Bureau of Ships	BuShips Rep. 65	June 3 1943
20.015 C	Some General Ideas Concerning the Transmission of Sound in the Deep Sea.	C. Eckart	UCDWR No. M108 NDRC Sec. 6.1-sr30	Sept. 28 1943
20.016 C	Interim Report on the Sound Field of Echo-Ranging Gear.	NRSL & U. of Calif.	UCDWR No. U113 NDRC Sec. 6.1- sr30-1206	Oct. 1 1943
20.017 C	Conclusions Derived from the Analysis of Transmission Data Obtained During Harbor Surveys (Preliminary Draft, Part I).	UCDWR	UCDWR No. U110 NDRC Sec. 6.1-sr30	Oct. 2 1943
20.018 C	Lloyd Mirror Effect in a Variable Velocity Medium.	R. R. Carhart U. of Calif.	UCDWR M 140 NDRC Sec. 6.1-sr30	Oct. 23 1943
20.019 C	A Survey of the Problem of Maximum Echo Ranges (Preliminary Draft).	C. Eckart U. of Calif.	UCDWR-U130 NDRC Sec. 6.1 sr30-1315	Nov. 20 1943
20.020 C	Use of Submarine Bathythermograph Observations (Revision of Rules for Predicting Maximum Sound Ranges).		NAVSHIPS 943-F	1944
20.021 C	Maximum Echo Ranges—Their Prediction and Use.	U. of Calif.	UCDWR-NDRC Sec. 6.1- sr30-1460	January 1944
20.022 C	Sound Transmission Through Destroyer Wakes.	Listening Section	UCDWR-M189 NDRC Sec. 6.1- sr30	Mar. 8 1944
20.023 C	Some Experiments on the Transmission of Continuous Sound in 100-Fathom to 600-Fathom Water.	Listening Section	UCDWR-M193 NDRC Sec. 6.1- sr30	Mar. 15 1944
20.024 C	Effect of the Thermocline on the Propagation of Sound.	P. S. Epstein U. of Calif.	UCDWR Rep. No. 5	Mar. 19 1944



<i>Bib. No.</i>	<i>Title</i>	<i>Author or Source</i>	<i>Number</i>	<i>Date</i>
20.000 UNDER-WATER SOUND PROPAGATION <i>(continued)</i>				
20.025 C	Prediction of Sound Ranges from Bathythermograph Observations. (Rules for Preparing Sonar Messages.)		NAVSHIPS 943-C2	March 1944
20.026 C	Preliminary Report on the Sonic Ray Plotter.	L. I. Schiff U. of P. for U. of Calif.	UCDWR M 207	Apr. 21 1944
20.027 C	Current Methods for Prediction of Maximum Sound Ranges.	Sonar Analysis Section	CUDWR Tech. Memo No. 1	May 1 1944
20.028 C	The Attenuation of Sound in the Sea.	C. Eckart U. of Calif.	UCDWR-U236 NDRC Sec. 6.1- sr30-1532	July 6 1944
20.029 C	The Sonic Ray Plotter.	L. I. Schiff U. of P. for U. of Calif.	UCDWR-U246 Sec. 6.1- sr30-1741	Aug. 8 1944
20.030 C	Sound Ranges under the Sea. (Revision of Report dated June 5, 1942.)	Sonar Analysis Section	CUDWR NDRC Sec. 6.1-sr11- 31-1880	November 1944
20.031 C	Prediction of Sonic and Supersonic Listening Ranges.	Sonar Analysis Section	CUDWR NDRC Sec. 6.1- sr1131-1884	December 1944
20.032 C	Relation Between Scattering & Absorption of Sound.	Sonar Analysis Section	CUDWR Memo for File SAS-8	Dec. 11 1944
20.033 C	Coherence of CW Reverberations.	Sonar Analysis Section	CUDWR Memo for File SAS-11	Dec. 20 1944
20.034 C	Distribution of Amplitude if Two Rays with Random Phase and Given Amplitude Distributions Interfere.	Sonar Analysis Section	CUDWR Memo for File SAS-13	Jan. 4 1945
20.035 C	Fluctuations of Transmitted Sound in the Ocean.	Sonar Analysis Section	CUDWR Tech. Memo No. 6	Jan. 17 1945
20.036 C	Lloyd Mirror Effect in the Presence of a Temperature Gradient.	Sonar Analysis Section	CUDWR Memo for File SAS-17	Jan. 22 1945
20.037 C	Change of Average Peak Echo Intensity with Changing Ping Length.	Sonar Analysis Section	CUDWR Memo for File SAS-30	Mar. 22 1945
20.038 C	The Wave Equation with Gravitational Terms.	Sonar Analysis Section	CUDWR Memo for File SAS-37	June 18 1945

<sup>a</sup>TM 11-486 (Apr. 25, 1945) together with TM 11-487—"Electrical Communication Systems Equipment." (Oct. 2, 1944) supersedes TM 11-486 (Feb. 25, 1944).

<sup>b</sup>See also 1.012 Part I.

<sup>c</sup>See also 1.012 Parts I, VIII, and XIV.

<sup>d</sup>See also 1.012 Part IV.

<sup>e</sup>See also 1.012 Parts III and IX, 5.049, 15.016, and 17.073.

<sup>f</sup>See also 1.012 Part XII and XIII, 6.028, 6.031, and 6.037.

<sup>g</sup>See also 1.012 Part VI and 6.035.

<sup>h</sup>See also 1.012 Parts V, VII, XII, and XV, 1.014 and 8.028.

<sup>i</sup>See also 1.012 Part II, 17.061 and 17.081.

<sup>j</sup>See also 13.012.

<sup>k</sup>See also 6.035 and 11.003.



## OSRD APPOINTEES

### COMMITTEE ON PROPAGATION

#### *Chairman*

CHAS. R. BURROWS

#### *Members*

H. H. BEVERAGE  
T. J. CARROLL  
J. H. DELLINGER

MARTIN KATZIN  
D. E. KERR  
J. A. STRATTON

#### *Consultants*

S. S. ATTWOOD

J. A. STRATTON

C. E. BUELL

#### *Technical Aides*

(Listed in the order they served.)

A. F. MURRAY  
S. W. THOMAS  
R. J. HEARON



# CONTRACT NUMBERS, CONTRACTORS AND SUBJECT OF CONTRACTS

<i>Contract Numbers</i>	<i>Name and Address of Contractor</i>	<i>Subject</i>
OEMsr-1207	Columbia University New York City, New York	Correlation, analysis and integration of data on radio and radar propagation.
OEMsr-728	State College of Washington Pullman, Washington	Develop meteorological equipment and conduct meteorological soundings in the Southwest Pacific and correlate it with radio propagation data.
OEMsr-1497	Humble Oil & Refining Company Houston, Texas	Development and construction of microwave field strength measuring sets.
OEMsr-1496	University of Texas Austin, Texas	Development of equipment for and making measurements of time and space deviations in radio wave propagation.
OEMsr-1502	Jam Handy Organization, Inc. Detroit, Michigan	Preparation of a General Outline of Training Material and the preparation of manuals, films and other training aids for use in instructing technical and other personnel in radio-weather and radio propagation.



## SERVICE PROJECTS

The Committee on Propagation did all of its work under Project Control SOS-9, which was originally set up through the request of the Combined Chiefs of Staff following recommendations submitted by the Combined Meteorological Committee: (a) That the Committee on Propagation of the National Defense Research Committee be requested to act as a coordinating agency for all meteorological information associated with short wave propagation; (b) That the Committee on Propagation be requested to forward periodically to the CMC a list of all reports and papers dealing with the meteorological aspects on short wave propagation which have been received or transmitted by that Committee.

Later the Combined Meteorological Committee in its 37th meeting on Tuesday, February 22, 1944, agreed, that "the National Defense Research Committee [NDRC], Committee on Propagation, be recognized as the supervising committee on all basic research being done in the United States on the related problems of radar propagation and weather, in addition it shall be the recognized channel whereby international exchange of papers of the two related sciences will be effected."

The Joint Communications Board therefore approved the following policy, which was concurred in by NDRC and by the Joint Meteorological Committee:

1. The NDRC Propagation Committee and its associated working groups will initiate and exercise technical supervision over such tests and investigations as they deem necessary to ascertain the nature of the above-mentioned propagation anomalies in the VHF, UHF, and SHF bands, to devise the most practicable methods to determine the occurrence and characteristics of these anomalies from appropriate meteorological forecasts, with a view to improving the interim solu-

tions offered by the Joint Wave Propagation Committee of the JCB.

2. The Army and Navy will furnish by direct coordination between them the basic staff guidance for such tests and investigations. They will accomplish this by determining:

a. The specific forms in which basic prediction data shall be presented, and

b. The method of use required for operational forecast of propagation anomalies in the VHF, UHF, and SHF bands.

3. When the NDRC requires the cooperation of the operating units of the Army and Navy in conducting such tests and investigations as it deems necessary and this cooperation is of such an extent and nature that it cannot be furnished by informal coordination, it will be requested through the Joint Wave Propagation Committee of the JCB. Such requests will be initiated by the NDRC representative on the Wave Propagation Committee and recommended to the Joint Communications Board by the Joint Wave Propagation Committee for consideration.

4. The Joint Wave Propagation Committee will be responsible for devising and furnishing immediately, interim operational forecasting guides based upon information already available.

On April 3, 1944, the Coordinator of Research and Development requested that the Army Project SOS-9 be made a joint Army-Navy project. Project No. AN-16 was assigned to this.

On May 23, 1944, the Chief Signal Officer requested that under Project AN-16 the following work be inaugurated:

Project AC 230.04 "Wave Propagation Study of Line-of-Sight Communication and Navigation."



# INDEX

The subject indexes of all STR volumes are combined in a master index printed in a separate volume. For access to the index volume consult the Army or Navy Agency listed on the reverse of the half-title page.

- Absorption of microwaves,
  - 82-90, 222-224
  - atmospheric gases, 89-90
  - rain and hail, 85-88
  - water drops, 222-224
- Advection, definition, 75-76, 212
- Advective ducts, coastal and maritime conditions, 77-78, 213-214
- Airplane radar cross sections, 83-84
- Angle-of-arrival measurements, 73-74
- Antenna patterns for ground radar, 162-167
  - earth curvature effect on lobe lengths, 166-167
  - factors, 164
  - local terrain effects, 164-166
  - reflecting screen, 163
  - vertical patterns, 162, 164
- Antigua transmission experiments, 71-73
- Atmospheric refraction
  - see Atmospheric stratification and refraction; Radar errors due to atmospheric refraction
- Atmospheric stratification and refraction, 75-76, 198-210
  - advection, 75-76
  - attenuation, 207
  - convection, 76
  - duct, superrefraction, 204-207
  - frictional turbulence, 76
  - measurement of refractive index, 200
  - nocturnal cooling, 75-76
  - operational applications, 208-210
  - origin of refractive index variations, 198-200
  - rays in stratified atmosphere, 202-204
  - reflection from elevated layer, 208
  - subsidence, 76
  - temperature inversions, 76
  - types of modified index curves, 202
  - wave picture of guided propagation, 207-208
- Attenuation diagrams for surface ducts, 240
- Bending of radio waves, 178-180
- Bilinear M curve, first mode, 228-232
  - completely trapped modes, 232
  - depth loss, 231
  - leaky modes, 232
  - surface barrier strength increase, 231
  - undiscovered solution, 231-232
- Bilinear M curve, second and higher modes, 234-236
- British transmission experiments, 58-60
  - Irish Sea experiment, 58-59
  - overland path, 59-60
- Calculations for second and higher modes of bilinear model, 234-236
- Calibration and testing of ground radars, 174-177
- Canadian transmission experiments, 67
- Captive balloons and kites, 52
- Characteristic values for bilinear M curve
  - first mode, 228-232
  - second and higher modes, 234-236
- Chronological record of Committee on Propagation activities, 13-24
  - 1943; 13-14
  - 1944; 14-20
  - 1945; 20-24
- Anderson's southwest Pacific Theatre work, 17-21
  - program adopted, 15-16
  - specific experiments outlined, 14-15
- Circuit reliability, 222
- Cloud echoes in radar, 184-185
- Coastal and maritime conditions, meteorology, 77-78
  - advection, 77, 213-214
  - duct formation, 77-78
- Contracts and projects, 11-12
  - Columbia University, 11
  - Combined Chiefs of Staff request, 11
  - Humble Oil Company of Texas, 12
  - Jam Handy Organization of Detroit, 12
  - State College of Washington, 11
  - University of Texas, 12
- Convection, 212
- Convergence effects in reflections from tropospheric layers, 258-259
  - conclusions, 259
  - convergence factor, 258-259
  - roughness effect, 259
- Cornu's spiral, 127-128, 131-132
- Coverage diagram, 190-193
  - complex cases, 193
  - definition, 190
  - magnitude of field intensity, 190-191
  - nomographic solutions, 95-105
  - simple cases, 191-193
- Diffraction of radio waves, 120-134
  - by terrain, 37-38
  - Cornu's spiral, 127-128, 131-132
  - Fresnel integrals, 125-127
- Fresnel zones, 121-123
  - limitations of Fresnel theory, 133-134
  - location of maxima and minima, 129-131
  - multiple slits and obstacles, 133
  - narrow obstacle, 132-133
  - obstacles, 124-125
  - over hills, 110-112
  - Rayleigh criterion, 123-124
  - rectangular slit, 131-132
  - reflection from rough surfaces, 123-124
  - shoreline, 158, 162
  - straight edge diffraction, 128-129
  - wave propagation, 121
- Diffraction zone, nonstandard propagation
  - see Nonstandard propagation in diffraction zone
- Divergence factor for reflected wave, 170
- Ducts
  - characteristics in nonstandard propagation, 46-47
  - fades, 220
  - formation, 79
  - over open ocean, 214-215
  - superrefraction, 204-207
  - surface, attenuation diagram, 240
- Dynamic effects in lower atmosphere fronts, 79
  - high pressure area, 79
  - low pressure area, 78-79
  - subsidence, 78-79
- Early warning heightfinding radar, 106-109
- Earth curvature effect on radar antenna lobe lengths, 166-167
- Electromagnetic field, 38-41
  - attenuation factor, 41
  - field strength distribution, 38-39
  - modes, 39-41
- Equipment tests for ground radar, 174-175
- Errors in radar due to atmospheric refraction
  - see Radar errors due to atmospheric refraction
- Fading on different wavelengths, 221-222
- Fixed echo control, shielding, 137
- Flat earth lobe angle calculations, 147-149



- Fog  
   effect on refractive index, 77, 216  
   effect on signal strength, 221
- Forecasting and meteorology  
   *see* Meteorology and forecasting
- Formula for lobe, radar, 171-174
- Formula for lobe angle, radar, 152-155
- Formula for reflection area, 160-162
- Fresnel formulas for reflection  
   coefficient, 32-33
- Fresnel integrals for diffraction  
   phenomena, 125-127
- Fresnel theory, limitations for  
   diffraction problems, 133-134
- Fresnel zones, 121-123, 158-162
- Fresnel-Kirchhoff diffraction theory, 37
- Frictional turbulence, 212-213
- Gaussian distribution, 259
- Graphical method for determination of  
   standard coverage charts, 93-94
- Ground and sea reflection, 28
- Ground radar, antenna patterns  
   earth curvature effect on lobe  
     lengths, 166-167  
   factors, 164  
   local terrain effects, 164-166  
   reflecting screens, 163  
   vertical patterns, 162, 164
- Ground radar, equipment, 106-109  
   conclusions, 109  
   derivation of formulas, 109  
   early warning heightfinding radar,  
     106-109  
   gunlaying (antiaircraft) radar,  
     106-107, 109  
   surface surveillance radar, 108  
   tests, 174-175
- Ground radar, siting and coverage,  
   113-177  
   calculation of vertical coverage,  
     145-174  
   calibration and testing, 174-177  
   diffraction of radio waves, 120-134  
   permanent echoes, 134-145  
   radar systems, 113-115  
   signal measurements, 175-176  
   topography of siting, 115-120
- Ground radar, test data analysis,  
   176-177  
   calibrated receiver method, 177  
   maximum free space range, 176-177  
   signal-to-noise graph, 176
- Ground radar, types, 113
- Ground reflection, 190-193
- Ground roughness estimation, 36-37
- Guided propagation, 179-182  
   *see also* Superrefraction  
   coverage, 181-182  
   critical angle, 181  
   definition, 190  
   duct, 181-182  
   equipment faults, 182  
   in nonhomogeneous atmosphere,  
     244-246  
   occurrence causes, 185  
   wave picture, 207-208
- Gunlaying (antiaircraft) radar,  
   106-107, 109
- Hankel functions in propagation  
   equation solution, 237-239
- Heightfinding radar, early warning,  
   106-108
- Height-gain functions, 255
- Historical background for nonstandard  
   propagation, 42
- History of Committee on Propagation,  
   5-27  
   chronological record of activities,  
     13-24  
   contracts and projects, 11-12  
   critique, 26  
   investigating bodies, 10  
   liaison channels, 8  
   objectives, 9-10  
   organization, 6-7  
   origin, 5-8  
   research recommendations, 26-27  
   results, 25-26
- Humidity and temperature in  
   meteorological measurements,  
     50
- Huyghens' principle, wave  
   propagation, 121
- Incipient leakage in surface duct,  
   233-234  
   attenuation constant, 233  
   conclusion, 234  
   Freehafer and Furry formula, 233
- Irish Sea transmission experiment,  
   58-59
- Leaky waveguide theory, 48
- Lobe angle calculations, 147-158  
   computing methods, 155  
   correction for standard earth  
     curvature, 149-152  
   diagrams of medium height sites,  
     158  
   flat earth, 147-149  
   formula, 152-155  
   general lobe formula, 171-174  
   lobe lengths, 166-167, 170  
   low site lobes, 155-156  
   reflection area, general formula,  
     160-162  
   sea reflection with diffuse land  
     reflection, 158-159  
   shoreline diffraction, 158, 162
- Lobes for medium height radar, 170
- Local terrain effects on antenna  
   pattern, 164-166  
   cliff edge diffraction, 166  
   land reflection and diffraction, 166  
   limited reflecting area, 165
- M curves, 43, 55-57
- Meteorological factors in radar  
   coverage, 182-184  
   air turbulence, 184  
   measurements, 184  
   occurrence frequency of guided  
     propagation, 184  
   over land, 183-184  
   over sea, 183  
   refraction causes, 182-183  
   subsidence, 184  
   temperature inversion, 182-184  
   trapping, 182-184
- Meteorological measurements, 50-57  
   anemometers, 55-56  
   M curves, 55-57  
   noncaptive radiosonde, 52-55  
   psychrometer, 52-55  
   refractive index measurements, 52  
   temperature and humidity elements,  
     50  
   wired sonde, 51
- Meteorology and forecasting, 75-81  
   atmospheric stratification, 75-76  
   coastal and maritime conditions,  
     77-78  
   conditions over land, 76-77  
   dynamic effects, 78-79  
   fog, 77  
   radar forecasting, 80-81  
   radio forecasting, 75  
   world survey, 79-80
- Microwave permanent echoes, 144-145
- Microwaves, scattering and absorption  
   *see* Scattering and absorption of  
     microwaves
- Moisture gradients, 210-212
- Nocturnal cooling, 75-77, 212, 215-216
- Nomographic solutions for coverage  
   diagrams, 95-105
- Nonoptical radio transmission path,  
   221-222
- Nonstandard propagation, 42-49  
   continuously varying modified index  
     curve, 247-248  
   duct characteristics, 46-47  
   historical background, 42  
   in ocean surface duct, 247  
   operational applications, 208-210  
   perturbation theory for exponential  
     M curve, 249-255  
   ray tracing, 44-45  
   reflection from elevated layers, 49



- refractive index, 42-44
- symbols, 255
- waveguide theory survey, 47-48
- Nonstandard propagation, operational applications, 208-210
- ground clutter interference, 208
- radio countermeasures, 210
- superrefraction, 208-210
- VHF navigational aids, 209-210
- Nonstandard propagation in diffraction zone, 226-227
- complex arguments, 227
- Eckersley modes, 226
- Gamow modes, 226
- horizontal attenuation of various modes, 226
- numerical integration method, 226-227
- phase integral methods, 227
- Oceanic surface duct, propagation in, 247
- Optical properties of earth surface and atmosphere, 32-38
- diffraction by terrain, 37-38
- electromagnetic properties of ground, 32-33
- Fresnel formulas, 32-33
- Fresnel-Kirchhoff diffraction theory, 37
- horizontal polarization, 32-34
- Rayleigh criterion for roughness of ground, 36-37
- reflection coefficients, 32-34
- roughness of ground, 36-37
- Snell's law, 36
- standard refraction, 34-36
- vertical polarization, 32-33
- Organization of propagation research program
- initial committee membership, 7
- liaison channels, 8
- program plan, 6-7
- Overland path transmission experiment, 59-60
- Permanent echo diagrams, 134-135
- plotting data, 135
- typical preparation, 134-135
- uses, 134
- Permanent echo prediction, 137-144
- methods of determination, 137
- profile method, 137-144
- radar planning device technique, 137-138
- supersonic method, 138
- Permanent echoes in radar siting diagrams, 134-135
- microwaves, 144-145
- prediction of permanent echoes, 137-144
- reasons for variations, 135-136
- shielding, 137
- testing uses, 135-137
- troublesome factors, 134
- Perturbation theory for M curve in nonstandard propagation, 249-255
- abstract, 249
- application to general class of M anomalies, 254
- computational program for exponential model, 254-255
- evaluation of indefinite integral, 251-252
- formal solution by perturbation method, 250-251
- iteration solution for characteristic values and coefficients, 253-254
- properties of indefinite integral, 252-253
- Power transmission in standard propagation, 31-32
- antenna gain, 31
- general transmission formula, 31-32
- thermal noise power, 32
- Precipitation echoes in radar, 184-185
- Profile method of permanent echo prediction, 137-144
- detailed example of difficult site, 141-144
- estimation of diffraction effects, 139-140
- general procedure, 140-141
- line-of-sight curve, 138-140
- plotting rules, 141
- principal requirements, 138
- Projects and contracts
- see* Contracts and projects
- Propagation, influencing factors
- guided propagation, 190
- refraction, 189-190
- standard refraction, 189-190
- superfraction, 190
- Propagation, nonstandard
- see* Nonstandard propagation
- Propagation, standard
- see* Standard propagation
- Propagation Committee
- see* History of Propagation Committee
- Propagation equation solution with Hankel functions, 237-239
- conclusions, 239
- exponential decay factor of horizontal waves, 237-238
- field of dipole source equation, 237
- given dependence of refraction index upon height, 237-238
- Stokes phenomenon, 238
- Propagation fundamentals, 189-198
- equivalent earth radius flat earth diagram, 195
- factors influencing propagation, 189-190
- ground reflection, 190-193
- horizon diffraction, 197-198
- refraction over curved earth, 194-195
- significance of propagation problems, 189
- Snell's law of refraction, 194
- Propagation in oceanic surface duct, 247
- Propagation research
- equipment problems, 26-27
- meteorological problems, 26-27
- organization, 6-7
- origin, 5-8
- propagation problems, 26
- recommendations, 26-27
- Radar, early warning heightfinding, 106-109
- absolute altitude errors, 107-108
- azimuth errors, 108
- range errors, 108
- relative altitude errors, 108
- tolerances, 106-107
- Radar, ground
- see* Ground radar, equipment
- Radar, precipitation echoes, 184-185
- Radar and radio transmission relationship, 63-65
- Radar coverage variations, 178-184
- cloud echoes in radar, 184-185
- guided propagation, 180-182
- meteorological factors, 182-284
- refraction of radio waves, 178-180
- summary of radar propagation facts 185
- Radar cross section, 82-84
- Radar data test flights, 176
- Radar errors due to atmospheric refraction, 106-109
- conclusions, 109
- derivation of formulas, 109
- early warning heightfinding radar, 106-109
- gunlaying (antiaircraft) radar, 106-107, 109
- refraction index variation, 106
- surface surveillance radar, 108
- Radar forecasting, 80-81
- Radar planning device (RPD), 137-138
- Radar range estimation over open ocean, 256-257
- attenuation constant, fractional change, 256-257
- duct thickness, 257
- low ducts, 256



- Radar siting  
 permanent echoes; *see* Permanent echoes in radar siting  
 technical aspects, 114-115  
 topography, 115-120
- Radar systems, tactical aspects, 113-114
- Radar vertical coverage calculations  
*see* Vertical coverage calculations for ground radars
- Radio and radar transmission relationship, 63-65
- Radio meteorology, 210-224  
 advective ducts, coastal conditions, 213-214  
 ducts over open ocean, 214-215  
 dynamic effects, 216-218  
 fluctuations in signal strength with time, 219-222  
 fog, 216  
 nocturnal cooling, daily variations, 215-216  
 physical causes of stratification, 212-213  
 scattering and absorption by water drops, 222-224  
 Snell's law, 224-225  
 subsidence, 216-218  
 superrefraction, seasonal and global aspects, 218-219  
 temperature and moisture gradients, 210-212  
 turbulence, 212-213
- Radio scintillations, 219-220
- Radio wave diffraction  
*see* Diffraction of radio waves
- Radio wave propagation research  
 origin, 5-8  
 historical background, 5-6  
 pertinent aspects of modern warfare, 5-6  
 plan of investigation, 5-6  
 purpose of Committee on Propagation, 5
- Radio wave refraction, 178-180
- Rain and hail absorption of microwaves, 85-88
- Ray tracing, 44-45
- Rayleigh criterion for roughness of ground, 36-37
- Rays in stratified atmosphere, 202-204
- Reflected beam, magnitude of field intensity, 190-191
- Reflected wave, divergence factor, 170
- Reflection area, general formula, 160-162
- Reflection coefficients, 32-34, 167-169
- Reflection from elevated layer, 208
- Reflection from ground, 190-193  
 complex cases, 193  
 coverage diagrams, 190  
 earth gain factor, 192-193  
 magnitude of field intensity, 190-191  
 simple cases, 191-193
- Reflection from rough surfaces, 123-124
- Reflection from tropospheric layers, convergence effects, 258-259
- Refraction, atmospheric  
*see* Atmospheric stratification and refraction; Radar errors due to atmospheric refraction
- Refraction of radio waves, 178-180
- Refraction over curved earth, 194-195
- Refractive index  
 fog effect, 77, 216  
 in nonstandard propagation, 42-44  
 M curves, 43  
 Snell's law, 42-43  
 temperature inversion, 43-44  
 variations, 198-200
- Refractive index measurements, 200  
 airborne installations, 52  
 captive balloons and kites, 52  
 stationary installations on towers, 52
- Remote shielding, 119-120
- Research recommendations, 26-27
- RPD (radar planning device), 137-138
- San Diego transmission experiments, 68-71, 208
- Scattering and absorption of microwaves, 82-90  
 absorption by atmospheric gases, 89-90  
 aircraft targets, 83-84  
 by water drops, 222-224  
 clouds, fog, rain, hail, snow, 85-90  
 radar cross section, 82-83  
 rain and hail absorption, 85-88  
 scattering echo, 88-89  
 ship targets, 84-85
- Scattering radar cross section, 82-83
- Scintillations, radio, 219-220
- Shielding as fixed echo control, 137
- Ship radar cross section, 84-85  
 aircraft carrier, 85  
 battleship, 84  
 cruiser, 84  
 submarine, 85
- Shoreline diffraction, 158, 162
- Signal measurements for ground radars, 175-176
- Signal strength fluctuations, 219-222  
 blackout, 220  
 circuit reliability, 222  
 duct fades, 220  
 effect of waves on sea, 219  
 fading on different wavelengths, 221-222  
 fog, 221  
 fronts and thunderstorms, 220-221  
 nonoptical path, 221-222  
 optical path, 221-222  
 scintillations, 219-220  
 target modulation, 219  
 tidal effects, 219
- Siting and coverage of ground radar  
*see* Ground radar, siting and coverage
- Snell's law of refraction  
 for curved earth, 42-43, 194-195, 224-225  
 general statement, 194, 224  
 rays in stratified atmosphere, 202-204
- Standard coverage charts, graphical  
 method of determination, 93-94
- Standard propagation, 31-41, 179-180, 185  
 atmospheric effects, 180  
 coverage diagrams, 179-180  
 deviations, 179-180  
 electromagnetic field, 38-41  
 height factor, 180  
 optical properties of earth's surface and atmosphere, 32-38  
 power transmission, 31-32  
 refraction, 179  
 summary, 185
- Standard refraction, 34-36, 189-190, 217  
*see also* Standard propagation
- Straight edge diffraction, 128-129
- Stratification, atmospheric  
*see* Atmospheric stratification and refraction
- Stratification causes, 212-213  
 advection, 212  
 convection, 212  
 frictional turbulence, 212-213  
 nocturnal cooling, 212  
 subsidence, 212  
 temperature inversions, 213
- Stratified atmosphere, rays in, 202-204
- Subsidence  
 definition, 76, 183-184, 212  
 duct formation, 216-217  
 fronts, 217-218  
 high pressure areas, 79  
 standard propagation, 217
- Superrefraction  
*see also* Guided propagation  
 causes, 185  
 definition, 190  
 duct, 204-207  
 operational applications, 208-210
- Superrefraction, world survey  
 Arabian Sea, 79-80, 218  
 Atlantic Coast of United States, 79, 218  
 Bay of Bengal, 80, 219  
 Mediterranean region, 79-80, 218  
 Pacific Ocean, 80, 219  
 Western Europe, 79-80, 218



- Surface duct, incipient leakage, 233-234
- Surface duct attenuation diagrams, 240
- Surface surveillance radar, 108
  - azimuth errors, 109
  - range errors, 109
- Symbols for use in theory of nonstandard propagation, 255
- Tactical aspects of radar systems, 113-114
- Temperature and humidity in meteorological measurements, 50
- Temperature and moisture gradients, 210-212
- Temperature inversions
  - coastal and maritime conditions, 77-78
  - conditions for occurrence, 76, 213
  - conditions over land, 76-77
  - M curves, 43-44
  - meteorological factors, 182-184
- Terrain effects on antenna
  - pattern, 164-166
  - cliff edge diffraction, 166
  - land reflection and diffraction, 166
  - limited reflecting area, 165
- Terrain reflection characteristics, 167-169
- Test flights for radar data, 176
- Testing of ground radars, 174-177
- Tidal effects on signal strength, 219
- Topography of siting, 115-120
  - azimuth of sun, 116-117
  - hour angle, 116
  - maps and surveys, 115
  - orientation, 116-117
  - profiles, 115-116
  - visibility problems, 117-120
- Transmission experiments,
  - angle-of-arrival, 73-74
- Transmission experiments, Antigua, 71-73
  - duct studies, 71
  - equipment employed, 71
  - field strength records, 71-73
  - M curve measurement, 71-72
- Transmission experiments, British, 58-60
  - Irish Sea experiment, 58-59
  - overland path, 59-60
- Transmission experiments, Canada, 67
- Transmission experiments, east coast, 60-65
  - Bell Telephone Laboratories, 60
  - Radiation Laboratory (MIT), 60
  - RCA Communications, Inc., 60
  - relationship between radio and radar transmission, 63-65
  - results, 60-65
  - signal occurrence frequency, 63
- Transmission experiments, southwest, 68-71, 208
  - Arizona desert, 71
  - San Diego, 68-71, 208
- Transmission experiments, State College of Washington, 65-67
- Trapping, 182-185
  - see also* Guided propagation
- Tropospheric propagation, 189-210
  - atmospheric stratification and refraction, 198-210
  - propagation fundamentals, 189-198
- Turbulence
  - see* Stratification causes
- Vertical coverage calculation for ground radars, 145-174
  - antenna patterns, 162-167
  - coefficient of reflection, 167-169
  - diagram construction, 146-147
  - divergence, 170
  - earth curvature effect on lobe lengths, 166-167
  - flat earth lobe angle calculations, 147-149
  - general lobe angle formula, 152-155
  - general lobe formula, 171-174
  - lobe angles corrected for standard earth curvature, 149-152
  - lobe diagrams of medium height sites, 158
  - lobe lengths, 170
  - local terrain effects, 164-166
  - low site lobes, 155-156
  - modified antenna pattern, 162
  - reflection area, general formula, 160-162
  - sea reflection with diffuse land reflection, 158-159
  - shoreline diffraction, 158, 162
- Visibility problems, 117-120
  - diffraction angle, 120
  - dip and rise, 118-120
  - horizon distance, 117-118
  - intervening obstructions, 119
  - remote shielding, 119-120
  - solution by computation, 119-120
  - vertical angles, 120
- Wave picture of guided propagation, 207-208
- Wave propagation, 121
  - see also* Nonstandard propagation; Standard propagation
- Waveguide theory survey, 47-48
- Wired sonde, 51

















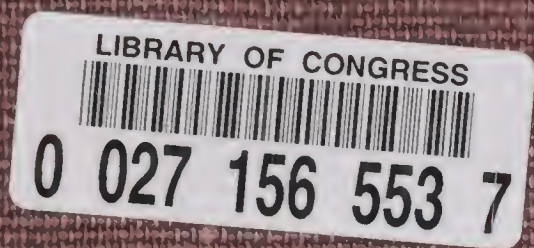




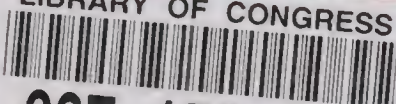








LIBRARY OF CONGRESS



0 027 156 553 7